Anatomy, phylogeny, and palaeoecology of the basal thalattosuchians (Mesoeucrocodylia) from the Liassic of Central Europe

Dissertation
zur Erlangung des Grades
Doktor der Naturwissenschaften

Am Fachbereich 09
Chemie, Pharmazie und Geowissenschaften
der Johannes Gutenberg-Universität Mainz

Inken Juliane Mueller-Töwe
geb. am 3.11.1971 in Bonn

Mainz, 2006

Dekan:

1. Berichterstatter:

2. Berichterstatter:

Tag der mündlichen Prüfung:

Erklärung

Hiermit versichere ich, die vorliegende Arbeit selbstständig und nur unter Verwendung der angegebenen Quellen und Hilfsmittel verfasst zu haben.

Inken Juliane Mueller-Töwe

Mainz, Juli 2006

That`s the advantage of space.
It`s big enough to hold practically *anything*, and so, eventually, it does.

Terry Pratchett

There is nothing amazing about size.
Turtles are amazing, and elephants are quite astonshing.
But the fact that there`s a big turtle is far less amazing than the fact that there is a turtle *anywhere.*

Terry Pratchett

Zusammenfassung

Die marine Krokodilgruppe der Thalattosuchia gehört in den jurassischen Meeresablagerungen Europas zu den häufig vorkommenden Reptilien. Sie ist vom Jura bis zur Unterkreide in ganz Europa weit verbreitet und auch weltweit nachzuweisen. Aufgabe war es, alle aus dem Lias Europas bekannten Arten zu untersuchen.

Die zahlenmäßig am häufigsten vorkommenden Arten *Steneosaurus bollensis* und *Pelagosaurus typus* werden anatomisch revidiert. Neue Erkenntnisse über den Schädel von *Pelagosaurus typus*, wie z.B. die Tatsache eines nicht vollkommen verschmolzenen Frontale, werden anhand von computertomographischen Untersuchungen gewonnen, und erstmals werden juvenile Exemplare dieser Art genauer untersucht.

Die selten vorkommende Art *Platysuchus multiscrobiculatus* wird erstmals detailliert anatomisch beschrieben. Sie weist sowohl im Schädel als auch im Postcranium morphologische Unterschiede zu *Steneosaurus bollensis* und *Pelagosaurus typus* auf. So besitzt *Pl. multiscrobiculatus* u. a. ein Ilium mit einem tieferen Acetabulum und einen Femur mit deutlich geneigtem Femurkopf. Ein juveniles Exemplar von *Pl. multiscrobiculatus* ist nun ebenfalls bekannt und wird in Teilen beschrieben.

Des Weiteren werden die aus England bekannten Arten *Steneosaurus gracilirostris* und *Steneosaurus brevior* untersucht und in Teilen neu beschrieben. *Steneosaurs brevior* wird in dieser Arbeit erstmals mit einem Exemplar aus dem Ober-Lias von Holzmaden belegt und liefert damit neue Erkenntnisse über die paläobiogeographische Verbreitung dieses Taxons.

Durch die hohe Zahl der bearbeiteten Exemplare ist es möglich Wachstumsreihen von juvenil bis adult bei *Steneosaurus bollensis*, *Pelagosaurus typus* und *Platysuchus multiscrobiculatus* zu erstellen. Biometrische Daten zur Erfassung der innerartlichen Variabilität und Ontogenie, als auch zur Artabgrenzung, werden sowohl an den fossilen als auch an einigen rezenten Vergleichs-Arten (z.B. *Gavialis gangeticus*) aufgenommen.

Die Schädel von *Platysuchus multiscrobiculatus* und *Steneosaurus bollensis* werden als Wachsmodell dreidimensional rekonstruiert. Die Rekonstruktion der Schädel bildet in Verbindung mit Vergleichsstudien an rezenten Krokodilen die Grundlage für die Kiefermuskel-Rekonstruktion von *Steneosaurus bollensis*. Mittels funktionsmorphologischer Analyse der Kiefermuskulatur, der Bezahnung, und des Bewegungsapparates von *S. bollensis* werden Rückschlüsse auf Beuteoptionen und Jagdverhalten gezogen.

Zur Klärung der verwandtschaftlichen Beziehungen innerhalb der Thalattosuchia wird eine computergestützte phylogenetische Analyse von 25 Thalattosuchia Arten durchgeführt. Für die phylogenetische Innengruppen-Analyse der Thalattosuchia werden folgende weitere Thalattosuchia-Taxa ebenfalls am Originalmaterial untersucht und verglichen: *Metriorhynchus superciliosus, Metriorhynchus hastifer, Metriorhynchus leedsi, Geosaurus gracilis, Geosaurus giganteus*, *Teleidosaurus calvadosi*, *Teleidosaurus gaudryi*, *Teleosaurus cadomensis*, *Teleosaurus geoffroyi, Steneosaurus priscus*, *Steneosaurus edwardsi, Steneosaurus heberti, Steneosaurus leedsi, Steneosaurus boutilieri*, *Steneosaurus megarhinus, Steneosaurus obtusidens* und *Machimosaurus hugii*. Die phylogenetische Innengruppen-Analyse ergibt auf der Basis von 115 Merkmalen eine eindeutige Trennung der monophyletischen Metriorhynchiden von den ebenfalls monophyletischen Teleosauriden, wobei sich innerhalb beider Gruppen einige Gattungen als paraphyletisch erweisen. *Pelagosaurus typus* ist eindeutig innerhalb der Teleosauriden anzusiedeln und nicht außerhalb oder innerhalb der Metriorhynchiden; letzteres wurde bisher von vielen Autoren angenommen. Auf der Basis dieser Ergebnisse wird ein vorläufiges paläobiogeographisch-evolutives Szenario entworfen.

Abstract

In the marine Jurassic deposits of Europe, a group of marine crocodilians, the Thalattosuchia, belongs to the frequently found reptiles. Thalattosuchia are widely spread in Central Europe from the Jurassic to Lower Cretaceous, and some taxa are also distributed worldwide. The task of the work was to examine all taxa known from the Liassic of Europe.

The most frequently known taxa *Steneosaurus bollensis* and *Pelagosaurus typus* are anatomically revised. New discoveries at the skull of *Pelagosaurus typus* e.g., the fact of a partly paired frontal are described by means of computed tomography investigations. In addition, juvenile specimens of this taxon are studied in detail for the first time.

The rarely occurring taxon *Platysuchus multiscrobiculatus* is anatomically described in detail for the first time. It shows both in the skull and in the postcranial material morphological differences to *Steneosaurus bollensis* and *Pelagosaurus typus*. Thus *Pl. multiscrobiculatus* possesses, e.g., an ilium with a deeper acetabulum and a femur with a distinctly flexed femoral head. A juvenile specimen of *Pl. multiscrobiculatus* is now discovered and is described in parts for the first time, too.

Furthermore, *Steneosaurus gracilirostris* and *Steneosaurus brevior* known from Lower Jurassic deposits of England are examined and in parts revised. In this work, *Steneosaurs brevior* is discovered with one specimen from the Upper Liassic of Holzmaden, Germany for the first time, and provides new evidence for the palaeobiogeographical distribution of the taxon.

Because of the high number of investigated specimens, it is possible to study ontogenetic development from juvenile to adult stage in *Steneosaurus bollensis*, *Pelagosaurus typus*, and *Platysuchus multiscrobiculatus*.

Biometric data are collected from thalattosuchians and extant crocodilians (e.g. *Gavialis gangeticus*) to investigate intraspecific variation, ontogenetic development, and taxa differentiation.

The skulls of *Platysuchus multiscrobiculatus* and *Steneosaurus bollensis* are reconstructed three-dimensionally as wax models. The skull reconstructions form the basis of the jaw muscle restoration of *Steneosaurus bollensis* in connection with comparative studies at extant crocodilians. By means of functional morphologic analysis of the jaw musculature, the dentition, and the locomotor system of *S. bollensis*, possible conclusions are drawn for the prey options and the hunting behaviour.

To clarify the relationships within the Thalattosuchia, a computer-based cladistic phylogenetic in-group analyse of 25 Thalattosuchia taxa is performed. For the analysis, following Thalattosuchia taxa are studied likewise at original material for comparisons: *Metriorhynchus superciliosus, Metriorhynchus hastifer, Metriorhynchus leedsi, Geosaurus gracilis, Geosaurus giganteus*, *Teleidosaurus calvadosi*, *Teleidosaurus gaudryi*, *Teleosaurus cadomensis*, *Teleosaurus geoffroyi, Steneosaurus priscus*, *Steneosaurus edwardsi, Steneosaurus heberti, Steneosaurus leedsi, Steneosaurus boutilieri*, *Steneosaurus megarhinus, Steneosaurus obtusidens,* and *Machimosaurus hugii*. The phylogenetic in-group analyse based on 115 characters, reveals a sister-group relationship of the monophyletic Teleosauridae and monophyletic Metriorhynchidae. Within the groups, some taxa are probably paraphyletic. The taxon *Pelagosaurus typus* is nested inside the Teleosauridae and not outside or within the Metriorhynchidae, as many authors suggested it so far. Based on these results, a tentative palaeobiogeographical-evolutionary scenario is developed.

Contents

List of figures:

Chapter 1

Introduction

1.1 Research history on Thalattosuchia and the aim of the present study

During the Early Jurassic, the first mainly aquatic crocodilians appeared: the Thalattosuchia. The group must have evolved during the Late Triassic, and probably were closely related to the Protosuchia. The Protosuchia as well as the Triassic Sphenosuchia are regarded as very primitive terrestrial crocodilians (WALKER 1968, FREY 1988b, CARROLL 1993). The sister group of the Thalattosuchia is still unknown and no further information is available due to the lack of finds in the Upper Triassic and the earliest Jurassic (see chapter 6). BUFFETAUT (1979a, 1980b, 1982) suggests that the ancestors of the Thalattosuchia might be found within the Upper Triassic protosuchians.

Thalattosuchia represent a monophyletic group of Mesozoic marine crocodilians referred to Mesoeucrocodylia (CLARK 1986, BENTON & CLARK 1988, CLARK 1994). Typical anatomical features of Thalattosuchia are: a mesorostrine to longirostrine rostrum, the separation of the nasals and premaxillae by the maxillae, the reduced dermal armour compared to *Protosuchus* and the short fore limbs with respect to the hind limbs (e.g. BRONN & KAUP 1841-1843; V. MEYER 1841; EUDES-DESLONGCHAMPS 1864; TATE & BLAKE 1876; BERCKHEMER 1928, 1929; WESTPHAL 1962; BUFFETAUT 1980a/b, 1985; GODEFROIT 1994; VIGNAUD 1995). While some taxa remained small, only reaching a size about one meter, the largest taxa grew up to seven meters. The secondary choanae lie at the posterior margin of the palatines and are mostly enclosed by the anterior margin of the pterygoids. Because of this position of the internal nasal aperture, Thalattosuchia have been referred to the Mesosuchia (BUFFETAUT 1982). The two major monophyletic groups inside the Thalattosuchia are the teleosaurids and the metriorhynchids, with *Pelagosaurus typus* as the sister taxon of both (BENTON & CLARK 1988). According to CARROLL (1993) and STORRS & EFIMOV (2000), up to 37 species are referred to the Thalattosuchia, but the in-group relationships are poorly known.

Thalattosuchia have a stratigraphic distribution from the Early Jurassic to the Early Cretaceous (VIGNAUD 1995, HUA et al. 1998), and have, at least during the Upper Jurassic, a nearly worldwide palaeogeographical distribution from Europe to South America, Africa, Madagascar, and probably Asia (BUFFETAUT 1982, GASPARINI 1985, LI 1993, VIGNAUD 1995, STORRS & EFIMOV 2000). However, in the Toarcian the palaeogeographical distribution of teleosaurids and *Pelagosaurus typus* is mainly limited to Central Europe, except for some

doubtful remains of teleosaurids from Asia, Madagascar and America (see chapter 7) (WESTPHAL 1962, LI 1993, VIGNAUD 1995, MAISCH & ANSORGE 2004).

The earliest-known metriorhynchid is *Teleidosaurus* cf. *gaudryi* and appears in the Bajocian of France (HUA & ATROPS 1995). According to JENSEN & VICENTE (1976), the oldest known specimen of *Metriorhynchus* sp. was also found in lower Bajocian levels near Copiapo, Chile. A comprehensive study on Jurassic metriorhynchids, mainly based on the French specimens, was presented by VIGNAUD (1995), but the relationships with the teleosaurids remain poorly known.

This work mainly focuses on the five valid thalattosuchian, i.e. teleosaurid taxa from the Upper Liassic (Toarcian) of Central Europe, *Steneosaurus bollensis*, *Steneosaurus gracilirostris*, *Steneosaurus brevior*, *Platysuchus multiscrobiculatus*, and *Pelagosaurus typus* (WESTPHAL 1961, 1962; VIGNAUD 1995).

Pelagosaurus typus is one of the stratigrapically oldest known thalattosuchians and first occurs in the Upper Liassic (Lower Toarcian) of the Schistes Carton in France. The taxon had originally been described from the Lower Toarcian, Posidonia Shale near Nabern in the Swabian Jura (BRONN 1841). French specimens from the Toarcian of Amaye–sur-Orne had formerly been described by EUDES-DESLONGCHAMPS (1864) as *Teleosaurus temporalis*. *Pelagosaurus typus* reaches a maximum length of two meters and represents the smallest of all Liassic crocodilian taxa. In the Toarcian of Central Europe *Pelagosaurus typus* coexisted with the teleosaurid taxa *Steneosaurus bollensis*, *S. gracilirostris*, *S. brevior*, *and Platysuchus multiscrobiculatus* (e.g. BERCKHEMER 1928, WESTPHAL 1961, 1962; GODEFROIT 1994, URLICHS et al. 1994, VIGNAUD 1995, HAUFF 1997, MAISCH & ANSORGE 2004).

The holotype of *Steneosaurus bollensis* was found near Bad Boll in the Swabian Jura in the year 1712. CUVIER (1812) was the first to describe the specimen as "Gavial de Boll" and for the first time mentioned its crocodilian nature. JAEGER (1828) investigated the specimen in detail and named it *Steneosaurus bollensis*. During the next almost 200 years, hundreds of *Steneosaurus* specimens were found in the Posidonia Shales around Holzmaden, and as a result, numerous taxa were established. The validity of these taxa was investigated by WESTPHAL (1962), in a paper about the systematic of the German and English Liassic crocodiles, and he reduced the number of taxa to five valid ones in the Upper Liassic.

Steneosaurus gracilirostris and *Steneosaurus brevior* both originally come from the Toarcian deposits of the Yorkshire Coast, England. *Steneosaurus gracilirostris* was erected by WESTPHAL (1961, 1962) based on four specimens from the Yorkshire Liassic, which had formerly been partly described by OWEN (1849/1884) and BUCKLAND (1836) as *Teleosaurus*

chapmanni. In addition, GODEFROIT (1994) referred several specimens from the Toarcian of Luxembourg to *Steneosaurus gracilirostris*.

Steneosaurus brevior was first described by TATE & BLAKE (1876) and revised by WESTPHAL (1962). Originally considered to be restricted to English deposits, the present study will show that this taxon also inhabited the Jurassic sea of the Holzmaden area of today (see chapter 3.3).

The Toarcian taxon *Platysuchus multiscrobiculatus*, exclusively known from the Holzmaden area, had been investigated by BERCKHEMER (1928, 1929) based on two specimens that he named *Mystriosaurus multiscrobiculatus*. WESTPHAL (1962) referred them to the new taxon *Platysuchus*, because the diagnostic features of the specimens, justified separation on genus level in his opinion.

The purpose of this work is to describe the anatomy of *Platysuchus multiscrobiculatus* in detail for the first time, and revise the anatomy of *Steneosaurus bollensis*, *Steneosaurus brevio*r, *Steneosaurus gracilirostris,* and *Pelagosaurus typus*. These taxa will be compared with each other as well as with other representative teleosaurid taxa from the Middle and Upper Jurassic of Europe. The results of the comparative anatomical study will be used to evaluate the in-group relationships, palaeobiogeography, and palaeoecology of the Liassic teleosaurids, in consideration of other thalattosuchians. In the phylogenetic analysis, also the metriorhynchid clade of the Thalattosuchia will be included.

1.2 Development of Central Europe during the Early Jurassic

Because in this work, the thalattosuchian fauna from the Early Jurassic of Germany, France, and England will be studied and the cosmopolitan distribution of thalattosuchians will be investigated, a short introduction of the general palaeogeography and the development of Central Europe during the Early Jurassic will be given.

The beginning of the Jurassic was marked by a break-up of Pangea. However, palaeomagnetic studies show that the distribution of the continents and oceans did not change significantly from the Late Triassic to the beginning of the Jurassic (Fig. 1.1). Together with Antarctica, the Gondwana-complex was drifting slightly northwards. The Tethys was expanding into the west and the Central Atlantic Ocean developed from an intercontinental rift zone to an ocean. The North Pole was situated in the Arctic Ocean and was probably free of ice, similar to the South Pole (HOHL 1985).

During the Late Triassic and Early Jurassic, tectonic activity intensified along the Tethys-Central Atlantic-Caribbean rift/wrench system. At the same time, the Tethys sea-floor spreading axis, which appeared already during the Early Triassic, propagated westward

(ZIEGLER 1990).

The first episode of intensive rifting began in the Middle Jurassic, about 180 million years ago (SCOTESE 2001, 2002). After an episode of igneous activity along the east coast of today's North America (part of Laurasia) and the northwest coast of what is now known as Africa (part of Gondwana), the Central Atlantic Ocean opened as Laurasia moved northwest. This movement also gave rise to the Gulf of Mexico of today as Laurasia moved away from today's South America (part of Gondwana). At the same time, on the East side of Gondwana, extensive volcanic eruptions along the adjacent margins of today's East Africa, Madagascar, and Antarctica heralded the formation of the western Indian Ocean (SCOTESE 2001, 2002). A small epicontinental sea extended from the Tethys across today's Central Arabia and Madagascar to Gondwana and the Jurassic sediments of today's Arabia and East Africa were deposited here. Madagascar has the most complete Jurassic deposits in this area. The first transgression took place in the Lower Toarcian and the second stronger transgression in the Bathonian (HOHL 1985).

As the Central Atlantic Ocean opened, Laurasia rotated clockwise, pushing North America northward and Eurasia southward. Coals, which were abundant in eastern Asia during the early Jurassic, were replaced by arid deposits during the Late Jurassic as Asia moved from the wet temperate belt to the dry subtropics. This clockwise motion of Laurasia also led to the closure of the wide, V-shaped Tethys that separated Laurasia from the fragmenting southern supercontinent Gondwana (SCOTESE 2001, 2002).

In Western and Central Europe the principal rift systems, which started during the Early Triassic, remained active during the Early Jurassic (ZIEGLER 1990). The sedimentary basins of Western and Central Europe deepened along patterns already established during the Triassic. Overall, a gradual overstepping of the Late Triassic basin edges became evident. Moreover, the main graben systems of Western and Central Europe continued to subside during the early Jurassic, whereas the volcanic activity was, like during the Triassic, at a very low level (ZIEGLER 1990). In Western and Central Europe, Rhaetian and Hettangian times were characterized by the regional transgression of the Tethys Sea, which resulted in a broad, open-marine shelf sea. This sea covered much of what is now known as southern Germany, the Paris Basin, the Celtic Sea-Western Approchaches area, the Irish Sea, the southern and central North Sea, Denmark, and northern Germany (ZIEGLER 1990). The Toarcian was marked by an active phase in the break up of Pangea (DE WEVER & BAUDIN 1996).
While the Sinemurian and Toarcian times were characterized by a cyclical rise of the sea level, the beginning of the Aalenian corresponds to a temporary low-stand sea level

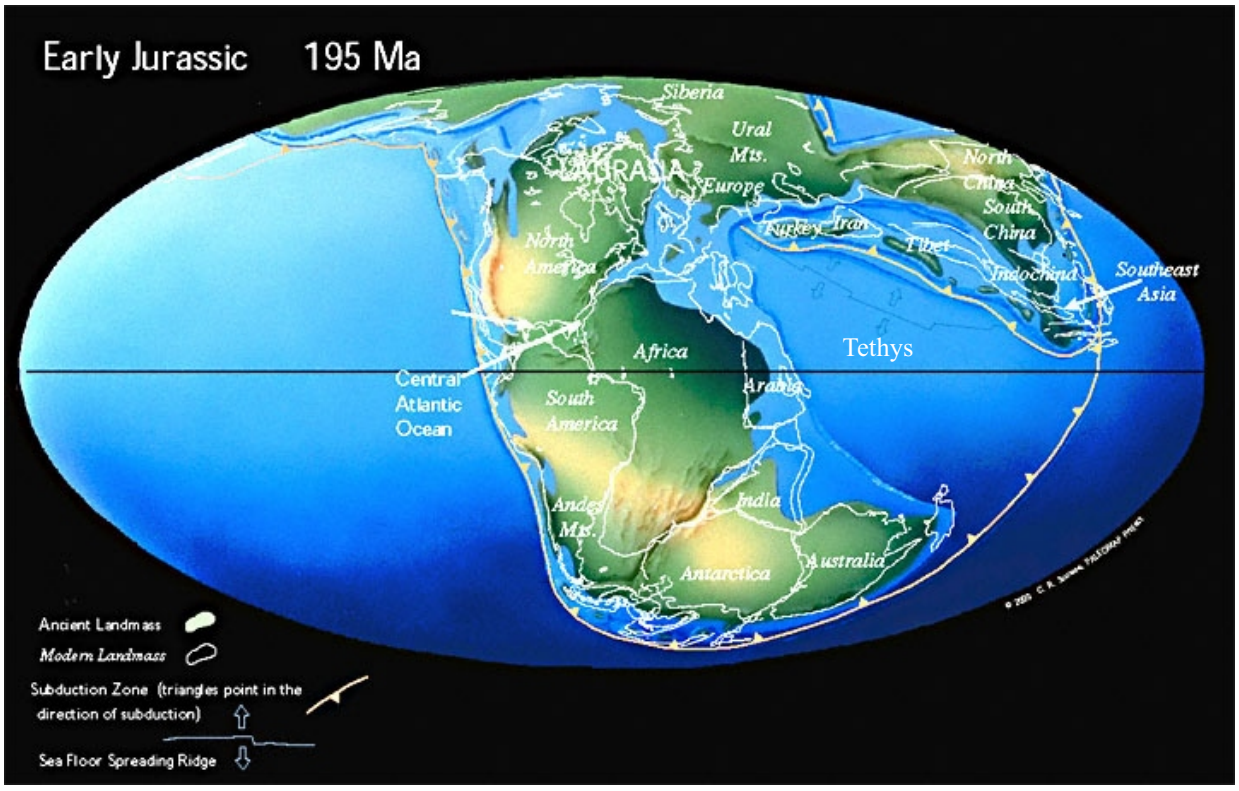

Figure 1.1: Paleogeographical world map in the Lower Jurassic after SCOTESE (2002).During the Jurassic period Europe formed an archipelago of islands separated by warm shallow seas resulting from transgression. The ancient ocean of Tethys was situated to the south and east.

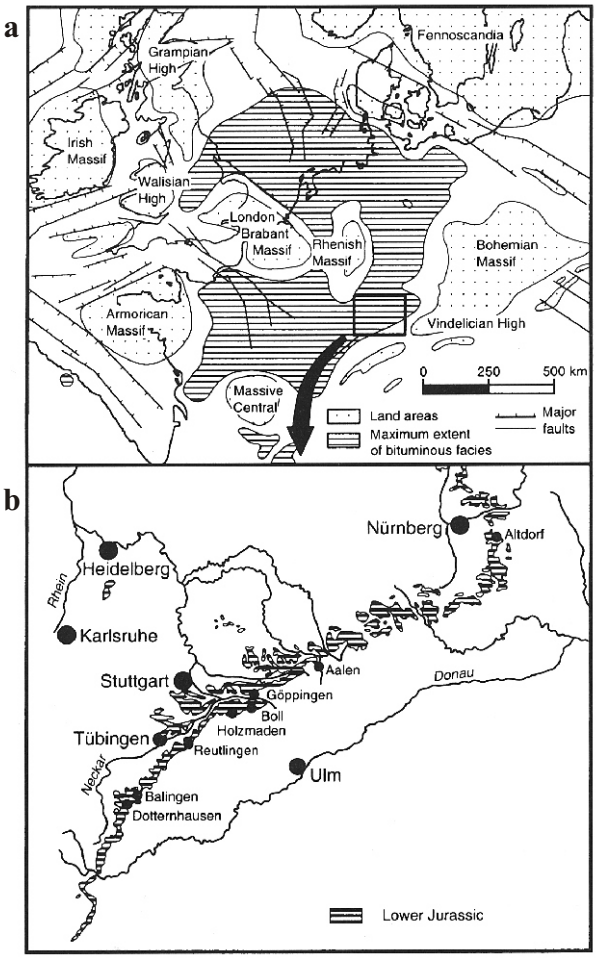

Figure 1.2a-b:
a - Paleogeographic map of Central Europe in the Toarcian and
b - the early Toarcian outcrops in South Germany (after ETTER & TANG 2002).

(ZIEGLER 1990). The development during the Early Toarcian anoxic conditions was accompanied by a biological crisis that affected both benthic and pelagic organisms. The effects of this crisis were also evident in basins that were characterized by well-aerated bottom conditions (ZIEGLER 1990).

By the end of the Early Jurassic large parts of what is now known as Western and Central Europe were covered by epicontinental seas that provided a free exchange between the Tethys shelf and the Arctic Sea. The southern North Sea and northwestern Europe formed a wide epicontinental platform where Toarcian deposits were well developed (Fig. 1.2a). These include the Jet Rock Formation in Great Britain, the Posidonia Shales in the southern North Sea, the Schistes Cartons in the Paris Basin, and the Posidonia Shales in Germany and Switzerland (DE WEVER & BAUDIN 1996), where most of the Liassic teleosaurids were found. This epicontinental sea was restricted in the Northeast by the Baltic Shield, in the West by the London-Brabant Massif and further in the West by the Amorican Massif, in the Southeast by the Hercynian-Bohemian Massif and the Vindelician landmass as well as the Alemannic High and the Massif Central in the South (Fig. 1.2a). The epicontinental sea was subdivided by the London – Brabant and Rhenish (Rhenian) Massif into three large basins: the northern Germanic Basin, the Paris Basin, and the southern Germanic Basin (HAUFF 1997) (Fig. 1.2a). This resulted partly in faunal provincialism, which also influenced the distribution of the teleosaurids and other marine reptiles in this area (GODEFROIT 1994, MAISCH & ANSORGE 2004). The connection to the open Tethys was situated in the South. The basins had probably only an occasionally connection with the open sea, so that the faunal exchange was limited (RÖHL et al. 2001, Seldon & Nudds 2004).

1.3 Geology of the Toarcian of the Holzmaden area, Germany

1.3.1 General conditions

The Holzmaden area in the Swabian Jura is famous for its fossil localities, which show excellent fossil preservation in organic-rich black shales. Quarrying in the Holzmaden region dates back for centuries, and the first early attempts to distil oil from the organic-rich black shales dates back to the late sixteenth century (SEILACHER 1990). In addition, fossils have been found since that time (URLICHS et al. 1994).

HAUFF (1921) provided the first comprehensive study of the Posidonia Shale of the Holzmaden region. The name "Posidonia Shale" refers to two bivalve taxa *Bositra buchi* and *Steinmannia bronni* both formerly referred to the taxon *Posidonia*, which are abundant in some layers (URLICHS et al. 1994). Today, an extensive literature exists about the origin, development, and taphonomy of the Holzmaden area. However, despite such extensive

examinations, there is still some controversy about the exact nature of the palaeo-environmental conditions, which existed during the deposition of this Lagerstätte, and the ecology of some fossil species (ETTER & TANG 2002).

1.3.2 Geological context

During the Toarcian (Lower Liassic) the Holzmaden area of today was placed approximately 100 km west of the coastline of the Vindelician High (Fig. 1.2a). It was situated in the subtropical zone at about 30° N (HAUFF & HAUFF 1981, SELDEN & NUDDS 2004). According to HAUFF (1997), the average depth of the Liassic Sea was about 200 to 300 m. The bituminous black shales were deposited, under stagnant and anoxic conditions which resulted in the extraordinary fossil preservation.

Today, Lower Toarcian Posidonia Shale of southwestern Germany outcrops in a southwest-northeast trending belt, extending from Waldshut to the Nördlinger Ries in the foreland of the Swabian Jura (URLICHS 1977, URLICHS et al. 1994). The best exposures in that area are found in quarries at Ohmden, Zell, Bad Boll, and especially Holzmaden (ETTER & TANG 2002) (Fig. 1.2b & 1.3). Today, Holzmaden lies at the foot of the Swabian Jura approximately 40 km southeast of Stuttgart (Fig. 1.2b). Holzmaden is inextricably linked to this Lagerstätte (HAUFF & HAUFF 1981).

The Posidonia Shale of the Swabian Jura is a 6 to 14 m thick succession of dark grey to black bituminous shales with intercalated bituminous limestones (ETTER & TANG 2002). It has long been recognized that each of the individual beds of the Posidonia Shale show distinct sedimentological, palaeontological, and taphonomical signatures (Fig. 1.4a) (ETTER & TANG 2002). The first detailed lithostratigraphy of the Posidonia Shale was made by QUENSTEDT (1858), who divided the Liassic in six layers: Lias alpha to zeta. The Posidonia Shale represents the Lias ε, which was divided in three subunits: Lower (ε I), -Middle (ε II) -, and Upper Lias ε (ε III). Today, the stratigraphy of the Lias ε is elaborated to the very detail. The layers are named according to the names the quarry workers used to characterize the units, based on the lithology and the main characters of the rocks (HAUFF 1921, URLICHS et al. 1994) (Fig. 1.4a).

The biostratigraphy of the Posidonia Shale is well established and based on both ammonites (RIEGRAF et al. 1984) and microfossils like ostracodes and foraminifers (RIEGRAF 1985). The biostratigraphic correlation with other Jurassic deposits in different areas of the world is based on ammonite zones. In the southern German Posidonia Shale there are three ammonite zones (from bottom to top): the *tenuicostatum*-, *falcifer(um)*-, and the *bifrons*-zone, based on the ammonite taxa *Dactylioceras tenuicostatum*, *Harpoceras falcifer*, and

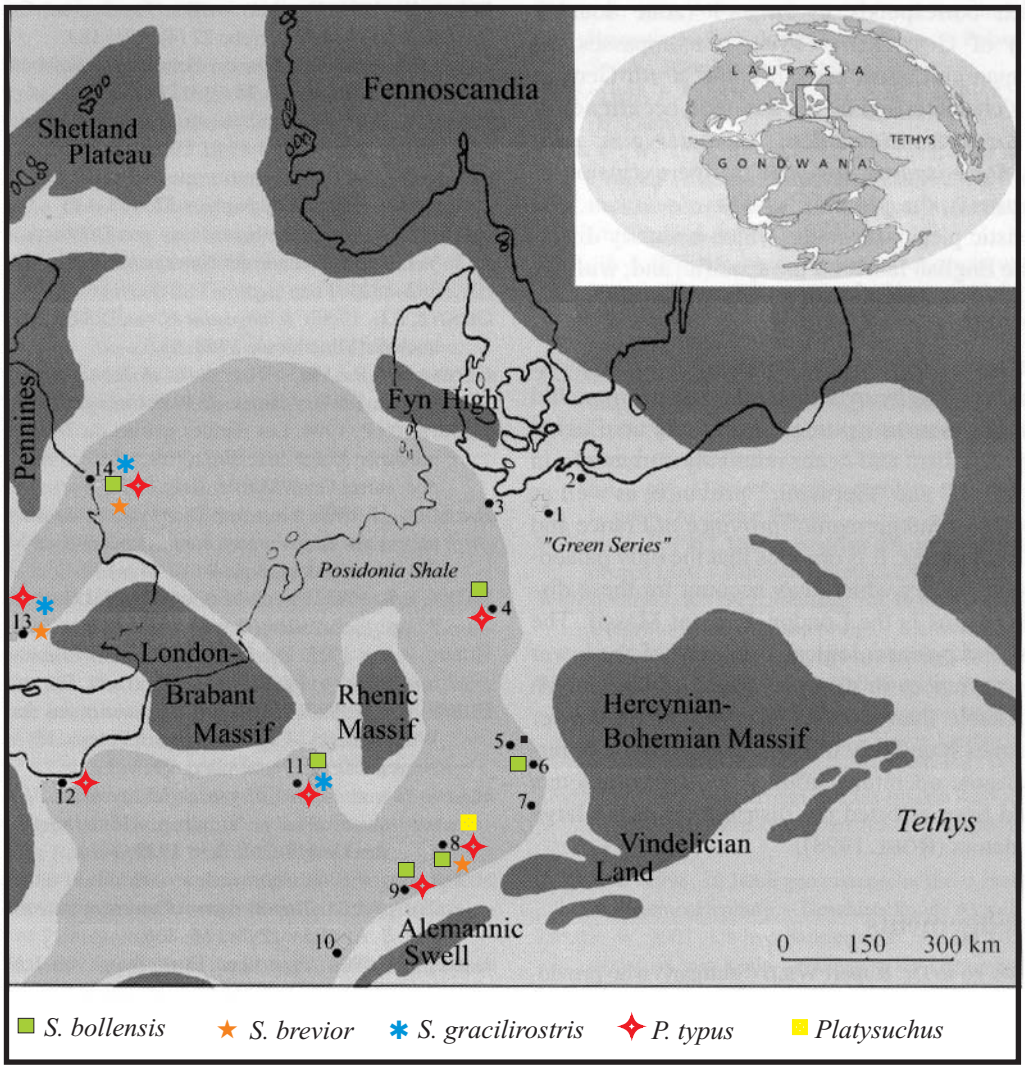

Figure 1.3: Lower Toarcian palaeogeography (dark grey = land, light grey = marine realm, medium grey = distribution of bituminous shales) and localities with marine reptile remains in Central and Western Europe (dots) and distribution of diagnostic thalattosuchia taxa (other symbols). - 1 Dobbertin, Mecklenburg-Vorpommern, Germany; 2 Grimmen, Meckelenburg-Vorpommern, Germany; 3 Ahrensburg, Schleswig-Holstein, Germany; 4 Schandelah, Lower Saxony, Germany; 5 Banz, 6 Mistelgau, 7 Kerkhofen, Franconia, Germany; 8 Holzmaden, Boll, Ohmden, 9 Dotternhausen, Swabian Alb, Germany; 10 Teysachaux; Fribourg; Switzerland; 11 Luxembourg; 12 Caen, Normandie, France; 13 Ilminster, Sommerset, England; 14 Whitby, Yorkshire, England. The figure is modified after MAISCH & ANSORGE (2004).

Hildoceras bifrons (URLICHS et al. 1994). Thus, the deposits of the Swabian Alb can be correlated with other organic-rich shales in Europe (Fig. 14a-c). According to the ammonite zones the Jet Rock Formation and Alum Shale Series of the Yorkshire Coast in England and the Schistes Cartons in France, from which thalattosuchians also were reported, are coeval with the southern German Posidonia Shale (Fig. 1.4a-c) (URLICHS et al. 1994, ETTER & TANG 2002).

In the Holzmaden area, most vertebrate fossils occur in the Lias ε II, whereas in the Lias ε III finds of invertebrates like ammonites and bivalves predominate (URLICHS et al. 1994). Finds of crocodilians are only known from the Lias ε II (Fig. 1.4.a). Apart from several bioturbated intervals, which are locally more clearly developed than in other places, e.g. in the *tenuicostatum*-zone or in the middle *falcifer(um)*-zone in Dotternhausen, the entire sequence is finely laminated (SEILACHER 1982; RIEGRAF et al. 1984, RÖHL et al. 2001). In addition to the differences between individual laminae, there are major geochemical differences between the calcareous beds and the bituminous shales. Generally, the middle Posidonia Shale (Lias ε) is more bituminous than the lower and upper parts of the sections (URLICHS et al. 1994). In the Lias ε II, bituminous black shales like "Fleins" (Lias ε II_3), "Unterer Schiefer" (Lias ε II_4) or "Schieferklotz" (Lias ε II $_6$) contain different percentage of organic matter. Between them limestones like "Unterer Stein" or "Oberer Stein" are inserted.

1.3.3 Palaeoenvironmental settings

During Liassic times, warm and humid climate predominated. The geographical poles were free of ice. Today's Holzmaden lied at about 30° N and had subtropical conditions with water temperatures of 25-30°C (RÖHL et al. 2001, BAILEY et al. 2003). Because the super-continent Pangea still existed in the early Jurassic, the unbalanced ratio of land- and ocean mass caused probably strong high and low pressure systems causing a pronounced monsoon-trade wind climate (PARRISH 1993, RÖHL et al. 2001).

The black and laminated bituminous Posidonia Shale has long been treated as the prototype stagnation deposit (POMPECKJ 1901, SEILACHER 1982, SEILACHER et al. 1985). The classical stagnant basin model introduced by POMPECKJ (1901), which is very similar to the recent conditions in the Black Sea, is supported with some modifications by SEILACHER

(1990). This classification still holds true, but other authors have questioned a strict application of the stagnant basin model. They restricted the stagnant conditions to the particular layers, which lack bioturbation or benthic life forms, and report the occurrence of deposited under aerated conditions with oxygenated bottom-waters favouring benthic life

forms like bivalves, gastropods, crustaceans, and echinoderms in other layers of the Posidonia Shale of Holzmaden (BEURLEN 1925, RIEGRAF et al. 1984, RÖHL 1998, RÖHL et al. 2001).

The current consensus is that the bottom waters of the Posidonia Shale Sea were severely oxygen depleted throughout the deposition of this formation, allowing the colonization of the seafloor by specialized or opportunistic taxa only at certain periods of time (ETTER & TANG 2002). However, the mechanisms that led to this unique and widespread deposition of black shales are still under discussion (ETTER & TANG 2002).

Several models have been developed to explain the widespread occurrence of black shales and the exceptional preservation of fossils in these settings. The first is a classic stagnant basin model, which favours long-term stagnant conditions with anoxic bottom waters and salinity stratification (POMPECKJ 1901, SEILACHER 1982).

HALLAM (1987) has applied a second model for developing a stagnant water mass, involving thermal stratification. While it is generally true that a thermally stratified water mass is less stable than a salinity stratified one, and is likely to experience seasonal mixing, a thermocline could be quite stable under equable climate (HALLAM 1987).

A third model called "the oxygen minimum zone model" (OMZ; JENKYNS 1988), assumes increased rates of marine productivity that stimulate oxygen consumption by aerobic bacteria, causing an oxygen minimum zone (OMZ) just below the zone of primary production (LANGROCK 2003). JENKYNS (1988) does not only try to explain the epicontinental black shale deposits in Holzmaden, but also those from other epicontinental black shales like the Jet Rock Series and Alum Shale Series in England or the Schistes Cartons in France. Contemporaneous epicontinental black shales are also known from northern Germany and from boreholes in the Netherlands and the North Sea (ETTER & TANG 2002). In addition, the model tries to explain the deep marine settings. In fact, organic-rich shales from the Lower Toarcian, which were deposited in deep-water settings in the Tethys, were also found in Austria, Italy, Switzerland, Hungary, Greece, and Tunisia (JENKYNS 1988). Worldwide deposits of early Toarcian age are often organic-rich, and according to JENKYNS (1988), the reason for this lies in the "Early Toarcian anoxic event". The most widespread development of these black shales can be recorded in the middle Posidonia Shale (Lias ε II), which corresponds to the *falcifer(um)*-ammonite zone (JENKYNS 1988). Worldwide, an abnormally high number of black shale deposits occur in the Toarcian, which could be the result of an Oceanic Anoxic Event (OAE), which lasted approximately 500 000 years (JENKYNS 1988). This Oceanic Anoxic Event (OAE) was preceded by a significant faunal turnover of ammonites in the Tethys. It was

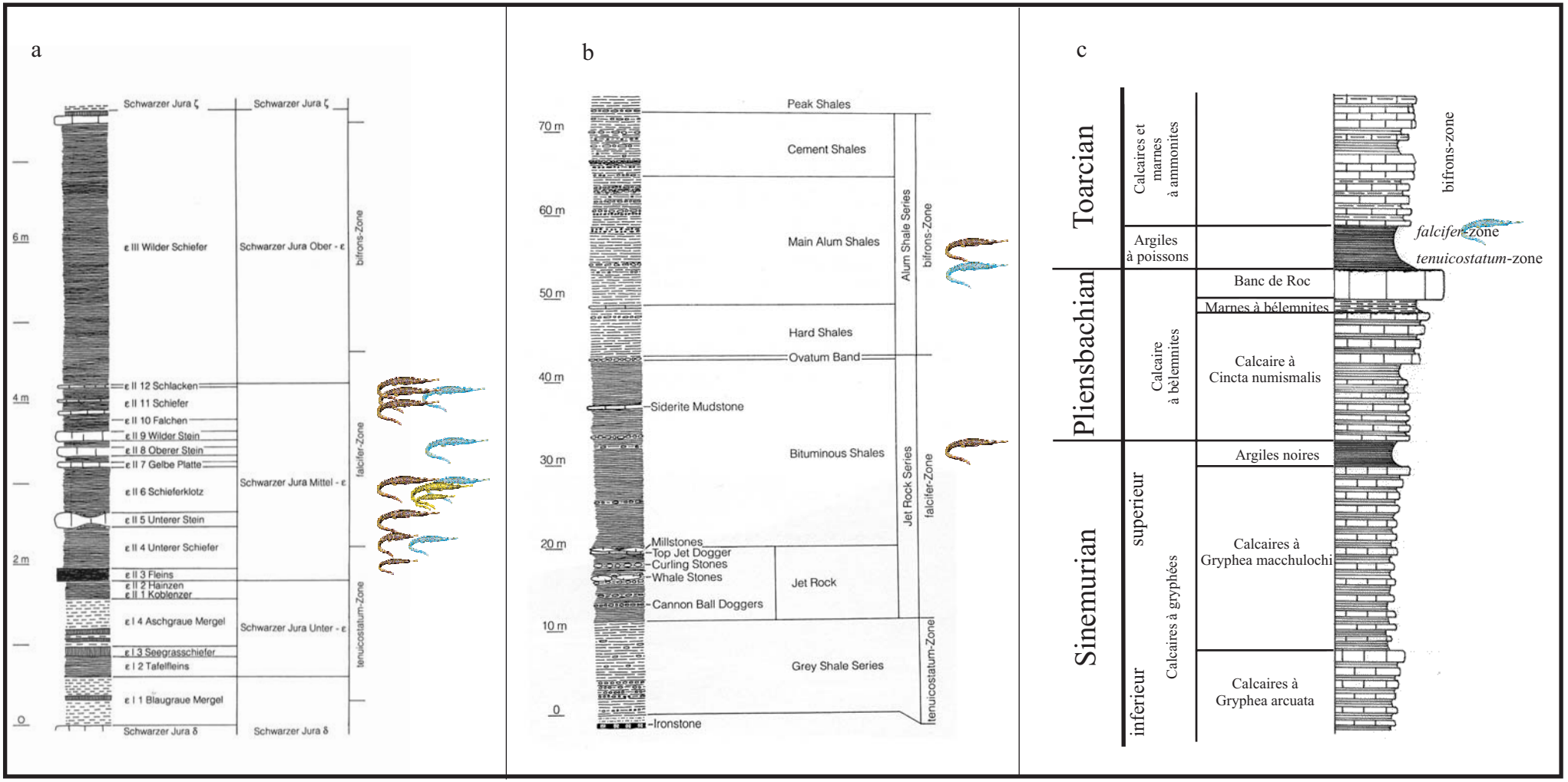

Figure 1.4a-c:
Thalattosuchia mark the layers with typical finds of marine crocodiles. Grey thalattosuchians = *Steneosaurus bollensis*, yellow thalattosuchians = *Platysuchus multiscrobiculatus*, blue thalattosuchians = *Pelagosaurus typus* (a small icon indicates juvenile specimens).
1.4a - The layers of Posidonia Shale at the quarry of G. FISCHER in Holzmaden. Left side shows the layer names and abbreviations after HAUFF (1921), the middle Part shows the names after QUENSTEDT (1858) at the right side shows the correlated ammonite zones. Modified after URLICHS et al. (1994).
1.4b - Stratigraphy of the Lower Toarcian at the Yorkshire Coast. Jet Rock Formation is correlated with the *falcifer*(*um*) –zone and the Alum Shale Formation with the *bifrons* – zone. Modified after URLICHES et al. (1994).
1.4c - Combined stratigraphy for the Lower. Liassic in the area of Calvados, France. The lower "Argiles a Poissons" is correlated to the *tenuicostatum*-zone and the upper part to the *falcifer(um)*-zone. The "Calcaires et marnes à ammonites" are correlated to the *bifrons*-zone. Modified after DUGUÉ et al. (1998).

accompanied by a widespread extinction of benthic life in northern Tethys, in response to the lateral spread of anoxic bottom waters during the transgression (JENKYNS 1988).

Recently, RÖHL et al. (2001) presented a detailed model for the deposition of the Posidonia Shale; based on investigations of the deposits in Dotternhausen, Swabian Alb (Fig. 1.5). They explain the different layers in the Toarcian sediments with variable oxygen availability in the water during deposition, which ranged from short oxygenated periods to long-term anoxia. According to RÖHL et al. (2001), the deposition of the Posidonia Shale probably was influenced by long-term trends like the sea level fluctuations and short-term trends like the occurrence of periodical monsoon rain.

It is assumed that oxygen availability during the early Toarcian was controlled by sea level changes. During seal level high stand, water exchange with neighbouring basins was possible and during sea level low stand a partial isolation of the basins occurred (RÖHL et al. 2001). Other important factors that probably controlled the depositional regime were the global palaeogeographical situation and the resulting climate conditions. The Early Jurassic was the latest period before the break-up of Pangea and was probably ruled by a strong meriodional atmospheric circulation system with pronounced seasonal changes of prevailing trade- and monsoon-wind systems (Parrish 1993, RÖHL et al. 2001).

RÖHL et al. (2001) suggested for the deposits of southern Germany, that during the Toarcian, anoxic conditions resulted in the deposition of black shales. However, these conditions were punctuated by various short periods (weeks to years) with oxygenated bottom water conditions. However, water column stratification reached its maximum during the early *falcifer(um)*-zone, probably related to low sea level stand. Therefore, the early *falcifer(um)*-zone was marked by extremely anoxic conditions, whereas well-oxygenated bottom water conditions existed during the sea level high stand in the late *falcifer(um)*-zone (RÖHL et al. 2001).

According to RÖHL et al. (2001), intense water exchange took place with the Tethys during sea level high stand (Fig. 1.5A & B). During summer, monsoon rainfall caused an estuarine circulation with an outflow of surface water of slightly reduced salinity towards the open Tethys. As a result, the corresponding counter current caused an inflow of higher salinity Tethyan waters. This water exchange established a density-stratified water body with water with reduced salinity at the top of the water column and high salinity water at the

bottom (Fig. 1.5A). The high rate of primary production caused the accumulation of large quantities of organic matter and accelerated consumption of oxygen within the bottom water, which resulted in suboxic, then anoxic conditions (Fig. 1.5A). During winter, high

evaporation rates favoured a water circulation in opposite direction (Fig. 1.5B). Because of the evaporation the surface water slightly increased in salinity, which caused an increase in density, and it sank to the bottom of the water column. As a result, the density stratification was destroyed and renewed oxygen-rich waters allow a colonization of the benthos. Anoxia was restricted to local areas in the deeper parts of the basin only (Fig. 1.5B).

During sea level low stand (like it is suggested for the lower *falcifer(um)*-zone) the water exchange between the epicontinental basins and the Tethys was largely restricted. During summer, estuarine circulation was characterized by intensive surface water mass outflow caused by the monsoon rainfall. Corresponding backflow was because of the low sea level stand presumably minimal (Fig. 1.5C). A permanent redox boundary was probably established within the water body. During winter, the weak anti-estuarine circulation was unable to disturb the water column and destroy the pycnocline (Fig. 1.5D). The benthic environment was predominantly anoxic precluding benthic life.

Short term colonization events, as they are partly observed in the sediments of the lower *falcifer(um*)-zone, were presumably caused by tropical storms that perturbated the stratified water. Stagnant conditions were interrupted and oxygen availability allowed short lived benthic colonization of the seafloor.

1.4 Geology of the Toarcian of the Yorkshire coast, Great Britain

The outcrops of Liassic marine sediments of Great Britain have been well known for many years (Fig. 1.4b, 1.6). Those of the Dorset coast are famous for ichthyosaurs and complete plesiosaur specimens in rocks of Lower Liassic (Hettangian) age (CADBURY 2000). The Liassic outcrops of the Yorkshire coast are more comparable to the Holzmaden Shale. The Upper Liassic (Lower Toarcian) sequence in this area is about the same age as the Holzmaden Shale and yields most of the marine reptiles (TATE & BLAKE 1876, SELDON & NUDDS 2004) (Fig. 1.4b).

The Lower Toarcian of the Yorkshire Coast is divided in the Grey Shale Series, the Jet Rock Series, and the Alum Shale Series (SIMMS et al. 2004). The Grey Shale Series is correlated with the *tenuicostatum*-ammonite zone (URLICHS et al. 1994) and until now, never yielded remains of marine reptiles. According to WESTPHAL (1962) the Jet Rock Series can be correlated with the *Hildoceras serpentinum* ammonite zone, but more recently BENTON & TAYLOR (1984) state that the Jet Rock Formation (= Series) is synonymous with the *Harpoceras falciferum* zone (Fig. 1.4). The upper Jet Rock Series consists mostly of hard grey bituminous shales with bands of calcareous concretions (SELDEN & NUDDS 2004). It is rich in

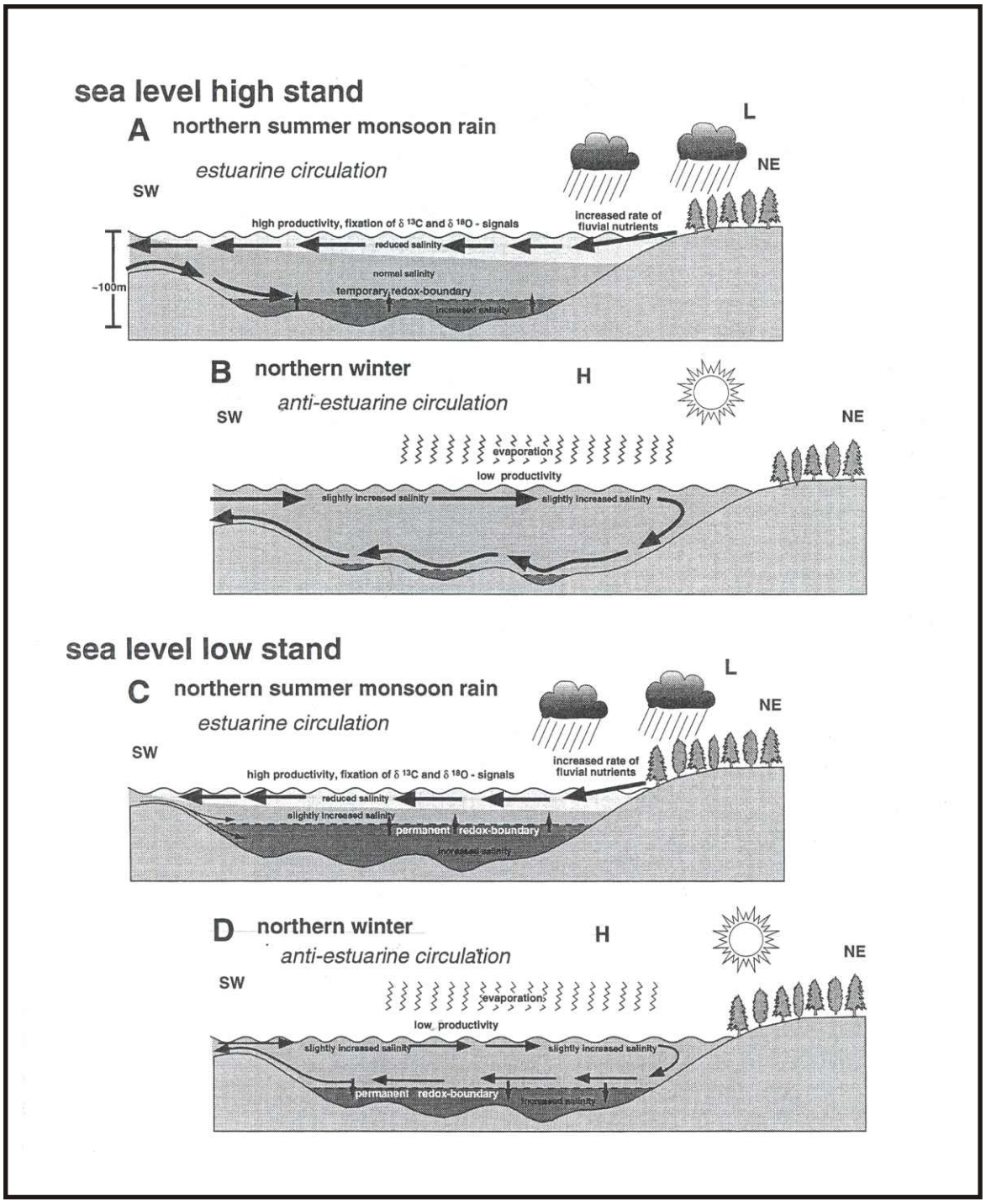

Figure 1.5: Schematic diagram illustrates the depositional model of the Posidonia Shale and is based on an alteration of humid conditions dominated by monsoonal rain (reduced salinity) and aridity with high evaporation rates (increased salinity). These seasonal variations caused an estuarine circulation in the summer (A, C) and an anti-estuarine circulation in the winter (B, D). During sea level high stand, an anti-estuarine circulation led improved oxygen conditions in the benthic environment (B). By contrast, during the summer month the redox boundary was situated within the water column and anoxic conditions prevailed (A). In the course of a sea level low stand, water exchange with the Tethys was restricted and a permanent redox boundary caused anoxia during the whole year (C, D). Only episodic storm events gave rise to the inflow of oxygenated water and favoured short-term benthic colonization (after RÖHL et al. 2001).

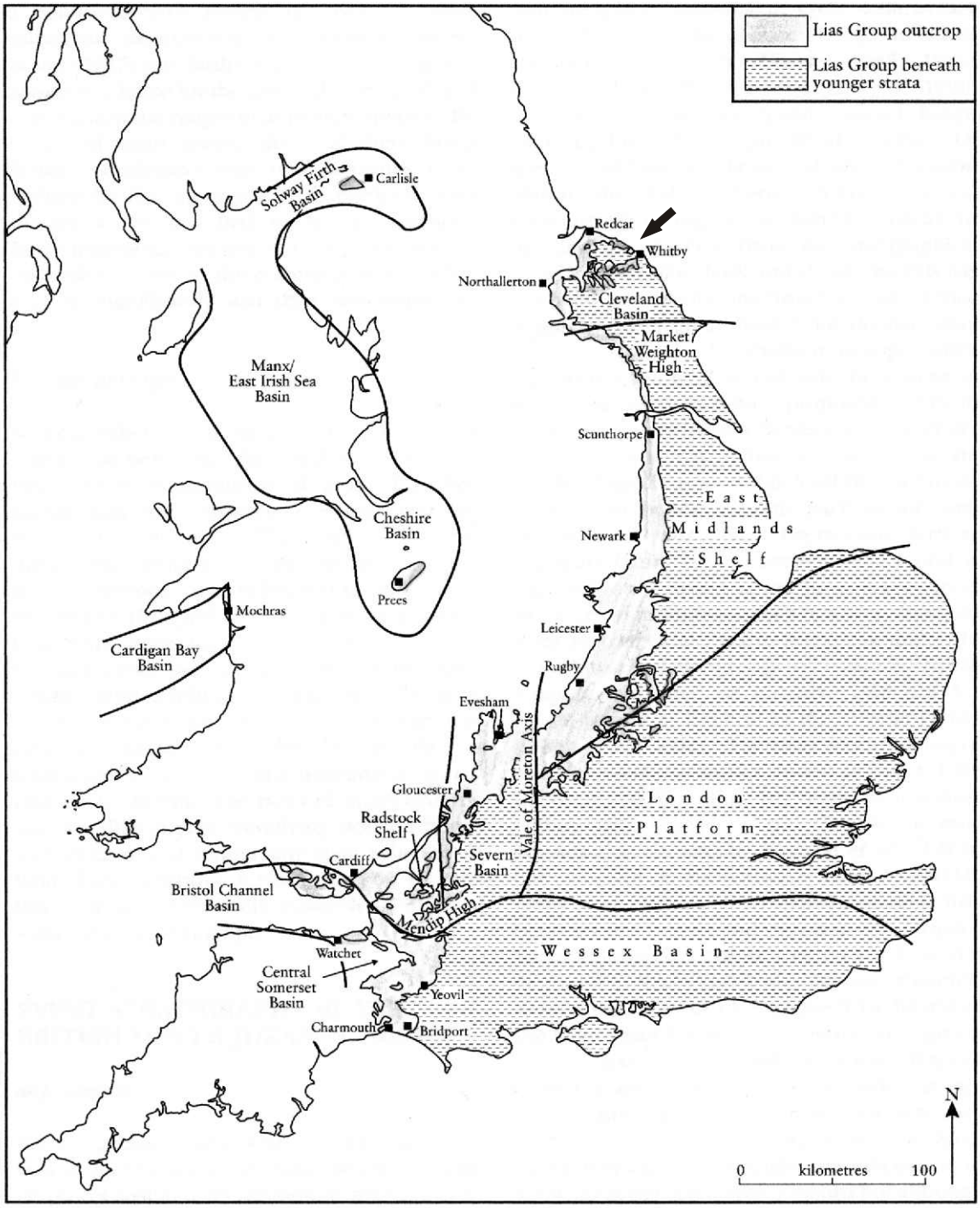

Figure 1.6: Outcrop map for the Liassic sediments in England and Wales (after COX et al. 1999). Arrow marks the area around Whitby at the Yorkshire Coast, where the main finds of teleosaurids occur in the Lower Toarcian.

bitumen, and the bottom conditions during deposition were anoxic (BENTON & TAYLOR 1984). The overlying deposits belong to the Alum Shale Formation (= Series) and are correlated with the *Hildoceras bifrons* and the *Dactylioceras commune* ammonite zone (WESTPHAL 1962, BENTON & TAYLOR 1984). According to BENTON & TAYLOR (1984), the *Dactylioceras commune* subzone is the lowest part of the Alum Shale Formation. The Alum Shale Formation consists of soft grey micaceous shales with a high content of pyrite, and show bands of calcareous concretions (SELDEN & NUDDS 2004).

The Jet Rock Formation and the Alum Shale Formation at the Yorkshire Coast have each a thickness about 30 m (HALLAM 1979, URLICHS et al. 1994). Thinner facies equivalents of the Jet Rock Formation occur in the British Midlands but pass in south-west England into non-bituminous marls and limestones (HALLAM 1979) (Fig. 1.6).

Most of the Liassic crocodilian specimens are reported from the Alum Shale Formation of Whitby, Saltwick section, with isolated finds from Sandsens, Runswick Bay and Kettleness (BENTON & TAYLOR 1984) (Fig. 1.4b, 1.6). However, some specimens of *Steneosaurus bollensis* and *S. brevior* were also found in the Jet Rock Formation of Whitby (e.g. TATE & BLAKE 1876, WESTPHAL 1962, BENTON & TAYLOR 1984, and WALKDEN et al. 1987) (Fig. 1.4b).

There are many more finds of thalattosuchians in British deposits, but most of them are younger and come, e.g., from outcrops of the Oxford Clay (Callovian) or Kimmeridge Clay (Kimmeridgian) (e.g. ANDREWS 1909, 1913; DELAIR 1957, ADAMS-TRESMAN 1987a/b, BENTON & SPENCER 1995, GRANGE & BENTON 1996).

1.5 Geology of the Toarcian of the Normandy, France

Toarcian outcrops in France are mainly restricted to the Normandy and eastern France (GALL 1979). However, the type locality lies near to Thouars (Poiton, Deux-Sevres, France), where the Toarcian consist of well-developed sandy and calciferous sediments (D' ORBIGNY 1849, GABILLY 1976).

At the northeastern margin of the Paris Basin, close to the east coast of the Amorican Massif, calciferous sediments and bituminous shales were deposited in the Toarcian (Fig. 1.4c & 1.7). The Toarcian deposits were settled here during a new transgressive episode followed upon the regressive tendency of the final Pliensbachian in the area of Calvados. The sedimentation basin deepened and bituminous shales were deposited under undisturbed and anoxic conditions. These black shales form the formation of Argiles à Poissons (Fish Clay). The deposit conditions at the sea bottom were unfavourable for life, which is marked by the absence of a benthic fauna and bioturbation in the formation. In the late Upper Toarcian, the

deposition of limestone and marl with ammonites indicates a return to carbonate sedimentation under open-sea conditions like in the Pliensbachian before, i.e. platform carbonates with oolites (DUGUÉ et al. 1998). The Lower Toarcian in the Normandy is therefore marked by bituminous shales called "Argiles à Poissons", which are correlated with the *tenuicostatum*-ammonite zone. The uppermost part of this horizon is also called "Schistes Cartons" and is referred to the *falcifer(um)*-ammonite zone (DANGEARD 1951) (Fig. 1.4c). The thickness of these shales is variable and ranges from two (i.e. in the Vendée) to 20 m (i.e. at Nancy) (DUGUÉ et al. 1998). There are only a few outcrops of these bituminous shales in the Paris Basin, and most information about thickness, exact age, and lithology of the depositions has been obtained from borehole data (URLICHS et al. 1994). Lower Toarcian outcrops in the Normandy with *Pelagosaurus typus* were reported by EUDES-DESLONGCHAMPS (1864) from Curcy, La Quaine, and in Amayé-sur-Orne, localities near Caen (Fig. 1.7). However, the Schistes Cartons are distributed throughout the entire Paris Basin, even though they are mostly not visible in surface outcrops.

The Upper Toarcian consists of calciferous deposits called "Calcaire à Ammonites", which is correlated with the *bifrons*- and *aalensis*- ammonite zone (DANGEARD 1951).

The fossil-rich deposits of the "Calcaire de Caen", which are famous for their beautifully preserved vertebrate fossils, including *Teleosaurus cadomensis* and different *Steneosaurus* taxa, are younger and of Middle Bathonian age that can be correlated with the *progracilis*-ammonite zone (DANGEARD 1951, DUGUÉ et al. 1998).

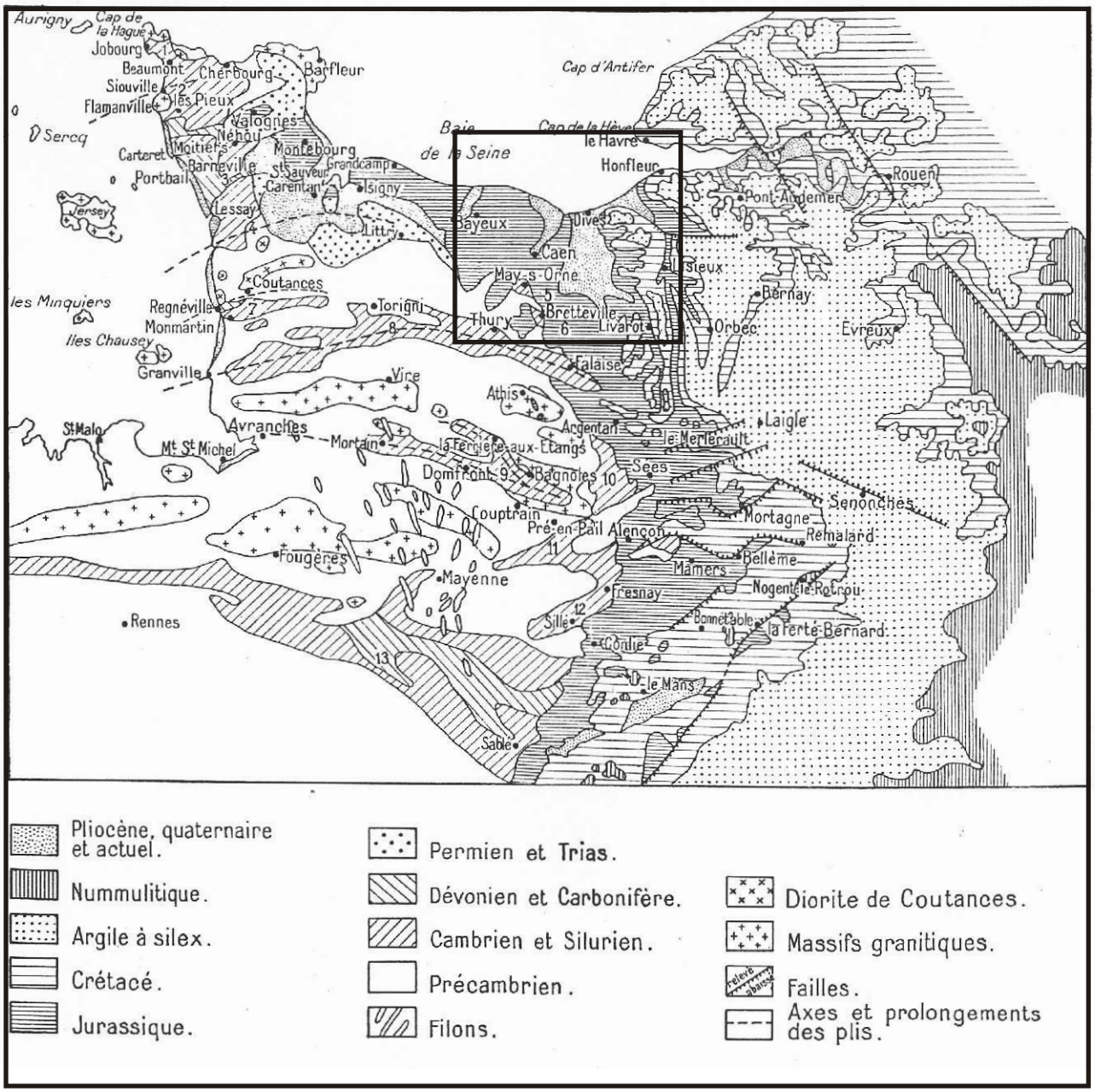

Figure 1.7: Geological map of the Normandy, France (after DANGEARD 1951). The surrounded area marks the main outcrops of the Lower Jurassic. Most finds of the French *Pelagosaurus typus* specimens occur there.

Chapter 2

Methods & Abbreviations

2.1 Methods

Short descriptions, sketches, and photographs were taken from original material in scientific collections in Germany, The Netherlands, Great Britain, France, Hungarian, and Denmark. The anatomical investigations were conducted either macroscopically or with stereomicroscope or hand lens for smaller specimens.

The photographs were taken by myself with an analogue Minolta Dynax 5 using a 28-80 mm zoom lens and a Nikon Coolpix digital camera. The photograph of SMNS 9930 in total view was provided by H. LUMPE (SMNS).

All drawings are based on these photographs and sketches of the original material (drawn with Rotring Rapidographs 0.25 and 0.35 mm). Based on the drawings three-dimensional restorations of the skulls were formed in wax. The reconstructions of the skulls of *Platysuchus multiscrobiculatus* and *Steneosaurus bollensis* are based on these wax models. All other reconstructions are based on drawings only.

For the computed tomography of the skull of the *Pelagosaurus typus* specimen BSGP 1890 I 5 a SOMATOM S medical scanner was used, by Dr. Stephan BOOR at the University Hospital of Mainz (Klinik für Neuroradiologie). Each of the 115 scans were 1.5 mm thick and were taken as coronal sections, in a 90° angle to the long axis of the specimen, and covered the entire skull fragment (see chapter 3.5).

Wherever it was possible, biometric data were taken directly from the specimens. If the specimens were not directly accessible, the measurements were taken from photographs. The biometric data were taken with a calliper (+/- 0.05 mm), a ruler (+/- 1.0 mm) or, if the measuring distance exceeded 100 mm, with a tape measure (+/- 1.0 mm). Measurements from photographs were taken in CorelDraw and afterwards converted into original size, after the photographs had been scanned (in the case of real photographs) or loaded in the computer (in the case of digital pictures).

The ratios of the biometric data were calculated with the software package Microsoft Excel 2000 and PAST.

The phylogenetic analysis was carried out with the software package PAUP 4.0b 10 (SWOFFORD 2003)

2.2 Material

A complete list of the investigated material is given in appendix I. In the respective chapters there is, a short list of the specimens examined therein.

2.3 Institutional abbreviations

BMNH: British Museum of Natural History London; **BSGP**: Bayrische Staatssammlung für Geologie und Paläontologie München; **FSL**: Collection of the University of Lyon, **GPIM**: Geologisches-Paläontologisches Institut der Universität Mainz; **GPIT**: Geologisches-Paläontologisches Institut der Universität Tübingen; **IPB**: Institut für Paläontologie der Universität Bonn; **MGUH**: Geologisk Museum København; **MNHN**: Museum National d'Histoire Naturelle Paris; **NHMUS**: Natural History Museum, Budapest; **OUM:** Oxford University Museum; **SMF**: Forschungsinstitut und Senckenberg Museum Frankfurt; **SMNK**: Staatliches Museum für Naturkunde Karlsruhe; **SMNS**: Staatliches Museum für Naturkunde Stuttgart; **SNSD**: Staatliche Naturhistorische Sammlungen Dresden**;** **TMH:** Teylers Museum Haarlem**; UH**: Urweltmuseum Hauff Holzmaden; **ZFMK**: Zoologisches Forschungsinstitut und Museum Alexander Koenig Bonn; **ZMUC**: Zoological Museum, University of Copenhagen.

2.4 Anatomical abbreviations

ac: acetabulum, **an**: angular, **AOF**: antorbital fenestra, **ar**: articular, **ar fc**: articular facet, **as**: astragal, **at**: atlas, **ax**: axis, **bs**: basisphenoid, **boc**: basioccipital, **c**: coronoid, **ca**: calcaneum, **cd rb**: caudal rib, **cn**: centrum, **CN**: cranial nerve, **co**: coracoid, **co f**: coracoid foramen, **cp:** carpal, **cr-q canal**: cranioquadrate canal, **cv rb**: cervical rib, **cv od**: cervical osteoderm, **cv vr**: cervical vertebra, **cy**: condyle, **d**: dentary, **da**: diapophysis, **dcp**: distal carpal, **dpc**: deltopectoral crest, **dt**: distal tarsal, **en**: external naris, **ecpt**: ectopterygoid, **eu f**-Eustachian foramen, **EMF**: external mandibular fenestra, **eo**: exoccipital, **f**: frontal, **fe**: femur, **fe hd**: femoral head, **fi**: fibula, **fi cy**: fibular condyle, **FM**: foramen magnum, **gl**: glenoid, **gl f**: glenoid fossa, **ga**: gastralia, **ha**: haemal arch (chevron), **hu**: humerus, **hu hd**: humerus head, **hy**: hyoid bone, **ic**: intercentrum (=hypocentrum), **icl**: interclavicle, **il**: ilium, **il cr**: ilium crest, **in:** internal naris (=secondary choana), **INF**: incisive foramen, **is**: ischium, **ITF**: infratemporal fenestra, **j**: jugal, **l**: lacrimal, **l r**: longitudinal row (of osteoderms), **m**: maxilla, **mcp**: metacarpal, **mt**: metatarsal, **n**: nasal, **na**: neural arch, **ncn**: neural canal, **nsp**: neural spine, **o**: orbit, **od**: osteoderm, **ol**: olecranon, **op**: opisthotic, **p**: parietal, **pa**: parapophysis, **ph**: phalanx, **pi**: pisiform, **pl**: palatine, **pmx**: premaxilla, **po**: postorbital, **poz**: postzygapophysis, **pr od**: odontoid process (dens), **pro**: prootic, **pro cr**: prootic crest, **pr tr**: transverse process, **prz**:

prezygapophysis, **pt**: pterygoid, **PTF**: posttemporal fenestra, **pu**: pubis, **q**: quadrate, **r**: radius, **ra**: radiale, **rap**: retroarticular process, **rb**: rib, **s**: stapes, **san**: surangular, **sc**: scapula, **sc rb**: sacral rib, **sk**: skull, **STF**: supratemporal fenestra, **sm**: septomaxilla, **sp**: splenial, **soc**: supraoccipital, **sq**: squamosal, **SUOF**: suborbital fenestra, **t**: tarsal, **th od**: thoracic osteoderm, **ti**: tibia, **ti cy**: tibial condyle, **tr pr**: transverse process, **tr r**: transverse row (of osteoderms), **u**: ulna, **ul**: ulnare, **vb**: vertebra, **v od**: ventral osteoderm

2.5 Biometric data definition

Measurements were taken from following 16 taxa: ***Steneosaurus bollensis*** (78), ***S. brevior*** (5), *S. boutilieri* (1), *S. edwardsi* (6), ***S. gracilirostris*** **(6)**, *S. heberti* (1), *S. baroni* (1), *S. lartifrons* (1), *S. leedsi* (5), *S. megarhinus* (1), *S. obtusidens* (1), *S. priscus* (1), *Teleosaurus* (14), ***Pelagosaurus typus*** (31), and ***Platysuchus multiscrobiculatus*** (4). A full list of all taken measurements is presented in appendix II. The taxa in bold letters are the Liassic taxa and the numbers refer to the quantity of measured specimens.

If possible, 62 measurements were taken, 31 measurements from the skull and 31 measurements from the postcranial material. The measurement definitions are according to ADAMS-TRESMAN (1987), VIGNAUD (1995), and from WESTPHAL (1962). Measurements without reference were defined or modified by me (Fig. 2.1 & 2.2).

2.5.1 Measuring sections at the skull (Fig. 2.1 & 2.2)

1. The skull length (**A**) is determined between the anterior margin of the premaxilla and the posterior edge of the squamosal parallel to the median line of the skull (Fig. 2.1a).
2. The rostral length (**B**) is determined between the anterior margin of the premaxillae and the fictive line tangential to the anterior margin of both orbits (ADAMS-TRESMAN 1987).
3. The skull width (**C**) is the maximum width and is defined by the posterolateral margins of the squamosals (ADAMS-TRESMAN 1987).
4. The supratemporal fenestra length (**D**) is the distance between the suture of the frontal and the postorbital to the posteromedial margin of the squamosal (ADAMS-TRESMAN 1987).
5. The supratemporal fenestra width (**E**) is the distance between the dorsolateral margin of the sagittal crest and the suture between the postorbital and the squamosal at their dorsomedial margin (ADAMS-TRESMAN 1987).
6. The rostral width (**F**) is taken in transverse direction at the level of the anterior margin of the nasals (ADAMS-TRESMAN 1987).

7. The antorbital width (**G**) means the maximum width of the skull right at the level of the anterior margin of the orbits (ADAMS-TRESMAN 1987).
8. The premaxilla-nasal distance (**H**) lies between the posterior margin of the premaxilla and anterior margin of the nasal (ADAMS-TRESMAN 1987).
9. The orbital length (**I**) is the maximum length of the orbit taken at its inner margin in longitudinal direction (ADAMS-TRESMAN 1987).
10. The orbital width (**J**) is the maximum width of the orbit taken at its inner margin in transverse direction (ADAMS-TRESMAN 1987).
11. The premaxillary width (**K**) is the maximum width of the paired premaxillae (VIGNAUD 1995).
12. The narrowing of the premaxillae (**L**) means the minimum width of the rostrum between the posterolateral margins of the premaxillae (Fig. 2.1.a).
13. The width of the sagittal crest (**M**) is the minimum widths of the sagittal crest (Fig. 2.1a).
14. The Infratemporal fenestra length (**N**) is the maximum length of the Infratemporal fenestra taken parallel to the median line of the skull (Fig. 2.1b).
15. The infratemporal fenestra height (**O**) is the maximum height taken vertically from the dorsal margin of the jugal to the ventral margin of the squamosal (Fig. 2.1b).
16. The interorbital space (**OD**) is the minimal distance between both orbits (Fig. 2.1a).
17. The antorbital fenestra length (**P**) is the maximum length taken at the inner margin parallel to the median line of the skull (Fig. 2.1b).
18. The antorbital fenestra height (**Q**) is the maximum height taken at the inner margin in transverse direction (Fig. 2.1b).
19. The suborbital fenestra length (**R**) is the maximum length taken parallel to the median line of the skull (Fig. 2.1c).
20. The suborbital fenestra width (**S**) is the maximum width taken in transverse direction (Fig. 2.1).
21. The skull height (**T**) is measured between the dorsal margin of the parietal and the ventral margin of the basioccipital (Fig. 2.1e).
22. The foramen magnum width (**Fm1**) is the maximum width measured at the inner margin in transverse direction (Fig. 2.1e).
23. The foramen magnum height (**Fm2**) is the maximum height measured at the inner margin in dorsoventral direction (Fig. 2.1e).

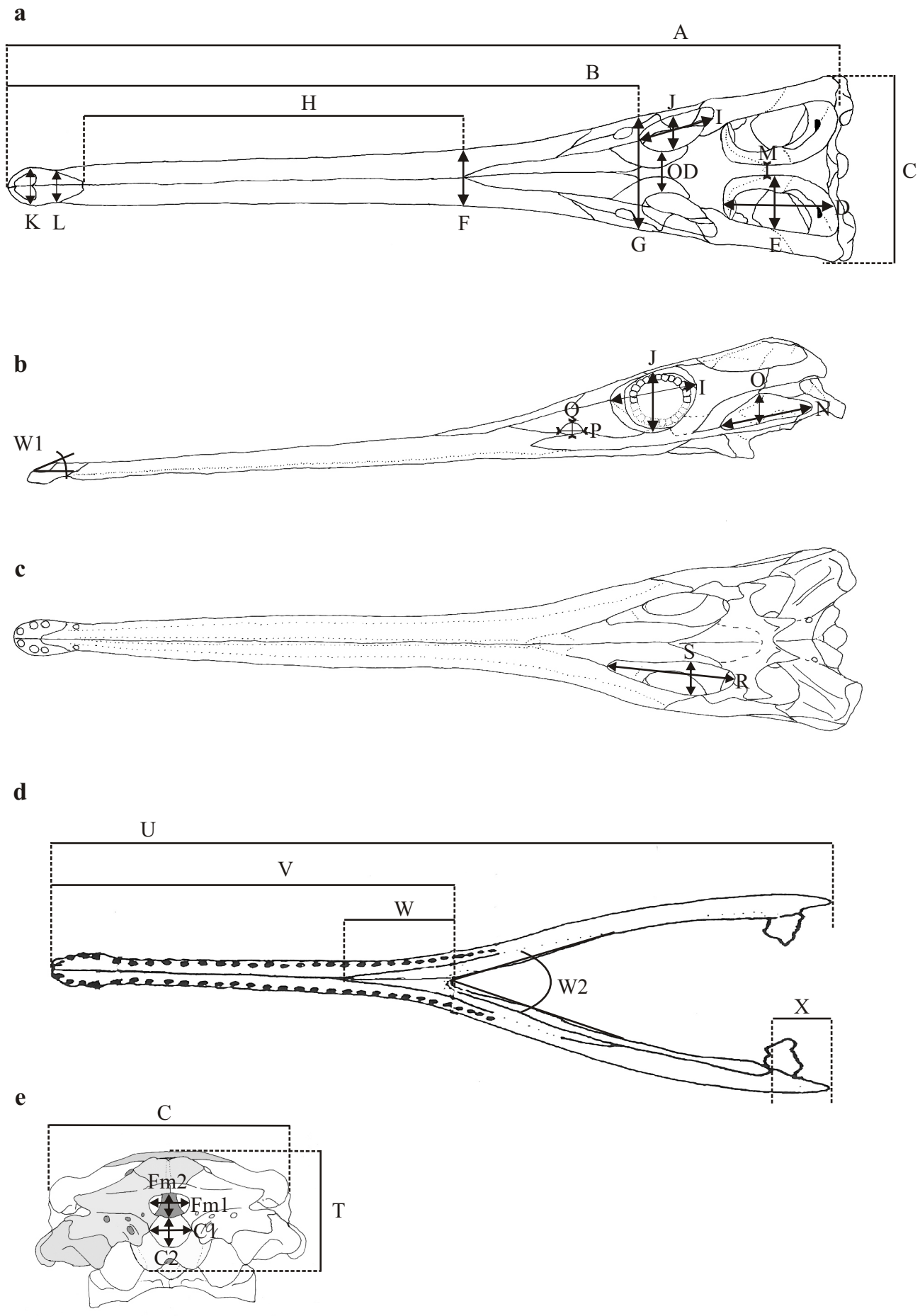

Figure 2.1a-e: Measurements of the skull. For further explanations see text.

24. The condyle width (**C1**) is the maximum width taken from the lateral margins in transverse direction (Fig. 2.1.e).
25. The condyle height (**C2**) is the maximum height taken between the dorsal and the ventral margin (Fig. 2.1e).
26. The mandibular length (**U**) is measured from the anterior tip of the dentary to the posterior end of the retroarticular process parallel to the median line of the lower jaw (Fig. 2.1d).
27. The length of the symphysis (**V**) is measured from the anterior tip of both dentaries until the end of symphysis (Fig. 2.1.d).
28. The splenial part of symphysis (**W**) is measured from the anteroventral margin of splenial to the end of symphysis (Fig. 2.1d).
29. The length of retroarticular process (**X**) is taken from the posterior margin of the articular facet to the end of the mandible (Fig. 2.1d).
30. The angle of the orientation of the external naris (**W1**) is measured between the outline plane of the external naris and the horizontal plane of the floor of the external naris (Fig. 2.1b).
31. The symphysis angle (**W2**) is measured between the mandibular rami at the posterior end of symphysis (Fig. 2.1d).

2.5.2 Measuring sections at the postcranial skeleton (Fig. 2.2)

32. The scapula length (**Sa1**) is the maximum length in proximal-distal direction parallel to the long axis of the bone (Fig. 2.2b).
33. The coracoid length (**Co1**) is the maximum length in proximal-distal direction (Fig. 2.2b).
34. The humerus length (**H1**) is defined as the maximum length of the humerus taken parallel to the long axis of the bone (Fig. 2.2d).
35. The humerus width (**H2**) is the maximum thickness of the bone shaft (Fig. 2.2d).
36. The radius length (**R1**) is the maximum length of the bone bar measured parallel to the long axis (Fig. 2.2d).
37. The radius with (**R2**) is the maximum thickness of the bone shaft (Fig. 2.2d).
38. The ulna length (**U1**) is the maximum length of the bone (Fig. 2.2d).
39. The ulna width (**U2**) is measured at the bend of the shaft (Fig. 2.2d).
40. The radiale length (**Ra1**) is the maximum length of the radiale taken parallel to the long axis of the bone (Fig. 2.2d).

41. The ulnare length (**Ul1**) is the maximum length of the ulnare measured parallel to the long axis of the bone (Fig. 2.2d).
42. The metatarsal length (**Mt1**) is the maximum length taken parallel to the long axis of the bone bar at the metatarsal one (Fig. 2.2c).
43. The length of the ilium (**P1**) is the maximum length of the bone taken in dorsoventral direction (Fig. 2.2a).
44. The width of the ilium (**P2**) is the maximum width determined between the anterior margin of the anterior process and the posterior margin of the posterior process of the ilium (Fig. 2.2a).
45. The ischium length (**Is1**) is the maximum length of the bone taken in proximal-distal direction parallel to the long axis of the ischium (Fig. 2.2a).
46. The ischium width (**Is2**) is the maximum width taken at the ventral margin (Fig. 2.2a).
47. The pubis length (**Pu1**) is the maximum length of the bone bar taken parallel to the long axis of the bone (Fig. 2.2a).
48. The pubis width (**Pu2**) is the maximum width taken at the ventral margin of the pubis (Fig. 2.2a).
49. The femur length (**Fe1**) is defined as the maximum length parallel to the long axis of the bone (Fig. 2.2c).
50. The femur width (**Fe2**) is defined as the minimum width of the shaft (Fig. 2.2c).
51. The tibia length (**Ti1**) is the maximum length taken parallel to the long axis of the bone (Fig. 2.2c).
52. The tibia width (**Ti2**) is the minimum width at the shaft (Fig. 2.2c).
53. The fibula length (**Fi1**) is the maximum length taken parallel to the long axis of the bone.
54. The fibula width (**Fi2**) is the minimum width of the shaft (Fig. 2.2c).
55. The shoulder-pelvic distance (**S-PL**) is the distance measured from the shoulder girdle to the pelvic girdle and is determined as the length between the thoracic vertebra at the level where the scapula is attached and the first sacral vertebra (WESTPHAL 1962).
56. The calcaneum length (**Ca1**) is the maximum length of the calcaneum (Fig. 2.2c).
57. The astragalus length (**As1**) is the maximum length of the astragalus (Fig. 2.2c).
58. The trunk length (**TRL**) is defined as the length of the cervical and thoracic spine including both sacral vertebrae (WESTPHAL 1962).

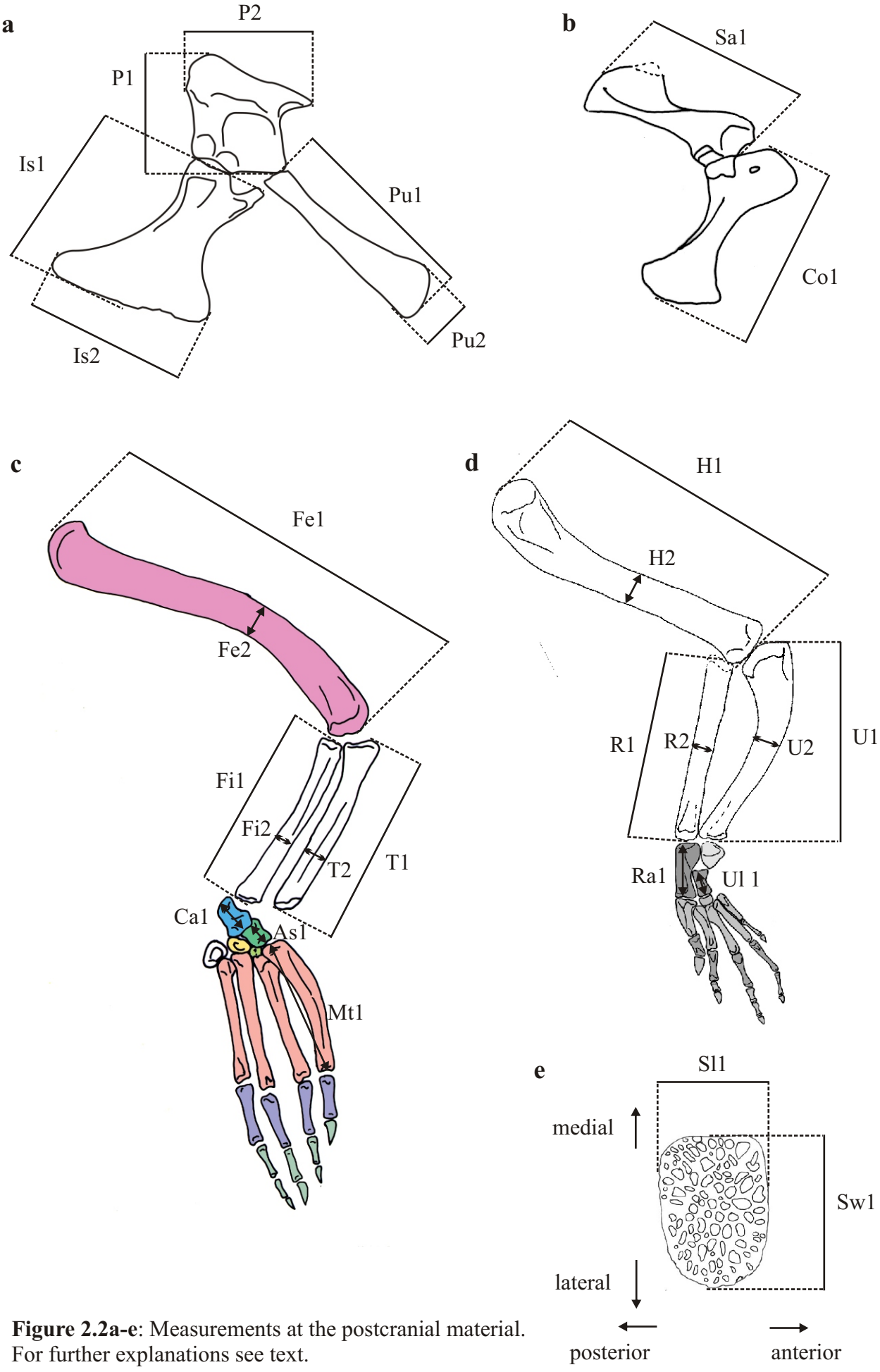

Figure 2.2a-e: Measurements at the postcranial material. For further explanations see text.

59. The caudal length (**CL**) is defined as the length of the caudal spine posterior to the sacral vertebrae (WESTPHAL 1962).
60. The total body length (**TL**) of the specimen is determined from the tip of the snout until the tip of the tail.
61. The osteoderm length (**Sl1**) is the maximum length of the osteoderms in anterior-posterior direction (Fig. 2.2e).
62. The osteoderm width (**Sw1**) is the maximum width of the osteoderms in medial-lateral direction (Fig. 2.2e).

Chapter 3

Anatomical descriptions

3.1 Osteology of *Steneosaurus bollensis* (JAEGER 1828)

3.1.1 Introduction

The Liassic crocodile *Steneosaurus bollensis* is the most common taxon in the Posidonia Shale (Lias ε) of South Germany. It is also known from Liassic localities in England and Luxembourg. The holotype was found in 1712 near Bad Boll and was bought by GMELIN for the Museum in Dresden, where it is still housed. CUVIER (1812) described the specimen as "Gavial de Boll". JAEGER (1828) reinvestigated it and named it *Steneosaurus bollensis*. A lot of teleosaurid material was found during the last two centuries in the Liassic deposits of the Swabian Jura and many new finds were established as new taxa (e.g. KAUP 1837, V. MEYER 1830, BRONN 1841; QUENSTEDT 1852). WESTPHAL (1962) reinvestigated the taxonomy of those taxa, provided a synonym list, and referred most taxa to *Steneosaurus bollensis*.

This description is a consensus of the examination of 89 specimens referred to *Steneosaurus bollensis* with certainty. Variation in the osteology is mentioned in the text, with the corresponding number of the specimen, which shows variation. The variation caused by ontogeny in *S. bollensis* is not described in this section, but discussed in chapter 4 "Intraspecific variation and Biometric data".

This anatomical revision of the taxon *Steneosaurus bollensis* was carried out to clear the influence of intraspecific variation on diagnostic characters, to establish characters, which are valuable for a phylogenetic analysis inside the Thalattosuchian, and to compare it with the poorly known taxon *Platysuchus multiscrobiculatus* (see chapter 3.4)

Eureptilia OLSON 1847

Diapsida OSBORN 1903

Mesoeucrocodylia WHETSTONE & WHYBROW 1983

Thalattosuchia FRAAS 1901

Teleosauridae GEOFFROY 1831

Steneosaurus bollensis (JAEGER 1828)

(Figures 3.1-3.18)

Holotype: SNSD uncatalogued, here labelled as SNSD 1

Locus typicus: Bad Boll, Germany

Stratum typicum: Lias ε (Lower Jurassic, Toarcian, Posidonia Shale)

3.1.2 Material

In total **89** specimens referred to *Steneosaurus bollensis,* well enough preserved to take measurements from (at least partially), were in detail investigated: **6** specimens housed in the BMNH; **4** specimens housed in the BSGP; **6** specimens housed in the GPIM; **17** specimens housed in the GPIT; **1** specimen housed in the MGUH; **1** specimen housed in the MNHN; **3** specimens housed in the NHMUS; **1** specimen housed in the SMNK; **40** specimens housed in the SMNS; **4** specimens housed in the SNSD; **4** specimens housed in the TMH, and **2** specimens housed in the UH.

A complete list of all the investigated material is provided in the appendix I.

3.1.3 Locality and horizon (Fig. 1.2b, 1.3, 1.4)

Steneosaurus bollensis is known from the Liassic layers (Toarcian) of the Swabian and Franconian Jura in South Germany (Fig. 1.2b) and from the Posidonia Shale (Toarcian) in Northern Germany (WINCIERZ 1967). New investigations show that *Steneosaurus bollensis* also occasionally occurred in the Liassic of Whitby, Yorkshire Coast in Great Britain (BENTON & TAYLOR 1984, WALKDEN et al. 1987) and in Luxembourg (GODEFROIT 1994, MAISCH & ANSORGE 2004) (see chapter 7).

However, most specimens of *Steneosaurus bollensis* come from the Lias ε, II, layers 1-12 (HAUFF 1921), from diverse localities of the Swabian and Franconian Jura in Southern Germany (Fig. 1.3). The holotype was found in Boll as well in the Lias ε (Posidonia Shale), but the exact layer is not reported (CUVIER 1812, JAEGER 1828, WESTPHAL 1962).

If possible, the exact location and layer of the individual specimens are provided in the appendix I.

3.1.4 Preservation

The Liassic specimens of *Steneosaurus bollensis* are preserved in a matrix of black shale. In most cases, overlying strata had compressed them, but the bones are often intact and still articulated. Because of the dorsoventral compression of the specimens, there is a lack of information about the particular height of the skull or the vertebrae, or the size and shape of the infratemporal fenestra in the skull. In addition, parts of the braincase and the palate were not available for closer investigation. Specimens preserved in lateral view are rare (e.g. SMNS 51753) and there is only one fragmentary isolated occipital in three-dimensional

preservation (SMNS 59558), which is tentative referred to *Steneosaurus bollensis*. There are numerous articulated and nearly complete skeletons. Most specimens are exposed from their dorsal side, but some specimens have been prepared ventrally (e.g. SMNS 15816, TMH 2741). Therefore, the information about the osteology of *Steneosaurus bollensis* is relatively complete.

Some specimens (e.g. GPIT Re 1193/1) consist of parts of more than one individual. In specimen GPIT Re 1193/1, the skull of one individual is glued to the body of another individual (pers. comment MAISCH). This fact has to be considered when using biometric data (see chapter 4), in order to avoid misleading information.

There are some specimens with preservation of skin texture and cartilage fragments. Specimen SMNS 10985 shows the skin outline at the leg and skin surface texture (BERCKHEMER 1928, figured there). SMNS 51555 and SMNS 20281 for example possess petrified tracheal rings of the primary cartilaginous trachea. In addition, there are several specimens with preserved stomach contents and/or gastroliths e.g., GPIT Re 1193/1, SMNS 51753, and SMNS 59736 (see also chapter 8, Fig. 8.8).

3.1.5 Diagnosis

Steneosaurus bollensis is a large thalattosuchian with a maximum length of five meters. The skull is flat, with an elongated, narrow rostrum and slightly broadened premaxillae (Fig. 3.1). The skull is up to 51%-65% of the total body length, without the tail (WESTPHAL 1962). The skull width (C) is about 27-30% of the skull length (A), and the rostral length (B) in ratio to the skull length (A) is between 69% and 75% (see chapter 4). The nasals do not contact the premaxillae. A lateral lacrimopostorbital contact is in some specimens present, but in most cases, the jugal separates them and participates in a small dorsal process at the lateral orbital margin. The orbit is longitudinal elliptic and the orbital length in adult specimens is in average 7.9 % of the skull length (A). The antorbital fenestra is very small, longitudinal slit-like or absent. The supratemporal fenestra (STF) is large with in average 15.2% of the skull length and elongated. It is usually twice as long as wide (STF length (D)/STF width (E) ~ 1.5, see also chapter 4). The cranial surface of the frontal, prefrontals, postorbitals, squamosals, the parietal, and sometimes the jugals is ornamented by a pattern of pits. The dentition is weakly heterodont, with an enlarged third premaxilla tooth, and visible replacement teeth in the maxilla and dentary. A diastema is present as a dorsolateral notch level with the ventrolateral premaxillary-maxillary suture. The dentition code is: $\frac{3-4+26-35}{24-35}$

A maximum of 76 amphicoelous vertebrae is present in the vertebral column. There are nine cervical vertebrae including the atlas-axis complex, 12 to 15 thoracic vertebrae and two to three lumbar vertebrae, two sacral vertebrae, and up to 55 caudal vertebrae. The number of cervical vertebrae is constant, as is the number of sacral vertebrae. The count of thoracic, lumbar, and caudal vertebrae show intraspecific variation (see chapter 4). Dorsal and ventral dermal armour is present. The dorsal armour starts posteriorly to the third cervical vertebrae and covers the animal up to the 50th vertebra with a double longitudinal row of osteoderms. Thus, the dorsal armour covers the tail up to the 23rd caudal vertebra. The ventral armour consists of six longitudinal rows, each possesses up to 16 osteoderms. The fore limbs are shorter than the hind limbs and the humerus length (H1) is between about 57% - 65% of the femur length (Fe1) (see chapter 4).

3.1.6 Osteology

Skull (Fig. 3.1-3.6)

About fifty skulls and skull fragments of *Steneosaurus bollensis* were investigated here, mainly coming from localities in southern Germany (see appendix I). Like all other teleosaurids, *Steneosaurus bollensis* has an elongated and narrow snout (rostral length (B) is in average 71.4 % of the skull length (A), see chapter 4). Contrary to many other extant and fossil crocodilians, the lateral margins of the maxilla are nearly straight and undulate not much. The premaxillae are broaden anteriorly and solely form a spoon-shaped enlargement at the anterior tip of the rostrum. The external naris is anterodorsally orientated. The premaxilla does not contact the nasals. The distance between the anterior margin of the nasal and the posterior margin of the premaxilla (H) in ratio to the rostral length (B) is between 22%, and 46%, and varies broadly intraspecifically (see also chapter 4). The skull widens gradually in posterior direction, beginning level with circa the 23rd alveolus of the maxilla and reaching maximum width at the posterior margin of the cranial table (Fig. 3.1a). The cranial table is trapezoidal and possesses elongated sub-rectangular to sub-trapezoid supratemporal fenestrae and longitudinal elliptic orbits (Fig. 3.1a). Anterior to the nasals, the cross-section of the upper part of the rostrum shows a convex dorsal surface and a slightly concave ventral surface, with a fused nasal canal inside and ventrally orientated alveoli. The parietal, frontal, prefrontals, postorbitals, squamosals, and in some specimens the jugals show ornamentation with a characteristic pattern of pits on their external dorsal surface (Fig. 3.1). The shape and the size of the pits are differently developed on the respective bones (see below, Fig. 3.1 & 4.2).

Cranial table

Openings

External naris (en, Fig. 3.1a)

The undivided margin of the external naris is completely formed by the premaxillae. In general, the external naris is transverse elliptic. In some cases, the outline of the external naris has anteromedially and posteromedially a small notch (e.g. GPIM 23a). In some specimens, the anterior margin of the external naris forms medially an anterodorsally orientated, small, pointed process (e.g. SNSD 4). The shape of the external naris varies intraspecifically. In addition, in some cases it appears different in shape because of diagenetic compression (for further discussion see chapter 4, Fig. 4.3).

The external naris opens anterodorsally, and the plane of the external naris aperture forms an angle of circa 45° (W1, Fig. 2.1b) with the horizontal plane of the floor of the external naris.

Antorbital fenestra (AOF, Fig. 3.1a)

In some specimens e.g. GPIT Re 1193/9, SMNS 81699, and BSGP 1949, XV 1 a small, longitudinal slit-like antorbital fenestra is visible. The medial margin is formed by the lacrimal, the lateral margin is formed by jugal, and the anterior margin is formed by the maxilla (Fig. 3.1a).

It is assumed that all specimens originally possessed antorbital fenestrae, but that the original condition is often obscured by the dorsoventral compression of the skull. In most cases, the maxilla is misaligned and overlies exactly the part of the rostrum where the antorbital fenestra is expected. However, in most cases, a slight depression is visible there. It seems that the maxilla preferentially moved towards this weak spot in the skull construction during diagenetical compression.

Orbit (o, Fig. 3.1)

The orbit is longitudinal ellipsoid. The longest axis extends from the point of the prefrontolacrimal suture up to the middle of the anterior margin of the postorbital. The orbits open almost dorsally and are only slightly laterally orientated. In the adult specimens, the orbits are much smaller than the supratemporal fenestrae (Fig. 3.1). The orbital length (I) is in average 52% of the supratemporal fenestra length (D) in adult specimens and about 63% in

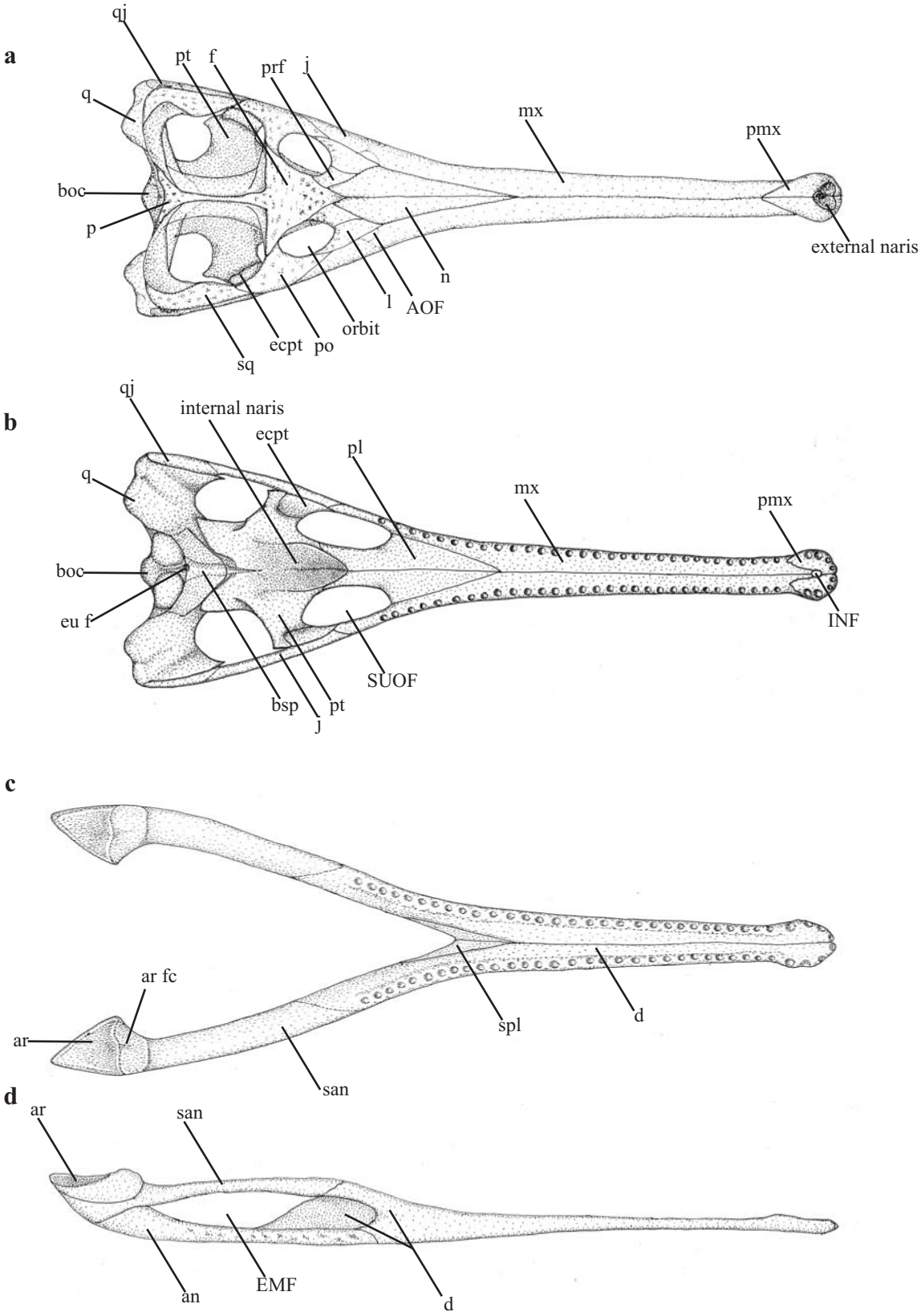

Figure 3.1a-d: Dorsal (a) and ventral (b) view of a hypothetical adult *Steneosaurus bollensis* skull. The skull is mainly reconstructed after GPIM 23a, SMNS 15816, SMNS 53422, and SMNS 80235. Lower jaw (c-d) reconstruction is mainly based on the adult specimens GPIM 23a, SMNS 80235, and SMNS 53422. Abbreviations see chapter 2.

juvenile specimens. The share of the orbital length (I) at the skull length (A) is about 7.9 % in adult specimens, but in average 9.6% in juvenile specimens (for further explanations see chapter 4, Fig. 4.1 & 4.5).

The anterior margin of the orbit is formed by the lacrimal and the prefrontal. The anterior margin is often slightly thickened, and in some cases, shows a small notch at the point of the prefrontolacrimal suture (e.g. SMNS 15951b, SMNS 20283). The smooth medial margin is formed by the frontal. Posteromedially, the margin is formed by the frontal and posterolaterally by the postorbital. Laterally, the margin is formed by the postorbital, jugal, and lacrimal. WESTPHAL (1962), WALKDEN et al. (1987), and GODEFROIT (1994) mention a direct contact between the postorbital and the lacrimal, excluding the jugal from the lateral margin of the orbit, for some *Steneosaurus bollensis* specimens from Southern Germany, England, and Luxembourg. In this work, it turns out that in some cases, the jugal is excluded from the lateral margin of the orbit (e.g. BSGP 1949 XV 1, GPIM 23a, OUM JZ 176), but more often it is included (Fig. 3.1). If the jugal is included, it forms a very small part of the lateral margin of the orbit and separates the postorbital from the lacrimal (for further discussion paragraph "jugal" and chapter 4).

Supratemporal fenestra (STF, Fig. 3.1a)

The large, elongated supratemporal fenestra in the cranial table is sub-trapezoid in adult specimens (Fig. 3.1a). Anteromedially, its margin is formed by the frontal and anterolaterally by the postorbital. Posterolaterally, it is formed by the squamosal and posteromedially by the parietal. The anteromedial corner of the supratemporal fenestra is right-angled and in most cases not rounded, whereas the anterolateral corner is right-angled but always rounded. The posterolateral corner is slightly posteriorly elongated and rounded, whereas the posteromedial corner has a blunt angle. The anterior part of the squamosal bulges out in medial direction into the supratemporal fenestra (see paragraph “squamosal”). This concavity in the lateral margin of the supratemporal fenestra gives the outline of the supratemporal fenestra often a somewhat kidney-like shape (Fig. 3.1a). The sagittal crest is formed by the frontal and the parietal. Up to 50 % of the crest is formed by the frontal. In adult specimens, the sagittal crest is very narrow, with a general width of 2-4 mm (see appendix II). However, the shape of the supratemporal fenestra and the sagittal crest varies ontogenetically in *S. bollensis* and the extension of the supratemporal fenestra depends mainly on the elongation of the posterior process of the frontal and the anterior process of the parietal during ontogeny (see chapter 4, Fig. 4.5).

Infratemporal fenestra (ITF, Fig. 3.2, Fig. 4.1)

This fenestra is difficult to detect because of the compressed preservation of all investigated skulls, but in some specimens e.g., SMNS 80235 (Fig. 3.2) the opening is visible. Anterodorsally the infratemporal fenestra is bordered by the postorbital, posterodorsally by the squamosal, anteroventrally by the jugal and posteroventrally by the quadratojugal. The opening lies nearly vertically in the skull and is only slightly laterally orientated. The infratemporal fenestra is almost as long as the supratemporal fenestra. Because of the flattening of the skulls, the original height of the infratemporal fenestra is questionable, but the wax reconstruction of a juvenile *S. bollensis* skull suggests an opening at least four times longer than high (see chapter 4; Fig. 4.1).

Cranial bones

Premaxilla (pmx, Fig. 3.1a, Fig. 3.2, Fig, 3.3)

The paired premaxilla is fully exposed in dorsal view, whereas the ventral face of the premaxilla is mostly hidden by the dentaries. Only in the specimens TMH 2741 and GPIT Re 1193-6, the ventral face of the premaxilla is entirely visible but poorly preserved. Dorsally, the paired premaxilla completely encloses the external naris (see above). Posterodorsal to the external naris the contralateral premaxillae meet medially in a straight suture. The dorsal premaxillary-maxillary suture runs obliquely from anterolateral to posteromedial. Thus, in dorsal view, the paired premaxilla tapers posteromedially between the maxillae, and ends medially at the level of the third maxillary tooth (counted from anterior). In dorsal view, the anterolateral external wall of the premaxilla is externally convex and posteriorly indented by a wide notch. As a result, the premaxillae form together a spoon-shaped expansion at the anterior tip of the snout (Fig. 3.1, 3.3). These lateral expansions of the premaxillae seem to be subject of individual variation (see chapter 4). Each premaxilla bears three to four teeth. The largest tooth is the third one (see paragraph “dentition”). It is situated directly in front of the notch (Fig. 3.2), which forms a diastema between the premaxillary and maxillary dentition. In lateral view, at this notch, the premaxillary-maxillary suture runs obliquely from anteroventral to posterodorsal. Thus, the premaxilla overlies the maxilla level with the diastema.

At the floor of the external naris, the straight interpremaxillary suture forms a low median crest (Fig. 3.1a, Fig. 3.3). It extends from the anterior margin nearly up to the posterior margin of the external naris.

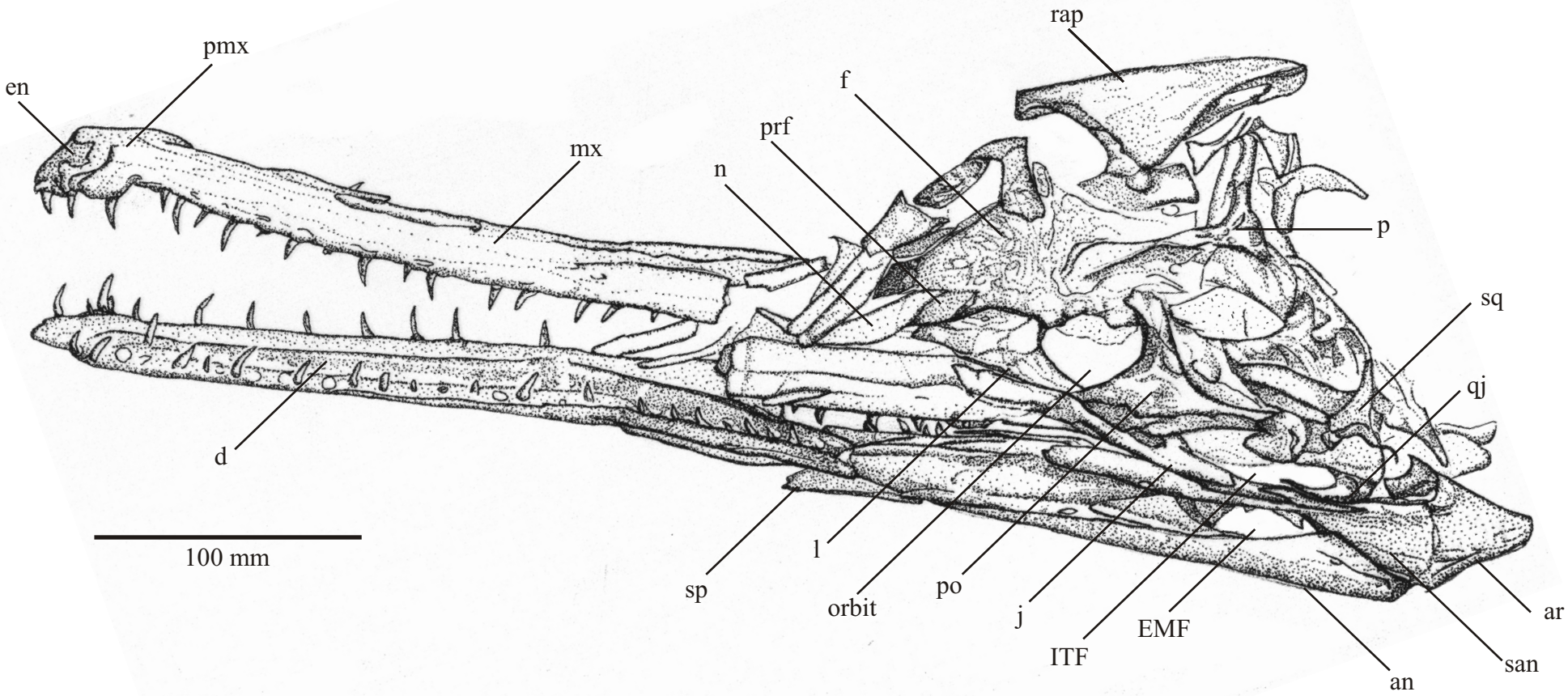

Figure 3.2: *In situ* drawing of the skull of SMNS 80235. Posterior part of lower jaw in lateral view with exposed external mandibular fenestra (EMF). The cranial table is disarticulated and the rostrum is broken. Original skull length about 450 mm. Scale bar 100 mm. Abbreviaions see chapter 2.

In dorsal view, a small, round incisive foramen is visible in the middle of this crest separating it at this point e.g., BSGP 149 XV 1a, SMNS 53422, TMH 2741, and OUM JZ 176 (Fig. 3.3). Dorsally, this foramen is entirely formed by the premaxillae, whereas ventrally, the maxillae form the posterior margin of it (see paragraph palate).

Maxilla (mx, Fig. 3.1, Fig. 3.2, Fig. 3.3)

The paired maxilla forms the largest part of the rostrum (see also paragraph "palate"). The lateral margin of the maxilla is straight in dorsal view and undulates only slightly in lateral view. Dorsally, the maxilla forms a straight median suture with the contralateral maxilla. Posteromedially, the paired maxilla contacts the nasals, which separate the maxillae in their posterior third. The maxillonasal suture is smooth and extends obliquely in mediolateral direction. Posteromedially, the maxilla is bordered by the lacrimal, which tapers off between the maxilla and the nasal. Posteriorly, the maxilla bifurcates in a dorsal and a ventral part. The dorsal part of the maxilla tapers posteriorly between lacrimal and jugal, while the ventral part of the maxilla posterolaterally descends posteroventrally, largely ventrally the jugal. Thus, the jugal overlaps the ventral part of the maxilla level with the anterior tip of the lacrimal. Anteriorly the paired maxilla contacts the paired premaxillae (see paragraph “premaxilla”). The maxillary number of alveoli ranges from approximately 26 to 30 (see also paragraphs “dentition” and “palate”). The dorsal surface of the maxilla is mainly smooth, only some weak longitudinal wrinkles are visible in some cases.

Nasal (n, Fig. 3.1)

The nasal is an elongated slender bone in the rostrum, which does not contact the premaxilla. Dorsally, the nasal meets its opposite in a smooth, straight median suture. Anteriorly the paired nasal terminates in the posterior third of the rostrum. Anteromedially, the paired nasal tapers deeply between the maxillae until the level of about the 20th maxillary tooth. Posterolaterally, the nasal is bordered by the lacrimal and the prefrontal, whereas the posterior and posteromedial parts are bordered by the frontal (see there). The frontal goes with a thin projection between the nasals and separates them at their posterior-most end. The posterior margin of the nasals terminates shortly posterior to the anterior margin of the orbits. The lateral margins of the paired nasal are slightly externally convex. The surface of the bones is smooth and does not possess any sculpturing.

Lacrimal (l, Fig. 3.1)

The lacrimal is a sub-triangular bone with a slender posterior process, which expands laterally to the orbit. The lacrimal is about as long as the orbit. Anterolaterally, it is bordered by the maxilla and forms there the medial margin of the antorbital fenestra (see there). Anteromedially, it is bordered by the nasal, and medially by the prefrontal. Posteriorly, the lacrimal forms the anterolateral margin of the orbit. The posterior margin of the lacrimal is slightly thickened. Posterolaterally and posteriorly, the lacrimal is bordered by the jugal. However, in some specimens, the posterolateral margin of the lacrimal contacts the postorbital in an oblique suture. The surface of the bone is mostly smooth, but on its posterior part, close to the anterior margin of the orbit, a pattern of small round pits or small grooves is visible. Because of the distinct ornamentation in that area and the flattened preservation, the exact run of the prefrontolacrimal suture is difficult to detect in that region.

Prefrontal (prf, Fig. 3.1)

The prefrontal is a small bone, which is situated medially to the lacrimal in the cranial table. It is a roughly rhombic bone, which is only half the size of the lacrimal. Anteriorly, it ends acute-angled between the lacrimal and the nasal. The anterior half of the lateral margin is bordered by the lacrimal, while the posterior half forms part of the anteromedial margin of the orbit. The medial margin of the prefrontal is bordered in its anterior two-thirds by the nasal and in the posterior third by the frontal. The exact run of the frontoprefrontal suture is hard to identify, because of the similar sculpturing of these bones in that area. If visible, the suture can be zigzag-shaped or straight and usually runs from the anterior margin of the orbit in anteromedial direction to the posterior end of the nasals. The ornamentation on the external surface of the prefrontal consists of a distinct pattern of circular pits at the posterior margin of the prefrontal and turns anteriorly into a pattern of flat elongated pits, whereas the surface of the anterior half is smooth.

Frontal (f, Fig. 3.1, Fig. 3.2, Fig. 3.3)

The unpaired frontal is a large triangular element, with a slender posteromedial process in adult specimens, which forms the medial surface of the cranial table. The shape of the frontal varies from rhombic to triangular during ontogeny and this variation is described and discussed in detail in chapter 4 (Fig. 4.5). The frontal forms the medial, the posteromedial, and the posterior margins of the orbits. In addition, it forms the anteromedial margin of the supratemporal fenestra. Anteromedially, the frontal projects with a short pointed process

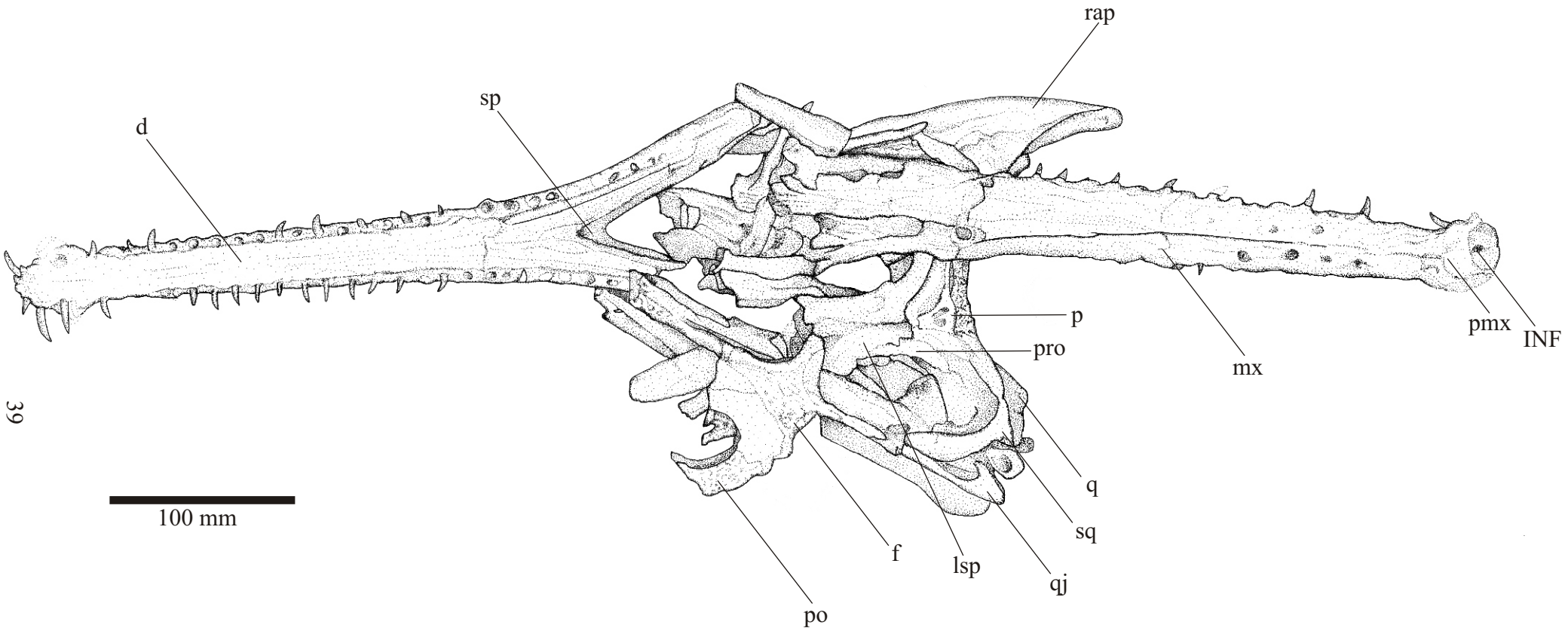

Figure 3.3: *In situ* drawing of the skull of SMNS 53422. Lower Jaw in ventral view, rostrum and posterior cranial table in dorsal view. Scale bar 100 mm. Abbreviations see chapter 2.

between the nasals (see paragraph "nasal"). Anterolaterally, it contacts the prefrontals and posterolaterally the postorbitals. Posteromedially it contacts the parietal with a slender process, which forms the anterior half of the sagittal crest. The prefrontofrontal sutures and the nasofrontal sutures are slightly interlocking. The heavy ornamentation on the external surface of the frontal consists of deep round pits in dens distribution. However, in some cases, the pits merge posteriorly into slender mediolaterally orientated grooves. Intermediate stages are often observed and the variability of the ornamentation is described in detail in chapter 4 (Fig. 4.2).

Parietal (p, Fig. 3.1a, Fig. 3.2, Fig. 3.3)

The parietal is an unpaired, triangular bone at the posterior end of the cranial table. Posterodorsally, it overlies the supraoccipital, while anteroventrally, the parietal is probably fused to the braincase, as no real suture to the prootic is visible there (see paragraph “braincase”). The slender anterior process of the parietal forms the posterior 50% of the sagittal crest and contacts anteriorly the frontal. In dorsal view, the posterolateral edge of the parietal contact each squamosal in an acute-angled suture and form together with them the posterior margins of the supratemporal fenestrae. The ornamentation of the parietal is slightly changing during the ontogenetic process (see chapter 4). In adult specimens, the dorsal surface of the posteromedial, triangular part of the parietal bears a pattern of round or ellipsoid pits, while the surface of the slender anterior process of the parietal is smooth. The ornamentation is very similar to the pattern of pits found on the prefrontal (see above).

Postorbital (po, Fig. 3.1, Fig. 3.2)

The postorbital is a large, triradiate bone at the lateral margin of the cranial table. It has three processes, one in anterior, one in posterior and one in dorsal direction. Anteriorly, the process is only one third of the height of the medial part of the postorbital and elongates from the medial part of the postorbital. A similar process emerges from the postorbital in posterior direction. The anterior process of the postorbital tapers between the lacrimal (see there) and the jugal and forms together with the posterior process of the lacrimal, the lateral margin of the orbit (see there). However, more often the anterior process of the postorbital contacts anteriorly a small dorsal process of the jugal in an oblique suture and therefore is separated from the lacrimal. The posterior process of the postorbital adjoins the anterior process of the squamosal in a smooth, oblique suture that runs from anterolateral to posteromedial. The postorbital lies medially and the squamosal laterally to this suture. Together they form

medially the lateral margin of the supratemporal fenestra (see there) and ventrally the dorsal margin of the infratemporal fenestra. The third process of the postorbital extends in dorsomedial direction, contacts the frontal, and forms anteriorly the posterolateral margin of the orbit and posteriorly the anterior margin of the supratemporal fenestra (see there). Ventromedially, the postorbital contacts the ectopterygoid. In addition, a ridge on the ventrolateral surface of the postorbital and the squamosal is noticed (Fig. 3.2). The ridge runs parallel to the long axis of the infratemporal fenestra and ventral to the ridge the ornamentation of both bones declines. The distinct ornamentation on the dorsal surface of the postorbital consists of a pattern of small, round to ellipsoid, deep pits in an equal dense distribution. The ventrolateral extension of the postorbital has a less pitted surface and appears almost smooth level with the postorbital-jugal contact.

Squamosal (sq, Fig. 3.1, Fig. 3.2, Fig. 3.3, Fig. 3.5)

The squamosal is situated posterolateral in the skull. The dorsal surface of the squamosal is somewhat L-shaped and slender. The squamosal forms the posterolateral margin and one-half of the posterior margin of the supratemporal fenestra. Anteriorly, it contacts the postorbital in an oblique, smooth suture (see paragraph "postorbital"). Posterior to postorbitosquamosal suture, the dorsomedial margin of the squamosal bulges out in medial direction, and its medial margin curves slightly medioventrally in the supratemporal fenestra. This convexity of the dorsal surface of the squamosal is less developed in juvenile specimens, and becomes more distinct in very large specimens (see chapter 4). Posteromedially, the squamosal contacts the parietal (see there).

The squamosal has its largest expansion in ventral direction. Posteroventrally, it broadly contacts the exoccipital, quadrate, and quadratojugal. The squamosal and the quadratojugal form the posterior margin of the infratemporal fenestra (Fig. 3.1). Laterally the squamosal forms together with the quadratojugal, quadrate, and exoccipital the cranioquadrate canal (Fig. 3.5). The squamosal, quadrate, and exoccipital form also the main part of the posterior wall of the supratemporal fenestra, but the exact course of the sutures in that area is hardly visible, because of the compressed preservation of the skulls. The distinct ornamentation on the dorsal surface consists of a pattern of small, deep, ellipsoid pits, which in some cases posteriorly merge to small, elongated grooves. These pits and grooves cover the entire dorsal surface of the bone. Next to the postorbitosquamosal suture, the pattern of pits is very similar to that of the postorbital (see there), while further posterior grooves appear more often. On the ventrolateral surface of the squamosal a ridge, which continues from the

postorbital (see there, Fig. 3.2), runs parallel to the long axis of the infratemporal fenestra. Ventral to the ridge, the ornamentation declines on the ventrolateral surface of the squamosal.

Jugal (j, Fig. 3.2)

Posteriorly, the jugal is a slender, rod-shaped, elongated bone, while anteriorly it doubles in height level with the anterior margin of the postorbital. Anteriorly, it is bordered by the maxilla, and dorsomedially, by the lacrimal and postorbital. Ventromedially, it contacts the ectopterygoid and posteriorly, the quadratojugal. Anteriorly, the jugal ends acute-angled, dorsally overlapping the posterior-most part of the maxilla (see there) until the level of the maxillolacrimal suture. Anteromedially, it lies parallel to the lacrimal and postorbital meeting them in a straight suture. In some specimens of *S. bollensis*, the jugal protrudes with a small dorsal process between the lacrimal and the postorbital and takes part at the lateral margin of the orbit (see there). Posterior to the orbit the jugal forms a thin, rod-shape process, which expand posteriorly and contacts the small hook-shaped quadratojugal posterior to the postorbitosquamosal suture. The jugoquadratojugal suture runs obliquely from anteroventral to posterodorsal. The jugal and quadratojugal form together the ventral bar of the infratemporal fenestra (see there). The sculpturing of the external surface of the jugal is poorly pronounced. Anteriorly, few circular pits cover the surface in irregular distribution, while posterior to the orbit the surface is smooth.

Quadratojugal (qj, Fig. 3.1, Fig. 3.2)

In dorsolateral view, the quadratojugal is a small, hook-shaped bone with a slightly elongated anteroventral process. Anteroventrally, this process contacts the jugal, in an oblique suture, which runs from posteroventral to anterodorsal. Posterodorsally, it has a contact to the squamosal and medially it meets the quadrate. The bone participates in the formation of the posteroventral and posterodorsal margin of the infratemporal fenestra (see there). Dorsally, it has broad contact to the squamosal, but does not reach the postorbital. The external surface of the quadratojugal is smooth.

Quadrate (q, Fig. 3.1, Fig. 3.5)

The quadrate is located in the posteroventral part of the skull. It has anteromedial contact with the basisphenoid, prootic, and pterygoid (see paragraph “palate” and “braincase”). Anterodorsally, it expands under the squamosal and dorsomedially, it has contact to the exoccipital-opisthotic complex. The quadrate forms the ventral part of the

posterior wall of the supratemporal fenestra. Laterally, the quadrate lies parallel to the entire quadratojugal and contacts it in a straight suture. There, the quadrate forms the floor of the cranioquadrate canal (Fig. 3.5). Posteroventrally, it forms two articular condyles for the mandibular joint. In ventral view, three crests for the attachment of the mandibular adductor are preserved on the ventral surface of the quadrate (see chapter 8).

Palate (pa, Fig. 3.1)

The secondary palate is formed by the premaxillae, maxillae, and palatines. The other palatal bones are the vomer, pterygoids, and ectopterygoids. The palatines and the maxillae cover the vomer, thus the vomer is not visible and cannot be described. Only few adult specimens expose the palate (e.g. GPIT Re 1193/8, SMNS 15816, SMNS 20281, SMNS 58876, SMNS 51555, and TMH 2742). The skull of the juvenile specimen SMNS 20286 is matrix-free and exposes the dorsal and ventral face of the skull. The specimen is discussed in chapter 4 (Fig. 4.1). In some cases, the dorsal face of the pterygoid and ectopterygoid, could be studied in dorsal view, through the openings of supratemporal fenestrae.

Palatal openings

Internal naris (in, secondary choana, Fig. 3.1, Fig. 3.4)

In the anterior half of the pterygoids, the internal naris is preserved as a deep, longitudinal, somewhat elliptic depression, which becomes shallower in posterior direction (Fig. 3.1, Fig. 3.6). Anteriorly, the internal naris tapers off between the palatines and separates them in their posterior sixth part. Thus, the anterior outline of the internal naris is pointed, and widens in posterior direction (Fig. 3.1, Fig. 3.6). In its anterior half, the confluent internal naris shows a low, longitudinal, median crest in its roof, which is formed by the dorsomedial pterygoid-pterygoid suture.

Suborbital fenestra (SUOF, Fig. 3.1b, Fig. 3.4)

In adult specimens of *Steneosaurus bollensis*, the suborbital fenestra is longitudinal elliptic and the largest of all Liassic *Steneosaurus* taxa. Its length is about 13.5% of the skull length. The anterior margin of the suborbital fenestra reaches the level of the last maxillary alveolus in adult specimens (Fig. 3.1). However, the shape of the suborbital fenestra varies ontogenetically and the suborbital fenestra is smaller and round in juvenile specimens (for further details, see chapter 4, Fig. 4.1). The lateral margin of the suborbital fenestra is formed

by the maxilla, the anterior and medial margin are formed by the palatine, the posterolateral margin is formed by the ectopterygoid and the posteromedial margin by the pterygoid.

Maxilla and premaxilla (Fig. 3.1b)

The presented palatinal premaxillary-maxillary suture in figure 3.1b is reconstructed after two specimens (GPIT RE 1193-6 and TMH 2741), which solely show this suture. The paired maxilla tapers between the premaxillae and separates them in their posteroventral half. Anteroventrally, the maxillae forms the posterior margin of the incisive foramen. The anterolateral margins of the incisive foramen are formed by the premaxillae. The ventral face of each premaxilla exposes four circular alveoli. The anterior two alveoli are about one-third smaller than the posterior two alveoli. The third alveolus (counted from anterior) is the largest one, but the fourth alveolus is only slightly smaller. Those two alveoli are similar in size to the maxillary alveoli. In ventral view, the lateral margin of the paired premaxilla undulates slightly forming slight external convexities lateral to the alveoli. In ventral view, the maxillae form the largest part of the secondary palate and meet medially in a long, straight suture. Posteromedially, the maxilla contacts the palatine in an oblique suture, which runs from anteromedial to posterolateral. Posterolaterally, the maxilla contacts the jugal and the ectopterygoid (Fig. 3.1b). Along the ventrolateral edge of the maxilla, 26 to 35 circular alveoli lie in a straight row. The interalveolar space is about the same size as the alveoli (for further details see paragraph “dentition”).

Prefrontal (prf, Fig. 4.1)

There is not much information about the ventral expansion of the prefrontal available, but very likely a ventral process of the prefrontal (prefrontal pillar) contacts the palatine anterior to the secondary choana. In some cases, this is indicated ventrally by a transversal ridge on the palatine in front of the secondary choana, at the level of the dorsal expansion of the prefrontals (Fig. 4.1).

Palatine (pl, Fig. 3.1b)

The palatines form the posterior third of the secondary palate. They are smooth, elongated, flat bones, which meet each other in a straight median suture. Anteriorly, the paired palatine tapers off between the maxillae and separates them in their last quarter. Posteriorly to this, the palatine widens out, and forms the anterior and medial margin of the suborbital fenestra (Fig. 3.1b). Posterolaterally, it contacts the pterygoid in a more slender

process. Posteromedially, the paired palatine forms the anteroventral margin of the internal naris.

Pterygoid (pt, Fig. 3.1b)

In the posterior portion of palate, the paired pterygoid form a somewhat butterfly-shaped structure with laterally and posteriorly elongated pterygoid flanges. Anteromedially, the paired pterygoid contacts the palatines and anterolaterally, it forms prominent, toothless transverse pterygoid flanges, which contact laterally the ectopterygoids in an L-shaped suture (see below). The anterior margin of the pterygoid flange forms together with the ectopterygoid, the posterior margin of the suborbital fenestra. Posterolaterally, the pterygoid broadly contacts the quadrate in a posterior elongated quadrate ramus. This pterygoid flange and the quadrate ramus extend nearly horizontal and are only slightly flexed ventrally from the horizontal plane of the secondary palate, in contrast to the ventrally flexed pterygoids of extant crocodilians (e.g. REESE 1915, IORDANSKY 1964). On the ventrolateral surface of each posterior quadrate ramus of the pterygoid, a shallow, slightly roughed facet is present (see chapter 8, Fig. 8.2). Posteromedially, the paired pterygoid contacts the basisphenoid at the lateral and ventral surface of the braincase. The anteromedial half of the pterygoids form the posterior part of the roof of the internal naris (see Fig. 3.1b). Here, the pterygoid-pterygoid suture forms a weak median ridge in its anterior half.

Ectopterygoid (ecpt, Fig. 3.1b)

In lateral view, the ectopterygoid lies almost vertically in the skull and contacts laterally the palate and ventrally the cranial table. In ventral view, it is a small, approximately rhombic bone, which a pointed process expanding in anterior direction (Fig. 3.1b). In adult specimens, the bone is about one-third the size of the suborbital fenestra. Anteriorly, the ectopterygoid meets the maxilla. Laterally, the ectopterygoid contacts the jugal in a straight suture. Anterodorsally it probably meets the postorbital. The ectopterygoid contacts the jugal level with the postorbitojugal suture (e.g. GPIT Re 1193/8), therefore a postorbital-ectopterygoidal contact is expected. Posteromedially, the ectopterygoid contacts the pterygoid in a smooth, L-shaped suture.

Hyoid apparatus (Fig. 3.4)

Parts of the hyoid apparatus (definition after ROMER 1956) are exposed, consisting of a paired tiny, slightly curved, elongated bone lying ventrolaterally to the pterygoid (e.g. SMNS

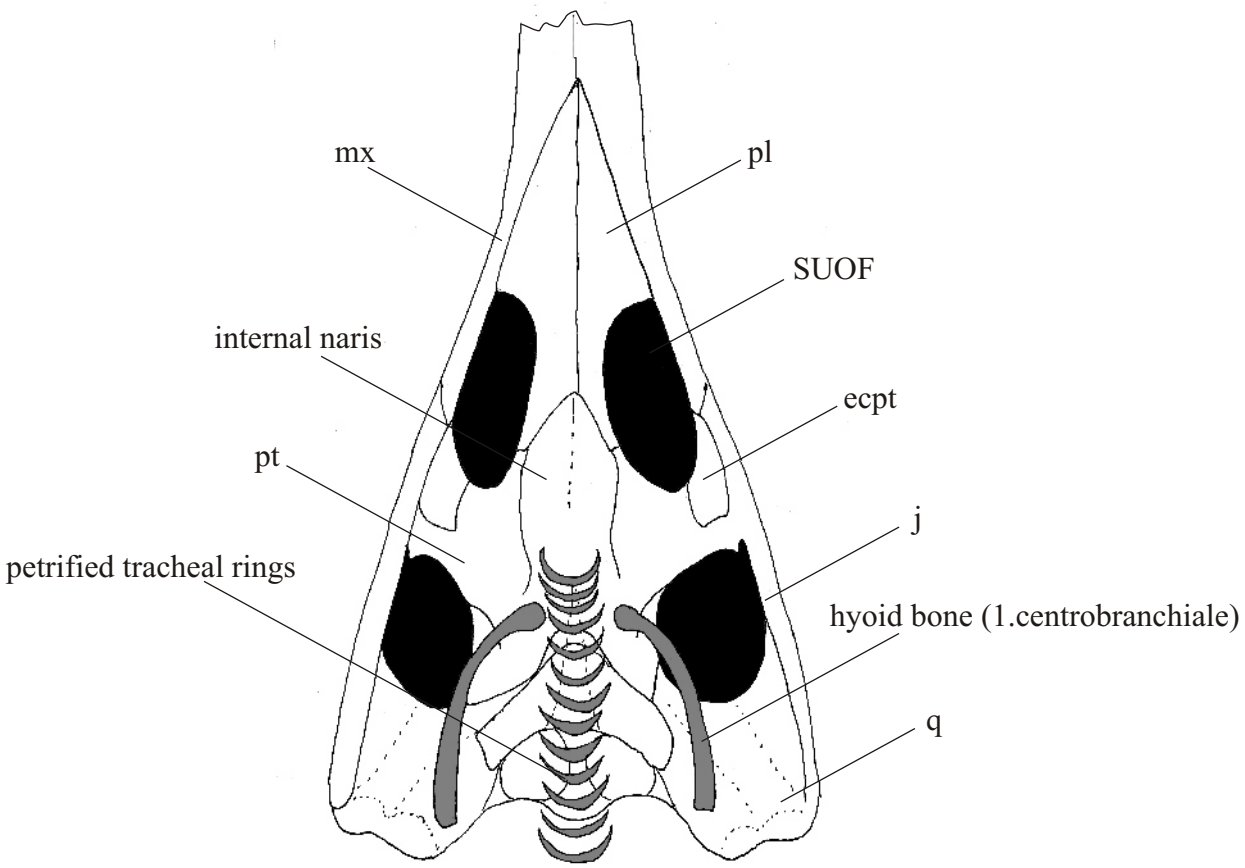

Figure 3.4: Sketch of the posterior part of the palate in *Steneosaurus bollensis* with petrified tracheal rings and first centrobranchialia (hyoid bone). Position and shape of tracheal rings and hyoid bones is reconstructed after SMNS 20281 & SMNS 51555. Abbreviations: ecpt-ectopterygoid, j-jugal, mx-maxilla, pl-palatine, pt-pterygoid, q-quadrate.

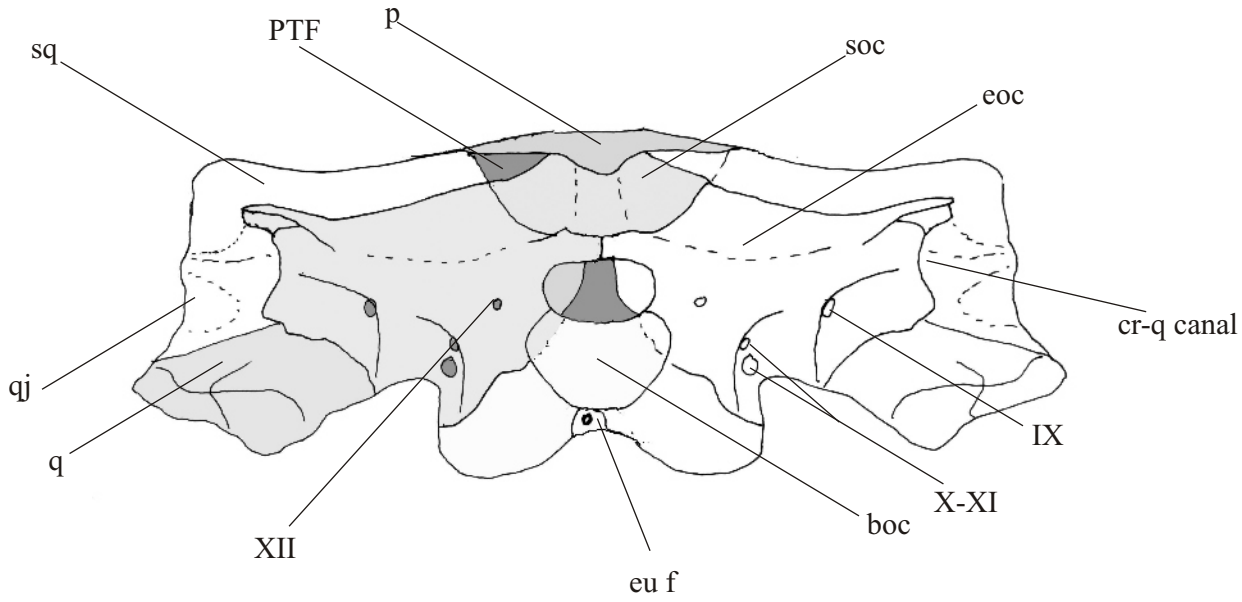

Figure 3.5: Reconstruction of the occipital region in posterior view of *Steneosaurus bollensis* (mainly after SMNS 59558). Abbreviations: boc-basioccipital, cr-q canal-cranioquadrate canal, eu f-Eustachian foramen, eoc-exoccpital, p-parietal, PTF-posttemporal fenestra, q-quadrate, qj-quadratojugal, soc-supraoccipital, IX-foramen for cranial nerve IX, X-foramen for cranial nerve X, XI-foramen for cranial nerve XI, XII-foramen for cranial nerve XII.

15951b, SMNS 20281, SMNS 20284, SMNS 20282, TMH 13288, TMH 2741, and GPIT Re 1193-3). Due to the shape and the position of these bones and compared to the conditions found in recent crocodilians (ROMER 1956, WESTPHAL 1962, BELLAIRS & KAMAL 1981), these bones are interpreted as the paired ceratobranchialis one. No other parts of the hyoid apparatus (e.g. corpus) are preserved. Because of the compressed preservation conditions, the original position of the ceratobranchialis one in *Steneosaurus bollensis* is uncertain. In ventral view, the specimen SMNS 20281 exposes two completely preserved bones, which each run from the posterolateral margin of the internal naris to the posteromedial margin of the quadrate (Fig. 3.4). Anteriorly, they lie closely to the preserved petrified tracheal rings (Fig. 3.4). According to ROMER (1956), the larynx lies in recent reptiles above the corpus of the hyoid, and cartilage, which is considered part of the visceral system develop in the walls of the larynx and as rings around the trachea. These tracheal rings may be incomplete and open dorsally (presumably a primitive condition) or may be complete hoops (ROMER 1956). Petrified tracheal rings are occasionally found in some specimens of *S. bollensis*. In ventral view, tracheal rings are exposed posterior to the internal naris, and in dorsolateral view, tracheal rings are visible lying ventrolaterally to the cervical column (e.g. SMNS 20281, SMNS 51555, and TMH 2741). They consist of incomplete rings, which open dorsally (Fig. 3.4), but occasionally also complete hoops are found. The exact number of the tracheal rings is unknown, due to fragmentary preservation. The preserved tracheal rings are exclusively exposed in large specimens. It is suggested, that the tracheal rings were probably ossified in life in older specimens and therefore preserved, whereas the probably full cartilaginous tracheal rings in younger (smaller) specimens are not preserved.

Braincase (Fig. 3.5)

The braincase consists of the basioccipital, the exoccipital-opisthotic complex, supraoccipital, prootics, laterosphenoids, and basisphenoid. It is enclosed dorsally by the frontal and parietal and ventrally by the pterygoids and the quadrates. Unfortunately, the braincase is barely exposed in most of the specimens. There is only one isolated occipital (SMNS 59558), which is tentatively referred to *Steneosaurus bollensis.* The description of the braincase is mainly based on this isolated occipital. In OUM JZ 176, the opening for the cranial nerve V is visible in the lateral wall of the braincase. Parts of the laterosphenoid and the prootic are exposed in e.g., SMNS 80235 and SMNS 53422. In some specimens e.g., SMNS 15951b and SMNS 20281, the basioccipital and basisphenoid are exposed in ventral view and in e.g., SMNS 59558, parts of the condyle is visible in posterior view, too.

Basioccipital (boc, Fig. 3.1, Fig. 3.5)

In posterior view, the basioccipital is an unpaired, triangular bone, which forms the main part of the occipital condyle and two basal ventral tubercles. Dorsomedially, the occipital condyle forms the concave ventral margin and the floor of the foramen magnum. Ventrally, the occipital condyle possesses a convex margin. At the ventral margin of the basioccipital between the paired basal tubercles, the median Eustachian foramen is exposed (Fig. 3.5). Laterodorsally, the basioccipital contacts the exoccipital-opisthotic complex in an oblique suture, which runs from dorsomedial to ventrolateral. In ventral view, it has anteroventrally contact with the basisphenoid in a deep groove and anterolaterally it has contact with the quadrates.

Exoccipital (eoc) and opisthotic (op) (Fig. 3.5)

In posterior view, the exoccipital is completely fused with the opisthotic. The exoccipital-opisthotic complexes meet each other in a short vertical suture dorsal to the foramen magnum and exclude the supraoccipital from the foramen magnum. The exoccipital-opisthotic forms the dorsal margin and the lateral wall of the foramen magnum, and at its ventromedial edge, it meets with the basioccipital. There it forms the lateral part of the occipital condyle, and ventrally, it unites with the lateral side of the ventrolateral process of the basioccipital, forming the lateral part of the basal tubercle. Anterolateral to this border the exoccipital-opisthotic turns sharply outwards, passing into the lower edge of the paroccipital wing. Dorsolaterally, the exoccipital-opisthotic complex has broad contact to the squamosal and dorsomedially it meets the supraoccipital. Ventrolaterally, it meets the quadrate and ventromedially the basioccipital. Most openings for the cranial nerves are situated in the exoccipital-opisthotic complex (Fig. 3.5). The openings for the cranial nerves IX-XII are identified based on comparison with the position of these openings in extant and fossil crocodilians (e.g. EDINGER 1938, IORDANSKY 1964, BROCHU et al. 2002)

Supraoccipital (soc, Fig. 3.5)

In posterior view, the unpaired supraoccipital is a trapezoid bone, which lies ventrally to the parietal. The dorsal margin of the supraoccipital, which contacts the parietal, is concave. Ventrally, it broadly contacts the paired exoccipitals in a slightly convex ventral margin, which. The exoccipitals exclude the supraoccipital from the foramen magnum. The dorsolateral edge of the supraoccipital has contact with the squamosal. In some cases, the

dorsolateral margin of the supraoccipital forms the ventral margin of a small posttemporal fenestra (see there).

Prootic (pro, Fig. 3.3, Fig. 3.2)

It is very difficult to identify an isolated prootic in the skull of *Steneosaurus bollensis* because of the flattened preservation of the skulls and the tendency of a fusion of the bones of the braincase during ontogeny (WESTPHAL 1962, IORDANSKY 1973). In posterolateral view, the prootic is a rectangular bone integrated in the lateral wall of the braincase. Dorsally it is bordered by the parietal and ventrally by the quadrate. Anteriorly it is bordered by the laterosphenoid and posteriorly by the exoccipital-opisthotic and the squamosal. In the disarticulated skull of specimen SMNS 53422 the prootic is exposed in dorsal view, being situated in the lateral wall of the braincase and the posterior wall of the supratemporal fenestra (Fig. 3.3), but the sutures are poorly pronounced and their exact course remain uncertain.

Basisphenoid (including parasphenoid) (bsp, Fig. 3.1b)

The basisphenoid is ventrally preserved for example in the specimens SMNS 15951b, SMNS 15816.

The basisphenoid is an unpaired bone and appears triangular in ventral view. It lies posterior to the pterygoids and continues with a very slender process in the posterodorsal part of the secondary choana, forming the wall of the median Eustachian canal. No single parasphenoid is identified; it appears to be fused with the basisphenoid. The basisphenoid is bordered anteriorly by the pterygoids, laterally by the quadrates, posteriorly by the basioccipital, and dorsally also by the quadrates (Fig. 3.1). Because of the compressed preservation, of all available *Steneosaurus bollensis* specimens, a contact of the basisphenoid to the laterosphenoid is not visible. The same holds true for the participation of the basisphenoid in the floor of the foramen magnum.

Laterosphenoid (lsp, Fig. 3.3, Fig. 3.2)

In lateral view, the laterosphenoid is a rectangular bone, which forms about 70% of the lateral wall of the braincase. It encloses large parts of the brain cavity and lies almost vertically in the skull. Because of the elongation of the posterior part of the skull, the laterosphenoid also is enlarged. Anterodorsally, the laterosphenoid contacts the frontal and posterodorsally, the parietal. The posterior contact to the prootic is only weakly pronounced and the ventral contact to the pterygoid and quadrate is rarely visible (e.g. SMNS 53422, Fig.

3.3). A possible contact to the basisphenoid is not exposed. On the external surface of the laterosphenoid, a weak ridge is visible, which runs medially horizontally over the complete length of the laterosphenoid and dividing it in a dorsal and a ventral half.

Stapes

A stapes is not visible in any of the investigated specimens. The cranioquadrate canal (cr-q canal), which leads to the middle ear cavity, is clearly visible at the lateral side of the skull, but a stapes is not exposed. Dorsally the cranioquadrate canal is enclosed by the squamosal, ventrally by the quadrate, medially by the exoccipital-opisthotic complex, and laterally by the quadratojugal (paragraph "squamosal" and Fig. 3.5).

Posttemporal fenestra (PTF, Fig. 3.5)

In some specimens (e.g. GPIM 23a, SMNS 15951b), a small posttemporal fenestra (PTF) is exposed. In posterior view, it is bordered ventrally by the supraoccipital, laterally by the squamosal and dorsally by the parietal (Fig. 3.5). In some case, the compressed posttemporal fenestra is visible, through the aperture of the supratemporal fenestra, in anterior view, too. There it is present as a transverse slit-like depression between the parietal and very probably the squamosal or possibly the anterior face of the exoccipital-opisthotic complex. A ventral contact to the quadrate is not visible.

Mandible (lower jaw, Fig. 3.1c-d, Fig. 3.2, Fig. 3.6)

Some specimens (e.g. GPIM 23a, SMNS 51957, SMNS 5175, SMNS 56370, and SMNS 80235) show a lateral embedding of parts of the mandible ramus (Fig. 3.1., 3.2 and 3.5). There the shape and borders of the external mandibular fenestra is visible (see there) and the presence of an internal mandibular fenestra is assured. The specimens SMNS 15816, SMNS 20286, and GPIM 23a present a ventral view of the lower jaw and the specimens SMNS 20283, SMNS 56370, SMNS 53422, and SMNS 80235 expose a dorsal to lateral view on the symphysis of the lower jaw (Fig. 3.1, 3.2, 3.3). The shape of the retroarticular process in dorsal view is visible in the specimens SMNS 15951, GPIT Re 1193 7/B, GPIT Re 1193/10, GPIT Re 1193/12, NHMUS 4, and UH 6.

The anterior two-thirds of the mandibular ramus of *Steneosaurus bollensis* is formed by the dentary. The dentary contact each other in their anterior two-thirds in a long symphysis. The symphysis angel is between 40 and 55 degrees in *Steneosaurus bollensis*. The posterior third of the mandibular ramus is formed by the splenial, the angular, surangular, articular and

probably a coronoid. The posterior third of the ramus possesses a prominent external mandibular fenestra and an elongated retroarticular process. The borders of the internal mandibular fenestra are not exposed because of the exclusive exposure of the external side of the mandibular rami. The same is true for the coronoids.

External mandibular fenestra (EMF, Fig. 3.1d, Fig. 3.2, Fig. 3.6)

An external mandibular fenestra is clearly visible in specimen GPIM 23a (Fig. 3.6), SMNS 80235 (Fig. 3.2), SMNS 51957, and SMNS 56370.

The external mandibular fenestra is bordered dorsally by the surangular, ventrally by the angular and anterior by the dentary. It is ellipsoid, longer than high, and at least two-thirds the length of the infratemporal fenestra.

Dentary (d, Fig. 3.1c-d, Fig. 3.2, Fig. 3.3, Fig. 3.6)

Specimens SMNS 53422, SMNS 80235, SMNS 59736, and SMNS 56370 show parts of the dentary in dorsal view (Fig. 3.2, Fig. 3.3).

In *Steneosaurus bollensis*, the dentaries are elongated slender elements, which are extensively fused to a prominent symphysis (Fig. 3.1c, Fig. 3.2). The paired dentaries are fused in their anterior two-thirds. The length of the symphysis, as compared to the length of the entire mandible ramus, is about 66% (see chapter 4). At the tip of the snout, the anterior 10% of the dentaries enlarge into a spoon-shape structure, similar to the structure formed by the premaxillae in the upper jaw. Posteromedially, the dentary contacts the splenial in an oblique suture, which runs from anteromedial to posterolateral. Posterolaterally, the dentary forms the anterior margin of the external mandibular fenestra and contacts the surangular dorsally and the angular ventrally. Until the level of the end of the symphysis (from anterior), the dentary is relatively flat and usually twice as wide as high. Posterior to the symphysis the dentary increases height and at the level of the external mandibular fenestra, the dentary is at least twice as high as wide. The dentary is the only tooth-bearing bone in the lower jaw. The number of alveoli varies from 24 to 35 (see also paragraph “dentition”). The round alveoli open dorsally. The medial margin of the dentary is slightly higher than the lateral part, where the alveoli lie. Due to this fact, the alveoli lie in a shallow lateral groove at the lateral margin parallel to the median interdentary suture. The external surface of the dentary is usually smooth and does not possess any ornamentation. The external ventral surface of the dentary is in some cases (e.g. GPIM 23a) slightly wrinkled by delicate, low ridges and grooves, while the external lateral and dorsal surface is smooth (Fig. 3.1, 3.2., 3.6).

Splenial (sp, Fig. 3.1c, Fig. 3.3)

In SMNS 15816, SMNS 20286, and GPIM 23a the splenial is ventrally exposed in the lower jaw. SMNS 56370 and SMNS 80235 expose the dorsolateral part of the symphysis of the lower jaw and the splenials are partly visible in lateral view (Fig. 3.2, Fig. 3.3). In ventral view, the splenial is a slender bone located in the ventromedial side of the mandible. Medially it contacts its contralateral in its anterior half. Anteriorly, posteriorly, and laterally it is bordered by the dentary. Anteriorly, the paired splenial tapers between the dentaries, separates them from each other, and forms circa the posterior 15 % of the symphysis. No ornamentation is visible at the dorsal surface of the splenial, but the external ventral surface is slightly wrinkled identical to the ventral surface of the dentary (e.g. GPIM 23a).

Surangular (san, Fig. 3.1c-d, Fig. 3.2, Fig. 3.3, Fig. 3.6)

The surangular is only exposed in dorsolateral view. It is an elongated bone that contacts the angular, the articular, and the dentary. A possible contact with a coronoid is not visible, because the internal side of the surangular is not exposed. Together with the articular and the angular, it forms the retroarticular process (see chapter 8 for further discussion).

Anteriorly, it is bordered by the dentary, posterodorsally by the articular, and posteroventrally by the angular. In lateral view, the surangular separates the angular completely from the articular. The surangular-articular suture runs horizontally and is straight and smooth. Posteroventrally, the surangular meets the angular in a long straight suture posterior to the external mandibular fenestra (see there). Anterodorsally, the surangular forms the dorsal margin of the external mandibular fenestra. In lateral view, the dentary-surangular suture is oblique and runs from anterodorsal to posteroventral. The surangular probably overlaps the dentary anterior to the external mandibular fenestra (Fig. 3.6). The external surface of the surangular is smooth, except of an anterior, shallow groove, which runs parallel to the external mandibular fenestra (Fig. 3.6). The groove probably indicates jaw muscle or tendon insertion marks.

Angular (an, Fig. 3.1c-d, Fig. 3.2, Fig. 3.3, Fig. 3.6)

The angular is exposed in lateral view. It is an elongated bone, which is slightly flexed posterodorsally. Therefore, the external ventral margin of the angular is slightly convex. Anteriorly, the angular contacts the dentary and posterodorsally, posterior to the external mandibular fenestra; it has a broad contact to the surangular. Anteromedially, the angular forms the ventral margin of the external mandibular fenestra. The angular-surangular suture is

straight, smooth, and slightly curving posterodorsally. In lateral view, the angular is separates from the articular by the surangular. Anteriorly, the angular thins out and contacts the dentary anterior to the external mandibular fenestra. The course of the angulodentary suture remains uncertain, because of insufficient preservation. In addition, the anterolateral surface of the angular is covered with a slight ornamentation of small, oval pits (Fig. 3.6). The pits are lying in irregular distribution ventral and anterior to the external mandibular fenestra and decline posteriorly. Therefore, it is impossible to identify the exact course of the angulodentary suture. A possible, internal anterior contact with the splenial is likely, but not visible.

Articular (ar, Fig. 3.1c-d, Fig. 3.2, Fig. 3.3, Fig. 3.6)

The articular is exposed in dorsal and lateral view. Anteriorly and ventrally, the articular is bordered by the surangular. In dorsal view, the articular is slightly rhombic and its dorsal surface is slightly concave, with a solid medial transversal crest, which divides the articular into two parts (Fig. 3.1c). The posterior two-thirds form the dorsal part of the retroarticular process and the anterior third forms the two mandibular articular facets for the quadrate condyles. In lateral view, the articular is a flat bone, which curves slightly posterodorsally in its posterior two-thirds (Fig. 3.1d). It is ventrally bordered by the surangular and has no contact to the angular.

Dentition

Tooth morphology

The dentition is weakly heterodont, because the size of the teeth is slightly variable. The teeth are slender, conical, pointed, and apically recurved. The tooth crown shows a fine vertical striation on their entire surface. In addition, it possesses one or two slightly developed faint carinae, one at the anterior and one at the posterior side (for further discussion of the tooth morphology, see chapter 8.1.3, Fig. 8.7).

Pattern of dentition (Fig. 3.2, Fig. 3.3)

In the upper jaw, the premaxilla and the maxilla are tooth bearing, while in the lower jaw it is the dentary. The number of alveoli in *Steneosaurus bollensis* varies from three to four in the premaxilla, 26 to about 35 in the maxilla, and 24 to 35 in the dentary. The dentition code is: $\frac{3-4+26-35}{24-35}$. Thus, the minimum alveoli count is 106 and the maximum count is 148 in the entire rostrum (see also chapter 4). In the dentary and the maxilla only every

second alveoli is occupied with a fully erupted tooth allowing the identification of different stages of tooth replacement. The maxilla bears the teeth until level with the anterior margin of the orbit.

A fully erupted tooth is, in an adult specimen, about 20 mm high, but fully erupted teeth only occupy every second alveolus. The alternated alveoli are either empty or in some cases occupied by a very small replacement tooth (Fig. 3.2, Fig. 3.3). In the premaxilla, usually the third tooth, counted from above, is larger than the other teeth and can reach almost double the size of them (see paragraph "premaxilla"). The first, second and in some cases the fourth tooth are usually very similar in shape to the teeth in the maxilla. Even though there is intraspecific variation in the specific development of the third premaxilla tooth, it is always the largest tooth in the upper jaw. In the dentary, the fully erupted teeth are identical to the fully erupted teeth in the maxilla. Only the third or fourth dentary tooth is enlarged like that of the premaxilla, which is in most cases indicated by an enlarged third or fourth alveolus almost double the size as the other alveoli. All alveoli are circular and open ventrally in the upper jaw and dorsally in the lower jaw. An exception is the anterior-three alveoli of the dentary, which are slightly laterally, in case of the first alveolus anteriorly orientated. The teeth are all vertically orientated. The lower and upper teeth occlude along the same line, and the teeth interfinger.

Postcranial elements

The axial skeleton

Armour (Fig. 3.7, Fig. 3.8)

The dermal armour in *Steneosaurus bollensis* consists of a dorsal and ventral osteodermal shield. The dorsal osteodermal shield forms one longitudinal row of 40-45 paired osteoderms and covers parts of the neck, the trunk, and the tail (see also BERCKHEMER 1929). The ventral osteodermal shield consists of about 100 osteoderms arranged in six longitudinal rows and it covers ventrally the thorax. In addition, ventral armour of the tail is present, which consists of about 20 paired osteoderms arranged in a longitudinal row.

The osteoderm count and the proportions of the single osteoderm considering its position in the osteodermal shield vary only slightly. In contrast, the osteodermal ornamentation varies broadly individually (see also chapter 4). In most cases, a longitudinal keel on the dorsal surface is developed level with or posterior to the lumbar vertebrae.

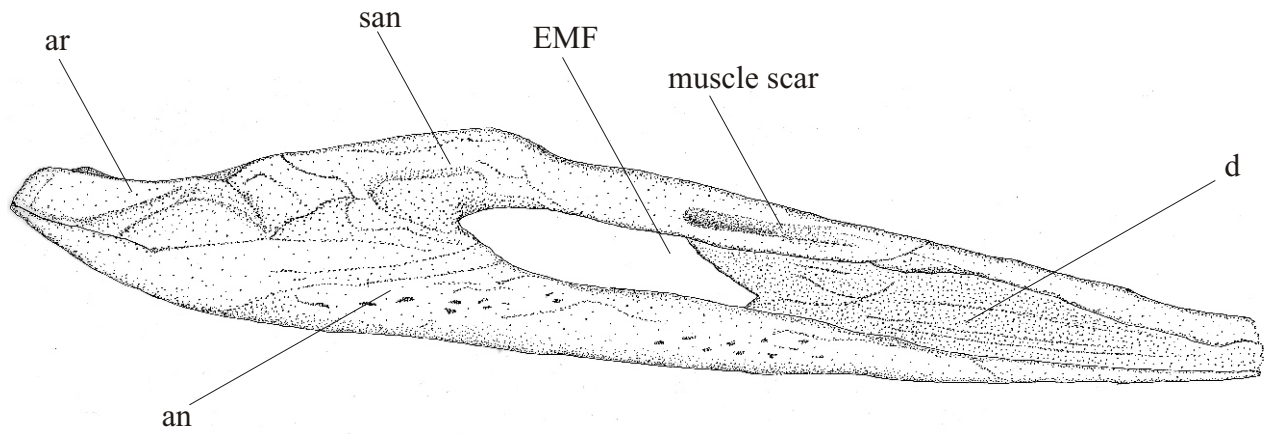

Figure 3.6: *In situ* drawing of the posterolateral part of the right mandibular ramus in lateral view of GPIM 23a. Original length of the fragment is 273 mm. Abbreviations: an-angular, ar-articular, EMF-external mandibular fenestra, d-dentary, san-surangular.

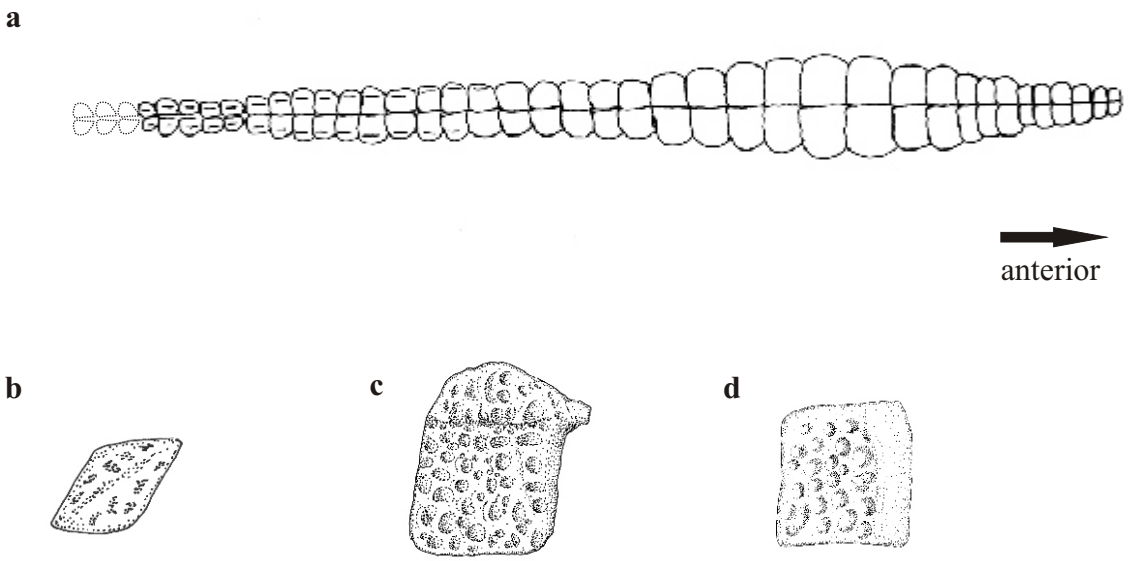

Figure 3.7a-d: Armour of *Steneosaurus bollensis.* **3.7a**-Reconstruction of the dorsal osteodermal shield. Ornamentation is not considered. **3.7b**-Caudal ventral osteoderm of NHMUS 4 (original length 30 mm). **3.7c**-Dorsal sacralosteoderm of SMNS 59736 (original width 40 mm). **3.7d**-Ventral thoracic odsteoderm of UH 5 (original length 30 mm).

Dorsal armour (Fig. 3.7, Fig. 3.8)

The dorsal osteodermal shield of *Steneosaurus bollensis* runs from the level of the anterior third or fourth cervical vertebra up to the 23rd caudal vertebra and consists of a longitudinal row of paired osteoderms (Fig. 3.7). The dorsal osteodermal shield starts small and slender and increases posteriorly continuously in width until the third or fourth thoracic vertebra, where it is twice as wide as in the cervical area. Posterior to the fourth thoracic vertebra, it slightly decreases in width until it terminates in the middle of the tail, where it is as wide as in the beginning (Fig. 3.7). Medially, the dorsal osteoderms meet each other horizontally in a straight suture. Anteriorly and posteriorly, the dorsal osteoderms overlap each other in a brick-like pattern. The posterior margin of each osteoderm overlaps the anterior margin of the adjacent posterior osteoderm.

The dorsal thoracic osteoderms are about 1.5 times wider than long, while the dorsal cervical, lumbar, and sacral osteoderms are almost square. The medial margin of the dorsal osteoderms is straight, whereas the lateral margin is externally convex. At the anterior margin of the osteoderms, a smooth, unsculptured area is recognized where the osteoderms overlap each other. This area develops a distinct peg (process) at the anterolateral margin. This peg is very characteristic for the Liassic taxon *Steneosaurus bollensis*, no other Liassic teleosaurid possesses this feature so distinctively (see also chapter 4). Equally distributed, large, round pits are present on the dorsal surface the osteoderms, but pit count and size may vary individually (see chapter 4). The dorsal osteoderms possess a slight keel on the dorsal surface, starting at the level of the sacral vertebrae, but in some cases start individually earlier (see chapter 4). The keel runs in anteroposterior direction and divides the external face of the osteoderms into two unequal sections: The lateral section is one-fourth of the osteoderm and semicircular, because of the convex lateral margin. The medial section consists of the remaining three-fourth of the osteoderm and is square.

Ventral armour (Fig. 3.7, Fig. 3.8)

The ventral thoracic armour reaches from the sixth thoracic vertebra up to the fifteenth thoracic vertebra. It consists of six longitudinal rows, with a maximum number of 19 osteoderms. The ventral armour of the tail consists of one longitudinal row of paired osteoderms, which starts at the anterior second or third caudal vertebra and which ends at the level of the 10th to 16th caudal vertebra. In specimen SMNS 849, there are six longitudinal rows with up to 19 osteoderms preserved. In specimen NHMUS 4, nearly the complete ventral armour is preserved (Fig. 3.16). In this specimen, the complete number of ventral

osteoderms is 110 (Fig. 3.16). The number of osteoderms in the longitudinal rows increases the middle rows. The lateral longitudinal rows (1, 2, 5, and 6) have 18 osteoderms each, while the medial longitudinal rows have 19 osteoderms each. Specimen GPIT Re 1193/10 possesses six longitudinal rows with up to 18 osteoderms, which fits well with the observation by BERCKHEMER (1929).

In some specimens, the ventral armour of the tail is preserved (Fig. 3.7). For example, specimen TMH 13287 is armoured with a double row of small rhombic osteoderms up to the level of Figure the 10th caudal vertebra, with a break in the area around the pelvic girdle. The same is true for NHMUS 4, except that the tail is covered by a double row of rhombic osteoderms ventrally up to the 16th caudal vertebrae (Fig. 3.8).

The thoracic ventral osteoderms are usually only half the size of the dorsal osteoderms. The ventral osteoderms are rectangular and only the two lateral rows of osteodermal shield possess osteoderms with a lateral externally convex margin. All other ventral osteoderms possess straight margins. In contrast to the dorsal osteoderms, the ventral osteoderms do not show any trace of a keel or a peg and overlap each other only slightly. Most of the ventral osteoderms, mainly those in the posterior part of the ventral thoracic armour, contact each other in interdigitating sutures. The ventral armour of the tail consists of a double row of small rhombic osteoderms, with a pronounced median keel in longitudinal direction. The pattern of the pits of the thoracic ventral osteoderms is similar to that of the dorsal osteoderms and consist of round to ellipsoid pits evenly distributed (Fig. 3.7). The caudal ventral osteoderms possess only a few small, elliptic pits at each side of the keel (Fig. 3.7).

Vertebral column (Fig. 3.8, Fig. 3.9)

The vertebral column consists of about 76 amphicoelous vertebrae. There are nine cervical vertebrae, including the atlas-axis complex, 12 to 15 thoracic vertebrae, two to three lumbar vertebrae, two sacral vertebrae, and up to 55 caudal vertebrae. The number of cervical vertebrae is constant. The number of thoracic vertebrae varies slightly, as well as the number of lumbar vertebrae. The number of sacral vertebrae is constant, while the number of caudal vertebrae is highly variable (see chapter 4 for further discussion).

Generally, it is difficult to distinguish the posterior-most cervical vertebrae from the first thoracic vertebrae. In the present study, the definition of the cervical and thoracic vertebrae is based on the articular facets of the ribs at the vertebra and the shape of the ribs themselves (MOOK 1921a, WETTSTEIN 1937, MATEER 1974). The cervical vertebrae possess diapophysial and parapophysial process for the attachment of the double-headed cervical ribs

a

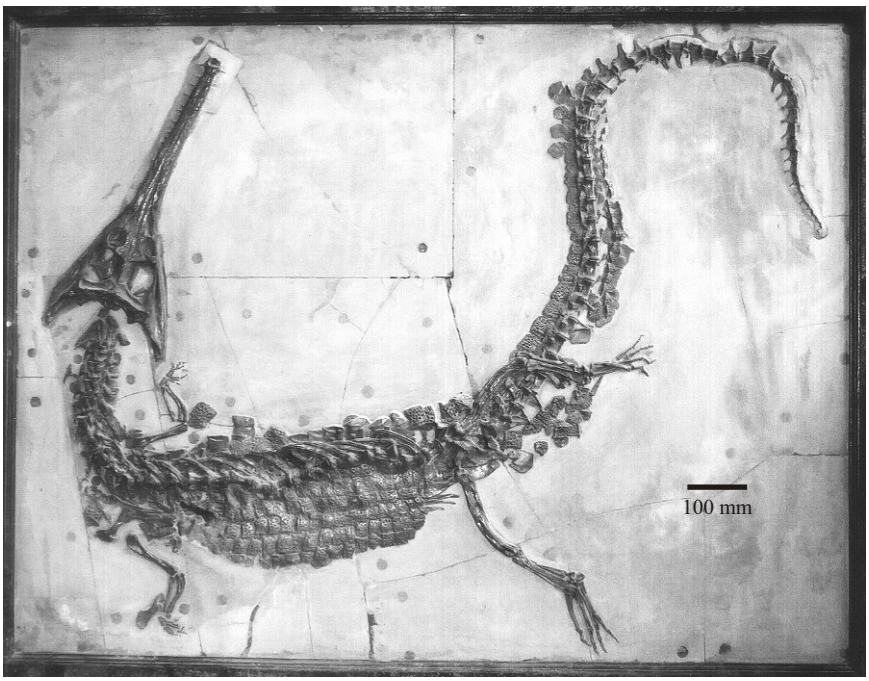

b

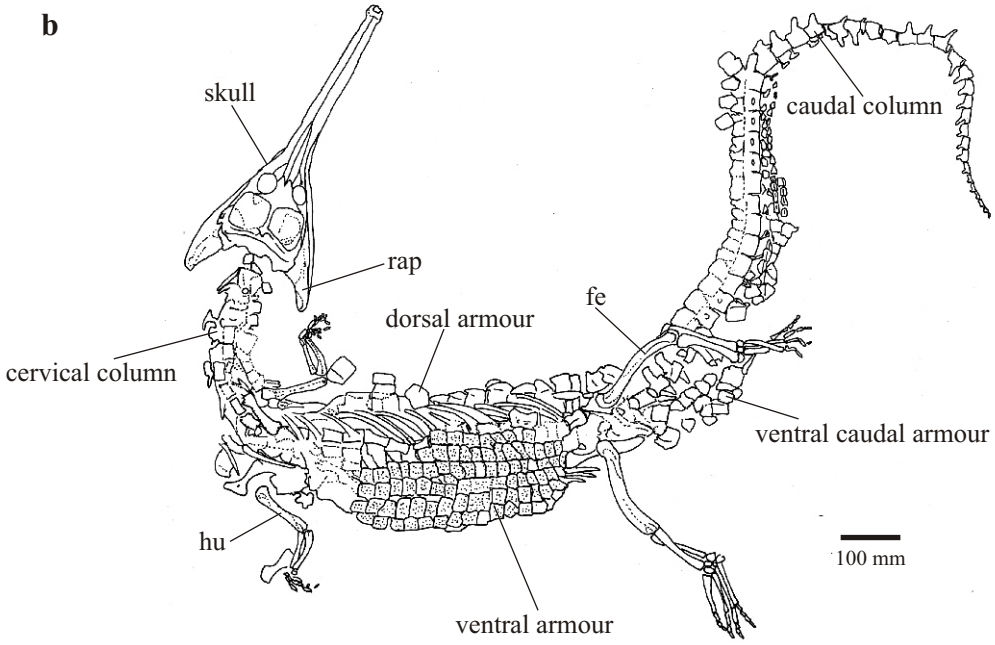

Figure 3.8 a-b: Pictures of *Steneosaurus bollensis* (NHMUS 4) **3.8a**-Photo of the original specimen in the collection of the NHMUS. Skull in dorsal view, the trunk is ventrally exposed. Total length about 2.7 m. **3.8b**- Overview sketch of the same specimen. Ventral osteodermal shield almost completely exposed with caudal ventral armour.

on the centrum, except of the ninth vertebra, which only possess the parapophysis at the centrum. In the posterior following thoracic vertebrae, both, the diapophysial and parapophysial process emerge from the lateral wall of the neural arch and form a transverse process.

Cervical vertebrae (Fig. 3.9a-d, Fig. 3.10)

The first two cervical vertebrae are always developed as an atlas-axis complex (Fig. 3.9a). Specimen SMNS 9428 consists of the anterior eight cervical vertebrae and in specimen GPIT Re 1193/3 a well-preserved atlas-axis complex is visible (Fig. 3.10a). The atlas is divided into four parts in *Steneosaurus bollensis*: The intercentrum, the paired neural arch, a possible proatlas, and the dens (=odontoid process) (WESTPHAL 1962). The hypocentrum is the anteroventral part of the atlas and contacts the occipital condyle of the skull. The two lateral parts of the atlas form the neural arch and a possible proatlas overlying dorsally the neural arch is visible (WESTPHAL 1962 and Fig. 3.9a-b, Fig. 3.10a). The odontoid process of the axis was originally the central part of the atlas (pleurocentrum), even though now fused with the axis (MOOK 1921a). The shape of the axis is similar to the shape of the following cervical vertebrae, except from the anteriorly attached dens and the reduced height of the neural spine. The connection for the anterior first cervical rib is on the ventrolateral margin of the dens, while the parapophysial process for the second cervical rib emerges laterally from the center of the axis centrum. The cervical vertebrae three to eight show diapophysis and parapophysis at the centrum, whereas the ninth cervical vertebra only shows the parapophysis on the centrum. Its diapophysis protrudes from the neural arch. The neural spine of the cervical vertebrae is as high as the vertebra centrum itself. Prezygapophyses and postzygapophyses are at the same height at the axis but the position of the postzygapophyses increase in height in the posterior cervical vertebrae and lying posterodorsally to the prezygapophyses (Fig. 3.9c, d).

Thoracic and lumbar vertebrae (Fig. 3.9e-h)

Posterior to the cervical vertebrae, there are 12 to 15 thoracic vertebrae bearing with elongated double-headed thoracic ribs (see paragraph “ribs”). The exact shape of a specific thoracic vertebra is mostly obscured by overlying osteoderms and three-dimensional preservation is unknown. In specimen NHMUS 4, some thoracic vertebras are partly exposed in lateral view. In SMNS 849, the ventral aspect of some thoracic vertebrae is shown.

In posterior and anterior view, the centra show round, deeply retracted articular areas. In ventral view, the vertebra centra are cylindrical with a shallow concave recess at their lateral margins. From the 12th-14th vertebrae (counted from anterior) diapophysis and parapophysis are fused to a synapophysis forming a transverse process, which protrudes horizontally from the ventrolateral wall of the neural arch (Fig. 3.9). In lateral view, the ventral margin of the central is externally concave. The prezygapophyses and the postzygapophyses lie at the antero- and posterodorsal margin of the neural arch at the same height.

In dorsal view, specimen GPIT Re 1193/6 shows isolated centra and separated neural arches, which bear a transverse process (Fig. 4.7). The fact that the thoracic vertebrae are decayed in two parts at their neurocentral suture is interpreted as a juvenile feature (BROCHU 1996, see also chapter 4).

Two to three lumbar vertebrae are present. The dorsal armour covers the lumbar vertebrae in most investigated specimens. However, in SMNS 56370 the posterior-most lumbar vertebra is exposed in posterior view (Fig. 3.9). The centrum is transverse ellipsoid in cross-section, and not circular or ventrodorsal ellipsoid like in thoracic vertebrae (WESTPHAL 1962, Fig. 3.9h). In addition, the anterior outline of the centrum shows instead a shallow concave recess at its dorsal margin forming the floor of the neural canal. The neural spine is as high as the vertebra centrum. The dorsal margin of the neural spine is slightly broader and blunt compared to that of the thoracic vertebrae, which show a pointed neural spine in anterior view (Fig. 3.9f and 3.9h).

Sacral vertebrae (Fig. 3.9i-j)

Two sacral vertebrae follow the lumbar vertebrae. The three-dimensional shape of the vertebrae is uncertain, because the vertebrae are often compressed and partly obscured by matrix in the specimens. The holotype SNSD 1 shows a well-preserved sacral vertebra in posterior view (Fig. 3.9i-j). In specimen BMNH R 3936 both sacral vertebra are exposed in ventral view. The sacroiliac joint is visible. The sacral vertebrae are connected to the ilia by prominent sacral ribs (see there). The shape of the centra of the sacral vertebra resembles that of the posterior-most lumbar vertebra. No transverse process is visible at the sacral vertebrae. The sacral ribs connect firmly with the entire lateral surface of the vertebra centra. The height of the neural spine is uncertain, because of insufficient preservation. However, it is estimated at least as high as the vertebra centrum.

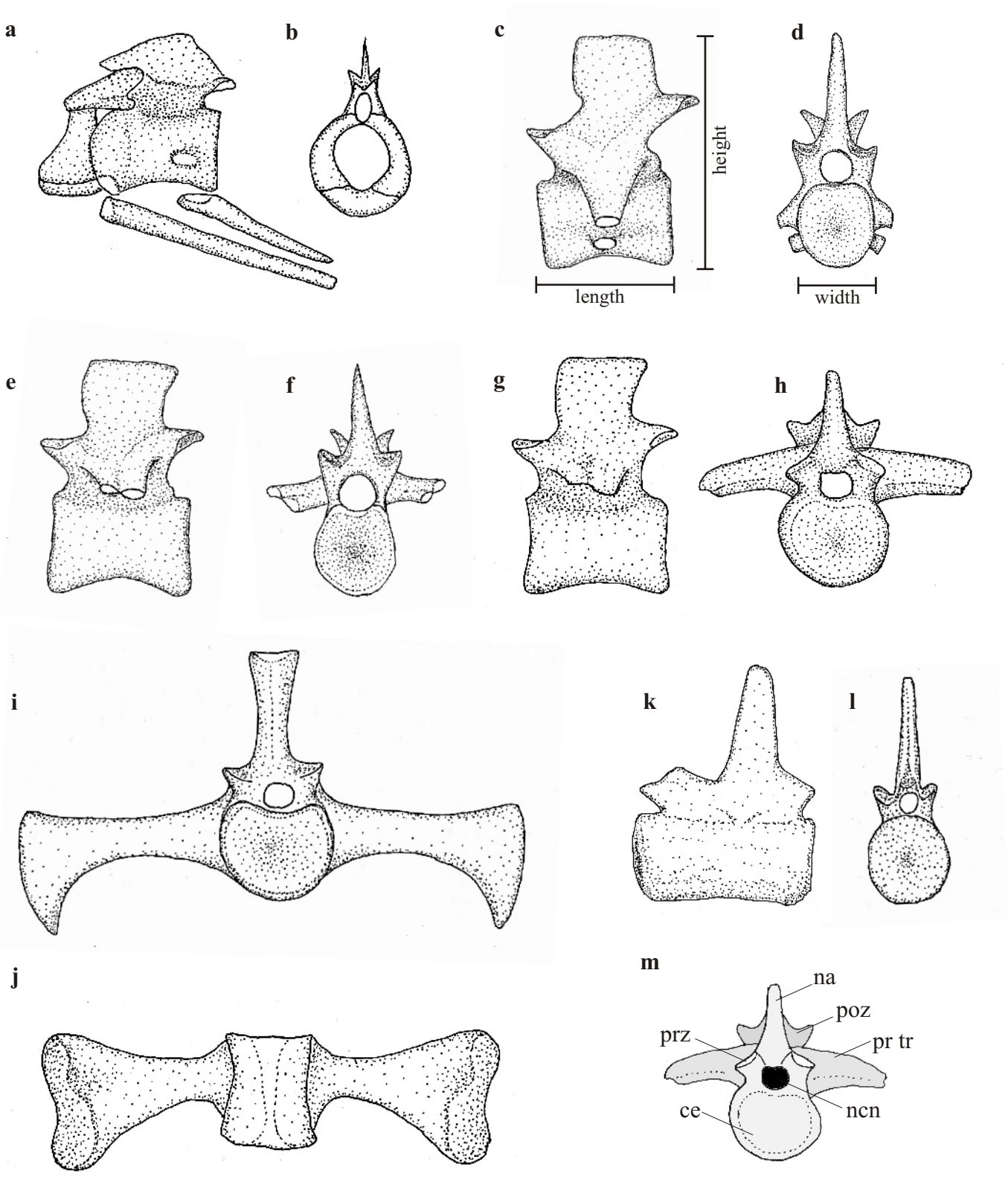

Figure 3.9a-m: Reconstructions of vertebrae of *Steneosaurus bollensis.*
3.9a-Shows the atlas-axis complex including the first and second cervical rib in lateral view. (Vertebrae are reconstructed after the specimens GPIT Re 1193/3 & SMNS 9428). **3.9b-S**hows the atlas-axis complex in anterior view. **3.9c-**Shows the lateral view of the fifth cervical vertebra. **3.9d-S**hows the anterior view of the fifth cervical vertebra. **3.9e-**Shows the lateral view of a thoracic vertebra. **3.9f-S**hows the anterior view of a thoracic vertebra. **3.10g-**Shows the lateral view of a lumbar vertebra. **3.9h-**Shows the posterior view of a lumbar vertebra (reconstructed after the specimen SMNS 56370). **3.9i-**Shows the first sacral vertebra with attached first sacral rib (mainly reconstructed after SNSD 1 (holotype)). **3.9j-**Shows the ventral view of the first sacral vertebra (with sacral rib). **3.9k-**Shows the lateral view of a posterior caudal vertebra (reconstructed after SMNS without number and NHMUS 4) and **3.9l-**Shows the anterior view of the same vertebra. **3.10m-**Sketch of a lumbar vertebra with the terms of the particular areas of the vertebra. All vertebrae scaled to the same size. Abbreviations see chapter 2.

Caudal vertebrae (Fig. 3.9k-l)

Caudal vertebrae are exposed in e.g., the adult specimens GPIT Re 1193-2, NHMUS 4, SMNS 51555, SMNS 51563, SMNS 18872, TMH 2741, and UH 5. The number of caudal vertebrae varies from about 45 to 55. The caudal vertebrae of *Steneosaurus bollensis* resemble those of other teleosaurids (see e.g. ANDREWS 1913). They possess an elongated, slender centrum, about three times longer than broad. In anterior view, the centrum is circular and in lateral view, it shows a straight ventral margin. In lateral view, in the anterior two-thirds of the caudal column, the neural spine is as high as the centrum is long and the neural spine is nearly as long as the centrum. The neural spines decrease rapidly in height and particularly in length posterior to the 20th caudal vertebra in the posterior third of the tail. The anterior ten caudal vertebrae possess transverse processes, which decrease posteriorly in size. Posterior to the 10th caudal vertebrae no transverse processes are visible. The pre- and postzygapophyses are smaller compared to those of the thoracic vertebrae.

The anterior 20 to 25 caudal vertebrae possess chevrons (haemal arches). All chevrons are somewhat "V"-shaped in anterior view, even though their size is decreasing posteriorly. Dorsally each proximal process of the chevron articulates with a small elliptic articular facet at the posteroventral edge of the caudal vertebra centrum. In lateral view, the ventral body of the chevron is mediolaterally compressed and anteroposterior slightly elongated.

The shape of the caudal vertebrae and the chevrons is very similar to those of *S. leedsi* and *S. durobrevensis* (see ANDREWS 1913, text-fig. 38 and text-fig. 40).

Ribs (Fig. 3.9a-b, Fig. 3.10)

The first cervical rib is a long, slender, and straight bar of bone with an acuminate distal end that attaches to the dens. The bone bar widens anteriorly slightly and bears a medial flat facet for union with the anteroventral facet at the dens. The rib extends posteriorly until the anterior half of the third cervical vertebra. The shape of the second cervical rib is similar, but it is only 65% of the length of the first cervical rib. The second cervical rib contacts the centrum of the axis (see there). Cervical ribs three to eight have distally a lateromedially-flattened body with a short, blunt anterior and a short, pointed posterior process and proximally an elongated diapophysial and parapophysial process to connect with the vertebra. The body of the rib is externally convex and internally concave. The two proximal processes are identical in shape, but the diapophysial process is slightly longer than the parapophysial process. The ninth cervical rib differs from the others cervical ribs. Its body is more elongated

and it thins out in posterior direction. Anteriorly, the body of the rib lacks most of the anterior process (Fig. 3.10c). The ribs are lying parallel to long axis of the vertebral column.

The number of thoracic ribs varies from 12 to 15 depending on the number of thoracic vertebrae. In general, the thoracic ribs possess a slender, elongated, curved body and are all double-headed (Fig, 3.10b-c). The tuberculum (diapophysial process) and the capitulum (parapophysial process) are unequal in size and shape. The tuberculum consist of a small, slightly arched proximal process. The capitulum is twice as long, and lies anteroventrally to the tuberculum. The elongated body of a thoracic rib is strongly curved. The external surface is convex and the internal is slightly concave. The body widens out at its distal end and is strongly anteroposterior compressed (ANDREWS 1913).

Heavy sacral ribs are firmly connected to the centrum of the sacral vertebrae. Externally, the rib expands broadly and terminates as broad as the centrum is long. Externally, it bears a rough articular facet to contact the internal side of the ilium. In case of the first sacral rib, the outline of the articular facet forms an ellipse with slight notches in its ventral and dorsal margin (Fig. 3.9j). The second sacral rib is not exposed in any investigated specimen of *S. bollensis* and therefore cannot be described.

Gastralia (g, Fig. 3.11 & Fig. 8.8)

WESTPHAL (1962) mentioned the presence of gastralia in some specimens of *Steneosaurus bollensis*. The particular specimen he referred to could not be investigated. However, in a couple of the examined specimens (e.g. GPIT Re 1193/1, SMNS 51555, SMNS 51563, SMNS 51753, and UH 5), slender bones interpreted as gastralia, are exposed. The thin bone bars are circa half as wide and long as the thoracic ribs. They are only slightly curved, and lie at the internal surface of the ventral osteodermal shield level with the lumbar vertebrae.

In addition, in the specimen UH 5, some triangular bony structures are exposed lying lateral to the ventral armour (Fig. 3.11). Compared to the conditions in *Crocodylus* (ROMER 1956), those structures are interpreted as the connected medial parts of the gastralia (Fig. 3.11).

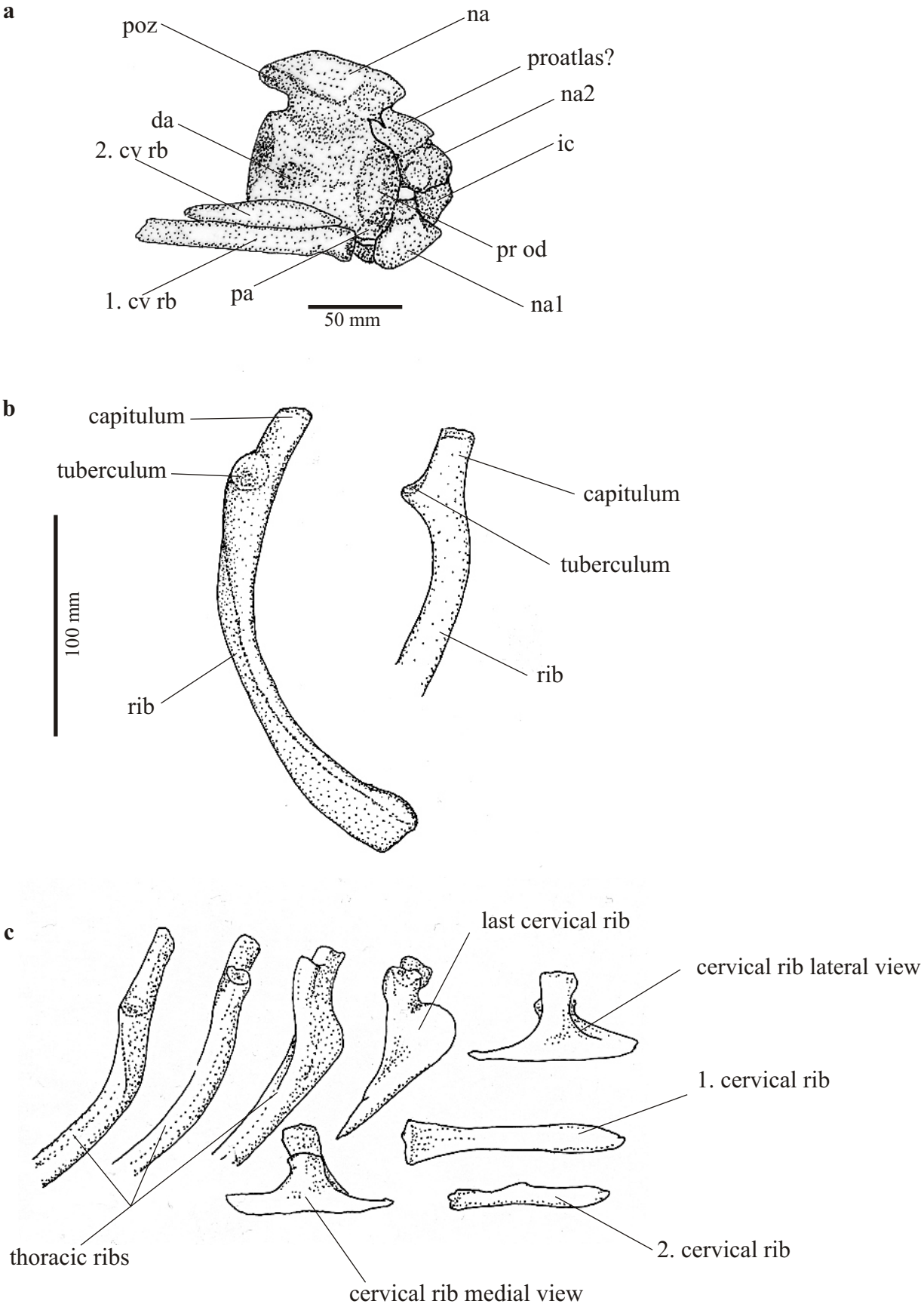

Figure 3.10 a-c: **3.10a**-*In situ* drawing of the atlas-axis complex with cervical ribs of *Steneosaurus bollensis* (GPIT Re 1193/3). **3.10.b-** *In situ* drawing of thoracic ribs in lateral and medial view of *S. bollensis* (NHMUS 4). **3.10c**-Different rib shapes in *Steneosaurus durobrivensis* (after ANDREWS 1913).

The appendicular skeleton

Pectoral girdle (Fig. 3.12, Fig. 3.13)

As it is typical for teleosaurids, the pectoral girdle consists of, a paired scapula, a paired coracoid, and an unpaired interclavicle, but lacks the clavicles and a sternum. The scapula and the coracoid are similar in size and general shape. Both are flat bones with a dorsal and ventral expansion emerging from a narrow shaft. Therefore, they appear hourglass-shaped in lateral view. The posteroventral margin of the scapula and the dorsolateral margin of the coracoid form together the glenoid fossa for articulation with the humerus. The interclavicle is a slender bone bar with a slight rhombic broadening at the anterior edge and a slightly pointed posterior end.

Scapula (sc, Fig. 3.12, Fig. 3.13)

The scapula is exposed in external view for example in the specimens SMNS 51753, SMNS 51563 (Fig. 3.12c), SMNS 53422, SMNS 56370, and SMNS 80235 (Fig. 3.12b). The scapula is exposed in internal view in specimens SMNS 51957, SMNS 51960, SMNS 59736, and SMNS 58876.

The scapula is a flat element with large expansions at the ventral and dorsal edges. It is roughly hourglass-shaped in external view. The dorsal expansion is three times as wide as the shaft and possesses an externally convex margin (Fig. 3.12b). The ventral expansion is only twice as wide as the shaft and its ventral margin is straight or slightly concave. In addition, at the anteroventral margin of the scapula, there is a thickened articular area for the joint between coracoid and scapula. A second articular facet lies at the posteroventral margin of the scapula, which forms the dorsal part of the glenoid fossa. The outline of this facet is round and its surface is slightly concave. A deep triangular depression with rugosities is recognized at the external surface of the ventral part of the scapula, which might represent a muscle attachment area for the coracobrachialis brevis dorsalis muscle (MEERS 2003). This muscle is inserting on the deltopectoral crest of the humerus and is stabilizing the humerus head in the glenoid fossa in extant crocodilians (MEERS 2003). The dorsal end of the scapula expands into a large, flat blade of nearly triangular shape with a distinct externally convex margin. The length of the scapula (Sa1) is in average 60% of the length of the humerus (H1) (see appendix II), but varies from 49% to 70%.

Coracoid (co, Fig. 3.12, Fig. 3.13)

Well-preserved coracoids are exposed in the specimens SMNS 849 (Fig. 3.11), SMNS 51753, SMNS 51960, SMNS 52563 (Fig. 3.11), SMNS 59736, and SMNS 80235.

The coracoid resembles in shape the scapula. It is a roughly hourglass-shaped bone, too. It has the same size as the scapula. Like the scapula, it has flatten, externally slightly convex dorsolateral and ventromedial expansions, which extend from a slender shaft. The shaft of the bone has an ellipsoid profile and is slightly flattened ventrodorsally. The flattened dorsolateral bone blade possesses at its posterior margin two arched articular facets. The anterior facet articulates with the anteroventral margin of the scapula and the posterior one forms the ventral part of the glenoid fossa. The anterior articular facet is formed by a slightly thickened, straight part of the margin and the posterior articular facet is a slight tubercle with a flat dorsal surface, which is slightly flexed in posteroventral direction. The coracoid foramen is situated anterior to the glenoid fossa in the center of the dorsolateral blade (Fig. 3.12, Fig. 3.13). The ventromedial blade is very thin in cross section and has a strongly externally convex edge.

Interclavicle (icl, Fig. 3.12, 3.13)

In specimen SMNS 849 (Fig. 3.12, Fig. 3.13), it is exposed in ventral view. The interclavicle is lying medially in proximity to the paired coracoids, probably close to its original position. Parts of the interclavicle are also visible in SMNS 80235.

The interclavicle is an elongated, straight bone, about 1.5 times the length of the coracoid. The anterior 15% -20% of the bone has laterally contact to the coracoids. There, it is flattened, slightly broadened, and rhombic, whereas it posteriorly thins out and possesses a pointed end. The interclavicle is situated ventrally to the vertebral column and it contacts laterally the coracoids, probably in a cartilaginous suture.

Pelvic girdle (Fig. 3.14, Fig. 3.15)

The pelvic girdle consists of the paired ilium, the paired ischium, and the paired pubis. On their internal side, the ilium is connected to the two sacral vertebrae by two prominent sacral ribs (see there). There was probably a cartilaginous connection between the ischia ventromedially, which is indicated in specimen SMNS 56370, where parts of the pelvic girdle are exposed in ventral view (Fig. 3.14). The same is probably true for the pubic bones.

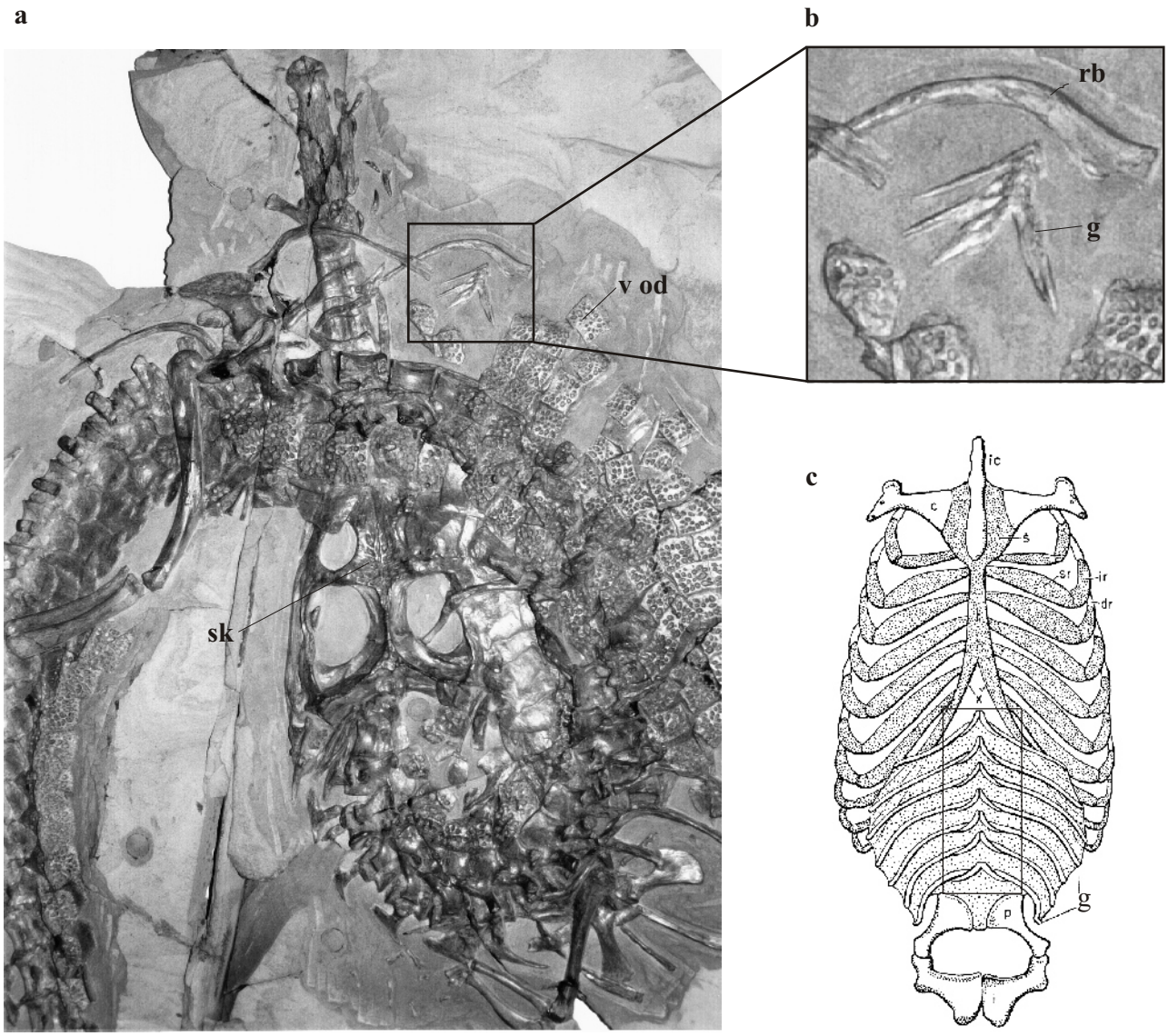

Figure 3.11: 3.11a-Photo of *S. bollensis*, part of the specimen UH 5 with a skull length of 415 mm. The frame in the photo marks the preserved medial parts of the gastralia. **3.11b-**On the right side the gastralia are enlarged (x 2.5) for better comparison with **3.11c**-The sketch of the gastralia of *Crocodylus* after ROMER (1956).The frame marks the triangular medial parts of the gastralia. Abbreviations: g-gastralia, rb-rib, sk-skull,v od-ventral osteoderms.

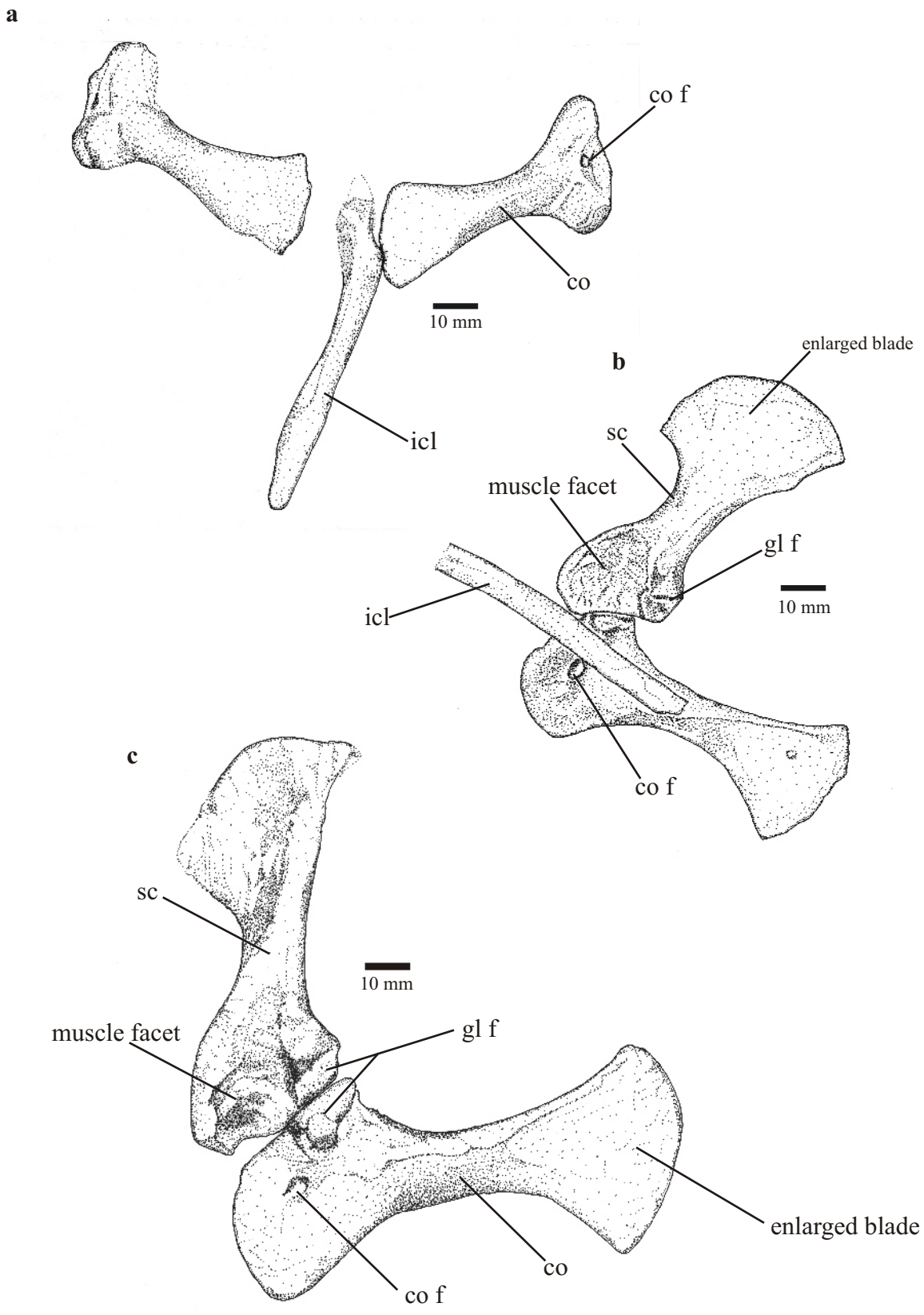

Figure 3.12a-c: Pectoral girdles of *Steneosaurus bollensis.* **3.12a**-*In situ* drawing of SMNS 849 coracoids and interclavicle in ventral view. **3.12b**-*In situ* drawing of left scapula, coracoid, and part of the interclavicle of SMNS 80235. **3.12c-***In situ* drawing of coracoid and scapula of SMNS 51563 in lateral view. Scale bar is 10 mm. Abbreviations: co-coracoid, co f-coracoid foramen, gl f-glenoid fossa, icl-interclavicle, sc-scapula.

Ilium (il, Fig. 3.14, Fig. 3.15)

The ilium is a rectangular bone, flat in mediolateral direction, which contacts ventrally the ischium and pubis. The length of the ilium (P1) is in average 80% of the width of the ilium (P2) (see chapter 2 and appendix II). The ilium possesses at its dorsal margin an anteroposteriorly running iliac crest. The anterior process of the iliac crest is projecting anteriorly to the anterior margin of the ilium, and the process is 15-20% of the iliac width (P2). The posterior process of the iliac crest is shorter or almost absent. The external side of the ilium forms the dorsal 80-90% of the shallow acetabulum, while the internal side is firmly connected to the sacral ribs (see also paragraph "ribs"). At the ventral margin of the ilium are three articular facets (e.g. UH 13, SMNS 51957, and SMNS 56370). The posterior two facets articulate with the ischium, the anterior facet probably with the pubis. The posterior-most articular facet is shallow concave and twice the size of the other posterior facet. It is longitudinal elliptic in outline and slightly divided in two equal portions by a low longitudinal median crest. The second posterior articular facet is round, shallow concave and contacts the anterior process of the ischium (see there). Anteroventrally, the small and slightly convex third facet probably contacts the pubis. Sometimes, this anterior facet is developed as a strongly convex tubercle (pubis peduncle) (UH 13, Fig. 3.15).

At the internal side of the ilium, which is exposed at specimen SMNS 59736 and SMNS 9428a, there are two rugose areas visible, which are the articular facets for the sacral ribs (Fig. 3.12d). The anterior articular facet for the first sacral rib is semi-circular in posterior direction, and the posterior articulations facet for the second sacral rib has an outline, which is shaped like an "8".

Ischium (is, Fig. 3.14, Fig. 3.15)

Well-preserved ischia are exposed in e.g., SMNS 51957, SMNS 58876, and SMNS 59736.

The ischium consists ventrally of an enlarged flat bone sheet, which forms dorsolaterally a slender neck, which is only about 30% of the width of the ischium (Is2). This neck forms the dorsal half of the ischium. At its dorsal margin, it bifurcates in a posterior and an anterior process. The posterior process is twice as large as the anterior process. The posterior process shows dorsally two shallow concave facets, which contact the ilium and externally participate in the formation of the acetabulum. The short anterodorsal process of the ilium forms a slightly convex facet at its dorsal margin, which contacts dorsally the ischium and probably anteriorly the pubis, too. The ventromedial bone sheet of the ischium

has a strongly convex margin. The surface of this margin is rough and was probably fringed with cartilage in life, like suggested by ANDREWS (1913) for *S. leedsi*. Therefore, the ischia met each other ventromedially in a probably cartilaginous suture (Fig. 3.14).

Pubis (pu, Fig. 3.14, Fig. 3.15)

The pubis is an elongated, flat bone with an enlargement at its ventromedial end. At its ventral margin the width of the enlargement (Pu2) is in average 35% of the pubis length (Pu1) (see appendix II). The pubis length (Pu1) is in average 1.6 times the length of the ilium (P1). The ventromedial half is roughly triangular with an externally convex margin. The margin has a roughened surface and was probably connected to the contralateral pubis by cartilage. The dorsolateral margin of the pubis has a small, thickened enlargement, with a rough surface on its edge, which is interpreted as a hint to a possible cartilaginous connection with the ilium. No distinct articular facet is visible on the dorsolateral margin. The pubis does not take part in the formation of the acetabulum nor is there evidence for a direct connection to the ilium or ischium.

Limbs

Forelimb (Fig. 3.16)

The fore limb consists of humerus, radius, ulna, and manus. It is shorter than the hind limb. In adult *Steneosaurus bollensis* specimens, the humerus length (H1) is about 60% of the femur length (Fe1). In addition, the humerus length (H1) is about 20-25% of the skull length (A) (see also chapter 4)

Humerus (hu, Fig. 3.16)

The humerus is a long and slender bone with a slightly expanded, curved proximal head and a weakly developed deltopectoral crest. The proximal articulation surface is a broadly oval and convex area, with a prominent ridge on the internal side of the head. The humerus head is curved slightly medially as well as it is tilted somewhat dorsally on the shaft, and the thickest portion of the articular area is toward the posterior margin of the head. Distal to the humerus head, at the internal side, lays a triangular rugosity, which probably represents the attachment area for the humeroradialis muscle (MEERS 2003). The distal end of the humerus has two articular facets connecting with radius and ulna. The articular areas for radius (condyle radialis) and ulna (condyle ulnaris) are only poorly separated from each other. They

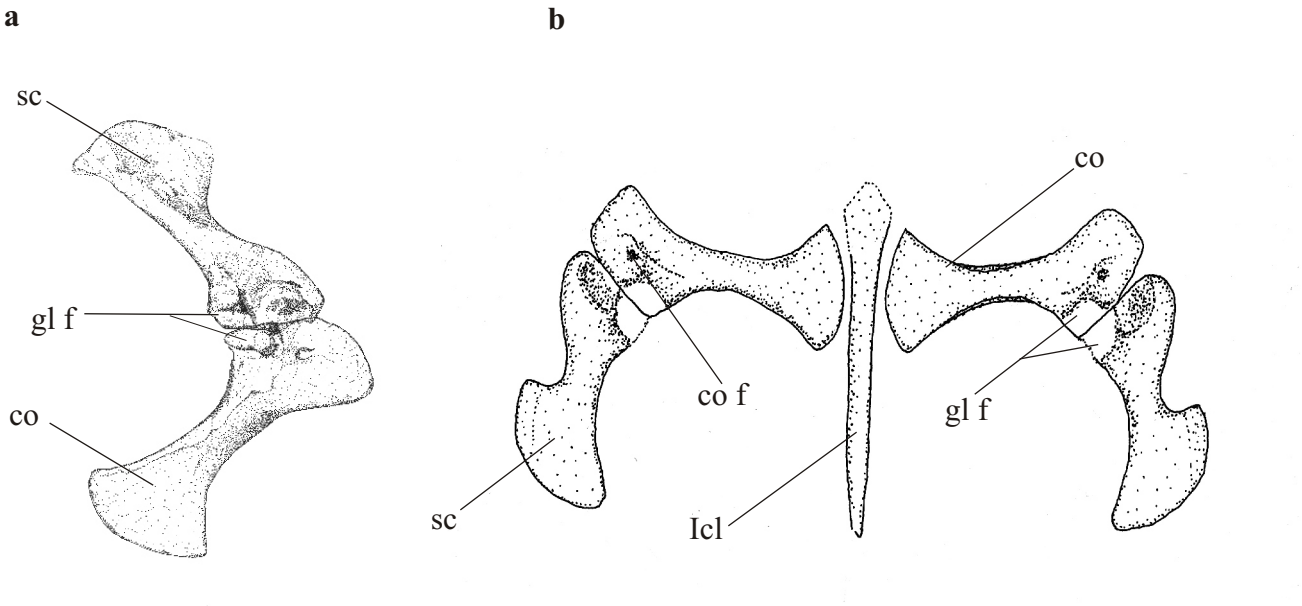

Figure 3.13a-b: Reconstruction of the pectoral girdle of *Steneosaurus bollensis*.
3.13a-Reconstruction of pectoral girdle in lateral view without interclavicle (after SMNS 51563).
3.13b-Reconstruction of the pectoral girdle in ventral view (after SMNS 849 & SMNS 80235).
Abbreviations see figure 3.12.

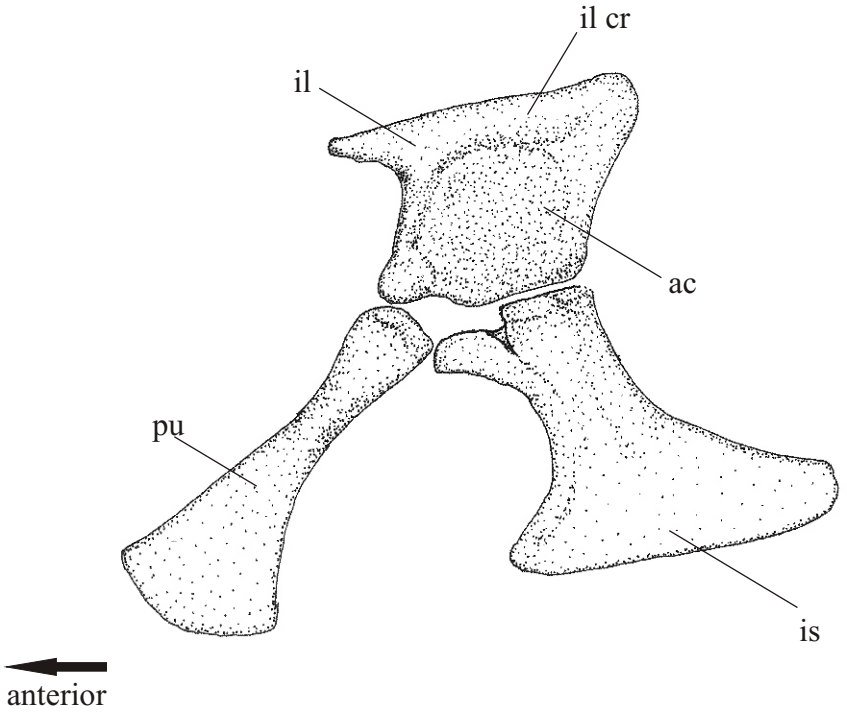

Figure 3.14: Reconstruction of the pelvic girdle of *Steneosaurus bollensis* in lateral view.
Abbreviations: ac-acetabulum, il-ilium, il cr-iliac crest, is-ischium, pu-pubis.

consist of two shallow convexities divided by a shallow intercondylar sulcus. The condyle radialis and the condyle ulnaris are of equal size.

Radius (r, Fig. 3.16)

The radius consists of a slender, cylindrical, slightly curved shaft that slightly expands at its proximal and distal end. The radius length (R1) is in average 59% of the humerus length (H1). The proximal margin articulates laterally with the ulna with a small circular, shallow concave facet and proximally with the humerus with a shallow convex facet. Distally, the radius connects with the radiale with a slightly convex articular facet (Fig. 3.16b).

Ulna (ul, Fig. 3.17)

The ulna is a slender bone that shows a posterior curvature in the proximal half of the shaft. The proximal end of the bone is three times the width of the minimum width of the shaft (U2) and twice as large as the distal end. The proximal end of the ulna is slightly flattened and possesses at the proximal margin two articular facets, which are divided by a shallow ridge. The anteroproximal facet is slightly convex, the posterior facet is slightly concave, and both articulate proximally with the humerus. In addition, the ulna contacts posteriorly the radius at its proximal and distal margin. The distal end of the ulna is only slightly enlarged and it contacts the ulnare and the pisiform with two slightly convex articular facets.

Manus (Fig. 3.16, 3.18a)

Directional terms for the manus including carpus and pes including the tarsus (as proximal or distal) are here used as if the manus and pes were vertically placed. The term "medially" refers to the direction of the radius ("radial") and the term "laterally" to the direction of the ulna (ulnar) (following ROMER 1956, p. 378).

The manus consists of the carpus, metacarpals, and phalanges. The carpus consists of four bones: the radiale, the ulnare, one single globular carpal bone, and the pisiform. The radiale is the largest bone in the carpus and about twice the size of the ulnare. The radiale is sub-rectangular with a slightly concave medial margin and a straight lateral margin. Proximally, it articulates with the radius with a slightly convex articular facet and distally with the first metacarpal with a slightly convex articular facet, too. Medially, it contacts the ulnare. The ulnare resembles in shape the radiale, but is only half the size. Proximally, the ulnare articulates with the ulna, laterally with the radiale, and medially with the pisiform.

Distally, it contacts the one globular carpal element. This small globular carpal bone represents some fused carpal elements. It is not exactly clear which of the carpal elements are fused in *S. bollensis*. In comparison to the carpus of the primitive crocodilian *Protosuchus* as well as to the carpus of the extant taxon *Crocodylus*, the preserved globular element should represent the fused carpals three and four (ROMER 1956). The pisiform is an anterodorsal flat, rectangular bone, articulating with the ulna proximally, the ulnare medially, and distally with the fifth metacarpal and probably with the carpal as well (Fig. 3.16, Fig. 3.18a).

The metacarpals I-V are similar in shape, but vary in length and in thickness. Each consists of a cylindrical shaft with a slight enlargement on each end (Fig. 3.18a). The metacarpal I is usually as long as the radiale, or in some cases slightly shorter. It is double as broad as the metacarpals III & IV and has a flatter cross-section. The metacarpal II is a fourth longer and slightly thinner than metacarpal I. The metacarpal III is again a fourth longer and slightly thinner than metacarpal II. The metacarpal IV is slightly shorter than metacarpal III but about the same width. The metacarpal V is about the length of metacarpal I or only slightly shorter, but it is always distinctly thinner than the other metacarpals. It is only half as broad as metacarpal I.

The manus has five digits (I-V). The phalangeal formula is 2-3-4-4-2. The phalanges share a similar hourglass-shape except of the terminal phalanges, which are distally pointed and claw-shaped (Fig. 3.16, Fig. 3.18).

Digit I (pollex) possesses two phalanges and is only two-thirds the length of digit III. However, it is the most distinctive one with phalanges as broad as the metacarpal I. Additionally, here the first proximal phalanx is only half the length of the first proximal phalanx of digit II. The terminal phalanx of digit I is as long and as wide as its proximal phalanx, but it is claw-shaped. Digit II has three phalanges and is longer than digit I but shorter than digit III. In digit II, the first proximal phalanx is twice the length as the second phalanx. The terminal claw-shaped phalanx is as long as the second phalange. Digit III & IV each have four phalanges. Anyway, digit III is always slightly longer than digit IV (Fig. 3.18a). In digit III, the first proximal phalanx is twice as long as the second phalanx and the third and fourth phalanx are only half the length of the second. The first proximal phalanx of digit IV is similar in shape and size to the first phalanx of digit III, while the second and third phalanx of digit IV are thinner and slightly longer than the corresponding ones of digit III. The fourth phalanx of digit IV is identical with the fourth phalanx of digit III. Digit V is about the same length as digit I and likewise possesses two phalanges. The first phalanx of digit V is as long as the metacarpal V and only slightly thinner. The second phalanx of digit V is claw-

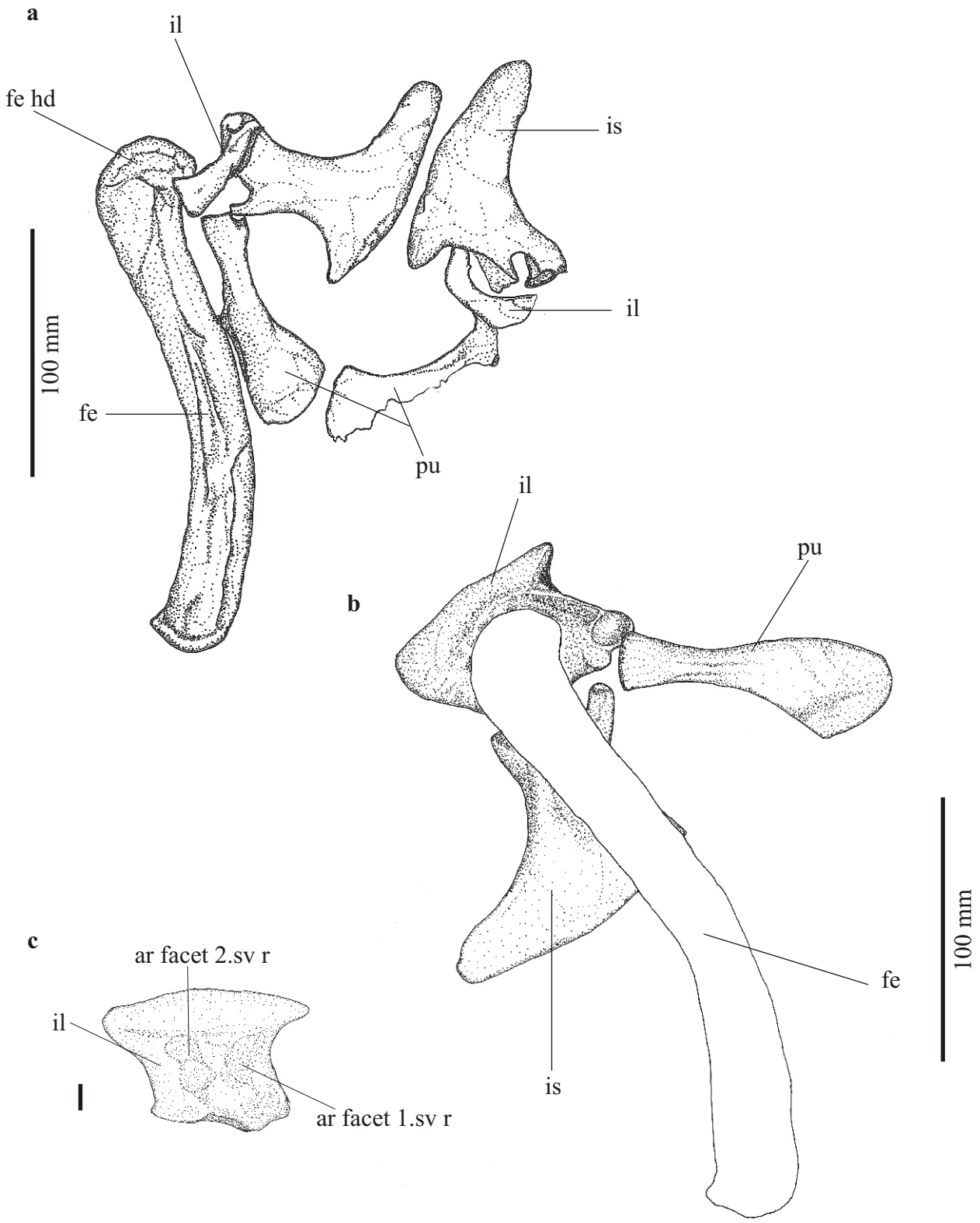

Figure 3.15a-c: *In situ* drawings of the pelvic girdle of *S. bollensis*. **3.15a**-SMNS 56370, pelvic girdle with left femur in ventral view. Scale bar is 100 mm. **3.15b**-UH 13, pelvic girdle with sketch of appending femur in lateral view. Scale bar is 100 mm. **3.15c**-Internal view of the ilum of SMNS 9428b, articular facets for the sacral ribs visible. Scale bar is 10 mm. Abbreviations see chapter 2.

shaped and identical in shape and size to the terminal phalanges of digit III and IV. In most specimens, only the proximal phalanges are preserved, while the terminal phalanx is lacking and is only indicated by an impression in the sediment.

Hind limb (Fig. 3.17, Fig. 3.18)

The hind limb consists of femur, tibia, fibula, and pes. As mentioned above, the hind limb is longer than the fore limb.

In adult *Steneosaurus bollensis* specimens, the femur length (Fe1) is about 36% of the skull length (A) (see chapter 4), and the tibia length (T1) is usually between 53-62% of the femur length (Fe1). In the holotype, however, the tibia length (T1) is 72% of the femur length (Fe1), which is very unusual for any *Steneosaurus* taxon (see chapter 4).

Femur (fe, Fig. 3.17b, 3.18b)

The proximal part of the femur is often covered by parts of the ilia or by osteoderms, but in specimen UH 13 and SMNS 56370 the femur is fully exposed in internal view. The shape of the femur is nearly identical to that of *Steneosaurus leedsi* described by ANDREWS (1913).

The femur is the longest of the limb bones. It is greatly elongated with proximal and distal expansions. In posterior view, the femur shows an open S-shaped curvature (Fig. 3.34). The femur is twisted, which means that the planes of the proximal and distal expansions are not parallel, but oblique to each other. The femoral head is only slightly bent towards the internal side. The lesser trochanter is clearly visible ventral to the femoral head at the shaft. It is marked by an area of rugosities on the internal side of the femur. At the external side ventral to the femoral head, an area of rugosities is visible as well. Distal to these areas, the shaft becomes more slender and is probably oval in cross-section. At the distal end of the bone, there are two condyles forming strong convexities separated by a deep intercondylar groove. The external fibular condyle is not much larger than the internal tibial condyle.

Tibia (ti, Fig. 3.17, Fig. 3.18b)

The slender tibia consists of a slightly curved, cylindrical shaft with a proximal and distal enlargement. Its length (Ti1) is in adults a 53-62% of the femur length (Fe1). The proximal and distal enlargement diverges about 10% from the minimum width of the shaft (T2). The dorsal margin of the proximal end forms a shallow convex articular area for the femur, which is divided into two very shallow condyles. The distal end of the tibia articulates

with the astragalus with a strongly convex articular facet. Medially, the proximal and distal ends of the tibia also contact the fibula by small, laterally aligned, and slightly concave articular facets.

Fibula (fi, Fig. 3.17, Fig. 3.18b)

The fibula is a slender bone bar with slightly enlarged convexities of nearly equal size at the proximal and distal end. The proximal end is about 5% larger compared to the minimum width of the shaft. (F1) It terminates in an elongated convex surface that serves for the articulation with the external portion of the lateral condyle of the femur. At its distal end, the fibula articulates distally with the calcaneum in a slightly internally concave articular facet, and medially, it meets the tibia (see there).

Pes (Fig. 3.17, Fig. 3.18b)

The pes consists of the tarsus, metatarsals, and phalanges. The tarsus consists of four bones: the calcaneum, astragalus, and tarsals 3 and 4. The calcaneum is a sub-rectangular bone with a slightly developed calcaneum tuber. It has nearly the same size as the astragalus, and its calcanean tuber is short (50% of the entire length of the calcaneum) and only slightly set off from the corpus by a circumference. The astragalus is similar to that of extant crocodiles. In posterior view, it is sub-rectangular with a pronounced, convex, lateral articular facet with the calcaneum (Fig. 3.17) and a slightly concave developed articular facet for contacting the tibia proximally. The joint between calcaneum and astragalus is developed as a ball-and-socket joint, with a "ball" at the astragalus and the "socket" at the calcaneum. *Steneosaurus bollensis* possesses a typical crurotarsal joint of the crocodile-normal type (ROMER 1956, PARRISH 1987).

The tarsal 3 is a small globular bone articulating with the astragalus proximally, the metacarpal I distally, and the tarsal 4 laterally. The relatively small tarsal 3 (only one-third in size of the tarsal 4) is often missing in the specimens**.** In dorsal view, the tarsal 4 is a dorsoventrally flattened, rectangular or in some cases sub-triangular bone. It is usually situated distally the calcaneum and contacts laterally the fifth metatarsal and medially the tarsal 3. Proximally, it articulates with the metatarsal II and III (Fig. 3.18b)

The pes generally has five digits, whereas the digit V is reduced here, and only a rudimentary flattened metatarsal V in rectangular or triangular shape is left (Fig. 3.17, Fig. 3.18b).

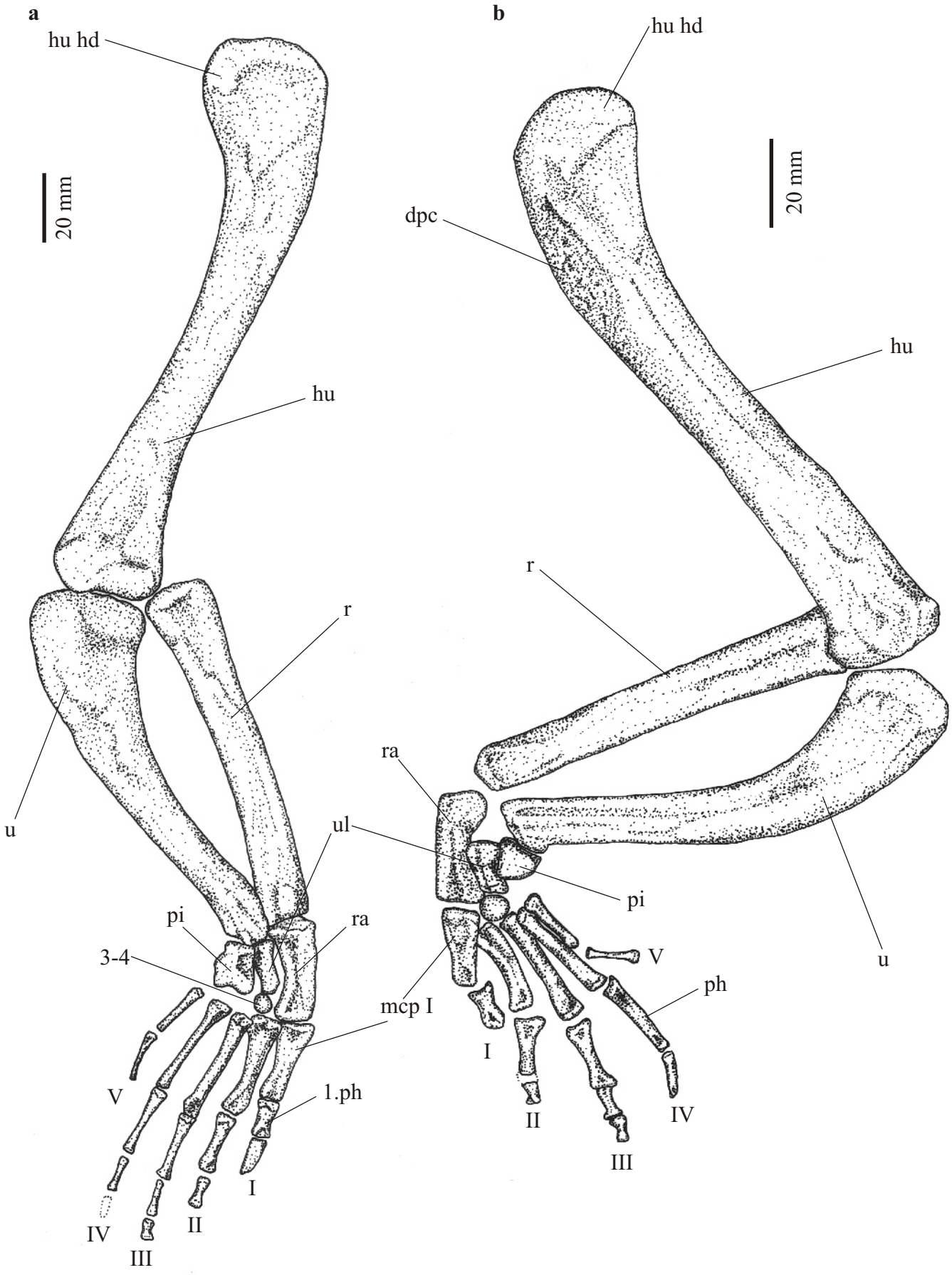

Figure 3.16a-b: Forelimb of *Steneosaurus bollensis*. **3.16a**-*In situ* drawing of the left forelimb of specimen UH 12. **3.16b**- *In situ* drawing of the right forelimb SMNS 52563. Original length of the humerus is 150 mm. Scale bars are 20 mm. Abbreviations see chapter 2.

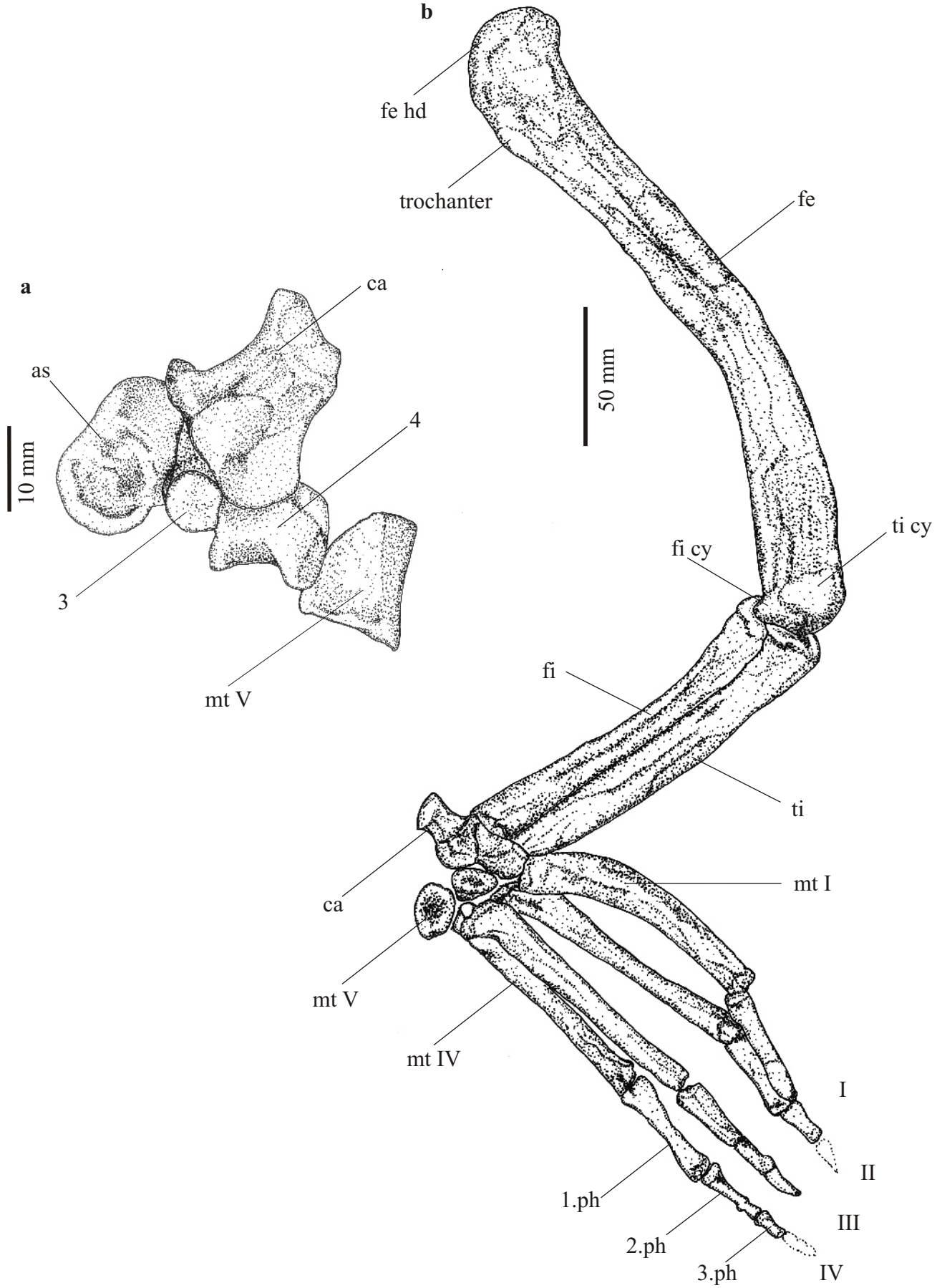

Figure 3.17a-b: 3.17a- *in situ* drawing of the left tarsus and fifth metatarsal of GPIM uncatalogued. **3.17b**-*In situ* drawing of the right hind limb of UH13. Abbreviations see chapter 2.

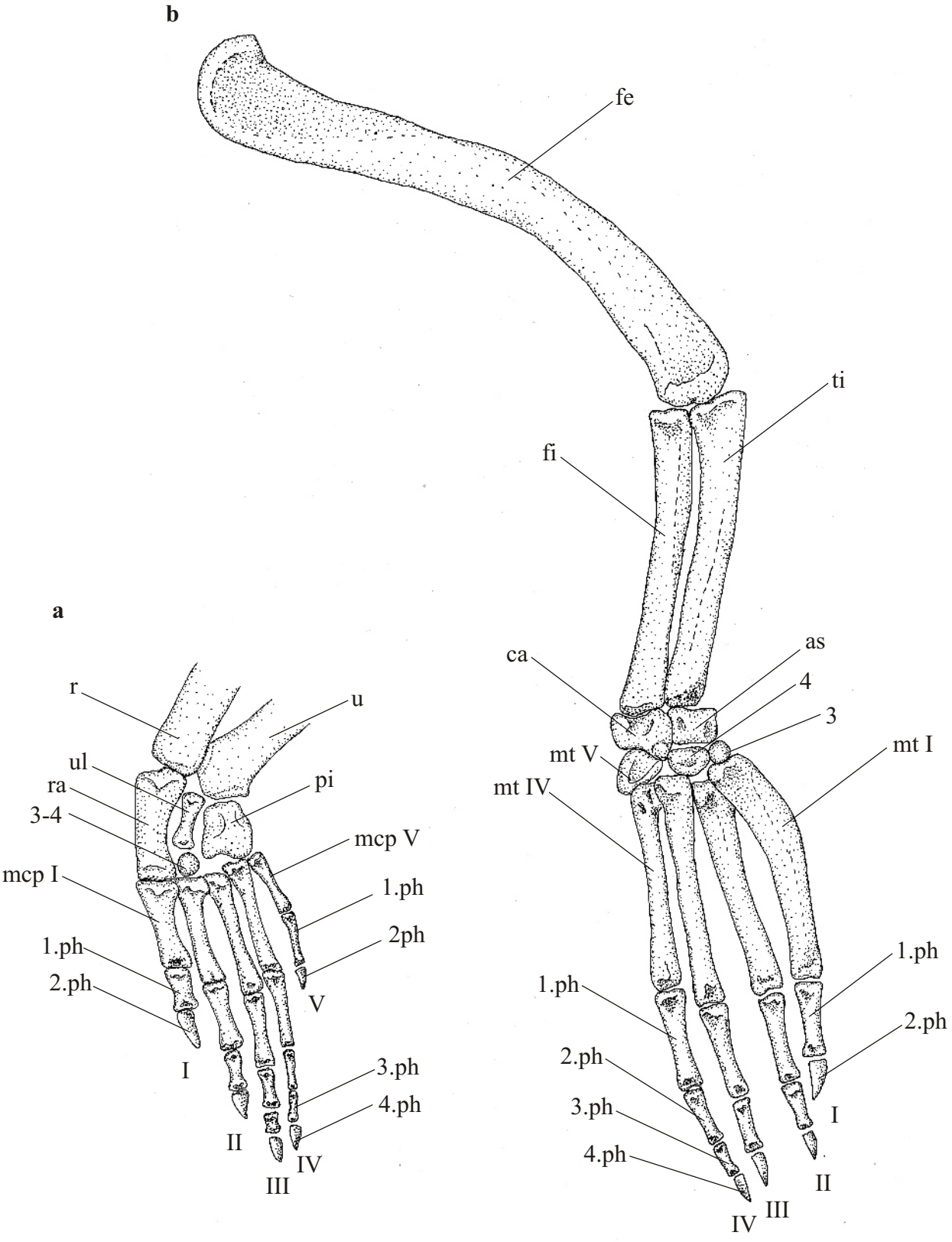

Figure 3.18a-b: Reconstruction of the manus and the hind limb of *Steneosaurus bollensis*. **3.18a**-Right manus with the phalangal formula 2-3-4-4-2. **3.18b**-Right hind limb with femur (fe), tibia (ti), fibula (fi), tarsus, and pes. Pes with the phalangal formula 2-3-3-4-0. Abbreviations see chapter 2.

The metatarsal V seems to be integrated in the tarsus. It contacts proximally the calcaneum, medially the tarsal 4 and distally the metatarsal IV. The remaining four long, slender metatarsals are circular in cross-section. Metatarsal I is shorter but broader than the remaining metatarsals. It is curved medially and is not straight as the other metatarsals. In cross-section, metatarsal I is more flattened than the other metatarsals. The metatarsals II-IV share the same shape. They consist of a cylindrical shaft with slight enlargements at the proximal and distal edges. The proximal articular facets are shallow concave, whereas the distal articular facets are slightly convex. Metatarsal II is about the same length as metatarsal I, while metatarsal III is slightly longer than the metatarsals I and II. Metatarsal IV is again slightly shorter than metatarsal III is.

Digit I possesses two phalanges and is the shortest digit. Digit II is slightly longer than digit I (about one tenth) and possesses three phalanges. Digit III is again about one tenth longer than digit II and possesses three to four phalanges. Digit IV is usually the longest one, even though it is only slightly longer than digit III. The phalangeal formula is 2-3-(3)4-4-0, but the numbers vary in some specimens due to intraspecific variation (see chapter 4).

The proximal phalanges are hourglass-shaped. The base of all phalanges is internally concave and the distal margin is developed as a trochlea, except for the unguals, which are distally pointed and claw-shaped. The first proximal phalanx of digit I is slightly shorter than the first phalanges in digits II-IV, which are all equal in length. The second phalanx of digit I is claw-shaped and only half the length of the first phalanx of digit I. The second phalanges of digit II-IV are only half the length of their first phalanges. The third phalanx of digit II and III are the terminal phalanges and claw-shaped. In digit IV, the third phalanx is only half the length of the second phalanx. The ungular phalanx of digit IV is as long as the third phalanx.

3.2 Osteology of *Steneosaurus gracilirostris* (WESTPHAL 1961)

3.2.1 Introduction

The taxon *Steneosaurus gracilirostris* was erected by WESTPHAL (1961) based on four specimens from the Yorkshire Lias, formerly partly described by BUCKLAND (1836) and OWEN (1849/1884) as *Teleosaurus chapmanni* and by DESLONGCHAMPS (1877) as *Pelagosaurus brongniarti.* Because the general appearance of all *Steneosaurus* taxa is similar, a detailed description of *Steneosaurus gracilirostris* is dispensable here, but it will be referred to the detailed description of *Steneosaurus bollensis* (see chapter 3.1). In the following a character diagnosis and a description of the unique features of *Steneosaurus gracilirostris* is presented.

Eureptilia OLSON 1847
Diapsida OSBORN 1903
Mesoeucrocodylia WHETSTONE & WHYBROW 1983
Thalattosuchia FRAAS 1901
Teleosauridae GEOFFROY 1831
Steneosaurus gracilirostris (WESTPHAL 1961)
(Figures 3.19-3.20)

Holotype: BMNH 14792
Locus typicus: Whitby, Yorkshire, Great Britain
Stratum typicum: Upper Liassic, Lower Toarcian, Alum Shale Series (WESTPHAL 1962)

3.2.2 Material

In total **10** specimens, all housed in the BMNH were investigated for this study: BMNH R 4, BMNH R 63 a, BMNH R 405, BMNH R 757, BMNH 14792, BMNH 15500, BMNH 33095, BMNH 33095 (2), BMNH 33095 (3), and BMNH 33097.

Of these, only few specimens can be referred to *Steneosaurus gracilirostris* with certainty: the holotype BMNH 14792, BMNH R 757, and BMNH 15500 (WESTPHAL 1961 & 1962, BENTON & TAYLOR 1984, VIGNAUD 1995). The other specimens are only tentatively referred to *S. gracilirostris*, because they are too fragmentary to show certain diagnostic features.

A complete list of all the investigated material is provided in appendix I.

3.2.3 Locality and horizon

Steneosaurus gracilirostris is known from Liassic sediments of Great Britain, Luxembourg and probably from France. It is certainly known from the Alum Shale Series of Whitby, Yorkshire Coast in Great Britain (WESTPHAL 1962), and from the Schistes de Grandcourt (Toarcian) of Luxembourg (GODEFROIT 1994). The specimen from the Upper Liassic sediments from La Caine (Calvados) was described by DESLONGCHAMPS (1877) as *Pelagosaurus brongniarti*. It is with reservations referred to *Steneosaurs gracilirostris*, but because of the missing skull in this specimen, certain evidence cannot be given (WESTPHAL 1962).

3.2.4 Preservation

The Liassic specimens of *Steneosaurus gracilirostris* are preserved in black shales. They are in some cases compressed by the overlying strata, whereas the bones are often not broken and still in articulated condition.

Only the skull is described in detail for this taxon, because postcranial material is only fragmentary preserved in one specimen (BMNH 14792). The holotype (BMNH 14792) consists of a partial skeleton with a nearly three-dimensional skull and it is exposed in dorsal view. Small parts of the lateral margin of the lower jaw are exposed in dorsal view, too. Parts of the limbs e.g., femur, humerus, and tibia are fragmentarily preserved and diagenetically flattened, as are some vertebrae and parts of the dorsal armour (figured in WESTPHAL 1962, Table 3, Fig. 2). Specimen BMNH 757 consists of a compressed skull free from matrix. Unfortunately, only the ventral side is exposed now, because the specimen is mounted on a wooden board. BMNH 15500 is a well preserved, three-dimensional, and almost complete skull including the mandible. However, the lower jaw is only fragmentarily preserved and the skull is fixed on a neuter; thus, only the lateral view of the mandible is exposed. Two other specimens are questionably labelled as cf. *Steneosaurus gracilirostris*. Specimen BMNH R 4 consists of several transverse sections of the posterior part of the skull taken from the anterior margin of the orbit until the occipital condyle and was formerly labelled as *Pelagosaurus brongniarti*. The other specimen, BMNH 33097, consists of a rostrum fragment (parts of maxillae and nasals) formerly referred to *Teleosaurus*. The other specimens do not show certain diagnostic features but resemble to *S. gracilirostris*: BMNH R 405 consists of a lower jaw fragment, specimen BMNH R 63a consist of some poorly preserved rostrum fragments,

BMNH 33095 consists of an fragment of the occipital region of the skull, and BMNH 33095 (1/2) consist of poorly preserved maxilla fragments.

3.2.5 Diagnosis

Steneosaurus gracilirostris is a medium-sized *Steneosaurus* taxon, which a total length of about 2.5 meter. Compared to *Steneosaurus bollensis* the skull of *Steneosaurus gracilirostris* is higher and more similar to the conditions in *Pelagosaurus typus* (see chapter 3.5). The total skull length (A) in ratio to the trunk length (TRL) is 67% in *Steneosaurus gracilirostris* (GODEFROIT 1994) and differs apparently from the ratio of in average 58% in *Steneosaurus bollensis*. The taxon *Steneosaurus gracilirostris* is characterised by a long, very slender rostrum. The ratio of the rostral length (B) to the total skull length (A) ranges between 74% and 77% in *S. gracilirostris* (GODEFROIT 1994), in comparison to 65% to 75% in *Steneosaurus bollensis* and only 65% in *Steneosaurus brevior* (see chapter 3.3 & 5). The narrowing in the rostrum posterior to the premaxillae (L) is 84 % of the premaxillae width (K) in BMNH 14792, in specimen BMNH 15500 it is about 88%. In adult *Steneosaurus bollensis* specimens, this ratio is in average 65% (see chapter 5). *S. gracilirostris* shows the larger antorbital fenestra than *S. bollensis*. The orbits of *Steneosaurus gracilirostris* are relatively large in comparison to the relative moderate size of the supratemporal fenestrae. The orbital length (I) is about 60% of the supratemporal fenestra length (D). In addition, the orbits open dorsolaterally in *S. gracilirostris*. These features differ distinctly from the anterodorsally orientated, relatively small orbit of adult *Steneosaurus bollensis*, where the ratio of orbital length (I) to supratemporal fenestra length (D) is only 40-55%, and is more similar to the configuration of adult *Pelagosaurus typus* (I/D~ 77%). The supratemporal fenestra length (D) in comparison to the skull length (A) is only 12.4% in *Steneosaurus gracilirostris*, which is similar to the conditions of *Pelagosaurus typus* but differs from that of *S. bollensis* (see chapter 3.5 & 5). The surface of the squamosal shows no ornamentation and is smooth, which differs distinctively from *Steneosaurus bollensis* and *Pelagosaurus typus* as well as *Platysuchus multiscrobiculatus.* The estimated number of teeth in the upper jaw is up to 60 on each side. In the dentary, the estimated tooth count is up to 60, too. This high number of teeth differs greatly from the other Liassic taxa, even though a high intraspecific variation in the tooth number is considered. In the palate, the posterior maxillary-maxillary suture forms a median ridge, which is accompanied by a parallel groove at each side. Such a median ridge is a unique feature within the Liassic teleosaurids.

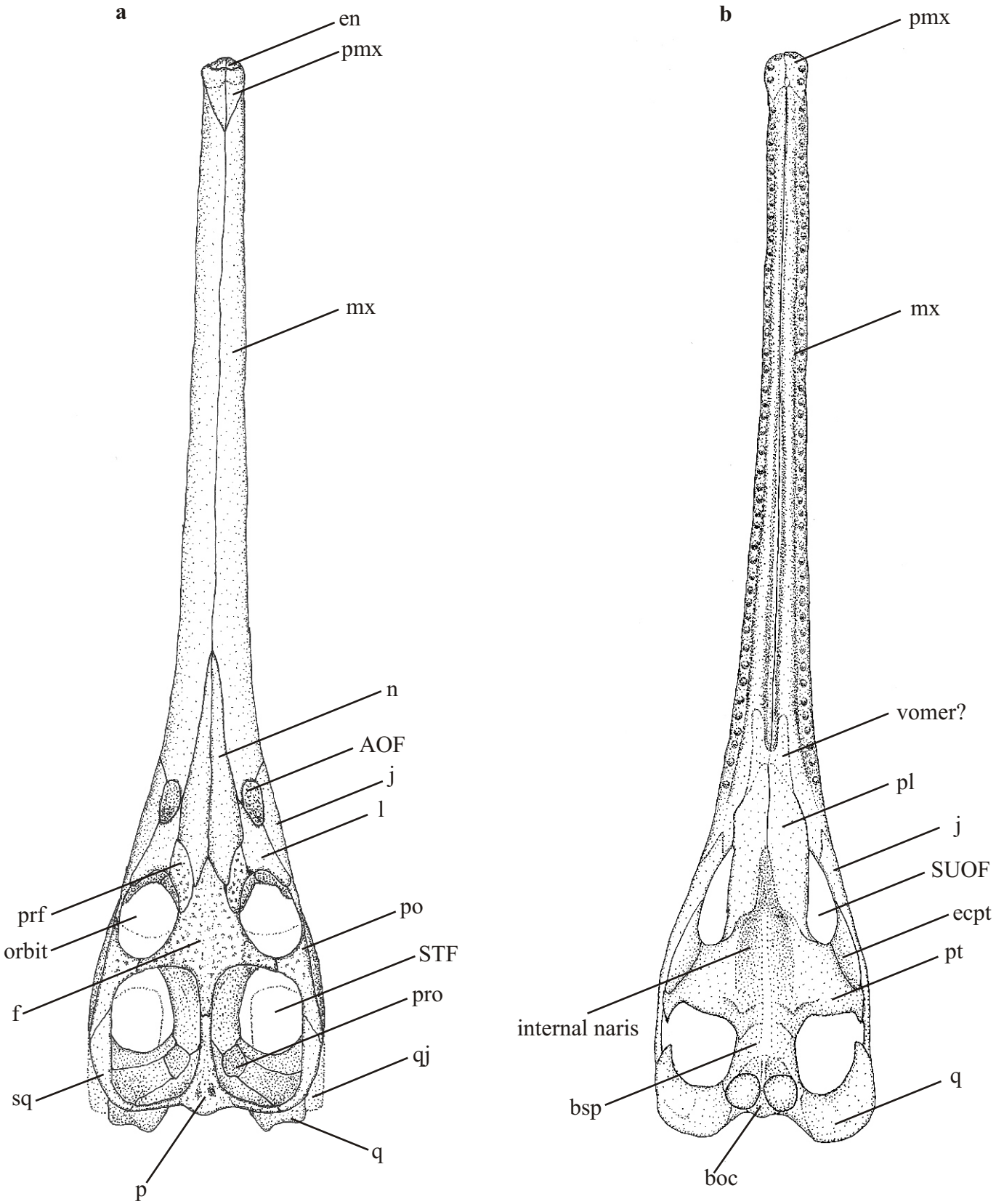

Figure 3.19a-b: Reconstruction of the skull of *Steneosaurus gracilirostris* in dorsal and ventral view .
3.19a-Dorsal reconstruction of the skull is mainly based on the specimen BMNH 14792.
3.19b-Ventral reconstruction of the skull is mainly bases on the specimen BMNH 757.
For abbreviations, see chapter 2.

3.2.6 Osteology

Skull (Fig. 3.19 & Fig. 3.20a)

Even though the skull of *Steneosaurus gracilirostris* has the some features of a typical *Steneosaurus* skull (see chapter 3.1), it is easy to distinguish it from the other *Steneosaurus* taxa. The entire skull is relatively slender and higher than in *Steneosaurus bollensis* or *Steneosaurus brevior* (see chapter 5). It is characterised by an elongated slender rostrum, which has no distinct anterior enlargement of the paired premaxilla. Large, dorsolaterally orientated orbits and distinct antorbital fenestrae are clearly different from the conditions of *Steneosaurus bollensis*. Large eyes in the skull can indicate a juvenile stage in teleosaurids, but in this case, the remaining characteristic features clearly belong to an adult specimen. In addition, due to the fact, that *S. gracilirostris* has a particular long skull, the ratio of orbital length (I) to skull length (A) is 7.4% in *Steneosaurus gracilirostris*, which fits well with the ratio of 7.9% for adult *Steneosaurus bollensis* and 7.7% for adult *Steneosaurus brevior* specimens. The thin sagittal crest in *Steneosaurus gracilirostris* also indicates an adult specimen, and differs from the broad sagittal area of juvenile specimens of *Steneosaurus bollensis* (see chapter 4 for further discussion). In fact, the general skull topography appears more similar to *Pelagosaurus typus* than to other *Steneosaurus* taxa.

Sculpturing of the cranial bones is only found on the frontal, parietal, postorbitals, and jugals. There is no ornamentation on the squamosals, lacrimals, or the nasals like in *Pelagosaurus typus* or *Platysuchus multiscrobiculatus* (see chapter 3.4 & 3.5). The particular pattern of ornamentation of the individual bones is described below.

Cranial table

Openings

External naris (en, Fig. 3.19, Fig. 3.20a)

The confluent external naris is directed anteriorly. The dorsal margin of the external naris forms an angle of about 60 degrees (W1), with the horizontal plane of the floor of the external naris (see also chapter 4). The external naris is wider than long and entirely enclosed by the premaxillae. The shape is almost identical with the shape of the external naris of *Steneosaurus brevior* (see chapter 3.3).

Antorbital fenestra (AOF, Fig. 3.19, Fig. 3.20a)

S. gracilirostris has relatively large, longitudinal elliptic antorbital fenestrae compared to that of *S. bollensis*. As usual in teleosaurids, it is bordered posteriorly by the lacrimal and jugal, medially by the lacrimal, laterally by the jugal and anteriorly by the maxilla (see chapter 3.1). The antorbital fenestra in specimen BMNH 15500 is three times longer than high. The maximum length of it (P) is 24 mm and the maximum height (Q) is 8 mm, whereas the total skull length (A) of this specimen is 700 mm. However, the antorbital fenestra shows no features distinguishing it from other *Steneosaurus* taxa except for its size.

Orbit (o, Fig. 3.19, Fig. 3.20a)

The large, ellipsoid orbit is dorsolaterally aligned (see paragraph "diagnosis" and “skull”). In specimen BMNH 14792, the anterior process of the postorbital is elongated and it forms the posterior third of the lateral margin of the orbit. The jugal forms the next third and the lacrimal forms the anterior third of the lateral orbital margin. Thus, the postorbital and the lacrimal do not contact each other, but are separated by the jugal. The anterior, posterior, and medial margin of the orbit is formed by the lacrimal, the prefrontal, the frontal, and the postorbital like that of *S. bollensis* (see chapter 3.1).

Supratemporal fenestra (STF, Fig. 3.19, Fig. 3.20a)

The supratemporal fenestra is sub-rectangular with slightly rounded corners. It is longer than wide and bordered by the frontal, the postorbital, the squamosal, and the parietal. The general appearance is similar to *Steneosaurus bollensis* (see chapter 3.1). Nevertheless, because of the minor difference of the shape of the squamosal (see there) the lateral outline of the supratemporal fenestra is straight and does not show a medial convexity at its lateral margin like *Steneosaurus bollensis.*

Infratemporal fenestra (ITF, Fig. 3.19)

The infratemporal fenestra is only visible in specimen BMNH 15500. It has a length of 82 mm (N) and is 28 mm high (O). It is bordered by the postorbital, the squamosal, the quadratojugal, and the jugal, like in *Steneosaurus bollensis*. The poor preservation in this part makes it impossible to determine diagnostic features at the infratemporal fenestra, which distinguishes it from the fenestra observed in *Steneosaurus bollensis*.

Cranial bones

Premaxilla (pmx, Fig. 3.19)

The borders of the premaxilla are the same as in *Steneosaurus bollensis* (see chapter 3.1). However, the premaxilla is only slightly laterally broadened compared to the maxilla. Therefore, the paired premaxilla does only form a slight enlargement at the tip of the rostrum and not a distinct spoon-shape enlargement like in *S. bollensis*. The specimens BMNH 14972 and BMNH 15500 show this slight enlargement well. Nevertheless, this feature differs clearly from *Steneosaurus bollensis*, *Steneosaurus brevior*, and *Platysuchus multiscrobiculatus*, which all possess a broad enlargement of the paired premaxilla; only *Pelagosaurus typus* shows similar premaxillae enlargement like *Steneosaurus gracilirostris* (see chapter 3.1, 3.3, 3.4, and 3.5 for comparison). The premaxilla bears three teeth.

Maxilla (mx, Fig. 3.19)

The maxilla has the same borders like in *Steneosaurus bollensis* (see chapter 3.1). The lateral margin of the maxilla is straight in ventral and dorsal view, but it slightly undulates in lateral view. There are at least 45 alveoli in each maxilla. The alveoli are small, circular, orientated ventrally and not visible in lateral view (see paragraph "palate"). The small, slender teeth are vertically orientated (see paragraph “dentition”). In contrast to *Steneosaurus bollensis* and *Pelagosaurus typus*, the maxilla in *Steneosaurus gracilirostris* carries teeth only until the level of the antorbital fenestra and not until the level of the orbit.

Nasal (n, Fig. 3.19)

The nasal in *Steneosaurus gracilirostris* is relatively slender compared to *Steneosaurus bollensis*, but otherwise the general features such as the adjacent bones and the shape are the same. There is no sculpturing on the surface, which differs from the conditions in *Pelagosaurus typus* (see chapter 3.5).

Lacrimal (l, Fig. 3.19)

The lacrimal forms the anterior margin of the orbit. Medially it shares a suture with the prefrontal and the nasal. Anteriorly it is bordered by the antorbital fenestra and laterally by the jugal like in *Steneosaurus bollensis*. Its general shape is trapezoidal and it is at least two times the size of the prefrontal. The surface of the lacrimal is completely smooth here, in contrast to

the pronounced ornamentation on the surface of the lacrimal of *Steneosaurus bollensis* and *Steneosaurus brevior*.

Prefrontal (prf, Fig. 3.19)

The small, slender prefrontal is slightly elongated in posterior direction. With the frontal, it shares a heavy ornamentation, which is much more distinct than the ornamentation of the prefrontal of *Steneosaurus bollensis* or *Steneosaurus brevior* (see chapter 3.1 & 3.3). The complete surface of the prefrontal is covers by small, rounded pits, which have a dense equal distribution.

Frontal (f, Fig. 3.19)

The general shape and the adjacent bones of the frontal are the same as in *Steneosaurus bollensis* (see chapter 3.1), but the ornamentation differs slightly from *Steneosaurus bollensis*. The ornamentation consists of a pattern of small, deep, round pits, which are densely distributed. In a medial line in longitudinal direction, the pits are more widely spreaded than in the rest of the frontal and form kind of a shallow medial groove. Due to this fact, the ornamentation on the frontal appears bilaterally symmetric.

Parietal (p, Fig. 3.19)

The parietal is bordered anteriorly by the frontal, and laterally by the squamosals like in *Steneosaurus bollensis* (see chapter 3.1). Medioventrally, it has broad contact with the prootic (see paragraph “braincase”) and lateroventrally with the squamosals. Posteroventrally, it is in contact with the supraoccipital. The bone is triangular with only faint ornamentation on its external surface. The ornamentation on the dorsomedial surface consists of two longitudinal elliptic, deep pits and some smaller, shallower pits around them. The posterior margin of the parietal is slightly externally convex and differs from the usual external concave margin of the parietal in other steneosaurs.

Postorbital (po, Fig. 3.19)

The postorbital shows the same general shape and is bordered by the same bones like in *Steneosaurus bollensis* (see chapter 3.1). In contrast to *S. bollensis*, the ornamentation of this bone is less developed in *S. gracilirostris*. The ornamentation consists of small rounded pits restricted to the medial part of the external surface of the postorbital. The remaining external surface is smooth.

Squamosal (sq, Fig. 3.19)

The position and the general shape of the squamosal are nearly identical with that of *Steneosaurus bollensis*. However, the surface of the squamosal is smooth without ornamentation, which differs distinctively from all other Liassic teleosaurids (see chapters 3.1, 3.3, 3.4, and 3.5). In addition, the squamosal has a broad ventral contact to the prootic, which cannot be confirmed for *Steneosaurus bollensis* because the suture is unknown.

Jugal (j, Fig. 3.19)

The position and the general shape of the jugal is nearly the same as in *Steneosaurus bollensis*. However, the jugal forms at least on third of the ventrolateral margin of the orbit, which is different from the conditions in *Steneosaurus bollensis* and *Steneosaurus brevior*, where the jugal does not or only slightly take part in the orbital margin (see chapter 3.1 & 3.3). In addition, the dorsal surface of the jugal is smooth, whereas the other Liassic teleosaurids show at least some slight ornamentation (see chapter 3.1).

Quadratojugal (qj, Fig. 3.19)

The poor preservation of the quadratojugal in all known *Steneosaurus gracilirostris* specimens makes it impossible to describe it in detail. It is only visible in specimen BMNH 15500, where the surface is eroded and the area is diagenetically stressed and shattered. However, the bone shows an anteroventral contact to the jugal, a posteromedial one to the quadrate, and an anterodorsal one to the squamosal. It is hook-shaped like in *Steneosaurus bollensis* and forms the posterior margin of the infratemporal fenestra (see there).

Quadrate (q, Fig. 3.19)

The preservation is even worse in the quadrate. Only parts of the quadrate are visible in specimen BMNH 757 (ventral view) and in specimen BMNH 15500 (lateral view). The exact shape and dimension can only be estimated, but the restrictions of the quadrate are close to the conditions in *Steneosaurus bollensis*, as well as the general appearance is.

Palate (pa, Fig. 3.19)

The available information about the palate is poor and only specimen BMNH 757 exposes the ventral side of the skull. The reconstruction of the palate as shown in figure 3.19 is mainly based on this specimen. The presence of an incisive foramen is not certain, the exact shape of the internal naris is difficult to determine, and the exact suture between basisphenoid

and pterygoid is missing in the specimen. The shape of the anterior margin of the palatine and its possible contact to the vomer could be also a consequence of the poor preservation of the skull.

Palatal openings

Internal naris (in, secondary choana, Fig. 3.19b)

The internal naris is larger than that of *Steneosaurus bollensis*. It tapers anteriorly between the palatines until the level of the anterior margin of the suborbital fenestra, and separates the palatines in their posterior half. The pterygoids enclose the largest part of the internal naris. The median suture of the pterygoidal-pterygoidal contact forms a distinct longitudinal bony ridge at the roof of the internal naris.

Suborbital fenestra (SUOF, Fig. 3.19b)

The slender suborbital fenestra is elongated with a round posterior and a pointed anterior margin. It is relatively small, because it does not extend anteriorly the ventral maxillojugal suture as it does in e.g., *S. bollensis* or *S. brevior*. It is bordered anteriorly by the maxilla, medially by the palatine, posteriorly by the pterygoid and ectopterygoid and laterally by the jugal. The shape of the suborbital fenestra differs distinctively from the shape in *Steneosaurus bollensis* (see chapter 3.1), but is similar to the shape in *Steneosaurus brevior* (see chapter 3.3).

Maxilla (mx, Fig. 3.19b)

Ventrally, the maxillae forms about 75% of the secondary palate and meet each other in their anterior third in a straight suture. In the posterior two-thirds, the maxillary-maxillary suture forms a median ridge, which has a parallel groove on each side. The palatinal maxillary-maxillary suture forming a median ridge is a unique feature within the Liassic teleosaurids. The ventral suture between the maxilla and premaxilla is not preserved in the specimens. The premaxillary-maxillary suture shown in the reconstruction (Fig. 3.19b) is based on known premaxillary-maxillary sutures of *S. bollensis* and Middle Jurassic teleosaurids and thus is hypothetical. Posteromedially, the maxilla contacts the palatine and posterolaterally the jugal. In addition, a possible palatine-vomer contact is exposed posteromedially (see paragraph "vomer"). The ectopterygoid does not contact the maxilla, as it does in *Steneosaurus bollensis* (see chapter 3.1). 50-60 circular alveoli with 4-5 mm

diameter lie in a straight row, in a shallow groove along the lateral edge of the maxilla (Fig. 3.19b). The interalveolar space is only half to two-thirds the size of the alveoli (for further details see paragraph “dentition”). Due to the poor preservation in the posterior part of the maxilla the exact number of alveoli is unknown.

Palatine (pl, Fig. 3.19b)

The palatine is a paired bone forming, together with the paired maxilla and the paired premaxilla, the secondary palate. Like in *Steneosaurus bollensis*, the paired palatine tapers off anteriorly between the maxillae, but only separates them in their last 15-20%. Probably they meet anteriorly the vomer, too (see paragraph "vomer"). Posteriorly the palatine is bordered by the pterygoids, posteromedially the internal naris tapers off between the palatines and separates them in their posterior half (see there). The palatine forms the medial margin of the suborbital fenestra (see there).

Vomer (v, Fig. 3.19b)

A possible vomer lies anterior to the paired palatine and forms an H-shaped structure. It cannot be excluded that this structure is a part of the palatine, but the position corresponds with the position observed for the vomer in *Tomistoma schlegelii*. However, no such structure is visible in *Steneosaurus bollensis.*

Pterygoid (pt, Fig. 3.19b)

The paired pterygoid forms a butterfly-shaped structure and lies in the same topographical position as in *Steneosaurus bollensis* and *Steneosaurus brevior* (see chapter 3.1 & 3.3). Due to the poor preservation of specimen BMNH 757 in this area, it can be only said that the paired pterygoids meet each other in a medial bone ridge in the roof of the internal naris, which is more distinctly developed than in *Steneosaurus bollensis* (see paragraph “internal naris”). The posterior pterygoid process is narrow and short in comparison to the broad, elongated posterior pterygoid process of *Steneosaurus bollensis*.

Ectopterygoid (ecpt, Fig. 3.19b)

The ectopterygoid is poorly preserved, but is similar in size and shape to the one of *Steneosaurus bollensis*. However, in *S. gracilirostris*, the ectopterygoid has definitely no contact with the maxilla (see there) and a possible contact to the postorbital is not exposed.

Braincase

Little information is available about the braincase of *Steneosaurus gracilirostris,* because of poor preservation of this part. Parts of the basioccipital, exoccipital-opisthotic complex, basisphenoid, laterosphenoid, and prootic are described based on the specimens BMNH 14792, BMNH 15500, and BMNH 757.

The specimen BMNH R 4, which shows transverse sections of the braincase is not described here, because it is only tentatively referred to *Steneosaurus gracilirostris*. However, the specimen is used for comparison with the braincase of *Pelagosaurus typus* in chapter 3.4 (Fig. 3.40).

Basioccipital (boc, Fig. 3.19)

Parts of the basioccipital are visible in BMNH 15500 and BMNH 757, but both specimens are in a very bad condition in that area. The occipital condyle is only slightly enlarged in posterior direction and not very distinct. The two basal ventral tubercles are round in ventral view and do not differ from the basioccipital tubercles seen in other teleosaurids.

Prootic (pro, Fig. 3.19a)

The prootic is exposed in BMNH 14972. Compared to the conditions found in recent crocodiles, the prootic of *Steneosaurus gracilirostris* is relatively large. The prootic is exposed on the braincase lateral wall as a rectangular bone, where it is bordered dorsally by the parietal, posteriorly by the squamosal, ventrally by the quadrate, and anteriorly by the laterosphenoid (Fig. 3.19a). A possible anterodorsal contact to the frontal cannot be confirmed, because of the uncertain course of the frontolaterosphenoid suture. The suture between parietal and prootic is well defined in *S. gracilirostris* and not fused as it is in *S. bollensis.*

Basisphenoid and parasphenoid (bsp, Fig. 3.19b)

Only parts of the basisphenoid are identifiable in specimen BMNH 757. Due to the compression of the specimen, the sutures are unclear, so no exact description is possible. In ventral view, it is bordered anteriorly by the pterygoid, posteriorly by the basioccipital, and a posterolateral contact to the quadrate is expected, but not visible.

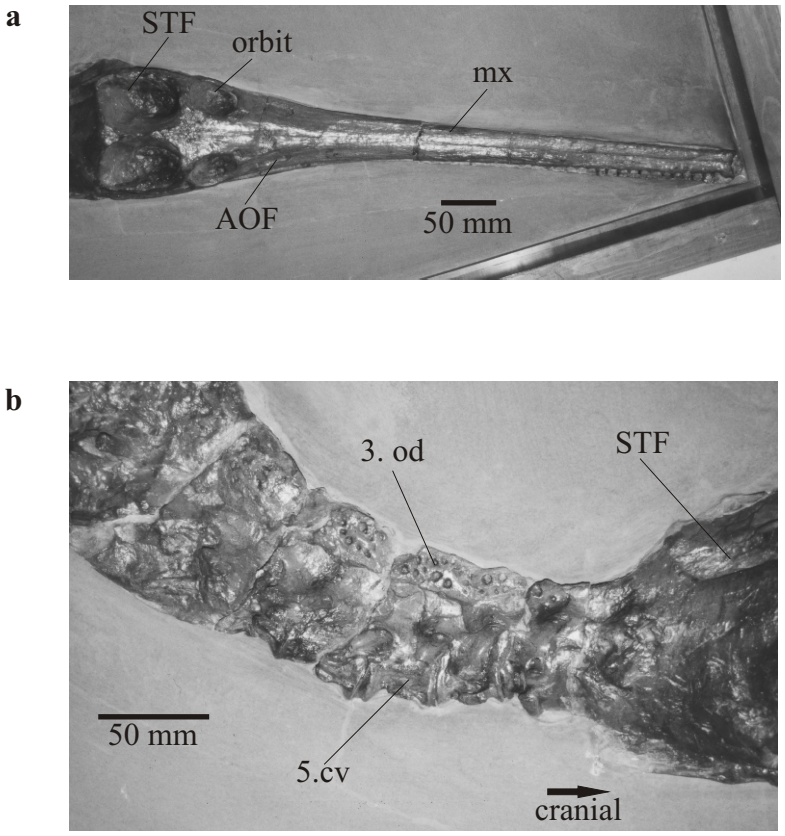

Figure 3.20a-b: Photos of the holotype of *Steneosaurus gracilirostris* (BMNH 14372). **3.20a-**Skull in dorsal view. **3.20b-**Cervical column posterior to the skull. Scale bars are 50 mm. The preservation is poor and the vertebrae are partly covered by dorsal osteoderms. Abbreviations: cv-cervical vertebra, AOF-antorbital fenestra, mx-maxilla, STF-supratemporal fenestra, od-osteoderm.

Laterosphenoid (lsp, Fig. 3.19a)

The laterosphenoid lies ventrally below the frontal and is probably fused dorsally to it. A clear frontolaterosphenoidal suture is not visible. Posteriorly, it contacts the prootic and ventrally the quadrate. The presumed contact to the pterygoid or the basisphenoid is too badly preserved to be determined. The shape and position of the laterosphenoid is similar to the laterosphenoid described for *Steneosaurus bollensis* (see chapter 3.1).

Mandible (Lower jaw)

The general structure of the mandible is similar to *Steneosaurus bollensis*, even though not all the parts of the mandible are visible in *Steneosaurus gracilirostris*. Because of the compressed mandible in BMNH 15500, a mandibular fenestra is not visible. The course of the sutures in the mandible remains uncertain. A description of the surangular, angular and articular is not given because of the insufficient preservation of these bones.

Dentary (d)

The general shape of the dentary is very similar to other teleosaurids. The anterior 70% of the dentary is firmly connected to the contralateral dentary forming a long symphysis. In the anterior 50% of the dentary, its cross-section is wider than high and increases suddenly in height posterior to the symphysis like in *Steneosaurus bollensis* (see chapter 3.1). The dentary of *Steneosaurus gracilirostris* shows at least 48 alveoli but the preservation is poorly in the posterior part and up to 12 more alveoli are expected. The lateral margin of the dentary slightly undulates. Slight lateral concavities at the lateral margin indicate the positions of the alveoli. At the level of the third dentary tooth (counted from anterior), there is a concavity, which inhabits the enlarged third tooth socket. The alveoli are not visible in lateral view.

Dentition

In the upper jaw, there are at least 48 teeth with an estimated maximum of 60 teeth on each side. The mandible very likely possesses the same number of teeth (see paragraph "dentary"). The estimated high tooth count differs from other Liassic teleosaurids. Circular, dorsoventrally orientated alveoli of equal size, lie in a straight row at the lateral margin of the maxilla separated by an interalveolar space about two-thirds the size of the alveoli. The teeth in the upper jaw only reach up to the level of the antorbital fenestra. The dentition code is: $\frac{3+45-57}{48-60}$.

Tooth morphology

The tooth crowns are very slender, conical, pointed, and apically recurved. They bear fine vertical striations on their surface and sometimes a very faint anterior and posterior carina. Nothing distinguishes these teeth from those of *Steneosaurus bollensis* (see chapter 3.1 and chapter 8).

Pattern of dentition

The pattern of dentition is different from *Steneosaurus bollensis* (see chapter 3.1). Almost every alveolus in the upper and lower jaw bears a tooth and the teeth are homogenously developed. The slender teeth stand vertically aligned and the teeth in the upper jaw obviously formed a rake with the teeth in the lower jaw. An enlarged third tooth is not exposed in the premaxilla, but expected in the dentary, because of the enlarged third alveolus.

Postcranial elements

Only parts of the postcranial skeleton are preserved in BMNH 14972. Of the vertebral column, almost half of the caudal vertebrae are missing.

According to WESTPHAL (1962), the vertebral column is preserved until the 26th caudal vertebra. However, the preservation of the postcranial material is poor and probably parts of the caudal column were added during preparation. Therefore, the number of caudal vertebrae is considered as uncertain, as is the measurement of the limb bones. The dermal armour is only partly preserved until the level of the fifth caudal vertebra.

The axial skeleton

Armour

In BMNH 14792, one longitudinal row of the dorsal armour and parts of one longitudinal row of the ventral armour are preserved. The dorsal armour must have consisted of two longitudinal rows of osteoderms, which reached the basal five to ten caudal vertebrae at least. In BMNH 14792, the dorsal armour extends along the entire length of the cervical column as well as over the thoracic column and the tail base (Fig. 3.20). The external surface of the dorsal osteoderms is sculptured by large, deep pits, which are regularly distributed. The osteoderms are only slightly wider than long and have a straight medial and a convex lateral margin. The anterior margin of the osteoderms in *S. gracilirostris* is straight and does not

possess an anterolateral peg. Thus, the osteoderm shape differs distinctly from that of *Steneosaurus bollensis* (see chapter 3.1 and 4).

Vertebral column (Fig. 3.20b)

Including the atlas-axis complex, there are nine cervical vertebrae in *S. gracilirostris*, which is typical for teleosaurids. An exception is *Pelagosaurus typus*, which has only eight cervical vertebrae (see chapter 3.5). The exact count of thoracic, lumbar, and sacral vertebrae is uncertain due to the overlying dorsal osteoderms and the poor preservation. Probably the basal 26 caudal vertebrae are preserved. At least 12 thoracic vertebrae bear a pair of thoracic ribs, which lies within the range of the number of thoracic ribs described for other teleosaurids (see chapter 3.1 & 4).

Limbs

The fore limbs are definitely smaller than the hind limbs. Parts of the right limbs are preserved in BMNH 14792, but the poorly preserved humerus, femur, and tibia should not be used for a definite comparison. Nevertheless, according to WESTPHAL (1962) and GODEFROIT (1994) the average ratio of the humerus length to the femur length is 72% in *Steneosaurus gracilirostris*, which differs from the average ratio in *Steneosaurus bollensis* (62%) and *Pelagosaurus typus* (53.4%) (see also chapter 5).

3.3 Osteology of *Steneosaurus brevior* (BLAKE 1876 ex Owen MS.)

3.3.1 Introduction

Steneosaurus brevior was first described in detail by TATE & BLAKE (1876) and later revised by WESTPHAL (1962). It was so far only known from English deposits. However, specimen UH 7 from Holzmaden, formerly labelled as *Steneosaurus chapmanni*, which is according to WESTPHAL (1962), synonym with *Steneosaurus bollensis*, is here referred to *Steneosaurus brevior*, too. It is housed in the Urweltmuseum Hauff (UH) and is the first record of *Steneosaurus brevior* outside of England.

Because the general appearance of all *Steneosaurus* taxa is similar, a detailed description of *Steneosaurus brevior* is not provided here, but it is referred to the detailed description of *Steneosaurus bollensis* (see chapter 3.1). In the following, a character diagnosis and a description of the unique features of *Steneosaurus brevior* as well as a short comparative description of specimen UH 7 is presented.

Eureptilia OLSON 1847
Diapsida OSBORN 1903
Mesoeucrocodylia WHETSTONE & WHYBROW 1983
Thalattosuchia FRAAS 1901
Teleosauridae GEOFFROY 1831
Steneosaurus brevior (BLAKE 1876 ex OWEN MS.)
(Figures 3.21-3.23)

Holotype: BMNH 14781
Locus typicus: Whitby, Yorkshire, Great Britain
Stratum typicum: Upper Liassic, Lower Toarcian, Alum Shale Series

3.3.2 Material

In total **9** specimens referred to *Steneosaurus brevior* were investigated. **8** specimens from BMNH and **1** specimen from UH. There are only few specimens, which can be referred to *Steneosaurus brevior* with certainty: the holotype BMNH 14781, BMNH 756, and BMNH 20691 (TATE & BLAKE 1876, WESTPHAL 1962, BENTON & TAYLOR 1984, VIGNAUD 1995). In

addition, one skull (specimen UH 7) of the Liassic deposits of Holzmaden is now referred to the taxon *Steneosaurus brevior*. Other specimens such as BMNH 14436, BMNH 39154, BMNH 5325, and BMNH 33095 are tentatively referred to *Steneosaurus brevior* with reservations, because most of the diagnostic characters are missing.

3.3.3 Locality and horizon

The taxon *Steneosaurus brevior* is known from the Liassic layers of Whitby, Great Britain and from the Liassic of Holzmaden, Germany. TATE & BLAKE (1876) referred the specimens of *Steneosaurus brevior* from Whitby to the zone of *A. serpentinus*. According to WESTPHAL (1962), the zone of *Hildoceras serpentinum* is synonymous to the Jet Rock Series. VIGNAUD (1995) notes additionally that the specimens are from the Toarcian, in particular the Jet Rock Series of Whitby. BENTON & TAYLOR (1984) mention that some specimens of *Steneosaurus brevior* come from the bituminous shales of the Jet Rock Formation, which is correlated with the ammonite zone of *Harpoceras falciferum.*

3.3.4 Preservation

The holotype BMNH 14781 is a nearly complete three-dimensionally preserved skull that is only slightly compressed. Specimen BMNH 756 is a partially preserved three-dimensional skull, the anterior 90% of the rostrum and parts of the lateral margins of the supratemporal fenestrae are missing, but the rest of the cranial table and the palatines, pterygoids, ectopterygoids, and basisphenoid are well preserved. BMNH 20691 consists of a 126 mm long fragment of the anterior part of the mandible. It shows the anterior spoon-shaped enlargement of the paired dentary and the anterior eight alveoli on each dentary are exposed. BMNH 39154 consists of three lower jaw fragments, which look very similar to BMNH 20691 (see paragraph “dentary’); therefore it will also be referred to *Steneosaurus brevior*.

The specimens UH 7 is preserved in black shales from Holzmaden. The overlying strata dorsoventrally compress it, but the bones in the skull are mostly intact and articulated. UH 7 consists of a skull with one mandibular ramus exposed in dorsolateral view, but the palate of this specimen is obscured by matrix and no data can be given for it. Furthermore, it possesses the anterior five cervical vertebrae with ribs, but apart from that, there is no further postcranial material certainly referable to *Steneosaurus brevior*. All other specimens only consist of the skull or skull fragments, therefore the taxon can be only partly described on the base of the skull material.

3.3.5 Diagnosis (Fig. 3.21-3.23)

Because the taxon *Steneosaurus brevior* is only known from skull material, all diagnostic characters are restricted to the skull. No diagnostic postcranial material is known; as a result, the total body length can only be estimated by using the skull length as an indicator. The largest known skull of *Steneosaurus brevior* is about 900 mm long; supposing similar body-skull proportion like in *Steneosaurus bollensis*, the total body length is estimated to 4.5 meters. *Steneosaurus brevior* has a broader and more robust skull than *Steneosaurus bollensis* or *Steneosaurus gracilirostris*. The ratio of skull width (C) to skull length (A) in *Steneosaurus brevior* is in average 33%. In *Steneosaurus bollensis,* it is 27-30% and in *Steneosaurus gracilirostri*s, it is only 20% (see chapter 4). The rostral length (B) is about 65% of the total skull length (A). In *Steneosaurus bollensis* and *Steneosaurus gracilirostris*, the ratio is between 71% and 76% (see chapter 4 & 5). The external naris opens anteriorly. The antorbital fenestra of *S. brevior* is about as large as that of *S. gracilirostris*. The orbits are circular and not longitudinal as in *S. bollensis.* The rectangular supratemporal fenestrae are elongated and large compared to the skull length (about 18.8% of the skull length).The teeth are robust and not as slender as in *Steneosaurus bollensis* or *Steneosaurus gracilirostris*. In *Steneosaurus brevior,* the number of alveoli in the rostrum varies from 23 to 30. In the palate, the paired palatine separates the maxillae in their posterior half.

Diagnosis of specimen UH 7 (Fig. 3.21)

The following features of specimen UH 7 are diagnostic for the taxon *Steneosaurus brevior*. UH 7 has a very robust and relatively short rostrum (about 69 % of the skull length), large supratemporal fenestrae (~ 18.7% of the skull length), a broad, robust skull with a cranial width being 33% of the skull length, and smaller, rounder orbits than *Steneosaurus bollensis* and its external naris opens pretty much anteriorly. The generally robust appearance of the skull and the biometric measurements are unlikely for *Steneosaurus bollensis* and are more suitable for *Steneosaurus brevior* (see chapter 4 “Intraspecific variation & Biometric data” for further discussion). The specimen UH 7 is therefore the first *Steneosaurus brevior* specimen described from deposits outside England.

3.3.6 Osteology

Skull (Fig. 3.21 - 3.23)

The general skull shape and ornamentation of the cranial bones is very similar to the one described for *Steneosaurus bollensis* (see chapter 3.1)

However, the skull is slightly broader than in *Steneosaurus bollensis*. It is characterised by a less elongated robust rostrum, which has distinct enlargement of the paired premaxilla, with an anterodorsal aligned external naris. Relatively small, round orbits, relatively large supratemporal fenestrae and distinct antorbital fenestrae are as well clearly different from the conditions of *Steneosaurus bollensis*. Furthermore, some differences in the palate are observed. Compared to *Steneosaurus bollensis* for example the internal naris is much larger and probably deeper, the suborbital fenestra is narrower and more drop-shaped, and the palatines projecting more deeply between the maxillae (see paragraph "palatine").

Cranial table

Openings

External naris (en, Fig. 3.21-3.23)

The external naris is transverse oval, with a small medial notch at the anterior and posterior margins. The premaxilla encloses the external naris completely, like in all teleosaurids. The shape is also common among steneosaurs, but the mainly anterior orientation of the external naris with a short and low anterior narial wall is only found in *Steneosaurus brevior* and *Steneosaurus gracilirostris.* The dorsal outline of the external naris forms an angel of about 70° (W1) with the horizontal plane of the floor of the external naris.

Antorbital fenestra (AOF, Fig. 3.21-3.23)

Like in *Steneosaurus gracilirostris* (see chapter 3.2), the antorbital fenestra in *Steneosaurus brevior* is well visible and large with an anteroposterior length of 22 mm and a dorsoventral height of 8 mm in BMNH 756.

According to TATE & BLAKE (1876), the antorbital fenestra should be bordered by jugal, maxilla, and nasal. However, the reinvestigation of these specimens shows that the posterior margin of the antorbital fenestra is formed by the lacrimal, the ventral margin by the jugal, and the anterior and parts of the dorsal margin by the maxilla. The nasal has at least no external contact to the antorbital fenestra like in all other Liassic teleosaurids. Specimen UH 7 does not show an antorbital fenestra, but there is a deep concavity at the posterior margin of maxilla and a small recess in the lacrimal, which most likely are the remnants of an antorbital fenestra (Fig. 3.21). The fenestra itself is not visible because of the compressed preservation.

Orbit (o, Fig. 3.21-3.23)

The margin of the orbit is formed by the lacrimal, prefrontal, frontal, postorbital, and by the ascendant dorsal process of the jugal. This coincides with the holotype (TATE & BLAKE 1876). The borders and the orientation of the orbit are identical to the configuration in *Steneosaurus bollensis.* However, the dorsally oriented orbit is almost circular and not ellipsoid as in *Steneosaurus bollensis*. The orbit is also very small compared to the supratemporal fenestra (e.g. BMNH 14436, BMNH 14781, BMNH 756, and UH 7). The ratio of the orbital length to the supratemporal fenestra length is only 42%, in contrast to an average of 55 % in *Steneosaurus bollensis* and 60 % in *Steneosaurus gracilirostris* (see also chapter 4 & 5).

Supratemporal fenestra (STF, Fig. 3.21, Fig 3.22)

The margin of the supratemporal fenestra is formed by the frontal, parietal, squamosal, and postorbital. The supratemporal fenestra differs not much from the typical teleosaurid conditions (see chapter 3.1). It is rounded rectangular in outline with a posterolaterally-elongated corner. The anteromedial and the anterolateral corners are right-angled whereas the posterolateral corner is acute angled and the posteromedial margin is rounded. The length of the supratemporal fenestra (D) is almost 19% of the skull length (A); therefore, it is the largest supratemporal fenestra among the Liassic teleosaurid taxa (see chapter 5). Specimen UH 7 possesses such a large supratemporal fenestra, which length is 18.7% of the skull length.

Infratemporal fenestra (ITF, Fig. 3.21, Fig. 3.23)

The infratemporal fenestra is bordered by the postorbital, squamosal, quadratojugal, and jugal similar to the conditions in *Steneosaurus bollensis*.

None of the specimens of *S. brevior* shows a complete, uncompressed infratemporal fenestra. Therefore, the length and height had to be reconstructed and is estimated in the lateral reconstruction of the skull (Fig. 3.23). However, in UH 7, the infratemporal fenestra can be confirmed as equally in length as the supratemporal fenestra (Fig. 3.21).

Cranial bones

Premaxilla (pmx, Fig. 3.21-3.23)

The premaxilla is preserved in BMNH 14781 and UH 7. The premaxilla is short and forms only the anterior 10-15% of the rostral length. In lateral view, the premaxilla inclines

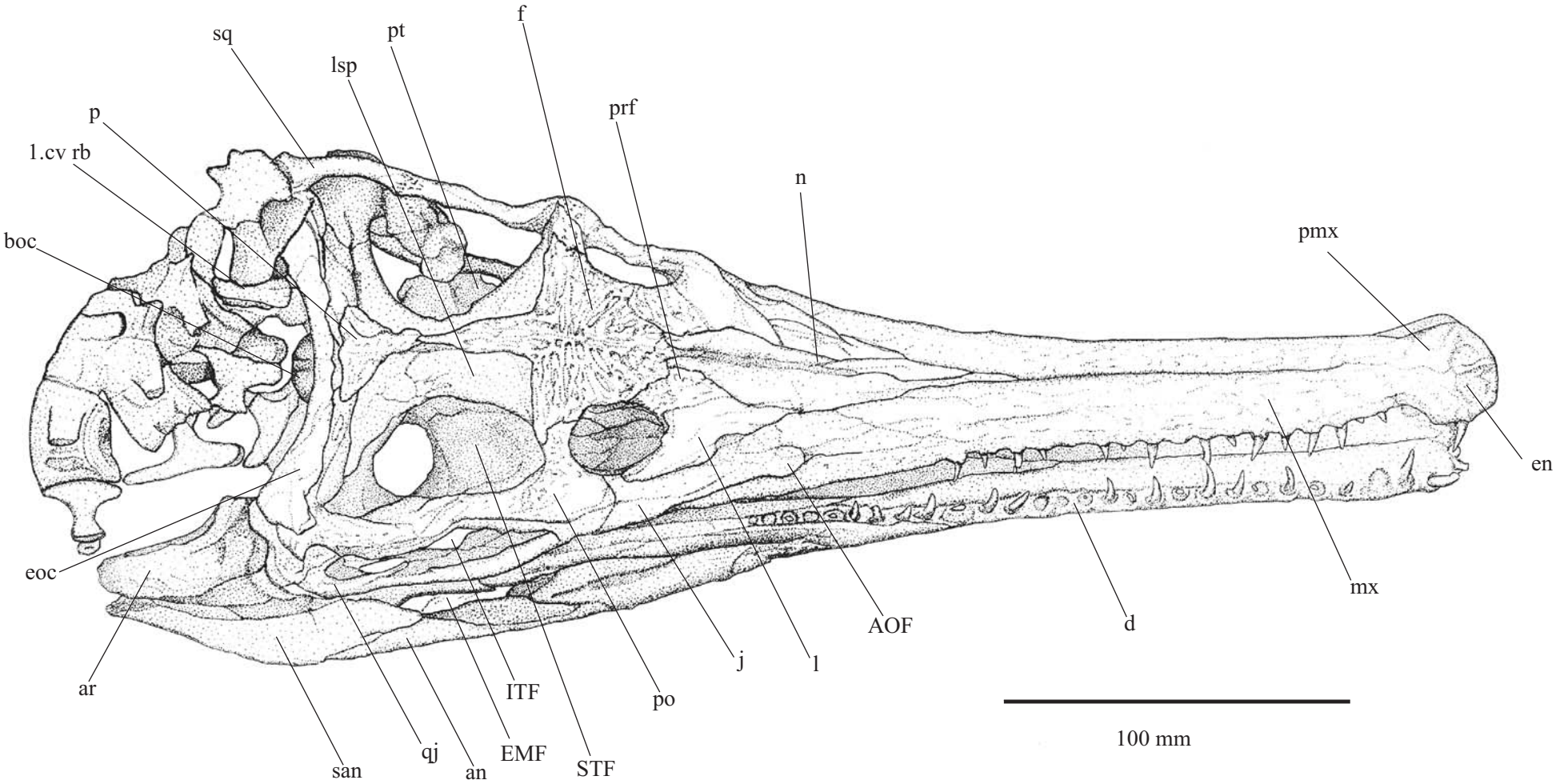

Figure 3.21: *In situ* drawing of *Steneosaurus brevior* (specimen UH 7). Skull in dorsolateral view with appending mandible and the anterior five cervical vertebrae. Abbreviations see chapter 2.

steeply in anterior direction, enclosing the external naris (Fig. 3.23). The contralateral premaxillae meet in a low median crest in the floor of the external naris. The paired premaxillae show a pronounced anterior enlargement, with a posterolateral notch at the lateral premaxillary-maxillary contact. The exact course of the dorsal premaxillary-maxillary suture is hard to determine, but it is supposed that the paired premaxilla probably projects posteriorly shortly between the maxillae like in other *Steneosaurus* taxa.

Maxilla (mx, Fig. 3.21-3.223)

The general shape and limiting bones are similar to the conditions described for *Steneosaurus bollensis* (see chapter 3.1). However, the anterolateral margin of the maxilla slightly undulates in lateral view (Fig. 3.23). Slight ventral convexities at the lateral margin of the maxilla indicate the position of the alveoli. In UH 7, 17 of those convexities are seen in the maxilla, marking the positions of the anterior 17 alveoli. However, up to 26 alveoli are reconstructed in the maxilla corresponding to the 29 alveoli visible in the dentary (for further explanation see paragraph “dentition”).

Nasal (n, Fig. 3.21 & Fig. 3.22)

The general shape and adjacent bones of the nasal are very similar to the conditions in *Steneosaurus bollensis* (chapter 3.1). Nevertheless, the paired nasal is relatively long with 40-45% of the length of the rostrum. The nasal length of *S. bollensis* is in average only 35% of the rostral length. The nasal in BMNH 14436 ends posteriorly level with the posterior margin of the prefrontal. In UH 7, the nasal terminates level with the middle of the prefrontal. In both cases, the nasal ends posteriorly on a level with the anterior margin of the orbit and does not extend further posterior as it does in *S. bollensis*.

Lacrimal (l, Fig. 3.21-Fig. 3.23)

The lacrimal is identical to that of *Steneosaurus bollensis* (see chapter 3.1), but differs in some cases in showing a shallow recess at its anteroventral margin, which forms the dorsal margin of the antorbital fenestra.

Prefrontal (prf, Fig. 3.21 &Fig. 3.22a)

The prefrontal is identical to that of *Steneosaurus bollensis* (see chapter 3.1).

Frontal (f, Fig. 3.21 & Fig. 3.22)

The general morphology (shape, borders, ornamentation) of the frontal resembles to that of *Steneosaurus bollensis*, but there are some minor differences:

The ornamentation on the external surface consists anteriorly of rounded pits and posteriorly the pits fuse to short transverse grooves. In addition, a shallow median groove runs in longitudinal direction on the external surface of the frontal. However, these differences in ornamentation of *S. brevior* are probably not diagnostic on its own, because of the observed broad intraspecific variability in the ornamentation of the frontal of *S. bollensis* (see chapter 4 & 5 for further discussion).

Parietal (p, Fig. 3.21 & Fig. 3.22)

The parietal is similar in shape and restriction to *Steneosaurus bollensis* (chapter 3.1), but its ornamentation is different. The ornamentation consists mainly of two large, ellipsoid pits on the posterodorsal, external surface of the parietal. The parietal is preserved in BMNH R 756, BMNH 14436, and UH 7.

Postorbital (po, Fig. 3.21-3.23)

The postorbital of *Steneosaurus brevior* has a very short anterior process compared to the anterior process of the postorbital of *S. bollensis*. Otherwise, the morphology of the postorbital is similar to that of *Steneosaurus bollensis* (see chapter 3.1).

Squamosal (sq, Fig. 3.21-3.23)

The squamosal is preserved in BMNH R 756, BMNH 14436, and UH 7. Even though the general shape and bordering bones of the squamosal are similar to *Steneosaurus bollensis*, some difference are visible.

The anterior process of the squamosal is slender and lacks the medial convexity seen in *S. bollensis* (see chapter 3.1). The ornamentation of the external surface of the squamosal is faint. The anterior process shows only few shallow pits on its external surface and on the posterior external surface of the squamosal, the pits are shallower and more widely distributed than in *S. bollensis*.

Jugal (j, Fig. 3.21-3.23)

Parts of the jugal are preserved in BMNH R 756, BMNH 14781, and UH 7. However, only UH 7 shows a complete jugal in dorsolateral view. Therefore, the reconstruction is

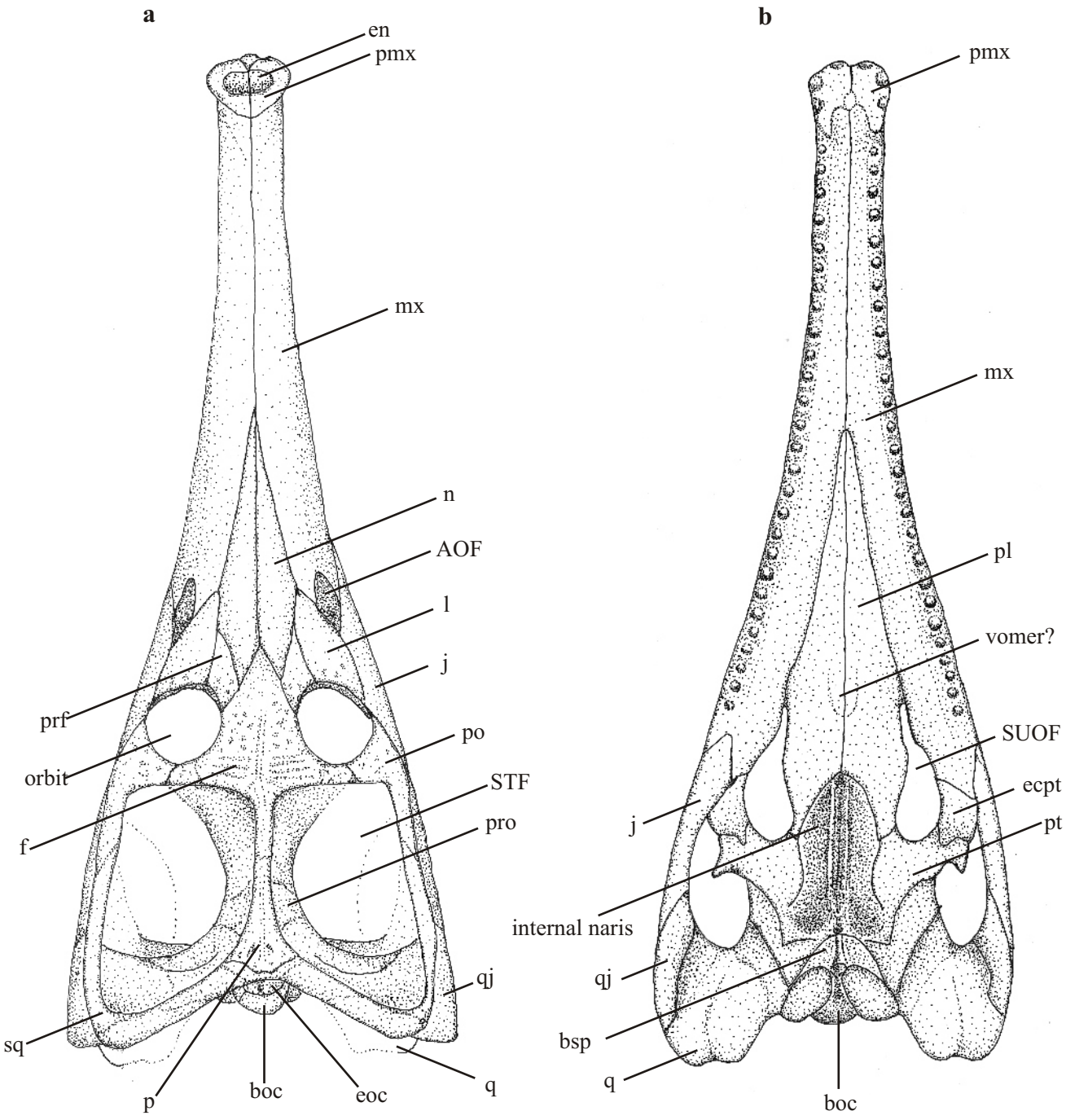

Figure 3.22a-b: Reconstruction of the skull in dorsal and ventral view of *Steneosaurus brevior* (after BMNH 14781 & BMNH 756). **3.22a-**Reconstruction of the skull in dorsal view. **3.22b**-The reconstruction of the skull in ventral view is mainly based on BMNH 756. For abbreviations, see chapter 2 .

mostly based on this specimen. Due to the deformation of the skull of UH 7, the exact outline of the margins remains unclear in the anterior part (Fig. 3.21). In the posterior part, the jugal is rod-shaped, forms the largest part of the ventral margin of the infratemporal fenestra, and contacts the quadratojugal posteriorly. Apparently, the bone resembles that of *S. bollensis*.

Quadratojugal (qj, Fig. 3.21 & Fig. 3.22)

The quadratojugal is only preserved in UH 7. Its shape coincides with the shape of the quadratojugal of *Steneosaurus bollensis* (see chapter 3.1).

Quadrate (q, Fig. 3.21-3.23)

The quadrate is only partially preserved in BMNH R 756 and UH 7 and the preservation is too poor for a detailed comparison. Concerning the adjacent bones, the topographical situation resembles that of *Steneosaurus bollensis*.

Palate (pa, Fig. 3.22b)

The reconstruction of the palate is mainly based on specimen BMNH R 756.
The palatinal premaxillary-maxillary suture is not completely preserved and its course in figure 3.22 is only being reconstructed according to that of other teleosaurids. The same holds true for the size and the bordering bones of the incisive foramen (Fig. 3.22b). The main differences in the palate of *Steneosaurus brevior* to *Steneosaurus bollensis* are that the palatines taper anteriorly more deeply between the maxillae (see paragraph “palatine”), that the secondary choana is larger with two longitudinal median crests in its roof (see paragraph "internal naris"), and that the suborbital fenestrae are smaller and drop-shaped (see paragraph "suborbital fenestra").

Palatal openings

Internal naris (in, secondary choanae, Fig. 3.22b)

The internal naris is larger and deeper than that of *S. bollensis*. Anteriorly, it is bordered by the palatines and posteriorly, it is enclosed by the pterygoids. The anterior margin of the internal naris is slightly pointed, but widens posteriorly. The pterygoids meet each other in a distinct median suture and form two parallel bony ridges in the roof of the internal naris, separated by a shallow median sulcus.

Suborbital fenestra (SUOF, Fig. 3.22b)

In ventral view, the suborbital fenestra is somewhat drop-shaped with a long, slender anterior notch. It is bordered anterolaterally by the maxilla, anteromedially by the palatine, laterally by the ectopterygoid, and posteriorly by the pterygoid. Anteriorly it ends approximate level with the posterior-most maxillary alveolus. It is much smaller and narrower than the supratemporal fenestra of *Steneosaurus bollensis*.

Premaxilla and Maxilla (Fig. 3.22b)

As described for *Steneosaurus bollensis* and *S. gracilirostris* the paired maxilla and premaxilla form most of the secondary palate. The contralateral maxillae meet each other in a straight median suture. Posteriorly, the medial margins of the maxillae diverge in their posterior half separated by the paired anterior process of the palatines. Anteriorly, the maxilla contacts the paired premaxilla, posteriorly it meets the jugal and the ectopterygoid. The alveoli lie along the lateral edge of the maxilla in a shallow longitudinal groove (see also paragraph “dentition”).

Pterygoid (pt, Fig. 3.22b)

The paired pterygoid has a somewhat butterfly-shaped structure similar to that of *Steneosaurus bollensis* (see chapter 3.1). The paired pterygoids meet each other in a median suture, forming two parallel longitudinal ridges (see paragraph “internal naris”). The anterior pterygoid wings are more slender than those of *S. bollensis*. They contact the ectopterygoids anterolaterally. The posterior pterygoid flanges are slightly broader than those of *S. bollensis* and form an oblique suture with the quadrates, which runs from anterolateral to posteromedial. Posteromedially, the pterygoid contacts the basisphenoid in a semicircular suture.

Ectopterygoid (ecpt, Fig. 3.22b)

The ectopterygoid is only poorly preserved in specimen BMNH 756 and UH 7. The exact shape remains therefore uncertain and could only be reconstructed tentatively (Fig. 3.22b). In ventral view, it is assumed roughly rectangular. Anteriorly, it contacts certainly the maxilla and the jugal and posteriorly, it contacts the pterygoid in a probably L-shaped suture.

Palatine (pl, Fig. 3.22b)

The palatines meet each other medially in a straight suture. The paired palatine tapers off anteriorly and reaches deeply between the contralateral maxillae until level with the 13th maxillary alveolus counted from anterior. Its posterior process laterally to the secondary choana is very short compared to *S. bollensis*. Laterally, the palatine forms the medial margin of the suborbital fenestra. Posterolaterally, the palatine contacts the pterygoid and posteromedially it forms the anterior margin of the secondary choana. Level with the anterior margin of the suborbital fenestra there lies a small depression at the median interpalatine suture. This depression may indicate the position of the vomer, but no further evidence is given.

Braincase (Fig. 3.21 & Fig. 3.22a)

The general features of the braincase are very similar to those of *Steneosaurus bollensis* (see chapter 3.1). However, there is a relatively large rectangular prootic similar to that of *Steneosaurus gracilirostris*, which is not seen in *Steneosaurus bollensis*.

Basioccipital (boc, Fig. 3.21 & 3.22)

The basioccipital are poorly and fragmentary preserved in BMNH R 756, BMNH 14781, and UH 7, therefore a detailed description is impossible. The occipital condyle and the ventral tuberosities are like those of *Steneosaurus bollensis*.

Exoccipital (eoc) & Opisthotic (op)

Only little information is available for the exoccipital-complex of *Steneosaurus brevior.* Like in *Steneosaurus bollensis*, the exoccipital is fused with the opisthotic and seems to have been similar in its topography, too.

Supraoccipital (soc)

The supraoccipital is poorly preserved. The outline in posterior view was most likely trapezoid. The supraoccipital is underlying the parietal and had a broad dorsal contact with it. Ventrolaterally, contact to the exoccipitals is expected but the exact course of the sutures is not identifiable.

Prootic (pro, Fig. 3.21 & Fig. 3.22b)

The exact course of the sutures is unclear, but an approximately rectangular prootic in the lateral braincase wall is preserved in BMNH R 756 and UH 7. It contacts the laterosphenoid and perhaps the frontal anteriorly, and the parietal and probably the squamosal posteriorly. A contact to the quadrate is not visible.

Basisphenoid and **parasphenoid (bsp, Fig. 3.22b)**

The basisphenoid is poorly preserved in BMNH R 756. Its exact shape is not preserved and a detailed description therefore impossible. The reconstruction in figure 3.22b is mainly an assumption, which is based on the basisphenoid of *S. bollensis*. However, it is bordered anteriorly by the paired pterygoid and posteriorly by the basioccipital. In ventral view, the basisphenoid is probably sub-triangular. On its ventral surface, the basisphenoid forms a median longitudinal ridge, which probably represents the wall of the median Eustachian canal.

Laterosphenoid (lsp, Fig. 3.21)

Poorly preserved laterosphenoids are visible at the specimens BMNH R 756, BMNH 14781, and UH 7. Like in *Steneosaurus bollensis*, the laterosphenoid is a large bone forming at least the anterior half of the lateral wall of the braincase. It probably fuses with the frontal anterodorsally, because a suture is not visible between them. In contrast, it contacts the prootic posteriorly in a straight vertical suture.

Mandible (lower jaw)

The mandible is partly preserved in specimens BMNH 14781, BMNH 20691, BMNH 39154, and UH 7. The reconstruction in lateral view of the mandible (Fig. 3.23) is combined from these specimens. Further mandibular fragments (BMNH R 282 (a), BMNH R 5325, and BMNH R 78) are too poorly preserved to be referred to *Steneosaurus brevior* with certainty, and therefore are not considered here.

External mandibular fenestra (EMF, Fig. 3.21 & Fig. 3.23)

The external mandibular fenestra is preserved in specimen UH 7 and BMNH 14781. The external mandibular fenestra is bordered anteroventrally by the dentary, posterodorsally by the surangular, and posteroventrally by the angular like in *Steneosaurus bollensis* (see

chapter 3.1). It is much smaller than in *S. bollensis* having only half the size of the infratemporal fenestra (Fig. 3.23).

Dentary (d, Fig. 3.21 & Fig. 3.23)

The right mandibular ramus is only entirely preserved in UH 7(Fig. 3.21). However, the posterior part of the dentary is broken in this specimen. The other specimens BMNH 20691 and BMNH 39154 are missing the posterior part of the mandible. Therefore, nothing definite can be said about the angular-dentary suture.

The general appearance of the dentary does not differ much from that of *Steneosaurus bollensis*. Anteriorly, the dentary meets its opposite in a long symphysis, which extends for half of the dentary length level with the 13th dentary tooth (counted from anterior). At the tip of the snout, the contralateral dentaries form a distinct spoon-shaped enlargement. Posteriorly, the dentary meets the splenial medially and the surangular and angular laterally. In cross-section, the paired dentary possesses a convex ventral margin and a concave dorsal margin. The dentaries meet each other dorsally in a shallow median groove.

In contrast to *Steneosaurus bollensis*, there is in *S. brevior* a deep medial notch between the dentaries level with the first alveolus in dorsal view (BMNH 20691, BMNH 39154, and UH 7). In lateral view, the tip of the dentary is slightly curving dorsally at an angle of about 15 degrees. Contrary to *Steneosaurus bollensis*, the first and second alveoli in the dentary of *Steneosaurus brevior* are inclined anterolaterally. The third alveolus is the largest alveolus in the dentary. The third alveolus is longitudinally elliptic in outline and dorsally orientated. In BMNH 20691, the third alveolus is 15 mm long and 10 mm broad. By contrast, in UH 7, the third alveolus is not enlarged but partly confluent with an additional fourth alveolus. Even though teeth three and four were probably separated from each other (see also 'dentition'). In lateral view, the dentary shows at the level of the third tooth a strong convexity in dorsal direction, which contains the enlarged third alveolus (Fig. 3.23). In dorsal view, the lateral margin of the dentary undulates slightly, and shows small interalveolar concavities.

Splenial (sp, Fig. 3.21)

Position and shape of the splenial are likely to resemble that of *Steneosaurus bollensis* (see chapter 3.1). However, only fragments of the splenial are preserved in *Steneosaurus brevior.* Specimen BMNH R 282 (a) (cf. *Steneosaurus brevior*) consists of a posterior symphysial fragment, in which the splenial participates. The splenial participates at the

symphysis in UH 7, too, but the upper jaw obscures the posterior topography of the symphysis. Thus, no exact sutures or proportions are available for it.

Angular (an, Fig. 3.23)

The angular is a slender bone located in the posteroventral part of the mandible. The general appearance and position of the bone is similar to *Steneosaurus bollensis*. In UH 7, it forms the ventral margin of the external mandibular fenestra and posteriorly, it expands ventrally below the surangular.

Surangular (san, Fig. 3.23)

The surangular is an elongated slender bone, which posteroventrally contacts the angular, posterodorsally the articular, and anteriorly the dentary like in *Steneosaurus bollensis*. Because of the poor preservation of the surangular, in all specimens of *Steneosaurus brevior*, diagnostic features are not visible, but the surangular morphology is probably similar to that of *Steneosaurus bollensis*.

Articular (ar, Fig. 3.21 & Fig. 3.23)

The articular together with the posterior part of the surangular forms an elongated retroarticular process, similar to the one observed in *Steneosaurus bollensis* (chapter 3.1). Only specimen UH 7 shows a complete articular in dorsolateral view and no differences to the conditions in *S. bollensis* is recognized.

Dentition

There are three alveoli in the premaxilla, probably 25 in the maxilla and 25-30 in the dentary. In specimen UH 7, 15 teeth in the maxilla are visible, but up to 25 teeth are supposed, because of the corresponding teeth in the mandible. Therefore, the maximum number of teeth in the upper jaw is estimated to 28 at each side (3 pmx + 25 mx). This number ranges within the specifications for the tooth count of *Steneosaurus bollensis*; and thus is undiagnostic on its own.

In the lower jaw, the estimated tooth count varies from 25 to 30 e.g., in specimen UH 7 at least 29 alveoli are counted. The variation in the tooth count within the *Steneosaurus* taxa will be further discussed in chapter 4 & 5.

The tooth morphology is similar to that of *Steneosaurus bollensis*, but the tooth crowns are slightly thicker and shorter.

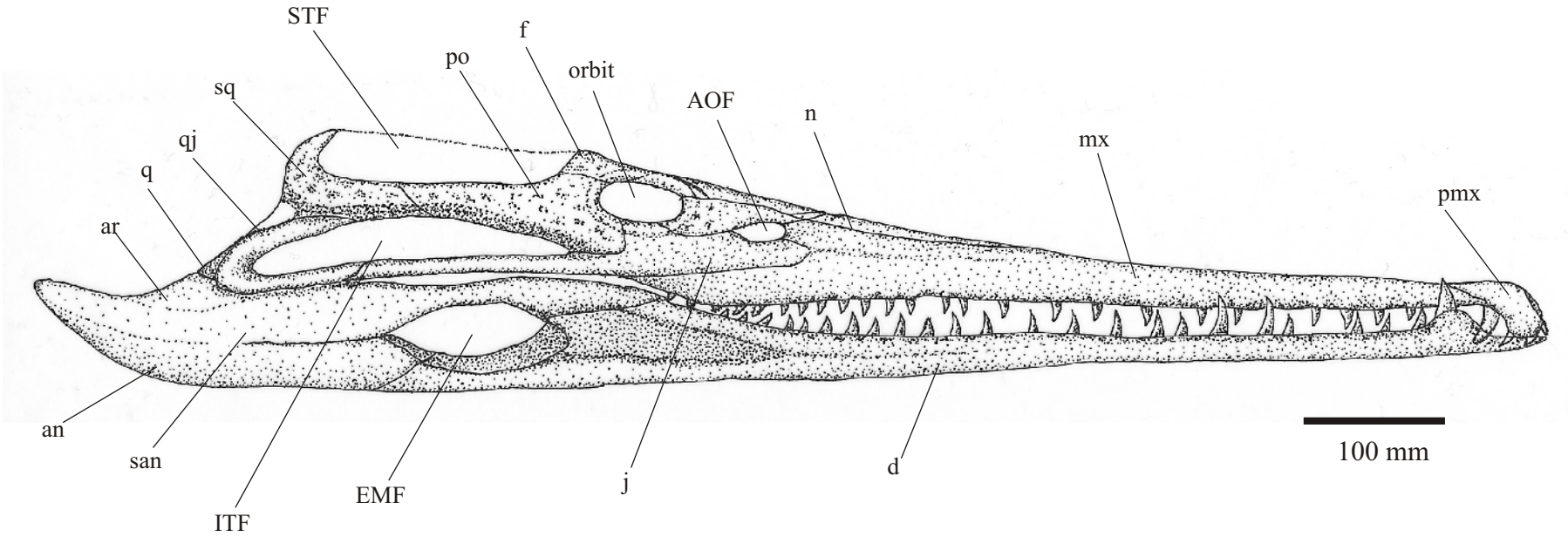

Figure 3.23: Lateral restoration of *Steneosaurus brevior* after the specimen BMNH 14781 (modified after TATE & BLAKE 1876) Abbreviations see chapter 2.

In the maxilla and dentary of UH 7, fully erupted teeth alternate with replacement teeth or empty alveoli (Fig. 3.21).

Postcranial material (Fig. 3.21)

The only postcranial material, which is referred to *S. brevior* with certainty, are the anterior-most five cervical vertebrae with associated ribs of specimen UH 7.

Cervical vertebrae and ribs (Fig. 3.21)

The atlas-axis complex is diagenetically compressed and partly obscured by ribs and the exoccipital-opisthotic complex. Therefore, it does not provide any diagnostic features. The remaining three cervical vertebrae are diagenetically compressed in lateral direction as well, so that a detailed description is impossible. Fragments of the first or second elongated cervical rib are also preserved, as well as four double-headed cervical ribs. The preserved and exposed parts of the cervical column do not show any significant differences to those described for *Steneosaurus bollensis* (see chapter 3.1). Size and general shape of the vertebrae and ribs are identical to those of other teleosaurids.

3.4 Osteology of *Platysuchus multiscrobiculatus* (BERCKHEMER 1928)

3.4.1 Introduction

Platysuchus multiscrobiculatus is a rare species of Jurassic crocodiles, which is exclusively known from the Lias ε of Holzmaden and Holzheim in South Germany. Until now only six specimens are known, which are certainly referred to *Pl. multiscrobiculatus*. The holotype SMNS 9930 is a well preserved, nearly complete skeleton (Fig. 3.23). It was first described by BERCKHEMER (1928) as *Mystriosaurus multiscrobiculatus*. Later WESTPHAL (1961) re-investigated the material and erected the new genus *Platysuchus*.

Because of the fact that BERCKHEMER (1928) and WESTPHAL (1962) mainly referred to the dermal armour as diagnostic for *Platysuchus multiscrobiculatus* and because of the discovery of two new specimens (UH 1 and UH 2) in the last years, an emended anatomical description of the taxon is now possible.

Eureptilia OLSON 1847
Diapsida OSBORN 1903
Mesoeucrocodylia WHETSTONE & WHYBROW 1983
Thalattosuchia FRAAS 1901
Teleosauridae GEOFFROY 1831
Platysuchus multiscobiculatus (BERCKHEMER 1928)
(Figures 3.24-3.34)

Holotype: SMNS 9930
Locus typicus: Holzmaden (BERCKHEMER 1929), Germany
Stratum typicum: Lias ε II, 6 (Lower Jurassic, Toarcian, Posidonia Shale)

3.4.2 Material

In total **7** specimens were investigated: **4** specimens housed in the SMNS: SMNS 9930, SMNS 50193, SMNS 15919b, and SMNS 15391. **1** specimens housed in the GPIT: GPIT Re 1193/16. **2** specimens housed in the UH: uncatalogued here UH 1 and UH 2. The specimen SMNS 15391 is only with reservations referred to *Platysuchus multiscrobiculatus*.
A complete list of all the investigated material is provided in the appendix I.

3.4.3 Locality and horizon

Platysuchus multiscrobiculatus is exclusively known from the Liassic layers (Toarcian) of Germany. The holotype SMNS 9930 was found in Holzmaden, Lias ε II, 6, South Germany (BERCKHEMER 1929). Specimens UH 1 and UH 2 were also found in Holzmaden in Lias ε, but the exact layers are unknown. The armour fragments of GPIT Re 1193/16 and SMNS 15919b were excavated in one piece in Holzheim near Göppingen (South Germany). The specimen was published under the name "Teleosauride von Holzheim" (BERCKHEMER 1928, 1929, WESTPHAL 1962). According to BERCKHEMER (1929), the material comes from the Lias ε II, 5 according to the stratigraphic order of HAUFF (1921). WESTPHAL (1962) refers these specimens to cf. *Platysuchus multiscrobiculatus* because of the similarities of shape and ornamentation of the osteoderms.

3.4.4 Preservation

All skeletons show the typical preservation of the locality of Holzmaden. The specimens are lying in a matrix of black shale (Posidonia Shale, Lias ε) and are compressed by overlying strata, but the bones are in most cases not broken.

Four almost complete skeletons including the skulls are preserved in dorsal view: two juvenile specimens (UH 2, Fig. 4.8 and SMNS 15391), and two adult specimens (SMNS 9930, Fig. 3.24 and UH 1, Fig. 3.25).

The palate is never exposed and the braincase is always diagenetically compressed in the skulls. The specimens UH 1 (Fig. 3.27), UH 2 (Fig. 4.8), and SMNS 9930 (Fig. 3.28) are well preserved, although dorsoventrally compressed. They are all more or less articulated and nearly complete except of some lacking or disarticulated parts of the limbs and the tail. In specimen SMNS 9930, the tail is completely preserved but the left manus is disarticulated and some phalanges and the carpus of the manus are missing (Fig. 3.24). The specimen UH 1 was only published as a photograph in the catalogue of the UH and not described before (HAUFF 1997). In specimen UH 1, only the anterior five caudal vertebrae are present (Fig. 3.25). Some parts of the pectoral and pelvic girdle are missing or not observable in both specimens (see paragraph "pectoral girdle" and "pelvic girdle"). The juvenile specimen UH 2 consists of a partial skeleton, which was recently found in Holzmaden (Fig. 4.8). In that specimen, only the anterior six caudal vertebrae are left and most of the fore limbs and parts of the hind limbs are missing. Of the fore limb only the left humerus, left ulna and one metacarpal is preserved. Of the hind limbs, both femora and the left tibia and fibula are preserved. The cervical column is disarticulated and two cervical vertebrae are missing. This specimen is a juvenile specimen and is further discussed in chapter 4 "Intraspecific variation and Biometric data".

The specimens SMNS 15919b (cast GPIT Re 1193/7a) and GPIT Re 1193/16 (cast SMNS 15919a) represent remains of one individual. GPIT Re 1193/16 is a fragment of the dorsal osteodermal shield, which also bears fragments of ribs, vertebrae, parts of the left fore limb (humerus, radius, and ulna), and the pectoral girdle. This specimen is described as the corresponding dorsal part to specimen SMNS 15919b (BERCKHEMER 1929, WESTPHAL 1962), which consist of parts of the ventral osteodermal shield (Fig. 3.29). Those armour fragments are nearly three-dimensional preserved.

3.4.5 Diagnosis

Platysuchus multiscrobiculatus is a medium sized teleosaurid with a maximum length of 3 meters. The general shape of *Platysuchus multiscrobiculatus* is similar to *S. bollensis*, but *Platysuchus multiscrobiculatus* is characterised by following features:

The skull is smaller than in *S. bollensis* and is only about 45% of the trunk length (TRL). The elongated rostrum possesses broadly enlarged premaxillae (see chapter 5). The circular to ellipsoid orbit opens in dorsal direction. All specimens show a direct contact between lacrimal and postorbital; therefore, the jugal is excluded from the lateral margin of the orbit. The orbital length (I) in adults is relatively small with 45% of the supratemporal fenestra length (D) (see chapter 4 & 5). The supratemporal fenestra length (D) is 15.6% of the skull length (A), but the supratemporal fenestra is only about one-third longer than broad (STF length (D)/STF width (E) ~1.45).

Pronounced ornamentation is present on the entire external surface of the prefrontals, lacrimals, postorbitals, squamosals, frontal, and parietal.

The vertebral column consists of about 64 amphicoelous vertebrae: nine cervical vertebrae, including the atlas-axis complex, 14 to 15 thoracic vertebrae, two to three lumbar vertebrae, two sacral vertebrae, and up to 38 caudal vertebrae.

The dorsal and a ventral osteodermal shield consist of deeply pitted osteoderms. The dorsal armour starts posterior to the atlas-axis complex, and runs in a longitudinal row of paired osteoderms caudally to the 26th caudal vertebra. However, posterior to the 18th caudal vertebra the longitudinal row consists only of single (and not paired) osteoderms. The ventral armour of the trunk consists of six longitudinal rows, each with a maximum of 18 single osteoderms. The tail possesses a ventral longitudinal row of paired osteoderms, which starts at the anterior third caudal vertebra and runs posteriorly to the 20th caudal vertebra. The posterior eight ventral tail osteoderms are probably unpaired, too.

The fore limbs are shorter than the hind limbs. The length of the humerus (H1) is 67.5%-72.5% of the length of the femur (Fe1) (see chapter 4 &5). The femur has a distinct

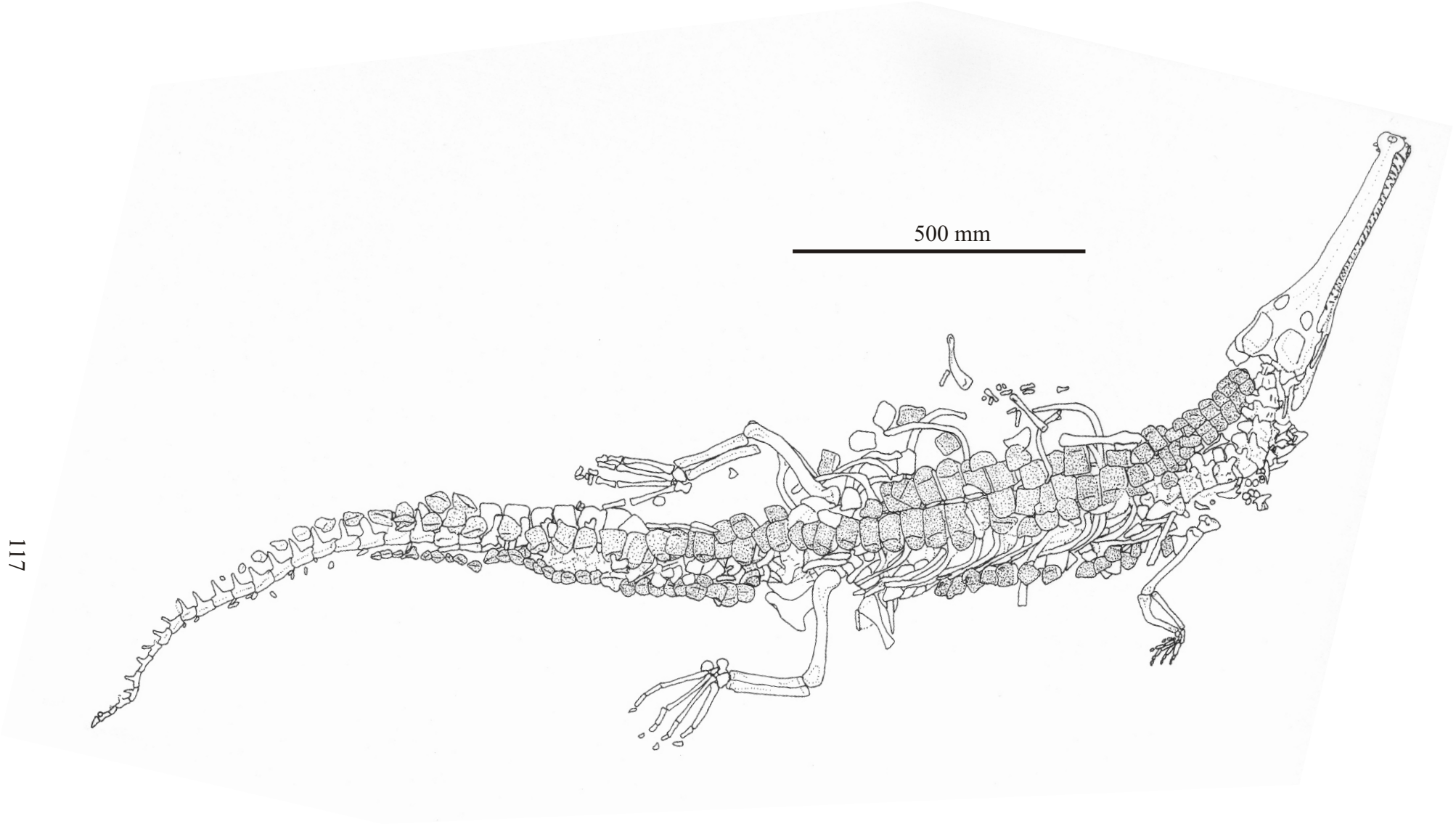

Figure 3.24: *In situ* sketch of SMNS 9930 (holotype of *Platysuchus multiscrobiculatus*). The skull is dorsalventrally compressed. Lateroventral to the cervical column some cervical ribs and some petrified tracheal rings are exposed. The left fore limb is disarticulated. The right fore limb is articulated, coracoid and scapula are present. The hindlimbs are well preserved, and the right ilium, ischium, and pubis are exposed. The dorsal armour is complete preserved. The ventral armour starts posterior to the coracoids at the level of the 11th vertebra. The tail is dorsally and ventrally heavily armoured until the 20th caudal vertebra.

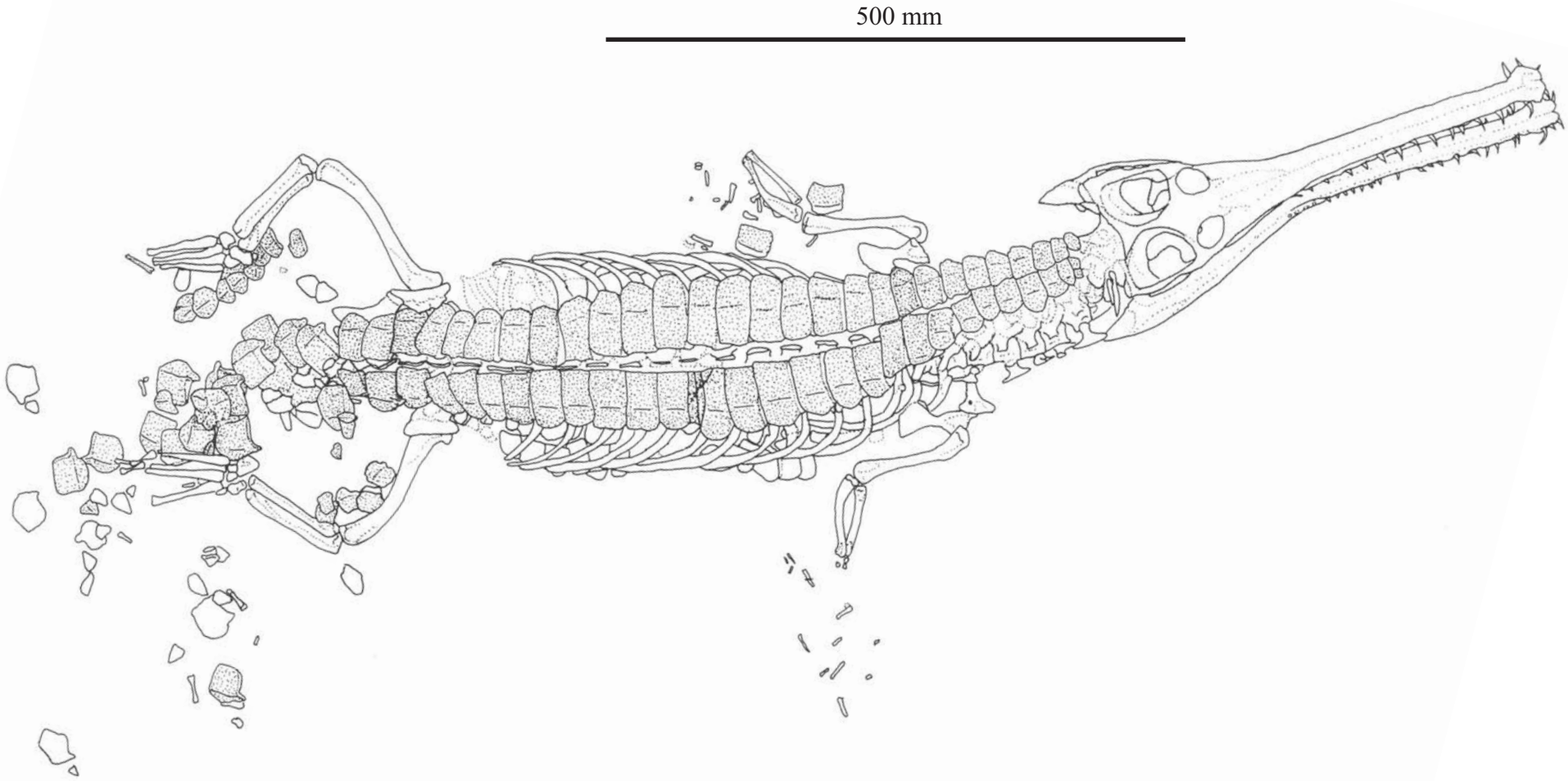

Figure 3.25: *In situ* sketch of the specimen UH 1 (*Platysuchus multiscrobiculatus*). The skull is completely preserved but dorsoventrally compressed. Both fore limbs are preserved, but the mani are disarticulated. Both scapulae and the distal part of the right coracoid are exposed. The 9th cervical rib is elongated, but do not yet show the usual thoracic rib shape. In the lumbar area faintly preserved elongated structures indicating gastral ribs. The dorsal armour is intact until the pelvic girdle. The main part of the caudal column is missing and only parts of the caudal armour are preserved. The ventral armour starts about the level of the 12th vertebra.

femoral head that fits well into the deepened acetabulum on the ilium. In addition, the ilium possesses a pronounced dorsal longitudinal iliac crest, which forms a distinct anterior and posterior process.

3.4.6 Osteology

Skull (Fig. 3.26-Fig. 3.28)

Like all other teleosaurid crocodiles, *Platysuchus multiscrobiculatus* has a very long and narrow snout, mainly formed by elongated maxillae. The rostral length (B) is in average 75% of the skull length (A). The dorsal anterior tip of the rostrum (~ 15%) is solely formed by the premaxillae similar to the conditions described for *Steneosaurus bollensis* and *Steneosaurus brevior*, but the premaxillae are more enlarged (see chapter 5). The skull widens into posterior direction posterior to the anterior margin of the nasals, and it reaches its maximum width at the posterior margin of the cranial table (Fig. 3.26). The cranial table is trapezoidal in shape, and the skull is very flat. The height of the skull (T) is about 15% of the skull length (A) (Fig. 3.26b). The external surface of parietal, frontal, prefrontals, lacrimals, squamosals, and postorbitals is ornamented by pits, while the surface of the nasals, maxillae, premaxillae, jugals, and quadratojugals is smooth. Shape and size of the pits are differently developed on the respective bones (see there). In specimen UH 1 a transverse break runs through the skull at the level of the orbits, therefore the ornamentation of the frontal is only partly preserved (Fig. 3.27). The orbits are sub-circular and open in dorsal direction. SMNS 9930 shows a small, collapsed antorbital fenestra (AOF) on the right side of the skull (Fig. 3.28).

For specific measurements of certain bones see the appendix II, and for further discussion of the biometric values of *Platysuchus multiscrobiculatus,* see chapter 4 & 5.

Cranial table

Openings

External naris (en, Fig. 3.26-Fig. 3.28)

The undivided margin of the external naris is formed by the premaxillae. The external naris is transverse ellipsoid, broader than long, and anterodorsally oriented. The posterodorsal side of the margin is smooth, while the anterior margin has a small indentation

at the premaxillary-premaxillary suture (in anterior view). The entire outline of the external naris has an angle of approximately 25° (W1) from posterior to the tip of the snout with the horizontal plane. At the floor of the external naris, the interpremaxillary suture is

marked by a median crest, which extends from the anterior margin posteriorly reaching the middle of the naris. There is an incisive foramen in the floor of the external naris.

Antorbital fenestra (AOF, Fig. 3.26-Fig. 3.28)

In the specimens, SMNS 9930 and UH 2 a very small, longitudinal slit-like depression indicates the antorbital fenestra. It lies between lacrimal, jugal and maxilla. The dorsomedial margin is formed by the lacrimal, which shows a shallow recess in all skulls. The ventrolateral margin is formed by the jugal and the anterior margin by the maxilla. Due to compression of the opening, its dimensions are not visible.

Orbit (o, Fig. 3.26-Fig. 3.28)

The anterior margin of the orbit is formed by the lacrimal and prefrontal. The medial margin is mostly formed by the frontal. The posterior margin is medially formed by the frontal and laterally by the postorbital. Laterally the orbit is bordered by the postorbital and lacrimal. The jugal is therefore excluded from the lateral margin of the orbit. The anterior margin is slightly reinforced by a small frill and, in some cases, shows a small recess at the lacrimal-prefrontal suture (see also paragraph “prefrontal”). The orbit is slightly ellipsoidal in shape. Its long axis extends from the lacrimal-prefrontal suture to the middle of the anterior margin of the postorbital. The orbit opens almost dorsally. In the adult specimens, the orbit is much smaller than the supratemporal fenestra (see paragraph "diagnosis"). The ratio between length and width of the orbit in comparison to the other skull measurements are described in detail and discussed in chapter 4 & 5. The typical juvenile characters of thalattosuchians in general are discussed in chapter 4.

Supratemporal fenestra (STF, Fig. 3.26-Fig. 3.28)

This large opening in the cranial table is rather elliptical than angular in shape. Its margin is composed anteromedially by the frontal, anterolaterally by the postorbital, posterolaterally by the squamosal, and posteromedial by the parietal. The anterolateral margin is angular, while all other parts of the margins are rounded. The sagittal crest consists of frontal and parietal. In the adult specimens SMNS 9930 and UH 1, a thin sagittal crest is developed between the supratemporal fenestrae (see the appendix II).

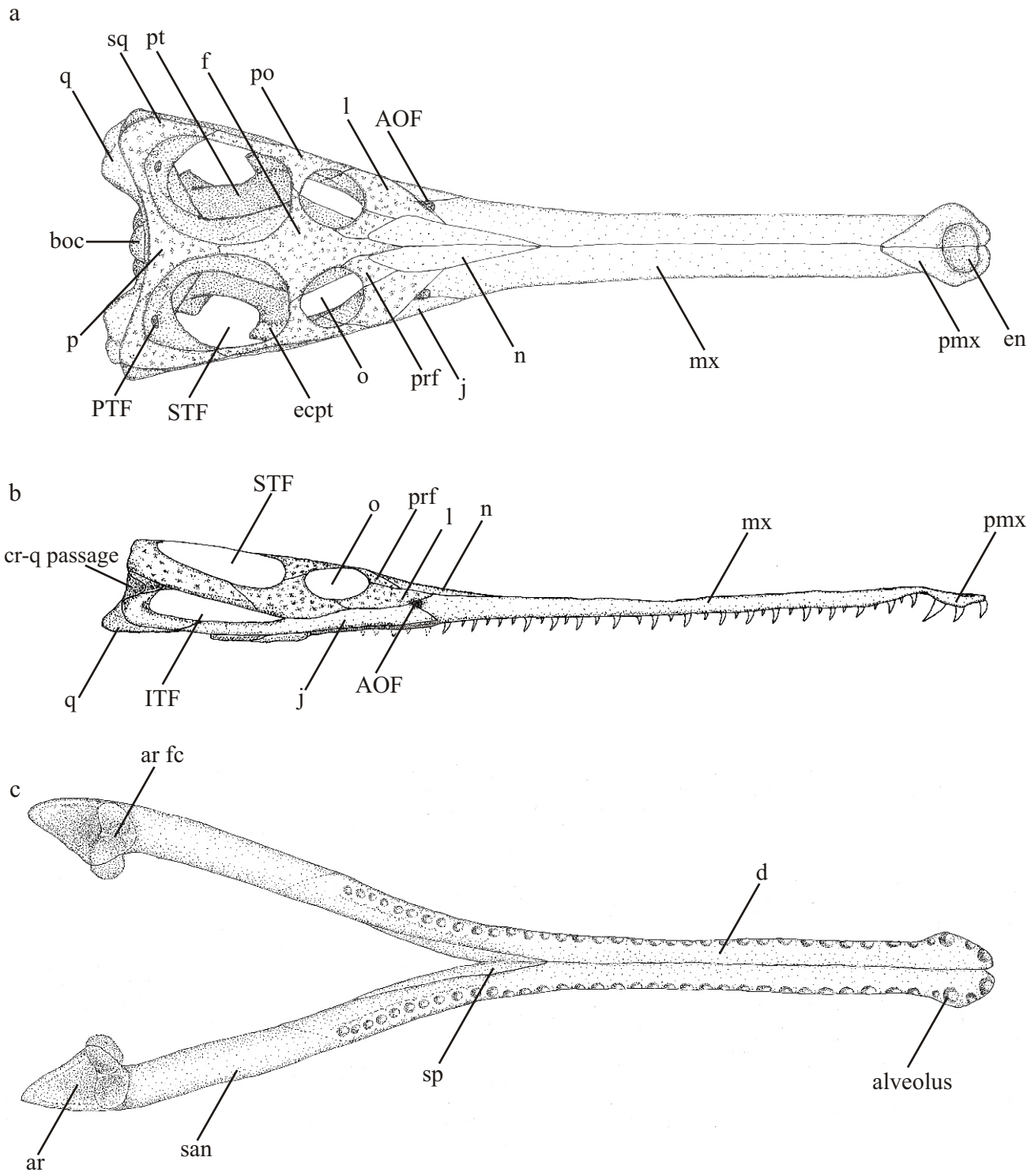

Figure 3.26a-c: The skull reconstruction of *Platysuchus multiscrobiculatus* is based on a wax model after SMNS 9930 and UH 1. **3.26a**-Skull in dorsal view. **3.26b**-Skull in lateral view. **3.26c**-Reconstruction of the lower jaw in dorsal view. Abbreviations: an-angular, AOF-antorbital fenestra, ar-articular, boc-basioccipital, d-dentary, eoc-exoccipital, f-frontal, EMF-external mandibular fenestra, j-jugal, l-lacrimal, lsp-laterosphenoid, mx-maxilla, n-nasal, p-parietal, pl-palatine, pt-pterygoid, po-postorbital, prf-prefrontal, PTF-posttemporal fenestra, q-quadrate, qj-quadratojugal, san-surangular, sp-splenial, sq-squamosal, STF-supratemporal fenestra, soc-supraoccipital.

Infratemporal fenestra (ITF, Fig. 3.26-Fig. 3.28)

This opening is hardly visible because of the dorsoventrally compression of the skulls in all respective specimens. In UH 1, the topography of the infratemporal fenestra is visible, but the original height of the opening is indiscernible (Fig. 3.27). Ventrally the infratemporal fenestra is bordered by jugal and quadratojugal. Quadratojugal and squamosal form its posterior margin. The dorsal margin is formed by squamosal and postorbital, and the anterior margin by the postorbital. The reconstruction of the skull suggests a longitudinal elongated opening, which is about four times longer than high (Fig. 3.26).

Cranial bones

Premaxilla (pmx, Fig. 3.26-Fig. 3.28)

The paired premaxilla is only exposed in dorsal view. It completely encloses the external naris (see above). At the floor of the external naris, the median straight interpremaxillary suture forms a median crest in its anterior half. Posterior to the external naris the premaxillae meet dorsally in a straight median suture. The external wall of the premaxillae is slightly undulated and a wide notch is developed posterior to the opening of the external naris. The premaxillae form a distinct spoon-shaped expansion at the anterior tip of the snout. Each premaxilla bears three teeth. The largest tooth is the third one (counted from anterior). It lies directly in front of the above-mentioned notch, which forms a diastema between the premaxillary and the maxillary dentition. At this notch, a lateral, obliquely suture runs between premaxilla and maxilla from anteroventral to posterodorsal, therefore the premaxilla overlays the maxilla at the diastema. In SMNS 9930 the fourth dentary tooth, counted from anterior, obviously fits the notch during jaw occlusion (Fig. 3.28). Posterodorsally the paired premaxillae deeply project between the maxillae in posteromedial direction, ending medially at the level of the third maxillary tooth (counted from anterior). The ventral premaxillary-maxillary suture is obscured by matrix in all specimens, and therefore cannot be described. The external dorsal surface of the premaxilla is smooth. Only the external lateral surface is slightly rugose.

Maxilla (mx, Fig. 3.26-Fig. 3.28)

The maxilla forms the largest part of the rostrum and probably of the secondary palate. The maxilla in all specimens is only exposed in dorsal view; therefore, no data can be given for the palate in ventral view. The lateral margin of the maxilla is nearly straight. Dorsally, it

meets in a straight median suture with the opposite maxilla. Posteromedially, the paired maxillae contact the paired nasals, which separate the maxillae in their posterior-most third. The maxillonasal suture is smooth and extends obliquely in mediolateral direction. Posteromedially, the maxilla is bordered by the lacrimal, which tapers off between the maxilla and the nasal. Posteriorly, the maxilla bifurcates in a dorsal and a ventral part. The dorsal part of the maxilla tapers posteriorly between lacrimal and jugal, while the ventral part of the maxilla posteroventrally descends below the jugal (Fig. 3.26b). The anterior-most fourth of the jugal extends dorsal to the posteroventral part of the maxilla up to the level of the anterior tip of the lacrimal. Anteriorly, the paired maxillae contact the paired premaxillae (see above).

The maxilla is tooth bearing and the number of alveoli ranges from 34 to 40 each (see also “dentition”). Because the maxilla is only preserved in dorsal view, the shape of the alveoli in the upper jaw is not visible. In lateral view, most alveoli contain fully erupted teeth. However, there are also teeth in an early growth stage in some alveoli, and some alveoli are empty. The dorsal surface of the maxilla is smooth. The lateral surface shows some delicate longitudinal wrinkles dorsal to the tooth bar.

Nasal (n, Fig. 3.26-Fig. 3.28)

The nasal is an elongated slender bone. It is anteriorly terminate in the posterior third of the rostrum. The lateral margin of the nasal is slightly externally convex, while the median suture between the contralateral nasals is smooth, straight and runs in the median line. Anteriorly and anterolaterally the nasal is bordered by the maxilla, anteromedially and medially by the opposite nasal, posterolaterally by lacrimal and the prefrontal, and posteromedially by the frontal. Anteriorly, the paired nasal deeply projects between the maxillae until circa the level of the 26th maxillary alveolus. Posteriorly, the frontal projects shortly between the nasals and separates them in their posterior fifth. The posterior margin of the nasal lies level with the anterior margin of the orbit. The surface of the bones is smooth and does not show any ornamentation in contrast to, e.g. the frontal or the lacrimal. Because of the compressed preservation of the skulls (SMNS 9930, UH 1, and UH 2) the posterolateral margin of the nasals are slightly obscured by the lacrimals. The lateral edge of the lacrimal is slightly diagenetically shifted dorsally over the posterolateral margin of the nasal and overlaps it.

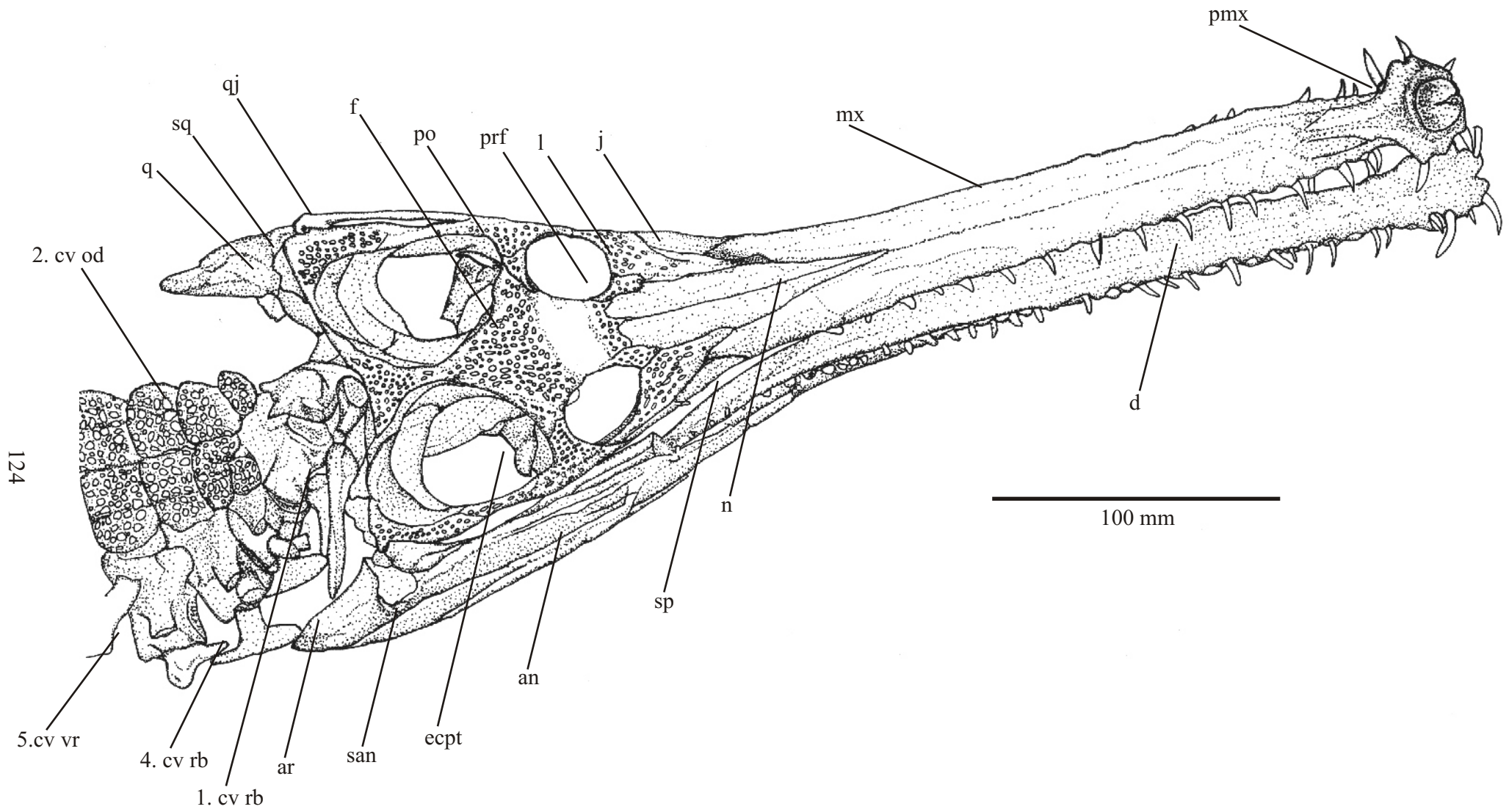

Figure 3.27: *In situ* drawing of the skull and part of the neck of *Platysuchus multiscrobiculatus* (specimen UH 1). The original skull length is 400 mm. Abbreviations see figure 3.26 and chapter 2.

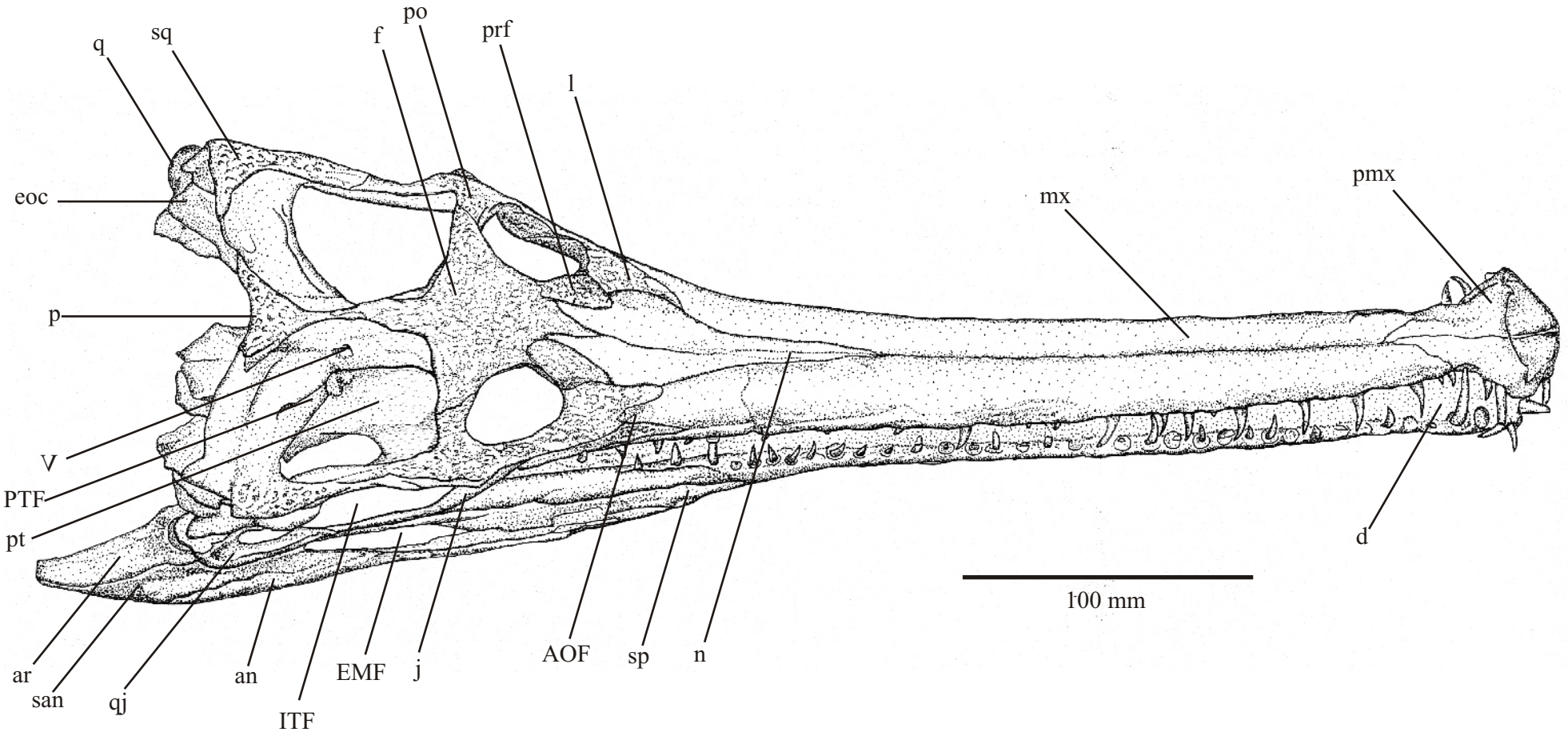

Figure 3.28: *In situ* drawing of the skull of *Platysuchus multiscrobiculatus* (holotype SMNS 9930). Ornamentation is visible on the frontal, lacrimal, parietal, prefrontal, and squamosal. An antorbital fenestra is exposed, but collapsed in dorsoventral direction.
Abbreviations: an-angular, AOF-antorbital fenestra, ar-articular, boc-basioccipital, d-dentary, eoc-exoccipital, f-frontal, EMF-external mandibular fenestra, j-jugal, l-lacrimal, lsp-laterosphenoid, mx-maxilla, n-nasal, p-parietal, pl-palatine, pt-pterygoid, po-postorbital, prf-prefrontal, PTF-posttemporal fenestra, q-quadrate, qj-quadratojugal, san-surangular, sp-splenial, sq-squamosal, STF-supratemporal fenestra, soc-supraoccipital, V-foramen for the trigeminal nerve (cranial nerve V).

Lacrimal (l, Fig. 3.26-Fig. 3.28)

The shape of the lacrimal is identical to the shape of the lacrimal of *Steneosaurus bollensis*, but in *Platysuchus multiscrobiculatus*, it shows a heavier ornamentation on its external surface. The lacrimal is a sub-triangular bone with a slender posterior process laterally to the orbit. Anterolaterally, the lacrimal contacts the maxilla and anteromedially the nasal. Medially, it has broad contact with the prefrontal in a straight longitudinal suture. Posteromedially, the lacrimal forms the anterior and anterolateral margin of the orbit. The posteromedial margin of the lacrimal is slightly thickened. Posterolaterally, the lacrimal is bordered by the jugal, and in the posterior part, it directly contacts the postorbital and thus excludes the jugal from the orbit. The posterior process of the lacrimal descends ventral to the anterior process of the postorbital. Both processes meet in a smooth oblique suture, which runs from anterodorsal to posteroventral. There is a recess at the anterolateral margin of the lacrimal, which indicates a rudimentary antorbital fenestra, formed by the lacrimal, the posteromedial margin of the maxilla, and the medial margin of the jugal (see paragraph “antorbital fenestra"). The distinct pattern of pits on the surface of the lacrimals consists mostly of small circular to ellipsoidal pits in a dense, nearly regular distribution. The density of the pits decreases slightly in anterior direction.

Prefrontal (prf, Fig. Fig. 3.26-Fig. 3.28)

The prefrontal is a heavily ornamented, roughly rhombic bone, which is only one-third the size of the lacrimal. Anterior it ends acute-angled between the lacrimal and the nasal. Anterolaterally the prefrontal meets the lacrimal in a straight suture, which runs slightly from anteromedial to posterolateral. The posterior 50% of the lateral margin of the prefrontal forms the anteromedial margin of the orbit. The posterior half of the lateral margin of the prefrontal is slightly thickened like the posteromedial margin of the lacrimal. Therefore, a small frill reinforces the anterior margin of the orbit (see there). In the two adult specimens (UH 1 and SMNS 9930), a small slit-like depression is visible in the anterior orbital margin at the suture between prefrontal and lacrimal, probably the aperture of the lacrimal duct (SHOEMAKER & NAGEY 1977). Anteromedially the prefrontal contacts the nasal, and posteromedially the frontal with its posterior third. The pattern of pits is similar to that of the lacrimal (described above).

Frontal (f, Fig. 3.26-Fig. 3.28)

The unpaired frontal is a rhombic bone, which forms a large part of the posteromedial surface of the cranial table. Its dorsal surface is heavily ornamented by a distinct pattern of pits. Anterolaterally, it contacts the prefrontals and anteromedially the nasals. As described above the frontal tapers anteriorly shortly between the nasals and separates them their posterior fifth. Posterolaterally, the frontal contacts the postorbitals, and posteriorly forms together with the parietal the sagittal crest. The frontal forms the medial and the posteromedial margins of the orbits. In addition, it forms the anteromedial margins of the supratemporal fenestra. Posteromedially, the frontal expands extensively and forms up to 50% of the sagittal crest. In dorsal view, the suture frontoparietal suture cannot be identified with certainty, because of the distinct external sculpturing on the surface of both bones. In lateral view, inside the supratemporal fossa, the frontoparietal suture runs obliquely from anteroventral to posterodorsal. In lateral view, the posterior end of the frontal overlays the parietal. The pattern of pits on the external surface of the frontal is nearly identical to the pattern on the surface of the prefrontal and lacrimal. It consists mainly of many regularly distributed small, circular pits. However, in the lateral parts of the frontal the transverse oval pits are sometimes confluent, and form in those cases short, shallow, delicate, transverse sulci (Fig. 3.28)

Parietal (p, Fig. 3.26-3.28)

The parietal is an unpaired triradiate bone of the cranial table. The parietal forms together with both squamosal the posterior margin of the cranial table. Posterolaterally, the parietal develops a slender process at each side, which contact the squamosals. Anteriorly, each lateral process of the parietal forms with the corresponding medial process of each squamosal the posterior margins of the supratemporal fenestrae (see above). The posterior margin of the entire margin of the parietal is externally shallowly concave (Fig. 3.26). In anteromedial direction, the bone contacts the frontal in another slender process and forms, in dorsal view, the posterior half of the sagittal crest. Anteriorly, the parietal contacts the frontal in an oblique suture, which runs in posterodorsal to anteroventral direction (see above). Ventrally, the parietal probably meets the laterosphenoid in an anteroventrally directed suture. In posterodorsal direction, the parietal is expected to overlie the supraoccipital, but this connection is not exposed in any of the investigated specimens (see also paragraph "supraoccipital"). Dorsally, the parietal possesses an ornamented surface. The ornamentation consists of a pattern of deep pits that is similar to that of the frontal. However, the pits on the

parietal are more spacious distributed. The pits in the center of the parietal are little deeper than the pits on the frontal. The depth of the pits declines on the lateral processes of the parietal.

Postorbital (po, Fig. 3.26-Fig. 3.28)

The postorbital of *Platysuchus multiscrobiculatus* is very similar in shape to that of *S. bollensis*. It is a triradiate bone at the lateral margin of the cranial table. It has three processes, one in anterior, one in posterior and one in dorsal direction. The anterior process of the postorbital tapers shortly between the lacrimal and the jugal and forms together with the posterior process of the lacrimal, the lateral margin of the orbit (see there). The posterior process of the postorbital adjoins the anterior process of the squamosal in a smooth, oblique suture that runs from anterolateral to posteromedial (in dorsal view). The dorsal process of the postorbital extends in medial direction, contacts the frontal in an oblique suture, which run from anteromedial to posterolateral. The dorsal process of the prefrontal forms anteriorly the posterolateral margin of the orbit and posteriorly the anterolateral margin of the supratemporal fenestra. The lateroventral margin of the postorbital forms the anterodorsal margin of the infratemporal fenestra. It is expected that the postorbital medioventrally contacts the ectopterygoid and the jugal, but the exact sutures cannot be identified, because of the compressed preservation and the dorsal preparation of the specimens. The postorbital possesses an ornamented external dorsolateral surface with a distinct pattern of small deep pits in a very dense distribution. Pronounced pits cover the anterolateral part and decline in posterior direction.

Squamosal (sq, Fig. 3.26-Fig. 3.28)

The squamosal is a large bone of the cranial table, which has its most extensive expansion in ventral direction. The cranial surface of the squamosal is L-shaped and heavily ornamented by a distinct pattern of pits. The squamosal forms the posterolateral margin and half of the posterior margin of the supratemporal fenestra. Anteriorly, it contacts the postorbital in an oblique, smooth suture, which runs from anterolateral to posteromedial (see paragraph “postorbital”). Posteromedially, it contacts the parietal in an oblique suture, which runs from anteromedial to posterolateral (in dorsal view). Posteroventrally, the squamosal has probably contact to the quadrate and the exoccipital and there is a contact to the quadratojugal, too. The squamosal and the quadratojugal form the posterior margin of the infratemporal fenestra as it is seen in SMNS 9930 (Fig. 3.26 & Fig. 3.28). Because of the

compressed preservation of all specimens, the exact run of the suture between the squamosal, the quadrate, and the exoccipital cannot be identified.

In specimen SMNS 9930 a possible posttemporal fenestra is preserved. The medial part of the anteroventral margin of the squamosal forms the dorsal margin of the posttemporal fenestra (see paragraph "braincase"). If the squamosal also contacts the supraoccipital is not visible. A distinct pattern of pits covers the dorsal and upper part of the lateral surface of the squamosal. It consists of circular pits, which are most distinct in the posterior part of the squamosal, while the pits decrease in size and become shallower in anterior direction. On the lateral surface of the squamosal, there is a longitudinal bony ridge, which leads to the cranioquadrate canal. Ventral to this ridge, the lateral surface of the squamosal is smooth (Fig. 3.26)

Jugal (j, Fig. 3.26-Fig. 3.28)

The jugal is an elongated bone, which is posteriorly rod-shaped and widens slightly level with the orbit. Because of the flattening of the skull in all studied specimens and due to the overlying of the postorbital and the lacrimal, the main medial part of the jugal is not exposed or badly damaged. The anterior part of the jugal, which lies parallel to the lacrimal and overlaps the maxilla, is preserved in UH 1 and SMNS 9930. In specimen SMNS 9930 the posterior part of the jugal is visible, even though poorly preserved.

The jugal is anteriorly bordered by the maxilla, anteromedially by the lacrimal and the postorbital, and posteriorly by the quadratojugal. Anteriorly, the jugal overlies dorsally acute-angled the posterior part of the maxilla (see paragraph "maxilla"). Anterior to the infratemporal fenestra, the jugal lies ventral to the postorbital and lacrimal. As described above the jugal forms together with the quadratojugal the ventral bar of the infratemporal fenestra. The jugal expands in a thin rod-shaped process in posterior direction and contacts the quadratojugal posterior to the level of the postorbitosquamosal suture. The exact course of the jugoquadratojugal suture cannot be reconstructed with certainty, but apparently, the jugal descends ventral to the quadratojugal. Ventromedially, the jugal probably has contact to the ectopterygoid, too (see paragraph "palate"). The ornamentation of the jugals is faint. A pattern of pits consists anteriorly of few very shallow, circular pits in irregular distribution, and posteriorly the surface is smooth.

Quadratojugal (qj, Fig. 3.26-Fig. 3.28)

Seen from dorsolaterally, the quadratojugal is a small, hook-shaped bone (Fig. 3.26) at the lateral side of the skull. It is clearly exposed in SMNS 9930, even though it is diagenetically compressed (Fig. 3.28). Anteriorly, it contacts the jugal in a slender process, but the exact run of the suture is camouflaged by compaction breaks. Posterodorsally, it has contact to the squamosal and posteromedially to the quadrate. The quadratojugal forms part of the ventral and posterior margin of the infratemporal fenestra (see there). The expansion of the quadratojugal in medial direction and the exact run of the sutures is not visible. The external surface is smooth.

Quadrate (q, Fig. 3.26-Fig. 3.28)

The quadrate is hard to identify because of the compressed preservation of the skull and the overlying squamosal and exoccipital. The posterior margin of the quadrate is exposed in SMNS 9930, UH 1, and UH 2. The quadrate condyles are therefore visible in dorsal view. These condyles are in dorsal view two slightly convex articular facets, which are separated by a shallow groove. Laterally, the quadrate broadly contacts the quadratojugal and anteroventrally, the squamosal. The quadrate expands diagonally in anterodorsal direction and forms, together with exoccipital and squamosal, the posterior wall of the supratemporal fenestra (see there). It has anteromedial contact with the pterygoid. A contact with the laterosphenoid is expected. It is supposed that the morphology of ventral connections of the quadrates is similar to that of *Steneosaurus bollensis* (see chapter 3.1), concerning its very similar topography of it in the cranial table and the position of the quadrate. However, no certain data is available for *Platysuchus multiscrobiculatus*, because the skulls are exclusively exposed in dorsal view.

Palate

The skull-bearing specimens of *Platysuchus multiscrobiculatus* UH 1, UH 2, and SMNS 9930 show all only their dorsal side. The palatal side of the cranium is obscured by matrix and therefore invisible. Only those parts, which are dorsally visible through the supratemporal fenestrae, are described here. In dorsal view, parts of the pterygoids and ectopterygoids are exposed in UH 1 and SMNS 9930. Therefore, at least the exact positions of these elements in the skull are known. There is no accurate data for the shape of these bones or the run of the sutures in ventral view. Data for the palatines, the internal naris, or the basisphenoid are not available. It is assumed that the topography of the palate of *Platysuchus multiscrobiculatus* is

similar to that of *Steneosaurus bollensis* (see chapter 3.1). Therefore, for the three-dimensional wax reconstruction of the skull, the palate of *Steneosaurus bollensis* was used. A slight change of the proportions was necessary for *Pl. multiscrobiculatus*; because of its less elongated posterior part of the skull compared to *S. bollensis.*

Pterygoid (pt, Fig. 3.26 & Fig. 3.28)

Parts of the pterygoid are seen through the supratemporal fenestra in SMNS 9930 (Fig. 3.28). The posterior margin of the pterygoid wing ends one-third posterior to the anterior margin of the supratemporal fenestra. The anterolateral margin of the pterygoid wing contacts the ectopterygoid. The pterygoid is broad and covers ventrally at least half of the aperture of the supratemporal fenestra (Fig. 3.26).

The exposed position of the pterygoid here is identical to what is seen in *Steneosaurus bollensis* (see chapter 3.1).

Ectopterygoid (ecpt, Fig. 3.26-Fig. 3.28)

The ectopterygoid is small sub-rectangular bone in the palate. The ectopterygoid is only exposed in dorsal view, inside the supratemporal fenestra, partly obscured by the frontal and postorbital. Dorsolaterally, it contacts the postorbital and most likely the jugal and ventromedially, the pterygoid. It lies almost vertically in the skull and connects the palate with the cranial table. The best-preserved ectopterygoid is that of UH 1, despite being slightly deformed (Fig. 3.26).

Hyoid apparatus and trachea

No parts of the hyoid apparatus are preserved. The holotype of *Platysuchus multiscrobiculatus* (SMNS 9930) possesses petrified tracheal rings (Fig. 3.24). They consist of small closed rings and were probably already partly ossified in life. About 12 tracheal rings are visible lying ventral to the sixth and seventh cervical vertebra. None of the other *Pl. multiscrobiculatus* specimens shows this feature. However, some larger specimens of *Steneosaurus bollensis* show petrified tracheal rings, too (see chapter 3.1).

Braincase (Fig. 3.28)

Because of the deformation of the skulls, the braincase of *Platysuchus multiscrobiculatus* is only fragmentarily preserved. In addition, the compressed skulls are only dorsally exposed, therefore only dorsal data of the braincase is available. Even the

occipital view is limited by the compressed preservation. Visible are parts of the basioccipital, exoccipital-opisthotic complex, supraoccipital, prootic, and laterosphenoid. In anterodorsal view, a shallow recess in the posterior wall of the supratemporal fenestra is seen in SMNS 9930. This recess is interpreted as a posttemporal fenestra and lies between the squamosal and the bone ventrally associated to it. This bone is most likely the quadrate, because the position is similar to the clearly identified posttemporal fenestra in *Pelagosaurus typus* (see chapter 3.5).

Basioccipital (boc, Fig. 3.26-Fig. 3.28)

Only the part of the basioccipital, which forms the occipital condyle, is visible in dorsal view. In UH 1 and SMNS 9930, the first cervical vertebra is overlying most of the condyle.

Exoccipital & Opisthotic (eoc, Fig. 3.27 & Fig. 3.28)

The exoccipital is completely co-ossified with the opisthotic. Only some parts of the exoccipital-opisthotic complex are exposed in UH 2 and, in very poor preservation in UH 1 and SMNS 9930. The exact sutures of the bone complex are therefore unclear. However, broad anterodorsal contact to the squamosal and parietal, which are both overlaying it, is visible in UH 2. Dorsomedially the exoccipital-opisthotic complex contacts the supraoccipital (Fig. 3.28). A ventral contact of the exoccipital-opisthotic complex to the quadrates and the basioccipital is expected as usual in teleosaurids (see chapter 3.1).

Supraoccipital (soc)

The supraoccipital is only exposed in dorsal view in the juvenile specimen UH 2 (Fig. 4.8). It is a rectangular bone anterodorsally bordered by the parietal and laterally, by the exoccipitals. No data exist for the restriction of the bone in ventral direction.

Prootic (pro, Fig. 3.28)

In the holotype of *Platysuchus multiscrobiculatus* (SMNS 9930), the right lateral wall of the braincase is exposed and the opening for the cranial nerve V is visible. The opening lies ventral to the frontoparietal suture in the middle of the lateral braincase wall. The prootic, which usually forms part of the posterior margin of this opening (IORDANSKY 1973), cannot be clearly identified. Clear sutures for the elements in the lateral braincase wall are not visible. The missing sutures could be the result of a real fusion of the bones in the braincase as

AUER (1909), ANDREWS (1913), and WESTPHAL (1962) have suggested it for other teleosaurids.

Laterosphenoid (lsp, Fig. 3.27 & Fig. 3.28)

The laterosphenoid forms the anteroventral half of the lateral braincase wall. The laterosphenoid has most likely posterodorsal contact to the parietal and anterodorsal broad contact to the frontal, but the sutures of the laterosphenoid with the parietal and frontal are only partly preserved in SMNS 9930 and UH 1 (Fig. 3.27 & Fig. 3.28). Posteriorly, it forms the anterior margin of the foramina of the cranial nerve V. An expected contact to the quadrate, prootic, or pterygoid is not visible.

Mandible (md, lower jaw, Fig. 3.26, Fig. 3.27 & Fig. 3.28)

The mandible is only partly exposed in SMNS 9930, UH 1, and UH 2. In dorsolateral view, the dentary, splenial, angular, surangular, and articular are partly exposed and show deformations (Fig. 3.26, Fig. 3.27 & Fig. 3.28). The anterior two-thirds of the mandible is formed by the dentary and the posterior third is mainly formed by the surangular, angular and articular. The mandible possesses a prominent external mandibular fenestra, and ends in an elongated retroarticular process. Because of the limited view to the external side of the lower jaw, no information is available about the existence of a coronoid or an internal mandibular fenestra. The external surface of the bones in the mandible is mostly smooth, only the posterior external surface of the surangular shows some roughness (see paragraph "surangular").

External mandibular fenestra (EMF, Fig. 3.27 & Fig. 3.28)

The external mandibular fenestra is very poorly preserved. Its dorsal margin is formed by the surangular, the ventral one by the angular and the anterior one probably by the dentary (Fig. 3.28). In SMNS 9930, UH 1, and UH 2 deep longitudinal depressions in the compressed mandible are identified as collapsed external mandibular fenestrae (Fig. 3.27 & Fig. 4.8). The prominent depression between angular and surangular suggests a long and slender external mandibular fenestra. The remnants of the external mandibular fenestra in SMNS 9930 shows that it has at least two-thirds of the length of the infratemporal fenestra, and ends anterior at the same level (Fig. 3.28).

Dentary (d, Fig. 3.26-Fig. 3.28)

The slender mandibular ramus possesses a flat, largely elongated tooth-bearing dentary, which is more than two-thirds of the whole length of the ramus. The dentaries are firmly fused to a prominent symphysis in their anterior half. The symphysis is preserved in SMNS 9930 and UH 1. Additionally, in UH 2, the left mandibular ramus is preserved in lateral view, the right is missing. In SMNS 9930 and UH 1, the anterior part of the dentary is exposed in dorsal view, while the posterior part is partly covered by parts of the upper jaw and the skull roof. In addition, the posterior part of the dentary is broken in UH 1 and compressed in SMNS 9930. The symphysis is only exposed in UH , but its posterior-most part is covered by the upper jaw. Therefore, the length of the symphysis can only be estimated.

The anterior 5% of the dentaries widens and forms a spoon-shaped end, similar in shape to the premaxillae but less distinctive. The anterior half of the dentary is flat and about twice as wide as high. In the posterior part, the cross-section of the bone increases constantly to twice as high as broad, similar to the conditions in *Steneosaurus bollensis* (see chapter 3.1). Posteromedially, the dentary contacts the splenial in a straight suture. Posterolaterally, it is dorsally bordered by the surangular and ventrally by the angular. The exact connection between the dentary, the surangular, and angular is poorly preserved, therefore it is impossible to reconstructed to which amount the dentary forms the ventral and dorsal margin of the external mandibular fenestra. The absolute length of the dentary cannot be measured, because its posterior suture is not clearly preserved.

Because the posterior-most part of the dentaries are always deformed and covered by other cranial elements the number of alveoli in the dentary cannot be certainly determined, but the number must lies between 35 and 40 (see paragraph “dentition”). The alveoli in the anterior two-thirds of the dentary are positioned along the lateral edge, ellipsoid, and open dorsolaterally; first level with the 28th tooth position, the alveoli open in dorsal direction and are circular in dorsal view (Fig. 3.27 & Fig. 3.28). Those dorsolateral orientations of the alveoli differ from the strict dorsal orientations of the alveoli observed in *Steneosaurus bollensis* (see chapter 3.1).

Splenial (sp, Fig. 3.26-Fig. 3.28)

The splenial is a long, slender bone situated at the ventromedial margin of the mandibular ramus (Fig. 3.26). It forms approximately the posterior 10 % of the symphysis. In UH 1, the posterodorsal part of the right splenial is visible (Fig. 3.27). Anteromedially, the splenials probably meet each other medially in a straight suture and anteriorly taper off

between the dentaries. Posterolaterally, the splenial is bordered by the dentary and surangular. In UH 2, the splenial is in its anterior part dislocated from the dentary and therefore observable in lateral view (Fig. 4.8.). However, because of the disarticulation the contact to the dentary and the angular remain unclear.

Surangular (san, Fig. 3.26-Fig. 3.28)

The surangular is exposed in dorsolateral view. It is an elongated bone with contact to the angular, the articular, and the dentary. A possible contact with a coronoid is not visible, because the internal side of the surangular is not exposed. Anteriorly, the surangular is bordered by the dentary and posterodorsally by the articular. The course of the dentary-surangular suture is uncertain. In contrary, the suranguloarticular suture runs well visible horizontally and is straight and smooth. Posteroventrally, the surangular meets the angular in a straight suture posterior to the external mandibular fenestra (see paragraph “angular”). Anteroventrally, the surangular forms the dorsal margin of the external mandibular fenestra. In lateral view, the surangular separates the angular completely from the articular. The surface of the surangular is smooth except of some rough areas at the posterior margin on the retroarticular process. The areas probably indicate jaw muscle or tendon insertion marks.

Angular (an, Fig. 3.26-Fig. 3.28)

The angular is exposed in lateral view. It is an elongated bone, which is slightly curving dorsally in its posterior part. Therefore, the external ventral margin of the angular is slightly convex. Anteriorly, the angular meets the dentary and posterodorsally it has broad contact to the surangular. Anteromedially, the angular forms the ventral margin of the external mandibular fenestra. The angulosurangular suture is straight, smooth, and curving posterodorsally. The connection between the dentary and angular is so badly preserved that it is impossible to identify the suture between these elements.

Articular (ar, Fig. 3.26-Fig. 3.28)

The articular is exposed in dorsal and lateral view. Anteriorly and ventrally, the articular is bordered by the surangular. In dorsal view, the articular is roughly rhombic and its dorsal surface is slightly concave with a solid transversal crest, which divides the articular in two parts. The posterior two-thirds form the retroarticular process, the anterior third forms the two articular facets at the mandible for the quadrate condyles. In the specimen UH 2, the lateral surface of the articular is sub-triangular. The articular forms with the posterior parts of

surangular and angular a prominent elongated retroarticular process (Fig. 3.26, Fig. 3.27 & Fig. 3.28). In SMNS 9930, the retroarticular process forms the posterior 11% of the entire mandibular ramus length (see chapter 4 for further details).

Dentition

Tooth morphology

The dentition is weakly heterodont, because the size of the teeth varies slightly. The teeth are slender, conical, pointed, and apically recurved. They are all covered with fine vertical striation. A particular carina is not recognized.

Pattern of dentition (Fig. 3.26-Fig. 3.28)

In the upper jaw, the premaxillae and the maxillae are tooth bearing. There are 3 alveoli in the premaxilla, and 30 to 34 alveoli in the maxilla. In the upper jaw are only every second alveoli is occupied with a fully erupted tooth. The other alveoli are empty or possess small replacement teeth. The fully erupted teeth in the upper and lower jaw are all similar developed. Exceptions are the third premaxillary tooth and the first and third dentary tooth (counted from anterior). They are larger and almost twice the size of the full erupted maxillary teeth. The shape of the alveoli in the upper jaw is not exposed and they are not visible in lateral view. The teeth in the upper jaw are vertically orientated. In the lower jaw, the dentary possesses anteriorly 26 dorsolaterally orientated alveoli; whereas posterior to the symphysis they are dorsally orientated. An exception is the first tooth in the dentary, which is pointing anteriorly (Fig. 3.26, Fig. 3.27 & Fig. 3.28).

In the mandible of UH 1, there is an estimate of 40 alveoli in each dentary. In SMNS 9930, the estimated number of alveoli in the dentary is 37. The exact number of dentary teeth is hard to tell because of the poor preservation of the specimens in these parts and overlying roof bones. The dentition code is: $\frac{3+30-40}{37-40}$.

Postcranial elements

The axial skeleton

Armour (Fig. 3.29, Fig. 3.30)

Platysuchus multiscrobiculatus possesses heavy dermal armour that is present both on the dorsal and on the ventral side of the animal. Both osteodermal shields consist of deeply pitted osteoderms. BERCKHEMER (1929) describes 42 dorsal rows of paired osteoderms and additionally, up to eight single dorsal osteoderms in the posterior part of the osteodermal shield for the holotype of *Platysuchus multiscrobiculatus* (SMNS 9930). He also notices a longitudinal keel on the dorsal osteoderms starting at the anterior first cervical osteoderm.

The ventral armour is also very distinctive; it consists of thoracic and caudal armour. The ventral armour of the thoracic consists of six longitudinal rows, each of it consisting of up to 18 osteoderms. The most lateral rows of the ventral armour, i.e. row one and six, are slightly curving laterodorsally, as it is seen e.g., in specimen SMNS 15919. The tail possesses ventral armour of about 50 osteoderms, too.

Dorsal armour (Fig. 3.29, Fig. 3.30)

The dorsal armour of *Platysuchus multiscrobiculatus* begins posterior to the atlas-axis complex (SMNS 9930 and UH 1), and runs in a longitudinal row of paired osteoderms posteriorly to the 18th caudal vertebra. Posterior to the 18th caudal vertebra, the longitudinal row only consists of single instead of paired osteoderms and ends level with the 26th caudal vertebra (Fig. 3.24, Fig. 3.25). The dorsal osteodermal shield is divided in eight pairs of cervical osteoderms, 17 to 18 pairs of trunk osteoderms, 17 pairs of caudal osteoderms, and seven or eight single, unpaired caudal osteoderms (Fig. 3.30).

A complete articulated dorsal shield is preserved in SMNS 9930 (Fig. 3.24). In specimen UH 1, osteoderms 1 to 29 are laying paired nearly in original position (counted from anterior). In the caudal region, there is also a minimum of 18 disarticulated dorsal osteoderms present, which are partly obscuring each other (Fig. 3.25). These 18 osteoderms should form a minimum of nine pairs and are part of the dorsal tail armour. Specimen GPIT Re 1193/16 consists of 15 pairs of almost unkeeled, but heavily sculptured osteoderms. The anterior first three pairs of the preserved osteoderms belong to the cervical dorsal armour, and the remaining 12 pairs of osteoderms are assigned to the dorsal armour of the thoracic region (Fig. 3.29a).

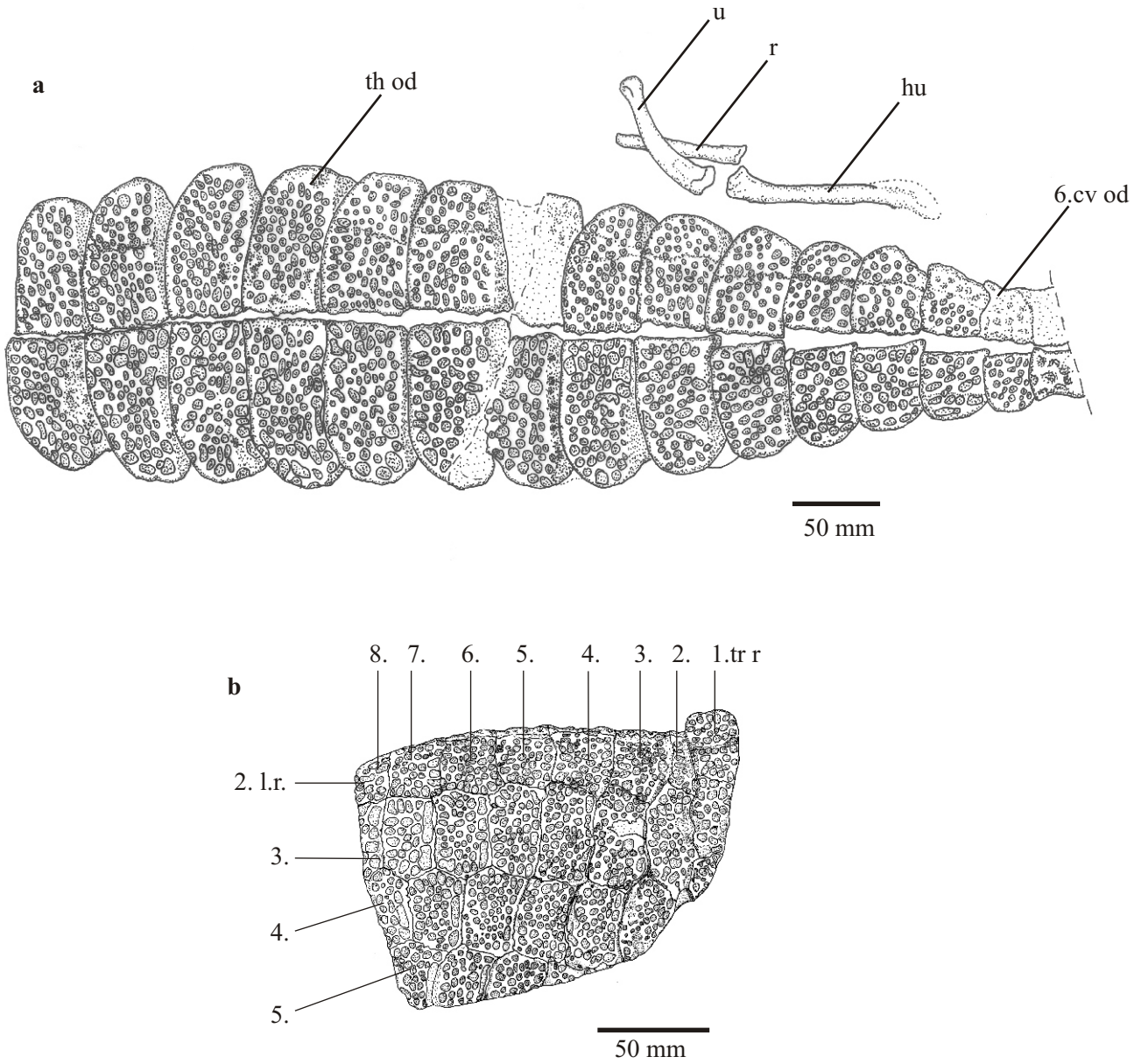

Figure 3.29a-b: *In situ* drawings of the armour of *Platysuchus multiscrobiculatus.* **3.29a**-Specimen GPIT Re 1193/16 shows part of the dorsal osteodermal shield and parts of the left fore limb in dorsal view. The last three pairs of cervical osteoderms (5.-7.) and 12 pairs of thoracic osteoderms (8.-19.) are preserved. A longitudinal row of heavily sculptured paired dorsal osteoderms is exposed. The osteoderms are two times longer than broad in the trunk region and possess a dense pattern of pits. A keel is slightly developed on the dorsal surface of the osteoderms.
3.29b-Specimen SMNS 15919 shows parts of the ventral osteodermal shield in ventral view.
The osteoderms are rectangular to rhombic and do not overlap each other. The dense pattern of pits on their external surfaces consists of equally distributed small pits. Parts of five longitudinal rows (l.r.) are visible, the sixth one is lacking. In addition, parts of eight transversal rows (tr.r.) are visible. Thus, parts of 32 osteoderms are observed.

In *Platysuchus multiscrobiculatus*, the dorsal thoracic osteoderms possess a dense pattern of circular, deep pits. The number of the pits depends on the size of the osteoderms, but the external surface is always completely covered with pits (Fig. 3.30b). All thoracic osteoderms are about twice as wider as long with a mostly straight, but in some cases slightly serrated medial margin and a smooth, convex lateral margin (Fig. 3.30). Starting from the anterior third pair of dorsal osteoderms, a low keel running in anteroposterior direction is recognized in SMNS 9930 and UH 1. Starting from the seventh pair of the dorsal osteoderms, the keel is well developed. This keel divides the external face of the dorsal osteoderms into two sections (Fig. 3.30c). The medial section is about two-thirds of the osteoderm and the lateral section is about one third of the osteoderm. The medial section of the osteoderms is nearly square, whereas the lateral section has a convex lateral margin (Fig. 3.30b). In UH 1, an anterior peg is visible at the anterolateral margin of the dorsal osteoderms, which lie posterior to the pelvic girdle (Fig. 3.25). The anterior edge of the osteoderms is slightly flexed in anteroventral direction and is overlapped by its anterior next osteoderm. The anterior edge is still covered by shallow pits, in contrast to that of *Steneosaurus bollensis,* where this area is smooth (see chapter 3.1). The dorsal armour of GPIT 1193/16 is very similar in size, shape, and sculpturing to that dorsal armour seen in UH 1 and SMNS 9930. Nevertheless, in specimen UH 1, a keel on the surface of the osteoderms is recognized, which is almost missing in specimen GPIT 1193/16. In SMNS 9930, the keel on the osteoderms is very prominent, and the osteoderms are often broken along this keel (Fig. 3.24).

UH 2 shows a prominent keel on all dorsal osteoderms, despite being a juvenile, therefore it is suggested that the development of a keel is more an individual character than an ontogenetic one (see chapter 4 for further discussion).

Ventral armour (Fig. 3.29b)

The ventral osteodermal shield of the thorax consists of six longitudinal rows, with a maximum of 18 osteoderms each. The tail possesses a ventral longitudinal row of paired osteoderms, which begins at the anterior third caudal vertebra and runs posteriorly to the 20th caudal vertebra. The posterior eight ventral tail osteoderms are probably unpaired.

Specimen SMNS 15919 allows to study part of the articulated ventral shield in ventral view. It consists of 32 articulated ventral osteoderms of rectangular to rhombic shape (Fig. 3.29b). The osteoderm are not flexible against each other, but contact each other in slight serrated sutures and do not overlap each other. The pattern of pits on the external face of the ventral osteoderms consists of almost regularly and densely distributed, circular pits. The 32

osteoderms are arranged in five longitudinal rows (l r) and eight transversal rows (tr. r). The expected sixth longitudinal row is here missing (see below).

The specimens UH 1 and SMNS 9930 show some disarticulated parts of the ventral armour like single ventral osteoderms in internal and external view. In UH 1, the area of the left fore limb shows two ventral thoracic osteoderms lying with the external side up. They are only half the size of the thoracic dorsal osteoderms and rectangular to rhombic with straight margins. The pattern of pits is similar to that seen on the external surface of the dorsal osteoderms.

In SMNS 9930, the smooth internal side of some ventral osteoderms is exposed between the thoracic ribs, and one longitudinal row of ventral osteoderms in external view is lying on the right side of the thorax nearby the ribs (Fig. 3.24). It is not possible to identify the exact number of ventral osteoderms, or the detailed shape of all osteoderms here, because of the overlying rib cage. However, a minimum of 16 transversal rows each consisting of a six ventral osteoderms is estimated. The ventral armour corresponds to the 15 pairs of thoracic ribs. In SMNS 9930, it starts about the level of the 12th vertebra (counted from anterior), immediately posterior the pectoral girdle. In addition, partial ventral armour of the tail is preserved in SMNS 9930 and UH 1. In SMNS 9930, it consists of a double row of rhombic osteoderms with a pronounced keel (Fig. 3.24). The osteoderms begin at the second caudal vertebra posterior to the pelvic girdle and terminate at the level of 25th caudal vertebra. The posterior-most eight to ten osteoderms of this posteroventral armour consist probably only of a single longitudinal row of osteoderms.

In this study, ventral armour of the tail consisting of a double row of keeled rhombic osteoderms is noticed in a couple of specimens of *Steneosaurus bollensis* (see chapter 3.1) and *Platysuchus multiscrobiculatus*. In contrast to the observations of BERCKHEMER (1929), specific lateral armour of the tail is not recognized in any teleosaurid specimen.

Vertebral column (Fig. 3.24)

The vertebral column consists of about 64 amphicoelous vertebrae. There are nine cervical vertebrae, including the atlas-axis complex, 14 to 15 thoracic vertebrae, two to three lumbar vertebrae, two sacral vertebrae, and up to 38 caudal vertebrae. In UH 1, the anterior-most 32 vertebrae, in UH 2 the anterior-most 34 vertebrae, and in SMNS 9930 64 vertebrae are preserved.

Only parts of the vertebral column are exposed in the known specimens of *Platysuchus multiscrobiculatus*. In SMNS 9930, the cervical and the posterior half of the caudal column

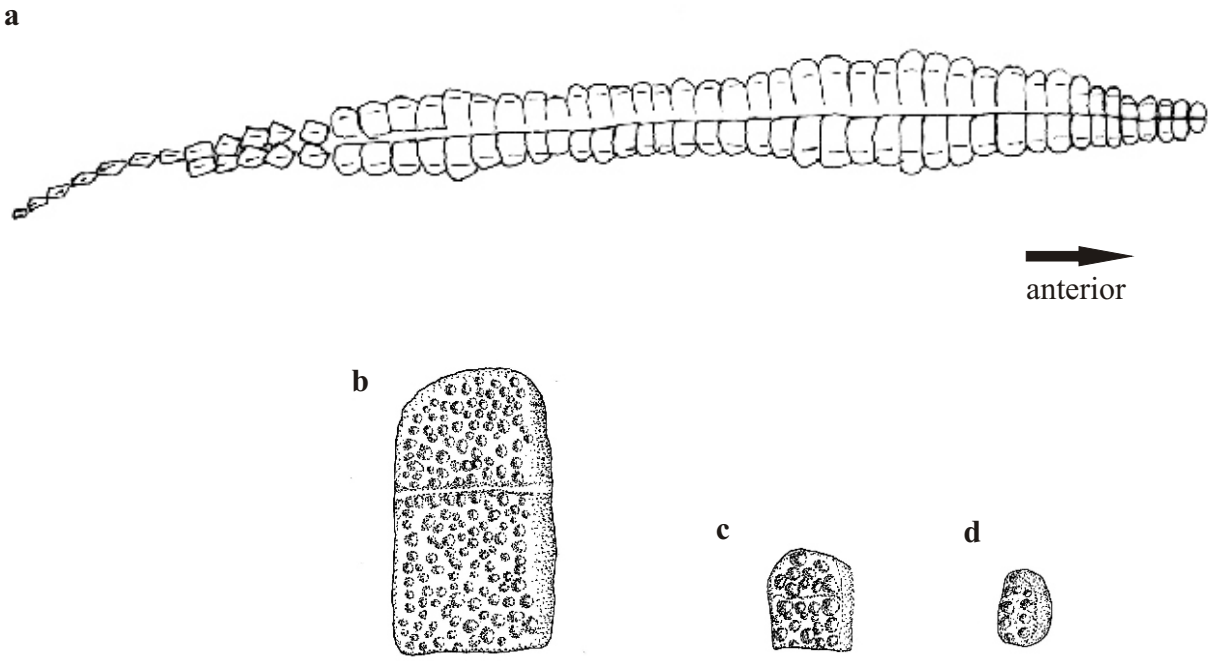

Figure 3.30: Armour of *Platysuchus multiscrobiculatus*.

3.30a-Restoration of the dorsal osteoderm shield (after SMNS 9930 und UH 1). A keel is developed on the surface of the osteoderms, posterior to the second cervical osteoderm. The last seven caudal osteoderms only form a single row. **3.30b-**Thoracic osteoderm, drawn after SMNS 9930. Original length is 35 mm. **3.30c-**Third cervical osteoderm with visible keel after specimen SMNS 9930. Original length is 25 mm. **3.30d-**First cervical osteoderm without keel and oval in shape after specimen UH 1. Original length is 12.5 mm.

are exposed in lateral view. In UH 1 the cervical vertebrae are partly exposed, but poorly preserved, because of the compression of the specimen. In UH 2, probably six cervical vertebrae are visible, but the neural arches are separated from their vertebra centra and partly obscured by matrix or other bones. In addition, four isolated caudal vertebra centra are exposed.

Cervical vertebrae (Fig. 3.27)

Due to compressed preservation and overlying osteoderms in the cervical area only parts of the cervical vertebrae are visible in the *Platysuchus multiscrobiculatus* specimens. The general morphology of the atlas-axis complex is similar to that of *Steneosaurus bollensis* (see chapter 3.1).

In lateral view, the atlas-axis complex is partly exposed in SMNS 9930 and UH 1(Fig. 3.27). A ventral semi-circular bone represents the intercentrum of the atlas and is exposed in UH 1 and SMNS 9930. The neural arch of the atlas cannot be identified with certainty. The axis possesses an odontic process and the height of its neural spine is only 65% of the length of the axis. It shows one articular facet for the second cervical rib at the anterolateral margin. The facet is semi-circular and slightly internally concave.

In SMNS 9930, the cervical vertebrae three to nine are also exposed in lateral view. Their shape is identical to the shape of the cervical vertebrae of *Steneosaurus bollensis* (see chapter 3.1, Fig. 3.10). The parapohyses and diapohyses protrude from the vertebra centra and the neural spines are low. An exception is the ninth cervical vertebrae vertebra, where the diapophysis emerges from the lateral wall of the neural arch, and the parapophysis protrudes from the centrum. The height of the neural spines is about the length of the vertebra centra. The exact height of the neural spines of the cervical vertebrae cannot be measured, because they are mostly diagenetically deformed and in their dorsal part obscured by the dorsal osteoderms. The prezygapophyses and postzygapophyses are as usual at the same height.

Because of these observations, the general conditions of the cervical column of *Platysuchus multiscrobiculatus* are most likely very similar to the conditions seen in *Steneosaurus bollensis* (see chapter 3.1).

Thoracic vertebrae & lumbar vertebrae (Fig. 3.24, Fig. 3.25)

Posterior to the cervical vertebrae there are 14 to 15 thoracic vertebrae, which possess elongated bicipital (double-headed) ribs (see paragraph “ribs”). The thoracic vertebrae possess

a transverse process, which consists of a synapohysis emerging from the lateral wall of the neural arch with a diapophysial process and parapophysial process.

In specimen UH 1, the anterior two thoracic vertebrae are partly visible in lateral view. The thoracic vertebrae possess a transverse process, which protrudes from the lateral wall of the neural arch. Their dorsal part of the neural arch is obscured by dorsal osteoderms. Of the posteriorly following thoracic and lumbar vertebrae, only the dorsal aspect of the neural spines is exposed in a longitudinal median line between the osteoderms. Therefore, the exact shape of the thoracic vertebrae is unknown. In UH 1, the exact number of thoracic vertebrae is determined by counting the neural spines and the corresponding ribs.

There are expected two to three lumbar vertebrae, but the dorsal armour covers them completely in all known specimens. Due to this fact, the shape of the lumbar vertebrae is unknown, but their position and number is determined by the lack of thoracic ribs and the number of corresponding dorsal osteoderms, in the area directly anterior to the sacral vertebrae (Fig. 3.24).

Sacral vertebrae

Two sacral vertebrae follow the lumbar vertebrae. The sacral vertebrae are connected with robust sacral ribs to the ilia. In the juvenile specimen UH 2, the sacroiliac articulation is visible, and is similar to that of *Steneosaurus bollensis* (see chapter 3.1). In SMNS 9930, vertebrae 26 and 27 are designated as sacral vertebrae, whereas in UH 1 vertebrae 25 and 26 are most likely connected to the ilia. In the juvenile specimen UH 2, the vertebrae 26 and 27 represent the sacral vertebrae. The sacral vertebrae themselves are not exposed, they are completely obscured by the dorsal osteodermal shield. Therefore, a description is impossible. The sacral vertebrae were determined by their contact to the ilia over sacral ribs and the position of the vertebrae in the vertebra column.

Caudal vertebrae (Fig. 3.24)

In UH 1, the anterior five caudal vertebrae are preserved. They are mostly covered by dorsal osteoderms and only their dorsal spine is visible in dorsal view. In UH 2, the anterior six caudal vertebrae are present. Three fragmentary vertebra centra are exposed and some chevrons determine the position of the other three vertebrae. In SMNS 9930, the entire caudal column with 38 vertebrae is preserved. However, the shape of the anterior 15 caudal vertebrae is unknown, because they are obscured by osteoderms and matrix.

The general shape of the posterior caudal vertebrae is identical with the shape described for *Steneosaurus bollensis* (see chapter 3.1, Fig. 3.10). The vertebra centra are elongated and twice as long as they are high and the neural spines are nearly as high as the centra are long.

Chevrons at the caudal vertebrae are partly exposed in SMNS 9930 and UH 2(Fig. 3.24). In the anterior half of the tail, the ventral armour obscures most chevrons. Only two chevrons are visible. The chevrons are "V"-shaped in anterior view. In lateral view, the ventral body of the chevron is compressed and anteroposterior slightly elongated. Dorsally each branch of the chevron articulates with a small elliptic articular facet at the posteroventral edge of the caudal vertebra centrum. The preservation in *Platysuchus multiscrobiculatus* is fragmentary, but the shape of the chevrons is similar to those of *Steneosaurus bollensis* (see chapter 3.1). The chevrons decrease posteriorly in size and end probably at the 28th caudal vertebra.

Ribs (Fig. 3.24, Fig. 3.27)

There are nine pairs of cervical ribs in the specimens UH 1 and SMNS 9930. The first and second cervical rib is exposed in dorsolateral view (Fig. 3.27). The first cervical rib is a long and slender, straight bar of bone with an acuminate distal end. It is connected to the first cervical vertebra (atlas) only with one head. The shape of the second cervical rib is similar to the first one but only tow-thirds the length of it. The second cervical rib is attached to the centrum of the axis. The third to eighth cervical vertebra has double-headed cervical ribs, which are identical in shape to those of *Steneosaurus bollensis* (see chapter 3.1, Fig. 3.10). The capitulum and the tuberculum are of equal extension. The body of the ribs is mediolaterally flattened with a short anterior and posterior process of equal size. The ninth cervical rib differs from the others. Its body is much more elongated posteriorly compared to the cervical ribs three to eight and has almost lost the anterior process. It is half the length and width of the thoracic ribs (Fig. 3.24).

The number of thoracic ribs varies from 14 to 15. The body of the thoracic ribs is significantly elongated, convex externally, and concave internally and show the typical shape for teleosaurids (e.g. ANDREWS 1913, WESTPHAL 1962). The capitulum and tuberculum are only exposed in the anterior three thoracic ribs in UH 1 and the 10th thoracic rib in SMNS 9930. The capitulum is larger than the tuberculum and more elongated. The tuberculum and capitulum articulate with the transverse process at the thoracic vertebrae like in *Steneosaurus bollensis* (see chapter 3.1).

The sacral ribs are mainly obscured by dorsal osteoderms or the ilia in all investigated specimens; therefore, no data for the exact shape is available. The lateral half of the anterior first sacral rib is exposed in SMNS 9930. It is diagenetically deformed and lies partly medially partly anteriorly to the ilium. The lateral articular facet of the rib is about 1.5 times wider than the body of the rib. In UH 1 the right sacroiliac joint is visible in dorsal view. The sacral ribs are poorly preserved at this joint and their shape is unknown.

Gastralia (Fig. 3.25)

Possible gastralia are described in some specimens of *Steneosaurus bollensis* (see chapter 3.1). In *Platysuchus multiscrobiculatus,* only in UH 1 and UH 2 are some structures exposed, which could represent gastralia (Fig. 3.25). In UH 1, some slightly curved, thin elements lie closely anterior to the right ilium. Due to the poor preservation of these structures, it is not to identify if they represent bone structures or not. It is also possible that these elements represent some stomach content or they may be artefacts of the preparation. In the juvenile specimen UH 2, some thin, short, bone bars are visible among the fourth to seventh thoracic rib. Those structures are interpreted as gastralia, but real evidence cannot be given.

The appendicular skeleton

Pectoral girdle (Fig. 3.31)

The pectoral girdle consists of a paired scapula, a paired coracoid, and an unpaired interclavicle. The scapula and the coracoid are similar in size and general shape. In external view, both are hourglass-shaped, flat elements with a slender middle part and dorsal and ventral expansions, twice as broad as the shaft. The posteroventral margin of the scapula and the dorsolateral margin of the coracoid form together the glenoid fossa for articulation with the humerus. The interclavicle is a slender bone bar with a slight rhombic broadening in its anterior 20%.

In UH 1, the right scapula and the ventrolateral part of the coracoid are present, while on the left side, only the scapula is exposed. All other parts are hidden or missing. In specimen SMNS 9930, the right scapula and coracoid are well preserved, but the right humerus obscures the medial part of the coracoid and the scapula is slightly deformed. The interclavicle is preserved in SMNS 9930 and UH 2. In the juvenile specimen UH 2, the left

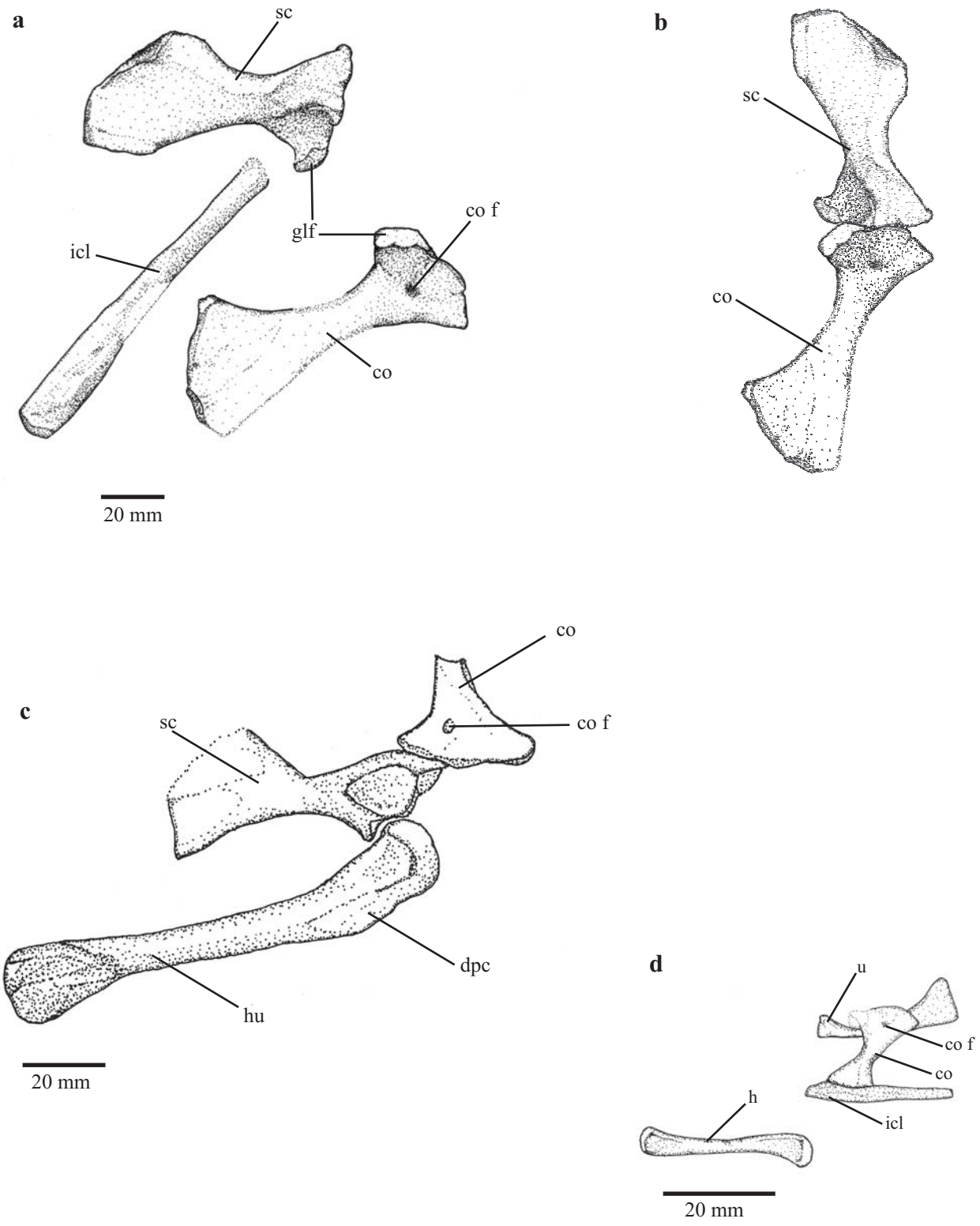

Figure 3.31a-d: Pectoral girdle of *Platysuchus multiscrobiculatus*. **3.31a**-*In situ* drawing of the right scapula (sc), the right coracoid (co), and the interclavicle (icl) of SMNS 9930. The coracoid foramen (co f) is visible in the dorsal part of the coracoid. **3.31b**-Reconstruction of the pectoral girdle in lateral view without interclavicle (after SMNS 9930). **3.31c-***In situ* drawing of the right scapula, coracoid and humerus (h) of UH 1. **3.31d**- *In situ* drawing of parts of the pectoral girdle and the left fore limb of the juvenil specimen UH 2. Scale bars are 20 mm each.
Abbreviations: co-coracoid, co f-coracoid foramen, dpc-deltopectoral crest, gl f-glenoid fossa, icl-interclavicle, h-humerus, u-ulna.

coracoid lies in contact to the interclavicle (Fig. 3.31d). In all specimens, the external sides of scapula and coracoid are exposed.

Scapula (sc, Fig. 3.31)

The scapula is exposed in external view in SMNS 9930, UH 1, and UH 2. The scapula is a mediolateral flat bone with a narrow shaft and broad dorsal and ventral expansions and resembles to that of *S. bollensis*. It is hourglass-shaped in lateral view. The dorsal end of the scapula expands into a large, flat nearly triangular blade with an externally convex margin. At the anteroventral margin of the scapula, there is a thickened articular facet, which contacts anteriorly the coracoid. At the posteroventral margin of the scapula, there is another articular facet, which forms the dorsal half of the glenoid fossa. Additionally, a deep depression is recognized on the external ventral face of the scapula, which indicates a large area for muscle insertion probably of the coracobrachialis brevis dorsalis muscle (MEERS 2003, see also chapter 3.1). The length of the scapula (Sa1) is about 50% of the length of the humerus (H1) (see appendix II).

Coracoid (co, Fig. 3.31)

Parts of the coracoid are exposed in SMNS 9930, UH 1, and UH 2. The internal surface of the coracoid is seen in UH 2 and UH 1, while in SMNS 9930 the coracoid is exposed in external view.

In external view, the coracoid is a roughly hourglass-shaped bone, similar to the scapula and the same size. It has flat externally convex dorsolateral and ventromedial expansions, which extend from a slender shaft. The shaft is circular in cross-section. The flattened dorsolateral part possesses two arched articular facets at its dorsolateral margin. The coracoid foramen lies in the center of the dorsolateral blade anterior to the glenoid fossa. The anterior articular facet is slightly externally concave and connects with the corresponding facet at the anteroventral margin of the scapula. The posterior articular facet of the coracoid is a slight tubercle with a flat dorsal surface and forms the ventral part of the glenoid fossa (see paragraph “scapula”). The ventromedial blade becomes ventrally flatter and its ventromedial margin is slightly externally convex.

Interclavicle (icl, Fig. 3.31)

In SMNS 9930, only the anterior two-thirds of the interclavicle are exposed. In the juvenile specimen UH 2, the interclavicle is seen in full length, and its anterior half contacts laterally the coracoid (3.31).

The interclavicle is a straight, slender bone bar. The anterior 20% -30% of the bone is flattened, slightly enlarged, and roughly rhombic, while the posterior section is more slender and possesses a blunt end. It lies ventrally to the vertebral column and connects in its anterior third the two coracoids medially. It is about twice the length of the coracoid.

Pelvic girdle (Fig. 3.32)

The pelvic girdle consists as usual of the paired ilium, the paired ischium, and the paired pubis. At their internal side, the ilia are connected to the sacral vertebrae over heavy sacral ribs. The external side of the ilia possesses each a large acetabulum to articulate with the femur. Posteroventrally, the ischia medially meet each other in a probably cartilaginous connection, the same is supposed for the pubic bones.

In UH 1, the left and right ilium and part of the left ischium are preserved. The pubic bones are not visible. The ilia are embedded vertically. In SMNS 9930, the right ilium and both ischia are preserved, and the right and the dorsolateral part of the left pubis is exposed, too.

Ilium (il, Fig. 3.32)

The ilium is visible in external view in SMNS 9930.

The ilium is a roughly rectangular, mediolaterally-flattened bone, which shows a prominent dorsal iliac crest extending from anterior to posterior direction. The length of the ilium (P1) is approximately 78% of the width of the ilium in SMNS 9930. The iliac crest possesses a pronounced anterior and posterior process and its dorsal margin is dorsally convex in the posterior half. The anterior process forms circa 15% and the posterior process circa 32% of the width of the ilium (P2). Laterally, two-thirds of the external face of the ilium forms the dorsal 80% of the acetabulum, while medially, the internal face of the ilium is connected to the sacral ribs. The ventral margin of the ilium possesses most likely three articular facets, but only the anterior-most facet is exposed in specimen SMNS 9930. Anteroventrally, the anterior-most facet is small, slightly convex and was probably connected to a cartilaginous dorsolateral part of the pubis. The supposed two posterior facets at the

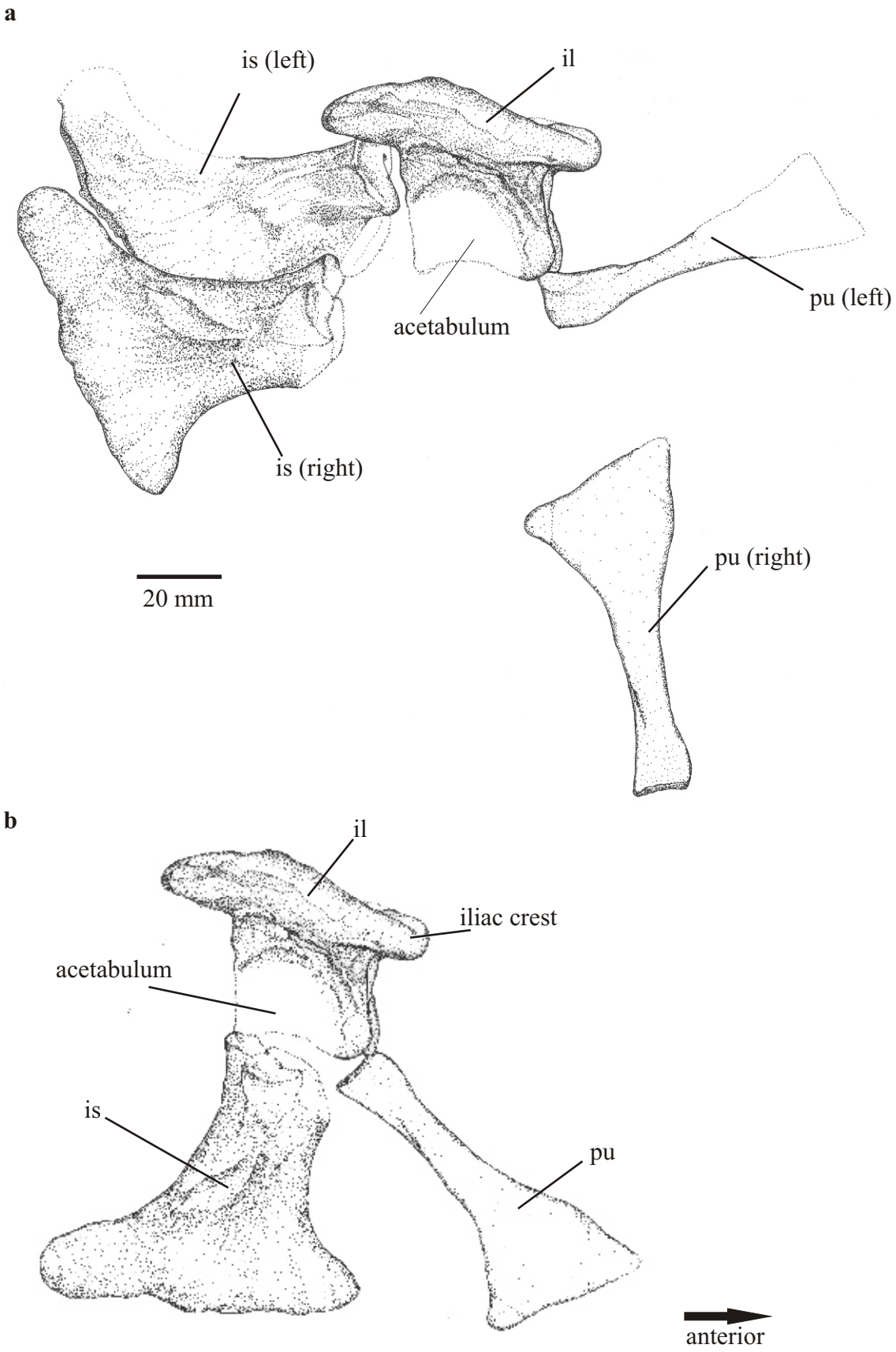

Figure 3.32a-b: Pelvic girdle of *Platysuchus multiscrobiculatus*. **3.32a**- *In situ* drawing of the right and part of the left pelvic girdle of specimen SMNS 9930 (holotype). The broken line suggests the shape of the non-exposed bone parts. **3.32b**-Reconstruction of the pelvic girdle (after SMNS 9930). Abbreviations: ac-acetabulum, il-ilium, is-ischium, and pu-pubis.

ventral margin of the ilium are not visible, but should fit with the corresponding articular facets visible at the ischium.

Ischium (is, Fig. 3.32)

Both ischia are exposed in lateral view in SMNS 9930. The ischium consists in its ventromedial third of a flat expansion. From this bone sheet develops dorsolaterally a slender shaft, which is only half as wide but triples in cross-section compared to the ventral bone blade. This dorsal shaft of the ischium split in three articulation areas. Posterodorsally, two articular facets connect the ilium and form together with it the acetabulum. They are identically developed, lying parallel at the posterodorsal margin of the ischium. Each consists of a small protrusion with a concave semicircle dorsal surface. The anterior articular facet is not exposed in the specimens. The ventromedial margin of the ischium possesses a rough external surface, which indicates a probably cartilaginous suture between the ischia, as ANDREWS (1913) suggested it for *Steneosaurus*.

Pubis (pu, Fig. 3.32)

The pubis is an elongated, flat bone with a sub-triangular expansion in its ventromedial third. At its ventral margin, the width of the expansion (Pu2) is approximately 55% of the pubis length (Pu1) (see appendix II). The pubis length (Pu1) is estimated to be 1.6 times the length of the ilium (P1). The expansion possesses a straight ventromedial margin, which is slightly fringed and rough at its surface. This indicates a probably cartilaginous connection to the contralateral pubis. The dorsolateral margin of the pubis has a small and thickened enlargement, with a rough surface on its dorsal edge. No articular facets are visible at the dorsal or ventral margin. It is supposed, that the pubic bones do not take part in the formation of the acetabulum and are probably only connected to the ilium over cartilage.

Limbs

Forelimb (Fig. 3.33)

The fore limb consists of the humerus, radius, ulna, and manus. It is shorter than the hind limb. In adult *Platysuchus multiscrobiculatus* specimens, the humerus length (H1) is about 70 % of the femur length (Fe1) (chapter 4). In addition, the humerus length (H1) is about 27% of the skull length (A) (chapter 4).

In specimen SMNS 9930, the right fore limb is preserved in completely articulated nature and exposed in dorsal view (Fig. 3.33). The left fore limb of the specimen is incomplete and disarticulated (3.24). The fore limbs in specimen UH 1 are both incompletely preserved. The left and right humerus, both radii, and both ulnae are exposed in dorsal view (3.25). Only some single metacarpals and phalanges, as well as a few unidentifiable elements of the manus are present. In GPIT 1193/16, most of the left humerus, the radius and the ulna are exposed (Fig. 3.29). In specimen UH 2, only the left humerus is exposed in ventral view (Fig. 3.31).

Humerus (hu, Fig. 3.31c-d, Fig. 3.33)

The humerus is an elongated bone bar with a slightly expanded proximal head. The proximal articulation surface is a transverse oval and convex area, with a prominent ridge at the internal side of the head. Ventral to this, at the internal side, lays a triangular rugosity, which probably indicates the attachment area for the humeroradialis muscle (MEERS 2003).

The humerus head is slightly curved medially, as well as tilted slightly dorsally on the shaft and the thickest portion of the articular area is toward the posterior margin of the head. The humerus only shows a weakly developed deltopectoral crest. The distal end of the humerus possesses two articular facets to connect the humerus to radius and ulna. The articular facets consist of two rounded convexities divided by a shallow sulcus. The capitellum, the articular area for the radius, is only slightly larger than the ulnar condyle, and the intercondylar sulcus between them is not very prominent.

Radius (r, Fig. 3.33)

The radius is preserved in SMNS 9930 and UH 1. The radius consists of a slender cylindrical shaft with enlargements of about equal size at the proximal and distal ends. The radius length (R1) is about 58% of the humerus length (H1). The bone broadens about 10% of its width at its proximal and distal end. The proximal end articulates medially with the ulna and dorsally with a slightly concave articular facet with the humerus. The distal end contacts the radiale.

Ulna (ul, Fig. 3.32d, Fig. 3.33)

The ulna is a slender bone that consists of a curved shaft with enlargements on the proximal and distal ends. The proximal enlargement is slightly flattened and triplicates its width compared to the shaft. It possesses two articular facets at its proximal margin. Medially,

a small, shallow convex facet contacts the radius, and dorsally, the twice as large, slightly convex facet articulates with the humerus. The distal end of the ulna is twice as wide as the shaft and possesses two shallow condyles, which contact the ulnare and pisiform.

Manus (Fig. 3.33)

Directional terms for manus including the carpus and pes including the tarsus (as proximal and distal) are here used again (see chapter 3.1) as if the manus and pes were vertically placed. "Medially" (radial) is in the direction of the radius and "laterally" (ulnar) defines the direction to the ulna (following ROMER 1956, p. 378).

The manus consists of the carpus, the metacarpals, and the phalanges. The carpus consists of radiale, ulnare, one globular carpal bone, and pisiform. The general configuration of the manus is nearly identical with the one described for *Steneosaurus bollensis* (chapter 3.1).

The radiale is the largest bone in the carpus and nearly twice as large as the ulnare. The radiale is sub-rectangular with a slightly concave medial margin and a slightly convex external margin. Proximally, it articulates with the radius and distally with the metacarpal I. Laterally, it has proximal and distal contact with the ulnare. The ulnare is similar to the radiale, but more hourglass-shaped, with a medial and lateral concave margin and only half the size. It is more robust than in *Steneosaurus bollensis.* Proximally, it articulates with the ulna, medially with the radiale, and laterally with the pisiform. Distally, it contacts the one globular carpal element. This globular carpal bone is only one-third the size of the ulnare. Like in *Steneosaurus bollensis* (see chapter 3.1), it is not exactly clear which of the carpal elements are fused to form this globular carpal. According to ROMER (1956), the small carpal bone should represent the fused carpal elements three and four. The pisiform is a flat, rectangular bone, about two-third the size of the ulnare. It is articulating with the ulna proximally, the ulnare medially, and distally with the metacarpal V and has probably contact with the single globular carpal bone as well (Fig. 3.33). Compared to S*teneosaurus bollensis* the pisiform of *Platysuchus multiscrobiculatus* has a slightly smaller diameter.

The manus has five metacarpals. The metacarpals are similar in shape, but vary in length and in thickness; each consists of a cylindrical shaft with a slight enlargement of about 30% at each end (Fig. 3.33). Metacarpal I is as long as the radiale, but is about twice as wide as the metacarpal III. Metacarpal II is one-fourth longer and slightly thinner than metacarpal I. Metacarpal III is as long as metacarpal II but slightly thinner than it. The metacarpal IV is

about one-tenth shorter and one-third broader than metacarpal III. Metacarpal V is as long as metacarpal I, but has the same width as metacarpal IV.

The manus has five digits (I-V), with the phalangeal formula 2-3-4-3-2. Digit I and digit V have only two phalanges, but the first proximal digit (pollex) is most distinctive, because the metacarpal I and the two appending phalanges are broader than the others. Digit II and digit IV have originally three phalanges. Digit III possesses most likely four very slender phalanges. Therefore, digit III is about 20-30% longer than the others are (Fig. 3.33).

The proximal phalanges share a similar hourglass-shape with two articular extremities and an intermediate shaft, but vary slightly in width and length. The terminal phalanges have an articular surface only at their proximal margin. They are distally pointed and therefore claw-shaped (Fig. 3.33). In digit I, the two phalanges share the same length and width, but are slightly broader than the phalanges of the others digits are. Additionally, the proximal phalanx of digit I is only two-thirds the length of the first phalanx of digit II and the distal phalanx of digit I is distally pointed. In digit II, the first proximal phalanx is twice as long as the second phalanx. The terminal third phalanx of digit II is lacking in all studied specimens, but according to impressions seen in the sediment should be claw-shaped In digit III, the first proximal phalanx is twice as long as the second and third phalanx. The terminal fourth phalanx is lacking but is supposed to be claw-shaped. In digit IV, the first and second proximal phalanx is similar in shape and size to the corresponding phalanges of digit II, but the terminal third phalanx of digit IV is distally pointed. The proximal phalanx of digit V is half as long as the metacarpal V and slightly thinner. The terminal phalanx of digit V is claw-shaped and slightly shorter than the first phalanx.

Hind limb (Fig. 3.34)

The hind limb consists of the usual parts femur, tibia, fibula, and pes. The hind limbs are well preserved in UH 1 and SMNS 9930, except for some of the terminal phalanges. Femora, tibiae, and fibulae are articulated, whereas the pes is slightly disarticulated. In the juvenile specimen UH 2, both femora are present, too, but only partly exposed. The ilia obscure the proximal ends of the femora in UH 2 and UH 1.

Femur (fe, Fig. 3.34)

The femur is the longest of the limb bones. It is greatly elongated with proximal and distal expansions. In posterior view, the femur shows an open S-shaped curvature (Fig. 3.34). The femur is twisted, which means that the planes of the proximal and distal expansions are

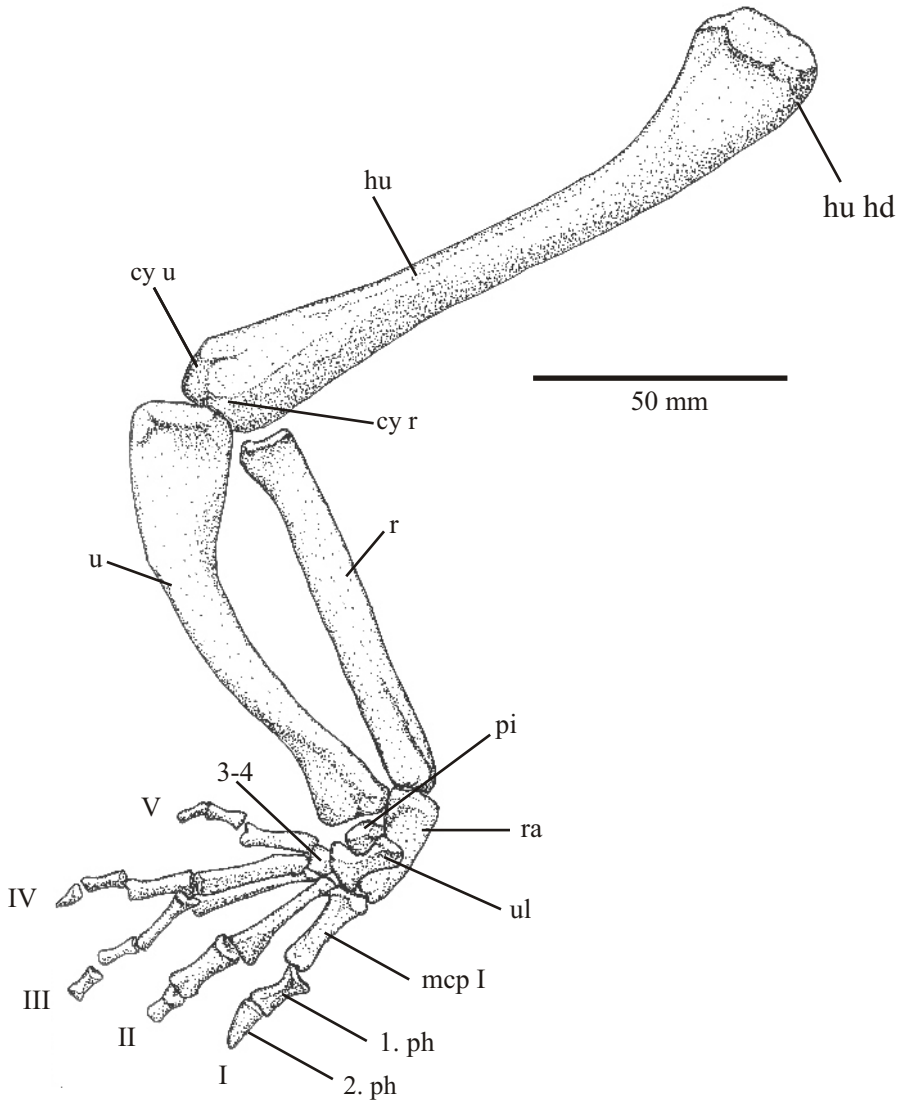

Figure 3.33: *In situ* drawing of the right fore limb of *Platysuchus multiscrobiculatus* (after SMNS 9930). Abbreviations: cp-carpal, cy r-condylus radialis, cy u-condylus ulnaris, hu-humerus, hu hd-humerus head, mcp-metacarpal, ph-phalange, pi-pisiform, ra-radial, r-radius, u-ulna, ul-ulnare, I-digit 1, II-digit 2, III-digit 3, IV-digit 4, V-digit 5.

not parallel, but oblique to each other. It has a more offset femoral head in comparison to *Steneosaurus bollensis* (see chapter 3.1). The femoral head is strongly convex, the surface being truncated on its external side by the flat external face of the bone.

The flattened external face of the distal end of the bone is marked by a series of longitudinal rugosities; the internal face ventral to the femoral head is also rough and internally concave. A rugose surface on the internal face of the shaft indicates the lesser trochanter. In distal direction, the shaft becomes more slender and has probably an oval cross-section. At the distal end of the bone, there are two condyles separated by an intercondylar sulcus. The external fibular condyle is not much larger than the internal tibia condyle.

Tibia (ti, Fig. 3.34)

The slender tibia consists of a cylindrical shaft with enlargements of about equal size at both ends. Its length (Ti1) is in adults about 65% of the femur length (Fe1), in juveniles it is about 74%. The proximal and distal enlargement diverges about 10% from the width of the shaft. The dorsal margin of the proximal end forms a shallow convex articulation area. This articulation surface for the femur is divided into two shallow condyles. The distal end of the tibia articulates with the astragalus. The surface of this distal articular facet is strongly convex. Medially, the proximal and the distal end of the tibia have contact to the fibula by small medial facets at the proximal and distal margin.

Fibula (fi, Fig. 3.34)

The fibula is a slender bone bar with slightly enlarged convexities of nearly equal size at both ends. The proximal end is about 5% larger compared to the width of the shaft. It terminates in an elongated convex surface that forms the articulation with the external portion of the lateral condyle of the femur. At its distal end, the fibula articulates distally with the calcaneum in a slightly internally concave articular facet, and medially, it meets the tibia (see there).

Pes (Fig. 3.34)

The pes resembles to that of *Steneosaurus bollensis* (chapter 3.1)and consists of tarsus, metatarsals, and phalanges. The tarsus consist of calcaneum, astragalus, and the tarsals 3 and 4. Like *Steneosaurus bollensis* (see chapter 3.1), the pes possesses a typical crurotarsal joint of the crocodile-normal type (ROMER 1956, PARRISH 1987). In contrast to extant crocodilians and other teleosaurids e.g., *Steneosaurus leedsi* (ANDREWS 1913), the calcaneum has nearly

the same size as the astragalus and its calcanean tuber is short (50% of the entire length of the calcaneum) and only slightly set off from the corpus by a circumference. The astragalus is similar to that of extant crocodiles. In posterior view, it is sub-rectangular with a pronounced, convex, lateral articular facet with the calcaneum (Fig. 3.34).

The tarsal 3 is a small globular bone articulating with the astragalus proximally, the metacarpal I distally, and the tarsal 4 laterally.

In dorsal view, the tarsal 4 is a ventrodorsally flattened, rectangular or in some cases sub-triangular bone. It is usually situated distally the calcaneum and contacts laterally the fifth metatarsal and medially the tarsal 3. Proximally, it articulates with the metatarsal II and III (Fig. 3.34)

The pes has five metatarsals, whereas metatarsal V is reduced to a flattened sub-rectangular bone (Fig. 3.34). Metatarsal V contacts proximally tarsal 4 and distally metatarsal IV. The remaining four metatarsals are long, slender bones with a circular cross-section. Metatarsal I is about 15% shorter than and twice as wide as the remaining metatarsals. It is slightly curved medially and not as straight as the other metatarsals. In cross-section, metatarsal I is more flattened than the other metatarsals. Metatarsals II-IV are identical in shape. They consist of a straight, narrow cylindrical shaft with slightly (about 10%) wider articular facets on both ends. Metatarsal II and III have the same length but are 10% longer than metatarsal IV, which is as long as metatarsal I.

Digit I consist of two phalanges and is the shortest and thickest digit. Digit II is slightly longer than digit I (about one tenth) and has three phalanges. Digit III is again about one tenth longer than digit II and has three phalanges, too. Digit IV is the longest one with four appending phalanges. It is probably one tenth longer than digit III. The phalangeal formula is 2-3-3-4-0.

The proximal phalanges are hourglass-shaped. The base of all phalanges is internally concave and the distal margin is developed as a trochlea, except for the unguals, which are distally pointed and claw-shaped. The first phalanx of digit I is about one-third shorter than the first phalanx of digit II. The second phalanx of digit I is the ungular phalanx, which is two-thirds the length of the first phalanx of digit I. The second phalanges of digits II-IV are hourglass-shaped like the first phalanges, but only half the length. The third phalanx of digits II and III are the unguals. In digit IV, the third phalanx is hourglass-shaped, but only half as long as the second phalanx. The fourth phalanx of digit IV is the ungular phalanx and as long as the third phalanx.

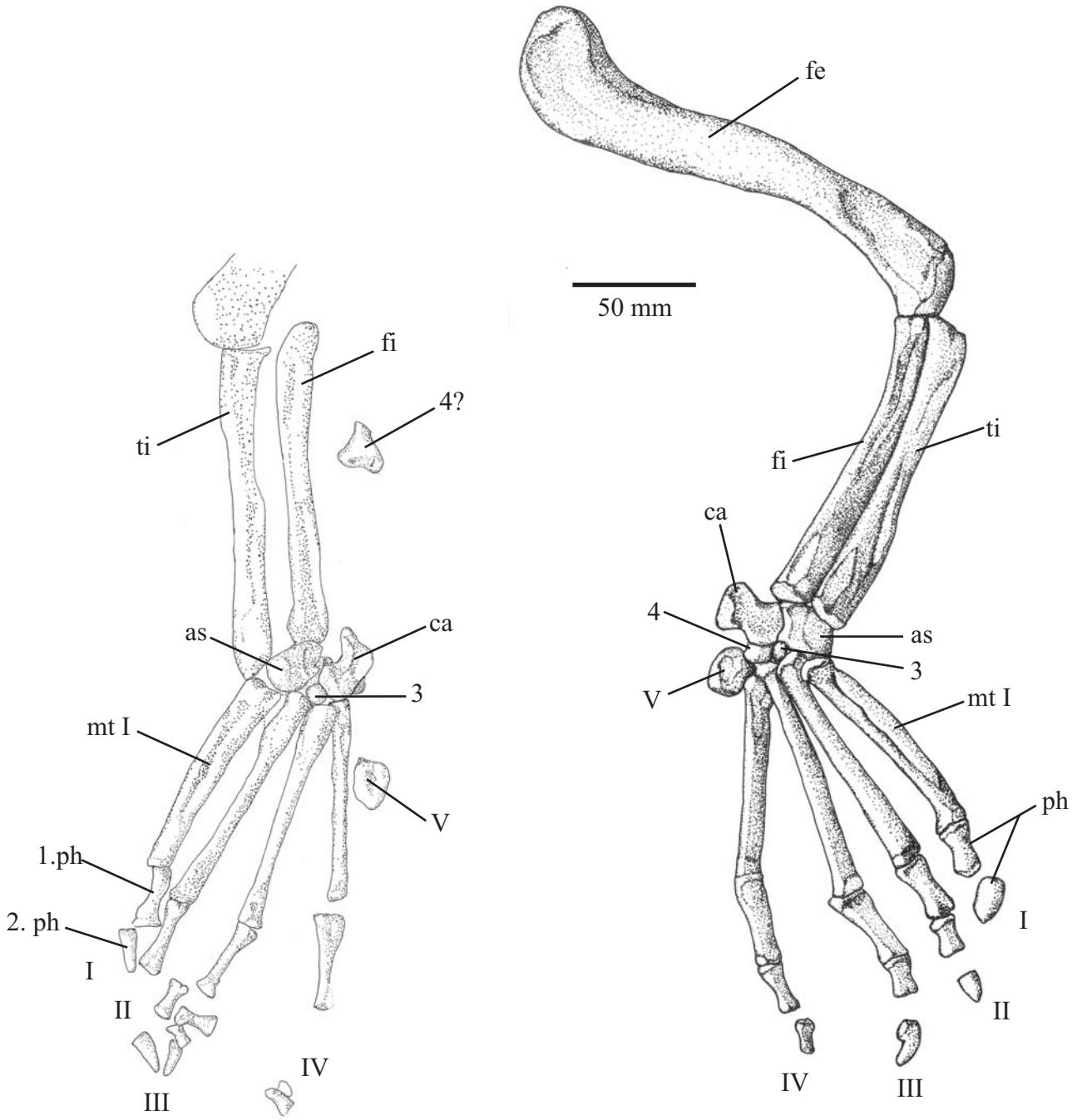

Figure 3.34a-b: *In situ* drawings of the hindlimb of *Platysuchus multiscrobiculatus*. **3.34a**-Tibia, fibula and parts of the pes of the left hindlimb of SMNS 9930. **3.34b**- Right hind limb of the same specimen. Abbreviations: as-astragalus, ca-calcaneum, fe-femur, fi-fibula, mt-metatarsal, ph-phalanx, ti-tibia, V-fifth metatarsal, I-digit one, II-digit two, III-digit three, IV-digit four, 3-tarsal 3, 4-tarsal 4.

3.5 Osteology of *Pelagosaurus typus* (BRONN, 1841)

3.5.1 Introduction

Pelagosaurus typus is a medium-sized thalattosuchian, which occurs in the Lower Jurassic of Europe. The taxon *Pelagosaurus typus* is the sole representative of *Pelagosaurus* and it is one of the oldest known thalattosuchian at all. It has originally been described from the Lower Toarcian, Posidonia Shale near Nabern in the Swabian Alb by BRONN (1841) as *Pelagosaurus typus*. French specimens from the Toarcian of Amaye–sur-Orne had formerly been described by EUDES-DESLONGCHAMPS (1864) as *Teleosaurus temporalis*.

Various finds exist of *Pelagosaurus typus* from the Liassic sediments of southern Germany (BRONN 1841, WESTPHAL 1962), France (DESLONGCHAMPS 1864, 1869, BUFFETAUT 1982, VIGNAUD 1995), Great Britain (WESTPHAL 1962, DUFFIN 1979a), and probably Portugal (VEIGA-FERREIRA 1959, ANTUNES 1967). The specimens from the Lower Jurassic of Portugal were formerly described as *Pelagosaurus tomarensis*, but probably belong to *Pelagosaurus typus*, too (ANTUNES 1967).

In the following a detailed description of the taxon *Pelagosaurus typus* is given, based on the investigation of 88 specimens. Additionally, one three-dimensional specimen (BSGP 1890 I 5) was examined with the aid of computed tomography (CT) to achieve more information about internal skull structures and the braincase (see paragraph “braincase”).

Eureptilia OLSON 1847

Diapsida OSBORN 1903

Mesoeucrocodylia WHETSTONE & WHYBROW 1983

Thalattosuchia FRAAS 1901

Pelagosaurus typus (BRONN 1841)

(Figures 3.35-3.49)

Holotype: TMH 2744

Locus typicus: Nabern near Kirchheim, South Germany

Stratum typicum: Lias ε II_5 (Lower Jurassic, Toarcian, Posidonia Shale)

3.5.2 Material

In total **88** specimens of *Pelagosaurus typus* were studied for this redescription: **12** housed in the collection of the BMNH; **19** specimens housed in the BSGP, **1** specimen housed in the FSL; **6** specimens housed in the GPIT; **1** specimen housed in the MGUH; **12** specimens housed in the MNHN; **1** specimen housed in the NHMUS; **20** specimens housed in the collection of the SMNS; **2** specimens housed in the TMH (including the holotype); and **4** specimens housed in the UH.

A complete list of all the investigated material is provided in the appendix I.

3.5.3 Locality and horizon

Pelagosaurus typus is known with certainty from Germany, France, and Great Britain. The holotype (TMH 2744) and numerous specimens of *Pelagosaurus typus* come from the Lias ε (Toarcian) from different localities e.g., Holzmaden, Bad Boll, Ohmden, and Ohmdenhausen in the Swabian Jura, South Germany. The French specimens were found in the Upper Liassic (Toarcian) layers of Amaye-sur-Orne, Caen, and Curcy (EUDES-DESLONGCHAMPS 1864, DESLONGCHAMPS 1877). Additionally one studied specimen (BMNH 14437) was found in the Upper Liassic of Whitby, Great Britain.

Further material of *Pelagosaurus typus* is known from the Lower Jurassic of Ilminster, Somerset in Great Britain (DUFFIN 1979a/b), and probably from the Late Toarcian from Portugal (VEIGA-FERREIRA 1959, ANTUNES 1967), but is not considered here.

3.5.4 Preservation

This taxon is almost complete preserved, except of parts of the carpus and tarsus, which are too fragmentary preserved for a close description.

The preservation of the specimens of the Holzmaden area is the typical one (see chapter 3.1 & 3.4). They are preserved in a matrix of black shale and compressed by overlying strata. Articulated preservation is common. In some cases, the bones are displaced but usually not broken (e.g. GPIT Re 1193/17, GPIT Re 1193/18, SMNS 8066, UH 4, and UH 8). From the German Posidonia Shale deposits, three-dimensional finds of *Pelagosaurus typus* are not reported, except for the specimen UH 10 from Holzmaden.

Even though the preservation of the French specimens is often three-dimensional, in most cases, the material is disarticulated and the correlation of the single teeth, osteoderms or bones to an individual specimen is therefore questionable (e.g. BMNH 32603, BMNH 32606). One of the best-preserved skulls of *Pelagosaurus typus* (BMNH 32599) from Amaye–sur-Orne in France was first described by EUDES-DESLONGCHAMPS (1864) as *Teleosaurus temporalis*. This specimen consists of a nearly complete three-dimensional skull

including the mandible, which only lacks the anterior parts of the rostrum including the premaxillae. It is acid-prepared and it shows excellently the sutures and the ornamentation of the cranial bones. Because of the three-dimensional preservation, the occipital is also visible.

Only one specimen (BMNH 14437) was investigated from the Liassic sediments of Whitby, England. It consists of a poorly and fragmentary preserved three-dimensional skull, which lacks most of the anterior rostrum, the mandible, and the occipital (DUFFIN 1979a).

3.5.5 Diagnosis

Pelagosaurus typus is a medium sized thalattosuchian with a maximum length of two meters. The skull length is about 57% of the trunk length (TRL)(WESTPHAL 1962). The skull is slender with a skull width (C) of 18-22% of the skull length (A). The rostrum is relatively long (about 74.4 % of the skull length) compared to the other Liassic teleosaurids. The paired premaxilla is not or only slightly spoon-shaped enlarged. The prefrontal is large and almost two-thirds the size of the lacrimal. The external naris opens anterodorsally or dorsally. The antorbital fenestra is visible and longitudinal ellipsoid. The lateral aligned orbit is relatively large in comparison to the skull size. The orbital length (I) in comparison to the skull length (A) is in average about 9.8%. The orbit is round or longitudinal ellipsoid depending on the ontogenetic stage of the specimen (see chapter 4). In some specimens, parts of the sclerotic rings are observable (EDINGER 1929, WESTPHAL 1961, VIGNAUD 1995). The jugal forms the ventral margin of the orbit. The supratemporal fenestra is longitudinal ellipsoid. The supratemporal fenestra is relatively small compared to the skull length (D/A~ 13.4%). The lateral margin of the supratemporal fenestra is one-third lower than the sagittal crest, therefore the supratemporal fenestrae open dorsolaterally.

Pronounced ornamentation consisting of a pattern of small round pits and elongated grooves is present on the external surface of following bones: Frontal, parietal, postorbitals, squamosals, prefrontals, lacrimals, nasals, and jugals. The upper jaw possesses about 36 teeth, while the in the lower jaw up to 32 teeth are present.

The vertebral column consists of up to 65 amphicoelous vertebrae. Only eight cervical vertebrae are present and the second cervical rib attached to the axis is double-headed. Up to 42 caudal vertebrae are described. The tail length is about 56% of the body length.

The dorsal armour consists of one longitudinal row of paired osteoderms and the ventral armour consists of four longitudinal rows of osteoderms. Posteriorly, the tail is only armoured up to the 10^{th} caudal vertebra and lacks ventral osteoderms.

The fore limbs are more slender and shorter than the hind limbs. The humerus length (H1) is about 53.4% of the femur length (Fe1). The ilium possesses only a short posterodorsal

process and has a small recess at the posterior margin ventral to this process. The shallow acetabulum lies closer to the anterior margin than to the posterior margin of the ilium. The pubis is long with 2.5 times the length of the ilium (Pu1/P1), slender and distally only slightly enlarged. The pubis width at the distal margin (Pu2) is about 30% of the pubis length (P1).

3.5.6 Osteology

Skull (Fig. 3.35)

The skull of *Pelagosaurus typus* is long and slender. The narrow rostrum widens gradually at the level of the anterior margin of the nasals in the cranial table. In transverse-vertical cross section, the posterior part of the skull has a more or less semi-round shape. In dorsal view, the cranial table is trapezoidal the complete skull shape appears therefore triangular. In lateral view, there is a gradually increasing in height of the skull visible. The upper rostrum is from the tip of the premaxilla to the anterior margin of the nasal wider than high in cross-section but at the level of the anterior margin of the nasals, the skull increases slightly but steadily in height. It reaches the highest point at the posterior margin of the parietal. Posteriorly, the height of the skull (T) is about 15.5% of the skull length (A), and is 49% of the skull width (C). Most of the cranial bones possess pronounced ornamentation on their external surface (see below).

Cranial table

Openings

External naris (en, Fig. 3.35)

The external naris is well preserved in specimens e.g., BSGP 1925 I 34, MNHN 1883-14, NHMUS M62 2516, UH 4, UH 8, and UH 10.

The paired premaxilla encloses the confluent external naris entirely. The external naris is circular to longitudinal ellipsoid and mainly dorsally orientated. The outline of the external naris forms an angle of about 10-20° with the horizontal plane. The margins are smooth. There is no internasal septum observable. In some cases, a small medial process extends from the posterior margin anteriorly in the external naris and gives it a more heart-shaped look in anterior view (Fig. 3.34a). There is no internasal septum visible. The paired premaxilla meets each other in a straight suture and no median ridge is developed like e.g., in *Steneosaurus bollensis* (see chapter 3.1).

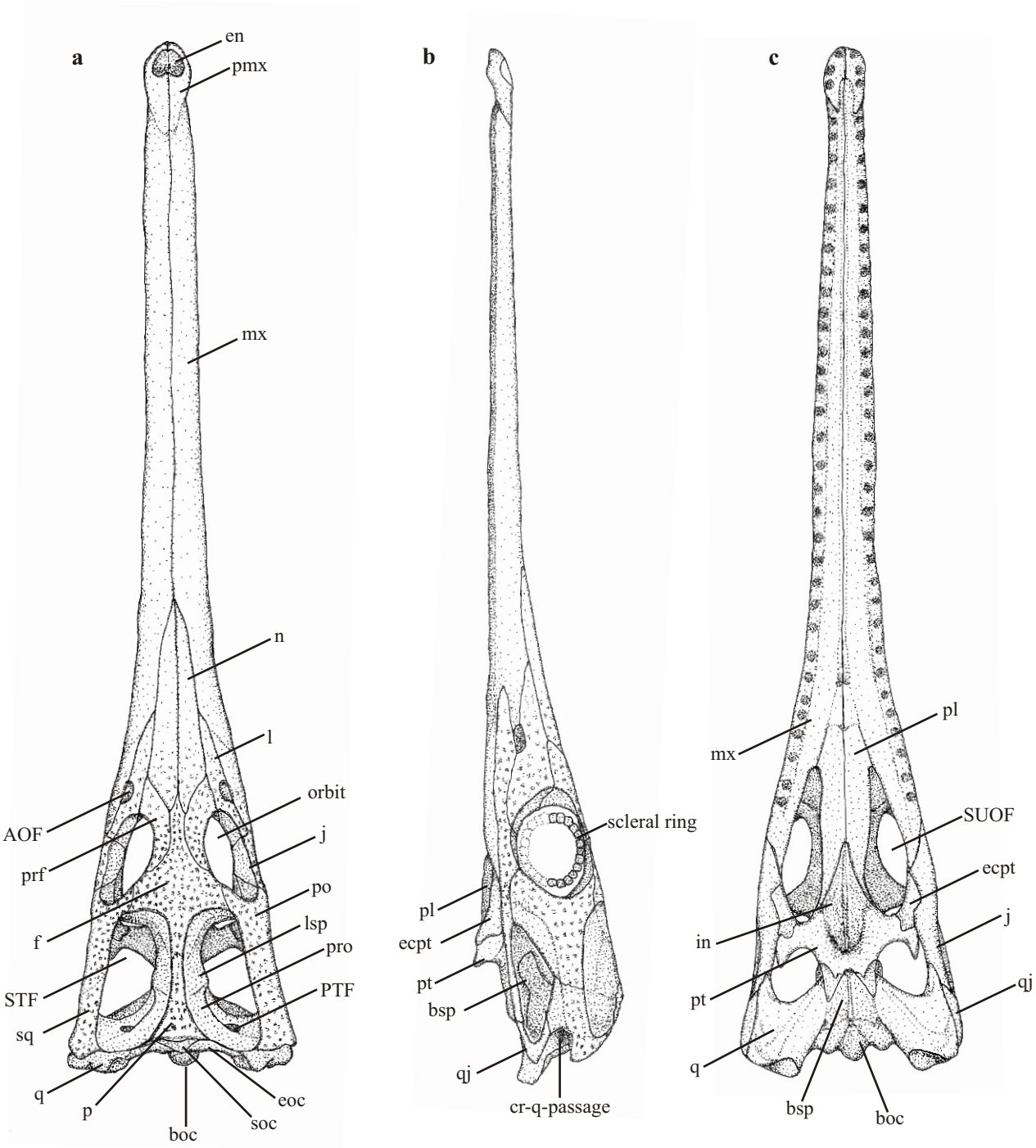

Figure 3.35a-c: Reconstruction of the skull of *Pelagosaurus typus* (mainly after BMNH 32599 and UH 10). **3.35a**-Skull in dorsal view. **3.35b**-Skull in lateral view, **3.35c**-Skull in ventral view. Abbreviations: AOF-antorbital fenestra, boc-basioccipital, bsp-basisphenoid, en-external naris, in-internal naris, j-jugal, eoc-exoccipital, ecpt-ectopterygoid, f-frontal, l-lacrimal, lsp-laterosphenoid, mx-maxilla, n-nasal, p-parietal, pl-palatine, pmx-premaxilla, pt-pterygoid, PTF-posttemporal fenestra, prf-prefrontale, pro-prootic,q-quadrate, qj-quadratojugal, sq-squamosal, soc-supraoccipital, STF-supratemporal fenestra, SUOF-suborbital fenestra.

Antorbital fenestra (AOF, Fig. 3.35)

Because of the three dimensional preservation of some of the skulls, small antorbital fenestra are visible at the specimens, e.g. BMNH 32599, UH 10, BSGP 1973 VII 592, BSGP 1925 I 34, MNHN 1914-9-9, MNHN 1883-14, and FSL 530238.

The antorbital fenestra is longitudinal ellipsoid and lies in the lateral side of the skull. Its length is about 25% of the orbit length (I). The dorsal margin is formed by the lacrimal, the ventral margin is formed by the jugal, and the anterior margin is formed by the maxilla. In some compressed specimens of *Pelagosaurus typus* from Holzmaden, the antorbital fenestra is collapsed and not clearly visible.

Orbit (o, Fig. 3.35, Fig. 3.36, Fig. 3.37)

The anterior margin of the orbit is formed by the lacrimal and prefrontal. The medial margin is formed by the prefrontal and frontal. Only one-fourth of the posterior margin is formed medially by the frontal and the remaining three-fourths are formed laterally by the postorbital. The posterior 80% -90% of the lateral margin is formed by the jugal and the anterior 10-20% is formed by the lacrimal. The orbit is relatively large compared to that of *S. bollensis*. The orbit length (I) is in average 9.8% of the skull length (A) and in average 77% of the supratemporal fenestra length (D). In the adult specimens, the orbits are usually smaller than the supratemporal fenestrae, while in the juvenile stages, the orbit can reach equal size to the supratemporal fenestra (I/D ~1, for further information, see chapter 4). The orbits open mainly laterally and are round or longitudinal ellipsoid. The longest axis of the orbit extends horizontal from the point of the prefrontolacrimal suture up to the middle of the anterior margin of the postorbital.

Scleral ring (Fig. 3.35b, Fig. 3.37)

A scleral ring inside the orbit of *Pelagosaurus typus* is described in the specimen BSGP 1925 I 34 by EDINGER (1929) and WESTPHAL (1962) as well as in one specimen housed in Budapest (EDINGER 1929). In addition, tiny rectangular bone plates, which are remains of a scleral ring, are exposed in the specimen UH 4 and specimen FSL 530238 (92812) (Fig. 3.37). The tiny rectangular bone plates form at least in the upper part of the orbit a scleral ring. In specimen FSL 530238, single, loose bone plates were collected during the preparation of the skull in the orbit area. They are very thin less than 0.5 mm in cross section. In UH 4 and BSGP 1925 I 34 they are still embedded in the sediment inside the orbit.

Supratemporal fenestra (STF, Fig. 3.35-3.37)

The supratemporal fenestra is longitudinal ellipsoid and opens dorsolaterally. It is bordered anteromedially by the frontal and anterolaterally by the postorbital. Posterolaterally, it is formed by the squamosal and posteromedially by the parietal. The squamosal and the postorbital form the lateral margin each with 50%. The wide lateral bar of the supratemporal fenestra lies ventrally to the level of the dorsal surface of the sagittal crest and possesses pronounced ornamentation (see paragraph "squamosal" and postorbital"). The anterior 25% of the sagittal crest is formed by the frontal and the posterior 75% by the parietal. The anteromedial corner of the fenestra is sub-angular, while all other edges of the margin are rounded. Compared with most other Liassic teleosaurids, the supratemporal fenestra is relatively small in *Pelagosaurus typus*. The supratemporal fenestra length (D) is in average 13.4% of the skull length, the holotype shows only 12.2%. In comparison, *Steneosaurus bollensis* and *Platysuchus bollensis* have a ratio of about 15-16%, while *Steneosaurus brevior* has a ratio of almost 19%. Only *Steneosaurus gracilirostris* shows a ratio similar to *Pelagosaurus typus* with an average 12.7% (for further information see chapter 4 & 5).

Infratemporal fenestra (ITF, Fig. 3.35-3.37)

In the specimens BSGP 1973 VII 592, BSGP 1890 I 5, FSL 530238, GPIT Re 1193/18, MNHN 1914-9-9, MNHN 1870-11-2 (cast), and MNHN 1883-14 the infratemporal fenestra is completely three dimensionally preserved. In BMNH 32599, the posterior end of the jugal is missing but the anterior part of the jugal and the quadratojugal still exist. Therefore, the infratemporal fenestra can be reconstructed (Fig. 3.35b). In addition, in the specimen UH 4 the infratemporal fenestra is exposed, because of the dorsolateral embedding of the specimen (Fig. 3.37).

The infratemporal fenestra is sub-triangular in lateral view (Fig. 3.35b & Fig. 3.36c). It is almost as long as the supratemporal fenestra. Its height is about one third of its length. For example, the specimen BSGP 1890 I 5 has an infratemporal fenestra length (N) of 34 mm and a height (O) of 12 mm (see chapter 2 and appendix II). It opens laterally and lies almost vertically in the skull. It is bordered anterodorsally by the postorbital, posterodorsally by the squamosal, posteroventrally by the quadratojugal, and anteroventrally by the jugal.

Cranial bones

Premaxilla (pmx, Fig. 3.35, Fig. 3.37)

The premaxilla configurations are exposed in good condition e.g., in the specimens MNHN 1883-14, UH 4, and UH 10 (Fig. 3.37).

The paired premaxilla is only slightly laterally enlarged and not very prominent in the rostrum (see chapter 4). Dorsally, the premaxilla completely encloses the confluent external naris (see there). The lateral margin of the premaxilla is smooth and slightly externally convex. In lateral view, the premaxillary-maxillary suture is oblique and runs from anteroventral to posterodorsal. The premaxilla therefore overlies the maxilla at the diastema like in *S. bollensis* (see chapter 3.1). At the floor of the external naris, the premaxillae meet each other in a straight suture. In dorsal view, no incisive foramen is visible. Posterodorsal to the external naris, the paired premaxilla meet each other in a straight median suture. The paired premaxilla tapers posteriorly between the maxillae and ends medially level with the third maxillary tooth.

The premaxilla possesses three to four homogenous teeth (see paragraph “dentition”). The external surface of the premaxilla is smooth and except of some weak longitudinal wrinkles in lateral view.

Maxilla (mx, Fig. 3.35-3.37)

The paired maxilla forms dorsally the largest part of the elongated rostrum and ventrally parts of the secondary palate (see paragraph “palate”). Dorsally, the maxillae broadly meet each other in a straight suture. The lateral margin of the maxilla is straight and do not undulate. Anterodorsally, the maxilla contacts the premaxilla in an oblique suture running from posteromedial to anterolateral. In anterior direction, the maxilla descends ventrally below the premaxilla. Posteromedially, the maxillae contact the paired nasal, which separates the maxillae in their posterior third. The maxillonasal suture is smooth and extends obliquely in mediolateral direction. Posteromedially, the maxilla is bordered by the lacrimal that anteriorly tapers off between the maxilla and the nasal. Posterolaterally, the maxilla bifurcates in a dorsal and a ventral part. The dorsal part of the maxilla tapers posteriorly between lacrimal and jugal, where it takes part in the anterior margin of the antorbital fenestra (see paragraph “antorbital fenestra”). The ventral part of the maxilla descends posteroventrally largely under the jugal up to the level of the orbit.

The maxilla is tooth bearing and possesses an estimate of up to 32 alveoli as visible in specimen UH 4 (Fig. 3.37). The teeth are running up to the level of the anterior margin of the orbit as it is visible in specimen FSL 530238 (see paragraph "dentition"). The external dorsal surface of the maxilla is generally smooth except of some faint wrinkles, in irregular distribution.

Nasal (n, Fig. 3.35-3.37)

The nasal is an elongated slender bone. It meets its contralateral nasal in a straight median suture. The paired nasal is restricted to the posterior fourth of the rostrum and has no contact to the premaxillae. The nasal length is an average 29% of the rostral length (B). Anteromedially, the paired nasal tapers off and deeply project between the maxillae until level with the 26th maxillary tooth. Posteromedially, the nasal contacts the frontal (see the paragraph "frontal"). Posterolaterally, the nasal is bordered by the prefrontal and more laterally by the lacrimal. The posterior margin of the nasals ends level with the anterior margin of the orbits. The ornamentation of the surface of the nasal varies slightly individually. In most cases, it is covered in its posterior part with similar pattern of pits as at the frontal and prefrontal (see there), which makes it complicated to find the exact run of the frontonasal and prefrontonasal suture, e.g. BMNH 32599 (Fig. 3.36). In rare cases, the ornamentation consists of a pattern of fine shallow pits covering the complete surface of the nasal (e.g. UH 10).

Lacrimal (l, Fig. 3.35-3.37)

The lacrimal is an ornamented and sub-triangular bone. Anterolaterally, it is bordered by the maxilla and anteromedially by the nasal. Posteromedially, it contacts the prefrontal on its entire length in a straight suture and posteriorly the lacrimal forms two-thirds of the anterior margin of the orbit. In some specimens, the posterior margin of the lacrimal is slightly thickened, forming a small bulge at the anterior margin of the orbit. Posterolaterally, the lacrimal is bordered by the jugal. In some specimens (e.g. BMNH 32599, BSGP 1925 I 34), the dorsal margin of the antorbital fenestra is visible as a recess, in the posterior third of the lacrimal (see paragraph "antorbital fenestra").

The lacrimal possesses a strongly ornamented external surface. The ornamentation consists of a pattern of small circular shallow pits and grooves, which are densely distributed in the posterior part of the lacrimal. In anterior direction, the pits get shallower and are more spacious distributed.

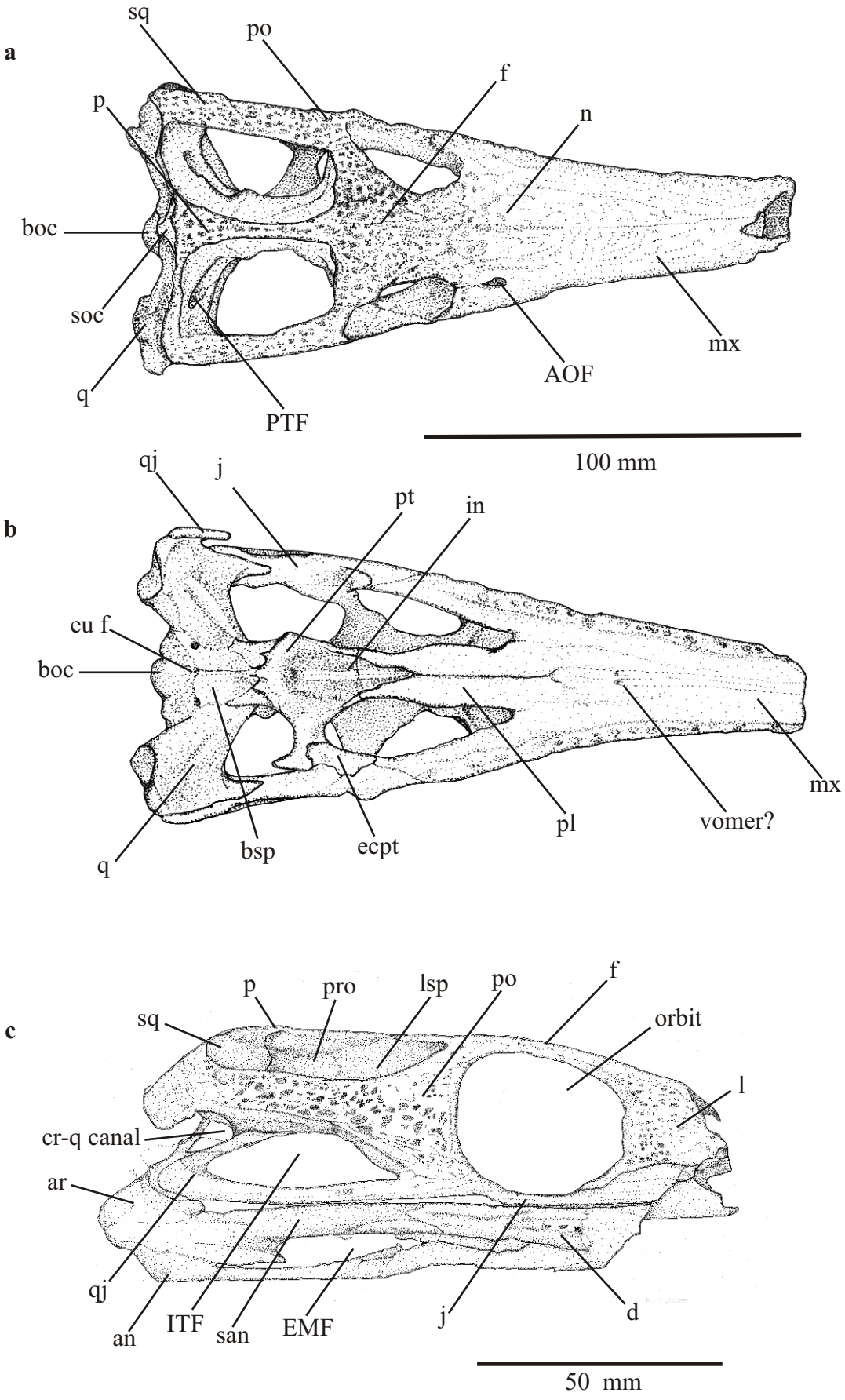

Figure 3.36a-c: *In situ* drawing of some skull fragments of *Pelagosaurus typus*. **3.36a**-Specimen BMNH 32599 in dorsal view, **3.36b**-Specimen BMNH 32599 in ventral view, **3.36**c-Specimen BSGP 1890 I 5 in lateral view. Abbreviations see figure 3.35 and EMF-external mandibular fenestra, ITF-infratemporal fenestra, lsp-laterosphenoid, pro-prootic, san-surangular.

Prefrontal (prf, Fig. 3.35-3.37)

The prefrontal is a roughly sickle-shape bone with pronounced ornamentation on its external surface. It is at least two-thirds the length of the lacrimal and expands anteriorly in front of the orbit. The medial margin of the prefrontal is medially convex and is posteriorly bordered by the frontal and anterior by the nasal. The posterolateral margin of the prefrontal is strongly laterally concave and forms the anteromedial margin of the orbit. The entire anterolateral margin of the prefrontal has contact to the lacrimal in a straight suture. The pronounced ornamentation on the external surface of the prefrontal is very similar to the ornamentation on the anterior part of the frontal (see there). It consists of a pattern of small circular to elliptic pits of all almost equal size in a dense, equal distribution. Because of the ornamentation in the area of the prefrontofrontal suture, the exact course of the suture is in some cases hard to determine.

Frontal (f, Fig. 3.35-3.37 & Fig. 3.42)

The unpaired frontal is roughly cruciform and forms the main medial part of the cranial table. It contacts posteriorly the parietal, posterolaterally the postorbitals, anterolaterally the prefrontals and the nasals. The frontal forms a pointed process, which projects anteriorly between the nasals. The short lateral processes of the frontal contact the postorbitals in a posterolaterally running oblique suture. In some specimens, the area around the frontopostorbital suture is thickened (e.g. GPIT Re 1193-18). The posterior process of the frontal is short and forms only one fourth of the sagittal crest.

The shape of the frontal varies during ontogeny from approximately rhombic to roughly cruciform; this variation is discussed in detail in chapter 4 (see there, Fig. 4.5).
The ornamentation of the frontal in adult and juvenile consists of numerous small, circular to ellipsoid, deep pits, which are evenly distributed on the external surface.

The CT scans of the skull of BSGP 1890 I 5 show the frontal in cross-section. A vertical median structure of less density is visible in the frontal in cross-section (Fig. 3.42). This vertical median structure in the frontal, indicates that the frontal is ventrally not totally fused (Fig. 3.42). It points to a later ontogenetic fusion of the bones and indicates probably a more primitive stage of *Pelagosaurus typus* than the other Liassic teleosaurids.

Parietal (p, Fig. 3.35-3.37)

The parietal is an unpaired triangular bone in the posterior margin of the cranial table. Anteriorly it forms a process, which forms the posterior three fourths of the sagittal crest and

contacts anteriorly the frontal. Laterally, it contacts the squamosal in an oblique suture, which runs from anteromedial to posterolateral. Posteroventrally it meets the supraoccipital, prootic, and anteroventrally the laterosphenoid. The anteroventral contact to the prootic and the laterosphenoid varies intraspecifically, in some specimens real sutures are found, in other specimens this area is completely fused. In specimen FSL 530238 and BSGP 1890 I 5, the parietal has broad ventral contact in a straight horizontal suture to the dorsal margin of the prootic and the laterosphenoid (Fig. 3.36c). In specimen MNHN 1914-9-9, the parietal fuses anteroventrally with the frontal and no suture is visible. The parietal fuses ventrally with the anterior part of the supraoccipital and the posterior part of the laterosphenoid. A contact with the prootic is likely but is not visible in this specimen.

The external dorsal surface shows a pattern of pits similar to that on the frontal. It consists of small circular deep pits in a dense distribution, which makes it impossible to determine the exact course of the frontoparietal suture.

Postorbital (po, Fig. 3.35-3.37)

The postorbital is a triradiate bone with pronounced ornamentation at the lateral margin of the cranial table. The posterior process contacts the squamosal. In lateral view, they meet each other in an oblique suture running in anteroventral-posterodorsal direction. Due to the pronounced ornamentation of the external surface of the postorbital and squamosal, the exact run of the suture is in some cases difficult to determine. Their medial margins form the lateral margin of the supratemporal fenestra (see paragraph “supratemporal fenestra”) and their ventral margins form the dorsal margin of the infratemporal fenestra (see paragraph “infratemporal fenestra”). Dorsomedially, the postorbital contacts the frontal with a medial process in an oblique suture running from anteromedial to posterolateral. It forms anteriorly 80% of the posterior margin of the orbit. Anteroventrally, it contacts the jugal in a slightly ventrally convex suture and medioventrally it meets the ectopterygoid.

The ornamentation on the dorsal surface of the postorbital consists of a dense pattern of deep rounded pits and small grooves (Fig. 3.36). In lateral view, the postorbital possesses in its ventral third a distinct ridge running parallel to the dorsal margin of the infratemporal fenestra (e.g. FSL 530238, BSGP 1890 I 5). This ridge continues also at the lateral surface of the squamosal. Ventral to this ridge, the surface of both bones is smooth (Fig. 3.35b, Fig. 3.36c).

Squamosal (sq, Fig. 3.35-3.37)

In dorsal view, the squamosal is an L-shaped bone situated posterolateral at the skull. The lateral part is oriented sagittally, whereas the medial part is transverse. The squamosal has its largest expansion in ventral direction and possesses pronounced ornamentation on its lateral and dorsal surface. The squamosal forms the posterolateral margin and at least half of the posterior margin of the supratemporal fenestra (see there). Anteriorly, it contacts the postorbital in an oblique, smooth suture, which runs from anteroventral to posterodorsal (see paragraph "postorbital"). The squamosal is anteriorly as wide as the postorbital and possesses an identical pattern of pits, too. In posterior direction, it deviates medially and contacts the parietal in a thin process in dorsal view. This process expands in ventral direction and has there wide contact to the parietal (see paragraph "parietal"). Posteroventrally, it broadly contacts the exoccipital in an oblique suture (Fig. 3.39) and the quadrate in a straight suture. Ventrolaterally is contacts the quadratojugal. The squamosal and the quadratojugal form the posterodorsal margin of the infratemporal fenestra (Fig. 3.36c and 3.37). Together with the quadratojugal, quadrate, and exoccipital it encloses posterolaterally the cranioquadrate canal (Fig. 3.36c). Together with the quadrate and prootic, it borders ventromedially the posttemporal fenestra (see there). In posterior view, a medial squamososupraoccipital contact is visible. The squamosal tapers medially between the dorsal parietal and the ventral supraoccipital. In posterior view, the external surface of the squamosal is smooth.

Jugal (j, Fig. 3.35-3.37)

The jugal is an elongated bone, which reaches from circa the level of the anterior margin of the lacrimal up to the last third of the infratemporal fenestra. Anterior to the postorbital, it is twice as high as in its posterior half. Posteriorly, the jugal extend in a thin rod-shaped process, and contacts the small hook-shaped quadratojugal posterior to the level of the postorbitosquamosal suture. In lateral view, the oblique jugoquadratojugal suture runs from anteroventral to posterodorsal. Posteriorly, the jugal forms at least the anterior two-thirds of the ventral margin of the infratemporal fenestra. Anteriorly, it forms the ventral margin of the antorbital fenestra and the main part of the ventral margin of the orbit. Anterior to the orbit, the jugal is anteroventrally bordered by the maxilla and anterodorsally by the lacrimal. Anterior to the infratemporal fenestra, the jugal lies ventrally to the lacrimal and postorbital and forms the lateral margin of the orbit. Dorsomedially, it has contact to the ventrolateral process of the postorbital (see there), medioventrally to the ectopterygoid (see paragraph "ectopterygoid").

The ornamentation on the external surface of the jugal is pronounced. The pattern of pits varies broadly in anterior-posterior direction. Anteriorly, a regular distribution of small pits and shallow grooves up to the level of the infratemporal fenestra is visible, whereas posteriorly the external surface of the rod-shaped process is completely smooth.

Quadratojugal (qj, Fig. 3.35-3.37)

In lateral view, the quadratojugal is a small, hook-shaped bone. Anteroventrally, it contacts the jugal with a slender process in an oblique suture (see paragraph "jugal"). Anterodorsally, it has contact to the squamosal in a straight, smooth suture, and medially it meets the quadrate. The quadratojugal forms the entire posterior margin and part of the ventral margin of the infratemporal fenestra (see "infratemporal fenestra"). It also forms the lateroventral floor of the cranioquadrate canal.

Quadrate (q, Fig. 3.35-3.37)

The general shape and position of the quadrate is very similar to those of *Steneosaurus bollensis* (see chapter 3.1).

The quadrate lies ventrally to the squamosal. Posteriorly, the quadrate forms two tubercles, which articulated with the mandible. The articular facets consist in dorsal view of two slightly convex prominences, separated by a shallow groove. The quadrate expands obliquely in dorsomedial direction and contacts posteromedially and mediodorsally the exoccipital and dorsally the squamosal (see there). Laterally, the quadrate meets the quadratojugal in a straight suture. In lateral view, it forms part of the braincase wall and meets anterodorsally the prootic in a straight suture. Anterolaterally, it forms the posterior margin of the foramen for the cranial nerve V. In ventral view, the quadrate meets anteromedially with the basisphenoid and the pterygoid in straight sutures.

Palate (pl, Fig. 3.35-3.37, Fig. 3.42)

The most complete palate is preserved in specimen BMNH 32599. Parts of a well-preserved palate are visible in e.g., BSGP 1890 I 5, FSL 530328, and GPIT Re 1193-18. The palate consists of the premaxillae, maxillae, palatines, pterygoids, ectopterygoids, and the unpaired vomer. The secondary palate is formed by the premaxillae, maxillae, and palatines.

Inside the secondary palate, ventral to the orbits the nasal canal is probably separated by the vomer dorsally and the palatinal septum ventrally, posterior to the orbits the nasal canal is fused (Fig. 3.42). Anteriorly, this nasal canal is formed by the premaxilla and maxilla.

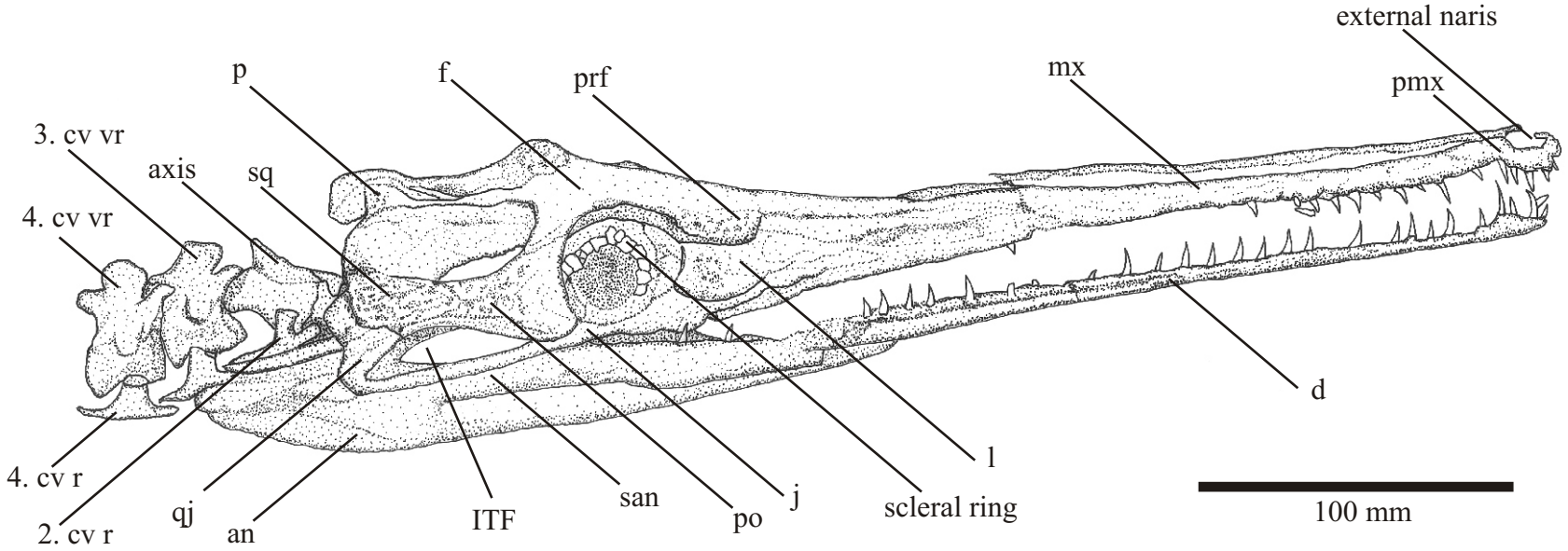

Figure 3.37: *In situ* drawing of the skull of *Pelagosaurus typus* with appending mandible and four cervical vertebrae of the specimen UH 4. This specimen is preserved in lateral view and is the largest known specimen of *P. typus* so far. Clearly visible are the small bone plates forming the scleral ring in the orbit. Another characteristic is the double-headed second cervical rib (2. cv r). Abbreviations see figure 3.35 and figure 3.36.

Palatal openings

Internal naris (in, secondary choana, Fig. 3.35c, Fig. 3.36b Fig. 3.42)

The longitudinal roughly drop-shaped internal naris is enclosed anteriorly by the paired palatine and posteriorly by the paired pterygoid. The internal naris is developed anteriorly as a narrow depression between the palatines and enlarges and deepens posteriorly widely into the pterygoids. Anteriorly, the internal naris tapers deeply between the palatines separating them in their posterior fourth. The depth of the internal naris is about 10 mm at its posterior margin, measured from the ventral surface of the pterygoid (Fig. 3.42). The median pterygoidal-pterygoidal suture forms a median pronounced ridge in the roof of the internal naris (Fig. 3.35c, Fig. 3.36b, and Fig. 3.42c).

Suborbital fenestra (SUOF, Fig.3.35c, Fig. 3.36b)

In ventral view, the suborbital fenestra is drop-shaped, which means it is longitudinal ellipsoid with an anterior pointed margin. It is bordered anteromedially by the palatine, laterally by the maxilla and ectopterygoid and posteriorly by the pterygoid. The suborbital fenestra ends anteriorly level with circa the 30th maxillary alveolus. Its length is about 15% of the skull length and therefore it is the largest suborbital fenestra within the Liassic teleosaurids.

Maxilla & Premaxilla (Fig. 3.35c, Fig. 3.36b)

The maxilla forms ventrally about 80% of the secondary palate. The maxillae meet each other in their anterior 70% in a straight median suture, which is developed as a shallow groove in its posterior half. The ventral premaxillary-maxillary suture is not exposed in any of the investigated specimens and is unknown. The shown premaxillary-maxillary suture in the reconstruction is hypothetical (Fig. 3.35c). It is an assumption based on the conditions observed in other teleosaurids. In dorsal view, no incisive foramen is visible in *P. typus*, therefore it is not reconstructed in ventral view.

Posteromedially the maxilla contacts the palatine, posterolaterally the jugal, and in most cases the ectopterygoid, too (Fig. 3.35c, Fig. 3.36b). In addition, a possible maxillary-vomer contact is exposed posteromedially in specimen BMNH 32599 (see paragraph "vomer").

Up to 32 circular alveoli lie in a straight row in a shallow groove along the lateral edge of the maxilla. The interalveolar space is about 1-1.5 times the length of the alveoli diameter.

Prefrontal (Fig. 3.41, Fig. 3.42)

Remains of the prefrontal pillars are visible in the specimen BMNH 32600 and BSGP 1890 I 5 (Fig. 3.41, Fig. 3.42).

The ventromedial process of the prefrontal (prefrontal pillar) is developed as a transverse oblique sheet of bone, which runs from anterolateral to posteromedial. The CT scans of BSGP 1890 I 5 show that the paired prefrontal pillar forms a somewhat heart-shaped structure in cross-section, probably to enclose anteriorly the ductus olfactorius (ZAHER et al. 2006). A ventral contact to the palatines is expected but not visible (Fig. 3.42a)..

Palatine (pl, Fig. 3.35c, Fig 3.36b)

The palatines form posteriorly circa 15% of the secondary palate. They are smooth, elongated, flat bones, which meet each other anteriorly in a straight median suture. Anteriorly, the paired palatine tapers off shortly between the maxillae and divides them in their posterior fourth to fifth. Anteromedially, an external contact to the vomer is indicated by two shallow depressions (see paragraph "vomer"). Posteriorly to this, it forms with its lateral margin the anterior and medial margin of the suborbital fenestra (Fig. 3.35c, Fig. 3.36b). Posteriorly, the palatines are separated in their posterior fourth by the internal naris and each palatine contacts posterolaterally the pterygoid in a slender pointed process. Posteromedially, the paired palatine forms the anteroventral margin of the internal naris and anteroventrally it encloses the paired nasal canal (Fig. 3.42a).

Vomer (v, Fig. 3.36b & Fig. 3.42a)

A possible vomer lies at the anterior margin of the paired palatine level with the 26th maxillary alveolus and forms a shallow paired depression parallel to the median interpalatinal suture. It cannot be excluded that this structure is part of the palatine or the maxilla, but the position resembles the position observed for the vomer in *Tomistoma schlegelii*. Thus, these depressions may indicate the position of the vomer, but no further evidence is available. In the CT slices is a paired nasal canal exposed, which is probably separated by the vomer ventrally to the orbits (Fig. 3.42a).

Pterygoid (pt, Fig. 3.35c, Fig. 3.36b)

The pterygoids meet each other dorsomedially in a straight suture and form together a roughly butterfly-shaped structure. It defines the posterior portion of the palate and contributes to the formation of the suborbital fenestra and the internal naris (see there).

Anteromedially it contacts the paired palatine (see there). Anterolaterally the paired pterygoid forms prominent, transverse pterygoid flanges, which contact the ventromedial margins of the ectopterygoids laterally (see there). Laterally, the transverse pterygoid flanges are strongly flexed ventrally, below the level of the jugal (Fig. 3.35c). Anteriorly, the pterygoid and ectopterygoid form, the posterior margin of the suborbital fenestrae. Posterolaterally, the paired pterygoid contacts the quadrates with slender posterior pointed processes (quadrate rami). On the lateral and posteroventral surface of the braincase, the pterygoid contacts the basisphenoid. In their anterior half, the paired pterygoid encloses the posterior half of the internal naris (see paragraph "internal naris").

Ectopterygoid (ecpt, Fig. 3.35c, Fig. 3.36b)

In ventral view, the ectopterygoid is a roughly rhombic bone, approximately one-third the size of the suborbital fenestra. It meets ventromedially the pterygoid in an L-shaped suture and dorsolaterally contacts the jugal, maxilla, and postorbital. The ectopterygoidal-jugal suture is roughly s-shaped. The pterygoidal-ectopterygoidal suture is well preserved in specimen FSL 530238 and BMNH 32599.

Hyoid apparatus (Fig. 3.38b)

In specimen FSL 530238 parts of the hyoid apparatus (definition see ROMER 1956) are preserved, consisting of a paired tiny, slightly curved elongated bone bar lying ventrolaterally to the pterygoid (in ventral view). The bone resembles that of *Steneosaurus bollensis.* It is interpreted as the ceratobranchialis one compared to the conditions in extant crocodilians (see chapter 3.1, ROMER 1956, and BELLAIRS & KAMAL 1981). The length of it is about 49 mm in this specimen. The original position is uncertain. However, in ventral view, the bone lies in the proximity of the lateral edge of the pterygoid and extends to the posterior edge of the quadrate. In specimen GPIT Re 1193/18 and BSGP 1890 I 5 likewise the ceratobranchialis one is exposed in ventral view. Position and shape are identical with those of specimen FSL 530238 (Fig. 3.38b). No other parts of the hyoid apparatus are preserved.

In some specimens of *Pelagosaurus typus*, petrified tracheal rings are preserved e.g., in specimen BSGP 1925 I 34 as formerly reported by EDINGER (1929) and WESTPHAL (1962). The shape of the tracheal rings is identical to that of *Steneosaurus bollensis* (see chapter 3.1). The original position and number of the tracheal rings cannot be reconstructed, due to their insufficient preservation.

Braincase (Fig. 3.38-Fig. 3.42)

Parts of the braincase are visible in detail in the specimens e.g., BMNH 32599, BMNH 32600, BMNH R4, BSGP 1890 I 5, BSGP 1925 I 34, BSGP 1990 XVIII 68, FSL 530238, GPIT Re 1193/17, MNHN 1914-9-3(9), and UH 10. Specimen BMNH 32600 consists of fragmentary posterior skull parts, which allow investigating parts of the internal surface of the braincase wall (Fig. 3.41). In addition, specimen BSGP 1890 I 5, a partly preserved three-dimensional skull, was studied with the aid of X-ray computed tomography and showed some internal features of the braincase (Fig. 3.38, Fig. 3.42).

The braincase consists of the unpaired basioccipital, the paired exoccipital-opisthotic complex, the unpaired supraoccipital, the paired prootic, the unpaired basisphenoid (fused with parasphenoid), and the paired laterosphenoid. Dorsally, it is bordered by the unpaired frontal and parietal and the floor is ventrally formed by the paired quadrate, pterygoid, and unpaired basisphenoid. The laterosphenoid, the prootic, and the quadrate contact each other broadly and form together with the basisphenoid the foramina for the Trigeminal Nerve (cranial nerve V) (Fig. 3.39). The main part of the lateral wall of the braincase is formed by the laterosphenoid and the prootic (Fig. 3.39, Fig. 3.41). Internally, the frontal encloses the ductus olfactorius (Fig. 3.41, Fig. 3.42b). In the posterior wall of the supratemporal fenestra, a small ellipsoid posttemporal fenestra is recognized mainly bordered by the squamosal and the prootic (Fig. 3.39). In posterior view, the squamosal and the exoccipital-opisthotic complex borders it (Fig. 3.40).

Basioccipital (boc, Fig. 3.38, Fig. 3.40, 3.41)

The basioccipital is an unpaired bone, which forms the main part of the occipital condyle and the ventral tubercles. In ventral view, it contacts anteroventrally the basisphenoid in an anteriorly convex suture and has anterolaterally contact with the quadrates. In posterior view, the occipital condyle contacts dorsolaterally the exoccipital-opisthotic complex in an oblique suture, which runs from dorsomedial to ventrolateral. Dorsomedially, basioccipital forms the ventral margin of the foramen magnum. Ventromedially, it encloses the median Eustachian foramen (eu f) between its two ventral tubercles. These basal tubercles possess a rough external surface in ventral view (Fig. 3.41b).

Exoccipital and opisthotic (eoc & op, Fig. 3.39-Fig. 3.42)

Like in extant crocodiles, the exoccipital of *Pelagosaurus typus* is completely fused with the opisthotic and a suture between them is not visible (e.g. IORDANSKY 1973, CURRIE &

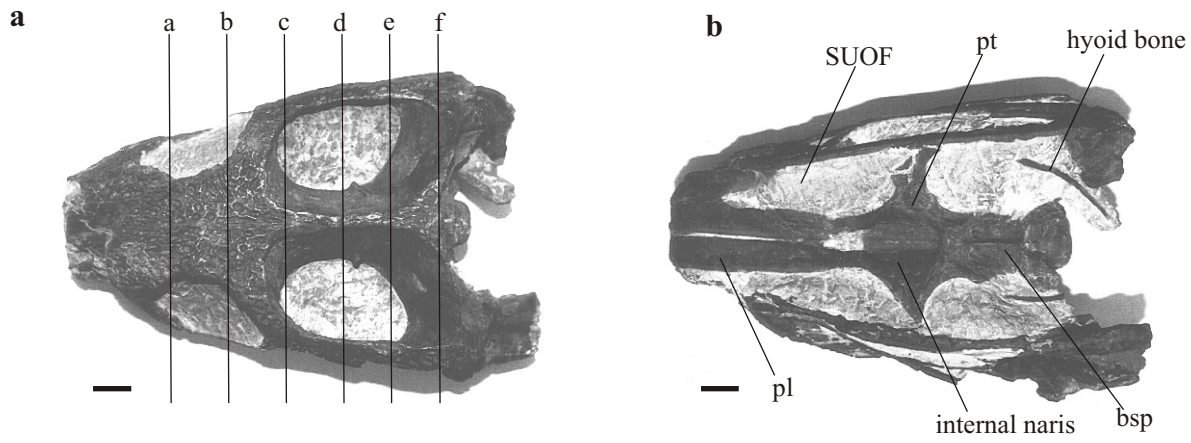

Figure 3.38a-b: Specimen BSGP 1890 I 5 in a-dorsal view and b-ventral view. **3.38a-**Pronounced ornamentation on the cranial bones is visible, as well as ellipsoid supratemporal fenestrae, and large lateral orientated orbits. The lines a-f mark the position of the CT scans shown in figure 3.42. **3.38b-**Internal naris shape and hyoid bones are exposed.Tthe pterygoid is fragmentary and the ectopterygoids are missing. Scale bars are 10 mm. Abbreviations: bsp-basisphenoid, pl-palatine, pt-pterygoid, SUOF-suborbital fenestra.

.

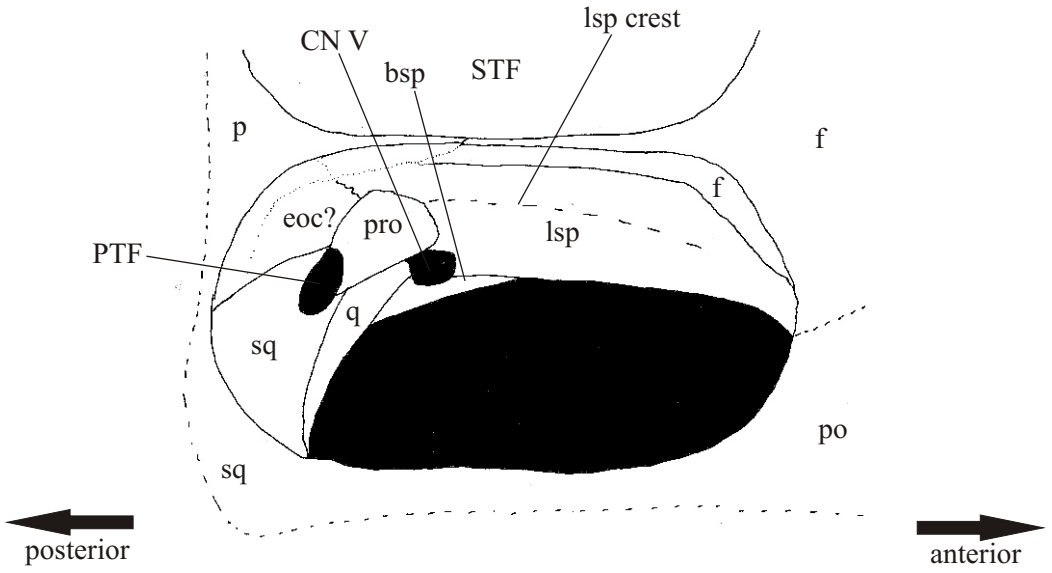

Figure 3.39: Sketch of the lateral and posterior configuration of the braincase wall in *Pelagosaurus typus* (after MNHN 1914-9-3(9)), seen through the opening of the right supratemporal fenestra. Sutures between the parietal and the braincase are not clearly visible.
Abbreviations: bsp-basisphenoid, CN V- foramina for the cranial nerve V, eoc-exoccipital, f-frontal, lsp-laterosphenoid, p-parietal, PTF-posttemporal fenestra, po-postorbital, pro-prootic, STF-supratemporal fenestra, sq-squamosal, q-quarate.

ZHAO 1993). Dorsomedially, the paired exoccipital-opisthotic complex meets each other in a vertical median suture dorsal to the foramen magnum (Fig. 3.40, Fig. 3.41, and Fig. 3.42f). Dorsomedially, the exoccipital-opisthotic complex meets the supraoccipital in an oblique suture and excludes it from the foramen magnum. Laterodorsally, the paroccipital process has broad contact to the squamosals. The exoccipital-opisthotic complex has medioventrally contact with the basioccipital and ventrolaterally, it meets with the quadrate. A possible anterior contact to the prootic is supposed, but cannot be clearly identified (Fig. 3.39).

In posterior view, it forms the dorsal and lateral margin of the foramen magnum. Its ventromedial margin contacts the basioccipital and forms there the dorsolateral part of the occipital condyle and the lateral part of the ventral tubercles of the basioccipital (Fig. 3.40, Fig. 3.41). In posterior and lateral view, the exoccipital therefore expands clearly ventrally below the level of the occipital condyle. In extant crocodiles, only *G. gangeticus* shows a similar ventral expansion of the exoccipital (IORDANSKY 1973).

The foramina for the cranial nerves IX-XII are visible in the exoccipital-opisthotic complex (see paragraph "foramina for the cranial nerves" and Fig. 3.40a, 3.41a, and 3.42f).

Supraoccipital (soc, Fig. 3.40)

In posterior view, it is an unpaired trapezoid bone completely shut off from the foramen magnum by the paired exoccipital-opisthotic complex. The ventral margin is slightly dorsally concave, smooth and meets broadly with the paired exoccipital-opisthotic complex. The dorsal margin of the supraoccipital is straight and has broad dorsal contact with the parietal. Dorsolaterally, it is bordered by the squamosals and ventrolaterally by the exoccipital-opisthotic complex. Probably, it forms laterally a small part of the medial margin of the posttemporal fenestra (see there). In the median vertical axis of the supraoccipital a faint ridge is visible.

Prootic (pro, Fig. 3.36, Fig. 3.39, Fig. 3.41)

The prootic is a sub-rectangular bone, which is integrated in the posterolateral braincase wall. Anteriorly it is bordered by the laterosphenoid, ventrally by the quadrate, posteriorly by the squamosal and probably the exoccipital. The latter could be also part of the supraoccipital, but its position points to the exoccipital-opisthotic complex. In addition, the dorsal sutures are

unclear. It is assumed that the prootic has dorsally contact to the parietal, but because of the missing sutures, no proof can be given. It is possible that the prootic is separated from the parietal by a dorsally lying exoccipital-laterosphenoidal contact (Fig. 3.39).

IORDANSKY (1973) supposes, based on his observations in *Gavialis gangeticus* that a large prootic exposed in the lateral wall of the braincase represents primitive conditions.

Basisphenoid (including parasphenoid) (bsp, Fig. 3.35c, Fig. 3.39)

The basisphenoid is an unpaired triangular bone, which forms part of the floor of the braincase cavity. In ventral view, its posterior margin has broad contact with the basioccipital. The basioccipital-basisphenoidal suture is slightly anteriorly convex and developed as a firm ridge (Fig. 3.35c). This transverse ridge is penetrated medially by the median Eustachian foramen (eu f). Anteromedially it has contact with the paired pterygoid and anterolaterally with the quadrate. The basisphenoid meets the quadrate in a straight suture. At the posterior tip of the quadrate-basispenoidal suture, the opening for the lateral Eustachian foramen is visible. A longitudinal median ridge is developed on the ventral surface of the basisphenoid. In lateral view, a dorsal contact with the laterosphenoid is present (Fig. 3.39). In lateral view, the basisphenoid develops a mediolateral flat basisphenoid rostrum (cultriform process) anterior to the pterygoid and the braincase (3.35c).

Laterosphenoid (lsp, Fig. 3.36, Fig. 3.39, Fig. 3.41)

In lateral view, the laterosphenoid is a rectangular, slightly laterally convex bone, which forms anteriorly circa 60-70% of the lateral wall of the braincase. Anterodorsally, it is bordered by the frontal, posteriorly it contacts the prootic, posterodorsally the parietal and perhaps the exoccipital, and posteroventrally the basisphenoid. A contact between the quadrate and the laterosphenoid is uncertain, but lies possibly inside the foramina for the cranial nerve V (Fig. 3.39). On the external surface of the laterosphenoid, a pronounced longitudinal crest runs horizontally over the entire length of the laterosphenoid and divides it in a dorsal and a ventral half.

Foramina for the cranial nerves (Fig. 3.36, Fig. 3.39-Fig. 3.42)

The largest openings in the braincase wall are beside the foramen magnum: the posttemporal fenestra (Fig. 3.39, Fig. 3.40) and the foramen for the Trigeminal Nerve (Cranial Nerve V, CN V) (Fig. 3.39). The position of the foramen for the Trigeminal Nerve (CN V) is clearly defined. It lies in the lateral wall of the braincase and varies negligible in its position within the Crocodilia. The margin of the foramen is usually formed by the laterosphenoid, prootic, quadrate, and basisphenoid while the portion of the particular bone can differ widely between the taxa (IORDANSKY 1973).

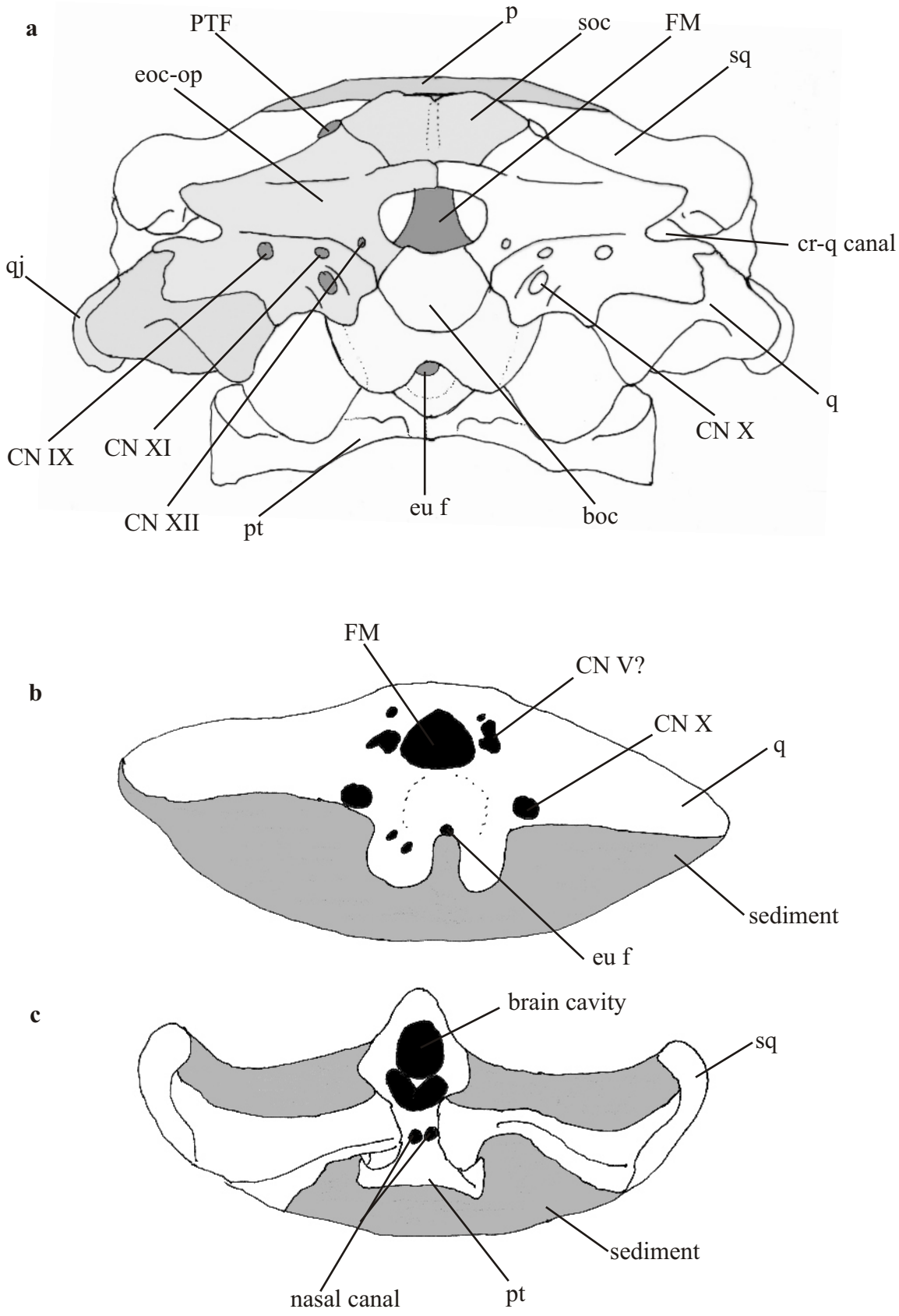

Figure 3.40a-c: **3.40a-**Reconstruction of the skull of *Pelagosaurus typus* in posterior view (mainly after the specimens BMNH 32599, BSGP 1890 I 5 and FSL 530238).
3.40b- Sketch after the cross-section of the skull of cf *Pelagosaurus typus* (after the specimen BMNH R4), 1 mm anterior to the occipital condyle. **3.40c**- Sketch of the cross-section of the skull of the specimen BMNH R4 in the middle of the supratemporal fenestra.
Abbreviations see figure 3.39.

In lateral view, in *Pelagosaurus typus*, the foramen for the Cranial Nerve V is circular and it is dorsally bordered by the laterosphenoid and prootic, anteriorly by the laterosphenoid, ventrally by the basisphenoid, and posteriorly by the quadrate. This position in the braincase wall is nearly identical with the position and the bordering bones of the foramen for the Trigeminal Nerve (CN V) in extant crocodilians (IORDANSKY 1973).

A lateral opening for the cranioquadrate canal is visible between the paroccipital process of the exoccipital-opisthotic complex, the quadrate, and the squamosal (Fig. 3.36c, Fig. 3.42e, f). This opening should provide the passage for the Cranial Nerve VII to the inner ear.

According to IORDANSKY (1973), the cranioquadrate canal in extant crocodilians provides passage for the main branch of the Cranial Nerve VII, the orbitotemporal artery, and the lateral cephalic vein. The positions of the foramina for the Cranial Nerves IX-XII are clearly defined in crocodilians. In general, the foramen, which lies medially closest to the foramen magnum, is considered as the foramen for the Hypoglossal Nerve (CN XII) (IORDANSKY 1973, BROCHU et al. 2002). The foramen for the Cranial Nerve XII lies in *Pelagosaurus typus* and *Steneosaurus bollensis* within the exoccipitals medially closest to the foramen magnum. Ventrolaterally to this foramen, usually the foramina for the Vagus Nerve (CN X), for the Accessorius Nerve (CN XI), and the Glossopharyngeal nerve (CN IX) are situated (IORDANSKY 1973). Those foramina are clearly exposed in posterior view of the skull (Fig. 3.40 and Fig. 3.42). In *Pelagosaurus typus*, one relatively large foramen for the Cranial Nerve X (Vagus group, CN X) is identified, lying at the medioventral margin of the exoccipital-opisthotic complex close to the dorsolateral margin of the basioccipital (Fig. 3.40. Fig. 3.41a, Fig. 3.42f). Laterodorsally to this foramen the smaller foramen for the Accessorius Nerve (CN XI) is situated. Laterally to the latter lies the foramen for the Glossopharyngal nerve (CN IX).

Posttemporal fenestra (PTF, Fig. 3.39, Fig. 3.40)

The posttemporal fenestra is reduced in *Pelagosaurus typus* to a small, transverse slit-like foramen. In posterior view, the exoccipital-opisthotic complex borders it ventrally and the squamosal borders it dorsally (Fig. 3.40). In some specimens, the supraoccipital forms laterally a small part of the medial margin of the foramen, too (see paragraph "supraoccipital"). In anterior view, through the supratemporal fenestra, the posttemporal fenestra is visible in the posterior wall of the supratemporal fenestra. It is bordered laterally,

by the squamosal and medially by the prootic (Fig. 3.39). In some specimens, it probably has dorsal contact to the exoccipital and ventral contact to the quadrate, too.

Mandible (lower jaw, Fig. 3.36c, Fig. 3.37, Fig. 3.43)

Parts of the mandible are three-dimensionally preserved in e.g., BMNH 32599, BSGP 1890 I 5 (Fig. 3.36c), and FSL 530238. In those specimens, the external mandibular fenestra is observable, too. Parts of the lower jaw and the symphysis are exposed in e.g., BMNH 32599, MNHN 1914-9-1, UH 4 (Fig. 3.37), UH 9, and UH 10.

In general, the configuration of the lower jaw of *Pelagosaurus typus* is similar to the ones described for the other Liassic teleosaurid taxa (see chapter 3.1-3.4). The mandible is anteriorly formed by the paired dentary, which meet each other in a long symphysis forming the anterior half of the lower jaw. The symphysis angel is 25-30 degrees. Furthermore, the mandible consists of the paired splenial, which takes part in the posterior-most part of the symphysis, the paired coronoid, the paired angular, the paired surangular and the paired articular. The dentary forms the anterior circa 75% of the mandibular ramus. The mandibular rami end in retroarticular processes, formed by the articular, surangular and angular. An external mandibular fenestra is visible in lateral view.

External mandibular fenestra (EMF, Fig. 3.36c, Fig. 3.43)

The external mandibular fenestra longitudinal ellipsoid is well preserved in the specimens e.g., BMNH 32599, BSGP 1890 I 5 (Fig. 3.36c), FSL 530238, MNHN 1914-9-9 and UH 9.

It is bordered anteriorly by the dentary, posteroventrally by the angular, and posterodorsally by the surangular. The external mandibular fenestra is three times longer than high and lies ventrally to the infratemporal fenestra in the skull (Fig. 3.36c).

Dentary (d, Fig. 3.37, Fig. 3.43)

The dentary is an elongated bone, which is wider than high in its anterior two-thirds and than as wide as high in its posterior third. It is posteromedially bordered by splenials, posterodorsally by the surangular and posteroventrally by the angular. It forms the anterior margin of the external mandibular fenestra (see there). The paired dentary is connected to each other in an elongated symphysis (see paragraph "mandible"). Approximately the anterior 4% of the paired dentary slightly enlarges laterally. Only the dentary is tooth bearing in the lower jaw. Up to 32 alveoli are found in the dentary, the alveoli are running up to the level of

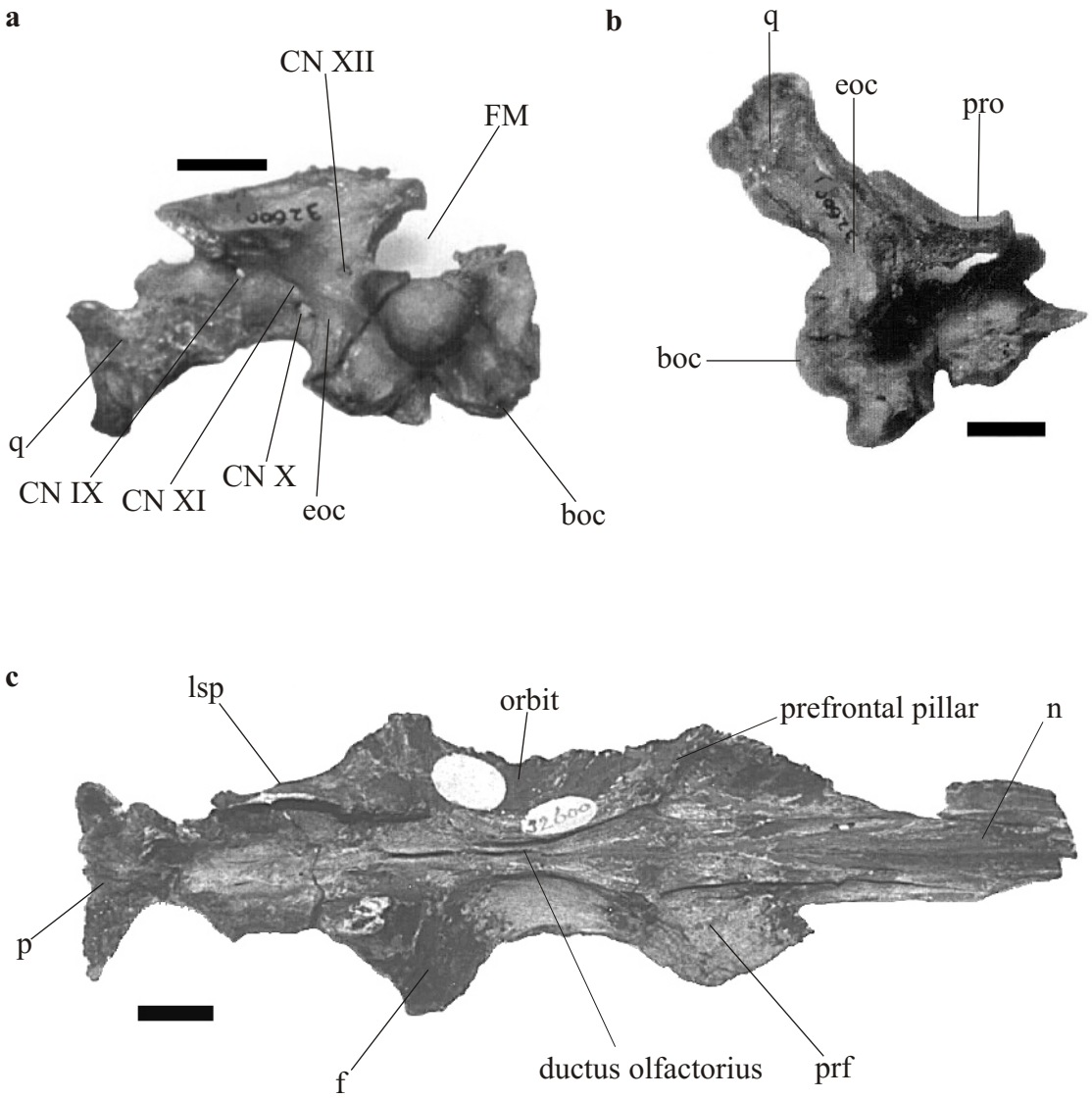

Figure 3.41a-c: Specimen BMNH 32600 (*Pelagosaurus typus*) posterior (a,b) and anterior (c) fragment. **3.41a-**Posterior view of the skull fragment. Basioccipital (boc), exocciptial-opistothic complex (eoc), and the quadrate (q) are clearly to identify. Foramina for the cranial nerves IX-XII (CN IX, CN X, CN XI, CN XII) as well as the foramen magnum (FM) are visible. Scale bar is 10 mm. **3.41b-**Skull fragment in dorsal view. View inside, the FM is open. Eoc and prootic (pro) are forming the posterior part of the lateral braincase wall. **3.41c-**Ventral (internal) view of parts of the cranial table. The ventral expansion of the prefrontal (prf), the prefrontal pillar, is visible anterior to the orbit. Ventral expansion of the frontal forms the ductus olfactorius. The laterosphenoid (lsp) forms the anterolateral wall of the braincase. Scale bar is 10 mm. Abbreviations see chapter 2.

the middle of the orbit. The symphysis is exposed in e.g., BMNH 32599, MNHN 1914-9-1, and UH 10. The symphysis angle (W2) is e.g., in MNHN 1914-9-1 30 degrees (see appendix II). The external surface of the dentary shows distinct ornamentation in some cases e.g., in BMNH 32599. Posteriorly, the ornamentation consists of a dense pattern of small circular pits, but the pits become more irregular distributed and shallower anterior to the symphysis (Fig. 3.43). In some cases, the surface of the dentary is smooth like in specimen UH 4 (Fig. 3.37) and UH 9. The feature is probably influenced by individual variation and it is further discussed in chapter 4.

Splenial (sp, Fig. 3.43)

Specimen BMNH 32599 as well as MNHN 1914-9-1 shows the splenial. The splenial is a slender bone located at the ventral and internal side of the mandibular ramus. It lies parallel to the dentary and is bordered anteriorly, laterally, and posteriorly by it. Anteriorly, the paired splenials forms the posterior 5% of the symphysis. They taper shortly between the fused dentaries and separated them in the posterior-most part of the symphysis. The external surface of the splenial is smooth.

Coronoid (cr)

A small coronoid is visible at the internal surface of the mandible in the specimen BMNH 32599. It contacts anteriorly the dentary and posterior the surangular. The sutures are weakly developed. However, it is hook-shaped with a posteriorly concave and anteriorly convex margin similar to that of extant crocodilians (IORDANSKY 1973). The concave posterior margin forms the anterior margin of the internal mandibular fenestra.

Surangular (san, Fig. 3.43)

Specimen BMNH 32599 shows the surangular in external view, as well as e.g., BSGP 1890 I 5, FSL 530238, MNHN 1914-9-9, and UH 9 (Fig. 3.37, Fig. 3.43).

The surangular is an elongated slender bone with anterior contact to the dentary, posterior to the articular and posteroventral to the angular. Because the surangular is only well preserved in external view, the run of the internal suture with the coronoid is uncertain. The suranguloarticular suture is horizontally straight, smooth, and clearly visible. Posteroventrally, the surangular meets the angular in a long slightly oblique suture (see angular) and anteroventrally; it forms the dorsal margin of the external mandibular fenestra. The exact run of the dentary-surangular suture is uncertain. In external view, the surangular probably thins

out in anterior direction and descends ventrally below the dentary, anterior to the external mandibular fenestra.

Unlike to the other Liassic teleosaurids, ornamentation is developed at the lateral external surface of the surangular. It consists of shallow grooves parallel to the external mandibular fenestra. Anteriorly and posteriorly, the ornamentation fades. However, not all specimens show this ornamentation. In the juvenile specimens UH 9 and UH 10, the external surface of the surangular is smooth. The variation of the ornamentation of the bones is further discussed in chapter 4.

Angular (an, Fig. 3.43)

In external view, the angular is an elongated bone, which is slightly curving posterodorsally. The external ventral margin of the angular is slightly convex. Anteriorly, the angular contacts the dentary in an oblique suture running from anterodorsal to posteroventral (Fig. 3.43). Posterodorsally, posterior to the external mandibular fenestra, it has ventral contact to the surangular in a straight horizontal suture. The angular forms the ventral half of the posterior margin of the external mandibular fenestra. In external view, the surangular separates the angular from the articular.. A possible, internal anterior contact with the splenial is likely, but could not be identified. In most cases, the lateral surface of the angular is smooth, but in some specimens (e.g. BMNH 32599), a dense pattern of shallow pits are visible on the anterolateral surface parallel to the external mandibular fenestra (Fig. 3.43).

Articular (ar, Fig. 3.43)

The articular are well preserved e.g., in BMNH 33599, BSGP 1890 I 5, UH 4, UH 9, and UH 10. They all show a well preserved articular in lateral view and one loose, single articular is found in FSL 530238 (Fig. 3.43c).

The articular is in dorsal view a triangular to rhombic bone, which overlies the surangular dorsally. Posteriorly, it forms with the surangular and angular the retroarticular process of the mandibular ramus. In dorsal view, a solid transversal crest is developed on surface of the articular, which divides it into two parts. The posterior part is circa 70% of the entire length of the articular and forms the retroarticular process. The small anterior part (30%) forms the articular facets at the mandible for the quadrate condyles. In addition, the posterior part of the articular shows dorsally two depressions divided by a pronounced longitudinal median ridge (Fig. 3.43c). In lateral view, the articular is sub-triangular. The posterior two-thirds of the articular expand obliquely in dorsoventral direction and curve

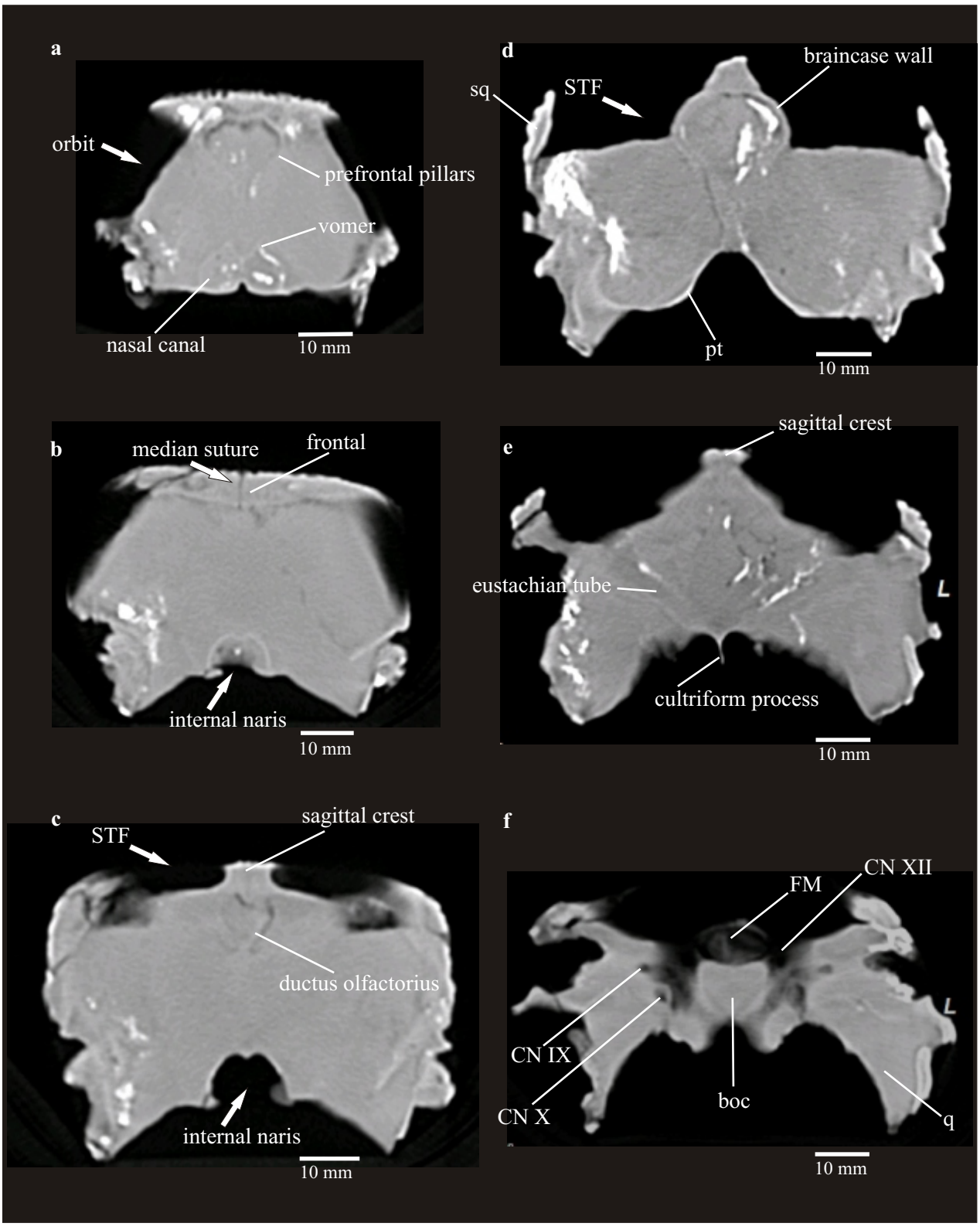

Figure 3.42a-f: Selected computed tomographic scans of the skull of *Pelagosaurus typus* (BSGP 1890 I 5). **3.42a**-Scan 10 mm posterior to the anterior margin of the orbits. **3.42b-**Scan 10 mm anterior to the posterior margin of the orbit. **3.42c**-Scan about 5 mm posterior to the anterior margin of the supratemporal fenestra. **3.42d**-Scan 20 mm posterior to scan c. **3.41e**-Scan 15 mm anterior to the posterior margin of the parietal. **3.42f-**Scan 10 mm anterior to end of the condyle. Abbreviations see figures 3.39 and 3.40. Scale bar is 10 mm.

slightly posterodorsally. Anteriorly, the bone extends in dorsoventral direction and is slightly concave. In lateral view, the articular is ventrally completely bordered by the surangular and has no contact to the angular. The length of the retroarticular process (X) is 6-10% of the skull length (A) (see chapter 4 & 5)

Dentition

Tooth morphology

The dentition is weakly heterodont, because the size of the teeth varies slightly. The tooth morphology of the teeth in the upper and lower jaw is identical. In addition, the alveoli are equally developed as circular pits in the upper and the lower jaw. The teeth are very slender, conical and apically recurved. The surface of the tooth crown is completely covered with very tiny vertical striation, but do not possess carinae like the teeth of *Steneosaurus bollensis*.

Because the carinae at the *Steneosaurus bollensis* teeth are only weakly developed and in some cases, even missing, this character does not have a great taxonomical importance (see chapter 3.1). VIGNAUD (1997) already notes that the teeth of *Pelagosaurus typus* are similar to the teeth of *Steneosaurus bollensis* and *Steneosaurus gracilirostris*.

Pattern of dentition

In the upper jaw, the premaxilla and the maxilla are both tooth bearing. The number of alveoli in the premaxilla is 3 to 4 and the number of alveoli in the maxilla is up to 32. According to DUFFIN (1979a), the juvenile *P. typus* specimen M 1418a from Ilminster possesses four premaxilla teeth, three anterior mature teeth and one small posterior replacement tooth. In this work, only specimens with three equally sized alveoli (as well as teeth) in the premaxilla were found.

The dentary in the lower jaw of *Pelagosaurus typus* possesses a maximum of 33 alveoli. About 8 to 10 alveoli lie posteriorly to the symphysis in the mandibular ramus.

In the upper jaw are only every second alveoli is occupied with a fully erupted tooth. The other alveoli are empty or possess small replacement teeth. The teeth are all vertical orientated. The teeth are running up to the level of the anterior margin of the orbit, as it is visible for example in specimen BSGP 1973 VII 592 and FSL 530238.

The exact number of teeth for this taxon is uncertain, because of the rudimentary preservation of some of the specimens and the high variability in the tooth count (see chapter

4). For example, specimens SMNS 80066 and UH 4 possess only 30 alveoli in the maxilla and in specimen UH 4, only 30 alveoli in the dentary are visible (Fig. 3.37, Fig. 3.43).

The dentition code is: $\frac{3-(4)+30-32}{30-33}$

Postcranial

The axial skeleton

Armour (Fig. 3.44)

The dorsal osteodermal shield of *Pelagosaurus typus* consists of one longitudinal row of paired osteoderms. The specimen BMNH 32598 shows a part of the dorsal thoracic armour, which consists of about twenty paired osteoderms (Fig. 3.44a). However, it is assumed that the specimen lacks parts of the dorsal cervical and tail armour. The tail is usually covered dorsally up to the level of the 10th caudal vertebra with a longitudinal row of paired osteoderms as visible in e.g., SMNS 19073 and UH 8.

Pelagosaurus typus possesses ventral armour in trunk region. This ventral osteodermal shield consists of four longitudinal rows of up to 18 rectangular osteoderms each. The ventral osteodermal shield is partly visible e.g., in BMNH 32601, SMNS 17758, TMH 2744, UH 8, and UH 4. In contrary to the other Liassic thalattosuchian taxa, ventral armour of the tail does not exist. This fits well with the observations of EUDES-DESLONGCHAMPS (1864) and BERCKHEMER (1929), who both noted that *Pelagosaurus typus* lacks ventral or lateral armour of the tail. Therefore, the armour of the tail is compared with the other Liassic teleosaurid taxa distinctly reduced.

Dorsal armour (Fig. 3.44a-d)

The complete dorsal osteodermal shield consists of about 64 osteoderms arranged in a paired longitudinal row. It extends level with the third cervical vertebrae to the 10th caudal vertebrae. The paired dorsal osteoderms meet each other medial in a straight suture. They form ventrally an obtuse angle of about 150° with each other (see chapter 8). The anterior three cervical dorsal osteoderms are longer than wide or square, and possess a straight or externally convex lateral margin. Posterior to the third dorsal osteoderms, the osteoderms are almost twice as wide as long and possess a straight medial and a strongly externally convex

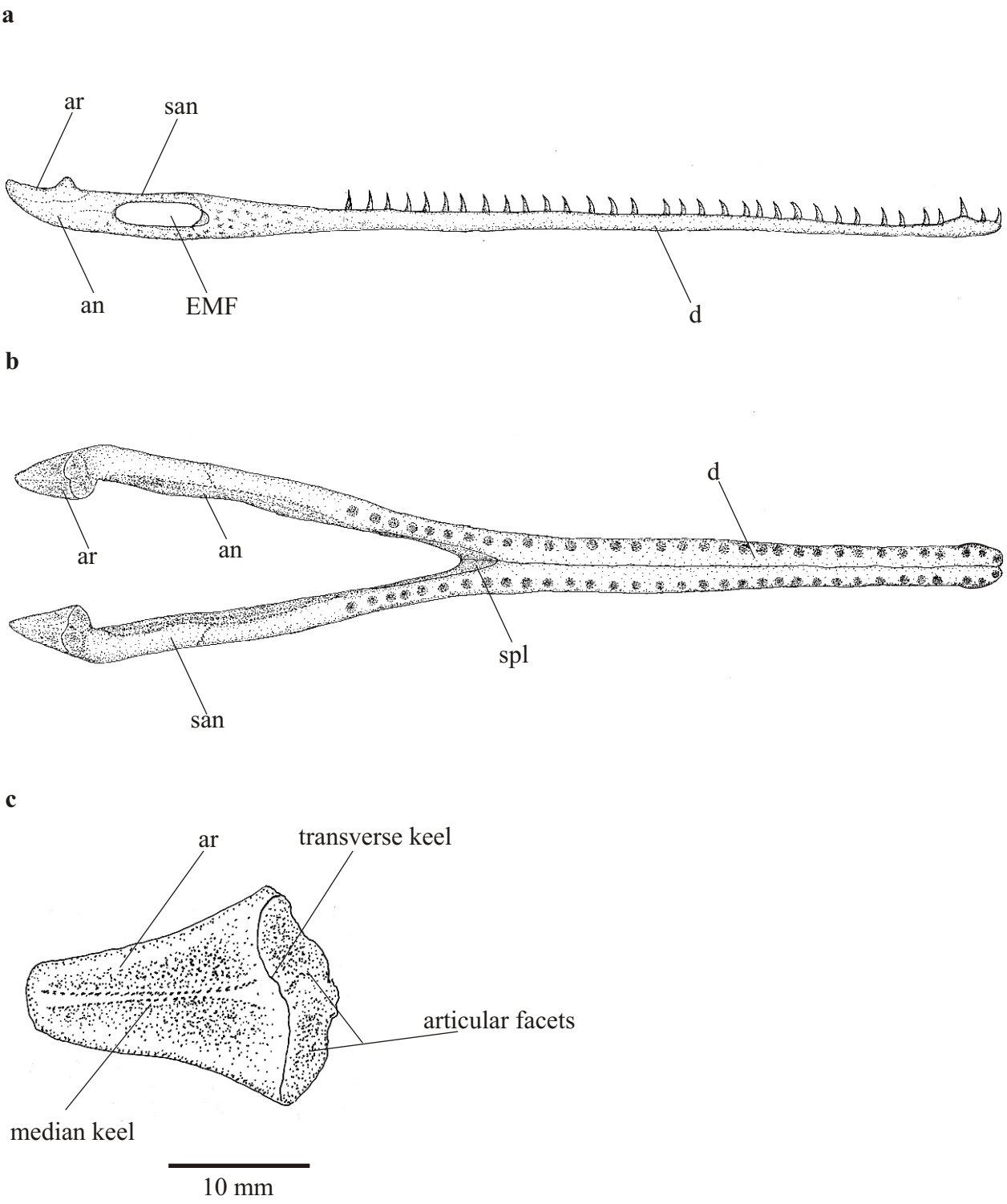

Figure 3.43a-c: The reconstruction of the lower jaw of *Pelagosaurus typus* is mainly based on the specimens BMNH 32599, BSGP 1925 I 34, UH 4, UH 9, and UH 10. **3.43a-**Reconstruction of the mandible in lateral view with appending teeth, supposing that every alveolus possesses a tooth. **3.43b**-Reconstruction of the lower jaw in dorsal view without teeth. Symphysis angle is about 30 degrees. **3.43c**-*In situ* drawing of the single articular of the specimen FSL 530238 in dorsal view. Abbreviations: an-angular, ar-articular, d-dentary, EMF-external mandibular fenestra, san-surangular, spl-splenial.

lateral margin. In the sacral and caudal region, the shape of the dorsal osteoderms become squarer again and the lateral margin is only slightly externally convex. The posterior-most 10 osteoderm are longitudinal ellipsoid. In cross-section, the osteoderms are relatively thin, and are only 2 to 4 mm thick. On the external surface of the osteoderms, the pronounced ornamentation consists of a dense pattern of small circular, deep pits. The ornamentation resembles that of *Platysuchus multiscrobiculatus* (see chapter 3.4), but in *Pelagosaurus typu*s, no keel is developed on the external surface of the dorsal osteoderms.

In contrast to *Steneosaurus bollensis* and *Platysuchus multiscrobiculatus*, a smooth articular area at the anterior margin or an anterolateral peg is not developed at the dorsal osteoderms of *Pelagosaurus typus*.

Ventral armour (Fig. 3.44e, f)

The ventral osteodermal shield consists of four longitudinal rows possessing each 16-18 rectangular osteoderms. The ventral osteoderms are quadratic to sub-rectangular in shape and has a similar ornamentation on their external surface than the dorsal osteoderms (see there). They are connected to each other in straight sutures, and do not overlap each other.

In the holotype TMH 2744, the ventral armour is completely preserved. It reaches from the 13th vertebrae (5th thoracic vertebra) to the 24th vertebra (16th thoracic vertebra). It consists of 14 transverse rows of osteoderms. The first three transverse rows consist each of two osteoderms, the next 10 transverse rows consist each of four osteoderms and the posterior-most row consists of two or three osteoderms. In this case, the complete ventral osteodermal shield consists of 49 osteoderms. In specimen SMNS 17758 the ventral armour is also well exposed, here are at least 15 transverse rows developed; each is consisting of four osteoderms. It is assumed that the specimen lacks the first three transverse rows and that therefore the complete ventral armour in this specimen consisted of 68 osteoderms. In specimen BMNH 32601 72 ventral osteoderms are reconstructed (Fig. 3.44)

Vertebra column (Fig. 3.45)

The vertebra column of *Pelagosaurus typus* consists of up to 65 vertebrae. There are eight cervical vertebrae, 13 to 15 thoracic vertebrae, two to three lumbar vertebrae, two sacral vertebrae, and up to 42 caudal vertebrae. The general shape of the vertebrae resembles those of other teleosaurids (see chapter 3.1).

Cervical vertebrae (cv vr, Fig. 3.45)

The definition of the cervical vertebrae is based on the same features as described for *Steneosaurus bollensis* and *Platysuchus multiscrobiculatus* (see chapter 3.1 & 3.4). The cervical vertebra three to eight possesses both articular facets (diapophysis and parapophysis) for the double-headed cervical ribs at the vertebra centrum. In contrary, the usual thoracic vertebra has no facet attached to the centrum. Only the very first thoracic vertebrae have still the parapophysial facet attached to the centrum (see "thoracic vertebrae").
The cervical column consists of eight cervical vertebrae. The atlas-axis complex and six following, almost equally developed cervical vertebrae. A well-preserved almost three dimensional atlas-axis complex is exposed for example in specimen BSGP 1890 I 510/1, MNHN 1890-14 (Fig. 3.45) and the holotype of *Pelagosaurus typus* TMH 2744.

The atlas consists of five parts: the intercentrum (=hypocentrum), the paired neural arch, an unpaired proatlas and the dens, which has a suture with the axis (Fig. 3.45). According to WESTPHAL (1962,) the dens (or odontoid process) of the axis is originally the pleurocentrum of the atlas. In *Pelagosaurus typus,* the dens is not totally fused with the axis, which is considered as a primitive feature. In BSGP 1890 I 510/1 and FSL 530238, the atlas-axis complex is exposed in ventral view (Fig. 3.45). In ventral view, the dens is closer attached to the atlas than to the axis. The dens nearly fuses with the intercentrum of the atlas and is ventrally divided from the axis by a transverse deep groove. The axis is similar in shape to the other seven cervical vertebrae. The centrum is slightly hourglass-shaped with a sharp keel on its ventral surface (see below). The neural spine is as long as the centrum and similar in height.

The connection for the first cervical rib is on the lateroventral margin of the dens, while the diapophysis and parapophysis for the second cervical rib is situated on the anterolateral margin and in the middle of the axis centrum. The total length of the axis-atlas complex is 30 mm in specimen MNHN 1890-14 and the height of the axis including the neural spine is 18 mm.

The third to eighth amphicoelous cervical vertebra are all very similar developed. In lateral view, the usual cervical vertebra possesses an elongated centrum with a sharply developed keel at the ventral side. Laterally, the centrum possesses a medial horizontal groove between the parapophysis and the diapophysis. The neural spine is slightly higher than in the axis and longer than high in lateral view. The height of the neural spine is maximum the height of the centrum. The pre- and postzygapophyses are circa at the same height. In ventral

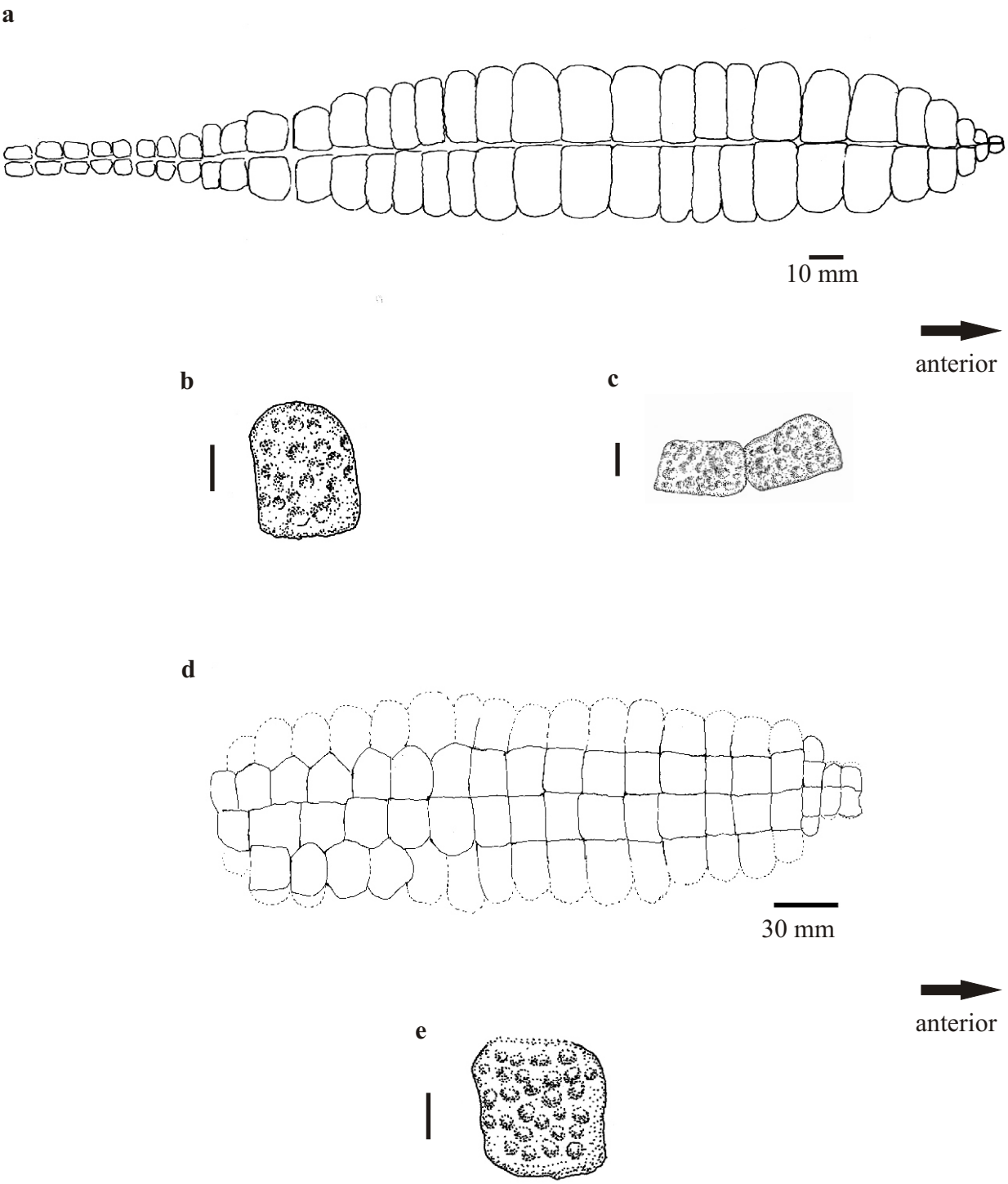

Figure 3.44a-e: Dorsal and ventral osteodermal shield of *Pelagosaurus typus*.
3.44a-Reconstruction of the dorsal osteodermal shield (mainly after BMNH 32598).
3.44b-thoracic dorsal osteoderm (after SMNS 19073). Scale bar is 10 mm. **3.44c**- *In situ* drawing of the cervical osteoderms two and three of UH 4. Scale bar is 10 mm. **3.44d-** Reconstruction of the ventral osteodermal shield (mainly after BMNH 32601). **3.44e**- *In situ* drawing of an ventral trunk osteoderm of SMNS 19073. Scale bar is 10 mm.

view, the vertebrae have a strongly developed hourglass-shape and posses a sharp longitudinal median keel on their ventral external surface (see above).

Thoracic & Lumbar vertebrae (Fig. 3.45)

Posterior to the cervical vertebrae there are 12 to 15 thoracic vertebrae, which possess elongated double-headed ribs. In the first thoracic vertebra, the parapophyses are not connected to the vertebra centrum, which is visible e.g., in specimen MNHN 1890-14. At about the 12^{th}-14^{th} vertebrae, the diapophysis and the parapophysis are fused to the transverse process protruding laterally from the neural arch. The former parapophysis lies now at the same height in front of the former diapophysis and is distinctly shorter than the latter. The form a transverse process. The prezygapophysis and the postzygapophysis are attached to the anterior and posterior dorsal margin of the neural arch. In specimen BSGP 1890 I 504, 513, 501, 502, 505, 503, and 506 the thoracic vertebrae are three-dimensional preserved. In anterior and posterior view, the outline of the centrum is circular. The neural spine is as high as the vertebra centrum and thins out dorsally. In ventral view, the vertebrae are hourglass-shaped like the cervical vertebrae, but a ventral longitudinal keel on the centrum is not developed here.

Two to three lumbar vertebrae are present. The general shape, in ventral view differs not much from the shape of the thoracic vertebrae. In specimen BSGP 1890 503 and 506, the lumbar vertebrae are exposed in ventral view. In specimen MNHN 1883-18, a lumbar vertebra is preserved in posterior and lateral view (Fig. 3.45). The vertebra is here 22 mm long and 34 mm high. The centrum is sub-circular in posterior view. It shows a shallow concave depression at the dorsal margin of the centrum. Pre-and postzygapophyses are at equal height. BMNH 32602 shows a fragmentary three-dimensional lumbar vertebra. In anterior view, the centrum outline is circular like in the thoracic vertebra. In posterior view, the centrum has a concave depression in the dorsal margin. The outline is almost heart-shaped, which is similar to that of the sacral vertebrae (see there). The neural spine is in its dorsal margin slightly broadened with small recess in the middle, in contrast to the thoracic vertebrae, which show in anterior view a slender neural spine without any recess.

Sacral vertebrae (Fig. 3.45)

Two sacral vertebrae are present. Three-dimensional sacral vertebrae are preserved in several specimens (e.g. BSGP 1890 506, BMNH 32598) showing the 26^{th} and 27^{th} vertebrae as the sacral vertebrae. The position of the sacral vertebrae in the vertebra column can vary

slightly between the 25th and the 28th vertebra (see chapter 4&5). Both sacral vertebrae are connected to the ilia by prominent sacral ribs (see "ribs"). The specimen MNHN 1880-14 shows the sacral vertebrae in dorsal view and the specimen BSGP 1890 506 shows both well-preserved sacral vertebrae in ventral view (Fig. 3.45d, e). In ventral view, the shape of the centra of the sacral vertebrae is similar to the shape of the lumbar or thoracic vertebrae (see above), but shows a low ventral longitudinal keel on the centrum. In anterior and posterior view, the centra of both sacral vertebrae are somewhat heart-shaped. The transverses processes are much stronger developed and nearly fused with the robust sacral ribs (see below).

Caudal vertebrae (cd vr)

The general shape of the caudal vertebrae of *Pelagosaurus typus* is similar to those of other teleosaurids (see chapter 3.1). However, the shape of the caudal vertebrae differs slightly from the anterior to the posterior one. All caudal vertebrae possess an elongated and slender centrum, twice as long as wide. . About the first 16 caudal vertebrae possess still a transverse process, posterior to that it is completely reduced (NHMUS M62 2516). In the anterior part of the caudal column, the neural spine is about 55% of the total height of the vertebrae, but posterior to the 16th vertebrae, its height decreases steadily towards the tip of the tail. In addition, the neural spines decrease rapidly in length (in lateral view, see figure 3.34) posterior to circa the 10th vertebra, when the tail is no longer armoured.

Specimen NHMUS M62 2516 consists of a complete skeleton exposed in dorsolateral view. Up to 49 caudal vertebrae are exposed here, but at least the posterior ten are most likely added during preparation. The anterior-most caudal vertebra bears no haemal arch posterior to that, chevrons are visible up to the 33rd caudal vertebra. The chevrons resemble those of *Steneosaurus bollensis* (see chapter 3.1).

Ribs (rb)

There are different kinds of ribs in *Pelagosaurus typus*: short double-headed cervical ribs, elongated double-headed thoracic ribs, and sacral ribs. The anterior two cervical ribs strongly differ from the other six pairs of cervical ribs. The first cervical rib is a slender straight bone bar with an acuminate proximal end and a pointed distal end. Anteriorly, it is attached to the atlas with its proximal end and extends posteriorly until the posterior margin of the axis centrum. The second cervical rib is double-headed and as long as the first cervical rib. It possesses a small capitulum, a dorsal tuberculum and a posterior elongated body (Fig. 3.37,

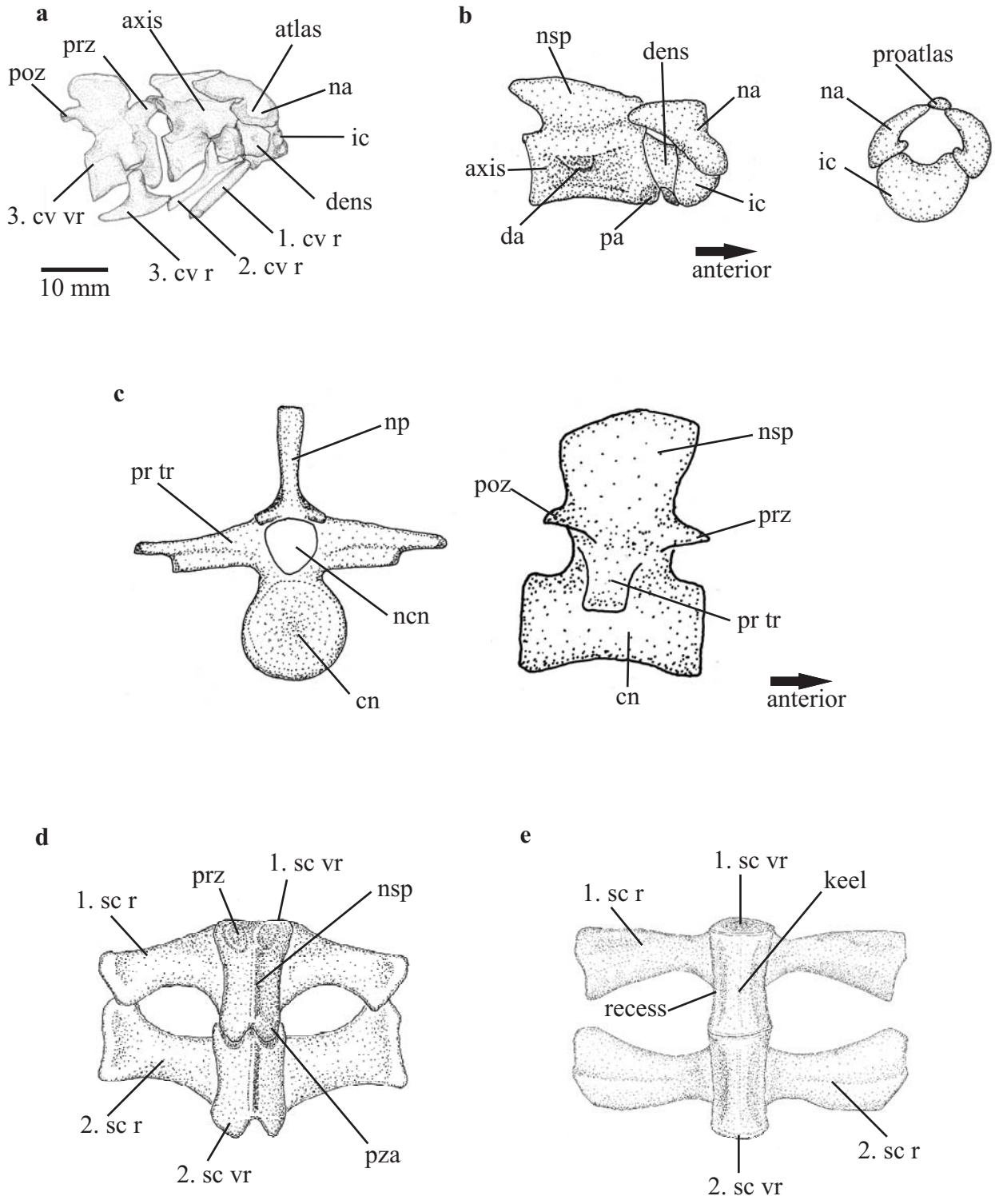

Figure 3.45a-e: Diverse vertebrae of *Pelagosaurus bollensis.*
3.45a-*In situ* drawing of the first three cervical vertebrae of specimen MNHN 1890-14. **3.45b**-Reconstruction of the atlas-axis complex in anterior and lateral view (mainly based on the specimen MNHN 1840-14 & BSGP 1890 I 510\1). **3.45c**-Reconstruction of a lumbar vertebra in anterior and lateral view based on the specimens MNHN 1883-18 (original centrum length is 22 mm) and BMNH 32602. **3.45d-**Reconstruction of the sacral vertebrae in dorsal view with appending sacral ribs after specimen MNHN 1840-14 (original length 1.sacral vertebra is 20 mm). **3.45e**-Reconstruction of the sacral vertebrae in ventral view with appending ribs after specimen BSGP 1890 I 506-502 (original length of the 1. sacral vertebra is 21.5 mm). Abbreviations see chapter 2.

3.45). It is attached with the capitulum and tuberculum to the centrum of the axis. e.g., in MNHN 1883-14 and UH 4 (Fig. 3.37, 3.45).

Cervical ribs three to eight have a very typical shape with two distal processes (diapophysial and parapophysial process) stretching out from the body, while the body of the ribs is very small and flattened with a short anterior and posterior process (Fig. 3.45a). The shape is nearly identical with the shape described for *Steneosaurus bollensis* (see chapter 3.1), except for the unequal height of the distal processes, the diapophysial process is distinctly longer than the parapophysial process here.

The number of thoracic ribs varies from 13 to 15 (see chapter 4 & 5). The thoracic ribs are slender, elongated, curved, and all double-headed. The capitulum (parapophysial process) and the tuberculum (diapophysal process) are unequal in size and shape. The general shape of the thoracic ribs is similar to the shape of ribs of *Steneosaurus bollensis* (see chapter 3.1). The thoracic ribs are all equally developed except of the first one. It has a slightly shorter body and the capitulum is less separated from the tuberculum than in the other thoracic ribs. The usual thoracic rib is an elongated bone bar, which is curving posteroventrally with an externally convex and internally concave margin. The cross-section of the shaft is ellipsoid. The anterior end of the rib is developed as an elongated capitulum and a shorter blunt tuberculum.

The sacral ribs are much shorter and more robust developed than the thoracic ribs and connect distally with the ilium in a sacroiliac joint (Fig. 3.45). The sacral ribs are not double-headed, but possess proximally one broad articular facet, which contacts the vertebra centrum laterally. Distally, the rib enlarges twice as wide as its body to an irregular shaped articular facet, which articulates with the internal side of the ilium. In ventral view, the body of the first sacral rib is curving in posterior direction, with an anteriorly convex and posteriorly concave margin. In general, the second sacral rib resembles the first sacral rib, but it is distally distinctly curving in anterior direction, with an anteriorly concave and a posteriorly convex margin (e.g. BMNH 32598, BSGP 1890 I 509/6-2, MNHN 1880-14).

Gastralia are unknown from *Pelagosaurus typus*.

The appendicular skeleton

Pectoral girdle (Fig. 3.46)

Parts of the pectoral girdle are exposed in specimens e.g. BSGP 1890 I 504, MNHN 1914-9-4, NHMUS M 62 2516, UH 4, and UH 8.

The pectoral girdle consists like in the other thalattosuchians of the paired coracoid, the paired scapula, and an unpaired interclavicle. In contrast to the other Liassic teleosaurid taxa, the coracoid is smaller than the scapula and reaches in most cases only two-thirds of the length of the scapula.

Scapula (sc, Fig. 3.46)

The scapula is well preserved in e.g., BSGP 1890 I 504, MNHN 1914-9-4, NHMUS M 62 2516 and UH 4.

It resembles in shape that of *Steneosaurus bollensis.* It is a flat element with broad expansions at its dorsal and ventral edges. The dorsal expansion is about twice as wide as the shaft, whereas the ventral expansion is only about 1.3 times the width of the shaft. It is roughly hourglass-shaped in external view. At the anteroventral margin of the scapula, there is a thickened articular area for the joint between coracoid and scapula. At the posteroventral margin of it, there is a sub-rectangular, convex facet forming the dorsal half of the glenoid fossa. The dorsal circa 60% of the scapula expands into a flat sub-triangular bone sheet, which has a dorsally convex margin (Fig. 3.46b).

Coracoid (co, Fig. 3.46)

Parts of a coracoid is exposed e.g., in the specimens NHMUS M 62 2516 and MNHN 1914-9-4.

The coracoid is a roughly hourglass-shaped bone, too, but is slightly shorter (only 75% the length of the scapula) and broader than the scapula. Its dorsolateral third is a flattened expansion, which is about three times the width of the shaft. Its ventromedially third is a expansions, which is about twice the width of the shaft. The shaft of the bone is elliptic in cross-section. The flattened dorsolateral part possesses two arched facets. The posterodorsal one is developed as a small tubercle with a flat dorsoposterior surface. It forms the ventral half of the glenoid fossa. The anterodorsal facet is slightly externally concave and articulates with the anteroventral facet of the scapula. The coracoid foramen is situated anterior to the glenoid fossa in the center of the dorsal blade (Fig. 3.46a, b).

Interclavicle (icl)

Only in UH 4, a small fragment of a straight slender bone bar is partly visible, which is interpreted as the remains of the interclavicle. The fragment lies in proximity to the coracoid,

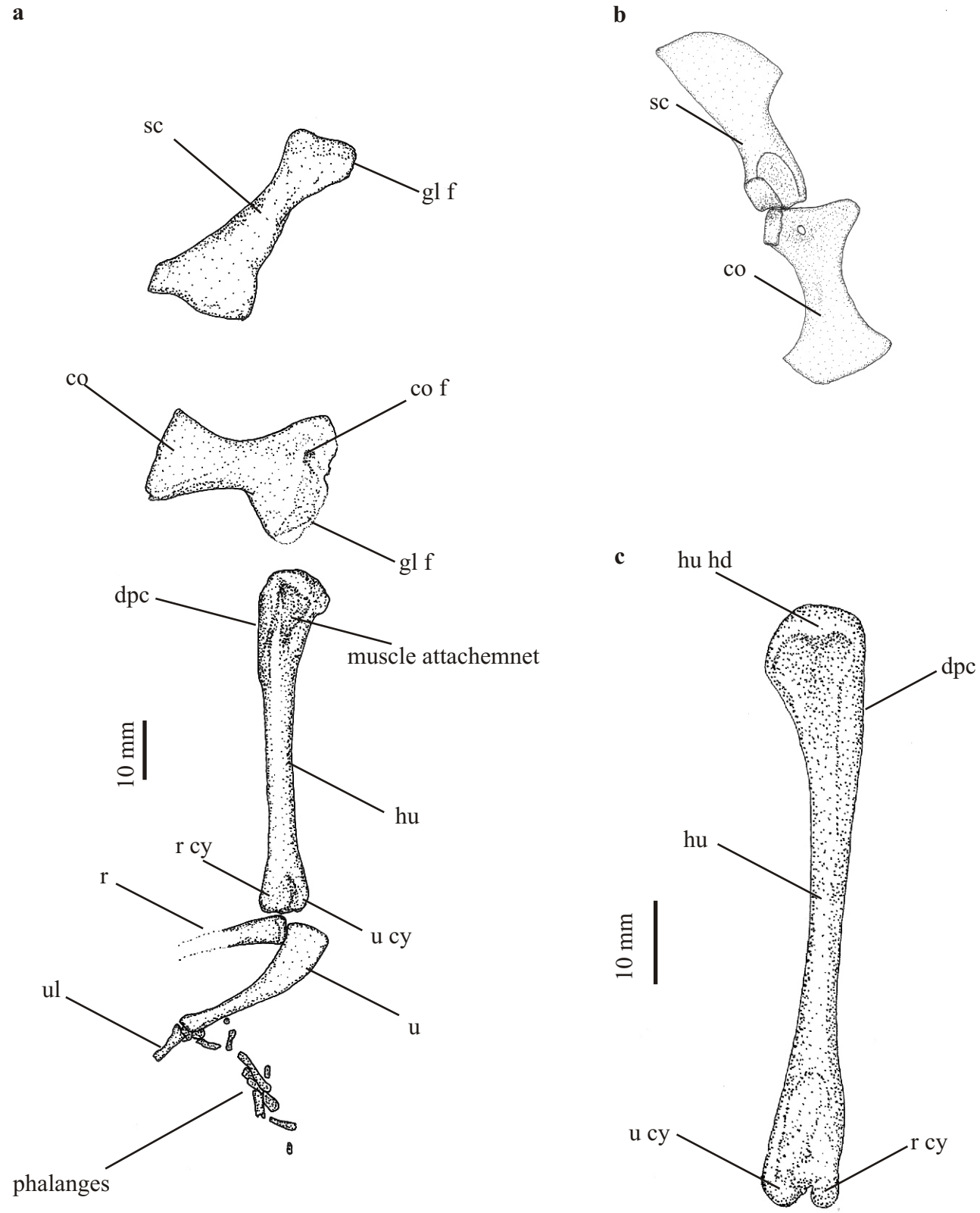

Figure 3.46a-c: Shoulder girdle and forelimb of *Pelagosaurus typus*. **3.46a-***In situ* drawing of the forelimb of the specimen NMHUS M62 2516. **3.46b-**Reconstruction of the shoulder girdle without interclavicle after specimen UH 4 in external view. **3.46c-***In situ* drawing of the forelimb of the specimen UH 4. Abbreviations: co-coracoid, hu-humerus, hu hd- humerus head, co f-coracid foramen, dpc-deltopectoral crest, gl f-glenoid fossa, sc-scapula, r-radius, r cy-radial condyle, u-ulna, u cy-ulnar condyle, ul-ulnare.

but has no distinct characters. Information that is more detailed is not available, because in all other specimens, the interclavicle is not exposed.

Pelvic girdle (Fig. 3.47-Fig. 3.48)

Parts of the pelvic girdle are exposed for example in e.g., MNHN 1883-18, MNHN 1883-14, MNHN 1914-9-8, NHMUS M 62 2516 and SMNS 17758.

The pelvic girdle is generally very similar to the pelvic girdle of *Steneosaurus bollensis* and consists as usual of the paired ilium, the paired ischium, and the paired pubis. However, minor differences are visible in the shape of the ilium in particular at the acetabulum, and in the shape of the pubis.

Ilium (il, Fig. 3.47a-c)

Well-preserved ilia are exposed e.g., in the specimens BMNH 32598, BSGP 1890 509/6 (Fig. 3.47c), MNHN 1883-18, MNHN 1914-9-8, NHMUS M 62 2516, and in BMNH R 1782a (Fig. 3.47b).

The ilium is a roughly rectangular, mediolaterally flattened bone similar to that of *Steneosaurus bollensis*. The iliac length (P1) is an average 78% of the iliac width (P2). However, the posterior process of the ilium crest is not as strongly developed as in *Steneosaurus bollensi*s and is only 2-10% of the entire ilium width. In addition, a small notch ventral to the iliac crest at the posterior margin of the ilium is visible in some specimens (Fig. 3.47a, b). The anterior process is about 20% of the ilium width. The shallow acetabulum lies closer to the anterior margin than to the posterior margin of the ilium. The external ventral part of the ilium has three articular facets; the two posterior facets articulate with the corresponding facets at the dorsal margin of the ischium. Anteroventrally, the small and slightly convex third facet was probably connected to the cartilaginous dorsal end of the pubis. At the internal side of the ilium two large rough areas below the iliac crest are visible, which are the articular areas for the sacral ribs (e.g. BSGP 1890 509/6, SMNS uncatalogued).

Ischium (is, Fig. 3.47a, d)

The ischium is well preserved e.g., in BSGP 1890 I 509/1, MNHN 1883-14, MNHN 1914-9-8, NHMUS M 62 2516, and SMNS 80066.

The ischium consists in its ventral half of an enlarged bone sheet with a rough, slightly convex margin. In its dorsal half, it forms a narrow shaft, which is about 35% the width of the bone sheet. At the dorsal margin, the ischium splits up into three articular facets. The

posterodorsal two facets contact posteriorly the ilium (see there). The anterior, square, and slightly convex facet probably had contact to the ilium and the pubis (Fig. 3.47a, d).

Pubis (pu, Fig. 3.47)

In ventral view, the pubic bones configuration in nearly original position is exposed e.g., in MNHN 1883-18. The pubis in lateral view is exposed e.g., in NHMUS M 62 2516 (Fig. 3.48).

The pubis is an slender, elongated bone with a flat ventromedial expansion. The ventromedial half widens gradually and possesses ventrally a convex margin. At the ventral margin, the pubis width (Pu2) is about 30% of the pubis length (Pu1). This convex margin has a rough surface and was probably connected to the opposite element by cartilage. The dorsal margin of the pubis has a small, thickened enlargement, with a rough surface on its edge, but no distinct articular area is visible at the dorsal margin of the pubis. This is considered as a hint of a possible cartilaginous connection with the ilium. The pubis did not take part in the formation of the acetabulum, and was probably only indirect connected to the ilium and ischium.

Limbs (Fig. 3.46, Fig. 3.47, Fig. 3.48)

Fore limb (Fig. 3.46)

Fore limbs or parts of them are preserved e.g., in the specimens NHMUS M 62 2516, UH 4, and UH 8.

The fore limb consists as usual of humerus, radius, ulna, and manus. It is much shorter and more slender than the hind limb. The distal part of the fore limb is very tiny compared to that of *S. bollensis*. In adult *Pelagosaurus typus* specimens the humerus length (Hl) is only about 53% of the femur length (Fel) in contrary to about 60% in *Steneosaurus bollensis* and in average 70 % *in Platysuchus multiscrobiculatus* (see chapter 4 & 5). In addition, the humerus length in *Pelagosaurus typus* is only about 18 -19% of the skull length (see chapter 4), which differs also widely from *Steneosaurus bollensis* (24%) and *Platysuchus multiscrobiculatus* (27%).

Humerus (hu, Fig. 3.46, Fig. 3.49)

A well-preserved humerus is exposed in the specimens e.g. NHMUS M 62 2516, UH 4, and UH 8.

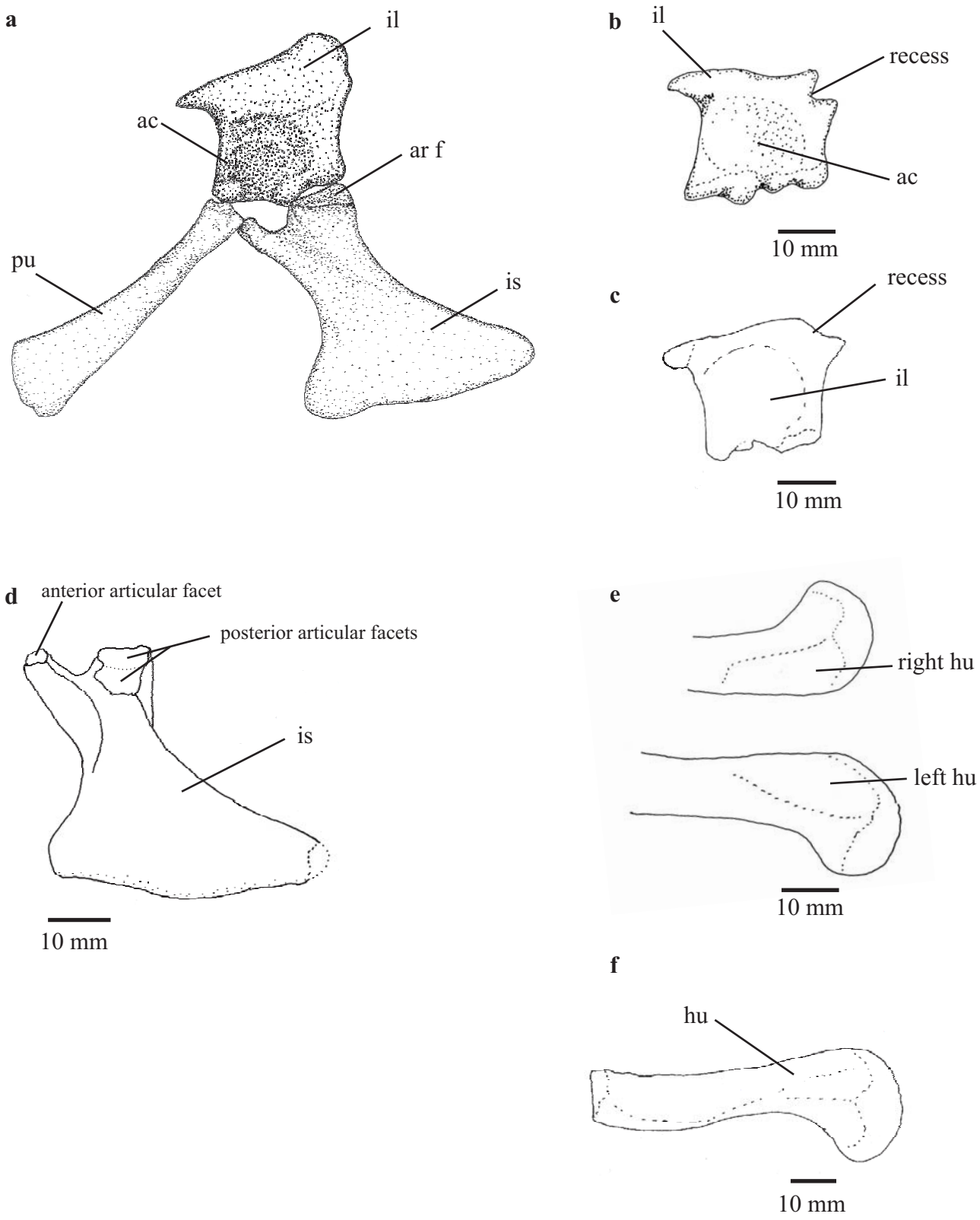

Figure 3.47a-f: Pelvic girdle and proximal femur parts of *Pelagosaurus typus*. **3.47a-**Reconstruction of the pelvic girdle of *Pelagosaurus typus* (after SMNS uncatalogued). **3.47b**-Ilium of specimen BMNH R 1782a in external view. **3.47c-**Sketch of the ilium of specimen BSGP 1890 I 509/6. The recess at the posterior margin is differently developed in the different ilia but always visible. **3.47d**-Sketch of the ischium of BSGP 1890 I 509/1 in internal view. **3.47e**-Sketches of the proximal femur parts of the specimen BMNH 32606 in external view. **3.47f**-Sketch of the proximal femur part of the specimen BSGP 1890 I 509/11 in external view. Abbreviations see chapter 2.

The humerus is an elongated bone with a slightly expanded proximal head and a weakly developed deltopectoral crest. The proximal articulations surface is strongly convex. Dorsally to this, at the internal side, lies a triangular rugosity, which is probably the attachment area for the humeroradialis muscle.

The distal end of the humerus has two articular facets for the connection to radius and ulna. The articular facets for radius (radial condyle) and ulna (ulnar condyle) are clearly separated from each other. They consist of two convexities, which are divided by a deep sulcus. Both the radial condyle and the ulnar condyle are equally developed in size and shape.

Radius (r) (Fig. 3.49)

In the specimens e.g., UH 8 and SMNS 80066, a well-preserved radius is exposed. The radius consists of a slender cylindrical slightly curved shaft that expands slightly both proximally and distally. The proximal margin articulates medially with the ulna in a slightly concave articular facet and with the humerus dorsally as well with a shallow concave articular facet. The distal end connects to the radiale. The radius length (R1) is circa 45% of the humerus length (H1).

Ulna (ul, Fig. 3.46, Fig. 3.49)

A well-preserved ulna is visible e.g., in NHMUS M 62 2516, UH 8, SMNS 80066, and MNHN 1883-14 .

The ulna is a slender bone that is distinctly curved in the proximal half of the shaft. The proximal end of the bone is twice as wide as the distal end. In addition, the proximal end of the ulna is slightly flattened and the proximal margin is slightly convex, with an articular facet for contact with the humerus. It contacts the radius laterally, and the humerus dorsally. The distal end of the ulna is only slightly enlarged and possesses two shallow condyles, which contacts the ulnare and the pisiform.

Manus (Fig. 3.49)

The manus consists of the carpus, the metacarpals, and the phalanges. Its general appearance is similar to those of *S. bollensis* and *Platysuchus multiscrobiculatus* (see chapter 3.1 & 3.4). The carpus consists as usual of the pisiform, the radiale, the ulnare, and one single globular carpal. The metacarpals share all the same elongated shape with slight enlargements for the proximal and distal articular facets (see chapter 3.1), but vary in length and thickness. The phalanges are only partly preserved, but there shape is similar to those of *S. bollensis.* In

most cases, the manus is disarticulated and the exact numbers of phalanges is not clear. The restoration of the phalanges in figure 3.49 is based on the conditions found in *S. bollensis*. The manus is very small and slender in *Pelagosaurus typus*, and possesses in most cases five digits. However, in two juvenile specimens (UH 8 & TMH 13288), only four digits are present. If that is a real intraspecific variation or only a preparation artefact is not to say (see chapter 4 for further discussion).

Hind limb (Fig. 3.47-Fig. 3.49)

The hind limb consists of femur, tibia, fibula, and pes. It shows only minor differences to the hind limb of *Steneosaurus bollensis*. The hind limb is longer than the fore limb (see paragraph "fore limb"). The shape of the femur is similar to the one of *Steneosaurus bollensis*, as well as the proportions of the femur to the tibia. In adult *Pelagosaurus typus* specimens, the femur length is about 30 % of the skull length (see also chapter 5), and the tibia length is usually about 57% of the femur length.

Femur (fe, Fig. 3.47-Fig. 3.49)

Well-preserved femora are exposed e.g., in BMNH 32606, SMNS 50090, and NHMUS M 62 2516 show all

The shape of the femur is very similar to the femur of *Steneosaurus bollensis*. The twisted femur is slender and greatly elongated forming in posterior view an open S-shaped curve (Fig. 3.49). The femoral head is only slightly bent towards the internal side. The muscle attachment for the lesser trochanter is clearly visible ventral to the femoral head. It is marked by an area of rugosities on the inner side of the femur. At the distal end of the bone, there are two condyles forming strong convexities separated by an intercondylar groove. The external fibular condyle is not much larger than the internal tibia condyle.

Tibia (ti, Fig. 3.48-3.49)

In lateral view, the tibia is exposed e.g., in NHMUS M62 2516 (Fig. 3.48) and SMNS 19073. The tibia is a slender slightly bent bone bar, consisting of a cylindrical shaft that is slightly expanding proximally and distally. The tibia length (T1) is about 57% of the femur length (Fe1). The proximal end is massive and about twice as wide as the shaft, forming the articular areas for the femur, which are developed as two very shallow condyles. The distal end of the tibia articulates with the astragalus. The articular facet is strongly convex.

Laterally, the proximal and the distal end of the tibia contact the fibula with a small, medially orientated and slightly concave articular facets.

Fibula (fi, Fig. 3.48-3.49)

The fibula is a slender, slightly bent bone with proximally and distally small, convex expansions. It is about the same length as the tibia. The fibula is nearly identical to that of *Steneosaurus bollensis*, except from the smaller diameter. At the proximal end, the fibula expands slightly (about 5% of its shaft width) and terminates in an elongated convex surface that serves for the articulation with the external portion of the lateral condyle of the femur. At the distal end, the fibula possesses a slightly concave articular facet for the articulation with the calcaneum. Medially, the fibula meets the tibia.

Pes (Fig. 3.48 and Fig. 3.49)

In general, the pes in *Pelagosaurus typus* is similar to that of *Steneosaurus bollensis*. The pes consists of the tarsus, metatarsals, and phalanges. The tarsus consist of the calcaneum, astragalus, and tarsals 3 and 4. The pes possesses a typical crurotarsal joint (see chapter 3.1 for details).

The calcaneum is not much elongated and has nearly the same length as the astragalus. The calcanum tuber is only slightly constricted. The very small, globular tarsal 3 is often missing in the specimens. Tarsal 4 is similar in size and shape to metatarsal V. It is a flat rectangular or triangular bone and about the same size as the metatarsal V. Usually it is situated below the calcaneum and has laterally contact to the metatarsal V and medially to tarsal 3. Ventrally, it articulates with the metatarsal II and III (Fig. 3.34)

The pes in general has five digits, whereas the fifth digit is reduced. Only a rudimentary metatarsal V in a nearly rectangular or in some specimens' triangular-shape is left.

Metatarsals I-IV are in general similar develops consisting of a long, narrow cylindrical shaft with slightly enlarged articular facets on both ends. Metatarsal I is slightly shorter and distinctly broader than the remaining metatarsals II-IV. It is slightly curved anteriorly and not as straight as the other metatarsals. In cross section, metatarsal I is more flattened and not as round as the other metatarsals. The metatarsals II-IV are identical in shape. Metatarsal II and III have the same length and are slightly longer than metatarsal I and IV.

The remaining four digits possess a different numbers of phalanges. The phalangeal formula is 2-3-3-(3)4-0 (e.g. NHMUS M 62 2516). The digit IV is usually the longest one, followed in length by digit III.

The phalanges resemble those of the other teleosaurids. The phalanges are hourglass-shaped, except for the terminal phalanx of each digit, which is developed as a blunt claw. The first phalanx of digit I is slightly shorter than the first phalanges in digits II-IV. The second phalanx of digit I is shaped like a claw and only half as long as the first phalanx of digit I. The second phalanx of digit II-IV are all hourglass-shaped like the first phalanges, but only half their length. The third phalanx of digits II and III are the unguals. In digit IV, the third phalanx is still hourglass shaped, but it is only half as long as the second phalanx. The fourth phalanx of digit IV is the ungual and as long as the third phalanx.

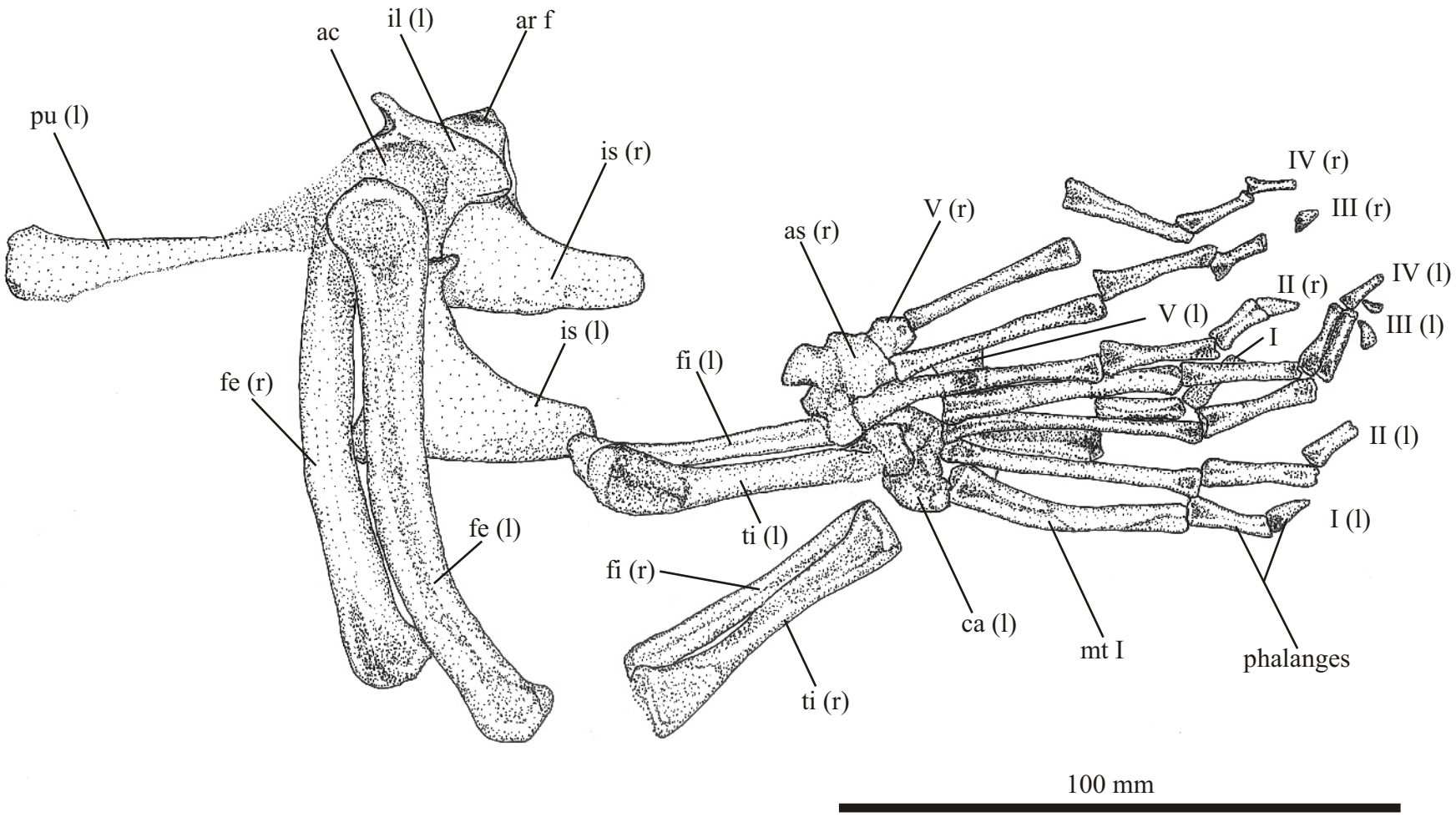

Figure 3.48: *In situ* drawing of the right (r) and left (l) hind limb and appending pelvic girdle of *Pelagosaurus typus* (NHMUS M 62 2516). Abbreviations: ac-acetabulum, as-astragalus, ca-calcaneum, fe-femur, fi-fibula, il-ilium, is-ischium, mt-metatarsal, ph-phalange, pu-pubis, ti-tibia, V- metatarsal V, I-digit one, II-digit two, III-digit three, IV-digit four, 3-tarsal 3, 4-tarsal 4.

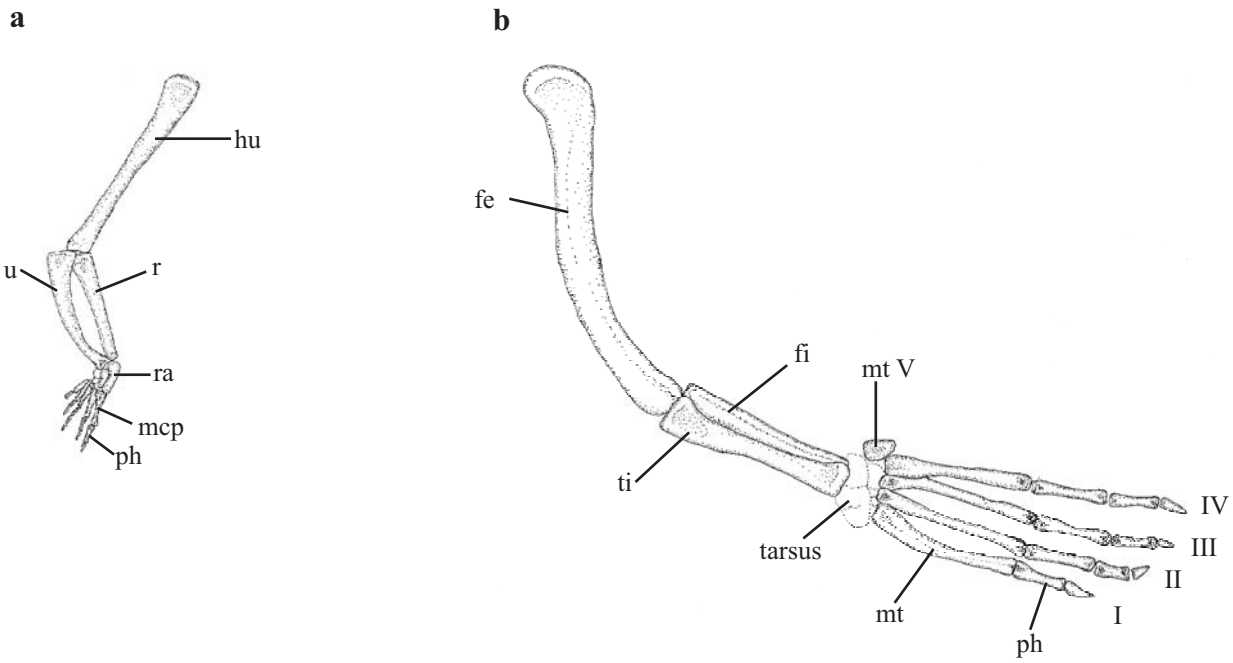

Figure 3.49a-b: Reconstruction of the fore- and hindlimb of *Pelagosaurus typus* in natural relation to each other (external view). Humerus length is about 53% of the femur length. **3.49a**-Fore limb reconstruction is based on the specimens UH 4, UH 8, SMNS 80066, and NHMUS M 62 2516. The carpus is only fragmentary preserved.

3.49b-Hindlimb reconstrucion in based on the specimens UH 4 and NHMUS M 62 2516. Abbreviations: digit I-V, fe-femur, fi-fibula, hu-humerus, mcp-metacarpal, mt-metatarsal, ph-phalange, r-radius, ra-radiale, ti-tibia, u-ulna, ul-ulnare.

Chapter 4

Intraspecific variation and biometric data

In the beginning of the last century, new species were erected by scientists, because of only slight variation of osteological characters (WESTPHAL 1962). Character differences because of individual variation, sexual dimorphism, or ontogenetic stage in the specimens were usually noted as possible, but because of the lack of proper evidence, mostly not considered (e.g. AUER 1909, BRONN & KAUP 1841). WESTPHAL (1962) revised the English and German Liassic teleosaurid fauna, and reduced them from the former over 30 taxa to now only five valid taxa.

In the following chapter the occurrence of intraspecific variation in the osteology of these five taxa, in particular, *Steneosaurus bollensis* (Fig. 4.1), *Platysuchus multiscrobiculatus* (Fig. 4.8), and *Pelagosaurus typus* (Fig. 4.9), as well as their ontogenetic development are described, and the resulting problems for the character definition and taxonomy are discussed. Furthermore, biometric data is compared to illustrate allometric growth rates and distinguish the taxa biometrically from each other.

4.1 Intraspecific variation in extant crocodilians

Intraspecific variation in extant crocodilians is known as ontogenetic and individual variation (MOOK 1921b). Sexual dimorphism among crocodilians is treated as an individual variation. Many ontogenetic studies of extant crocodilians focus on the early embryonic development (e.g., KLEMBARA 1991, 2001, 2004, LARSSON 1998). Unfortunately, these studies could not be considered for comparison, because embryonic material of teleosaurids is not preserved. The post-hatching ontogenetic features of extant crocodilians often deal with soft tissue, which gives further problems for comparison with fossilized material. However, typical juvenile features like large orbit or shorter rostrum size in comparison to the skull size are osteologically and biometrically described, and therefore suitable for comparison with fossil specimens (e.g., KÄLIN 1941, KRAMER & MEDEM 1955, BUSTARD & MAHARANA 1983, MÜLLER & ALBERCH 1990, RIEPPEL 1993, BROCHU 1995, 1996, MONTEIRO & SOARES 1997, MONTEIRO et al. 1997).

The variation of proportions during growth is well known both in extant crocodilians and in thalattosuchians (KRAMER 1955, KRAMER & MEDEM 1955, WESTPHAL 1962, ADAMS-TRESMAN 1987, VIGNAUD 1995). Allometric growth describes morphological proportion changes through time, i.e. changes, which are dependent on age. Because the age is not directly measurable, the total body length is generally used as the standard measure of the age.

However, this leaves a general uncertainty, because, particularly in fossils, no real evidence for isometric growth of the body length is available.

KRAMER & MEDEM (1955) describe the ratio between the total skull length and the total body length of *Gavialis gangeticus* during ontogeny and report a negative allometric growth rate for the skull. They also measure the rostral length in ratio to the total skull length of *G. gangeticus* and note a positive allometric growth of the rostral length in the first years, and afterwards, at an older age, a change into a negative allometric growth.

Main ontogenetic characters for *G. gangeticus* are a negative allometric growth rate of the orbits and the sagittal crest, and a positive allometric growth of the supratemporal fenestrae in ratio to the skull (WESTPHAL 1962).

According to KRAMER & MEDEM (1955), measurements on *Caiman sclerops juscus* and *Caiman sclerops humboldi* show that the growth rate of the skull is only slightly slower than the growth rate of the rest of the body. Respectively the measurements show only slightly negative allometric growth of the skull. The deviation of the isometric growth is very small in these taxa, but they note that the rostrum region of the skull clearly grows faster, i.e. positive allometric, than the brain region of the skull and the trunk region of the animals. Nevertheless, in most extant crocodilians the growth rate of the rostrum region slows down as they get older (KÄLIN 1941, KRAMER & MEDEM 1955). Therefore, KRAMER & MEDEM (1955) record that very large specimens of *Gavialis gangeticus* and *Tomistoma schlegelii* always have relatively shorter snouts in comparison with smaller, which means most of the times also younger, specimens of their own species.

They also recognize that the length of the limbs varies with age in most extant crocodilian taxa. The limbs become proportionally shorter in ratio to the body size in specimens of older age, which means the limbs possess a negative allometric growth rate.

Sexual dimorphism is known with certainty in a couple of extant crocodilian taxa, like for example *Alligator* or *Gavialis* (FREY 1988a, WHITAKER & BASU 1982). However, the description of recent sexual dimorphism consists mostly of the difference in total body length considering the individual age of the adult animals (KRAMER & MEDEM 1955, DODSON 1975, TRUTNAU 1994, BEHLER & BEHLER 1998). KRAMER & MEDEM (1955) describe that the only observable difference between male and female *Caiman sclerops,* reflected by biometric data, is that the females have a smaller body size. DODSON (1975) provides an explanation for the reduced body size and notes that the female crocodilians are usually earlier pubescent than the males, and after reaching sexual maturity, the growth rate slows down. Therefore, the females

are usually kept smaller than the males after sexual maturity (DODSON 1975, TRUTNAU 1994, BEHLER & BEHLER 1998).

The only osteological character for sexual dimorphism known in extant crocodilians is the missing chevron at the first caudal vertebra and the occurrence of a reduced chevron at the second caudal vertebra in the female *Alligator mississipiensis* (FREY 1988a).

Other distinctive signs for sexual dimorphism consist of soft tissue, like the premaxillary swelling in large male individuals of *Gavialis gangeticus* (WHITAKER & BASU 1982). The male Indian gharial (*Gavialis gangeticus*) develops a bulbous appendage on the end of its snout (MARTIN & BELLAIRS 1977, WHITAKER & BASU 1982, BEHLER & BEHLER 1998). This structure is said to resemble an Indian pot called ghara, hence the animal's common name (BEHLER & BEHLER 1998). However, this bulbous consists of connective tissue and forms something like a lid over the external naris (WHITAKER & BASU 1982, MAGNUSSON et al. 2002). Depending on the fact that this swelling consists of soft tissue, a structure like this is usually not fossilized and left hardly any traces on the bony structure ventrally.

4.1.1 The body size problem

Determination of the total body size in fossil taxa is often problematic because of insufficient preservation. Even though the absolute length can be determined in fossil crocodiles, the main problem is that the individual age belonging to the body size is not known. When comparing animals of similar size, there is no guarantee that the compared animals are of similar age (BROCHU 1996). It is therefore possible to compare mistakenly, for example a large female with a small male and vice versa. Additionally, even in extant crocodilians the same age does not guarantee same body size. The growth rate can be retarded or accelerated e.g., by the food situation during the development, climate conditions, population size, or habitat (BUSTARD & MAHARANA 1982, 1983, CHOUDHURY & BUSTARD 1983, ACHARJYO et al. 1990, BROCHU 1996). Due to this fact, it is not surprising that, according to ACHARJYO et al. (1990), in the Indian gharial the limiting factor for the sexual maturity is not the age, but the size of the individual. Depending on food and other environment conditions, the growth rate can vary widely, but no sexual activity is reported for female Indian gharials with a body size of less than 2.6 meters (WHITAKER & BASU 1982, ACHARJYO ET AL. 1990). Similar observations are reported for *Crocodylus niloticus* (COTT 1961, BUSTARD & MAHARANA 1982). Therefore, the total body size does not necessarily provide information about a specific individual age for fossil specimens, but can contain information about juvenile or adult stages or even the point of sexual maturity.

In this study, the first problem is to determine the total body size. In most cases, it is only an estimate, because of the often insufficient preservation, especially of the tail (i.e. caudal column) of the specimens. Therefore, the length of the shoulder-pelvic distance (S-PL) is used instead as standard length for an allometric growth rate of the skull (see chapter 2.5 for measurement definitions). This measurement is more often well preserved and in most cases unaffected by diagenetic deformation. In all other cases the skull length (A) is used as standard length (see chapter 2.5 and Fig. 2.1). However, in *Steneosaurus bollensis* and *Pelagosaurus typus*, where a sufficient large group of individuals was measured, a statistically statement of the proportion changes and growth rate is reasonable, and can for example provide information about the point of reaching sexual maturity (see chapter 5). In this case, smaller specimens (in skull length (A) or S-PL) are usually treated as relatively younger than large specimens, even though the individual age of a particular specimen cannot be determined.

4.2 Intraspecific variation in teleosaurids

VIGNAUD (1995) discusses three different types of intraspecific variation in thalattosuchians: Variations caused by sexual dimorphism, variations caused by individual characters, and variations caused by different geographic distribution.

In the following, two different types of possible causes of intraspecific variation are investigated: Firstly, ontogenetic variation during the development in proportion and shape of bones and secondly, the individual variation of proportion and shape of bones, because of individual or pathological differences. The individual variations are particularly studied for characters possibly based on sexual dimorphism.

The variation caused by geographic distribution is negligible for *Steneosaurus bollensis* in this study, because the taxon is mostly restricted to the southern part of Germany and only specimens from the Holzmaden area were used for comparison.

Because of the few certain *Platysuchus multiscrobiculatus* specimens (2 adults, 1 juvenile), mainly the ontogenetic intraspecific variation is described. The quantity of individuals is too small to set up a general pattern for individual variation.

For *Pelagosaurus typus* individual as well as ontogenetic variation is described and discussed. Even though the investigated individuals are coming from localities in England, France and Germany, particular variation caused by geographical distribution are not recognized. The former described differences in cranial bone ornamentation between French and German specimens by BERCKHEMER (1928) and WESTPHAL (1962) is not visible here.

Observed minor differences in bone ornamentation are probably caused by individual, diagenetic or preparation conditions. A relation of different bone ornamentation to a specific ontogenetic stage or geographical distribution is not recognizable.

4.2.1 Morphological features

The following morphological features were closely studied for intraspecific variations:

- The orbit shape (Fig. 4.1, Fig, 4.8, Fig. 4.9, Fig. 4.5, and diagram 6, 7, and 8)
- The ornamentation of the cranial bones (Fig. 4.2)
- The shape of the external naris (Fig. 4.3)
- The shape and ornamentation of the osteoderms (Fig. 4.4)
- The supratemporal fenestra (STF) shape (Fig. 4.5 and diagram 9)
- The shape of the frontal regarding the development of a sagittal crest (Fig. 4.5)
- The shape of the parietal, squamosal, and quadrate regarding the posterior margin of the skull (Fig. 4.5)
- The number of teeth in the rostrum
- The number of ribs and vertebrae
- The closure of the neurocentral suture at the vertebrae (Fig. 4.7)

The development of the closure of the neurocentral suture at particular vertebrae are studied for thalattosuchians, because BROCHU (1996) describes that neurocentral sutures are not totally fused in juvenile specimens of extant crocodilians (e.g. *Alligator mississipiensis*, *Crocodylus acutus*). The vertebral ossification run from cranial to caudal in all reptiles, but the neurocentral suture closure sequence is caudal to cranial in crocodilians (BROCHU 1996). Therefore a certain sign for a juvenile or at least immature specimen in the fossil record is the separation of the vertebra centrum from the neural arch in the presacral column, indicating that the vertebrae suture were open at the time of death (BROCHU 1996).

4.2.2 Size and proportion

For definition of the single measurements and explanation of the used values, see chapter 2.5 and figures 2.1 and 2.2. The following biometric values were compared for some Thalattosuchia taxa, to find possible difference in the ratios as well as to study intraspecific variation in the Liassic taxa:

- Skull length (A) to shoulder-pelvic distance (S-PL) (Diagram 1)
- Skull width (C) to skull length (A) (Diagram 2)

- Rostral length (B) to skull length (A) (Diagram 3)
- Premaxilla-nasal distance (H) to rostral length (B) (Diagram 4)
- Enlargement of the premaxillae (K/L) in ratio to skull length (A) (Diagram 5)
- Orbital length (I) to skull length (A) (Diagram 6)
- Orbital length (I) to supratemporal fenestra length (D) (Diagram 7)
- Orbital width/orbital length (J/I) to skull width/skull length (C/A) (Diagram 8)
- Supratemporal fenestra (STF) width/STF length (E/D) to skull width/skull length (C/A) (Diagram 9)
- Retroarticular process length (X) to skull length (A) (Diagram 10)
- Symphysis length (V) to mandibular length (U) (Diagram 11)
- Splenial part of the symphysis (W) to symphysis length (V) (Diagram 12)
- Humerus length (H1) to femur length (Fe1) (Diagram 13)
- Humerus length (H1) to skull length (A) (Diagram 14)
- Femur length (Fe1) to skull length (A) (Diagram 15)
- Tibia length (T1) to femur length (Fe1) regarding the proportion of the hind limb (Diagram 16)
- Quotient of humerus length/femur length (H1/Fe1) to skull length (A) (Diagram 17)

All diagrams show the absolute values as measured, or in some cases the percentages or quotients of the absolute values. In the diagrams, the values are not logarithmised. Using the absolute values and not logarithms have two main advantages: The metric interspecific differences of the taxa remain more obvious and the standard length is not needed for comparison. Nevertheless, to make a statement about allometric growth for the skull length within one species, the shoulder-pelvic distance (S-PL) is taken as standard length. The total body length (TL) is in most case, not measurable or at least too uncertain to use as standard length, mostly because of insufficient preservation, disarticulation, or artificially added parts. To investigate allometric growth, for the rostral length, orbital length, retroarticular process, humerus length, and femur length, the skull length (A) was defined as standard length. Allometric growth rate was calculated after $\log y = a \log x + \log b$, with $a = 1$ isometric growth rate, $a < 1$ negative allometric growth rate, and $a > 1$ positive allometric growth rate. The variable "x" represents here the standard length and "y" is the variable for the particular values of the studied body parts (e.g. orbital length).

Most of these characters were chosen after WESTPHAL (1962) and VIGNAUD (1995), who already have mentioned individual and ontogenetic variation of osteological characters

and proportions in some thalattosuchians. Furthermore, investigations by KRAMER (1955) and KRAMER & MEDEM (1955) show different proportions changes during growth, both in extant crocodilians and in *Steneosaurus bollensis*.

4.2.3 General individual variation of *Steneosaurus bollensis*

For this investigation, 89 specimens of *Steneosaurus bollensis* were studied (see appendix I). The largest known *S. bollensis* specimen reaches five meters. However, more common are specimens with a total body length of three to four meters.

In *Steneosaurus bollensis*, growth independent, individual variations are noted as following: The number of teeth in the premaxilla varies from three to four, in the maxilla from 26 to 35, and in the dentary from 24 to 35. The number of thoracic vertebrae varies from 12 to 15, the number of lumbar vertebrae varies from two to three, and the number of caudal vertebrae varies from about 45 to a maximum of 55.

The shape and the enlargement of the premaxillae are almost independent of the ontogenetic stage**.** The growth independent variability in premaxillae enlargement is high and shows only a very slight tendency to increase during ontogeny (Diagram 5). The enlargement of the premaxillae is expressed by the percentage quotation of the premaxillae width (K) divided through the narrowing posterior of the premaxillae (L). A value of about 100% indicates no enlargement; a value of about 200% indicates broad enlargement of the premaxillae (Diagram 5). The orientation of the external naris is anterodorsal with an angle (W1) of 30°- 45° to the horizontal plane, while the premaxillae are not or only slightly flexed ventrally (Fig. 4.1).

The shape of the external naris varies broadly (Fig. 4.3). It is obvious that the variation is influenced by ontogenetic, individual, and unfortunately diagenetic factors as well. The external naris in juveniles are mainly posterior heart-shaped or rectangular longer than wide (Fig. 4.1 and 4.3), whereas in adults the external naris is anterior heart-shaped, posterior drop-shaped, or transverse ellipsoid, with an anterior and posterior small recesses. A clear statement is impossible because of the compressed preservation of all specimens, which make the feature hardly usable for comparative studies.

The symphysis angle (W2) varies in *S. bollensis* between 35° and 50° (see Fig. 3.1.). Too few measured values of the lower jaw of *S. bollensis* were available, to make a statement about ontogenetic development. However, they indicate a linear development of the symphysis length (V) in ratio to the entire mandibular length (U) (Diagram 11).

Ornamentation on the cranial bones varies individually, but is probably partly related to ontogenetic development. However, a clear connection between ornamentation of the cranial

bones and age cannot be confirmed with certainty. The ornamentation of the frontal in some large specimens (e.g. SMNS 51957, NHMUS 4) consists of elongated transverse grooves and faint ridges and does not consist of round pits like in most other specimens (e.g. SMNS 15951, Fig. 4.2). For a detailed description of the ornamentation in the adult specimens, see chapter 3.1. In some but not all juvenile specimens of *S. bollensis* (e.g. UH 6, SMNS 115, and GPIT Re 1193/7b), the ornamentation is restricted to the parietal and frontal and the pits are shallower and fainter than in the adult specimens.

The ornamentation of the osteoderms varies slightly with the position of the osteoderm in the armour itself, and in the individual specimen (Fig. 4.4). The ornamentation consists of large regular distributed circular pits, but the definite number of the pits varies individually and with the size of the osteoderm (see chapter 3.1 and Fig. 4.4). A dorsal keel is developed on the surface of the posterior dorsal osteoderms usually beginning level with the sacral vertebrae. This keel is most pronounced on the osteoderms covering the sacral and the caudal column, but it can also start individually earlier already in the middle of the thoracic region.

The shape of the osteoderms is relatively constant, considered their position in the osteodermal shield, and varies individually only little from rectangular to more elongated osteoderms (see chapter 3.1 and Fig. 4.4).

4.2.4 Ontogenetic variation in *Steneosaurus bollensis*

The smallest known specimen of *Steneosaurus bollensis* has a skull length of about 130 mm (SMNS 15712a/b) and the largest known individual has a skull length of about 1030 mm (GPIT Re 1193/3).

Juvenile specimens are defined as specimens, which possess a skull length (A) of less than 250 mm. Based on this definition, the following 10 certain juvenile specimens of *S. bollensis* were personally studied: BSGP (uncatalogued), GPIT Re 1193/10, GPIT Re 1193/12, GPIT Re 1193/6 (Fig. 4.7), GPIT Re 1193/7b, SMNS 10000, SMNS 15712a/b, SMNS 20280, SMNS 20286 (115) (Fig. 4.1), and UH 6 (Fig. 4.5 and Fig. 4.6). Some complementary data were taken from the literature (WESTPHAL 1962) (see appendix II).

According to WESTPHAL (1962), the estimated age for an individual of *S. bollensis* with a skull length of about 130 mm is two years, compared with growth rates of *Crocodylus porosus*. Extant crocodilian hatchlings possess in average a total body length of 250 mm, except of the Indian gharial (*Gavialis gangeticus*), which has an average hatchling size of 370 mm (BOLTON 1989). The common growth rate of extant crocodilians, under optimal nutrition conditions in captivity, lies in the first three years by 40-50 mm per month (BOLTON 1989). Extant crocodilians usually need at least one year, to reach a body length of about 700 mm

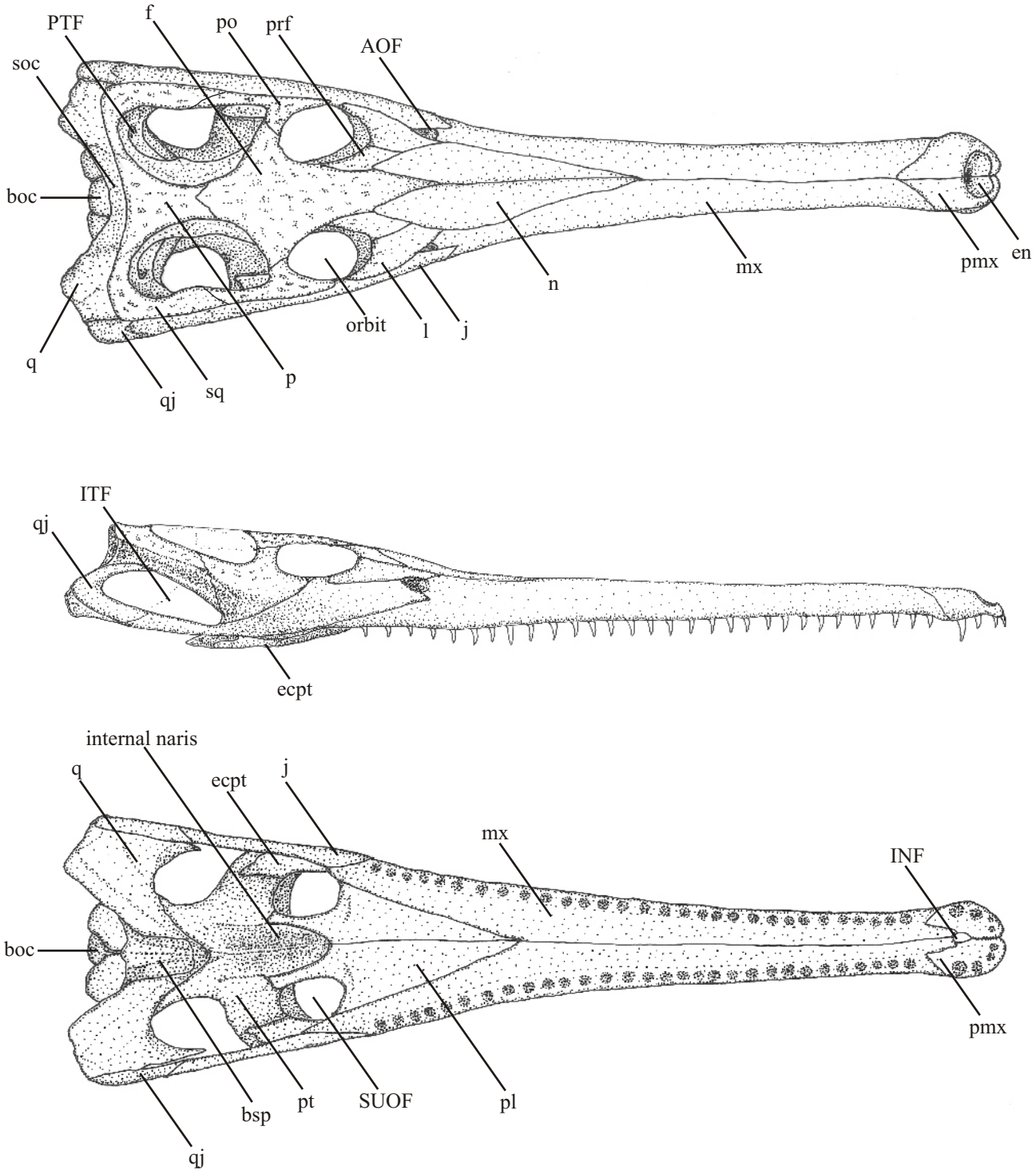

Figure 4.1a-c: Reconstruction of a juvenile *Steneosaurus. bollensis* skull modeled in wax after specimen SMNS 115 (SMNS 20286). **4.1a-**Skull in dorsal view. The ornamentation of the cranial bones can vary and is in some cases restricted to frontal and parietal. **4.1b**-Skull in lateral view. **4.1c**-Skull in ventral view without hyoid bones. The original skull length is 138.4 mm. Abbreviations: **AOF-** antorbital fenestra; **bsp-**basisphenoid; **boc-**basioccipital **d-**dental; **en-**external naris; **ecpt-**ectopterygoid; **eo-**exoccipital; **f-**frontal; **FM-**foramen magnum; **ITF-**infratemporal fenestra; **INF-**incisive foramen; **is-**ischium; **j-**jugal; **l-**lacrimal; **m-**maxilla **n-**nasal; **o-**orbit; **op-**opisthotic; **p-**parietal; **pl-**palatine, **pmx-**premaxilla; **po-**postorbital; **prf-**prefrontal; **pro-**prootic; **pt-**pterygoid; **PTF-**posttemporal fenestra; **q-**quadrate; **STF-**supratemporal fenestra; **soc-**supraoccipital; **sq-**squamosal; **SUOF-**suborbital fenestra.

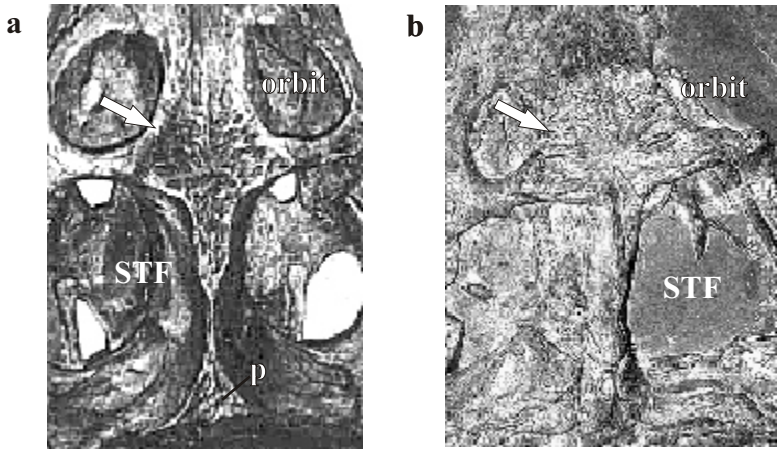

Figure 4.2a-b: Dorsal view of the frontal and parietal of two different *Steneosaurus bollensis* specimens. **4.2a-**SMNS 15951 with round and elongated pits in dense distribution on the frontal (orbit length 30 mm). **4.2b-**SMNS 51957 with elongated grooves on the surface of the frontal (orbit length 43 mm). Arrows mark the frontals.
Abbreviations: p-parietal, STF-supratemporal fenestra.

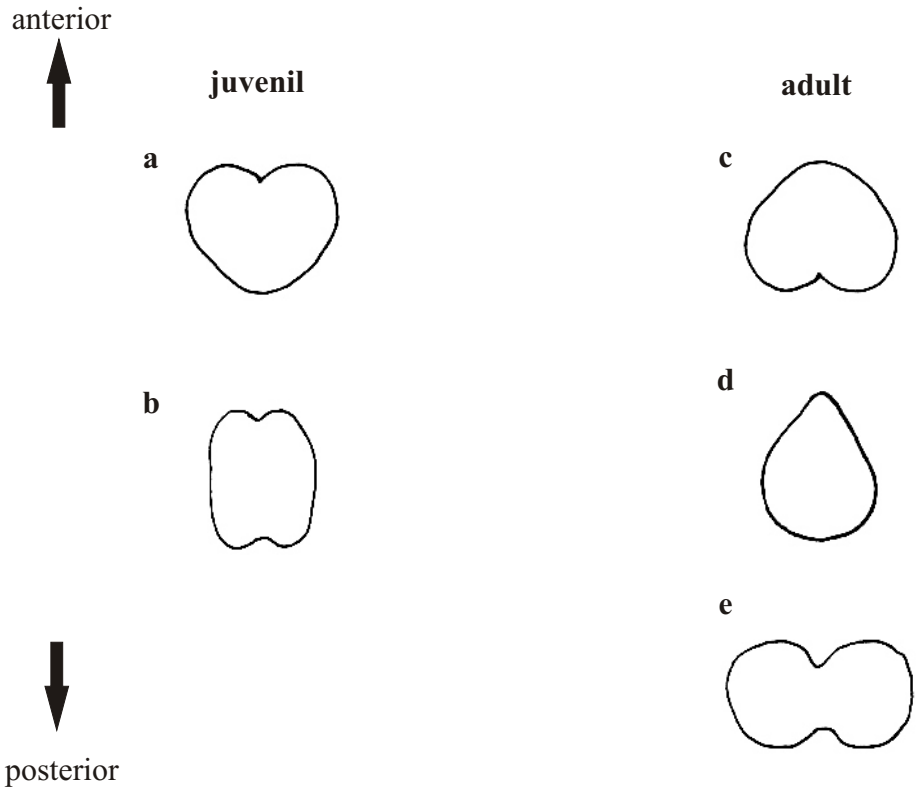

Figure 4.3a-e: Often observed variation of the shape of the outline of the external naris in *Steneosaurus bollensis.* The variation is probably caused by intraspecific and ontogenetic variation as well as diagenetic deformation (see text). **4.3a-**Shape as it is visible e.g, in SMNS 10000 (juvenile). **4.3b**-Shape as it is visible e.g., in UH 6 (juvenile), **4.3c**- Shape as it is visible e.g., in GPIM 23a (adult). **4.3d**-Shape as it is visible e.g., in specimen SNSD 4 (adult), **4.3e**-Shape as it is visible e.g., in SMNS 51555 (adult).

Steneosaurus bollensis

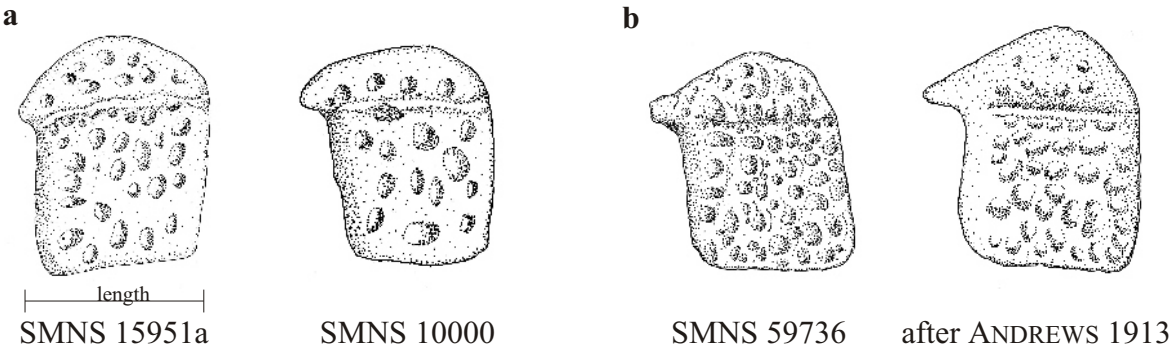

Platysuchus multiscrobicualtus

Pelagosaurus typus

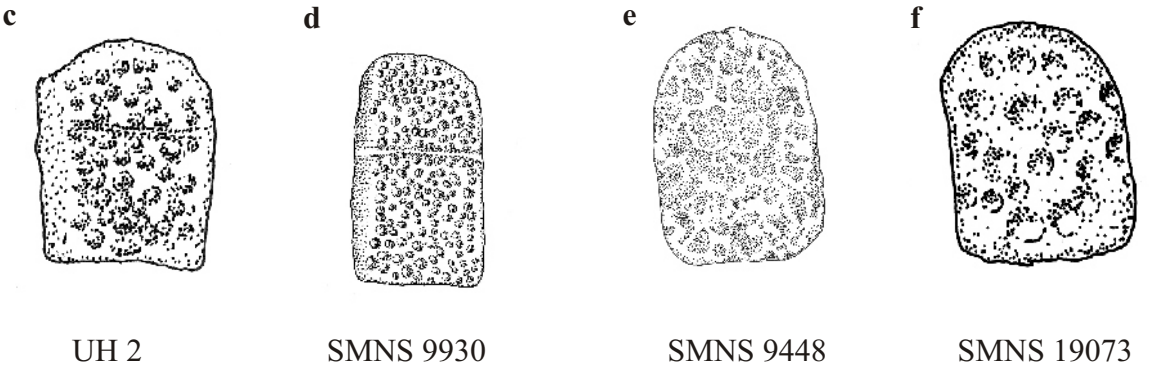

Figure 4.4a-f: Dorsal posterior thoracic osteoderms of: **4.4a**- juvenile *Steneosaurus bollensis* (original length of the osteoderms are 12 mm and 10 mm), **4.4b-**an adult *S. bollensis* (original length of the osteoderm are 32 mm and 30 mm), **4.4c**-a juvenile *Platysuchus multiscrobiculatus* (original length of the osteoderm is 10 mm), **4.4d**-an adult *Pl. multiscrobiculatus* (original length of the osteoderm is 35 mm), **4.4e** and **4.4f-** adult *Pelagosaurus typu*s (original length of the osteoderm 4.4e is 28 mm and original length of the osteoderm 4.4f is 22 mm). Osteoderms are scaled to similar size for better comparison. The specific specimen, which the osteoderm belongs to, is written under each osteoderm.

(BOLTON 1989), which is until now the smallest known body size for *S. bollensis* (GPIT Re 1193/7b). It is likely that the growth rate in the wild is even slower because of unfavourable nutrition conditions.

Based on this assumption, it is most likely that the earliest ontogenetic stages of *Steneosaurus bollensis* are missing, and that the smallest known specimens with 130-250 mm skull length represent an individual age between one and three years. Thus, embryonic or hatchling material is unknown of *S. bollensis* so far (see chapter 8 for further discussion). Nevertheless, total body size depends on many different factors and must be interpreted with caution (see paragraph 4.1.1.).

Growth related variation in the skeleton of *S. bollensis* is observed as following:
Slight negative allometric growth is noticed for the skull length in ratio to the shoulder-pelvic distance. The percentage of the skull length (A) at the shoulder-pelvic distance (S-PL) varies between 80-95% in adults and 77-82% in juvenile specimens (Diagram 1).

In the skull, negative allometric growth is observed for the rostral length (B), the orbital length (I), the supratemporal fenestra length (D), and the sagittal crest width (compared to the skull length (A)). In juvenile specimens, the rostral length (B) in ratio to the skull length (A) does not vary much from the value measured for the adult specimen (average 71.4%). The variation is almost superimposed by the individual, growth independent variation of the rostral length (B). However, the proportion shows a linear development (Diagram 3) with a calculated slight negative allometric growth rate. In addition, large juvenile orbit size compared to the skull size and the supratemporal fenestra length (D) is visible (Diagram 6, 7, 8). The average of the orbital length (I) to the skull length (A) is 9.6% in juvenile specimens of *Steneosaurus bollensis*, while it is only 7.9 % in adult specimens (Diagram 6). This results in a negative allometric growth rate of the orbit in ratio to the skull length.

Morphologically, the orbital shape of juveniles is more circular than in adults, who possess longitudinal elliptic orbits. This fact is reflected and confirmed by the ratio of orbital width (J) to orbital length (I) (Diagram 7, Fig. 4.5). A percentage of 100-80% indicate circular orbits, while a percentage of less than 80% indicates elliptic orbits. Orbital length (I) to supratemporal fenestra length (D) is in average 63% in juveniles and only 52% in adult specimens (Diagram 6 and appendix VI).

The supratemporal fenestra (STF) length (D) is in average 16.2% of the skull length (A) in juveniles and about 15% in adults. A slight negative allometric growth rate is calculated here.

S. bollensis. At the same skull length, the intraspecific variation of the percentage of the retroarticular process length is relatively high with up to 3%.

Isometric growth is noted for the skull width (C) in ratio to the skull length (A).The skull width (C) is in average 28.6% of the skull length (A) (Diagram 2).

Morphologically, the shape of the STF is reflected by the percentage of the STF width (E) in ratio to the STF length (D). If the percentage is higher, the STF is more squarely (Diagram 8). Obviously, the shape of the supratemporal fenestra (STF) directly depends of the frontal shape. In juvenile individuals, the supratemporal fenestra is more ellipsoid than the rectangular supratemporal fenestra in adult specimens (Fig. 4.5). In *Steneosaurus bollensis*, the shape of the frontal varies most obviously during ontogenetic development. In juvenile specimens, the frontal is roughly rhombic or cruciform, whereas in adult specimens it is triangular with a narrow posterior process (Fig. 4.5). This is linked to a decrease of width in the sagittal crest, which shows a negative allometric growth rate compared to the skull length.

Another morphological, typical juvenile character is the less posteriorly extended quadrates and squamosals, compared to adult specimens. This results in a straighter outline of the posterior margin of the cranial table in juvenile specimens, in contrast to an externally concave outline in adult specimens (Fig. 4.5). KRAMER & MEDEM (1955) first described this difference in the development of the posterior margin of the skull in extant crocodilians. An anatomical comparison of a particular juvenile specimen of *S. bollensis* (UH 6, skull length about 180 mm) and an adult specimen of *S. bollensis* (UH 9, skull length about 900 mm), show only minor changes in the general skull shape, except of the posterior outline of the skull. Obviously, the larger changes lie in the shape of the particular cranial bones like the frontal, parietal, squamosals, and quadrates (Fig. 4.5).

Positive allometric growth in the skull is calculated for the maxillae and the retroarticular process. Even though the rostral length develops slightly negative allometric (see above), the premaxilla-nasal distance (H) increases during the growth. In the juvenile specimens, "H" is measuring about one third of the rostrum, while it is half of the rostral length in adult individuals (Diagram 4). This indicates that the elongation of the rostral length (B) mainly depends on the elongation of the maxillae. The growth rate of the maxillae is therefore slightly positive allometric.

According to WESTPHAL (1962) the growth of the retroarticular process in the lower jaw is positive allometric in *Gavialis gangeticus*. In this study, a positive allometric growth rate of the retroarticular process in the lower jaw is confirmed for *S. bollensis*, too. A slight increase in the retroarticular process length is observed relatively to the skull length (Diagram 10).

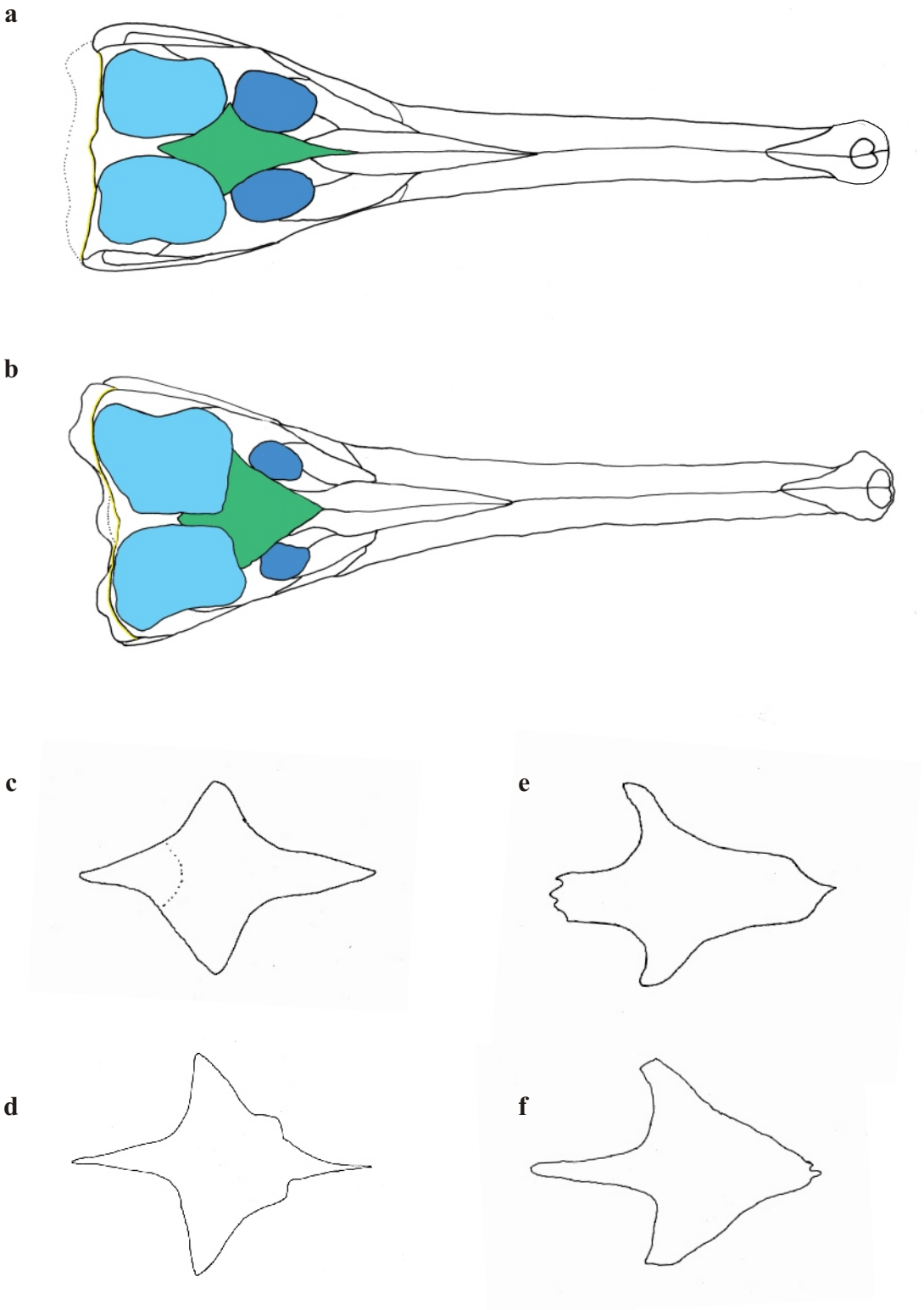

Figure 4.5a-f: Comparison of the skull and cranial bones shape of a juvenile skull (skull length 180 mm) and an adult skull (skull length 900 mm) of *Steneosaurus bollensis*. For easier comparison the skulls are scaled to the same size. **4.5a-***In situ* sketch of a juvenile *Steneosaurus bollensis* skull (UH 6). Orbits are coloured in light blue, supratemporal fenestrae in dark blue, and frontal in green. Posterior outline of the skull is marked in yellow. **4.5b**-*In situ* sketch of an adult *S. bollensis* skull (UH 3). Colours are identical with 4.5 a. Comparison of the frontal shape in **4.5c-** juvenile *Platysuchus multiscrobiculatus.* **4.5d-**adult *Platysuchus multiscrobiculat*us. **4.5e-**juvenile *Pelagosaurus typus*, **4.5f**-adult *Pelagosaurus typus*. The frontal shape changes from rhombic or cruciform to triangular with a narrow posterior process. During growth almost all intermediate forms can appear. Bone ornamentation is not considered.

This feature is observable in several other taxa as well, but because of the high scattering of the values, it is not useful for taxa differentiation within the teleosaurids (Diagram 10). The percentage of the retroarticular process length at the skull length lies between 8% and 18% in the postcranial of *S. bollensis*, positive allometric growth is noted for the humerus length (H1) and the femur length (Fe1) compared to the skull length (A). The percentage of the humerus length (H1) at the skull length (A) is about 19% to 30%. The average is about 23.7%. The highest percentage values are not related to the largest skull length but to medium-sized skulls. Therefore, the humerus is growing obviously positive allometric compared to the skull, at least in an early ontogenetic stage. The highest scattering of the values in the Diagram 14 are visible between skull sizes of 400 to 750 mm. This could indicate sexual dimorphism after reaching sexual maturity. However, a clear differentiation in two separated lines is not visible (Diagram 14).

The absolute values of the femur length (Fe1) in ratio to the skull length (A) are shown in Diagram 15. The percentage of the femur length at the skull length is in average 41.3 %. The femur has as well a calculated positive allometric growth rate.

The ratio of humerus length (H1) to femur length (Fe1) shows a linear development and is in average 67.2% in juvenile and 60.3% in adult specimens. The length of the humerus is therefore a little larger in juveniles compared to the femur length than in adults, even if the individual variation can be up to 4% of the average in both juvenile and adult specimens (Diagram 13, Diagram 17, appendix II).

The tibia length (T1) is 68%-70% of the femur length (Fe1) in juveniles and only 53%-62% in adults (see appendix II & VI). Therefore, the tibia length decreases distinctly during growth in ratio to the femur length. Nevertheless, the development of the tibia is linear (Diagram 16) and the observed ratios are a result of the positive allometric growth of the femur (relatively to the skull).

Additionally, morphological ontogenetic features are observed as following: In the juvenile specimen UH 6, the articular areas at the fore limb between humerus and ulna show unusual roughness and even slight deformation in comparison with the fore limb of an adult specimen (Fig. 4.6). Thus, it is assumed that the articular facets were not fully ossified at the time of death, which indicates a juvenile stage of development (RIEPPEL 1993).

Separated neural arches from the vertebrae centra in the presacral column are visible in *S. bollensis* (specimen GPIT Re 1193/6) and as well as in *Pelagosaurus typus*, and *Platysuchus multiscrobiculatus* (see below). All specimens, in which such a separation of the vertebrae is visible, possess a skull length less than 250 mm and other certain juvenile

characters, like a broad ornamented region between the STF's instead of a sagittal crest, and relatively larger orbits in comparison to larger specimens. In GPIT Re 1193/6, only some caudal vertebrae are found intact. All other preserved vertebrae were disaggregated into the centrum and the neural arch (Fig. 4.7). According to BROCHU (1996), this is a clear sign of a juvenile specimen (see paragraph 4.2.1).

4.2.5 Intraspecific variation in *Steneosaurus brevior* and *Steneosaurus gracilirostris*

Because only three adult specimens of *S. brevior* were investigated, a general statement about intraspecific variation is impossible. However, some of the biometric values show differences in comparsion to the other Liassic teleosaurid taxa like e.g., the percentage of the skull width (C) at the skull length (A) (Diagram 2) or rostral length (B) to skull length (A) (Diagram 3) (see chapter 5).

Intraspecific variation in *S. gracilirostris* could not be studied in detail, because of the insufficient number of specimens available. However, the biometric values show differences in comparison to the other Liassic teleosaurid taxa like e.g., the ratio of skull width (C) to skull length (A) (see chapter 5 and appendix III).

4.2.6 Intraspecific variation in *Platysuchus multiscrobiculatus*

Pl. multiscrobiculatus reaches a total body length of three meters. Two adult specimens and two juveniles were investigated. Only one juvenile specimen UH 2, with a skull length of 132 mm, is referred to *Platysuchus multiscrobiculatu*s with certainty (Fig. 4.8). The second juvenile specimen SMNS 15391 (skull length 168 mm), shows osteoderms with a well-developed keel and a particular dense pattern of pits on the surface. Both features are very similar to the features found in *Platysuchus multiscrobiculatus* (see chapter 3.4 and Fig. 4.4). Unfortunately, the cervical column as well as the armour in that particular part is artificially added in SMNS 15391. In addition, the skull might belong to another specimen (personal comment WILD). The specimen is probably a chimera. Nevertheless, because of the nearly identical armour in the trunk, it is tentatively referred to *Platysuchus multiscrobiculatus*, but will not be further considered in the following.

The smallest known specimen of *Platysuchus multiscrobiculatus* possesses a skull length of 132 mm (UH 2, Fig. 4.8) and the largest known a skull length of 450 mm (SMNS 9930, Fig. 3.24); so far no specimens of intermediate size are known.

Because of the few numbers of individuals, growth independent variation could not investigated in detail and the following analysis focus on the possible ontogenetic differences.

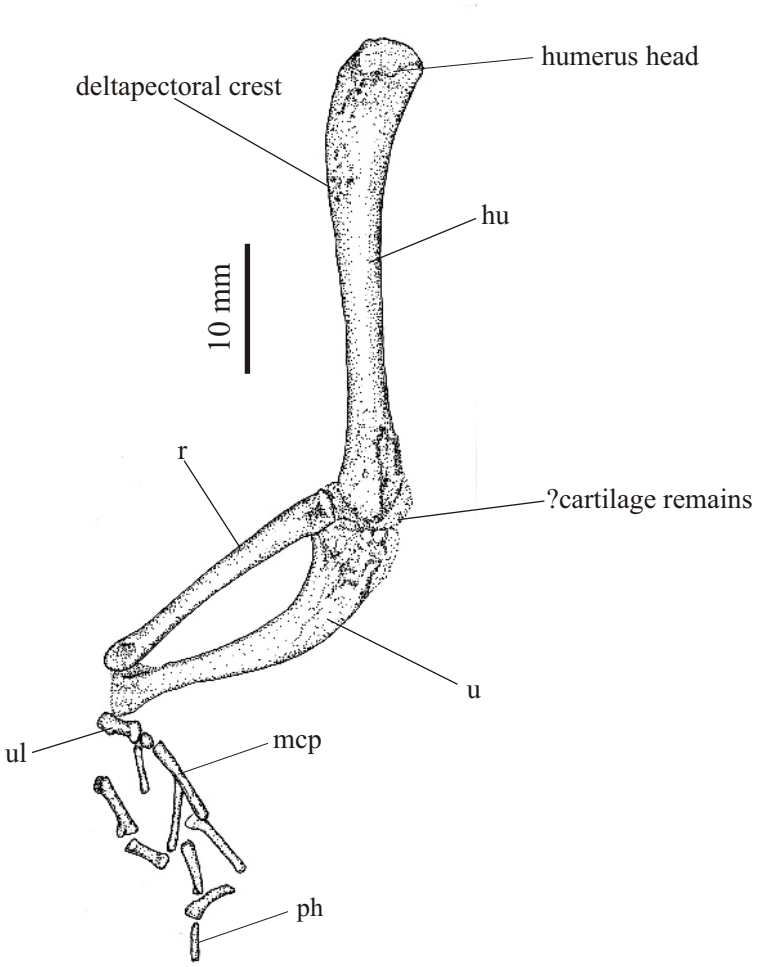

Figure 4.6: *In situ* drawing of the left forelimb of a juvenile *Steneosaurus bollensis* (UH 6) with only partly petrified articular facets on the proximal margin of the ulna and the distal margin of the humerus indicating poor ossification at the time of death. Abbreviations: hu-humerus, mcp-metacarpal, ph-phanlanx, r-radius, u-ulna, ul-ulnare.

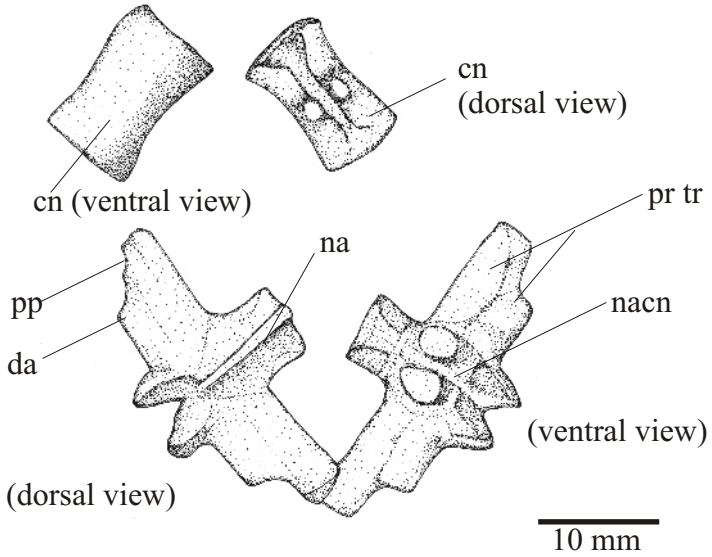

Figure 4.7: In situ drawing of separated thoracic vertebrae of a juvenile *Steneosaurus bollensis* specimen (GPIT Re 1193/6), indicating open neurocentral sutures at the time of death. Abbreviations: na-neural arch; cn-centrale (vertebra centrum), poz-postzygapophysis, prz-prezygapophysis, da-diapohysis, pr tr-processes transverses.

In general, the ontogenetic changes in *Platysuchus multiscrobiculatus* are similar to those of *Steneosaurus bollensis* (see paragraph 4.2.4). Even though some proportions are different in *Platysuchus multiscrobiculatus,* like e.g. the skull length (A) in ratio to the shoulder-pelvic distance (S-PL) (Diagram 1). In the two adult specimens, the skull length is only 44% and 48% of the S-PL, while the juvenile (UH 1) shows the same percentage of the skull length as juvenile *S. bollensis* specimens of about 80% of the S-PL (Diagram 1). The ratio of skull length (A) to trunk length (TRL) is about 72% in the juvenile *Platysuchus multiscrobiculatus* specimen (UH 2) and about 45% in the adults (appendix III), which indicates a negative allometric growth rate for the skull.

In the skull, negative allometric growth rate is calculated for the orbital length and the sagittal crest width. The average percentage of the orbital length (I) at the skull length (A) changes from 9.1% in juveniles (with a skull length less than 250 mm) to only 7.5% in adult specimens (Diagram 6). The orbit grows negative allometric compared to the skull. In addition, the shape of the orbit in the juvenile differs from the orbital shape in the adult specimens like in *S. bollensis*. In the juvenile specimen, the orbit is sub-circular and not as longitudinal elongated as in the adult specimens (Diagram 8, Fig. 4.2 & Fig. 3.26). The orbit of the juvenile is relatively large in comparison with the supratemporal fenestra. In the juvenile specimen, it is 60%, while the two adults show only an orbital length of about 45% of the length of the supratemporal fenestra (Diagram 7).

In contrast to the adult specimens, the juvenile specimen possesses no sagittal crest between the supratemporal fenestrae (STF) but a broad, ornamented region similar to the conditions found in juvenile *Steneosaurus bollensis* specimens (see paragraph 4.2.4). The frontal of the juvenile *Platysuchus multiscrobiculatus* (UH 2) is rhombic, whereas the frontal of the adult specimens is sub-triangular with a narrow posterior process (Fig. 4.5, Fig. 4.8).

Positive allometric growth in the skull is supposed for the rostral length, the premaxillae width, the supratemporal fenestra length, and the quadrates. Because of the few numbers of specimens, the calculation of the values is insufficient.

The rostral length (B) is 70.45% of the skull length (A) in the juvenile specimen (UH 2) and 75% in the adult specimens and develops slightly positive allometric (Diagram 3, appendix II and VI), whereas the rostral length develops slightly negative allometric in *Steneosaurus bollensis*.

The supratemporal fenestra (STF) length (D) is in average 15.6% of the skull length (A). In the juvenile specimen UH 2, the supratemporal fenestra length is 15.2% of the skull length, and in the adult specimens, it is 15.4% (UH 1) and 16.5% (SMNS 9930).

The posterior large extension of the squamosal and quadrate in the adult specimens SMNS 9930 and UH 1 and the small expansion of these bones in the juvenile specimen (UH 2) cause the change in the outline of the posterior margin of the skull, like in *S. bollensis* (Fig. 4.5).

Isometric growth is supposed for the skull width (C) compared to the skull length as it is observed in *S. bollensis*. However, the number of *Platysuchus multiscrobiculatus* specimens is too small to confirm this fact. The skull width (C) is in average 27.6% of the skull length (A) (Diagram 2).

In the postcranial, the percentage of the humerus length (H1) at the skull length (A) is in average 27.17% (Diagram 14). In the juvenile specimen UH 2, the humerus is 23.5 % of the skull length (A), while it is 30.8% and 27.2% in the adult specimens.

The femur length (Fe1) is in average 37.7% of the skull length (A) (Diagram 15). In the juvenile specimen, the femur length (Fe1) is 32.6% of the skull length (A), while in the adult specimen the femur length (Fe1) is 45.1% and 37.6%. Therefore, positive allometric growth is supposed for the humerus as well as for the femur of *Platysuchus multiscrobiculatus* as it is observed in *Steneosaurus bollensis*.

The humerus length (H1) is in average 70.1% of the femur length (Fe1), and varies from 67.5% to 72.5% (Diagram 13). However, the ratio of humerus length (H1) to femur length (Fe1) shows no significant difference between the juvenile and the adult stage. Both stages show here a humerus length (H1) about 72% of the femur length (Fe1) (Diagram 13).

In contrast, the tibia length (T1) decreases in comparison with the femur length (Fe1) during growth and is up to 74% in the juvenile specimen UH 2 and only 61% in adult specimens (Diagram 16).

Additional morphological differences between juvenile and adult specimens are the ornamentation of the cranial bones and the less ossification of the vertebrae.

In comparison with the adult specimens, the juvenile *Platysuchus multiscrobiculatus* (UH 2) shows partially differences in its ornamentation of the cranial bones (Fig. 4.8). The ornamentation is less distinctive in the juvenile specimen, and consists of shallow pits and grooves instead of deep round pits like in the adults (see chapter 3.4, Fig. 3.26). In the juvenile specimen, ornamentation is only found on the frontal, parietal, squamosal, prefrontal, and lacrimal. The postorbital is smooth and does not bear a pattern of pits in contrast to the ornamented postorbitals of the two adult specimens (Fig. 4.8)

Separated neural arches from the vertebrae centra are visible in the juvenile specimen UH 2 in the sacral region and at the cervical vertebrae. This is similar to the conditions of

juvenile *Steneosaurus bollensis* specimens (e.g., GPIT Re 1193/6, see paragraph 4.2.4, and Fig. 4.7).

In contrast to the observed ontogenetic differences in the ornamentation of the cranial bones, the ornamentation of the osteoderms is strikingly similar in all *Platysuchus multiscrobiculatus* specimens independent of their size. Both the juvenile specimen UH 2 (as well as SMNS 15391) and the adult specimens (SMNS 9930, UH 1) show a prominent keel on all dorsal osteoderms lying posteriorly to the 7th osteoderm; as well as a dense regular distribution of small round pits on the external surface of the osteoderms. Therefore, it is assumed that at least the development of a keel is independent from growth, because it is steadily observed in all ontogenetic stages (Fig. 4.4).

4.2.7 Intraspecific variation in *Pelagosaurus typus*

For this investigation, in total 80 specimens of *Pelagosaurus typus* were studied (see appendix I). *P. typus* reaches a total body length (TL) of maximum two meters. Juvenile specimens are defined as specimens with a skull length (A) less than 250 mm (see appendix II). The analysis of the juvenile characters of *Pelagosaurus typus* is mainly based on the investigation of four certain juvenile specimens: SMNS 17758, SMNS 4554, UH 8 (Fig. 4.9), and GPIT RE 214, all with a skull length less than 150 mm. Furthermore, two personally studied specimens (UH 9 & GPIT Re 1193/17) with a skull length of 250 mm and the description by DUFFIN (1979a) of a juvenile *Pelagosaurus typus* specimen from England (M 1418a) were considered.

One of the smallest known specimens of *Pelagosaurus typus* is the specimen UH 8, with a skull length of 134 mm. The largest known individual of *Pelagosaurus typus* (UH 4) possesses a skull length of 380 mm (see appendix II). Interestingly, even though adult specimens of *P. typus* are much smaller than adult *Steneosaurus bollensis* or *Platysuchus multiscrobiculatus* specimens, the smallest known individuals of each taxon are almost of the same size.

Growth independent variations are similar to the described changes in *S. bollensis*. In *Pelagosaurus typus* the number of ribs varies from 12-15 and the number of thoracic (including lumbar) vertebrae from 16-18. The number of teeth varies in the premaxilla from three to four, in the maxilla from 25-32, and in the dentary from 30-32 (see chapter 3.5).

The pronounced ornamentation of the cranial bones (see chapter 3.5 and Fig. 4.9) is almost unaffected by individual variation and only minor differences are observed, which are most likely a result of preservation or preparation conditions. The same is true for the dermal

armour (Fig. 4.4). Only minor differences are visible in shape and ornamentation of the osteoderms considering their position in the osteodermal shield.

Furthermore, scleral rings in the orbit are only noticed in a few specimens of *P. typus* (e.g. BSGP 1925 I 34, FSL 530238, UH 4). The lack of scleral rings in the other specimens is probably caused by individual preservation and preparation conditions (see chapter 3.5 and 5). It is assumed that scleral rings have existed in all specimens.

In the lower jaw the length of the retroarticular process (X) is steadily 10% of the skull length (A), with a single exception in specimen NHMUS M62 2516, were X is only 6.3% of the skull length (Diagram 10). Too few data is available to provide any suggestion about the allometric growth rate. The symphysis angle in the lower jaw varies from 28°-30° in *Pelagosaurus typus*.

Ontogenetic variation in *Pelagosaurus typus* is, in its general appearance, similar to *Steneosaurus bollensis* and *Platysuchus multiscrobiculatus* and differs mainly in the proportion of the particular values (see 4.2.4 & 4.2.7).

The percentage of the skull length (A) is in the adult specimens 69% to 90% of the shoulder-pelvic distance (S-PL). The only completely preserved juvenile specimen UH 8 shows 95% skull length of the SP-L (Diagram 1 & Table 1). The relation of skull length (A) to shoulder-pelvic distance (SP-L) is highly individually variable and the number of measurements available is too small for a certain statement. Nevertheless, the calculation of the logarithms values indicates a negative allometric growth rate.

Specimen of *P. typus*	**Skull length (A)**	**Shoulder-pelvic distance (S-PL)**	**A/S-PL%**
UH 8	134	140	95,7142857
TMH 2744	270	380	71,0526316
NHMUS M62 2516	275	400	68,75
MNHN 1883-14	285	400	71,25
UH 4	380	420	90,4761905

Table 1: Percentage of the skull length (A) at the length of the shoulder girdle - pelvic girdle distance (S-PL).

A negative allometric growth rate is supposed for the skull width (C), the rostrum length (B), the orbital length (I), and the supratemporal fenestra length (D), too.

The skull width (C) of *P. typus* is 18%-23% of the skull length (A). In juveniles the average is 22.8% and in adults 21.9%. A slight negative allometric growth rate is calculated, which is close to an isometric development.

The rostral length (B) is 70% to 76% of the skull length (A). The average is 74.4%, which is only slightly larger than in *S. bollensis*. The rostrum has a linear development and shows a negative allometric growth rate.

In juvenile specimens, the orbital length (I) has an average of 11.5% of the skull length (A), while it is an average 9.5% in adult specimens. However, the ratio of orbital length (I) to skull length (A) varies growth independently, too. For example, in the semi adult holotype of *Pelagosaurus typus* TMH 2744 (skull length 270 mm), the orbital length is still 11.1% and in the largest know specimen UH 4 (skull length 380 mm), the orbital length is with 10.8% of the skull length relatively large compared to other adult specimens. Therefore, the ontogenetic variation of the orbital length (I) relative to the skull length (A) is sometimes superimposed by the individual, growth independent variation. However, this could be also a sign of heterochrony in *Pelagosaurus typus*.

Growth related development of the orbital length (I) is more obvious compared to the supratemporal fenestra length (D). In juvenile specimens, the orbit can be up to the same size of the supratemporal fenestra (100%) (Fig. 4.9), in adult specimens, the orbital length (I) reaches maximal 77% of the supratemporal fenestra length (D).

The supratemporal fenestra length (D) is in average 13.4% of the skull length (A). In juveniles, the average is 13.4% (deviation 0.9%) and in adults, 13.5% (deviation 1.4%), but the calculated logarithms show a slight negative allometric growth for the supratemporal fenestra.

Interestingly enough, the orbit and supratemporal fenestra shape do not change much during development in *Pelagosaurus typus* as it does in *Steneosaurus bollensis* and *Platysuchus multiscrobiculatus*. Both the orbit and the supratemporal fenestra stay ellipsoid, whereas the frontal shape changes from rhombic to triangular in *P. typus* similar to the conditions described for *S. bollensis* and *Platysuchus multiscrobiculatus* (see paragraphs 4.2.4, 4.2.7, and Fig. 4.5).

The posterior outline of the skull is changing as well. The posterior enlargement of the quadrates and squamosals increases during ontogeny and indicate a positive allometric growth rate like described in *S. bollensis* (see paragraph 4.2.4, Fig. 4.5).

Positive allometric growth is also assumed for the development of the premaxilla enlargement in *P. typus*. The premaxillae is less enlarged in *Pelagosaurus typus* as it is in

Steneosaurus bollensis, until a skull length of 300 mm. The absolute values in Diagram 5 (not logarithms) show an increase of premaxillae enlargement (K/L) in ratio to the skull length (A).

In the postcranial, the humerus length (H1) is in average 15% of the skull length (A) in juveniles and 18 % in adults. The humerus length (H1) shows a positive allometric growth rate in *P. typus* like it does in *S. bollensis*.

In the juvenile specimen UH 8, the femur length (Fe1) is 25.6% of the skull length (A), whereas the femur length has an average 32.6% in the adults. The femur length (Fe1) shows in *P. typus* a positive allometric growth rate, too.

The ratio of humerus length (H1) to femur length (Fe1) is 51% in UH 8 (juvenile specimen) and up to 61.7% in adults (Diagram 13 & 17).

The ratio of tibia length (T1) to femur length (Fe1) changes only slightly during growth in the juvenile specimen SMNS 17758 it is 58.3% and in the adult specimens it varies from 51.5% (NHMUS M62 2516) to 60% (MNHN 1883-14). Therefore, the individual variation is higher than the growth change (Diagram 16). The average of the tibia length (T1) is 57.3% of the femur length (Fe1) in adult specimens.

Open neurocentral sutures at the presacral vertebrae, respectively separated vertebra centra from the neural arches are visible in juvenile specimens of *Pelagosaurus typus*, too (e.g. SMNS 17758).

4.3 Special pathological and preservational features

Individual variation can be caused as well by pathological changes and particularly in the case of fossils, different preservation conditions can influence the individual appearance. Pathological changes in fossil specimens mean mainly inborn malformation, injuries, or illness, which causes changes in the bone structure.

From some extant crocodilians species (e.g. *Crocodylus porosus*, *Caiman crocodilus*, *Crocodylus vulgaris, Paleosuchus niloticus, Caimain latirostis*, *Melanosuchus niger*, and *Alligator mississipiensis*) a couple of pathological features are described, which influences the appearance of the skeleton (KÄLIN 1937). Kälin (1937) mentions deformation on the skeleton by e.g., brachychephaly (abnormally short broad skull), healed fractures, and partly regenerated tails.

Personally, a juvenile skull of *Gavialis gangeticus* (skull length 196 mm, lower jaw length 333 mm) with a pathological shortened upper jaw was investigated (SMF 1914/28131) (Fig. 4.10). The upper jaw lacks anteriorly about 50% of its length and no premaxillae are preserved. Nevertheless, the upper jaw shows a slight enlargement at the anterior margin

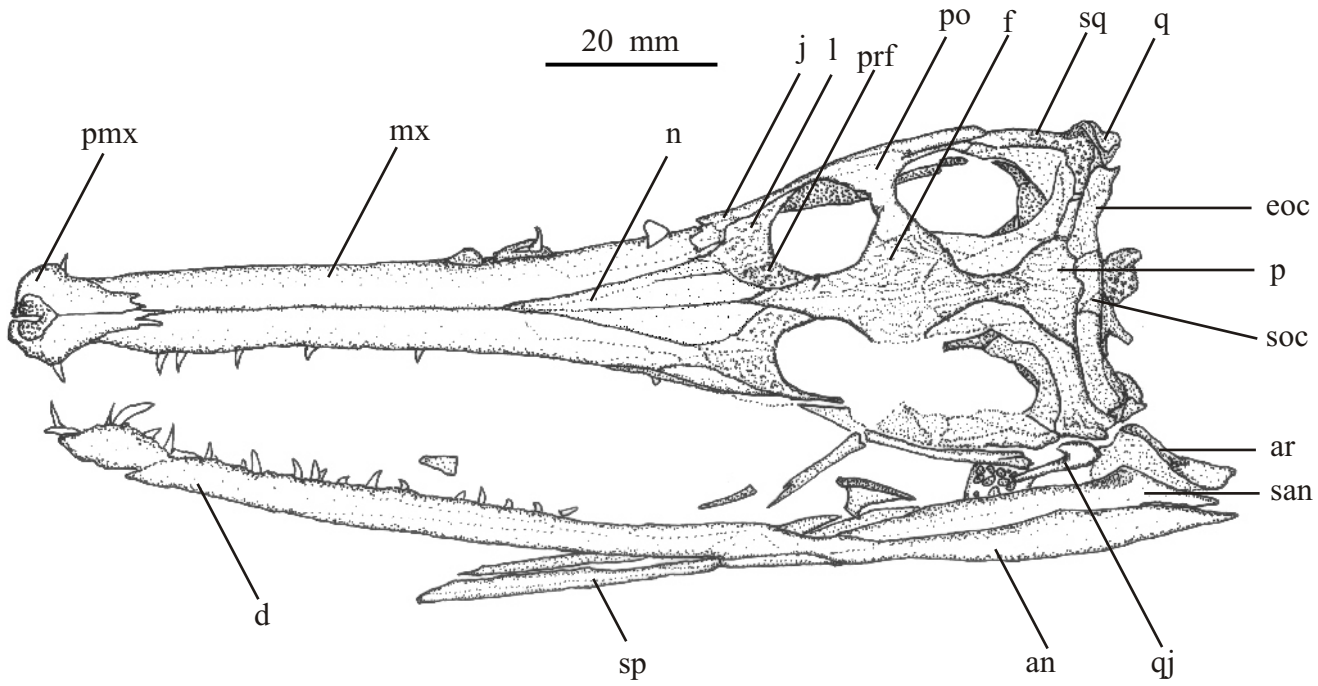

Figure 4.8: *In situ* drawing of a juvenile *Platysuchus multiscrobiculatus* specimen (UH 2). The skull is shown in dorsal view, with the left branch of the lower jaw in lateral view. Skull length is 132 mm in the original. Scale bar is 20 mm. Abbreviations see figure 4.1 and **ar**: articular; **an**: angular; **d**: dental; **san**: surangular; **sp**: splenial.

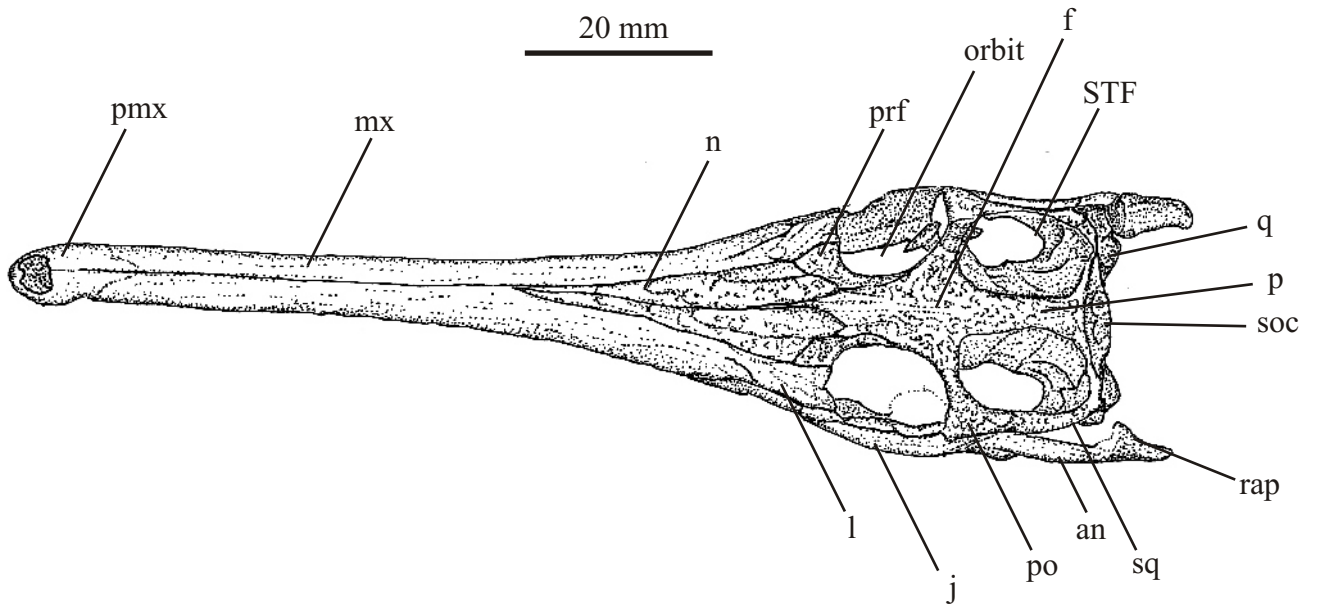

Figure 4.9: *In situ* drawing of a juvenile *Pelagosaurus typus* specimen (UH 8). The skull is shown in dorsal view. Skull length is 134 mm in the original. Scale bar is 20 mm. Abbreviations see Fig. 4.1. Characteristic juvenile features are the large orbits and the broad area between the STF's. Heavy ornamentation is visible on the surface of n, prf, p, po, and sq, less distinctive also on l, and j.

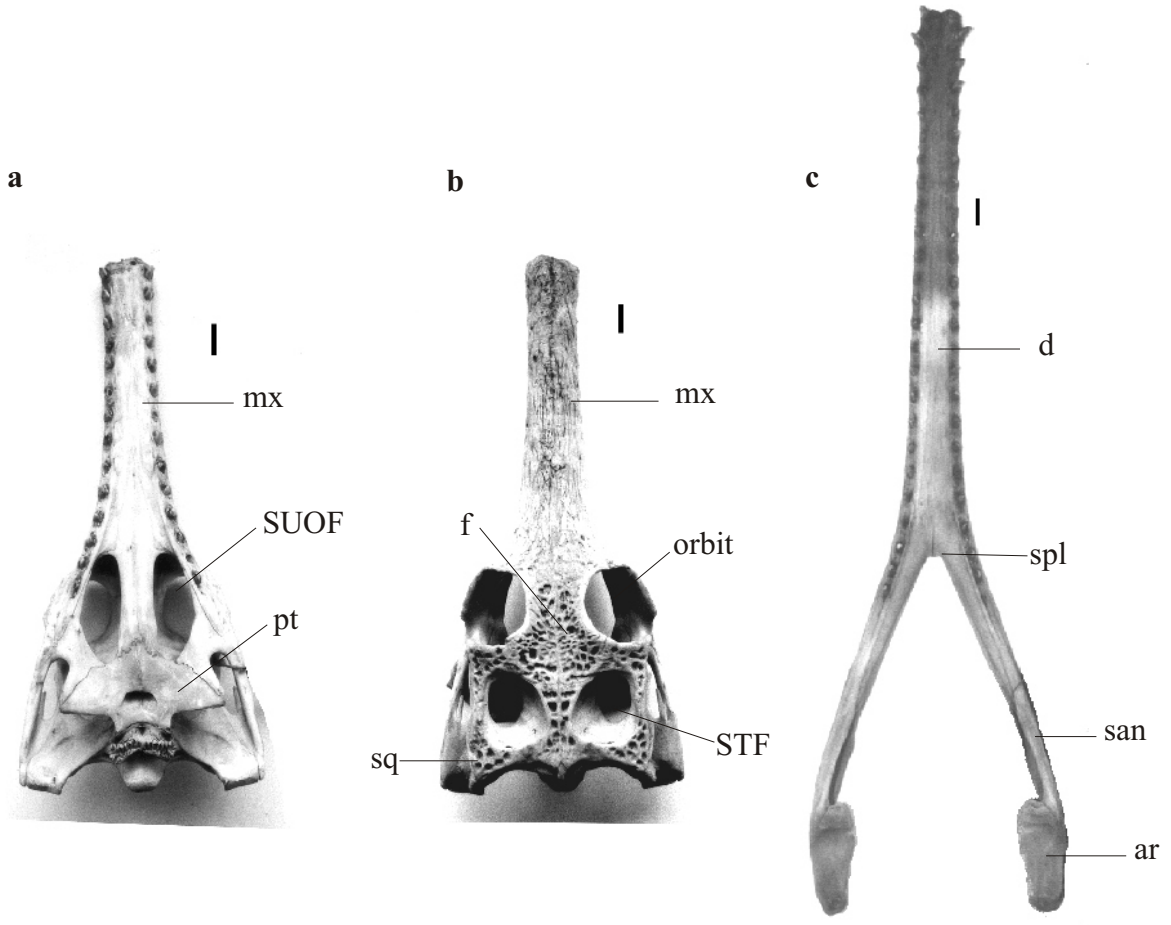

Figure 4.10a-c: Skull of a juvenile *Gavialis gangeticus* (SMF 1914). Scale bar 10 mm. **4.10a**-Skull in ventral view, **4.10b**-Skull in dorsal view, **4.10c**-Lower jaw in dorsal view. The skull length is 196 mm, the lower jaw length is 333 mm. A pathological change of frontal-nasal suture is observed, the pemaxillae are missing. Anteriory, the maxilla is slightly enlarged and shows additional bone material. The lower jaw is normally developed. Abbreviations: ar-articular, d-dentary, f-frontal, mx-maxilla, san-surangular, spl-splenial, STF-supratemporal fenestra, SUOF-suborbital fenestra, sq-squamosal.

formed by the maxilla, which indicates that the bone healed here; therefore, the deformation was not immediately deadly for the animal (Fig. 4.10a, b). It is uncertain whether this defect is a result of an inherent deformation, or whether it was caused by a later injury. The mandible of the specimen is normally developed (Fig. 4.10 c). Such major pathological changes at the skull cannot be reported for *Steneosaurus bollensis*, *Platysuchus multiscrobiculatus*, or *Pelagosaurus typus*. However, some *Steneosaurus bollensis* specimens show deformation at the rostrum that could be a result of former injuries, but the observed breaks could also be a result of diagenetic deformation (Fig. 3.3). In addition, the *Steneosaurus bollensis* specimen SMNS 51555 shows some regenerated caudal vertebrae (BUFFETAUT 1985).

Furthermore, an extraordinary observation is made at the fore limb of a juvenile specimen of *Pelagosaurus typus* as well as in one cf *S. bollensis* specimen. Here the manus only consist of four digits instead of five (UH 8, TMH 13288). Unfortunately, it is indeterminably, whether this is a general intraspecific variation, a pathological feature, or perhaps a result of preservation or preparation conditions. The fifth digit just seems to be totally missing, while the other four digits remain the same as usual. However, this was never observed in an adult specimen, which suggests the possibility of an incomplete preservation of the delicate manus of the juveniles.

A clearly preservational feature is the in some cases visible petrified tracheal rings in *Steneosaurus bollensis*, *Platysuchus multiscrobiculatus*, and *Pelagosaurus typus* (see chapter 3). The appearance of petrified tracheal rings depends most likely mainly on the preservation conditions of the specimens. Another main factor could be the body size (i.e. the age) of the individual. Petrified tracheal rings are only observed in specimens with a total body length larger than 1.7 m (see chapter 3). Nevertheless, they are not observed in every specimens of this size.

The following 17 diagrams show inter- and intraspecific variation of different Thalattosuchia. For further explanations, see chapter 4 and chapter 5.

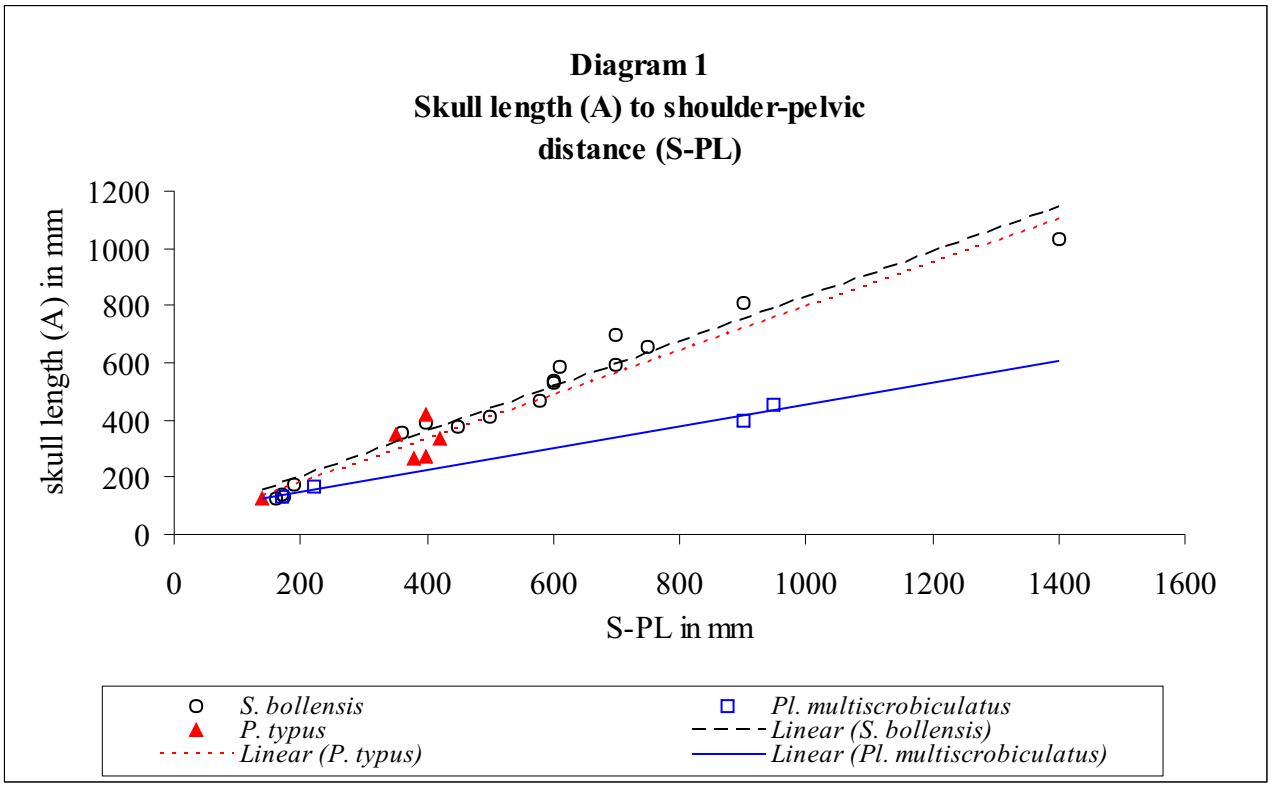

Diagram 1: The diagram shows the ratio of the skull length (A) to the shoulder-pelvic distance (S-PL) in absolute values, to make the differences between the three taxa more apparent for the eye. The skull of *S. bollensis* shows a larger ratio in adult age as *Platysuchus multiscrobiculatus* does.

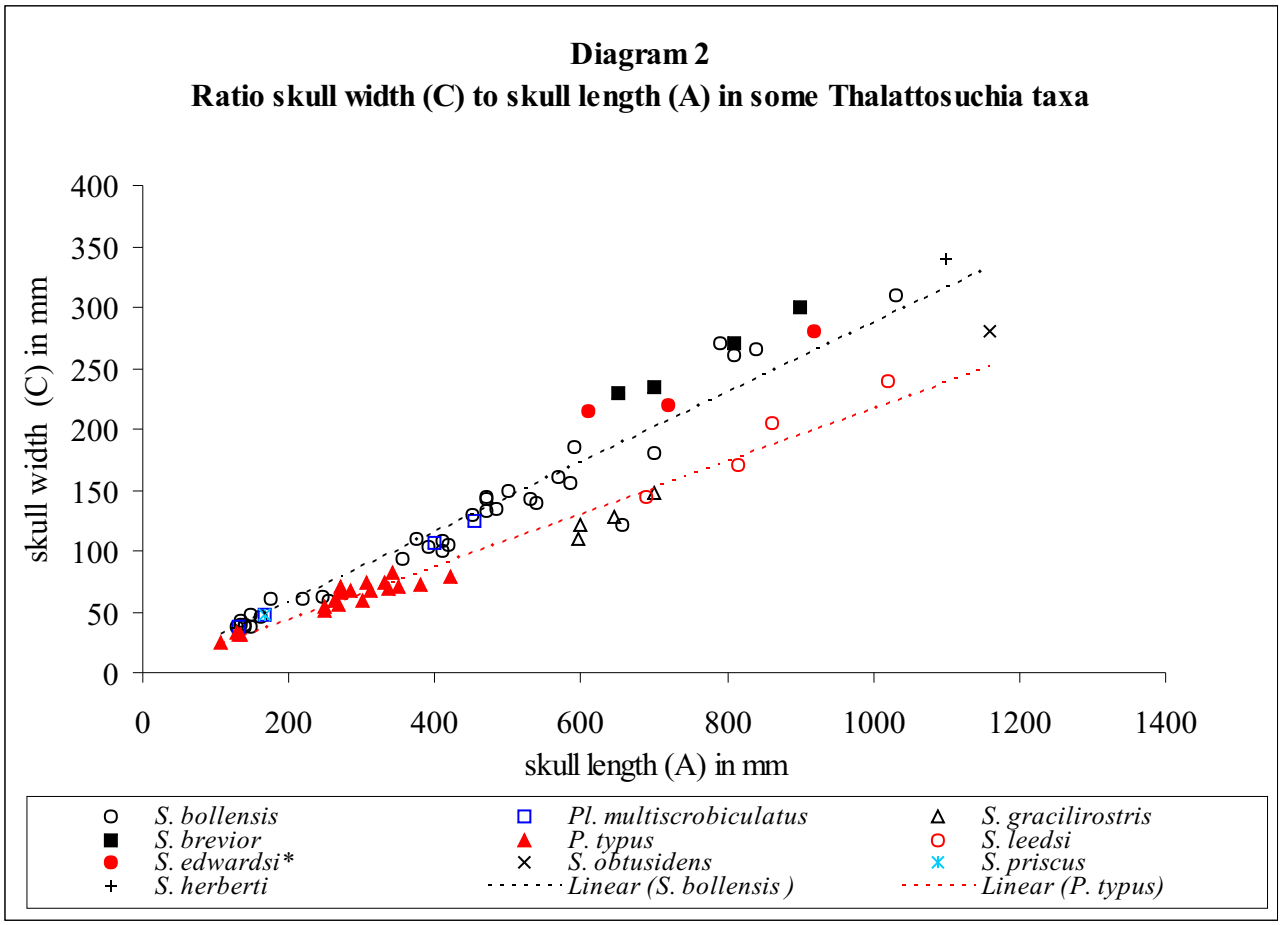

Diagram 2: Comparisons of the values for 10 Thalattosuchia taxa show basically two lines. The ratios for *S. bollensis*, *S. brevior*, *Platysuchus multiscrobiculatus*, *S. edwardsi* and *S. heberti* all show the same linear development with flat, relatively broad skulls. The ratios for *Pelagosaurus typus*, *S. gracilirostris* and *S. leedsi* show linear development, too, but differ from the other taxa by having a much narrower skull.

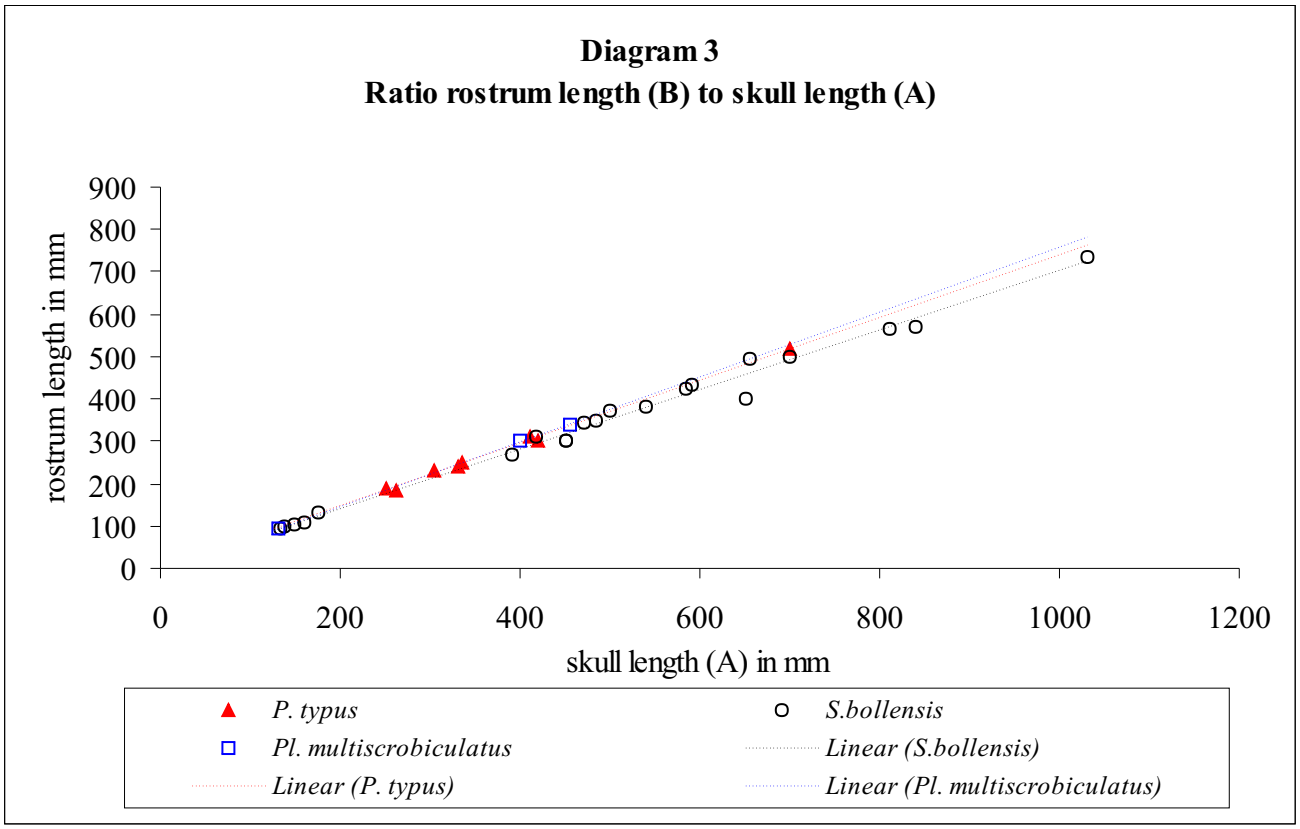

Diagram 3: The rostral length (B) shows a linear development compared to the skull length (A). All taxa show very similar ratios. It is therefore almost impossible to distinguish the taxa from each other because of the rostral length. All values lie within the scattering range.

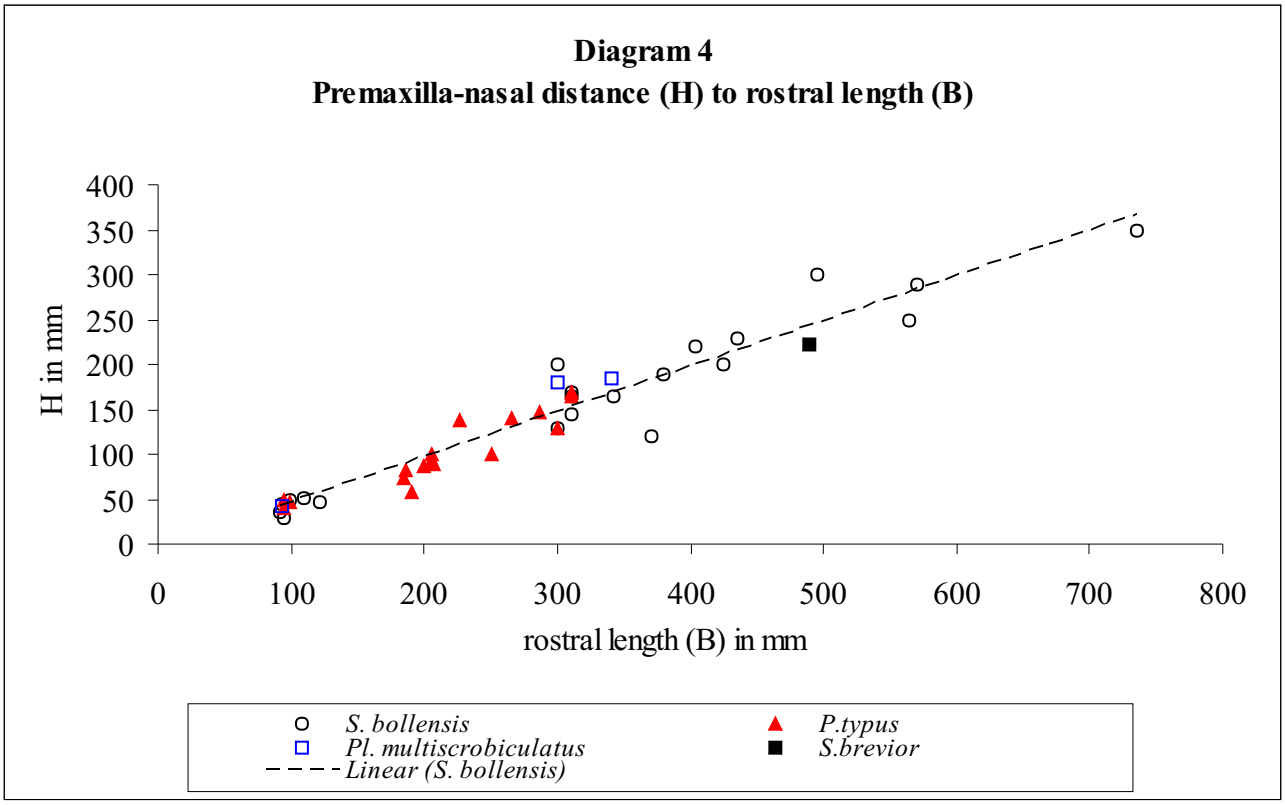

Diagram 4: The values indicate a linear development of the premaxilla-nasal distance (H) compared to the rostral length (B) of the four studied taxa. The differences between the taxa are minor and provide only little information for taxa differentiation.

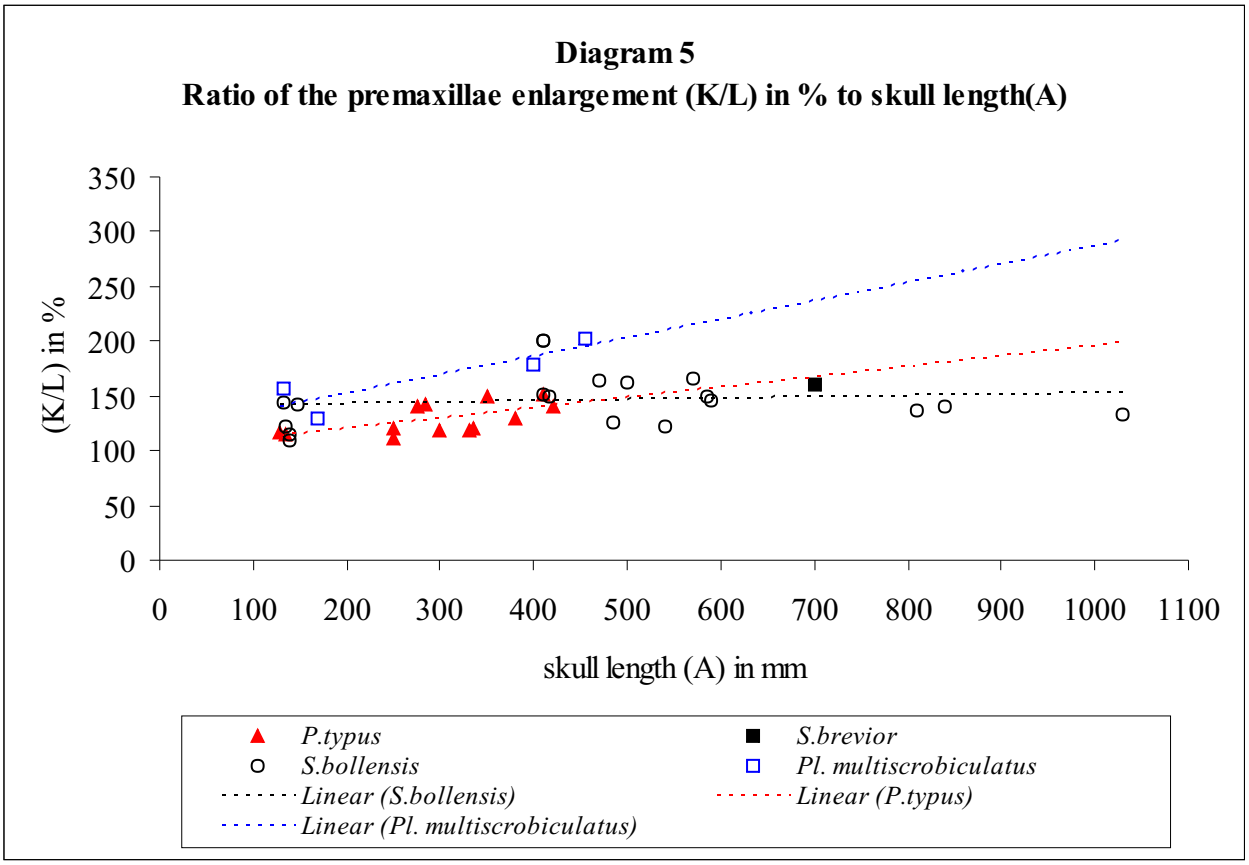

Diagram 5: The degree of the enlargement of the premaxillae (K/L) is relatively independent from the skull length (A) in *S. bollensis.* In contrast, the values of *Pelagosaurus typus* and *Platysuchus multiscrobiculatus* show a trend of increasing premaxillae enlargement during development. However, the values show a high intraspecific variation during the entire ontogenetic development in all taxa. The percentage of the premaxilla width (K) at the narrowing of the premaxillae (L) reflects the enlargement of the premaxillae. 200% reflects broad enlargement, while 100% reflects no enlargement of the premaxillae.

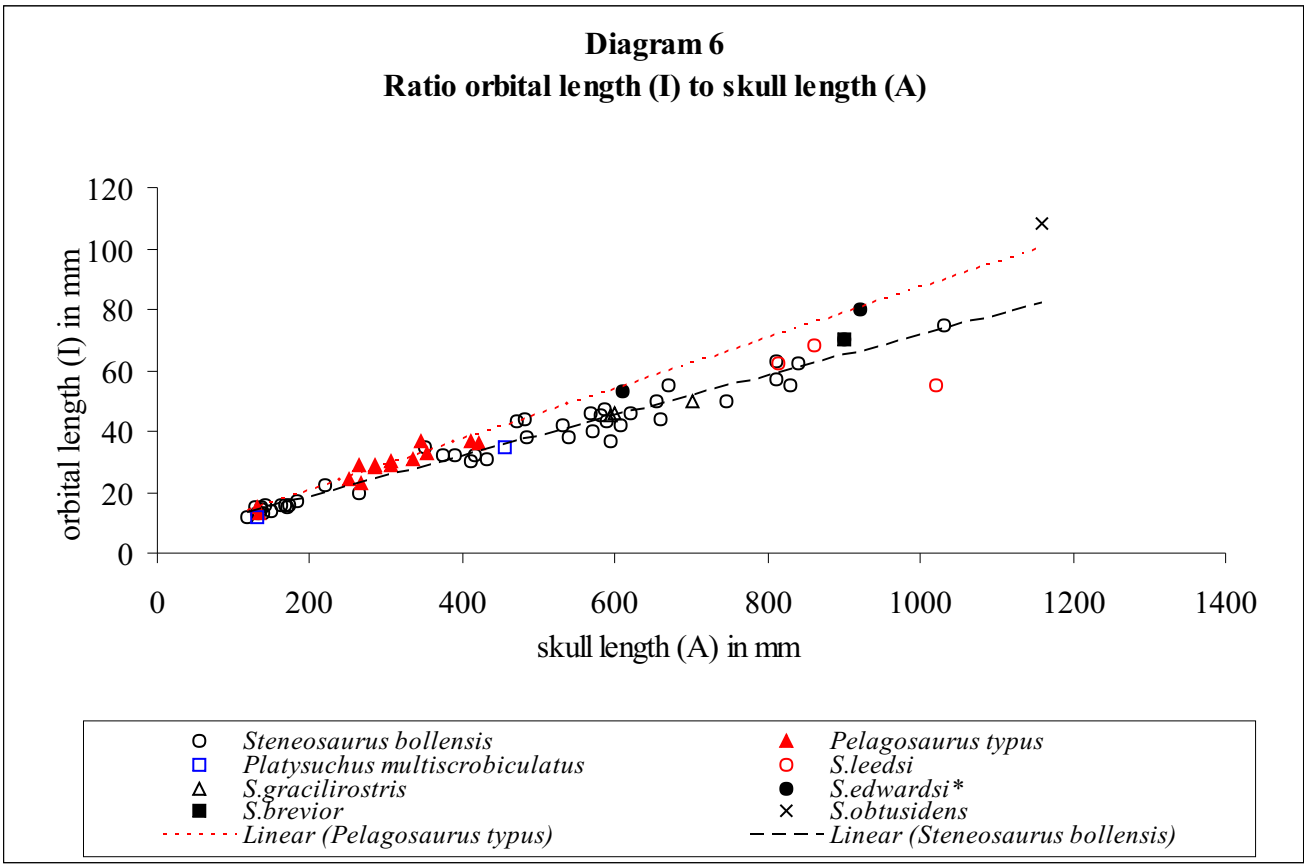

Diagram 6: All eight studied taxa show a linear development of the orbital length (I) compared to the skull length (A). While *S. bollensis* and *Platysuchus multiscrobiculatus* cannot be distinguished by this ratio, the orbital length in *P. typus* is slightly higher. The juvenile specimens, all show very similar ratios independent of their species. The scattering of the values for the orbital length (I), increase with increasing skull length (A). In particular, in *S. bollensis* specimens, which have a skull length of over 500 mm, the values show high scattering. This could indicate possible sexual dimorphism.

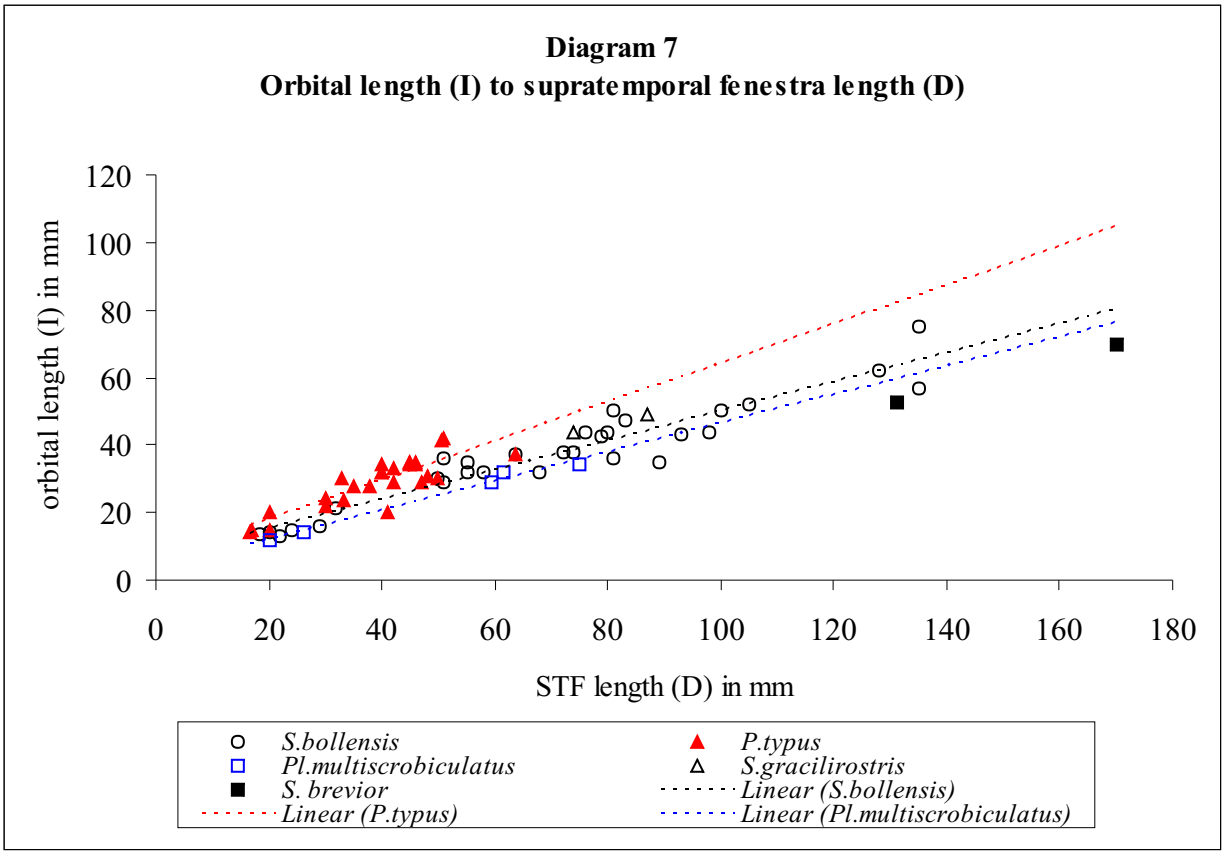

Diagram 7: All five studied taxa show a linear development of the orbital length (I) compared to the supratemporal fenestra length (D). However, in *Pelagosaurus typus* the orbital length in ratio to the supratemporal fenestra length is larger than in *Steneosaurus bollensis* and *Platysuchus multiscrobiculatus*. The latter two are similar in their ratios and cannot be distinguished by these values. The values of *S. bollensis* shows again a quite high scattering with increasing size, and the values of *S. gracilirostris* lie within scatter range.

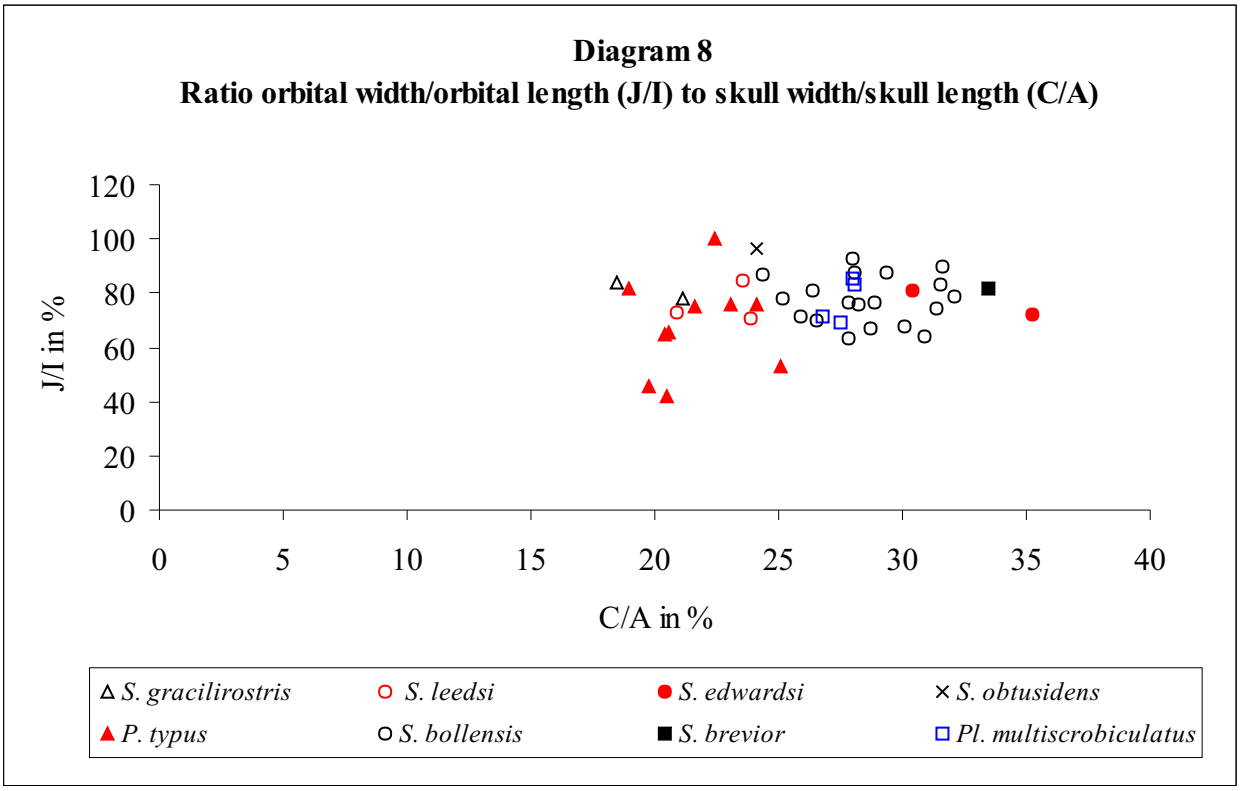

Diagram 8: The shape of the orbit is expressed by the ratio of the orbital width (J) to the orbital length (I) in percent. An orbital width of 100-80% of the orbital length indicates circular orbits, which is the case in most juvenile specimens. A smaller percentage share indicates elliptic orbits, which is usually the case in adult specimens of the eight investigated taxa. The orbit shape is strongly ellipsoid in adult *P. typus.* The value (red triangle), which show a narrow skull (C/A= 22%) with circular orbits (J/I=100%), are reflecting a juvenile *P. typus* specimen. The biometric values e.g., of *P. typus* and *S. bollensis* differ most obviously in the width of the skull relatively to the skull length (C/A in % > 24% in *S. bollensis*), but also in the shape of the orbit. *S. gracilirostris* and *S. leedsi* show similar orbit shape to *S. bollensis*, but have a much narrower skull, which place them here in one group together with *P. typus*. In contrast, the skull width of *S. brevior* is very high (C/A~34%) but the orbits are relatively circular (~ 80%). This is, particularly interesting, because the *S. brevior* specimen is an adult specimen and do not represent a juvenile of *S. bollensis* like the other values in the area.

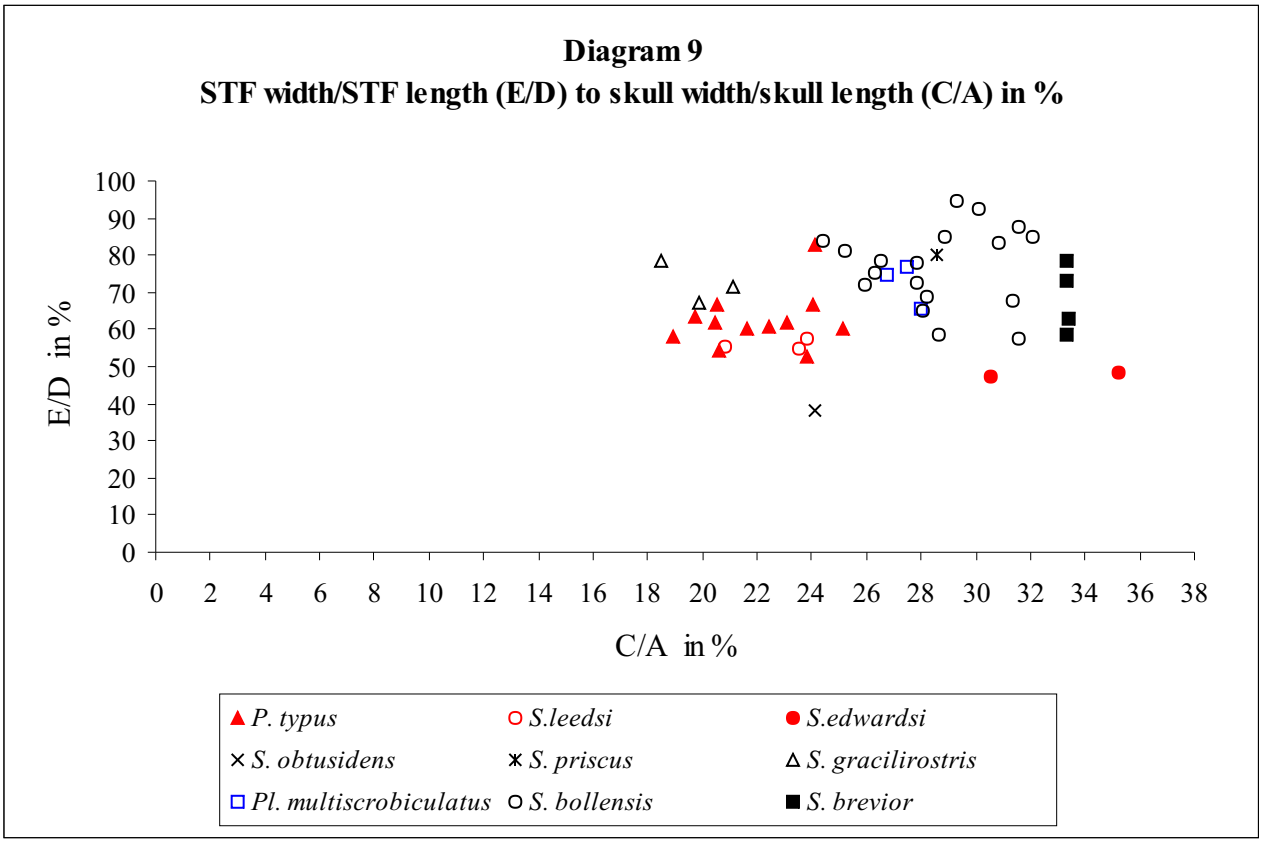

Diagram 9: The ratio E/D characterise the shape of the STF in ratio to the skull width (C) to skull length (A) in percent. As previously explained for the orbit, the ratio of STF width (E) to STF length (D) in percent, indicates a square (80-100%) or more elongated (79-45%) shape of the supratemporal fenestra, whereas the difference between ellipsoid and square shape is not visible in this diagram. *P. typus* ((E/D)% = 50-70%) is clearly distinguished from *S. bollensis* (60-95%). Considering the skull length (A) and the percentage share at the skull width of the skull length (C/A in %), the separation between these taxa becomes more clearly. C/A is between 18% and 24% in *P. typus*, while in *S. bollensis* the value is between 26 and 32%, which indicates broader skulls is *S. bollensis*. Furthermore, the diagram shows that the Upper Jurassic taxa *S. edwardsi* and *S. obtusidens* have more elongated supratemporal fenestrae than the Lower Jurassic taxa.

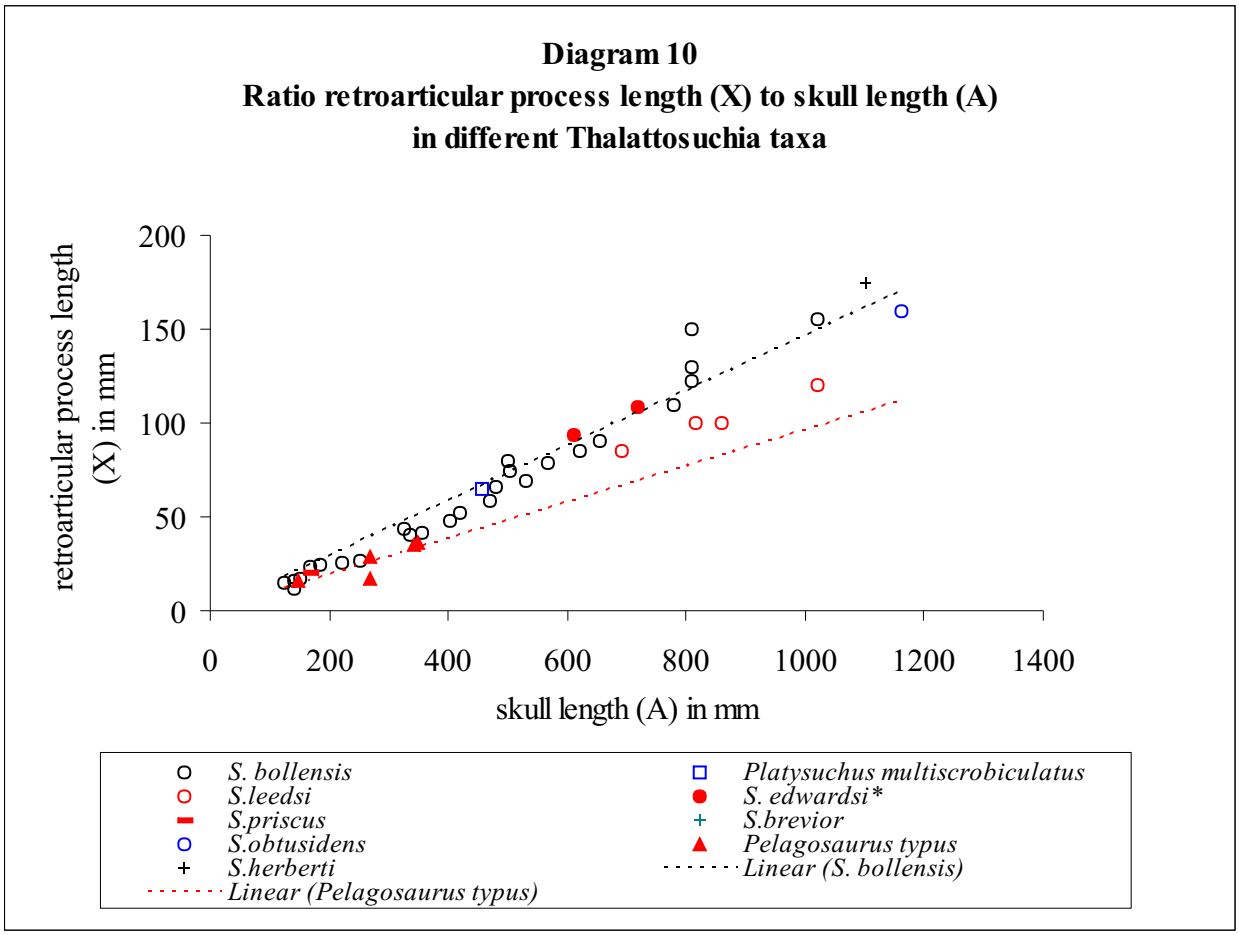

Diagram 10: The ratio of the retroarticular process length (X) to the skull length (A) of nine different Thalattosuchia taxa is shown. Most obviously, *Pelagosaurus typus* possesses a much shorter retroarticular process than the other described Thalattosuchia taxa. However, all other taxa show the same linear development in the length of the retroarticular process, but the scattering of the values is particular high in the larger specimens of *S. bollensis* with a skull length of more than 750 mm. Sexual dimorphism could be a possible explanation, but cannot be confirmed with the existing data at the moment.

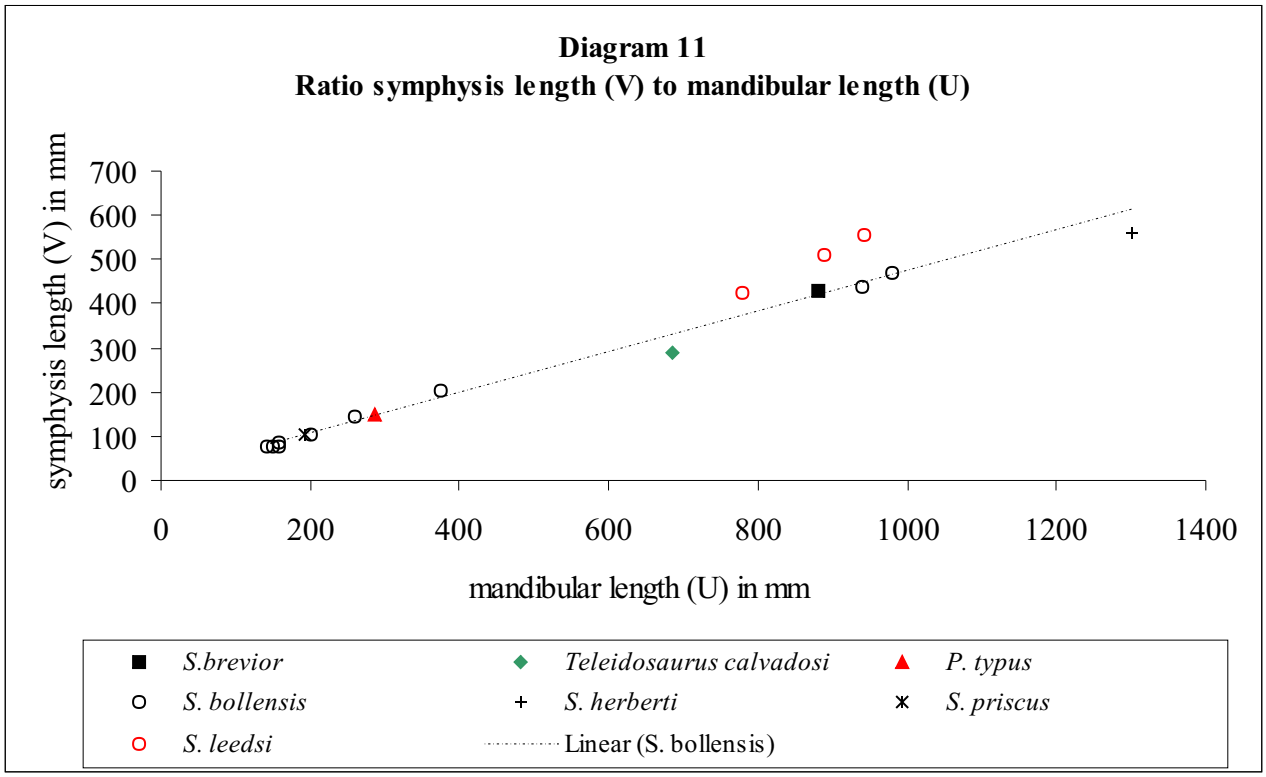

Diagram 11: A comparison of seven Thalattosuchia taxa is shown, regarding the length ratio of the symphysis to the lower jaw. Only few data of each taxon were available. They indicate a linear growth of the symphysis in comparison of the lower jaw. Interspecificly, *S. leedsi* and *S. heberti* show the biggest deviation from *S. bollensis*, but the metriorhynchid *Teleidosaurus calvadosi* shows a shorter symphysis than the teleosaurid taxa.

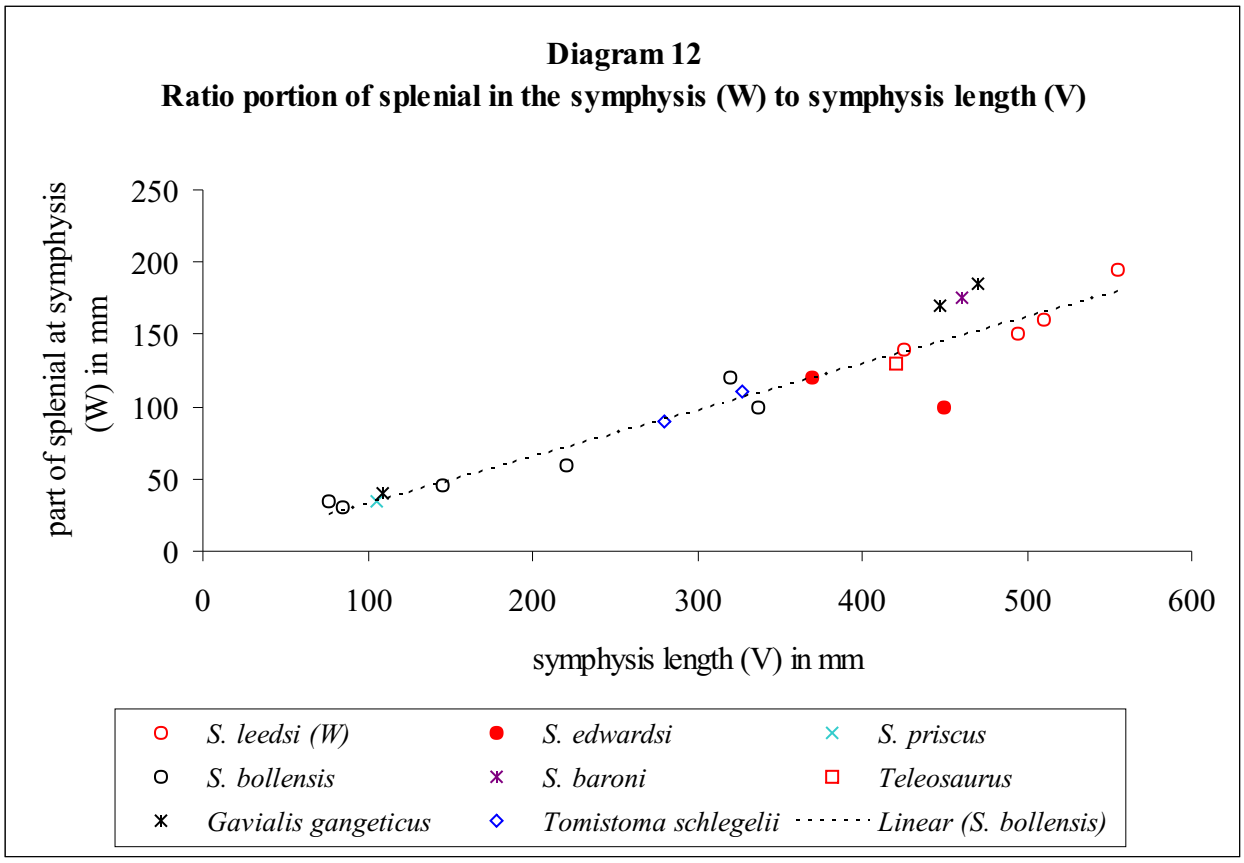

Diagram 12: Comparison of the ratio of the portion of the splenial (W) to the symphysis length (V) of six Thalattosuchia taxa and in addition, two extant long-snouted crocodilians *Gavialis gangeticus* and *Tomistoma schlegelii*. The extant taxon *Gavialis gangeticus* possesses a large splenial portion at the symphysis, whereas in the Upper Jurassic taxon *S. edwardsi,* the splenial has only a small portion at the symphysis length, compared to the ratios of *Steneosaurus bollensis.* A comparison of seven Thalattosuchia taxa is shown, regarding the length ratio of the symphysis to the lower jaw. Only few data of each taxon were available. They indicate a linear growth of the symphysis in comparison of the lower jaw. Interspecificly, *S. leedsi* and *S. heberti* show the biggest deviation from *S. bollensis*, but the metriorhynchid *Teleidosaurus calvadosi* shows a shorter symphysis than the teleosaurid taxa.

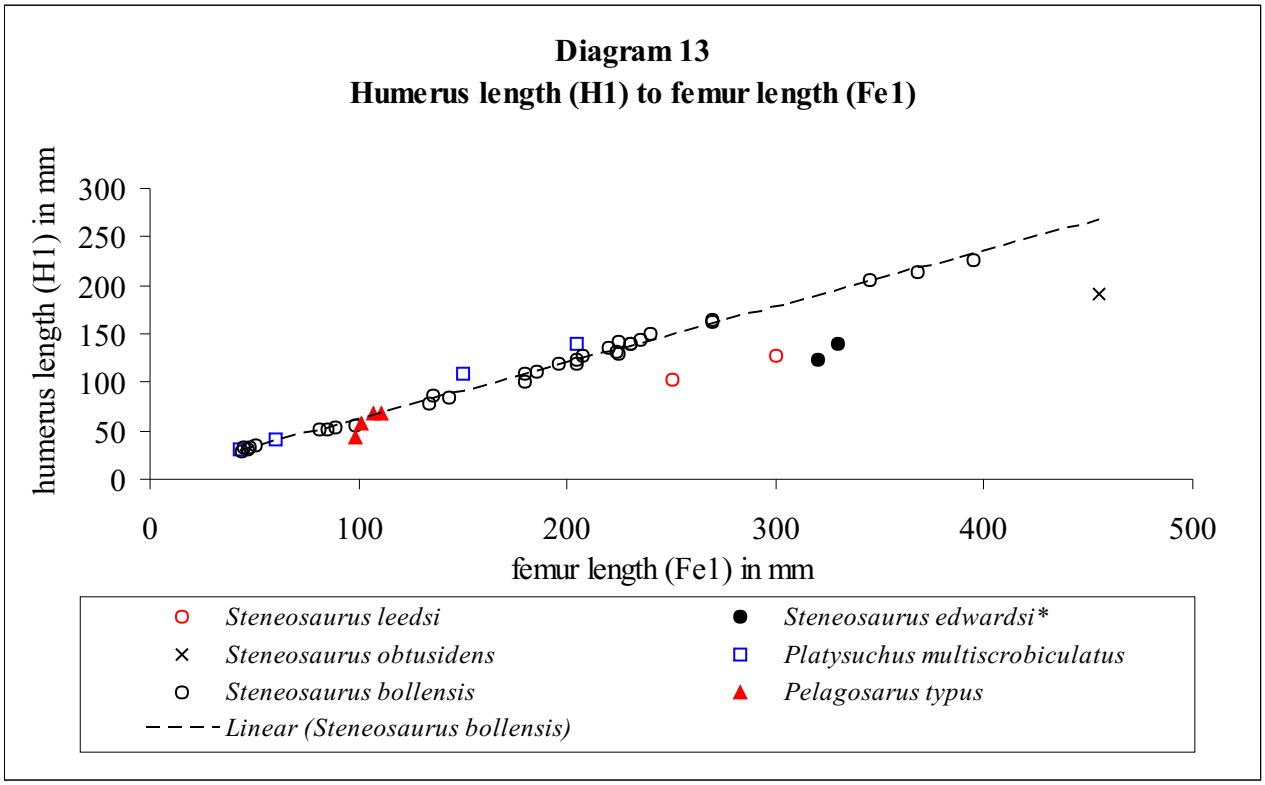

Diagram 13: The diagram shows the ratio of the humerus length (H1) to the femur length (Fe1) in six Thalattosuchia taxa. All taxa show a similar linear development of the humerus length in comparison to the femur length. However, the humerus of *Platysuchus multiscrobiculatus* is slightly larger compared to the humerus in *S. bollensis* at the same femur length. Interestingly, the Middle Jurassic taxa *S. leedsi* and *S. edwardsi* show a particular short humerus compared to *S. bollensis* at the same femur length.

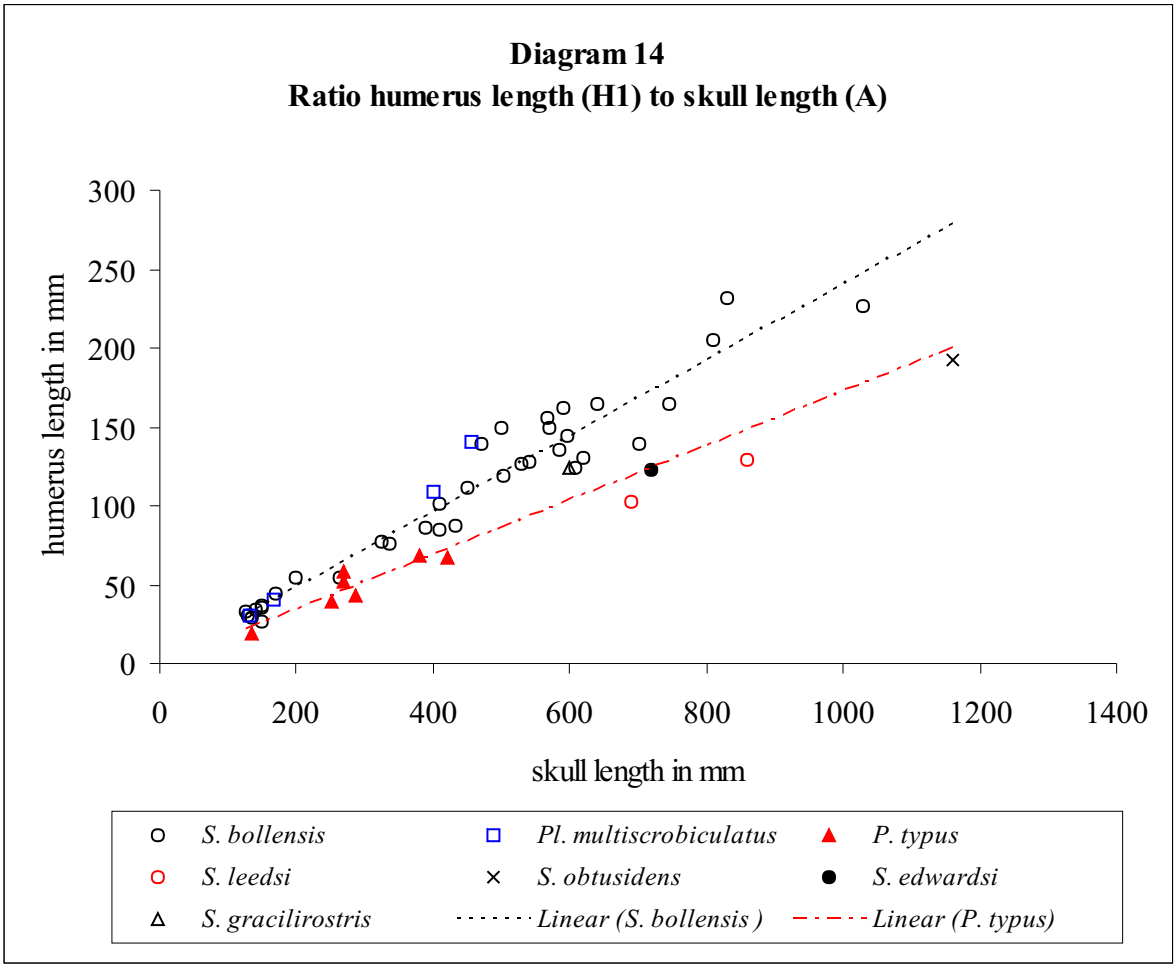

Diagram 14: The ratio of the humerus length (H1) to the skull length (A) of seven Thalattosuchia taxa is compared in this diagram. Again, *Pelagosaurus typus* is distinguished by its smaller humerus length in ratio to the skull length (A). Surprisingly, also the Middle and Upper Jurassic *Steneosaurus* taxa (*S. leedsi*, *S. obtusidens*, and *S. edwardsi*) show a small humerus compared with their skull length. Again, *S. bollensis* shows high scattering of the values in specimens with a skull length of over 600 mm. *Platysuchus multiscrobiculatus* possesses a relatively long humerus compared to the skull length, even though the values appear still within the scattering pattern of the values of *S. bollensis*.

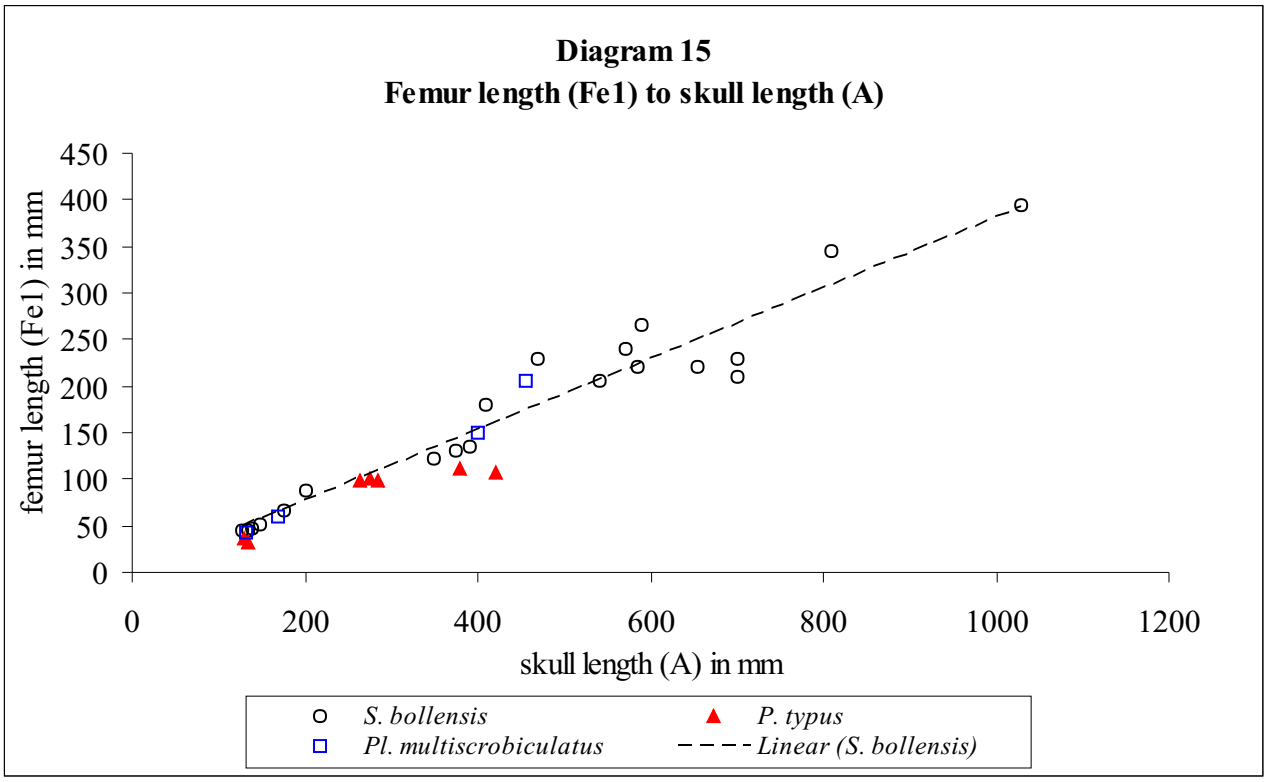

Diagram 15: The ratio of the femur length (Fe1) to the skull length (A) in three Liassic Thalattosuchia taxa are compared. In the larger specimens of *S. bollensis*, slight variations in the femur size are observed. The femur of *Pelagosaurus typus* stays smaller compared to the femur of *Steneosaurus bollensis* and *Platysuchus multiscrobiculatus.* For further explanations, see text.

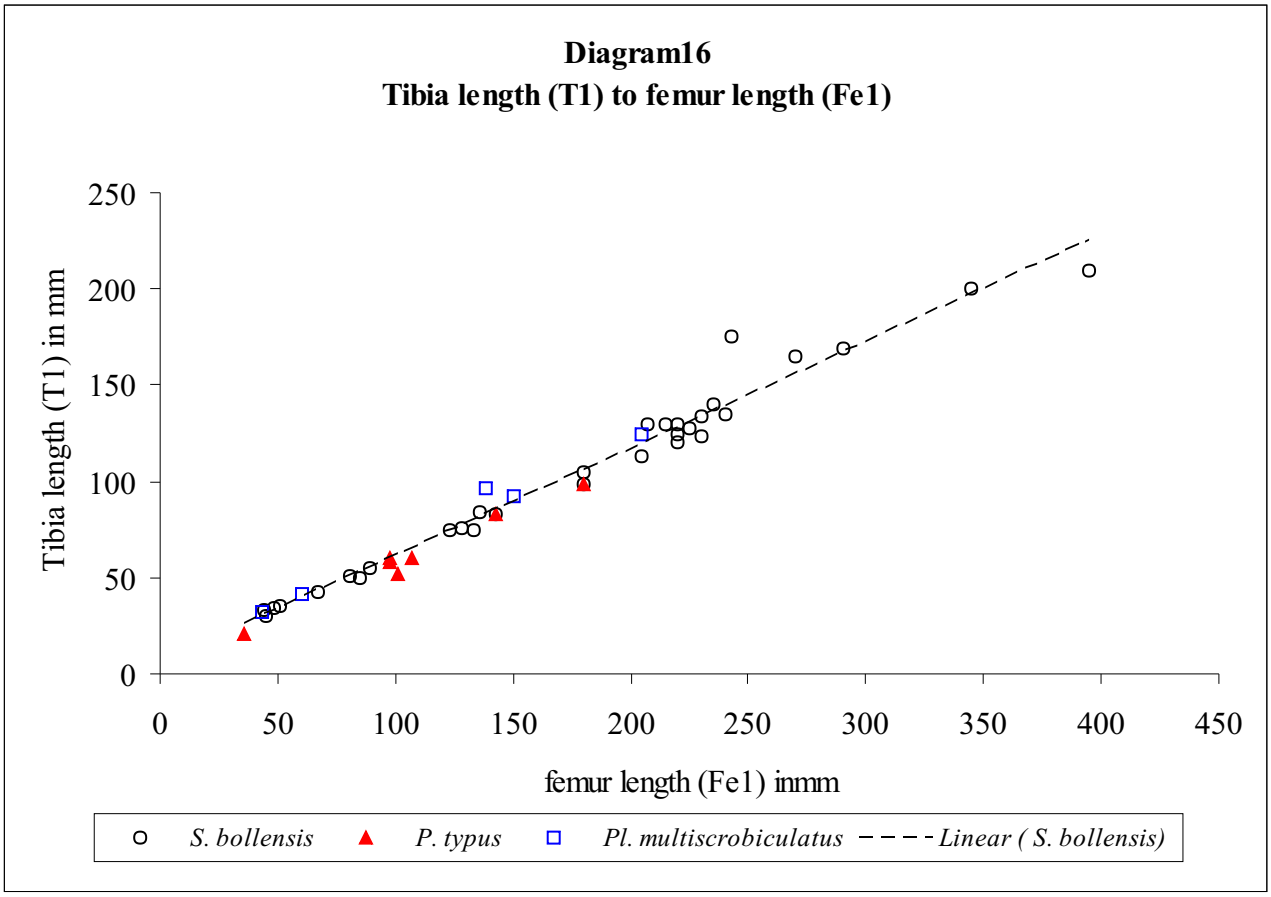

Diagram 16: The ratio of tibia length (T1) to femur length (Fe1) in three Liassic thalattosuchians is compared. The development of the femur length in comparison with the tibia length shows in all taxa similar linear development. There is almost no difference in the three studied taxa.

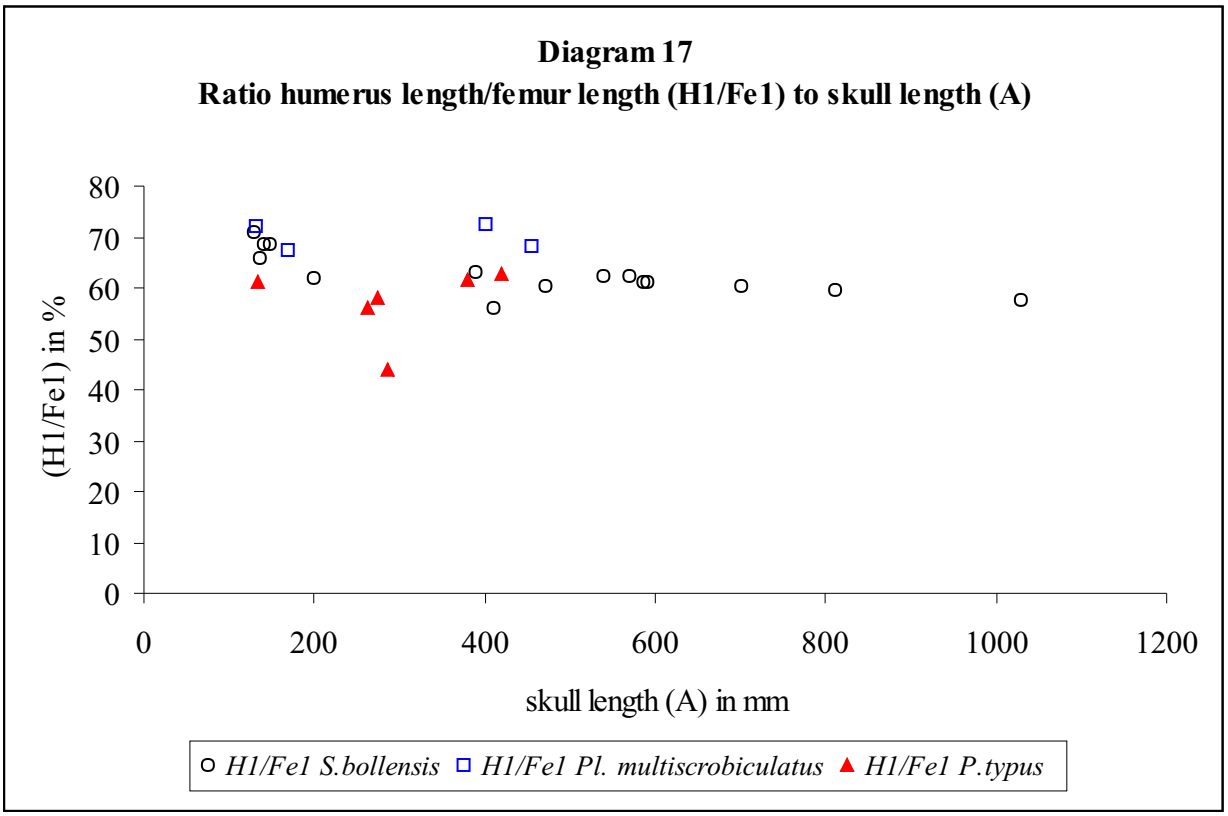

Diagram 17: The ratio of humerus length (H1) to femur length (Fe1) in percentage to the skull length (A) of three Liassic taxa is compared. The humerus length (H1) is up to 75% of the femur length (Fe1) in *Platysuchus multiscrobiculatus*, while the ratio is only 60% in *S. bollensis* at a similar skull length. *Pelagosaurus typus* possesses a relatively small humerus length in comparison to the femur length of about 57%. However, in adult *P. typus* specimens with a skull length larger than 350 mm, the values are similar to the values of *S. bollensis*.

Chapter 5

Discussion of intraspecific and interspecific variation

5.1 Discussion of the diagnostic features of the Liassic thalattosuchians

The five valid Liassic taxa differ in general size, proportions and in shape from each other (Fig. 5.1 and appendix III). Nevertheless, in some cases the minor differences between the taxa are hard to identify without a close investigation of the intraspecific variation of the specimens. The main diagnostic features are listed in appendix III and the following comparison is mainly based on that table.

5.1.1 Biometric data as use for taxa differentiation

The bivariate plots seldom show the presence of different genera, more often they show convergent development in all taxa (Diagram 1-17). Noticeable is the absence of possible biometric values for taxa differentiation in a juvenile stage. The biometric data of all juvenile specimens (skull length less than 250 mm) provide no useful data for taxa separation (Diagram 1-17). Especially, in the smallest specimens with a skull length from 100 mm to 160 mm, the ratios hardly differ and cannot be distinguished from intraspecific scattering of the values. Therefore, no significant difference in the biometric ratios is shown in the skull proportions of the juvenile specimens of *Pelagosaurus typus*, *Steneosaurus bollensis*, and *Platysuchus multiscrobiculatus*. In the adult specimens, in particular in Steneosaurus bollensis, the high scattering of the values makes it difficult to interpret the results especially for taxa differentiation. Therefore, some osteological differences, which are not reflected by the biometric data, in the skull and in some parts of the postcranial, are more useful for distinguishing the taxa (see chapter 3, 4 and appendix III). Furthermore, in all studied taxa similar ontogenetic variation superimpose the data sets for taxa separation. Ontogenetic variation can be certainly reported for e.g., the shape and size of the orbit, the supratemporal fenestra, the frontal, and the posterior outline of the skull (see figure 4.5), as well as the tibia length (T1) compared to the femur length (Fe1) (Diagram 16).

In addition, the sagittal crest is distinctly decreasing in width during the growth process in all studied taxa and shows a negative allometric growth rate, which is also reflected by the morphological change of shape of the frontal (Fig. 4.5). Those shape changes in the frontal are also known from extant crocodiles, like e.g. *Crocodylus niloticus* (BUFFRENIL 1982) and should be therefore carefully considered for the taxa differentiation.

5.2 Variation in teleosaurids

5.2.1 Body proportions

The entire length of the adult specimens of the Liassic taxa differs considerably. While *Steneosaurus bollensis* is the largest taxon with a length of up to 5 meters, followed by *Steneosaurus brevior* with an estimated body length of 4.5 meters, the maximum body length of *Platysuchus multiscrobiculatus* is only up to 3 meters. *Steneosaurus gracilirostris* still reaches 2.5 meters, but *Pelagosaurus typus* is the smallest Liassic taxa with a maximum body length of 2 meters (see appendix III). However, in most cases, the body length can hardly be used to distinguish the taxa from each other, mostly because of the lack of information about the individual age and the often-insufficient preservation. In the case of *Steneosaurus gracilirostris,* postcranial material is only poorly and in the case of *S. brevior,* not preserved at all; therefore, exact information about the body proportions is not available.

For adult specimens the skull length (A) in ratio to the trunk length (TRL) of *Platysuchus multiscrobiculatus* is with 45% the smallest for the Liassic taxa. *Steneosaurus bollensis* and *Pelagosaurus typus* with 51-65% skull length at the trunk length (TRL) are the average and *Steneosaurus gracilirostris* possesses with estimated 67% skull length at the trunk length (TRL) the relative largest skull (see appendix III). *Steneosaurus brevior* is only preserved with cranial material; therefore, no ratio can be given in this case.

In addition, negative allometric growth is calculated for the skull length (A) compared to the shoulder-pelvic distance (S-PL) at least for *Pelagosaurus typus* and *Pl. multiscrobiculatus* (see. 4.2.8). *Steneosaurus bollensis* show only very slight negative growth, which means almost isometric growth for the skull. This is contrary to the observation of WESTPHAL (1962), who describes a slightly positive allometric growth of the skull up to a skull length of about 300 mm, and afterwards isometric growth for *S. bollensis*. However, WESTPHAL (1962) uses the trunk length (TRL) as standard length instead of the shoulder-pelvic distance (S-PL), which is used here.

The ratio of skull length (A) to shoulder-pelvic distance (S-PL) provides only for adult specimens some usable data for taxa differentiation. Adult specimens of *Platysuchus multiscrobiculatus* and *Pelagosaurus typus* possess smaller skulls compared to the S-PL than adult *S. bollensis* specimens possess, while the juvenile specimens all show similar ratios (Diagram 1).

Another difference is the percentage of the tail length at the total body length (TL) in the different Liassic teleosaurids (see appendix III). *Steneosaurus bollensis* and *Platysuchus multiscrobiculatus* share a tail length of about 49% of the total body length (TL), whereas it is

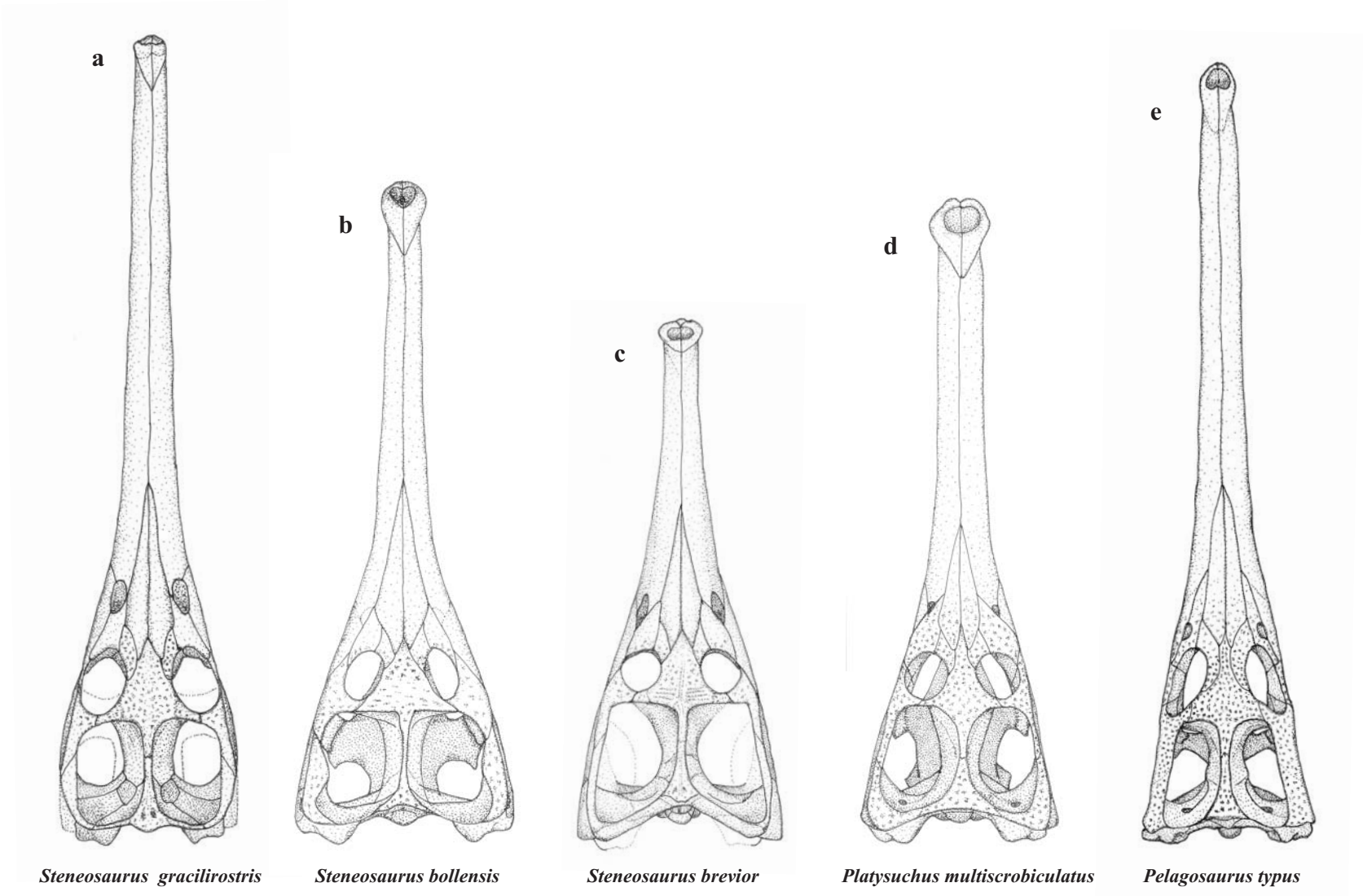

Figure 5.1a-e: Comparison of the skull shape of the five Liassic Thalattosuchia taxa. Skulls are scaled to the same size for better comparison. **5.1a**-Largest known skull length 700 mm (*S. gracilirosrtis*). **5.1b**-Largest skull length 1030 mm (*S. bollensis*). **5.1c**-Largest skull length about 900 mm (*S. brevior*). **5.1d**-Largest skull length 450 mm (*Pl. multiscrobiculatus*). **5.1e**-Largest skull length 380 mm (*P. typus*)..

56% in *Pelagosaurus typus*. Because the tail preservation is often incomplete in teleosaurids, it is rarely used for taxa differentiation and only a few data were available. *Steneosaurus gracilirostris* and *S. brevior* are only known from incomplete material; therefore, data for the tail length was not available at all.

5.2.2 Skull shape and proportions

More important and more significant for taxa differentiation, is the ratio of the skull width (C) to the skull length (A) (Diagram 2 and appendix VI). All teleosaurids possess a longirostrine, relatively flat and in dorsal view triangular skull (see chapter 3 and Fig. 5.1). Even though considered the compressed preservation of some specimens especially from Holzmaden, the relative skull width still provides information to separate some of the taxa. For example, *Pelagosaurus typus* has a much narrower (C/A ~20%), in this case also higher, skull (T/C~ 45%) than most of the *Steneosaurus* taxa have. Only *Steneosaurus gracilirostris* and *Steneosaurus leedsi* have similar ratios as *Pelagosaurus typus* in the skull width (Diagram 2). *Steneosaurus brevior* possess the broadest skull compared to the skull length (C/A~33%) of the other Liassic teleosaurid taxa, even though there are always overlapping values with *S. bollensis*. Unfortunately, *Platysuchus multiscrobiculatus* cannot be distinguished from *Steneosaurus bollensis* based on the ratio skull width to skull length (Diagram 2).

However, comparing the skull width (C) to the skull length (A) in different Thalattosuchia taxa, basically, two lines can be distinguished (Diagram 2). The ratio for *S. bollensis*, *S. brevior*, *Platysuchus multiscrobiculatus*, *S. edwardsi,* and *S. heberti* are showing the same linear development with relatively broad skulls. The ratio for *Pelagosaurus typus*, *S. gracilirostris* and *S. leedsi* are showing linear development, too, but differ from the other taxa in a much narrower skull shape. The narrower skull shape of *S. gracilirostris* and *Pelagosaurus typus* is obviously reflected by the ratio of skull width to skull length, whereas the other *Steneosaurus* taxa including *Platysuchus multiscrobiculatus* possess broader skulls. In addition, the skulls of *P. typus* and *S. gracilirostris* possess a very elongated, narrow rostrum, with only hardly broadened premaxillae and more laterally orientated orbits compared to the other Liassic teleosaurids. These data reflect a more streamlined shape of the skull and could indicate a more pelagic way of life (see chapter 8).

However, the difference in skull width is not used as a character in the phylogenetic analysis (see chapter 6), because of the lack of definite information about the height of the skull in *S. bollensis* and *Pl. multiscrobiculatus* and the fact, that the signal is probably influenced by preservational conditions.

The elongated rostrum is reflected by the data of the rostral length (B) in ratio to the skull length (A) (Diagram 3). In this study, slight negative allometric growth rate of the rostral length (B) compared to the skull length (A) is noticed in all investigated taxa, except of *Platysuchus multiscrobiculatus*, which shows a slight positive allometric growth rate (see chapter 4). Because the percentage of rostral length (B) at the skull length (A) changes during ontogeny, it can only be partly used as a distinguish character for the teleosaurids. In adult *Platysuchus multiscrobiculatus*, *Steneosaurus gracilirostris,* and *Pelagosaurus typus* the rostral length is with an average of 75% of the skull length relatively high, compared to the rostral length of adult *Steneosaurus bollensis* with an average of 71.4% and *Steneosaurus brevior* with only 65% (see appendix III). However, the scattering of the values superimposes the differences between the taxa (Diagram 3). Even though the signal of the rostral length is not very clear on its own, it is used as an additional character in the phylogenetic analysis (see chapter 6 and appendix V, character 175).

The distance between the posterior margin of the premaxilla and the anterior margin of the nasal (pmx-n distance "H") is equally developed in *Pelagosaurus typus* and *Steneosaurus bollensis* (Diagram 4). The premaxilla-nasal distance (H) in *Platysuchus multiscrobiculatus* is up to 55% of the rostral length (B), and therefore is larger than in *Steneosaurus bollensis and Pelagosaurus typus* (Diagram 4). In adult specimens of *S. bollensis* and *P. typus,* H reaches a maximum of 50% of the rostral length (see chapter 4). The scattering of the values in all studied taxa is a result of individual variation and the difficulty to identify the exact run of the dorsal premaxilla-maxilla suture. For *S. gracilirostris* and *S. brevior* the exact run of this suture could not be identified, therefore, no data for "H" was available.

Enlargement of the premaxillae is individually variable within the species and cannot be certainly referred to a typical size or gender (Diagram 5). Nevertheless, the values in *Pelagosaurus typus* and *Platysuchus multiscrobiculatus* indicate a slight increase in premaxillae enlargement during growth. The premaxillae enlargement is largest in *Platysuchus multiscrobiculatus,* with a maximum of 202% of the premaxillae width (K) of the narrowing posterior to the premaxillae (L) and smallest in *Pelagosaurus bollensis* with an average of 129%. *Steneosaurus gracilirostris* shows with 135% a relatively small premaxilla enlargement, too. The value of *Steneosaurs brevior* differs not from the values of *S. bollensis,* which has an average of 147% premaxillae enlargement (Diagram 5).

Additionally, in *Pelagosaurus typus*, the external naris opens dorsally with an angle (W1) of less than 30° to the horizontal plane, whereas the external naris in *Platysuchus multiscrobiculatus* and *Steneosaurus bollensis* opens anterodorsally with an average angle of

45° to the horizontal plane. In all three taxa, the premaxillae are not or only slightly flexed ventrally. In contrary, *Steneosaurus brevior* and *S. gracilirostris* share an anterior orientated external naris, with an estimated angle (W1) of 60°-70° to the horizontal plane and the premaxillae are flexed ventrally at least in *S. brevior* (Fig. 3.23). The orientation of the external naris is therefore used as a character in the phylogenetic analysis (see chapter 6 and appendix V, character 146).

All investigated thalattosuchians show obvious ontogenetic changes in orbital size compared to the size of the skull, and less distinctive also in orbital shape (see chapter 4 and Diagram 6, 7, and 8). The orbital length (I) shows negative allometric growth compared to the skull length (A) in all investigated taxa (see chapter 4). Interestingly, all taxa show similar ratios in their juvenile specimens and cannot be distinguished there. However, the ratio orbital length (I) to skull length (A) shows larger orbits in adult *Pelagosaurus typus* specimens than in adult *Steneosaurus bollensis, S. brevior, S. gracilirostris,* and *Platysuchus multiscrobiculatus* specimens (Diagram 6 and appendix III). Even though, the signal is partly superimposed by the high intraspecific variation of the values of *S. bollensis* (Diagram 6). The Middle Jurassic teleosaurids, *Steneosaurus leedsi* shows here similar ratios to *S. bollensis*, while *S. edwardsi* and *S. obtusidens* shows distinct larger orbital length, similar to the ratios of *Pelagosaurus typus*.

The ratio orbital length (I) to supratemporal fenestra length (D) in the five Liassic taxa *Steneosaurus bollensis*, *S. gracilirostris*, *S. brevior*, *Platysuchus multiscrobiculatus,* and *Pelagosaurus typus* confirm the larger orbits in *Pelagosaurus typus* even more clearly (Diagram 7). Even in a juvenile stage, the differentiation of the values from the other teleosaurids is clearly noticeable here. *S. brevior* shows relatively smallest orbits in the Liassic taxa (see also appendix III).

The orbital shape reflected by the percentage of the orbital width (J) of orbital length (I) changes in *Steneosaurus bollensis* slightly from round (J/I 80-100%) to ellipsoid (J/I > 80%) (Diagram 8). An orbital width of 100-80% of the orbital length indicates round orbits, which is the case in most juvenile specimens. A lesser percentage share indicates ellipsoid orbits, which is usually the case in adult specimens of the investigated taxa. The orbital shape is most ellipsoid in adult *P. typus* (J/I ~ 40%). *S. gracilirostris* and *S. leedsi* show similar orbital shape to *S. bollensis*, but have a much narrower skull (C/A~18-25%), which place them in the diagram 8 in one group together with *P. typus* (Diagram 8). In contrary, the skull of *S. brevior* and *S. edwardsi* is very broad (C/A~34-36%) but the ratio orbital width (J) to orbital length (I) (I/J~65%-80%) lies in the scattering range of the ratios of *S. bollensis*. The orbit shape is

therefore only partly useful for taxa differentiation. However, in the phylogenetic analysis the orbit shape and its orientation in the skull was use as an additional character for adult individuals (see chapter 6, appendix V, character 149, and 150).

The percentage of the supratemporal fenestra length (D) to the skull length (A) reflects the size of the supratemporal fenestra in the skull and varies obviously inside the Liassic teleosaurids (see appendix III). *Steneosaurus gracilirostris* possesses the smallest supratemporal fenestra (D/A =12.7%) compared to the other Liassic teleosaurids (see appendix III). Only *Pelagosaurus typus* has similar ratios of the supratemporal fenestra length (D) to the skull length (A). It is in average 13.4 %, but only 12.2% in the holotype of *P. typus*. The average ratios of *Steneosaurus bollensis* and *Platysuchus multiscrobiculatus* are larger and lie by 15.2% and 15.6%. *Steneosaurus brevior* possesses the largest supratemporal fenestra with 18.8% supratemporal fenestra length (D) of the skull length (A) (see appendix III).

The size and partly the shape of the supratemporal fenestra are reflected in the ratio supratemporal fenestra width (E) to supratemporal fenestra length (D) (Diagram 9). The ratio E/D in percentage indicates a square (80-100%) or more elongated (79-45%) shape of the supratemporal fenestra, whereas the difference between ellipsoid and rectangular shape is not visible. *Pelagosaurus typus* is clearly distinguished by its more elongated supratemporal fenestrae (E/D~50-70%) from *Steneosaurus bollensis, S. brevior, S. priscus,* and *Platysuchus multiscrobiculatus* with broader supratemporal fenestrae (E/D~60-95%). Furthermore, the Middle and Upper Jurassic taxa *Steneosaurus leedsi*, *S. edwardsi,* and *S. obtusidens* have more elongated supratemporal fenestrae (E/D~ 35-50%) than the Lower Jurassic taxa (Diagram 9). Additionally, the ratio of skull width (C) to skull length (A) in *Pelagosaurus typus*, *Steneosaurus gracilirostris*, and *S. leedsi* fall together in a group, while *Steneosaurus bollensis*, *S. brevior, S. priscus,* and *Platysuchus multiscrobiculatus* form another group. Even though, the biometrical data of the supratemporal fenestra provides information for taxa differentiation, the outline shape has to be considered, too (appendix III).

According to WESTPHAL (1962), *Steneosaurus bollensis* shows a distinctive change in the relative orbit size during the development, but not in the proportion of the supratemporal fenestra compared to the skull size. According to him, even the outline shape of the supratemporal fenestrae does not change. In contrary, in this study a distinct change in the shape of the STF of *Steneosaurus bollensis* as well as in *Platysuchus multiscrobiculatus* is noted (Fig. 4.5). The shape of the STF changes from ellipsoid in juveniles to sub-rectangular in adults (see chapter 4). Additionally, a distinct elongation at the posterolateral corner and a

notch at the lateral margin, because of the shape change of frontal and squamosal during the development, are noted. However, in adult specimen of *Platysuchus multiscrobiculatus* and *Steneosaurus bollensi*s specimens the supratemporal fenestra is usually rectangular in contrary to the supratemporal fenestra in *Pelagosaurus typus*, which is constantly ellipsoid during development (see chapter 4 and appendix III).

In consideration of the ontogenetic variations within each taxon (see chapter 4), the differences in shape and size of the supratemporal fenestra are used as characters in the phylogenetic analysis (see chapter 6 and appendix V, character 68, 138, 173, 174).

Additional morphological differences in the cranial table of the taxa are: the size of the antorbital fenestra, the configuration of the lateral margin of the orbit, the orientation of the orbit in the skull, the shape and configuration of the postorbital, and the frontal (see chapter 3 and 6 for details and Fig. 5.1).

The antorbital fenestra is very small or missing in *Platysuchus multiscrobiculatus* and *Steneosaurus bollensis*, whereas it is relatively large in *Steneosaurus brevior*, *Steneosaurus gracilirostris*, and *Pelagosaurus typus*. *Steneosaurus gracilirostris* possesses the largest antorbital fenestra (see appendix V, character 67).

The orbit of *Pelagosaurus typus* and *Steneosaurus gracilirostris* is laterally orientated and the lateral margin of the orbit is mainly formed by the jugal. In contrary, the orbit of *S. bollensis*, *S. brevior*, and *Platysuchus multiscrobiculatus* is dorsally orientated in the skull, and the lateral margin of the orbit is mainly formed by the postorbital and the lacrimal (see appendix V, character 139 and 149, see above).

Additionally, the postorbital of *Steneosaurus gracilirostris* possesses a thin anterior process, which forms the posterior third of the lateral margin of the orbit, which is not the case in *Pelagosaurus typus* (see chapter 3). In *Steneosaurus bollensis* and *Platysuchus multiscrobiculatus,* the anterior process of the postorbital is long and contacts the posterior process of the lacrimal in some cases (see chapter 3.1 & 3.4). The shape and ornamentation of the postorbital is used as characters in the phylogenetic analysis (see chapter 6, appendix V, character 25, 26, and 31).

The frontal in the adult specimens has a longer posterior process and forms up to the half of the sagittal crest in *Steneosaurus gracilirostris*, *S. bollensis*, and *Platysuchus multiscrobiculatus,* while it is only one-third in *Pelagosaurus typus* (see appendix V, character 23). In adult specimen, the anterior process of the frontal tapers off between the nasals in all taxa (see appendix V, character 20, 140), but differ in the length of this process

(see chapter 3 for details). Furthermore, the frontal of the single taxa shows minor differences in ornamentation.

In the palate, the internal naris (=secondary choana) shape differs in the Liassic taxa as well as the paired pterygoid shape, which are used as characters in the phylogenetic analysis (see chapter 6, appendix III, and appendix V, characters 141, 142, 143).

The ratio of the retroarticular process length (X) to the skull length (A) of nine different Thalattosuchia taxa is shown in diagram 9. Most obviously, *Pelagosaurus typus* possesses a much shorter retroarticular process than the other described Thalattosuchia taxa (see chapter 4). *S. leedsi* also shows a relatively small retroarticular process compared to *S. bollensis*. However, all other taxa show the same linear development in the length of the retroarticular process and differ not in there ratios. Additionally, the scattering of the values is particular high in the larger specimens of *S. bollensis* with a skull length of more than 750 mm. Differences because of sexual dimorphism in old specimens of *S. bollensis* could be a possible explanation, but cannot be confirmed with the existing data, and is therefore highly speculative.

Noticeable is furthermore, the almost equal development of the lower jaw regarding the symphysis length and the portion of the splenial at the symphysis in all studied thalattosuchians as well as in the two extant crocodile species *Gavialis gangeticus* and *Tomistoma schlegelii* (Diagram 11 & Diagram 12). The values of seven different Thalattosuchia taxa are compared in diagram 11, but unfortunately, only few data of each taxon is available. The length of the symphysis (V) in ratio to the total length of the lower jaw (U) differs not much in the chosen Thalattosuchia taxa (Diagram 11). The measured values indicate a linear growth of the symphysis length (V) in comparison of the mandibular length (U). The Middle Jurassic taxon *Steneosaurus heberti* and the metriorhynchid *Teleidosaurus calvadosi* possess a slightly shorter symphysis in comparison to *S. bollensis*, whereas the symphysis of *S. leedsi* is slightly longer. However, due to the fact of the small data set and the usual high scattering of the intraspecific values in *S. bollensis* these readings remains uncertain.

A few more data is available for the participation of the splenial (W) at the symphysis length (V). Six Thalattosuchia taxa and additionally two recent crocodilian taxa (*Gavialis gangeticus, Tomistoma schlegelii*) are compared with each other (Diagram 12). Interestingly, *Tomistoma schlegelii* falls exactly on the line calculated for the development in *Steneosaurus bollensis*. *Gavialis gangeticus* and *Steneosaurus baroni* show a larger portion of the splenial taking part in the symphysis in comparison to the ratios of *S. bollensis*, whereas one value of

S. edwardsi is distinctly smaller. Nevertheless, the diagram shows that the biometric values are not helping much to distinguish Thalattosuchia taxa from each other.

The symphysis angle (W 2) differs among the Liassic taxa and is up to 50° in *Steneosaurus bollensis*, while it is only about 30° in *Pelagosaurus typus*. The symphysis angle (W2) in *S. brevior* is about 40°. Therefore, it is used for taxa differentiation, even though an intraspecific variation of up to 10° of the symphysis angle should be considered (see appendix V, character 152).

5.2.3 Limb & general body proportions

The morphology of the shoulder and pelvic girdle as well as the fore- and hind limbs is partly different in the teleosaurid taxa from Holzmaden (see chapter 3, and Fig. 5.2 and 5.3). In the postcranial a reduction of the fore limb length (respectively humerus length) compared to the femur length, is observable in *Steneosaurus bollensis*, *S. gracilirostris*, *Platysuchus multiscrobiculatus*, and *Pelagosaurus typus*. This reduction differs slightly in its degree among the taxa (Diagram 13). The fore limb is more reduced in *P. typus* than in *S. bollensis* or *Pl. multiscrobiculatus* (Diagram 13, 14, and 17). The humerus length in ratio to the femur length is in adult specimens about 70% in *Steneosaurus gracilirostri*s (WESTPHAL 1962), at least 67.5% in *Platysuchus multiscrobiculatus*, in average only 61.9% in *Steneosaurus bollensis*, and no more than 53.4% in *Pelagosaurus typus* (Diagram 13, appendix III). Interestingly, the Middle and Upper Jurassic teleosaurids *Steneosaurus leedsi*, *S. edwardsi*, and *S. obtusidens* show all smaller ratio of the humerus length (H1) to femur length (Fe1) than the Lower Jurassic taxa (Diagram 13). Therefore, the difference in humerus length to femur length is used as a character in the phylogenetic analysis (see chapter 6, appendix V, character 187).

For *Steneosaurus bollensis, Platysuchus multiscrobiculatus*, and *Pelagosaurus typus* a positive allometric growth rate is calculated for the humerus length (H1) in ratio to the skull length (A). However, comparing the absolute values of the humerus length (H1) in ratio to skull length (A), *P. typus* shows a smaller humerus than *S. bollensis*, while *Pl. multiscrobiculatus* shows a larger one (see Diagram 14 and appendix III). Again, the Middle and Upper Jurassic teleosaurids *S. leedsi*, *S. edwardsi*, and *S. obtusidens* show a distinctly smaller humerus than *S. bollensis* (Diagram 14).

The scapula of *Steneosaurus bollensis*, *Platysuchus multiscrobiculatus*, and *Pelagosaurus typus* possesses all similar broad and deep muscle insertions area at the ventral external surface, but their dorsal blades show differences in its expansion (see chapter 3, appendix III, and Fig. 5.2). It is least expanded in *Pl. multiscrobiculatus*. The coracoid

possesses a thinner shaft in *Pl. multiscrobiculatus* than in *S. bollensis* or *P. typus*. Additionally, the scapula length/coracoid length ratio is 1:1 in *S. bollensis* and *Pl. multiscrobiculatus*; whereas it is only 1: 0.75 in *Pelagosaurus typus* (see Fig. 5.2 and appendix III). Different characters at the pectoral girdle are therefore used in the phylogenetic analysis (see appendix V, character 153, 154, 155, 180).

In this study, positive allometric growth for the femur length (Fe1) in ratio to the skull length (A) is confirmed for *Steneosaurus bollensis*, *Platysuchus multiscrobiculatus*, and *Pelagosaurus typus*. Already WESTPHAL (1962) described the tendency of the femur of *S. bollensis* to increase its relative length with age. In contrary, KÄLIN & KNÜSEL (1944) note a negative allometric growth rate in the hind limb and especially in the femur of extant crocodilian taxa. In addition, KRAMER & MEDEM (1955) describe progressive negative allometric growth for the fore- and the hind limb in some *Caiman* and *Paleosuchus* species. However, a direct comparison to the measurements of extant crocodilians is difficult, because those measurements are taken from the complete fleshy limb, including manus and pes in comparison to the total body length, whereas in the fossil specimens, only the single length of the humerus or femur is measured and compared to the skull length. Anyway, it is confirmed that the proportion changes of the limbs in *Steneosaurus bollensis* are relatively small in comparison to the changes in extant crocodilian species like previously noted by KRAMER (1955) and WESTPHAL (1962). For interspecific taxa differentiation, the ratio femur length (Fe1) to skull length (A) is not very helpful, because the scattering of the values are particularly high in *S. bollensis* (Diagram 15).

The proportion of the tibia length (T1) to the femur length (Fe1) is similar in *Platysuchus multiscrobiculatus* (60% in adults) and *Steneosaurus bollensis* (in average 60.7%) but differ slightly from the proportions found in *Pelagosaurus typus,* in average 57.3% (Diagram 16). Nevertheless, the values lie closely together and the growth rate inside the leg shows a linear development in all taxa (Diagram 16).

Morphologically, the pelvic girdle and the femur shape in the studied thalattosuchian taxa differs obviously from the pelvic girdle and the femur in modern crocodilians, like for example *Crocodylus porosus* (Fig. 5.3), even though the pelvic bones of *Pelagosaurus typus*, *Steneosaurus bollensis*, and *Platysuchus multiscrobiculatus* are also slightly different from each other (see chapter 3 and fig. 5.3). *C. porosus* possesses a far more enlarged posterior process of the iliac crest, a relatively deeper acetabulum, and an ischium with a much smaller ventromedial enlargement in comparison to the Liassic teleosaurids (Fig. 5.3).

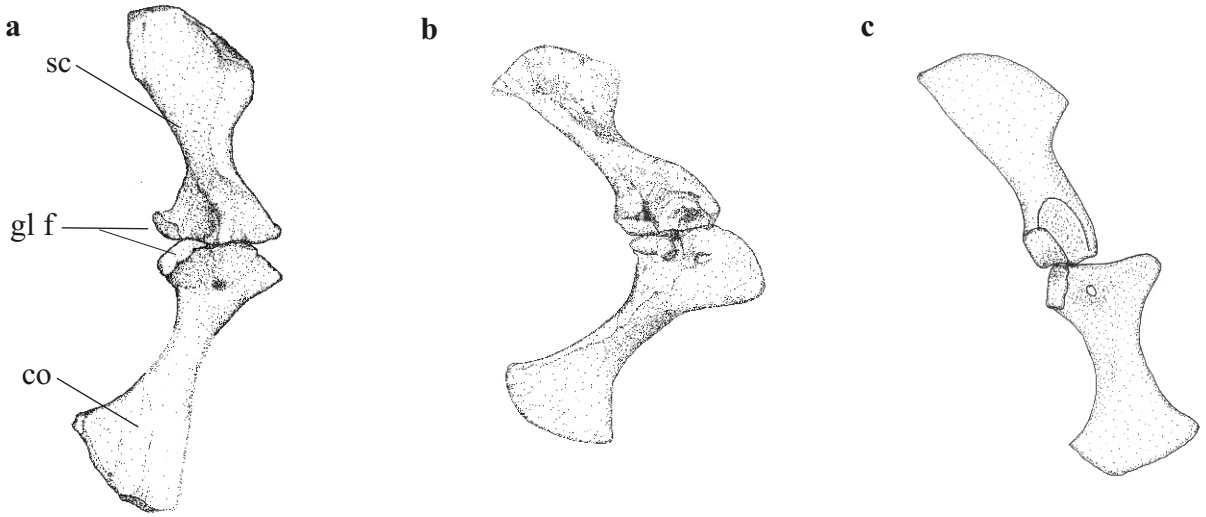

Figure 5.2a-c: Pectoral girdle in lateral view of *Platysuchus multiscrobiculatus* (a), *Steneosaurus bollensis* (b), and *Pelagosaurus typus* (c). The scapula is scaled to the same size for better comparison. Abbreviations: co-coracoid, gl f-glenoid fossae, sc-scapula.

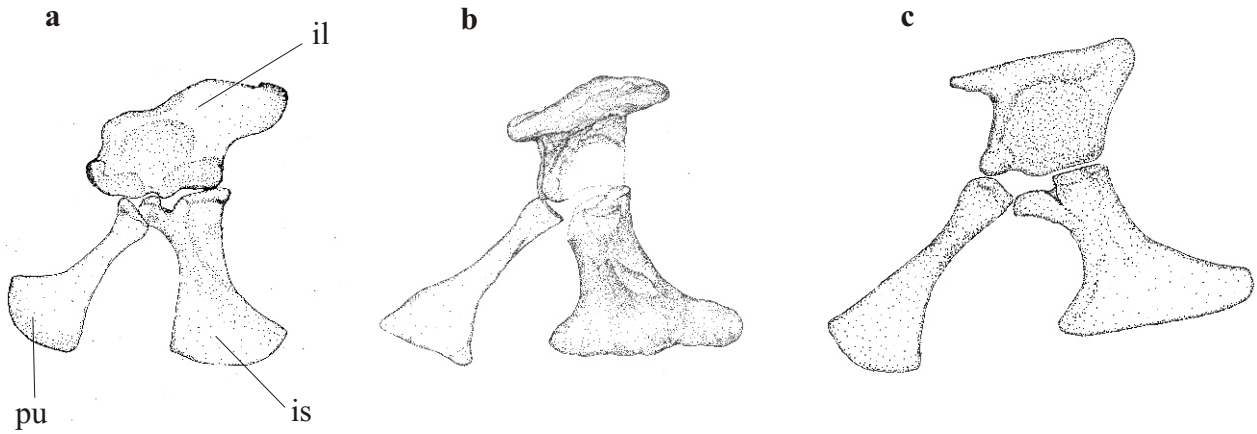

Figure 5.3a-c: Pelvic girdle in lateral view of the extant saltwater crocodile *Crocodylus porosus* (a) in comparison with the pelvic girdle of *Platysuchus multiscrobiculatus* (b) and *Steneosaurus bollensis* (c). Scaled to the same size for better comparison.

However, the ilium differs only very slightly in shape between *Steneosaurus bollensis* and *Pelagosaurus typus.* They share a mediolateral flat ilium with a shallow acetabulum (see chapter 3, Fig. 3.12 & Fig. 3.46), while in *Platysuchus multiscrobiculatus* the ilium possesses a pronounced iliac crest with one well-developed dorsoanterior and one dorsoposterior process (see appendix V, character 183). The acetabulum is here much deeper developed and probably more similar to the conditions in extant crocodilians. The femur of *Platysuchus multiscrobiculat*us possesses, in contrary to the one in the other Liassic taxa, a relatively distinct femoral head, which inserts in the relative deep acetabulum (see Fig. 3.31, Fig. 3.33 and appendix IV, character 157). The femur of *Platysuchus multiscrobiculatus* is s-shaped (in posterior view) and possesses a distinct flexed femoral head, whereas the femoral head in *Steneosaurus bollensis* and *Pelagosaurus typus* is less developed (see chapter 3 for a detailed description). In addition, the shape of the pubis differs within the Liassic taxa. *Pelagosaurus typus* possesses a longer, more slender pubis than *Steneosaurus bollensis* and *Platysuchus multiscrobiculatus* (see chapter 3, Fig. 3.47, and appendix V, character 156).

5.2.4 Tooth count and tooth shape

The teeth in the Liassic teleosaurids are generally slender, conical and apically recurved and the tooth crown is covered with a fine vertical striation. Usually but not always, the teeth of *Steneosaurus bollensis* and *S. gracilirostris* possess one or two weak carinae, one at the anterior, and one at the posterior side. The teeth of *S. brevior*, *Platysuchus multiscrobiculatus*, and *Pelagosaurus typus* lack a carina (see also chapter 3 and 8).

The number of teeth in the rostrum varies within a certain limit in the Liassic teleosaurids (see also chapter 3, 4 and appendix III). The number of teeth in the snout differs both inter- and intraspecific (see table 2 and appendix III).

Taxa/ Tooth count	***Steneosaurus bollensis***	***Steneosaurus gracilirostris***	***Steneosaurus brevior***	***Platysuchus multiscrobiculatus***	***Pelagosaurus typus***
premaxilla	3-4	?	3	3	3-4
maxilla	26-35	45-?60	23-28	40-44	32
dentary	24-35	48-?60	23-28	~40	30-32

Table 2: Intraspecific variation of the tooth count in the single bones of the rostrum in the Liassic teleosaurid taxa.

The number of teeth (respectively alveoli) is variable within a certain range, in all taxa. The number of available specimens of *Platysuchus multiscrobiculatus*, *S. brevior*, and *S. gracilirostris* is too small to discover a specific variation pattern in the tooth number.

However, in *Steneosaurus bollensis* and *Pelagosaurus typus*, an ontogenetic variation of the tooth number is not noted, nor can it be directly linked to the absolute rostrum length. Thus, no specific variation pattern is visible. According to ADAMS-TRESMAN (1987) and VIGNAUD (1995), such intraspecific variation in tooth number is also typical for Middle and Upper Jurassic teleosaurids as well as for metriorhynchids. It is therefore agreed with ADAMS-TRESMAN (1987), who already notes, "[...] the tooth number never provides the sole basis on which species are recognized, rather they occur together with clear morphological differences in the skull". In the Liassic teleosaurid taxa, the number of teeth is intraspecifically variable and is not useful as a certain diagnostic character of its own. Nevertheless, in consideration of the variation, the tooth count is used as additional character in the phylogenetic analysis (see chapter 6 and appendix V characters 169, 170, 184).

It is useful as an additionally character, used together with other morphological characters like the orientation and arrangement of the teeth or alveoli in the jaw, the particular shape of the jaw bones, and the specific tooth shape (see chapter 6 as well as appendix V, characters 177, 179, 181, 182, 186).

For example, the alveoli in the premaxilla are circular in all Liassic taxa and the teeth are orientated vertically in *Steneosaurus bollensis, S. gracilirostris,* and *Pelagosaurus typus*. In contrast to the first premaxilla alveolus and the appending tooth of *S. brevior,* which is slightly anteriorly orientated. No data for the orientation of the alveoli in the premaxilla of *Platysuchus multiscrobiculatus* are available. Furthermore, the third premaxilla tooth is larger developed in *S. bollensis*, *S. brevior*, and *Pl. multiscrobiculatus*, whereas *S. gracilirostris* and *P. typus* do not show enlargement of the third premaxilla tooth. The alveoli in the maxilla are round and the teeth are vertically aligned in all Liassic teleosaurids. The alveoli in the dentary are round and vertically orientated in *S. bollensis, S. gracilirostris*, *S. brevior*, and *Pelagosaurus typus*, whereas *Platysuchus multiscrobiculatus* shows slightly lateral aligned alveoli in the dentary and particularly, the third tooth in the dentary is laterally orientated (see chapter 3 and 8 for more details).

5.2.5 Ribs and vertebrae

Extant crocodilians possess steadily 9 cervical vertebrae, 10 thoracic (rib-bearing) vertebrae, 5 lumbar vertebrae, 2 sacral vertebrae, and about 35 caudal vertebrae (LEVY 2003). In contrast, the number of thoracic, lumbar, and caudal vertebrae is variable within a certain limit in all investigated Thalattosuchia taxa. The number of thoracic ribs, respectively the number of thoracic vertebrae, varies in *S. bollensis* and *P. typus* from 12-15 (see chapter 3), while the number of lumbar vertebrae varies from 2 to 3. Thus, the number of trunk vertebrae

can generally vary from 14 to 18. The number of caudal vertebrae is even more variable and lies usually between 30 and 40 vertebrae, not to forget the problem of artificial added vertebrae during preparation. *Platysuchus multiscrobiculatus* possesses probably about 38 caudal vertebrae, while *Pelagosaurus typus* usually have 42, and *Steneosaurus bollensis* possesses up to 55. Interestingly, the percentage of the tail length to the body length is in *P. typus* with 56% higher than in *S. bollensis* and in *Pl. multiscrobiculatus*, where the length of the tail is only about 49%.

Nevertheless, the number of cervical vertebrae is constant 9 in *S. bollensis* and *Pl. multiscrobiculatus* and constant 8 in *P. typus* (see appendix III and appendix V, character 160). The shape of the cervical, thoracic, lumbar, sacral, and caudal vertebrae is regarding to their position intraspecifically constant. In consideration of weathering and diagenetic conditions of the fossil specimens, it is almost impossible to find diagnostic characters at the vertebrae to distinguish the Liassic taxa from each other. An exception is the atlas-axis complex. The axis of *Pelagosaurus typus* bears two articular facets for the second cervical rib instead of only one, like in all other teleosaurids (see chapter 3, Fig. 3.44 and appendix V, character 171, 172). In fact, the axis of *P. typus* shows more similarity with the axis of the metriorhynchids (ARTHABER 1907a). In addition and in contrary to all other teleosaurids, which possess a single headed second cervical rib, is the second cervical rib of *P. typus* double-headed, which is as well similar to the conditions described for metriorhynchids (ARTHABER 1907a, BUFFETAUT 1980a).

A missing chevron, as a sign for sexual dimorphism, like at the first caudal vertebra in alligators, cannot be verified in any of the investigated taxa, because of mostly unfavourable preservation or overlying armour in some other cases. In specimen SMNS 19073 (cf *P. typus*) both at the first and the second caudal vertebrae a normal developed chevron is observed. Because those particular vertebrae are not exposed at any other *Pelagosaurus typus* specimen, it is impossible to make a statement about variation or sexual dimorphism.

5.2.6 Ornamentation

The ornamentation of the cranial bones within the single studied Thalattosuchia taxa depends only slightly on ontogenetic but more on individual variation. However, it varies obviously interspecifically.

The individual variability of the pattern of pits on the osteoderms and on the cranial table is relatively high in *Steneosaurus bollensis* but cannot be referred with certainty to a specific gender or a specific size (Fig. 4.2). In contrast, *Pelagosaurus typus* shows only minor variation of the ornamentation on the surface of the osteoderms and the cranial bones (see

chapter 3.5). *Platysuchus multiscrobiculatus* shows also few variations in the ornamentation, the only exception is the smooth surface of the postorbital in the juvenile specimen (Fig. 4.9). However, the number of specimens is too small to determine this as an ontogenetic character.

The ornamentation of the cranial table is most pronounced in *Pelagosaurus typus* and *Platysuchus multiscrobiculatus*. The cranial ornamentation is spread over the frontal, parietal, postorbital, squamosal, prefrontal, lacrimal, and in some specimens even the nasal and jugal (see appendix V, character 137). The Liassic *Steneosaurus* taxa have a less developed ornamentation on the cranial bones and sculpturing is restricted to the parietal, frontal, prefrontal, postorbital, and squamosal. The prefrontals of *Steneosaurus gracilirostris* are long, slender, with a smooth surface, and not as broad and sculptured as in *Pelagosaurus typus*. The nasals of *Steneosaurus gracilirostris* are more slender than in *Pelagosaurus typus* and without any ornamentation on the surface. In addition, the lacrimal of *Steneosaurus gracilirostris* does not show ornamentation on the surface, contrary to *Pelagosaurus typus* where the lacrimal is strongly ornamented.

Within a certain taxon, the ornamentation can vary within certain limits, like individual form of the pits or density of the pit pattern. In some cases, even some cranial bones can be with or without ornamentation. Nevertheless, the ornamentation of certain cranial bones, especially whether ornamented or not can be used as a character in the phylogenetic analysis (see chapter 6 and appendix V, characters 25, 31, 33, 35, 137).

BUFFRENIL (1982) notes for extant crocodilians, like e.g. *Crocodylus niloticus* that "[...] during skeletal growth pit dimensions are constantly adapted to skull size [...]". This observation fits fine with the observations in the Liassic taxa. It is obviously resulting in a similar ornamentation patterns during growth. Reported variation of ornamentation is in most cases individually and a clear relation between ontogeny and cranial bone ornamentation cannot be observed. In contrary, WESTPHAL (1962) reports for the dorsal surface of the rostrum in *Gavialis gangeticus* stronger ornamentation in older states, but, no such increasing ornamentation of the rostrum of large steneosaurs is observed.

Furthermore, BUFFRENIL (1982) describes the absence of ornamentation on skulls less than 120 mm long for recent crocodilians. Because the smallest known individuals of *S. bollensis*, *Pelagosaurus typus*, and *Platysuchus multiscrobiculatus* possess at least a skull length of 130 mm, no comparative data is available in this case. Interestingly, *S. bollensis* shows generally slightly less distinct ornamentation in juveniles (see paragraph 4.2.3), whereas there is almost no variation in *Pl. multiscrobiculatus* or *P. typus* between juvenile and adult specimens (see chapter 3 and paragraphs 4.2.7 and 4.2.8). According to BUFFRENIL

(1982) and MOOK (1921b), the first occurrence of ornamentation in a juvenile crocodilian is usually on the parietal, squamosal, postorbital and the jugal, while the frontal first shows ornamentation later with increasing size. All studied specimens of the teleosaurids, even the smallest ones, possess ornamentation on the frontal, even though the ornamentation is slightly weaker in some juveniles, than in the adult specimens. In addition, the juvenile Platysuchus multiscrobiculatus (specimen UH 2) shows no ornamentation on the postorbital, but pronounced ornamentation at the frontal, parietal, lacrimal, prefrontal, and squamosal. Therefore, the development of ornamentation in the teleosaurids probably differs from the observed conditions in extant taxa.

The occurrence of transverse grooves instead of pits especially on the frontal is explained for extant crocodilians as a faster resorption than reconstruction of bone material on the surface during the spatial shift of pits (BUFFRENIL 1982). According to BUFFRENIL (1982) the occurrence and appearance of transverse grooves are highly individual variable. This observation fits well with the observations made for *S. bollensis*. Transverse grooves on the external surface of the frontal are only occasionally observed and are not related to an absolute skull size, even though the grooves appear only in adult skulls (Fig. 4.2).

The ornamentation and the shape of the osteoderms work well to distinguish teleosaurid taxa from each other, like *Steneosaurus bollensis*, *Platysuchus multiscrobiculatus,* and *Pelagosaurus typus*. However, within the Liassic species the ornamentation at the osteoderm surfaces can be individually variable, even though an ontogenetic variation is improbable (see appendix V, characters 161, 162, 163, 164, 165, 166, 167, 189).

In particular, *S. bollensis* shows a high individual variation of the ornamentation of the osteoderms. WESTPHAL (1962) mentions three main types of osteoderm ornamentation inside the taxon and refers the third type tentatively to a juvenile stage. In this study, a definite relation of a particular pit pattern to a juvenile stage of *S. bollensis* was not observed. The three ornamentation types appear with all kind of transitional stages and should only be carefully used as a diagnostic character. However, *S. bollensis* possess larger and less pits on the surface of the dorsal osteoderms than *Platysuchus multiscrobiculatus* and *Pelagosaurus typus* (see chapter 3 and 4, Fig. 4.4).

However, considering the position of the single osteoderm in the osteodermal shield, the particular shape is much more constant and thus more useful as a diagnostic character. The ornamentation alone is influenced by too many factors, like the individual variation, the preservation, and the preparation of the fossil.

The single osteoderms differ also in shape among the taxa. The taxon *Platysuchus multiscrobiculatus* is characterized by lateral elongated dorsal osteoderms with a well-developed longitudinal keel, a pattern of small round pits in dense distribution on the surface and a small articulations surface at the anterior margin without a distinct peg (Fig. 4.4). While *Pl. multiscrobiculatus* has thoracic dorsal osteoderms, which are one-third broader than long and show a distinct keel on the surface; the thoracic dorsal osteoderms of *Steneosaurus bollensis* are squarer with a peg at the anterolateral margin and only a slightly developed keel at the surface of the pelvic osteoderms (see chapter 3).

The dorsal osteoderms of *Pelagosaurus typus* are in the trunk region two times broader than long and have a similar ornamentation like *Platysuchus multiscrobiculatus* osteoderms. However, the dorsal osteoderms of *P. typus* possess no keel on the surface and show only very small articulations areas at the anterior margins (Fig. 4.4).

The position and the shape of the complete osteodermal shields differ interspecifically. *Platysuchus multiscrobiculatus* possess a higher number of osteoderms than *Steneosaurus bollensis* and in particular than *Pelagosaurus typus* (see chapter 3 and 4, and Fig. 4.4).

5.2.7 Special features for taxa differentiation

One important character, which distinguishes *Pelagosaurus typus* from all *Steneosaurus* taxa and from *Platysuchus multiscrobiculatus* as well, is the occurrence of a scleral ring in the orbit (see appendix IV, character 168). Only a couple of specimens of *P. typus* (UH 4, BSGP 1925 I 34, and FSL 530238) show this feature (Fig. 3.35 & Fig. 3.37). However, it is assumed that all specimens have possessed those tiny bone plates forming a scleral ring in the orbit. The specimen FSL 530238 is the first specimen known from France that possesses scleral rings. The reason of the rare preservation of the scleral rings in *P. typus* is unknown. Most likely, the tiny bone plates have been lost during preservation or even earlier during fossilization.

Inside the Thalattosuchia, the occurrence of a scleral ring in the orbit is typical for metriorhynchids (EDINGER 1929, BROILI 1932, WESTPHAL 1962). However, the occurrence of a scleral ring in the orbit is common for many marine reptiles like ichthyosaurs and mosasaurs, as well as for certain birds, fishes, and pterosaurs (EDINGER 1929). Therefore, even though the occurrence of a scleral ring is definitely a diagnostic character for *P. typus* within the Thalattosuchia, it must be considered that the occurrence of a scleral ring in the orbit is a plesiomorphic character and occurs in many other taxa, too.

5.3 Results

The ratio between the skull length (A) and the shoulder-pelvic distance (B) can only be used for taxa differentiation in adult specimens (Diagram 1). The ratio between skull width (C) and skull length (A) is in some cases useful for taxa differentiation and show two "lines" of skull types (Diagram 2). However, this could reflect different preservational conditions and not real morphological differences. The ratio between the skull length (A) and the rostral length (B) can be poorly used for taxa differentiation (Diagram 3). The overlap between the single species is large. Therefore, it should not be used as a single diagnostic character; nevertheless, it can provide useful information together with other morphological features like for example the tooth count. It also turned out that the ratio between the premaxilla-nasal distance (H) and the rostral length (B) is not really significant to distinguish taxa, because of the high intraspecific scattering of the values (Diagram 4). The values for the premaxillae enlargement show such a high scattering in *Steneosaurus bollensis* that it is almost useless as a single diagnostic feature (Diagram 5). Generally, the premaxillae are less enlarged in *P. typus* than in *S. bollensis, S. brevior,* and *Platysuchus multiscrobiculatus*. The ratio orbital length (I) to skull length (A) shows a clear separation of *Pelagosaurus typus* from the other taxa and can provide useful information for taxa separation in adult specimens (Diagram 6). The same is true for the ratio orbital length (I) to supratemporal fenestra length (D) (Diagram 7). Different groups of thalattosuchians can be produced by using the orbit shape (I/J) or STF shape (E/D) in comparison with the skull shape (C/A) (Diagram 8, 9). The diagrams shows basically the same splitting in the narrow skull group and in the broad skull group, like diagram 3 in ratio to orbit and STF shape. The retroarticular process is slightly shorter in *Pelagosaurus typu*s and *Steneosaurus leedsi* than in the other investigated taxa (Diagram 10). However, the absolute length of it changes during ontogeny (see chapter 4), thus this feature should not be used as a single diagnostic character.

The ratio of the rostral length (B) in comparison to the skull length (A) (Diagram 3), the ratio of the orbital length (I) to supratemporal fenestra length (D) (Diagram 7), and orbit shape (J/I) to skull shape (C/A) (Diagram 8) is obviously influenced by ontogeny in all investigated thalattosuchians as well as in extant crocodilians (see chapter 4). Therefore, these features have to be carefully considered before entering them in a phylogenetic analysis.

The ratios of the symphysis length (V) to the mandibular length (U) and the splenial length (W) in the symphysis (Diagram 11, 12) do not provide any data for taxa differentiation among the Liassic thalattosuchians. The proportions of humerus, femur, and tibia to each other are only slightly different in the single taxa (Diagram 13-17). The most useful character

here is the proportion of the humerus length (H1) compared to the length of the skull (A) (Diagram 14), which shows distinct separation of, e.g. *Pelagosaurus typus*, *Steneosaurus bollensis* and *Platysuchus multiscrobiculatus* from each other.

Intraspecific variation is found in all investigated taxa in the ornamentation pattern of the cranial bones. Nevertheless, the particular bones, which bear ornamentation, are almost constant in the single taxa. Therefore, for example, the ornamentation of the nasal is a feature, which only occurs in *Pelagosaurus typus* with certainty (see appendix III). The number of teeth and vertebrae is not useful as single diagnostic feature, except of the number of cervical vertebrae, which are constant in each taxon.

As described for the teleosaurids before (e.g. AUER 1909, ANDREWS 1913, BERCKHEMER 1928, and WESTPHAL 1962) and therefore not unexpected; the dermal armour is useful for distinguishing the taxa from each other, considering the shape of the entire osteodermal shields and the shape and position of the single osteoderms.

The main differences between the five Liassic teleosaurid taxa are only partly reflected by the chosen biometric data, but they occur in specific morphological differences of particular bones, like already described for the osteodermal shield (see chapter 3, and BERCKHEMER 1928, WESTPHAL 1962). The differences are visible in the skull by, e.g. orbit shape, frontal shape, postorbital shape, supratemporal fenestra shape, and ornamentation of the cranial bones. Other differences are the shape of the internal naris, the shape of the pterygoid, the suborbital fenestra shape, the shape of the supraoccipital, the shape of the prootic, the orientation of the external naris, the incisive foramen, the size of the external mandibular fenestra and the shape and size of the prefrontal (see appendix III for a brief comparison).

Nevertheless, ontogenetic changes of specific configurations in the skull must be considered in the analysis e.g., in *Steneosaurus bollensis*, the shape of the suborbital fenestra changes from circular (Fig. 4.1) to longitudinal ellipsoid (Fig. 3.1) during ontogeny or the change of the change of frontal shape in the taxa (see chapter 4, Fig. 4.5). If the ontogenetic stage of the specimen cannot be determined, only features unaffected by ontogenetic development have to be considered.

In the postcranial, the atlas-axis complex, the shape of the bones in the pectoral and pelvic girdle, and the femur can be used for taxa differentiation (see also chapter 3 and appendix III).

Clear signs of sexual dimorphism are not noticed in the biometric values or in the morphological appearance of the Liassic thalattosuchians. Nevertheless, there are at least in

*Steneosaurus bollensi*s hints of a higher variation in particular body proportions, like skull width (C), orbital length (I) or humerus length (H1), after reaching a specific size. This specific size, here represented by a skull length larger than 400 mm, probably indicates maturity, as it is similar observed in recent crocodilians (MONTAGUE 1984). The diagrams show high scattering of the values in that area, but a clear division in two opposite lines (genders) cannot be confirmed (e.g. Diagram 2, 5, 14). Because of the missing data for the specific individual age of the specimens, any statement is very speculative. Therefore, the assumption that some characters of the observed intraspecific variation in *Steneosaurus bollensis* are results of sexual dimorphism can be neither confirmed nor denied.

Chapter 6

Phylogenetic analysis

6.1 Systematic and in-group relationships of the Thalattosuchia

The aim of the following study is to investigate the relationships inside the monophyletic group of the Thalattosuchia (BENTON & CLARK 1988, CLARK 1994).

Despite the wealth of material, the relationships among the genera and species are unclear because cladistic methodology has only insufficiently been applied to them. Here the phylogenetic in-group relationships of metriorhynchids and teleosaurids as well as their relation to the taxon *Pelagosaurus typus* are presented. In the past, these relationships only have been very rarely investigated (BUFFETAUT 1980a/b, VIGNAUD 1995) and this study presents a detailed computer-based cladistic in-group analysis in particular of the Teleosauridae for the first time. An tentative attempt to clarify the phylogenetic relationships of the Thalattosuchia was made by me (MUELLER-TÖWE 2005), but the matrix used now is modified and the phylogenetic analysis turns out to be slightly different.

Most recently, GASPARINI et al. (2006) published a phylogenetic analysis, which shows in-group relationships of the Metriorhynchidae, but considers for the Teleosauridae only *Pelagosaurus typus* and *Steneosaurus bollensis*.

According to VIGNAUD (1995), 48 valid taxa of thalattosuchians are present, but here only 25 of them were considered as sufficient preserved and described. Because of this, the following taxa were excluded: *Steneosaurus jugleri* MEYER, 1845, *Steneosaurus megistorhynchus* (GEOFFROY, 1831), *Steneosaurus larteti* (DESLONGCHAMPS, 1868), *Steneosaurus obtusidens* ANDREWS, 1909, ?*Steneosaurus* ?*deslongchampsianus* (LENNIER, 1887), *Steneosaurus* ?*rudis* SAUVAGE, 1872, and ?*Steneosaurus* ?*nowackianus* (HUENE, 1938), *Machimosaurus mosae* SAVAGE & LIENARD, 1879 , *Peipehsuchus* YOUNG, 1948, *Teleidosaurus bathonicus* (MERCIER, 1933), *Metriorhynchus palpebrosus* (PHILLIPS, 1871), *Metriorhynchus acutus* LENNIER, 1887, *Metriorhynchus geoffroyi* MEYER, 1832, *Metriorhynchus brachyrhynchus* (DESLONGCHAMPS, 1868), *Metriorhynchus potens* (RUSCONi, 1948), *?Metriorhynchus ?incertus* DESLONGCHAMPS, 1868, *?Metriorhynchus littoreus* SAUVAGE, 1874, *Dakosaurus lissocephalus* SEELEY, 1869, *Dakosaurus lapparenti* DEBELMAS & STRANNO-LOUBSKY, 1957, and *Dakosaurus* nov.sp. VIGNAUD, 1995, *Metriorhynchus casamiquelai* GASPARINI & CHONG, 1977, *Metriorhynchus westermanni* GASPARINI, 1980, and *Geosaurus araucanensis* GASPARINI & DELLAPÉ, 1976.

In total, the original matrix in this study consists therefore of 29 taxa including 2 out-group taxa *Gracilisuchus* and *Protosuchus*; 2 non-thalattosuchian, longirostrine Crocodyliformes taxa *Pholidosaurus* and *Dyrosaurus*, and 25 Thalattosuchia taxa (see appendix V). Following 25 Thalattosuchia taxa are considered: *Geosaurus giganteus* (SOEMMERING, 1816); *Geosaurus gracilis* (MEYER, 1830); *Geosaurus suevicus* (FRAAS, 1902); *Geosaurus vignaudi* FREY et al., 2002; *Machimosaurus hugii* MEYER, 1837; *Metriorhynchus superciliosus* (BLAINVILLE, 1853); *Metriorhynchus hastifer* (DESLONGCHAMPS, 1868); *Metriorhynchus leedsi* ANDREWS, 1913; *Pelagosaurus typus* BRONN, 1841; *Platysuchus multiscrobiculatus* BERCKHEMER, 1929; *Steneosaurus baroni* NEWTON, 1893; *Steneosaurus bollensis* (JAEGER, 1828); *Steneosaurus boutilieri* (EUDES-DESLONGCHAMPS, 1868); *Steneosaurus brevior* (BLAKE, 1876); *Steneosaurus edwardsi* (EUDES-DESLONGCHAMPS, 1868)*; Steneosaurus gracilirostris* WESTPHAL, 1961; *Steneosaurus heberti* GLASVILLE, 1876; *Steneosaurus leedsi* ANDREWS, 1909 (including *Myceterosaurus natus* after VIGNAUD 1995); *Steneosaurus megarhinus* (HULKE, 1871); *Steneosaurus obtusidens* ANDREWS, 1909; *Steneosaurus priscus* (SOEMMERING, 1814); *Teleidosaurus calvadosi* DESLOMGCHAMPS, 1866; *Teleidosaurus gaudryi* COLLOT, 1905; *Teleosaurus cadomensis* LAMOUROUX, 1820, and *Teleosaurus geoffroyi* DESLONGCHAMPS, 1868.

6.2 Method

The phylogenetic analysis was performed with PAUP 4.0 b 10 (SWOFFORD 2003). The original data matrix consists of 29 taxa (see above), and in total 189 characters were used in the analysis (see appendix V). The first 136 characters and coding were taken from CLARK (1994), TYKOSKI et al. (2002), and POL & NORELL (2004) but were modified if necessary (see appendix IV and V). Additionally, 53 new, personally defined characters were added. The data matrix, character list, and full coding are found in the appendices IV-VI. The character codes for 21 taxa were determined by personal examinations of original material and by data from the literature, whereas the character codes for the remaining taxa derived from the literature only (appendix IV). Due to the large size of the data matrix, the heuristic search option with random stepwise addition and tree-bisection-reconnection (TBR) was used. Character optimisation was accelerated (ACCTRAN) or delayed (DELTRAN). All characters were unordered and not weighted, multi-state characters were treated as polymorph. 37 characters proved to be constant during the analysis, additionally 37 characters were parsimony-uninformative, therefore the remaining 115 characters entered into the analysis as parsimony-informative.

The here presented consensus trees are derived from 123 equally parsimonious trees (tree length 423) under DELTRAN character optimisation with a consistency index (CI) of 0.6312, homoplasy index (HI) of 0.5414, retention index (RI) of 0.6549, and a rescaled consistency index (RI) of 0.4134 (Fig. 6.1 & Fig. 6.2). Figure 6.1 shows the consensus tree calculated after the 50% majority rule and figure 6.2 shows the strict consensus tree derived from 123 equally parsimonious trees. The results under DELTRAN character optimisation were chosen to be presented here, because it assumes that a change in character state occurs at the latest possible location on the cladogram, leading to the more conservative diagnoses than the ACCTRAN option. The DELTRAN option is generally used in analyses of palaeontological data (SANDER 2000).

6.3 Phylogenetic analysis

6.3.1 Analysis 1 (Fig. 6.1 & Fig. 6.2)

In the following each node within the Thalattosuchia will be described, including a list of the most important synapomorphies, if not noted otherwise, the description represents the analysis under DELTRAN character optimisation. Unambiguous synapomorphies occur both under ACCTRAN and DELTRAN character optimisation.

All analyses confirm a distinct separation between the Metriorhynchidae and the Teleosauridae. The teleosaurids and the metriorhynchids turned out to be monophyletic sister-groups as expected (BENTON & CLARK 1988, CLARK 1994).

The monophyly of the Teleosauridae (node ***1***) is supported by the following six unequivocal characters, which are also unambiguous synapomorphies: A sculptured lateral surface of the postorbital bar (character 25, consistency index (ci) = 0.5, coded 0), the postorbital bar is transversely flattened (character 26, ci = 0.25, coded 0), the dorsal end of the postorbital bar broads dorsally, continuous with the dorsal part of the postorbital (character 30, ci = 0.333, coded 0), the basisphenoid is exposed on the ventral surface of the braincase (character 56, ci = 0.333, coded 0), a transversely expanded dentary, almost as wide as high (character 108, ci = 0.5, coded 1), and slender, conical, pointed and apically recurved teeth (character 182, ci = 0.667, coded 0).

Pelagosaurus typus, which is assumed basal to the Teleosauridae and the Metriorhynchidae (BENTON & CLARK 1988, CLARK 1994, BUCKLEY et al. 2000), occupies here basal position within the teleosaurids. It shows a stable sister-group relationship with all other remaining teleosaurids. The taxon is supported by following six unambiguous unequivocal autapomorphies: The dorsal, primary head of the quadrate articulates with the squamosal, otoccipital, and the prootic (character 47, ci=0.25, coded 0), the choana is partly

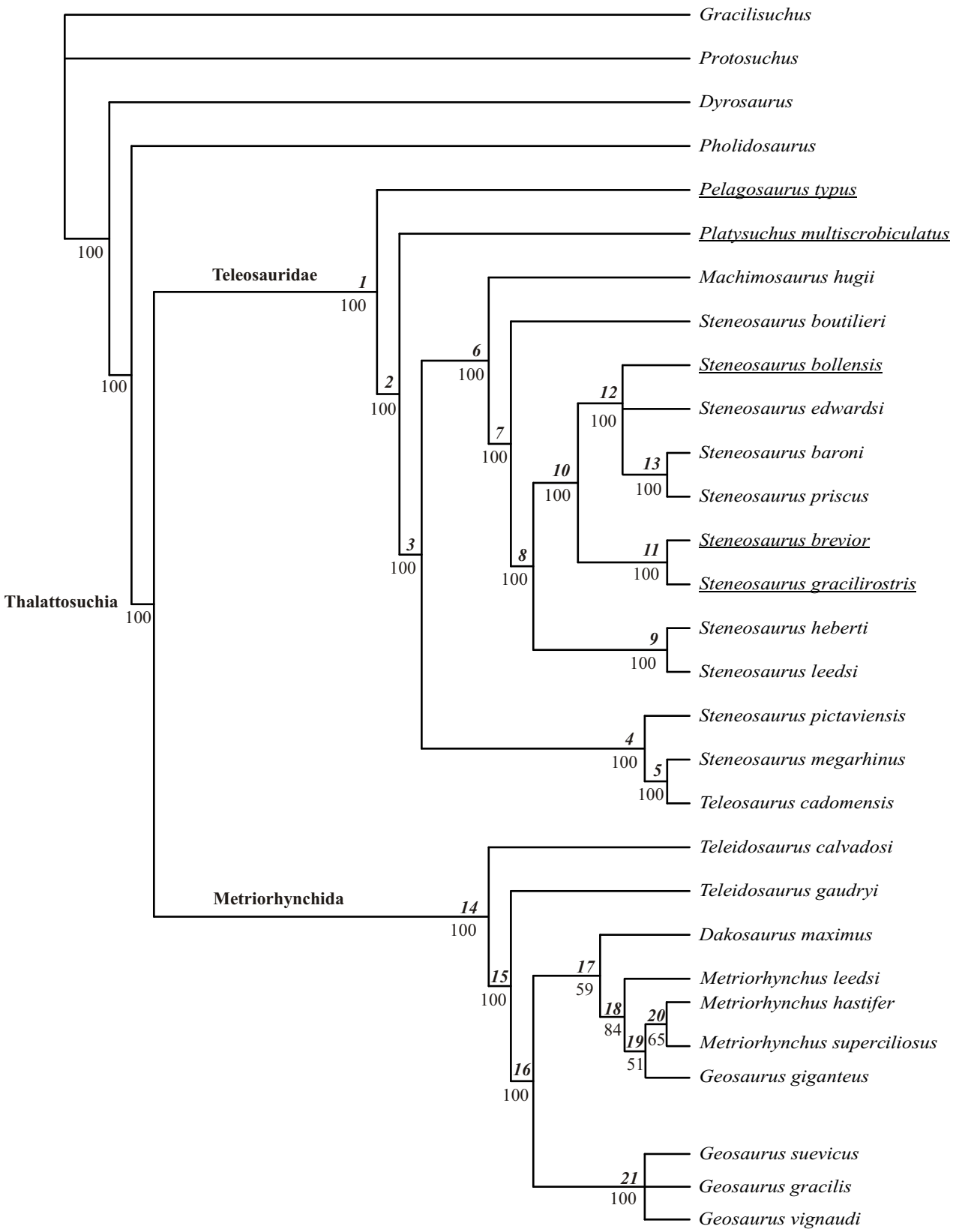

Figure 6.1: The 50% majority rule consensus tree was calculated after 123 equally parsimonious trees (tree length 423) with a consistency index (CI) of 0.6312, homoplasy index (HI) of 0.5414, retention index (RI) of 0.6549, and a rescaled consistency index (RI) of 0.4134. The matrix consists of 29 taxa. In total 189 characters were used in the analysis and 115 characters entered into the analysis as parsimony-informative. Character optimisation was DELTRAN. The Liassic taxa are underlined. The nodes are numbered in italics and described with the appending percentages of appearance.

divided by a midline ridge (character 69, ci=0,667, coded 2), osteoderms without longitudinal keels on the dorsal surface (character 101, ci=1.0, coded 1), the dorsal surface of the nasals is sculptured (character 137, ci=0.667, coded 0), in posterior view is the supraoccipital rhombic shaped and fused (character 144, ci=0.75, coded 2), and the ventral armour consist of four longitudinal rows (character 162, ci=1, coded 1). One additional unequivocal character only occurs under DELTRAN character optimisation: The distal end of the pubis is paddle-shaped (character 156, ci=0.667, coded 0).

The next node (***2***) consists of a sister-group relationship between *Platysuchus multiscrobiculatus* and all other remaining teleosaurids. The node is diagnosed by the following eight unambiguous unequivocal synapomorphies: The rostrum is wider than high (character 3, ci=0.625 coded 2), the premaxilla is anterior the nares similar in breadth to the lateral part to the nares (character 5, ci=0.25, coded 1), the anterior and posterior scapula edges are dorsally narrow with straight edges (character 82, ci=0.667, coded 2), the coracoid is (sub)equal in length to the scapula (character 83, ci=0.6, coded 1), the tail is completely surrounded by osteoderms (character 99, ci=1, coded 1), the orbits are dorsally aligned (character 149, ci=0.667, coded 1), the axis possesses only one parapophysis for the second cervical rib (character 171, ci=1, coded 1), and the prefrontal is about half size of the lacrimal (character 178, ci=0.75, coded 0).

The following three unambiguous unequivocal autapomorphies support the taxon *Platysuchus multiscrobiculatus*: The postorbital possesses a well-developed long, acute anterolateral process (character 28, ci=0.4, coded 1), the proximal end of the femur possesses a well-developed head (character 157, ci=0.5, coded 0), and the ilium shape is mainly rectangular with a well-developed posterodorsal and anterodorsal process (character 183, ci=0.667, coded 0).

The next node (***3***) consists of a sister-group relationship of a branch comprising two *Steneosaurus* taxa together with *Teleosaurus cadomensis* and the branch with the remaining *Steneosaurus* taxa together with *Machimosaurus hugii*. There is only one unambiguous unequivocal synapomorphy found which support this node: The external surface of the cranial bones is slightly grooved (character 1, ci=0.333, coded 1). Under DELTRAN character optimisation, following three equivocal synapomorphies are also found: The ventromedial part of the quadrate does not contact the otoccipital (character 51, ci=0.25, coded 0), Ilium possesses no posterior process (character 84, ci=0.6, coded 2), and the dorsal osteoderms develop a longitudinal keel level with or posterior to the pelvic girdle (character 163, ci=1, coded 1). Under ACCTRAN character optimisation, following three equivocal

synapomorphies are found: The jugal is excluded from the lateral margin of the orbit or only slightly participating (character 139, ci=0.333, coded 1), half of the tail is covered with dorsal osteoderms (character 161, ci=0.75, coded 2) and the maxillary teeth possess one smooth carina (character 179, ci=0.857, coded 1).

In the present analysis, *Steneosaurus pictaviensis* occurs repeatedly in a direct sister-group relation with *Teleosaurus cadomensis* and *Steneosaurus megarhinus*. This branch forms a sister-group to all other *Steneosaurus* taxa and *Machimosaurus hugii*. The node (***4***) places *Steneosaurus pictaviensis* in a sister-group relationship with *Steneosaurus megarhinus* and *Teleosaurus cadomensis*. This node (***4***) is supported by the following three unambiguous synapomorphies: The choanal opening continues with the pterygoid ventral surface expect for anterior and anterolateral borders (character 39, ci=0.333, coded 0), the posterior surface of the supraoccipital shows bilateral posterior prominences (character 64, ci=1, coded 1), and a round choana shape (character 141, ci=0.833, coded 0).

The taxon *Steneosaurus pictaviensis* is diagnosed by the following three unequivocal unambiguous autapomorphies: The depression on the primary pterygoidean palate posterior to choana is wider than the palatine bar (character 42, ci=0.5, coded 1), the basisphenoid rostrum (cultriform process) is slender (character 53, ci=1, coded 0), and the orbits are ellipsoid (character 150, ci=0.4, coded 1).

The dichotomy (***5***) between *Teleosaurus cadomensis* and *Steneosaurus megarhinus* is supported by only one unambiguous unequivocal synapomorphy: The prefrontals are relatively short and broad, oriented posteromedially-anterolaterally in the skull (character 122, ci=0.333, coded 1). Under DELTRAN character optimisation one additional equivocal synapomorphy is found: It possesses four premaxilla teeth (character 169, ci=0.778, coded 1). Under ACCTRAN character optimisation the characters 2, 41, 50, 59, 136, 142, and 173 are reported as equivocal synapomorphies, too.

The taxon *Teleosaurus cadomensis* is supported by one unambiguous unequivocal autapomorphy: The shape of the alveoli in the maxilla is ellipsoid (character 177, ci=0.2, coded 1). Under DELTRAN character optimisation, additionally a couple of equivocal autapomorphies occur: 2, 22, 31, 38, 41, 50, 59, 131, 136, 139, 142, 173, and 175.
The taxon *Steneosaurus megarhinus* is only weakly supported by one equivocal autapomorphy: The external naris is anterior aligned (character 146, ci=0.5, coded 2). Under ACCTRAN character optimisation, no autapomorphies are found.

The next node (***6***) comprises the remaining *Steneosaurus* taxa and *Machimosaurus hugii*. Only one unambiguous unequivocal synapomorphy support this node: The number of

teeth in the maxilla is between twenty-one and thirty (character 170, ci=0.583, coded 2). Under DELTRAN character optimisation, two-more equivocal synapomorphies are found: The jugal is excluded from the lateral margin of the orbit or only slightly participating (character 139, ci=0.333, coded 0) and the teeth in the maxilla possess one smooth carina (character 179, ci=0.857, coded 1). Under ACCTRAN character optimisation, two other equivocal synapomorphies are reported: The dorsal osteoderms possess a well-developed process located anterolaterally (character 96, ci=0.8, coded 2) and large pits in dense surface distribution cover the dorsal osteoderms (character 164, ci=1, coded 1).

Within the Teleosauridae, *Machimosaurus hugii* proves to be consistently the sister taxon to all *Steneosaurus* taxa, excluding *Steneosaurs megarhinus* and *Steneosaurus pictaviensis*, which fall with *Teleosaurus cadomensis* (see above). The taxon *Machimosaurus hugii* is well supported by 11 unambiguous unequivocal autapomorphies: The rostrum narrow anterior to the orbits, broading abruptly at orbits (character 2, ci=0.25, coded 0), premaxilla narrow anterior to naris (character 5, ci=0.25, coded 0), external naris facing anterior (character 6, ci=0.556, coded 0), dorsal primary head of quadrate articulates with squamosal, otoccipital and prootic (character 47, ci=0.25, coded 0), quadrate, squamosal, and otoccipital meet broadly lateral to cranioquadrate canal (character 49, ci=0.5, coded 2), pterygoid ramus of quadrate with deep groove along ventral edge(character 50, ci=0.25, coded 1), basisphenoid virtually excluded from the ventral surface of the braincase by pterygoid and basioccipital (character 56, ci=0.333, coded 1), otoccipital with lateral flange descending ventral to the subcapsular process (character 58, ci=0.333, coded 1), the anterior ilium process is one-quarter or less the length of the posterior process (character 84, ci=0.6, coded 1), the choana is ellipsoid (character 141, ci=0.833, coded 2), the teeth are blunt and broad (character 182, ci=0.667, coded 1).

The next node (***7***) comprises all remaining *Steneosaurus* taxa. Two unambiguous unequivocal synapomorphies diagnose this dichotomy: An incisive foramen is present (character 148, ci=0.5, coded 0) and the orbits are ellipsoid (character 150, ci=0.75, coded 1). The taxon *Steneosaurus boutilieri,* which is in this dichotomy the sister taxon to all remaining *Steneosaurus* taxa, is diagnosed by two unambiguous unequivocal autapomorphies as well: The supraoccipital is paired in posterior view (character 144, ci=0.75, coded 0) and the alveoli in the maxilla are mainly laterally aligned (character 186, ci=0.5, coded 1).

The next node (***8***) comprises the remaining *Steneosaurus* taxa and is characterized by only one unambiguous unequivocal synapomorphy: The postorbital has a well-developed elongated anterolateral process (character 28, ci=0.4, coded 1). Additionally, under

DELTRAN character optimisation two more equivocal synapomorphies are reported: The dorsal osteoderms possess a well-developed anterolateral process (character 96, ci=0.8, coded 2) and the size of the calcaneum is nearly double the size of the astragalus (character 159, ci=0.5, coded 1).

The Upper Jurassic taxa *Steneosaurus leedsi* from England and *Steneosaurus heberti* from France occur constantly as sister groups, which fits well with their stratigraphic background. This node (***9***) is characterized only by one unambiguous unequivocal synapomorphy: The number of teeth in the maxilla is more than forty (character 170, ci=0.583, coded 4). Under ACCTRAN character optimisation, three additional equivocal synapomorphies are reported: The proximal edge of the scapula is smaller than its distal edge (character 153, ci=0.667, coded 2), four premaxilla teeth (character 169, ci=0.778, coded 1), and the ratio of humerus length to femur length is less than 54% (character 187, ci=0.5, coded 2). Under DELTRAN character optimisation, the taxon *Steneosaurus leedsi* is supported by the following three equivocal autapomorphies: Character 153, character 169, and character 187 all already described before under the additional ACCTRAN characters for the dichotomy (see there). *Steneosaurus heberti* is only defined by missing these characters. Under ACCTRAN character optimisation, the taxa *Steneosaurus leedsi* and *Steneosaurus heberti* do not show any autapomorphies.

The next node (***10***) comprises the three Liassic *Steneosaurus* taxa with *Steneosaurus baroni* and *S. edwardsi* and is characterized by three unambiguous unequivocal synapomorphies: the posterior pterygoid flanges are well developed with broad quadrate contact (character 142, ci=0.333, coded 0), the lateral pterygoid processes are not flexed posteriorly (character 143, ci=0.5, coded 0), and the number of teeth in the dental is between twenty-one and thirty (character 184, ci=0.667, coded 1). Under DELTRAN character optimisation, one additional unequivocal synapomorphy is found: the symphysis angle is more than 50° (character 152, ci=0.5, coded 1), this character appears also under ACCTRAN character optimisation but only as an equivocal synapomorphy.

The Liassic taxa *Steneosaurus brevior* and *Steneosaurus gracilirostris* occur repeatedly in a sister-group relationship, which fits well with the stratigraphic background (Yorkshire Lias). However, the dichotomy (***11***) is weakly supported by two unambiguous unequivocal synapomorphies: The external naris are facing anterolaterally (character 6, ci=0.556, coded 0), the fused external naris is anterior aligned (character 146, ci=0.5, coded 2), and an incisive foramen is absent in dorsal view (character 148, ci=0.5, coded 1).

The taxon *Steneosaurus brevior* is supported by two unambiguous unequivocal autapomorphies: the dorsal surface of the frontal and parietal has a narrow midline ridge (character 22, ci=0.667, coded 1) and the depression on the primary pterygoidean palate posterior to the choana is wider than the palatine bar (character 42, ci=0.5, coded 1). Under DELTRAN character optimisation two additional equivocal autapomorphies are found: The choana is partly divided by a midline ridge (character 69, ci=0.667, coded 2) and the orbits are round (character 150, ci=0.4, coded 0).

The taxon *Steneosaurus gracilirostris* is well supported by eight unambiguous unequivocal autapomorphies: The rostrum is higher than wide or nearly tubular (character 3, ci=0.625, coded (01)), the premaxilla narrow anterior to the naris (character 5, ci=0.25, coded 0), jugal forms large part of the lateral margin of the orbit (character 139, ci=0.333, coded 0), orbits are laterally aligned (character 149, ci=0.667, coded 0), the number of teeth in the maxilla is more than forty (character 170, ci=0.583, coded 4), the shape of the supratemporal fenestra is mainly ellipsoid (character 174, ci=0.333, coded 0), the ratio of rostral length to skull length is more than 75% (character 175, ci=0.8, coded 2), and the number of teeth in the dental is more than forty (character 184, ci=0.667, coded 3).

The next node (***12***) comprises *Steneosaurus bollensis*, *S. edwardsi*, *S. priscus*, and *S. baroni*. This node (***12***) is supported by only one unambiguous unequivocal character: The dorsal primary head of the quadrate articulates with the squamosal, the otocipital and the prootic (character 47, ci=0.25, coded 0). Under ACCTRAN character optimisation it is additionally supported by an unequivocal synapomorphy: The external naris possesses equal width and length (character 147, ci=0.5, coded 1).

In the presented consensus trees (strict & 50% majority rule) the taxa *S. bollensis* and *S. edwardsi* fall, together with the *Steneosaurus baroni* - *S. priscus* dichotomy (***13***), in an unsolved polytomy.

Steneosaurus edwardsi is supported by the following unambiguous unequivocal autapomorphy: The prefrontals are narrow and long (character 111, ci=0.667, coded 2).

The taxon *Steneosaurus bollensis* is under DELTRAN character optimisation supported by one unequivocal autapomorphy: The symphysis angel is less than 50° (character 152, ci=0.5, coded 0). Additionally, six equivocal autapomorphies are found: the supraoccipital is rhombic and fused in posterior view (character 144, ci=0.75, coded 0), the coracoid shaft is about the same width as the scapula shaft (character 154, ci=0.6, coded 1), pubis distal part is paddle-shaped (character 156, ci=0.667, coded 0), the dorsal armour begins at the level of the fourth vertebra (character 166, ci=1, coded 1), and the cervical vertebrae have a reduced

midline ridge in ventral view (character 172, ci=1, coded 1). Under ACCTRAN character optimisation, one unequivocal autapomorphy is found: The ventral osteoderms are rhombic (character 165, ci=1, coded 1). Additionally, one more equivocal autapomorphy is found, which appears as unequivocal under DELTRAN conditions, too: The symphysis angel is less than 50° (character 152, ci=0.5, coded 0).

The dichotomy (***13***) of *Steneosaurus priscus* and *Steneosaurus baroni* is characterized by two unambiguous unequivocal synapomorphies: The ventromedial part of the quadrate contacts the otoccipital to enclose carotid artery and form passage for cranial nerves IX-XI (character 51, ci=0.25, coded 1) and the prefrontal is short and broad, orientated posteromedially-anterolaterally in the skull (character 122, ci=0.333, coded 1).

The taxon *S. baroni* is characterized by one unambiguous unequivocal autapomorphy: The number of teeth in the dental is between thirty-one and forty (character 184, ci=0.667, coded 2).

The taxon *S. priscus* possess under DELTRAN character optimisation only one equivocal autapomorphy: It possesses eight cervical vertebrae (character 160, ci=0.75, coded 1). Under ACCTRAN character optimisation, no autapomorphies are reported.

The monophyly of the Metriorhynchidae (node ***14***) is supported by the following four unequivocal characters (only under DELTRAN character optimisation): The external surface of the cranial bones is only slightly grooved (character 1, ci =0.333, coded 1), the dorsal edge of the surangular is arched dorsally (character 74, ci = 0.5, coded 1), the snout is relatively broad and shorter than the remainder of the skull (character 122, ci = 0.333, coded 1), and the prefrontal lateral edge is convex and overlaps the orbit (character 188, ci =1, coded 1). Under ACCTRAN character optimisation, unequivocal synapomorphies are not found. The only equivocal synapomorphy, which is found under both character optimisations is character 174, which describe the shape of the supratemporal fenestra here as mainly rectangular (ci = 0.333, coded 1).

The taxon *Teleidosaurus cadomensis* falls in a sister group relation ship with all remaining metriorhynchids. It is characterized by the following three unambiguous unequivocal autapomorphies: the external naris is facing anterolaterally or anterior (character 6, ci=0.556, coded 0), the supratemporal fenestra is as long as broad (character 173, ci=0.333, coded 1), and the size of the prefrontal is half the size of the lacrimal (character 178, ci=0.75, coded 0).

The next node (***15***) comprises all remaining metriorhynchids and is diagnosed by two unequivocal synapomorphies (only under DELTRAN character optimisation): the lacrimal contacts the nasal on medial and anterior edges (character 12, ci=0.333, coded 1) and the orbits are ellipsoid (character 150, ci=0.4, coded 1). The only synapomorphy, which is found under both character optimisations is that the quadrate, squamosal and otocipital enclose together the cranioquadrate canal near the lateral edge of the skull (character 49, ci=0.5, coded 1). Additionally, following equivocal synapomorphies are found under DELTRAN character optimisation: The anterior part of the jugal is as broad as the posterior part (character 17, ci=0.5, coded 0), osteoderms absent from ventral part of the trunk (character 100, ci=0.5, coded 0), no armour at the tail (character 161, ci= 0.75, coded 3), and dorsal armour absent (character 189, ci=1, coded 1).

The taxon *Teleidosaurus gaudryi* falls in a sister group relation ship with all remaining metriorhynchids and is diagnosed by one unambiguous unequivocal autapomorphy: The antorbital fenestra is much smaller than the orbit (character 67, ci=0.75, coded 2). One other equivocal autapomorphy occurs as well under DELTRAN as under ACCTRAN character optimisation: The shape of the alveoli in the maxilla is ellipsoid (character 177, ci=0.2, coded 1).

The next node (***16***) comprises the remaining metriorhynchids, excluding the genus *Teleidosaurus*. This node is characterized by two unequivocal synapomorphies (only under DELTRAN character optimisation): The postorbital bar is transversely flattened (character 26, ci=0.25, coded 0) and the size of the prefrontals are double or more the size of the lacrimals (character 178, ci=0.75, coded 2). Both synapomorphies appears also under ACCTRAN conditions as equivocal synapomorphies. Additionally, there are four equivocal synapomorphies, which are found both under DELTRAN and ACCTRAN character optimisation: A mandibular fenestra is absent (character 75, ci=1, coded 1), the ilium possesses no posterodorsal process (character 84, ci=0.6, coded 2), lateral bar of supratemporal fenestra is thin in dorsal view (character 138, ci=0.333, coded 1), and a sclerotic ring is present in orbit (character 168, ci=0.5, coded 0).

The next node (***17***) is only present in the 50% majority rule consensus tree (59%); it comprises *Dakosaurus maximus,* the three *Metriorhynchus* taxa, and Geosaurus *giganteus*. It is diagnosed by one unambiguous unequivocal synapomorphy: the teeth are laterally compressed (character 116, ci=1, coded 1). Under ACCTRAN character optimisation twenty-one additional equivocal synapomorphies are found for this node, under DELTRAN condition only one additional equivocal synapomorphy occurs: The shape of the alveoli in the maxilla is

ellipsoid (character 177, ci=0.2, coded 1). In the strict consensus, this node turns out as an unsolved polytomy of these taxa. However, in the consensus tree after the 50% majority rule *Dakosaurus maximus* turns out as a sister to all the remaining taxa (node ***17***).

Dakosaurus maximus is characterized by the following seven unambiguous unequivocal autapomorphies: The premaxilla is anterior similar in breadth than at its lateral margin (character 5, ci=0.25, coded 1), the basioccipital des not possess well-developed bilateral tuberosities (character 57, ci=0.5, coded 0), the splenial is not involved in the symphysis (character 77, ci=0.8, coded 0), the teeth are serrated (character 104, ci=1, coded 1), the lateral surface of the dentary shows a longitudinal groove (character 109, ci=0.5, coded 1), the external naris is wider than long (character 147, ci=0.5, coded 0), and orbits are open dorsally (character 149, ci=0.5, coded 1).

The monophyly of the taxon *Metriorhynchus* within the Metriorhynchidae is not confirmed. The next node (***18***) is only present in the 50% majority rule consensus tree (84%) comprises the three *Metriorhynchus* taxa and *Geosaurus giganteus*. It is characterized by the following unequivocal synapomorphies (under DELTRAN character optimisation): A robust splenial posterodorsal to the symphysis (character 110, ci = 0.5, coded 1), the anterior margin of the choana is rectangular (character 141, ci = 0.83, coded 3). Under ACCTRAN character optimisation, no unequivocal characters are found, only two equivocal synapomorphies support this node here: The shape of the supratemporal fenestra is mainly ellipsoid (character 174, ci=0.333, coded 0) and the teeth in the maxilla possess one smooth cutting edge (carina) (character 179, ci=0.857, coded 1).

The taxon *Metriorhynchus leedsi* turns out as a sister to the remaining *Metriorhynchus* taxa and *Geosaurus giganteus* and is supported by one unambiguous unequivocal autapomorphy: The external surface of the cranial bones is smooth (character 1, ci=0.333, coded 0). Additionally, occur under both character optimisations the character 170 (ci=0.583, coded 3), which means that the number of teeth in the maxilla is between twenty-one and thirty. Under DELTRAN character optimisation, one additional equivocal autapomorphy occurs: A prearticular is present (character 72, ci=0.5, coded 0).

In the 50% majority rule consensus tree *Geosaurus giganteus* falls with 51% (node ***19***) in a sister group relationship to the taxa, *Metriorhynchus hastifer* and *M. superciliosus*, which fall with 65% together in a dichotomy (node ***20***) .

The taxon *Geosaurus giganteus* is supported by the following four unambiguous unequivocal apomorphies: The rostrum is higher than wide (character 3, ci=0.625, coded 0), the postorbital bar is cylindrical (character 26, ci=0.25, coded 1), transversely expanded

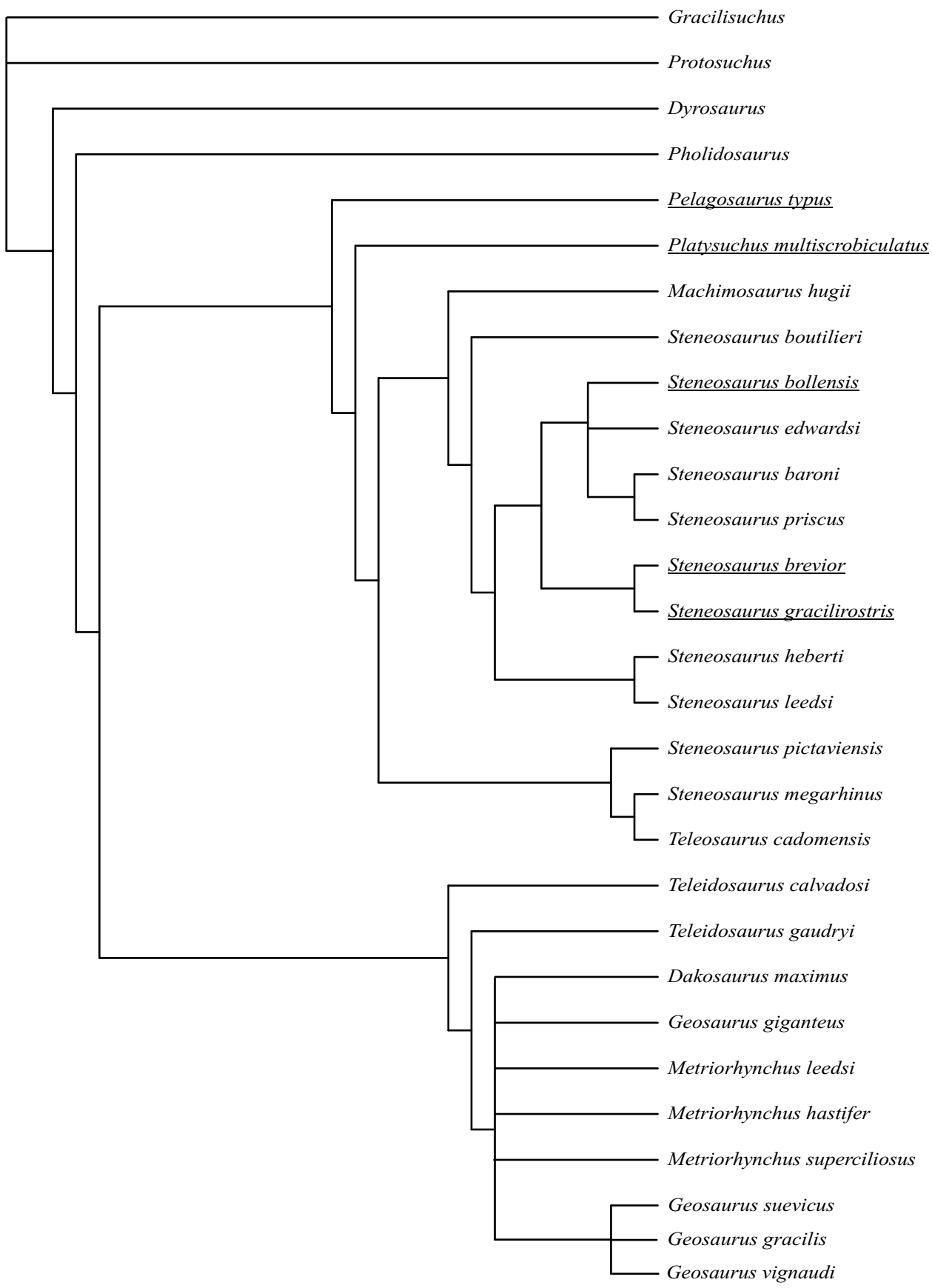

Figure 6.2: The strict consensus tree derived from 123 equally parsimonious trees (tree length 423) with a consistency index (CI) of 0.6312, homoplasy index (HI) of 0.5414, retention index (RI) of 0.6549, and a rescaled consistency index (RI) of 0.4134. The matrix consists of 29 taxa. In total 189 characters were used in the analysis and 115 characters entered into the analysis as parsimony-informative. Character optimisation was DELTRAN. The Liassic taxa are underlined.

dentary, almost wide as high (character 108, ci=0.5, coded 1), and the orbits are round (character 150, ci=0.4, coded 0).

*Metriorhynchus hastife*r and *Metriorhynchus superciliosus* fall together as sister taxa (node ***20***). This node is diagnosed (with 65%) by the unequivocal synapomorphy, that the lacrimal contacts the nasal along the medial edge only (character 12, ci=0.333, coded 0).

The taxon *Metriorhynchus hastifer* is characterized by one unambiguous unequivocal autapomorphy: The shape of the alveoli in the maxilla is round (character 177, ci=0.2, coded 0).

The taxon *Metriorhynchus superciliosus* is supported by one unambiguous unequivocal autapomorphy: The coracoid length is equal in size or bigger than the scapula length (character 83, ci=0.6, coded (12)). Additionally, occur following equivocal apomorphies under DELTRAN character optimisation: The dorsal surface of the nasal is sculptured (character 137, ci=0.667, coded 0), the maxilla bears twenty-one to thirty teeth (character 170, ci=0.583, coded 2).

In the present consensus trees, *Geosaurus gracilis* falls with *Geosaurus vignaudi* and *Geosaurus suevicus* in an unsolved polytomy (node ***21***). This node (***21***) is characterized by the following three unequivocal synapomorphies (under DELTRAN character optimisation): The dorsal end of the postorbital bar broads dorsally, continuous with the dorsal part of the postorbital (character 30, ci = 0.333, coded 0), the retroarticular process is very short and robust (character 71, ci = 0.667, coded 1), and Geosaurus possesses slender, conical, pointed and apically recurved teeth (character 182, ci = 0.667, coded 0). Under the ACCTRAN character optimisation, unequivocal synapomorphies are not found, but the node is supported by about twenty equivocal synapomorphies.

The taxon *Geosaurus vignaudi* is diagnosed with the following two unambiguous unequivocal autapomorphies: The postorbital possesses a well-developed elongated anterolateral process (character 28, ci=0.4, coded 1), and the lateral surface of the dentary is marked with a longitudinal groove (character 109, ci=0.5, coded 1).

The taxon *Geosaurus gracilis* is characterized by the following five unambiguous unequivocal autapomorphies: The rostrum is higher than wide (character 3, ci=0.625, coded 0), the lacrimal contacts the nasal along the medial edge only (character 12, ci=0.333, coded 0), the posterodorsal corner of the squamosal possesses an unsculptured “lobe” (character 35, ci=1, coded 1), antorbital fenestra about half the diameter of the orbit (character 67, ci=0.75, coded 1), and orbits round (character 150, ci=0.4, coded 0). The taxon *Geosaurus suevicus* is characterized by three unambiguous unequivocal autapomorphies: The external surface of the

cranial bones is smooth (character 1, ci=0.333, coded 0), teeth in the maxilla are twenty-one to thirty (character 170, ci=0.583, coded 2), and the teeth in the maxilla possess two smooth carinae (character 179, ci=0.857, coded 2). Additionally, three apomorphies occur under DELTRAN character optimisation, which occur under ACCTRAN conditions as well: a premaxilla bar dorsally separates the external naris (character 6, ci=0.556, coded 2), coracoid shaft is thinner than the scapula shaft (character 154, ci=0.6, coded 2), and scapula smaller than coracoid (character 180, ci=0.75, coded 2).

6.3.2 Analysis with an additional all-0-ancestor (Fig. 6.3 & Fig. 6.4)

To confirm the analysis 1 (described above), a second analysis was performed, using an additional hypothetical all-0-ancestor as out-group. A heuristic search option with random stepwise addition, and DELTRAN character optimisation was used again. As out-group is only the hypothetical all-0-ancestor ("Ancestor") defined. The data matrix consist therefore now of 30 taxa (including the hypothetical ancestor). Of the used 189 characters, now only 31 characters turn out to be constant and 28 to be parsimony-uninformative. The remaining 130 characters entered in the analysis as parsimony-informative. All other settings are the same as described for analysis 1 (see paragraph 6.2 "methods"). The number of saved trees increases from 123 to 1214 equally parsimonious trees. The 50% majority rule consensus tree shows still the monophyletic clades of the Metriorhynchidae and the Teleosauridae, whereas the strict consensus tree shows only the Metriorhynchidae, as a monophyletic clade and the Teleosauridae appear paraphyletic. In the strict consensus tree, *Pelagosaurus typus* appears together with the other teleosaurids in an unsolved polytomy. The dichotomy of *Steneosaurus brevior* and *Steneosaurus gracilirostris* is stable as well as the dichotomy of *Steneosaurus leedsi* and *Steneosaurus heberti*. Within the metriorhynchids *Teleidosaurus cadomensis* falls still as a sister group to all remaining metriorhynchids. The remaining taxa turn out in an unsolved polytomy.

However, in the 50% majority rule consensus tree, the addition of an all-0-ancestor has only a slight effect at the in-group relationships of the teleosaurids. The main difference to analysis 1 is that, *Platysuchus multiscrobiculatus* falls now repeatedly within the branch of *Teleosaurus cadomensis* and the branch of the remaining Teleosauridae, but in the 50% majority rule consensus trees the polytomy between them is not solved. The relationships within the Metriorhynchidae are not as stable as the turned out before (analysis 1).

The other obvious difference is that *Teleidosaurus gaudryi* falls here together with *Dakosaurus maximus* and the group of the *Metriorhynchus* taxa and *Geosaurus giganteus* in an unsolved polytomy.

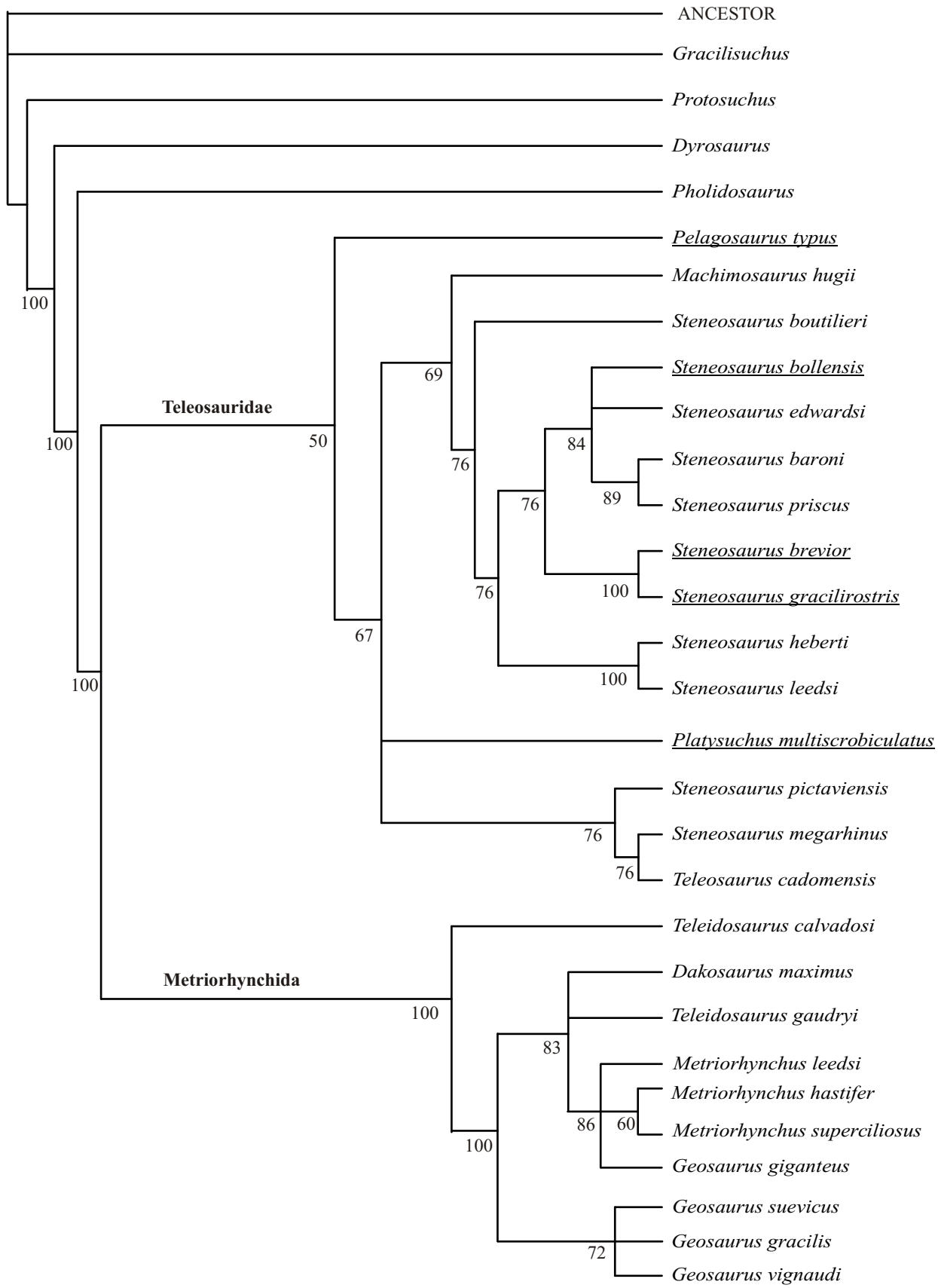

Figure 6.3: The 50% majority rule consensus tree was calculated after 1214 equally parsimonious trees (tree length 453) under DELTRAN character optimasition, with CI = 0.6159, HI = 0.5475, RI = 0.6686, and RC = 0.4118. The matrix consists of 30 taxa including now the hypothetical all-0-ancestor as out group.189 characters were coded, 130 remained as parsimonious-informative in the analysis. The Liassic taxa are underlined. The nodes are described with the appending percentages of appearance.

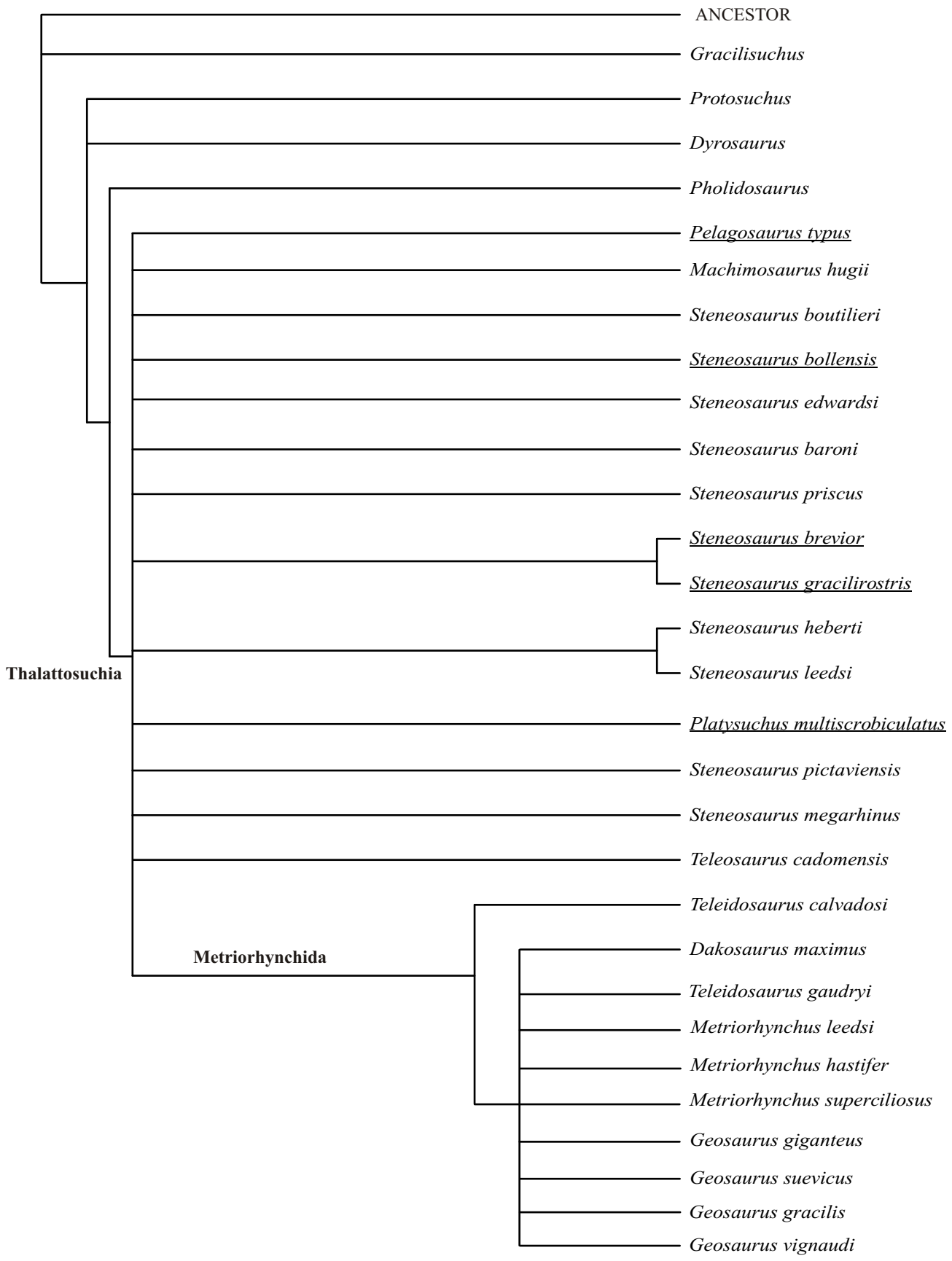

Figure 6.4: The strict consensus tree derived from 1214 equally parsimonious trees (tree length 453), under DELTRAN character optisimation, with CI = 0.6159, HI = 0.5475, RI = 0.6686, and RC = 0.4118. The matrix consists of 30 taxa including now the hypothetical all-0-ancestor as out group. 189 characters were coded, 130 remained as parsimonious-informative in the analysis. The Liassic taxa are underlined.

6.3.3 Bootstrap analysis

Different Bootstrap analyses of the Analysis 1 were attempted. The first bootstrap analysis was performed under the heuristic search option, but broke down after about 6 weeks running time without any result. The second bootstrap analysis performed under the fast step search option, took for 100 replicas only 12 seconds, but resulted only in an unsolved polytomy for all Thalattosuchia (50% majority rule). A higher number of replicas (10 000) was performed as well. It took about five minutes and came to the same result. *Gracilisuchus* and *Protosuchus* remained as out-groups (98%), and *Dyrosaurus* and *Pholidosaurus* as sister-group (58%) to the Thalattosuchia.

A possible explanation is that the data matrix possesses a high number of "?", coding the unknown character stage of the taxa. It is assumed that the high number of unknown character stages influenced the bootstrap analysis and is therefore responsible for the unsolved polytomy of the Thalattosuchia here.

6.4 Discussion

The in-group relationships of the Thalattosuchia had not been studied with the help of the computer before. Because of this, the results will be mainly discussed in comparison with the Linnaean systematic suggests by VIGNAUD (1995) for the thalattosuchians. Only the status of *Pelagosaurus typus* (BENTON & CLARK 1988, CLARK 1994) was discussed based on a cladistic analysis before. Most recently, GASPARINI et al. (2006) present a phylogenetic analysis where *Steneosaurus bollensis* and *Pelagosaurus typus* together form a sister group to the Metriorhynchidae. In the following, the phylogenetic relationships of the Liassic thalattosuchians on the base of the present cladistic analysis are discussed in particular, as well as the relationships inside the genus *Steneosaurus*. Furthermore, a brief discussion of the relationships within the metriorhynchids is given.

6.4.1 The status of *Pelagosaurus typus*

In general, *Pelagosaurus* including the only existing taxon *Pelagosaurus typus* is in a basal position with the Metriorhynchidea and the Teleosauridea (BENTON & CLARK 1988, CLARK 1994). Nevertheless, according to BUFFETAUT (1980a, 1982) *P. typus* belongs very likely to the Metriorhynchidea and therefore represents in his opinion a basal metriorhynchid. VIGNAUD (1995) refers *P. typus* as well to the Metriorhynchidea, in a new family the Pelagosauridae. There is obviously a significant difference in the position of *P. typus* between the Linnaean systematic BUFFETAUT (1980a, 1982) and VIGNAUD (1995) use and the phylogenetic systematic BENTON & CLARK (1988) and CLARK (1994) suggest.

In contrast to both opinions, in this work, *Pelagosaurus* turns out to be repeatedly nested inside the teleosaurids, as a basal sister taxon to all other remaining teleosaurids (Fig. 6.1 & Fig. 6.2). Six unequivocal synapomorphies (see paragraph 6.3.1) define the teleosaurids quite well, even though three of those characters refer to the shape of the postorbital. The taxon *Pelagosaurus typus* is well supported by six unambiguous unequivocal autapomorphies, too (see paragraph 6.3.1). In the analysis including a hypothetical all-0-ancestor, the strict consensus tree shows *Pelagosaurus typus* nested inside Teleosauridae and Metriorhynchidae in an unsolved polytomy (Fig. 6.4). In the 50% majority rule consensus tree, *P. typus* falls in 50% (DELTRAN) or 69% (ACCTRAN) in basal position to the remaining teleosaurids (Fig. 6.3). It does not turn out within the metriorhynchids in any case. Therefore, the suggestion by BUFFETAUT (1980a/b, 1982) and by VIGNAUD (1995) that *Pelagosaurus typus* is a basal metriorhynchid itself cannot be confirmed in the present analyses. Even though in the analysis with the hypothetical all-0-ancestor *Pelagosaurus typus* falls sometimes outside the remaining thalattosuchians, more often it occurs inside the teleosaurids. Therefore, neither can be agreed with BENTON & CLARK´S (1988) opinion about the position of *P. typus*. Recently, GASPARINI et al. (2006) presented a phylogenetic analysis where *Steneosaurus bollensis* and *Pelagosaurus typus* form together a sister group to the Metriorhynchidae. Thus, their result mainly corresponds with the result of this work.

6.4.2 The relationships of *Platysuchus multiscrobiculatus*

The status of the taxon *Platysuchus multiscrobiculatus* only had been a marginal subject of former discussions (BERCKHEMER 1928, 1929, WESTPHAL 1962). However, VIGNAUD (1995) suggests referring *Platysuchus multiscrobiculatus* together with all *Teleosaurus* taxa in the subfamily Teleosaurinae.

In this study, *Platysuchus multiscrobiculatus* falls from time to time in one branch with *Teleosaurus cadomensis*, too, in particular if a hypothetical all-0-ancestor is added, but a lot more often it occurs as a sister taxon to all remaining Teleosauridae taxa like shown in the first analysis (Fig. 6.1 & 6.2). The addition of an all-0-ancestor to the analysis nests *Platysuchus multiscrobiculatus* (in the 50% majority rule consensus tree, Fig. 6.3) in an unsolved polytomy with the branch comprising *Teleosaurus cadomensis*, *Steneosaurus pictaviensis*, and *S. megarhinus* (see paragraph 6.3.2) and the branch comprising *Machimosaurus hugii* and the remaining *Steneosaurus* taxa (Fig. 6.3). The node (***2***), which excludes *Platysuchus multiscrobiculatus* in the first analysis (analysis 1) from the remaining taxa, is supported by the fact that the cranial surface of the bones is only slightly grooved in the remaining taxa and not heavily as in *Pl. multiscrobiculatus* (see paragraph 6.3.1), and that

the dorsal osteoderms in the other taxa first develop a keel from the level of the pelvic girdle and not before that.

In the second analysis including the all-0-ancestor, the node (67%) comprising *Platysuchus multiscrobiculatus* with *Machimosaurus hugii* and the remaining *Steneosaurus* taxa and is supported by two synapomorphies (ci=1), first, that the tail is completely surrounded by osteoderms and second, that the cervical rib is only single headed. The sister group relationship to the branch including *Teleosaurus cadomensis* is here only based on two equivocal synapomorphies: The premaxilla is broad anterior of the naris (character 5, ci=0.25, coded 1) and that the dorsal osteoderms only show a discrete convexity at the anterior margin and not a real process (character 96, ci=0.833, coded 1).

Due to the fact, that mostly palatal features support the relationships between *Steneosaurus pictaviensis*, *Teleosaurus cadomensis,* and *Steneosaurus megarhinus* (see above), it is not surprising that the exact status of *Platysuchus multiscrobiculatus* cannot be solved. A palate is unknown of *Pl. multiscrobiculatus* and therefore can be neither described nor coded.

Platysuchus multiscrobiculatus is characterized by three autapomorphies (see above). The distinct femoral head and the ilium with a well-developed anterodorsal and posterodorsal process are different from the typical teleosaurid condition and considered as primitive conditions. The other autapomorphy that the postorbital possesses a well-developed long, acute anterolateral process is probably a convergent developed structural feature, because of the dorsal orientation of the orbits in the skull.

Therefore, *Platysuchus multiscrobiculatus* is considered a basal teleosaurid probably closer related to *Teleosaurus cadomensis* and *S. pictaviensis* than to the remaining steneosaurids. The suggestion by VIGNAUD (1995) that *Platysuchus multiscrobiculatus* should be put in a close relationship with the *Teleosaurus* taxa therefore can only be partly confirmed in the present investigation.

6.4.3 Relationships within the steneosaurids

VIGNAUD (1995) suggests for the Teleosauridae based on Linnaean systematic two different subfamilies: The subfamily Teleosaurinae, in which he refers *Platysuchus multiscrobiculatus* together with all *Teleosaurus* taxa, and the subfamily Steneosaurinae including all known *Steneosaurus* taxa. In the present analyses, the *Steneosaurus* taxa turned out to be paraphyletic on a certain level. *Steneosaurus pictaviensis* falls with *Teleosaurus cadomensis* and *Steneosaurus megarhinus* (Fig. 6.1& Fig. 6.2) as a sister group to all remaining *Steneosaurus* taxa including *Machimosaurus hugii*.

Therefore, the present analysis indeed shows two major subclades, but the monophyly of the *Steneosaurus* taxa cannot be confirmed.

6.4.4 Relationships of *Steneosaurus bollensis*

Steneosaurus bollensis mostly falls together with *Steneosaurus edwardsi* from the French Callovian and Oxfordian and the branch comprising *Steneosaurus priscus* from the Tithonian of the Swabian Alb and *Steneosaurus baroni* from the Callovian of Madagascar in an unsolved polytomy. The Liassic taxon *Steneosaurus bollensis* shows therefore surprisingly closer relationships with the Middle Jurassic taxon *Steneosaurus edwardsi* and the Upper Jurassic taxon *S. priscus* and *S. baroni* as with the other Liassic taxa *S. brevior* and *S. gracilirostris*. Nevertheless, is the node (***12***) only weakly supported by one character, which appears four times in the analysis (ci=0.25). The fact that the dorsal primary head of the quadrate articulates with the squamosal, occipital and prootic, is obviously quite often the case. Additionally, this is a problematic feature, because of its position in the skull. It is often not to identify, because of compressed fossil preservation and fused sutures. Additionally, *S. edwardsi* is only characterized by one autapomorphy; whereas *S. bollensis* is well supported by seven autapomorphies (see paragraph 6.3.1).

6.4.5 Relationships of *Steneosaurus brevior* and *Steneosaurus gracilirostris*

The sister-group relation ship of these taxa is based on the orientation of the external naris and the absence of an incisive foramen in dorsal view (see above). The anterior alignment of the external naris is a stable feature (synapomorphy), while for example the premaxillae enlargement can vary broadly intraspecifically (see chapter 4 & 5). The absence of an incisive foramen in dorsal view is a questionable character, because the fossil report for these taxa is poor, and the skulls often miss the anterior part of the rostrum. The incisive foramen for example in *S. bollensis* is often not visible because of the flattened preservation of the skulls, too, and only the high number of specimens allows verifying the existence of an incisive foramen. *S. brevior* is characterized by four autapomorphies (under DELTRAN character optimisation); while *S. gracilirostris* is well supported by eight autapomorphies (see paragraph 6.3.1).

6.4.6 Relationships of *Steneosaurus leedsi* and *Steneosaurus heberti*

S. leedsi and *S. heberti* fall in a stable dichotomy in all performed analyses. The dichotomy is supported by one unambiguous unequivocal synapomorphy that the number of teeth in the maxilla is over forty. Even though the number of teeth varies slightly intraspecifically, this feature is considered as steady in this case. The variation of tooth

number was already considered in the character definition. The taxon *S. leedsi* is supported by three autapomorphies (DELTRAN) while *S. heberti* is only defined by the absence of autapomorphies (see paragraph 6.3.1) and its status is therefore unclear.

6.4.7 Relationships within the Metriorhynchidae

The relationships inside the metriorhynchids turn out to be not as stable as the relationships for the teleosaurids in the present analyses. Quite stable relationships are that the *Teleidosaurus* taxa are basal to the remaining metriorhynchids. Only in the second analysis (including an all-0-ancestor), *Teleidosaurus gaudryi* falls with *Dakosaurus* in an unsolved polytomy. The *Metriorhynchus* taxa turn out to be monophyletic, in most cases but fall together with the taxon *Geosaurus giganteus*. Therefore, the genus *Geosaurus* turns out to be paraphyletic within the Metriorhynchidae. *Geosaurus giganteus* shows a closer relationship with *Metriorhynchus* and *Dakosaurus maximus* than to *Geosaurus gracilis*, which occurs, together with *Geosaurus giganteus,* in the Kimmeridgian of the Swabian Alb. *Geosaurus gracilis* falls steadily together with *Geosaurus vignaudi* and *Geosaurus suevicus* in an unsolved polytomy as a sister group to the branch comprising the *Metriorhynchus* taxa, *Geosaurus giganteus* and *Dakosaurus*.

According to GASPARINI et al. (2006), *Dakosaurus* (with *D. maximus* and *D. andiniensis*) and *Geosaurus* (with *G. araucanensis* and *G. suevicus*) fall together in a dichotomy as a sister group to *Metriorhynchus* (with *M. superciliosus* and *M. casamiquelai*).

Because in the present work, *Dakosaurus maximus* was only coded after data from the literature (FRAAS 1902 and appendix IV,) and the strict consensus trees show an unsolved polytomy with the *Metriorhynchus* taxa (Fig. 6.2 and Fig. 6.4), a closer relationship to *Geosaurus* like suggested by GASPARINI et al. (2006) cannot be entirely excluded.

To explain the poor resolution of the metriorhynchids in the present analysis two explanations are most likely:

1. This study is mainly focused on the teleosaurids, therefore the coding for the metriorhynchids are probably less informative and less exact than for the teleosaurids. Some of the data have only derived from the literature, while the data for the teleosaurids base mainly on personal observations.
2. The metriorhynchids represent a specialized group of marine crocodiles, which are highly adapted to aquatic environment. This probably leads to much convergence as well as to many autapomorphic features as it is known for other marine reptiles, for example in ichthyosaurs (SANDER 2000).

Chapter 7

Thalattosuchia in time and space (Fig. 1.3, Fig. 7.1, Fig. 7.2, Fig. 7.3)

The thalattosuchians were not only distributed in time but naturally also in space. After their first appearance in the early Lower Jurassic, they spread widely and had an almost worldwide distribution during the Upper Jurassic (Fig. 7.1) (e.g., BUFFETAUT 1982, VIGNAUD 1995, GASPARINI et al. 2000). The last few representatives became extinct in the Lower Cretaceous (Fig. 7.2). In the following, the palaeogeographical distribution of the group during Jurassic time is described and discussed, considering the phylogenetic relationships and the stratigraphic background. A phylogenetic-palaeobiogeographical scenario is developed, which indicates where the group possibly originated and how it spread over the world. In addition, special attention is paid to the distribution in Central Europe during the Toarcian.

7.1 Distribution during the Lower Jurassic

In the Lower Jurassic thalattosuchian finds occur in several localities all over Europe (Fig. 1.3): In the Swabian and Franconian Jura (southern Germany), northern Germany, Yorkshire and Dorset (Great Britain), Normandy (France), Lorraine (Belgium and Luxembourg), Portugal, and Italy (e.g. EUDES-DESLONGCHAMPS 1864, ANDREWS 1913, WESTPHAL 1962, ANTUNES 1967, BUFFETAUT 1980a/b, BENTON & TAYLOR 1984, BARDET 1994, GODEFROIT 1994, BIZZARINI 1995, VIGNAUD 1995, DELFINO 2001, DELFINO & DAL SASSO 2003).

However, the knowledge about the worldwide distribution of the oldest thalattosuchians in the early Lower Jurassic is incomplete. There are early Lower Jurassic finds from Europe, South America, and probably China, which most likely, belong to the Thalattosuchia (Fig. 7.1). Little later in the Toarcian suddenly a quite various thalattosuchian fauna appear. The splitting up of the thalattosuchians must therefore have taken place very early in the Lower Jurassic.

At the time of their first well-documented appearance in the fossil record (in the late Lower Jurassic) (Fig. 7.1), thalattosuchians are already a diverse group, with some species (*Pelagosaurus typus*) mere highly marine adapted than others (e.g. *Platysuchus multiscrobiculatus*).

Their remains are mainly found in shelf marine sediments, except of the finds of the questionable thalattosuchian *Peipehsuchus* in China, which is found in fluvial fresh water sediments (LI 1993). In most cases, the Lower Jurassic teleosaurids are found together with ichthyosaur and plesiosaur remains in shelf marine sediments with a water depth less than 200 meters. It is unknown, whether the thalattosuchians avoided the open ocean or not, because of the unfavourable vertebrate preservation in this environment.

7.1.1 Hettangian, Sinemurian & Pliensbachian

In the early Lower Jurassic, the fossil record regarding marine crocodilians is scanty. All finds are fragmentary and only provide few diagnostic features, which hardly allow referring them to the Thalattosuchia.

The oldest representatives, who are referred with certainty to the Thalattosuchia are: Teleosauridae indet. from the Upper Sinemurian of Lorraine, Europe (HUENE & MAUBEUGE 1952, 1954, GODEFROIT 1994) and Thalattosuchia indet. from the Sinemurian of Chile and South America (GASPARINI 1985, GASPARINI et al. 2000). Additionally, fragmentary remains are reported from the Lower Liassic of Argentina and referred to Teleosauridae indet. (GASPARINI 1981, 1985), and from the Lower Liassic of India as Thalattosuchia indet. (OWEN 1852, JAIN et al. 1962, KRISHNA 1987, KUTTY et al. 1987) (Fig. 7.1). In addition, the oldest *Steneosaurus* specimen appears in Lorraine in the uppermost Pliensbachian or the lowest Toarcian (GODEFROIT 1994).

It must be considered that the fossil record in the early Lower Jurassic is not extremely poor only for the marine crocodilians, but also insufficient for other marine reptiles. Ichthyosaurs, well known from Triassic and in general from Jurassic times, show a gap here, too. However, there are ichthyosaurs finds of Sinemurian age from the "Blue Lias" in England (SANDER 2000). Plesiosaurs are also known from the Hettangian and Sinemurian deposits in England (OWEN 1840, 1865; STORRS & TAYLOR 1996, STORRS 1997). Interestingly enough, marine crocodilian finds have never been reported from those sites. According to BARDET (1994), the completeness of the fossil record of marine reptiles (SCM) is in particular low (only 16%) in the Pliensbachian in the Lower Jurassic, while it is 87% in the Toarcian.

7.1.2 Toarcian

In the Toarcian various Thalattosuchia taxa like *Steneosaurus*, *Platysuchus* and *Pelagosaurus* occur mainly restricted to Europe, except of some fragmentary, mostly undiagnostical remains of teleosaurids from Madagascar (NEWTON 1893, BUFFETAUT et al. 1981, FARA et. al 2002), North America (BUFFETAUT 1979b, STRICKER & TAYLOR 1989) and

South America (GASPARINI 1985). Furthermore, some remains of *Peipehsuchus* from the Ziliujing Formation in China are referred to the Thalattosuchia (LI 1993, VIGNAUD 1995).

In the Toarcian, the oldest certain finds in Europe consist mainly of *Steneosaurus*, less frequently appears *Pelagosaurus typus* and seldom *Platysuchus multiscrobiculatus*. Among the three known Toarcian *Steneosaurus* taxa, *Steneosaurus bollensis* is the most common one, while *S. gracilirostris* and *S. brevior* occur less frequently and show a more restricted palaeogeographical distribution.

In the *tenuicostatum*-ammonite zone of the Lower Toarcian, no thalattosuchian finds are reported so far. In the *Harpoceras falcifer(um)* ammonite zone of the Lower Toarcian, finds are reported from Great Britain, France and Germany. *Steneosaurus bollensis* is reported from the Jet Rock Series in Great Britain (BENTON & TAYLOR 1984, WALKDEN et al. 1987). *Pelagosaurus typus* is reported from Whitby and Somerset in Great Britain (DUFFIN 1979a/b). The specimens of *Steneosaurus bollensis*, *Pelagosaurus typus* and *Platysuchus multiscrobiculatus* from the Swabian Jura (e.g. Holzmaden) come from the *falicfer*- ammonite zone (Lias ε II), too. In this study, one Holzmaden specimen (UH 7) has been referred to *Steneosaurus brevior* (see chapter 3.3); therefore, the oldest find of *S. brevior* occur now in the *falcifer*-ammonite zone, Lias ε II in Holzmaden. According to GODEFROIT (1994) *Steneosaurus bollensis*, *S. gracilirostris*, and *Pelagosaurus typus* specimens are found in the Schistes de Grandcourt of Luxembourg, which lies as well in the *falcifer*- ammonite zone and is therefore the same age as the deposits from the Swabian Jura. However, *Pelagosaurus* typus is found on the base of this deposits and appears thus little earlier in the stratigraphy (GODEFROIT 1994). From France *Pelagosaurus typus* is reported from several Lower Toarcian localities in the Normandy (EUDES-DESLONGCHAMPS 1864, BUFFETAUT 1982, VIGNAUD 1995). However, an exact correlation to an ammonite zone is not available.

In the Upper Toarcian corresponding to the *bifrons*-ammonite zone, *Steneosaurus* finds are mostly reported from Great Britain. *S. brevior* and *S. gracilirostris* come mainly from the Alum Shale Series in Whitby, which is correlated with the *bifrons*-ammonite zone, and are therefore slightly younger than the finds from Holzmaden (WESTPHAL 1962, BENTON & TAYLOR 1984).

From the Toarcian of Italy finds of cf. *Pelagosaurus* and cf. *Steneosaurus* are known from at least six localities (DELFINO & DEL SASSO 2003). Recent discovery of a probable juvenile specimen from the Toarcian of the Sogno Formation in the Lecco Province, Italy, support the assumption that the distribution of thalattosuchians in northern Italy was far from being sporadically (DELFINO & DEL SASSO 2003). The exact ammonite zone correlation of the

Italian finds is still under discussion; therefore, an exact age of the specimens cannot be determined.

Based on the variation of the marine reptile fauna GODEFROIT (1994) suggests for Western Europe in the Lower Toarcian a pattern of four marine reptile provinces ("zones"), which show a remarkable provincialism. MAISCH & ANSORGE (2004) simplify this into a scheme of three provinces: The south-eastern or **"Germanic" province**, which corresponds to "zone 1" of GODEFROIT (1994), a north–western or **"British" province** which corresponds to "zone 2" ("zone de Yorkshire") of GODEFROIT (1994), and an intermediate **"Subgermanic" province**, which contains "zone 3" ("zone luxenbourgoise") and "zone 4" ("zone normand") of GODEFROIT (1994). According to MAISCH & ANSORGE (2004), the latter two "zones" of GODEFROIT (1994) yield relatively few different taxa; therefore, they are summarized to only one zone. The definition of these three marine reptile provinces is mainly based on the occurrence of typical ichthyosaur or plesiosaur taxa, which do not occur in one of the other provinces.

However, for the "British" province MAISCH & ANSORGE (2004) also mention the very common occurrence of *Steneosaurus gracilirostris* and the very rare occurrence of *Steneosaurus bollensis*. Nevertheless, *Steneosaurus gracilirostris* occurs according to GODEFROIT (1994) also in the intermediate "Subgermanic" province, while *Steneosaurus brevior* is much more restricted to the British province, except for the one new *Steneosaurus brevio*r specimen from Holzmaden ("Germanic" province). *Steneosaurus bollensis* appears to have been a rather widespread taxon, with definite records from Germany, Luxembourg, and England. Even though, it most frequently occurrence is in the "Germanic" province. In contrary, *Platysuchus multiscrobiculatus* is clearly restricted to the Swabian Alb respectively to the "Germanic" province. It is so far only known from the Posidonia Shale around Holzmaden, and even there it is by far the rarest of the five known species from the Lower Jurassic. Some taxa, such as the leptonectic ichthyosaur *Eurhinosaurs longirostris* and the well aquatically adapted thalattosuchian *Pelagosaurus typus*, are apparently unaffected by this provincialism and occur relatively commonly in all three provinces (MAISCH & ANSORGE 2004).

Palaeogeographically, only the London-Brabant Massif may be responsible for these distributional patterns (MAISCH & ANSORGE 2004). It could have acted as a barrier for the spreading pass ways. According to RÖHL (1998), the lithological and palaeoecological similarity of the Lower Toarcian in all three areas ("provinces") makes it unlikely that there were major differences in palaeotemperature, salinity or other parameters, which otherwise

could have effected the distribution of the large marine predators. In contrary, to the highly aquatically adapted ichthyosaurs and plesiosaurs, the marine crocodilians show different stages of aquatic adaptation, which may have caused limitation in the distribution pattern, too. Obviously, the higher aquatically adapted thalattosuchian *Pelagosaurus* is more widespread than the other thalattosuchian taxa. The more "robust" forms like *Steneosaurus brevior* or *Platysuchus multiscrobiculatus* are palaeogeographically very restricted and the intermediate forms like *Steneosaurus bollensis* and *S. gracilirostris*, show less provincialism than the "robust" forms. It is supposed that the "robust" forms were still more terrestrial adapted than the other forms (see chapter 8).

7.2 Distribution in the Middle Jurassic

There is a distinct gap in the fossil record of the thalattosuchians during Aalenian and Bajocian time, which results in prominent ghost lineages for these stratigraphic layers (Fig. 7.3). Even though all known *Steneosaurus* taxa would have been considered in the phylogenetic analysis (see chapter 6), the gap would still remain. However, the gap in the fossil record fits well with the fall of sea level during this time. According to BARDET (1994), the stratigraphic interval Aalenian-Bathonian is known for yielding scanty fossil remains in all other marine reptile groups, too. The completeness of the fossil record (SCM) for marine reptiles is according to BARDET (1994) only 20% in the Aalenian.

The second broad documentation of the teleosaurids occurs first in the upper Middle Jurassic beginning in the Bathonian again, with rising sea level.

In the Middle Jurassic, the taxon *Steneosaurus* is still represented by several taxa. The first *Teleosaurus* appear in Europe while *Pelagosaurus* became extinct in the early Middle Jurassic or perhaps even already in the latest Toarcian. The first metriorhynchids appear and spread out.

7.2.1 Aalenian

Only scanty fossil remains of marine reptiles are known from the Aalenian. According to ANTUNES (1967), the finds of cf *Pelagosaurus* (formerly described as *Mystriosaurus* cf. *bollensis*) in Portugal come from the upper most Toarcian or the base of the Aalenian, and thus, seem to be little younger than the finds of *Pelagosaurus typus* in Germany, England and France.

Interesting enough, the oldest known *Steneosaurus* sp. specimen from Switzerland is first reported from Lower Aalenian (RIEPPEL 1981, KREBS 1962) and is therefore clearly

younger, too. Some sporadic *Steneosaurus* sp. finds are also reported from South Dagestan, Asia in the Aalenian (STORRS & EFIMOV 2000).

7.2.2 Bajocian

Additionally, the poor fossil record of marine crocodilians in the Bajocian of Central Europe can be explained by a decrease of the sea level and therefore fewer marine deposits (VIGNAUD 1995). Nevertheless, in the Bajocian the first metriorhynchids appear with the taxon *Teleidosaurus* in Europe and *Metriorhynchus* sp. in Chile (HUA & ATROPS 1995, GASPARINI et al. 2000). Fragmentary *Steneosaurus* sp. finds are reported from Europe and Russia (STORRS & EFIMOV 2000).

7.2.3 Bathonian

In the Bathonian, the fossil record of the thalattosuchians becomes much better than in the beginning of the Middle Jurassic. *Steneosaurus* finds (e.g. *S. boutilieri*, *S. baroni, S.* sp) are reported from Europe, Madagascar, and Tunisia in Africa (e.g., EUDES-DESLONGCHAMPS 1867-69, FARA et al. 2002, NEWTON 1893, PHIZACKERLEY 1951, and VIGNAUD 1995). The first *Teleosaurus* (e.g. *Teleosaurus cadomensis*) appear in Europe and metriorhynchids finds (*Teleidosaurus* and *Metriorhynchus*) are mainly known from Europe (GODEFROIT et al. 1995). However, GASPARINI et al. (2005) also describe *Metriorhynchus* aff. *M. branchyrhynchus* from Argentina.

7.2.4 Callovian

The fossil record in the Callovian is excellent especially from France and England (Oxford Clay), and from South America (HUA et al. 1994, VIGNAUD 1995, GASPARINI et al. 2000). In general, a rich diversity of Thalattosuchia taxa is known. *Metriorhynchus* as well as *Steneosaurus* taxa show a broad diversity (e.g. *Metriorhynchus casamiquelai, M. superciliosus, S. heberti*, *S. leedsi*, *S. edwardsi*, *S. pictaviensis*), while other thalattosuchian taxa are almost unknown during this timeperiod (VIGNAUD 1993, 1995, GASPARINI & DIAZ 1977). Some scanty finds of steneosaurs (cf *S.* sp.) are also reported from Russia and India (OWEN 1852, KRISHNA 1987, KUTTY et al. 1987, STORRS & EFIMOV 2000). *Peipehsuchus teleorhinus* is reported from Changet, Ferganga Basin, Kirgizstan (STORRS & EFIMOV 2000).

7.3 Distribution in the Upper Jurassic

The fossil record in the Upper Jurassic is good, but generally marked by less diversity of the taxa. The highly aquatically adapted metriorhynchids have almost worldwide distribution in the Upper Jurassic and the metriorhynchids *Dakosaurus* and *Geosaurus* appear for the first time in the fossil record. *Steneosaurus* and *Teleosaurus* taxa still represent the teleosaurids but

are mostly restricted to Europe (MICHELIN et al. 1985, VIGNAUD 1995). The first finds of the robust teleosaurid *Machimosaurus* are reported from the Oxfordian.

7.3.1 Oxfordian

The fossil record of the marine crocodilians is mainly restricted to Europe in the Oxfordian. According to BARDET (1994), the completeness of the fossil record for all marine reptile groups (SCM) lies by 42% in the Oxfordian. The first *Machimosaurus (hugii)* specimens appear in Europe and Africa (e.g. KREBS 1967, BARDET & HUA 1996). *Steneosaurus* finds (e.g. *S. heberti*, *S. edwardsi*, *S. megarhinus*) are only reported from Europe (e.g. EUDES-DESLONGCHAMPS 1864, SAUVAGE 1879, BUFFETAUT & THIERRY 1977, VIGNAUD 1995). Rare metriorhynchid finds (*Metriorhynchus*) are particularly reported from France (BUFFETAUT 1977, VIGNAUD 1995), but one is also recently reported from Cuba as the oldest *Geosaurus* sp. specimen (GASPARINI & ITURRALDE-VINENT 2001). Additionally, FARA et al. (2002) describe Thalattosuchia indet. finds from the Oxfordian/Kimmeridgian strata in southern Tunisia.

7.3.2 Kimmeridgian

The first *Dakosaurus (maximus)* specimens appear in Europe, Russia, and Argentina (FRAAS 1902, DEBELMAS 1957, HUA et al. 1998, GASPARINI et al. 2000). Other metriorhynchids have been reported especially from England and France (GRANGE & BENTON 1996). Fragmentary *Steneosaurus megarhinus, S.* sp., and a couple of *Teleosaurus* sp. finds are reported from Europe, as well (SELENKA 1867). In contrary, the teleosaurid *Machimosaurus* (*hugii, mosae*) is a common taxon in the crocodile fauna of the Kimmeridgian of Europe (KREBS 1967, HUA 1999). However, it is often only represented by its striking teeth. *Geosaurus* sp. occurs in England for the first time (VIGNAUD 1995).

7.3.3 Tithonian

Geosaurus (*G. araucanensis, G. vignaudi, G. gracilis, G. giganteus, and G. suevicus*) finds are now reported from diverse localities in Europe (i.e. Solnhofen) and South- and Middle America (SOEMMERING 1816, FRAAS 1901, 1902, GASPARINI et al. 2000, FREY et al. 2002) and show almost worldwide distribution. *Metriorhynchus* is only reported from Argentina and became extinct at the end of the Jurassic. *Dakosaurus andiniensis* is recently reported from the Jurassic-Cretaceous boundary of Patagonia, Argentina (GASPARINI et al. 2006).

Steneosaurus priscus is reported from Europe (SOEMMERING 1816) and *Machimosaurus* (*hugii*) is now reported from Portugal (KREBS 1967, MATEUS 2002).

7.4 Distribution in the Lower Cretaceous

In the Lower Cretaceous, only a few Thalattosuchia taxa are still present. The only certain representative of the teleosaurids, *Machimosaurus*, is restricted to Europe and was extinct in the Valanginian (CORNÉE & BUFFETAUT 1979, VIGNAUD 1995). *Dakosaurus* and *Geosaurus* represent the metriorhynchids in the Lower Cretaceous and as the last representative of the metriorhynchids. *Dakosaurus andiniensis* is known from Berriasian levels of Argentina (GASPARINI et al. 2006). *Dakosaurus* was extinct in the Hauterivian (VIGNAUD 1995, HUA & BUFFETAUT 1997).

7.5 Hypothetical pass ways for the Thalattosuchia in the Lower Jurassic **(Fig. 7.2)**

Because the geographical origin of the Thalattosuchia is still unknown, the earliest distribution in the Lower Jurassic is not easy to explain. According to the fact that the first thalattosuchians occur contemporaneously in Central Europe and at the South American west coast, it is necessary to develop a hypothesis about the early spreading of the Thalattosuchia.

BUFFETAUT (1981a) does so, by suggesting a direct marine connection between Europe and South America as early as in the Toarcian or even earlier (Fig. 7.2). In contrary, according to VIGNAUD (1995) it is very unlikely that a direct seaway from Europe to the west coast of South America has existed before the Middle Jurassic. He notes that all more recent palaeogeographical reconstructions of the Lower Liassic deny a direct connection between the east and west coast of Gondwana, and he mentions a possible connection deep down in the south of Gondwana or in the north for faunal exchanges.

It is correct that no real sedimentary evidence for a marine pass way in the Lower Jurassic exists so far, which proves a connection between the Tethys and the west coast of America. The most western marine sediments are known from between the South of Morocco and the North of Senegal (BASSOULET et al. 1993). However, BONAPARTE (1981) and GASPARINI (1985, 1992) postulate an episodical connection between Europe and the American west coast, based on certain molluscs distribution. This early sporadic development of the so-called "Hispanic corridor" should be connected with strong eustatic sea level changes during the Sinemurian - Pliensbachian transgression. SHA (2002) also demonstrates with bivalve taxa that "[...] the Hispanic epicontinental seaway became established along the rifting area between North America and South America and Africa of the Pangaean supercontinent as early as Hettangian or even earlier, connecting western Tethys and eastern Palaeo-pacific and providing a corridor for migration and exchange of creatures between

Tethys and Palaeo-pacific". In addition, according to ABERHAN (2001, 2002) was "[...] the opening of the Hispanic Corridor, an embryonic seaway between the eastern Pacific and western Tethys oceans, coincided with the mass extinction [...]" in the Late Pliensbachian. According to BLODGETT & FRYDA (2001), the Hispanic Corridor was already open in the late Triassic based on the distribution of some gastropod taxa. Nevertheless, the palaeogeographical situation in the Lower Liassic is still under discussion, and because the first thalattosuchians were probably not highly aquatically adapted, a distribution partly over land seems to be possible, too.

However, considering the new biostratigraphic evidence for the existence of the Hispanic corridor as early as in the Late Triassic but at least sporadically in the early Lower Jurassic, the migration hypothesis through this pass way is preferred here (Fig. 7.2).

Interestingly, the main distribution of ichthyosaurus is also restricted to Central Europe during the Lower Jurassic (SANDER 2000, MONTANI 2005). The same is true for plesiosaurs, even though some remains of plesiosaurs are reported from the Lower Jurassic of Australia (THULBORN & WARREN 1980). In contrast, during the Middle and Upper Jurassic, ichthyosaurs and plesiosaurs are known from diverse localities of America e.g. Oregon, Chile, Cuba, and Argentina (CAMP & KOCH 1966, GASPARINI 1997, FERNÁNDEZ 1997, FERNÁNDEZ & ITURRALDE-VINENT 2000, SHULTZ et al. 2003). It seems therefore likely that the Hispanic corridor still represented a barrier in the Lower Jurassic, which was impossible to pass by strictly aquatic reptiles.

The distribution of the thalattosuchians in Asia and Russia is fragmentary during the entire Jurassic. According to VIGNAUD (1995), the taxon *Peipehsuchus* from the Lower Liassic of China must also be referred to the thalattosuchian clade. However, *Peipehsuchus* is a problematic taxon. Because of the insufficient description, it was not added to the phylogenetic analysis, so its phylogenetic relationships could not be tested. STORRS & EFIMOV (2000) clearly refer *Peipehsuchus* to the teleosaurids, too, with reference to BUFFETAUT (1982) and LI (1993). However, according to LI (1993) *Peipehsuchus* comes, in contrary to all other teleosaurid fossils, from non-marine deposits. In addition, *Peipehsuchus* is, according to NESOV et al. (1989), first reported from the Callovian of Changet (Fergana) and does not occur in Toarcian sediments (in STORRS & EFIMOV 2000). However, the specimen described by NESOV et al. (1989), was recently revised by AVERIANO (2000) as *Sunosuchus* sp., a member of the Goniopholididae. *Sunosuchus* is a common freshwater crocodilian in the Jurassic of Asia (YOUNG 1948, BUFFETAUT & INGAVAT 1980, BUFFETAUT 1986, MAISCH et al.

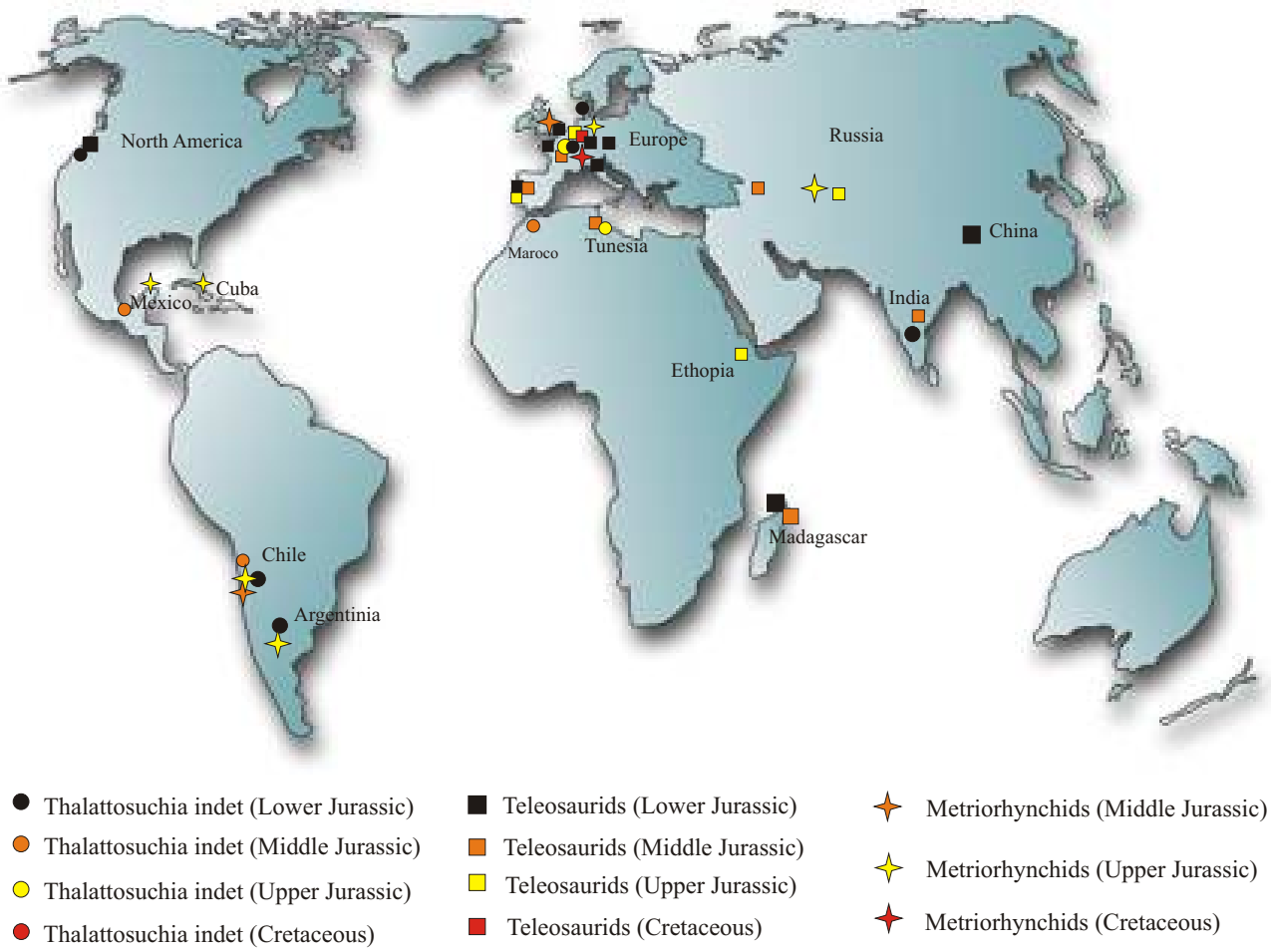

Figure 7.1: Finding localities of thalattosuchians worldwide. The specific colour indicates the stratigraphical background: Black for Lower Jurassic, orange for Middle Jurassic, yellow for Upper Jurassic, and red for Lower Cretaceous.

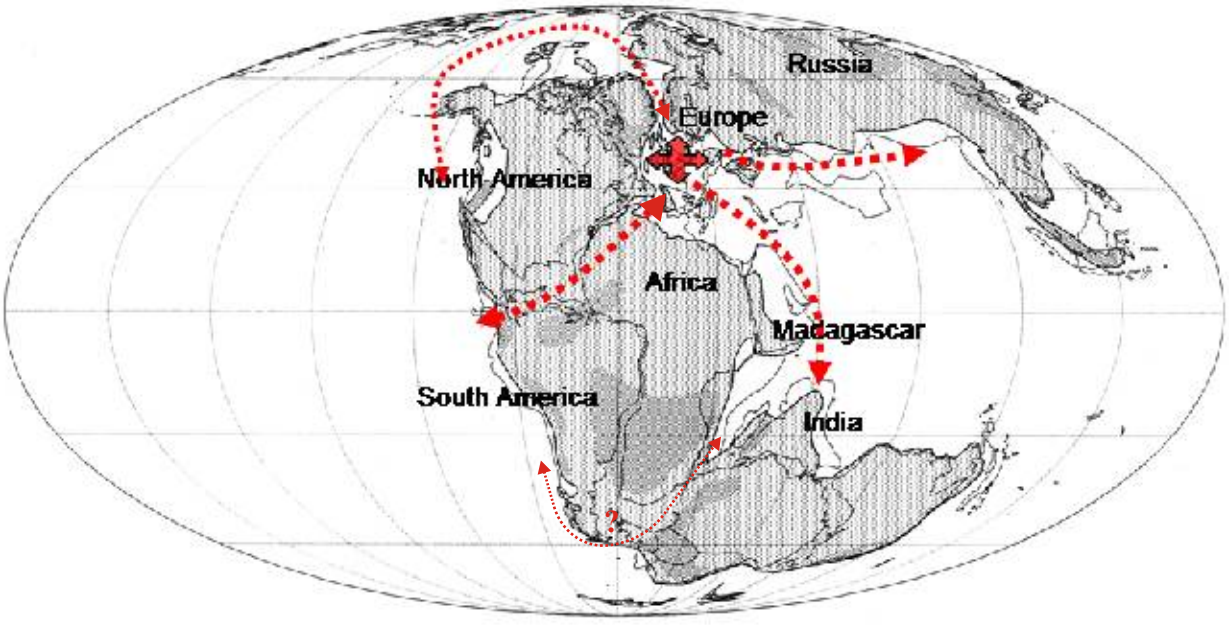

Figure 7.2: Possible spreading passes (red arrows) of the thalattosuchians in the Lower Jurassic (Toarcian). The coastline map in the Toarcian is taken after SMITH et al. (1995).

2003). However, STORRS & EFIMOV (2000) report, that the islands and north coast of the Tethys seaway (Russia to China) were home to at least two taxa of Thalattosuchia (*Steneosaurus* and cf. *Dakosaurus*) in the Middle to Upper Jurassic. They do not mention *Peipehsuchus* in particular here, nor report them any finds of thalattosuchians from the Lower Jurassic of Russia. Due to this uncertain status of *Peipehsuchus*, it is not further considered here.

However, the palaeogeographical distribution of Thalattosuchia was probably widespread already in the Lower Jurassic. The spreading to Asia might have taken place along the northern margin of the Tethys.

The fragmentary remains from India (OWEN 1852, KRISHNA 1987, KUTTY et al. 1987) are even on the familial level dubious (GASPARINI et al. 2000). Nevertheless, in the Lower Jurassic, a possible spreading in the Tethys from Europe to India, which was still connected in the south to Gondwana, should have been unproblematic along the eastern Gondwanan margin (Fig. 7.2). This way of spreading would likewise explain the plesiosaur finds from Australia in the Lower Jurassic (THULBORN & WARREN 1980).

In contrast, VIGNAUD (1995) tentatively suggests a spreading from South America to India along the western Gondwanan coast with a passage in the south of today's South America in the Lower Jurassic. This migration seaway between southern South America and western Africa is at least known during the Late Middle Jurassic associated with the break-up of the southern sector of Gondwana. This seaway would be the southern counterpart to the Hispanic Corridor (SHULTZ et al. 2003)**.**

However, the distribution along the east coast of Gondwana has sedimentary evidence, which makes the first hypothesis more probable. A small epicontinental sea was spreading from the Tethys over today's Central Arabia and Madagascar to India and the Jurassic deposits of Arabia and East Africa were settled here. The first transgression took place in the Lower Toarcian, and the second stronger transgression in the Bathonian (HOHL 1985). These events coincide well with the finds of teleosaurid remains in the Toarcian and Bathonian deposits of Madagascar, and represent probably two immigration events of thalattosuchians in this area. According to FARA et al. (2002), only few crocodilian remains from the Toarcian of Madagascar exist. BUFFETAUT et al. (1981) describe a jaw fragment of *Steneosaurus* sp. of Toarcian age on Madagascar. All the other remains of teleosaurids, including *Steneosaurus baroni*, are first described from the Bathonian of Madagascar (NEWTON 1893). During the Middle and Upper Jurassic also sporadic findings of teleosaurids are reported from Tunisia (FARA et al. 2002), Morocco (LAPPARENT 1955), and Ethiopia (East Africa) (HUENE 1938,

BARDET & HUA 1996). FARA et al. (2002) interpret "[...] the paucity of the south Tethysian fossil record as mainly reflecting poor sampling".

Since the Middle Jurassic until the Cretaceous, the faunal exchange for the thalattosuchians was less complicated, because the connection between Tethys and western Pacific was wide open. The metriorhynchids were most widely spread, probably because of their better swimming abilities, compared to the teleosaurids.

7.6 Phylogenetic-palaeobiogeographical scenario

The comparison of the stratigraphic occurrence of the Thalattosuchia with the here suggested phylogeny (chapter 6 and Fig. 7.3), allows some new conclusions about the in-group relationships inside the Thalattosuchia.

The origin of the Thalattosuchia is still unclear, because of the scanty fossil record in the lowermost Liassic. Some time during the Triassic the Thalattosuchia, originate probably from some kind of protosuchian, which is referred to be a terrestrial primitive crocodilian (BUFFETAUT 1982, CARROLL 1993).

The first sister group, the Teleosauridae, is with its basal taxon *Pelagosaurus typus*, restricted to the Upper Liassic of Central Europe. The taxon *Pelagosaurus* is only described from the Toarcian of Europe and perhaps, additionally, from the lowest Aalenian of Portugal (ANTUNES 1967). The placement of *Pelagosaurus typus* at the base of the teleosaurid clade seems therefore stratigrapically reasonable, because it appears very early in the Toarcian. However, the first occurrence of *Pelagosaurus typus* from Germany (e.g. WESTPHAL 1962), France (e.g. VIGNAUD 1995), and England (e.g. DUFFIN 1979a) coincides with the first occurrence of *Steneosaurus bollensis*, *S. brevior*, and *Platysuchus multiscrobiculatus*. *S. gracilirostris* probably occurs slightly later in the Toarcian of England. Nevertheless, *Pelagosaurus typus* is not a primitive teleosaurid, but a highly specialized marine crocodilian for its time. It is in basal relationship to the remaining teleosaurids, because it shows primitive characters together with highly derived features.

In contrast, *Platysuchus multiscrobiculatus* mostly shows basal features for teleosaurids, and occur as well early in the Toarcian. The placement of this taxon at the base of the teleosaurids seems therefore sensible. However, it is only known locally from the Swabian Alb.

The first certain appearance of *Steneosaurus* happened by the three taxa *Steneosaurus bollensis*, *S. brevior* und *S. gracilirostris* almost simultaneous in the Toarcian in Central Europe, together with the taxon *Pelagosaurus typus* and the taxon *Platysuchus*

multiscrobiculatus. The Toarcian taxa *Steneosaurus brevior* and *S. gracilirostris* fall together in a sister group relationship (see chapter 6), which corresponds well with their stratigraphic and geographical background.

One major problem in the current hypothesis is the occurrence of long ghost lineages. For example, the Toarcian taxon *Steneosaurus bollensis*, shows a sister group relationship with *S. edwardsi*, which appears for the first time in the Callovian.

During the entire Jurassic period, the genus *Steneosaurus* is widely distributed in Europe and can be sporadically found in Tunisia, Madagascar and perhaps in Asia (e.g., NEWTON 1893, BUFFETAUT et al. 1981, STORRS & EFIMOV 2000, FARA et al. 2002). Certain finds from the Cretaceous period are not known so far. The taxon *Steneosaurus* appears suddenly in the Upper Liassic of Europe with a couple of taxa and remains probably until the Lower Cretaceous. The remains of thalattosuchians from the Toarcian of America (BUFFETAUT 1979b, STRICKER & TAYLOR 1989) are so fragmentary and undiagnostic that a hypothesis about their relationships to the European specimens is impossible

There is so far only one certain *Steneosaurus* taxon known from outside Europe, *Steneosaurus baroni* from the Bathonian of Madagascar (NEWTON 1893). STORRS & EFIMOV (2000) mention possible *Steneosaurus* sp. finds earlier from the Aalenian of Asia (South Dagestan). The restriction of these taxa on mainly Central Europe also might reflect the poor preservation of Lower Jurassic marine deposits in other parts of the world. During the Lower Jurassic, also ichthyosaurs, plesiosaurs, and other marine reptiles are mainly restricted to Central Europe (SANDER 2000, GROSSMANN pers. comment)

The basal sister to most of the *Steneosaurus* taxa, *Machimosaurus* appears first in the Oxfordian of Europe and probably Africa (KREBS 1967, BARDET & HUA 1996). Stratigrapically, it is so far restricted to the Upper Jurassic and the Lowest Cretaceous and is therefore the youngest known representative of the teleosaurids (VIGNAUD 1995). According to CORNÉE & BUFFETAUT (1979), *Machimosaurus* was extinct in the Valanginian, as the last of the teleosaurid taxa. However, considering the phylogenetic analysis, is has to be one of the first to emerged, which requires a prominent ghost lineage in the Lower Jurassic (Fig. 7.3). The taxon remains until the Lower Cretaceous, quite likely not leaving Central Europe (BUFFETAUT et al. 1985). However, there, it is widely distributed (e.g. VON MEYER 1840, KREBS 1967, HUA 1999, MATEUS 2002). According to BARDET & HUA (1996) the teleosaurid findings from the Oxfordian of Ethiopia belong to *Machimosaurus* sp., too. This is the first reference for *Machimosaurus* outside Europe. The material is scanty and as long as no further finds are made, the evidence for this genus outside Europe is quite poor.

The taxon *Steneosaurus boutilieri* appears first in the Bathonian, but must have been emerged early in the Lower Jurassic, due to the present phylogenetic analysis (see chapter 6 & Fig. 7.3). It falls in close relationship with *S. leedsi* and *S heberti*, which appear together a little later in the Callovian (Fig. 7.3). The sister group relationship of the latter two is convincing and corresponds well with their stratigraphic background.

The taxon *Teleosaurus* is a sister-group to the steneosaurs and appears first in the Middle Jurassic of France and England (VIGNAUD 1995). Nevertheless, EFIMOV & CHKHIKVADZE (1987) and STORRS & EFIMOV (2000) mention remains of *Teleosaurus* from the uppermost Jurassic or lowermost Cretaceous of the Fergana Basin in Kirgizstan. The taxon *Teleosaurus* exists therefore certainly from the Bathonian of Europe and remains probably until the Lower Cretaceous in Russia (Fig. 7.3). Nevertheless, the taxonomy of these specimens is uncertain due to the fragmentary preservation. However, the *Teleosaurus* clade probably originates in Central Europe during the Middle to Upper Liassic and developed perhaps afterwards widely. Only a few representatives probably left Central Europe later in the Middle Jurassic and emigrated to Asia.

The occurrence of *Steneosaurus pictaviensis* at the base of the "*Teleosaurus*" branch, seems to be slightly problematic, because of the stratigraphic younger position of it than *Teleosaurus* itself, but the resulting ghost lineage is still much shorter than the ghost lineage e.g. for *Machimosaurus*. Because the fossil record in the Aalenian and Bajocian is fragmentary, the exact development during this timeperiod remains unclear.

The second sister-group, the Metriorhynchidae, is first known from the Middle Jurassic, with the basal taxon *Teleidosaurus*. The Metriorhynchidae must have derived already some time during the Lower Jurassic like the teleosaurids, what results also in a prominent ghost lineage until the first known occurrence of the metriorhynchids in the Bajocian (Fig. 7.3). Once the Metriorhynchidae occur, the phylogenetic hypothesis and the stratigrapically background correspond well. The oldest known representatives appear first in the Bajocian as *Teleidosaurus* cf. *gaudryi* in France (HUA & ATROPS 1995) and as *Metriorhynchus* in Chile (GASPARINI et al. 2005). *Teleidosaurus,* only described from the Middle Jurassic (Bajocian-Bathonian) of France (EUDES-DESLONGCHAMPS 1867-69, COLLOT 1905), is certainly restricted to Europe and appears stratigrapically as well as in the phylogenetic analysis at the base of the Metriorhynchidae (Fig. 7.3).

The taxon *Dakosaurus* is described from the Upper Jurassic (Kimmeridgian) until the Lower Cretaceous in Central Europe (FRAAS 1902, CORROY 1922, DEBELMAS 1957, VIGNAUD

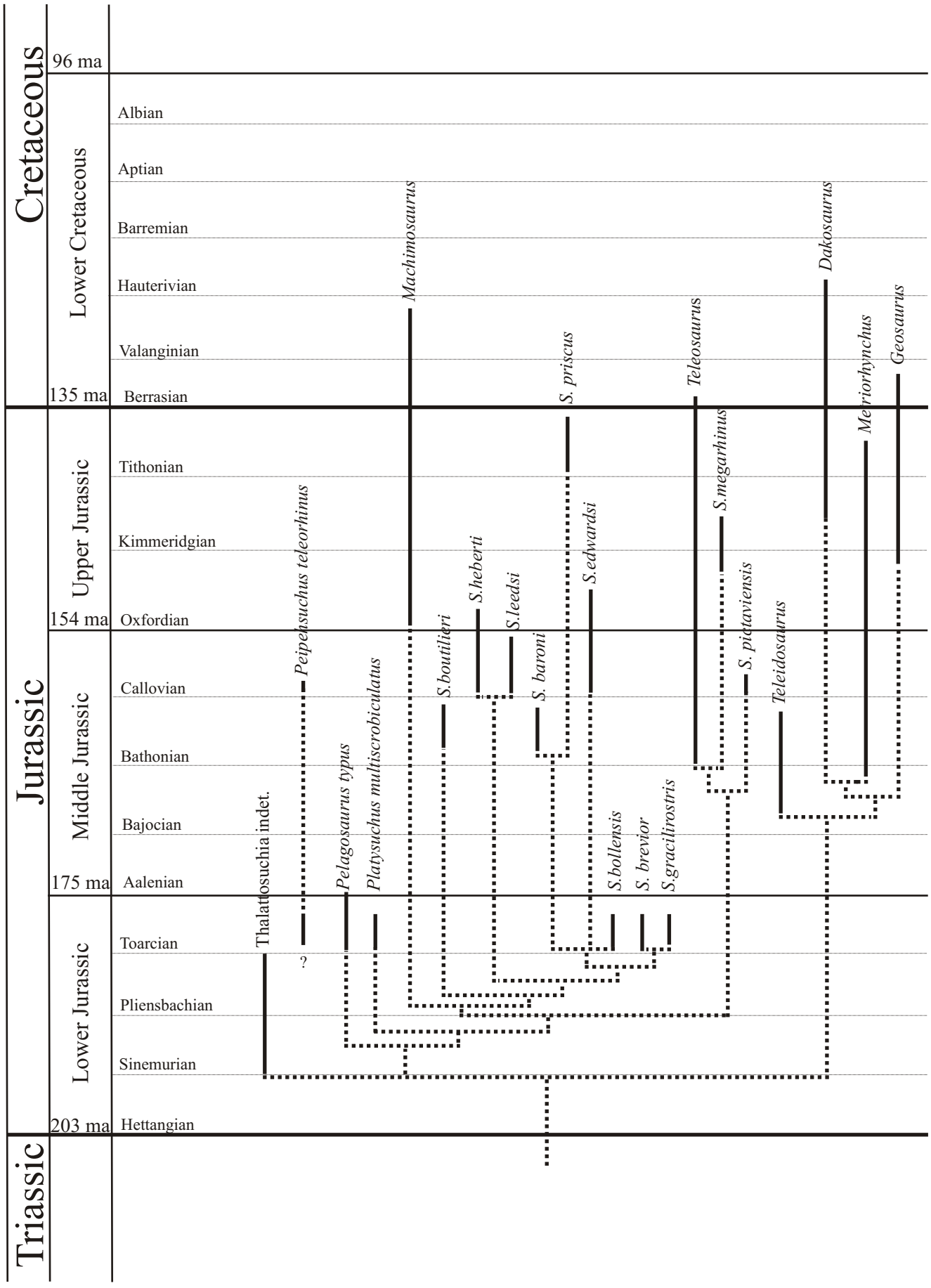

Figure 7.3: Ghost lineage diagram presenting the stratigraphical occurrence of the studied Thalattosuchia, based on the phylogeny proposed by the presented analysis (see the chapter 6). Certain stratigraphic occurrence is marked by full lines, while ghost lines are doted. For a better understanding *Geosaurus* as well as *Metriorhynchus*, *Teleosaurus* and *Machimosaurus* are treated as a single taxon.

1995). In the last decade, new finds of cf. *Dakosaurus* are reported from the Upper Jurassic of Russia (STORRS & EFIMOV 2000). In addition, finds of cf. *Dakosaurus* and *Dakosaurus andiniensis* are reported from the Upper Jurassic and Lower Cretaceous of Argentina (VIGNAUD & GASPARINI 1996, GASPARINI et al. 2006), which expands the palaeogeographical distribution of the taxon. It was the last representative of the metriorhynchids in the Lower Cretaceous and became extinct as far as known in the Hauterivian (HUA & BUFFETAUT 1997). Nevertheless, it emerges early within the metriorhynchids together with the *Metriorhynchus* taxa. As a sister-group to the *Metriorhynchus* and *Geosaurus* taxa, the ghost lineage therefore reaches back to the Early Middle Jurassic (Fig. 7.3).

The taxon *Metriorhynchus* (here including *G. giganteus*) is known from the Middle and Upper Jurassic (Bajocian -Tithonian) of Europe (VIGNAUD et al. 1994, GRANGE & BENTON 1996) and South America (GASPARINI & CHONG 1977, GASPARINI 1980, GASPARINI et al. 2000). In Europe, it is first certainly known from the Bathonian (VIGNAUD et al. 1994). However, JENSEN & VICENTE (1976) refer to a fragmentary *Metriorhynchus* sp. specimen, in early Bajocian levels near Copiapo in Chile. GASPARINI et al. (2000) confirm this fact, so *Metriorhynchus* appears certainly in the Bajocian of Chile and is therefore the oldest find of the genus *Metriorhynchus* so far. Nevertheless, it seems unlikely that *Metriorhynchus* originated there, because the most basal metriorhynchid *Teleidosaurus* comes from the Bajocian of Europe. Therefore, *Metriorhynchus* probably originate in Europe as well. Additionally, it appears first frequently in South America in the Tithonian. However, it is likely that there were more than one immigration event of *Metriorhynchus* taxa from Europe to South America (GASPARINI et al. 2000).

The paraphyletic taxon *Geosaurus* seem to be a special case. The taxon *Geosaurus* (here excluding *G. giganteus*) appears with the oldest *Geosaurus* sp. specimens in the Oxfordian (Upper Jurassic) of Cuba (GASPARINI & ITURRALDE-VINENT 2001) and than little later in the Kimmeridgian of Great Britain (VIGNAUD 1995). The taxon *Geosaurus* became extinct probably during the Lower Cretaceous (BROILI 1932, VIGNAUD 1995, GASPARINI & ITURRALDE-VINENT 2001, FREY et al. 2002). The stratigraphic youngest finds of *Geosaurus* are so far reported from the Wealden (Lower Cretaceous) of Germany (STEEL 1975). In South America, Mexico, and Argentina, it is first frequently known from Tithonian deposits (GASPARINI 1985, GASPARINI et al. 2000, GASPARINI & ITURRALDE-VINENT 2001, FREY et al. 2002). The immigration of *Geosaurus* to Europe probably happened during the Kimmeridgian and afterwards it might have emigrated again to South America during the late Upper Jurassic (Tithonian). Obviously, the pelagic taxon *Geosaurus* was here most successful (GASPARINI et

al. 2000). From the Upper Bajocian until the Upper Oxfordian a prominent ghost lineage is assumed for this taxon. Due to the presented phylogeny, it must have emerged little earlier than its sister groups, the *Metriorhynchus* and *Dakosaurus* taxa (Fig. 7.3).

Interestingly enough, the holotype for *Geosaurus giganteus* (SOEMMERING 1816), known from the Tithonian of Germany, falls in the phylogenetic analysis (see chapter 6) together with *Metriorhynchus* and not with the other *Geosaurus* taxa (and is therefore excluded there).

HUA et al. (1998) report the find of an indeterminate metriorhynchid from the upper Tithonian of Russia. This is the first known representative of this group in Russia, before that it was restricted exclusively to Europe and South America.

In the Lower Cretaceous, the last appearance of thalattosuchians is known sporadically from Europe. Reported are *Enaliosuchus* sp., *Machimosaurus* sp., and *Dakosaurus* sp. as Lower Cretaceous taxa from Europe (CORNÉE & BUFFETAUT 1979, VIGNAUD 1995, HUA et al. 2000).

Chapter 8

Palaeoecology

8.1 Feeding

To understand possible feeding options in Jurassic marine crocodiles, particularly in *Steneosaurus bollensis*, a reconstruction of the jaw muscles will be presented in the following chapter, together with their functional interpretation. In addition, tooth morphology and stomach contents will be interpreted with regard to possible prey.

8.1.1 Methods of jaw muscle reconstruction

In general, jaw muscle reconstruction in fossil animals can be accomplished by using analogies with closely related extant and fossil forms, comparing the position and shape of muscle scars on the particular bones (BRYANT & SEYMOUR 1990), and comparing the general configuration of the skull, respectively the inference of muscle anatomy as suggested by functional reasons (RIEPPEL 2002).

Muscle or tendon attachment are usually indicated by crests on the surface of the bone, distinctly flattened surfaces or slight depressions on the surface of the bone, and by irregular rugosities on the bone surface (MÜLLER 2002).

8.1.2 Jaw muscle reconstruction in *Steneosaurus bollensis*

Muscle reconstruction in *Steneosaurus bollensis* was undertaken by comparison with extant crocodilian jaw muscles, based on data from the literature (POGLAYEN-NEUWALL 1953, IORDANSKY 1964, SCHUMACHER 1973, BUSBEY 1989, SHIMADA ET AL. 1993, SATO et al. 1994, CLEUREN & DE VREE 2000, ENDO et al. 2002).

Additionally, because of some significant osteological differences of *Steneosaurus bollensis* in comparison to alligators or the extant long-snouted crocodilians *Gavialis gangeticus* and *Tomistoma schlegelii*, the fossil long-snouted crocodile *Dyrosaurus* was likewise considered (SCHWARZ 2003).

Steneosaurus bollensis has a much flattener, dorsoventrally compressed skull than extant crocodiles, with enlarged supratemporal and infratemporal fenestrae, features that are shared with *Dyrosaurus.*

In comparison to extant forms like, e.g. *Gavialis gangeticus*, *Tomistoma schlegelii*, and *Alligator mississipiensis* or the fossil crocodile *Dyrosaurus, Steneosaurus bollensis* possesses an extremely large external mandibular fenestra in the lower jaw, which can reach the size of the infratemporal fenestra (see chapter 3; Fig. 3.1).

Even though a long retroarticular process in the lower jaw is common among crocodilians, the specific shape of the retroarticular process in *Steneosaurus bollensis* differs from extant forms as well as from *Dyrosaurus* (Fig. 8.1). In lateral view, the elongation of the process is relatively horizontal and only slightly extended in dorsal direction, in comparison to the retroarticular process in e.g., *Dyrosaurus* or *Gavialis gangeticus*, which is distinctly dorsally bent (Fig. 8.1).

Unlike all other crocodilians, *S. bollensis* possesses an extremely flat pterygoid. The complete pterygoid lies almost horizontal in the skull (see chapter 3 & 4, Fig. 3.1 & 4.1). The transverse pterygoid flanges are broad but only slightly bent in ventral direction (see chapter 3).

8.1.3 Insertion areas at the cranial and mandibular bones of *Steneosaurus bollensis*

Reconstruction of the jaw muscles as indicated by muscle scars is difficult, because in most specimens of *Steneosaurus bollensis,* the lateral part of the skull is not exposed, because of its dorsoventrally compressed preservation. Therefore, it provides only a few data about muscle scars. However, on the ventrolateral surface of the postorbital and the squamosal a ridge is recognizable, running parallel to the infratemporal fenestra (see chapter 3.1), and on the surface of the laterosphenoid, a weak ridge, running parallel to the sagittal crest, is recognizable, too (see chapter 3.1). In addition, muscle scars are identified in ventral view on the quadrate and the pterygoid, and in lateral view on the lower jaw (see chapter 3, Fig. 3.1 & Fig. 8.2).

On the ventral surface of the quadrate of *Steneosaurus bollensis* three crests are identified and interpreted as A-, B-, and C-crest, in analogy to extant crocodilians by IORDANSKY (1964) (SMNS 15816, Fig. 8.2). The A-crest runs in anteromedial to posteroventral direction and forms in extant crocodilians the insertion area for a broad and strong tendinous sheet, which BUSBEY (1989) calls the cranial adductor tendon ll (CATll = lamina lateralis SCHUMACHER 1973, A-tendon IORDANSKY 1964). The B-crest runs in anteroposterior direction and provides the insertion area for a large flat tendinous sheet called B-tendon (IORDANSKY 1964). According to SCHUMACHER (1973), this is synonymous to the lamina medialis, which according to BUSBEY (1989), also is part of the cranial adductor tendon (=CATlm). The C-crest runs roughly parallel to the posteromedial margin of the quadrate, and provides a further attachment area for the lamina medialis (SCHUMACHER 1973).

CAT is situated in the lateroposterior part of the skull roof, arising from the ventral surface of the quadrate and expanding vertically in anteroventral direction (BUSBEY 1989).

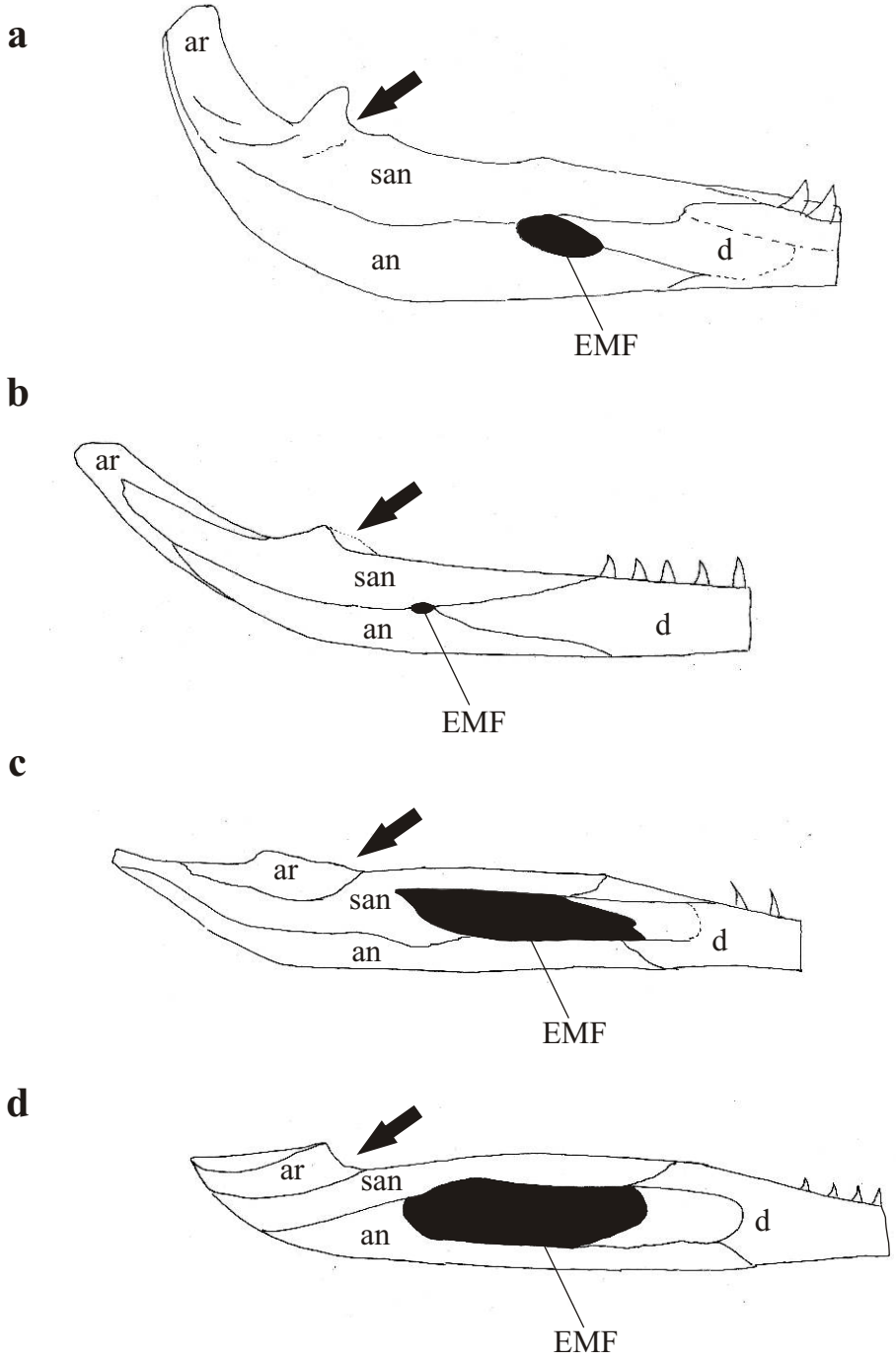

Figure 8.1a-d: Posterior part of the right mandibular ramus with retroarticular process and external mandibular fenestra (EMF) of **a**-*Gavialis gangeticus*, **b**-*Dyrosaurus*, **c**-*Steneosaurus heberti* and **d**- *Steneosaurus bollensis*. The arrows mark the articular areas for the quadrate condyles. For better comparison of the shape of the retroarticular process, all specimens are scaled to the same size and the articular facets are on a vertical line. Abbreviations an-angular, ar-articular, d-dental, EMF-external mandibular fenestra, and san-surangular.

In *Steneosaurus bollensis*, the A-crest is well developed on the ventral surface on the quadrate and runs in anteromedial to posterolateral direction (Fig. 8.2a, b). The strongly developed B-crest runs in anteroposterior direction and the short, weakly developed C-crest runs parallel to the posteromedial margin of the quadrate. It is assumed that these crest in *S. bollensis* provided similar attachment areas for the CAT as they do in extant crocodiles.

In lateral view, the surangular of *S. bollensis* shows anteriorly a small groove dorsal to the external mandibular fenestra (Fig. 3.6). It is interpreted as a possible insertion area of the

M. adductor mandibulae externus superficialis (see paragraph MAMES, Fig. 3.6, and Fig 8.3).

On the lateral side of the angular of *S. bollensis*, a weak crest runs parallel to the external mandibular fenestra; furthermore, a slight ornamentation here indicates insertion of muscle fibers of the M. adductor mandibulae posterior (MAMP) or tendons (Fig. 3.6).

In dorsal view, the posterior part of the articular of *S. bollensis* exposes a smooth, convex surface, only parted by a weak median keel, running in anteromedial-posterolateral direction (see chapter 3.1, Fig 3.1). According to IORDANSKY (1964), in extant crocodilians the M. depressor mandibulae (MDM) and the M. pterygoideus posterior (MPT (p)) insert in that area, therefore it assumed that these muscles inserted likewise in *S. bollensis* (see paragraph MDM & MPT (p)).

M. adductor mandibulae externus (MAME) of *Steneosaurus bollensis* (Fig. 8.3-8.5)

The M. adductor mandibulae externus (**MAME**) is situated laterally to the trigeminal nerve (LAKJER 1926), and is usually subdivided into the M. mandibulae externus superficialis (**MAMES**), M. mandibulae externus medialis (**MAMEM**), and M. mandibulae externus profundus (**MAMEP**) in extant crocodilians (IORDANSKY 1964, BUSBEY 1989).

In extant crocodilians, the MAMES is an undivided muscle unit, which arises from the upper temporal bar. It originates from the postorbital near the postorbital bar, the ventral surface of the quadratojugal, and posteriorly from the lateral part of the quadrate and inserts on the dorsal surface of the surangular (IORDANSKY 1964, BUSBEY 1989, MÜLLER 2002). According to POGLAYEN-NEUWALL (1953) and IORDANSKY (1964), the dorsoventral muscle fibers of the MAMES fill the complete infratemporal fenestra.

Similarly, the MAMES in *S. bollensis* is reconstructed as a muscle mass filling the infratemporal fenestra, arising from the posteroventral surface of the postorbital and the ventral surface of the upper part of the quadratojugal and inserting on the anterior dorsolateral surface of the surangular (Fig. 8.3a, b). Because the infratemporal fenestra is much larger in *S.*

bollensis than in extant crocodilians, the MAMES was probably thicker and therefore stronger compared to extant crocodiles.

In extant crocodilians, the fibers of the MAMEM often are hard to distinguish from the MAMES and therefore, its absolute size is not clear (IORDANSKY 1964, SCHUMACHER 1973, MÜLLER 2002, SCHWARZ 2003). The MAMEM arises from the ventral surface of the quadrate medial to the MAMES and from the anterior and lateral faces of the lateral and medial lamina of the cranial adductor tendon (A- and B-tendon according to IORDANSKY 1964) (BUSBEY 1989). The MAMEM insert on the inner edge of the medial face of the surangular medial to the MAMES insertion. The anterior fibers of the MAMEM insert into a tendon, which fastens upon the surangular above the attachment of the mandibular adductor tendon (MAT = stem tendon IORDANSKY 1964) (BUSBEY 1989). According to CLEUREN & DE VREE (2000), the MAMEM inserts by means of a small apneurosis (a part of the MAT) on the Cartilago transiliens (CT).

In *Steneosaurus bollensis*, the MAMEM probably also arose from the ventral surface of the quadrate and the cranial adductor tendon (CAT). The described well-developed crests on the ventral surface of the quadrate (see 8.1.3), makes the existence of a cranial adductor tendon (CAT) in *Steneosaurus bollensis,* as it is observed in extant crocodilians, very likely (Fig. 8.2a-c). Therefore, the MAMEM is reconstructed as a bundle of muscle fibers, which stretched out slightly anteroventrally. It inserted anteriorly on a tendinous sheet perhaps attached to a Cartilago transiliens (CT), medially it inserted probably on the medial surface of the surangular and angular, and posteriorly on a lamina of the mandibular adductor tendon (MAT) (Fig. 8.4a). Unfortunately, the internal side of the mandible of *S. bollensis* is unknown, therefore the insertion areas for the MAMEM are only speculations.

The M. adductor mandibulae externus profundus (MAMEP) is separated from the other portions of the M. adductor mandibulae externus by a thin fascial sheet in extant crocodilians (BUSBEY 1989). According to IORDANSKY (1964) and BUSBEY (1989), the MAMEP is divided into two portions of fibers with slight different orientations. The anterior portion originates from the lateral surface of the laterosphenoid and from a thin tendinous sheet, which is attached to the oblique crest of the laterosphenoid (IORDANSKY 1964, BUSBEY 1989). The posterior muscle portion arises from the lateral surface of the parietal, the medioventral surface of the squamosal and postorbital, and the ventral surface of the quadrate and the posttemporal wall (BUSBEY 1989). Both portions insert on the strap-shaped lamina lateralis of the mandibular adductor tendon (MATll, part of stem tendon after IORDANSKY 1964), which inserts along the dorsolateral edge of the CT (BUSBEY 1989). The mass of the MAMEP

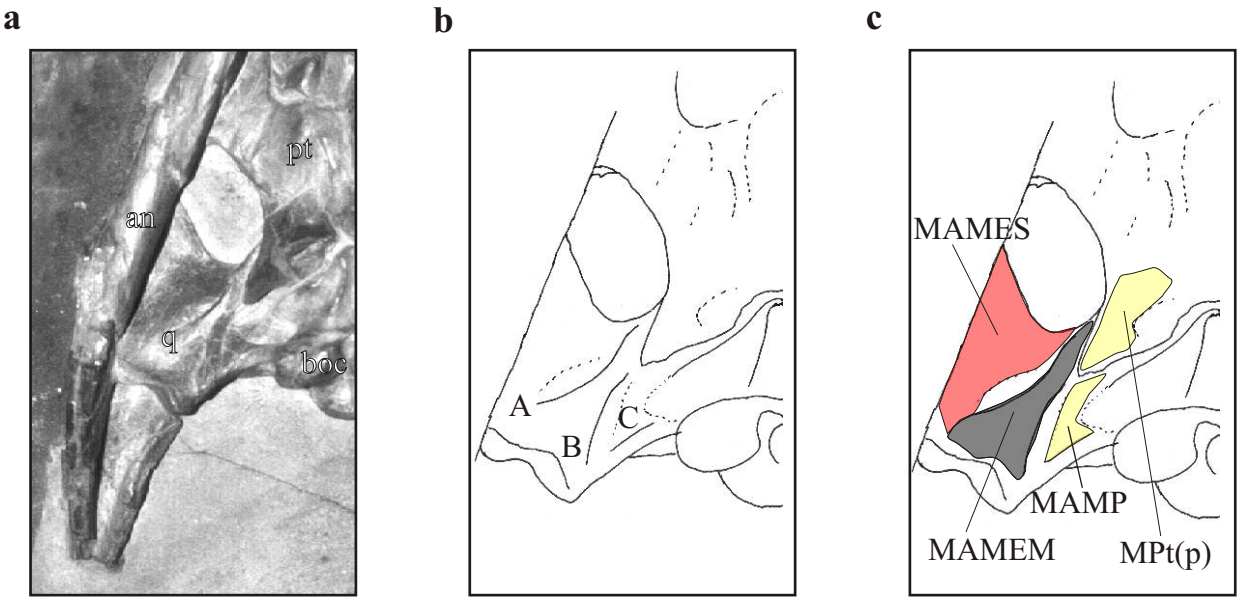

Figure 8.2a-c: Quadrate of *Steneosaurus bollensis* (SMNS 15816) in ventral view with potential insertions of the laminae of the cranial adductor tendon, respectively the corresponding muscles. **8.2a-**Photo of the left quadrate in ventral view, in articulation with the adjacent bones and overlying mandible. Abbreviations: an-angular, boc-basioccipital, pt-pterygoid, and q-quadrate. **8.2b**- Schematically presented crests on the ventral surface of the quadrate (definition after IORDANSKY 1964). **8.2c-**Corresponding attachment areas of the cranial adductor tendon with corresponding muscles (for muscle abbreviations see text).

depend on the dimensions of the supratemporal fenestrae (IORDANSKY 1964). By contrast, SCHUMACHER (1973) and ENDO et al. (2002) refer most of the muscle mass in the supratemporal fenestra to the M. adductor mandibulae internus pseudotemporalis (MPS), particularly in case of the Indian gharial.

Following the description by IORDANSKY (1964) and BUSBEY (1989) of the MAMEP in extant crocodilians, the MAMEP in *Steneosaurus bollensis* is reconstructed as a partly divided muscle mass (anterior and posterior portion), which filled the supratemporal fenestra almost completely. The anteriormost part of the supratemporal fenestra was probably filled by the MPS in *S. bollensis*, following the description by SCHUMACHER (1973) and ENDO et al. (2002) of extant longirostrine crocodilians (Fig. 8.3a & Fig. 8.4b). It is therefore assumed for *S. bollensis* that the main part of the supratemporal fenestra was filled by the MAMEP, but that in the anteriormost part of the supratemporal fenestra also the MPS arose (see also paragraph MPS, Fig. 8.5a). In the posterior portion of the MAMEP, the fibers probably ran in slight posterodorsal to anteroventral direction and in the anterior portion vice versa. The entire muscle mass itself must have pulled almost vertically downwards, because the infratemporal fenestra and the mandible lie almost vertically ventral to the lateral bar of the supratemporal fenestra.

M. adductor mandibulae posterior (MAMP) of *Steneosaurus bollensis* (Fig. 8.1a, Fig. 8.5a)

In extant crocodilians, the superficial fibers of the MAMP arise from the ventral parts of the quadrate and from the lateral surface of the cranial adductor tendon (CAT) (SCHUMACHER 1973, BUSBEY 1989). Furthermore, some fibers arise from the posterior part of the medial lamina (B-tendon, IORDANSKY 1964) of the cranial adductor tendon (CAT) (BUSBEY 1989). The muscle inserts posteriorly on the anteromedial surface of the articular and angular, and, more anteriorly, on the posterior wall of the Meckelian fossa. Moreover, the deepest parts of the MAMP, i.e. those fibers originating from the medial lamina of the cranial adductor tendon, insert into the posterior lamina of the mandibular adductor tendon (MAT) (SCHUMACHER 1973, BUSBEY 1989, CLEUREN & DE VREE 2000, MÜLLER 2002).

In *Steneosaurus bollensis*, the MAMP had probably its origin on the ventral surface of the quadrate and the cranial adductor tendon (CAT) and inserted on a broad mandibular adductor tendon (MAT), which was probably attached to the jugal. Because of the large size of the mandibular fenestra, it is supposed, that the tendon (MAT) was likewise enlarged (Fig. 8.1a & Fig. 8.5a). It is most likely that the anterior muscle fibers of the MAMP also inserted

directly on the anteromedial part of the angular, because of the observed faint crest and the rugosities on the lateral surface of the angular of *S. bollensis* (see 8.1.3). A larger physical cross-section for the MAMP is supposed for *S. bollensis*, because of the enlarged mandibular and infratemporal fenestrae compared to extant crocodilians.

M. adductor mandibulae internus of *Steneosaurus bollensis* (Fig. 8.5)

In extant crocodilians, the M. adductor mandibulae internus is subdivided into three major portions, the M. pseudotemporalis (MPS), the M. pterygoideus anterior (MPT (a)), and the M. pterygoideus posterior (MPT (p)) (POGLAYEN-NEUWALL 1953, IORDANSKY 1964).

The muscle fibers of the **MPS** originate from the supratemporal fenestra, in particular from the crest of the laterosphenoid and the surrounding bones like the lateral surface of the parietal, the anterior surface of the squamosal, and the anterior surface of the supraoccipital as well as from the alisphenoid. From there, the fibers run ventrolaterally and insert on the Cartilago transiliens (CT), in some cases via narrow tendinous laminae (SCHUMACHER 1973). The most deeply situated fibers insert on the dorsal surface of the mandibular adductor tendon (IORDANSKY 1964, SCHUMACHER 1973, BUSBEY 1989, MÜLLER 2002, SCHWARZ 2003). Furthermore, in extant longirostrine crocodilians the MPS enlarges at the expense of the MPT (a) (SCHUMACHER 1973, ENDO et al. 2002).

In *Steneosaurus bollensis*, the MPS should be similar developed to the extant longirostrine crocodiles, but real osteological evidence is not available. However, it arose probably only from the posterolateral surface of the frontal, the lateral crest of the laterosphenoid (see chapter 3) and the posterior surface of the postorbital, because the supratemporal fenestra is greatly enlarged in *S. bollensis* compared to extant crocodilians (Fig. 8.5a). Whether the MPS was enlarged in order to compensate a weak MPT (p) in *S. bollensis*, as SCHUMACHER (1973) describes it in general for longirostrine crocodilians and ENDO et al. (2002) particularly for *Gavialis gangeticus,* cannot be determined.

In extant crocodilians, the **MPT (a)** originates from the most anteroventral part of the quadrate, the dorsomedial part of the pterygoid, the cultriform process of the basisphenoid, the cartilaginous part of the interorbital septum, the prefrontal pillars, the maxilla, and the ventrolateral part of the palatine, completely filling the palatal opening. The posterior deeper fibers insert on the angular, the articular, and on the posterior lamina of the mandibular adductor tendon (MAT). The anterolateral fibers are attached to the dorsal surface and the anterior lamina of this tendon (MATlas BUSBEY 1989), which insert on the dorsal edge of the Cartilago transiliens (CT) (BUSBEY 1989, CLEUREN & DE VREE 2000, MÜLLER 2002).

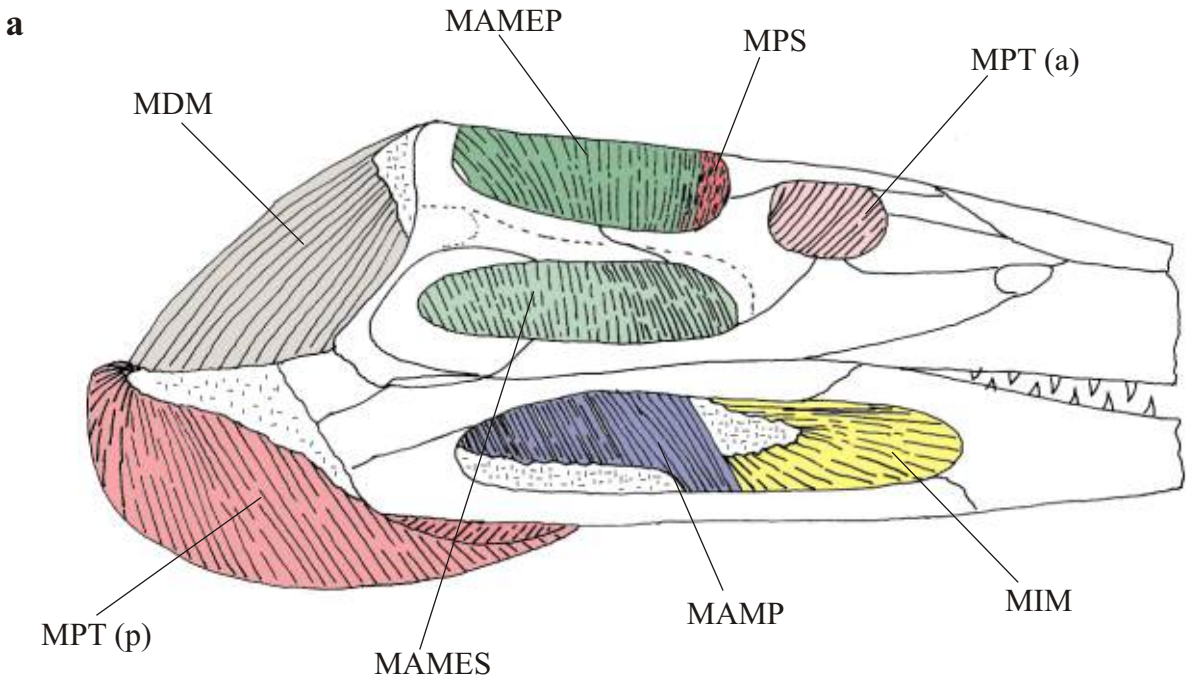

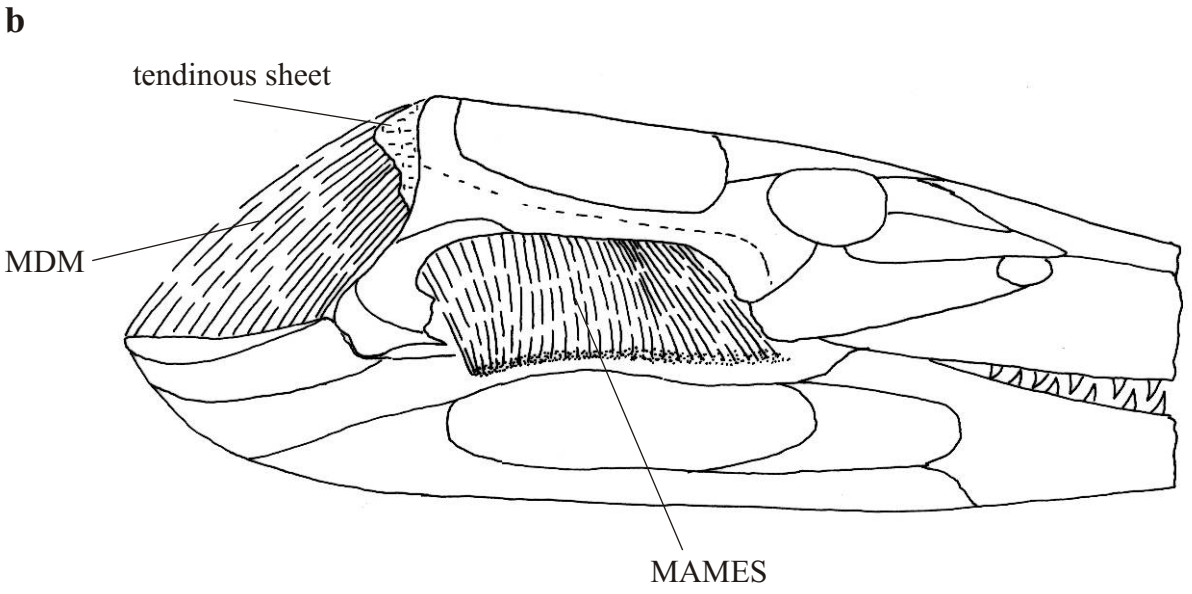

Figure 8.3a-b: Hypothetical reconstruction of the jaw adductor musculature in *Steneosaurus bollensis*. **8.3a-**Possible outer layer of the jaw musculature. **8.3b-**Reconstruction of the MDM and the MAMES after removing the lower temporal bar. Abbreviations see text.

In *Steneosaurus bollensis*, the MPT (a) was probably running through the palatal opening (=suborbital fenestra) like in extant crocodilians (see above). The suborbital fenestra is large in *S. bollensis* (see Fig. 3.1), which indicates a well developed MPT (a). The existence of a Cartilago transiliens (CT) is assumed in analogy with the conditions in extant crocodilians, but no real evidence can be given.

In extant crocodilians, six large apneuroses form the origin and insertion of the **MPT (p)** (SCHUMACHER 1973). Its muscle fibers arise from the dorsal and ventral surface of the pterygoid and three aponeuroses are attached to the posterior part of the pterygoid wing. The fibers merge into three further aponeuroses, which insert on the surangular and articular (CLEUREN & DE VREE 2000).

According to ENDO et al. (2002), in *Gavialis gangeticus* the M. adductor mandibulae internus pterygoideus (MPT (p)) consists of a single huge belly on the medial side of the lower jaw. The muscle arises from the dorsal surface of the pterygoid and the ventral side of the quadrate, and inserts on the entire area of the medial side of the articular, angular and surangular. The muscle belly also reaches the caudal part of the coronoid. In *Tomistoma schlegelii*, the MPT (p) also possesses a lateral extension and inserts on the lateral surface of the articular, surangular and angular. In addition, ENDO et al. (2002) note that the lateral extension of the M. pterygoideus posterior (MPT (p)) is much weaker in the extant long-snouted species than in latirostrine *Alligator* or *Crocodylus* species. The stronger developed M. pseudotemporalis (MPS) may compensate for the weak M. pterygoideus posterior (MPT (p)) in the role of mastication, at least in *Gavialis gangeticus*.

In *Steneosaurus bollensis*, the MPT (p) was probably relatively thin. The broad transverse pterygoid flanges do not extend much ventrally in *S. bollensis*, whereas the pterygoids in extant crocodilians expand distinctly in ventral direction. The flat pterygoids in *S. bollensis* probably limited the diameter of the MPT (p) by reducing the space between the pterygoid and the internal face of the skull table, where the muscle originates. However, in *S. bollensis* the MPT (p) probably originated additionally at the ventral surface of the pterygoid, which is indicated by an ancillary small crest on the ventral surface of the pterygoid (see Fig. 8.2). In that way, the muscle diameter of the MPT (p) could have been increased in *S. bollensis*, but probably were still thinner than in extant crocodilians (Fig. 8.2). In addition, the muscle probably expanded posteriorly to the lateral surface of the retroarticular process in *S. bollensis*. At the lateral surface of the retroarticular process, at the level of the articular-surangular suture, a slight depression is visible, which indicates muscle attachment in this area, probably by means of a tendinous sheet (see 8.1.3 and Fig. 8.5b).

M. intramandibularis (MIM) in *Steneosaurus bollensis* (Fig. 8.5b)

In extant crocodilians, the muscle originates at the ventral surface of the Cartilago transiliens (CT) by means of an tendon (intramandibular tendon SCHUMACHER 1973) and inserts on the medial surface of the angular, coronoid and splenial, the dorsal surface of Meckel´s cartilage, and on the posteromedial surface of the dentary (SCHUMACHER 1973, CLEUREN & DE VREE 2000).

It is supposed here that in *S. bollensis* the fibers of the MIM were running from a Cartilago transiliens (CT) to the lateral surface of the angular like in extant crocodilians (Fig. 8.5b), because on the lateral surface of the angular of *S. bollensis* a small crest and slight ornamentation is visible, which probably indicates some muscle attachment there. Furthermore, it is assumed that the muscle runs anterior into the Meckelian fossa like in extant forms, but due to the lack of preservation of the internal side of the mandible of *S. bollensis*, no evidence can be given.

M. depressor mandibulae (MDM) in *Steneosaurus bollensis* (Fig. 8.3)

In extant crocodilians, the depressor mandibular muscle is not subdivided. The fibers arise from the posterior edge of the parietal, squamosal, supraoccipital, and the posterodorsal part of the quadrate and from a tendonious sheet, which is attached to the lateral tip of the exoccipital wings. The fibers run posteroventrally to insert on the dorsal surface of the retroarticular process (IORDANSKY 1964, BUSBEY 1989, CLEUREN & DE VREE 2000, MÜLLER 2002).

Because of the horizontal alignment of the retroarticular process of *Steneosaurus bollensis* (Fig. 8.1) compared to extant crocodilians, the muscle fibers of the MDM probably extended steeply, in an angel of 50-60 degrees, in posteroventral direction (Fig. 8.3b). The muscle probably arose similar to extant crocodilians at the posterior surface of the skull and inserted on the dorsomedial surface of the retroarticular process. A slight keel on the dorsal surface of the retroarticular process of *S. bollensis* (see 8.1.3) indicates muscle attachment of the MDM there.

8.1.4 Functional interpretation

Extant crocodilians possess strongly developed adductor muscles for closing the mouth and only one jaw muscle for jaw abduction (and opening of the mouth, respectively) (IORDANSKY 1964, SCHUMACHER 1973, BUSBEY 1989). However, jaw opening is achieved by a depression of the lower jaw by contraction of the M. depressor mandibulae (MDM) and simultaneously, the upper jaw is elevated by the contraction of several dorsal cervical muscles

a

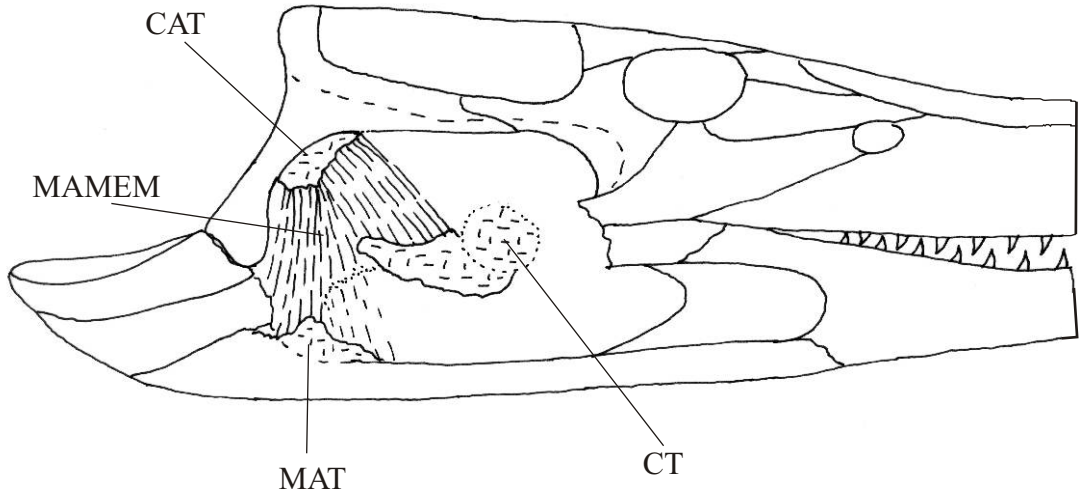

b

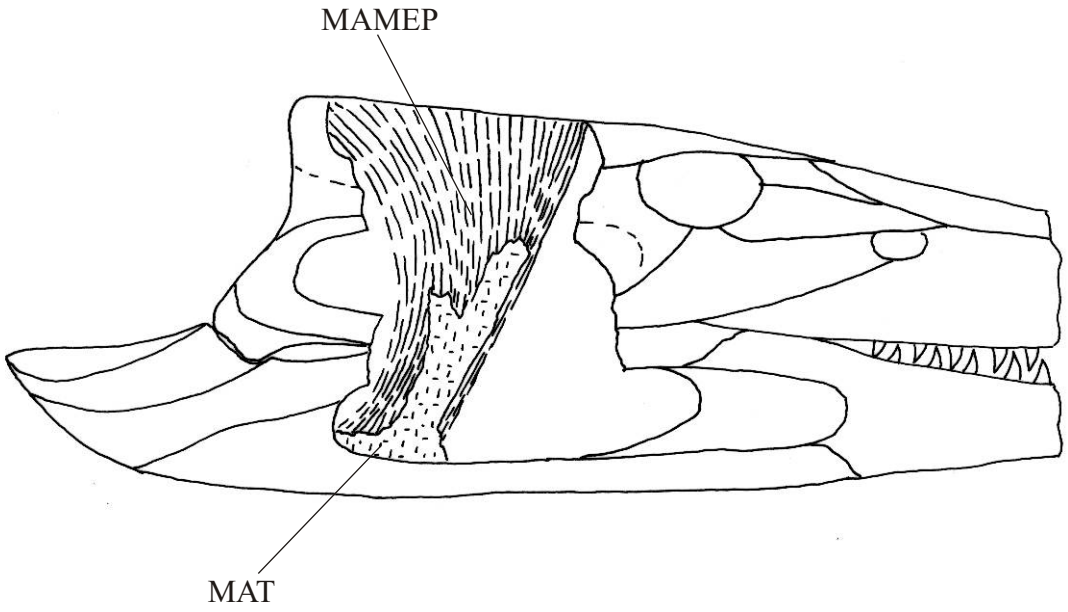

Figure 8.4a-b: Hypothetical reconstruction of the successively deeper lawers of the adductor mandibulae externus muscle. **8.4a-**The possible run of the adductor mandibulae externus medialis muscle (MAMEM). **8.4b-**Reconstruction of the adductor mandibulae externus profundus muscle (MAMEP). Abbreviations see text.

(CLEUREN & DE VEER 2000). This system is basically also suggested for fossil crocodilians (SCHWARZ 2003) and is here likewise assumed for *S. bollensis*.

For biomechanical considerations the jaw of crocodilians can be regarded as a lever model with the pivot (center of rotation) in the jaw joint, and the mandible as the movable lever arm (SCHUMACHER 1973, PREUSCHOFT et al. 1985, SCHWARZ 2003, WESTNEAT 2003). It is regarded as a third-order lever, which has the input force and the load on the same side of the fulcrum (pivot), with the force closer to the fulcrum than the weight. This mechanism is used to gain a velocity advantage (WESTNEAT 2003). Even though this does not completely reflect the movement in the crocodile jaw as described by e.g. BUSBEY (1989) or CLEUREN & DE VREE (2000), the model allows interpretations of the jaw mechanism.

8.1.5 Jaw adduction

Following the law of the lever, the distance between the jaw joint (pivot) and the attachment of the corresponding adductor mandibulae muscle is defined as the force arm, and the distance between the jaw joint (pivot) and a prey item between the jaws is defined as the load arm (SCHWARZ 2003). Provided, that the force arm is constant, the longer the load arm in relation to the force arm is the smaller is bite force working on the object. As a result, the bite force is stronger closer to the jaw joint (short load arm) than at the tip of the snout (long load arm) (SCHWARZ 2003). Therefore, in general in the longirostrine skull type, the bite force at the tip of the rostrum is lower than in short-snouted crocodiles.

However, force output at the tip of the lower jaw depends on the muscular input force, the angle of insertion of the muscles onto the jaw, and the ratio of force arm to load arm (WESTNEAT 2003). The angle of insertion of the jaw adductor muscles changes during jaw closure, depending on their position and orientation in the jaw. According to BUSBEY (1989) the quotient of muscle mass/fiber length is an indicator of the potential output force of a muscle, alternative the physiological cross-section of the muscle, i.e. the number of fibers working in parallel, can be used to calculate the force output (MARTIN et al. 1998, RIEPPEL 2002). Thus, the resulting force, i.e. the bite force, is the ratio of force arm to load arm in the model, under consideration of the respective insert angle at the mandible and the physiological cross-section of the adductor muscles.

It is assumed, that *Steneosaurus bollensis* possessed a weakly developed MPT (p), which probably was compensated by a strongly developed MAMEP and an enlarged MPS. Similar to the conditions found in *Tomistoma schlegelii* and *Gavialis gangeticus* (SCHUMACHER 1973, CLEUREN & DE VREE 2000, ENDO et al. 2002). However, in *Steneosaurus bollensis,* the assumed larger physiological cross-section of the MAMES,

MAMEP, and probably the MPS (see 8.1.4) indicates an increased force output of these muscles, compared to the conditions in extant longirostrine crocodilians (e.g. *Gavialis gangeticus* and *Tomistoma schlegelii*).

The changes in the lines of action of the main jaw muscles in *Steneosaurus bollensis,* during closed or opened jaw, are illustrated in Figures 8.6a-b. The MAMP, MAMES, and MAMEP were probably pulling in almost vertical direction, when the jaw was closed (Fig. 8.6a). The MPS pulled in anteroventral direction, while the MPT (a) pulled mainly anteriorly, at closed jaw position (Fig. 8.6a). It is assumed, that during opening of the jaws, the MAMP was only slightly tensioned, but then pulled slightly posteriorly (Fig. 8.6b). The MAMES, MAMEP, and MPS were largely tensioned. The latter probably doubled its length. All of them were pulling mainly vertically. The MPT (a) showed the most striking changes, because of its anterior position in the skull. During jaw opening, it was probably largely tensioned, and pulled then nearly vertically and only slightly anteriorly (Fig. 8.6b).

No definite statement can be made about the possible force output of the single muscles, because important parameters such as fiber length, physiological cross-section, origin, and insertion angle of the muscles are mainly suppositions.

However, the main adductor muscles showed probably a strong extension during jaw opening (Fig. 8.6b), and a small jaw rotation angle resulted in a large gape distance at the tip of the rostrum, due to the longirostrine conditions in *S. bollensis*. According to SCHUMACHER (1973), a strong extension of the adductor muscles is achieved during opening of the mandible in extant crocodilians. The more the adductors are tensioned, the quicker is the contraction of the muscles and quick muscle contractions of the adductor muscles allow a fast closing of the jaws (SCHUMACHER 1973). The suggested strong extension of the adductor musculature and the most likely increased cross-section of the MAMES, MAMEP, and MPS in *Steneosaurus bollensis* compared to *Gavialis gangeticus,* result in the assumption, that *S. bollensis* could close its jaws quickly and had most likely a more forceful bite than *G. gangeticus*, in consequence of increased force output due to the larger adductor muscle diameters.

8.1.6 Lower jaw abduction

In extant crocodilians, opening of the jaw is mainly achieved by contraction of the MDM and partly the M. branchiomandibularis (MB), and by the contraction of several cervical muscles (BUSBEY 1989, CLEUREN & DE VREE 2000, SCHWARZ 2003). According to CLEUREN & DE VREE (2000), e.g. straight lifting of the cranium during fast opening is mainly caused by a bilateral contraction of the muscles of the transversospinalis system.

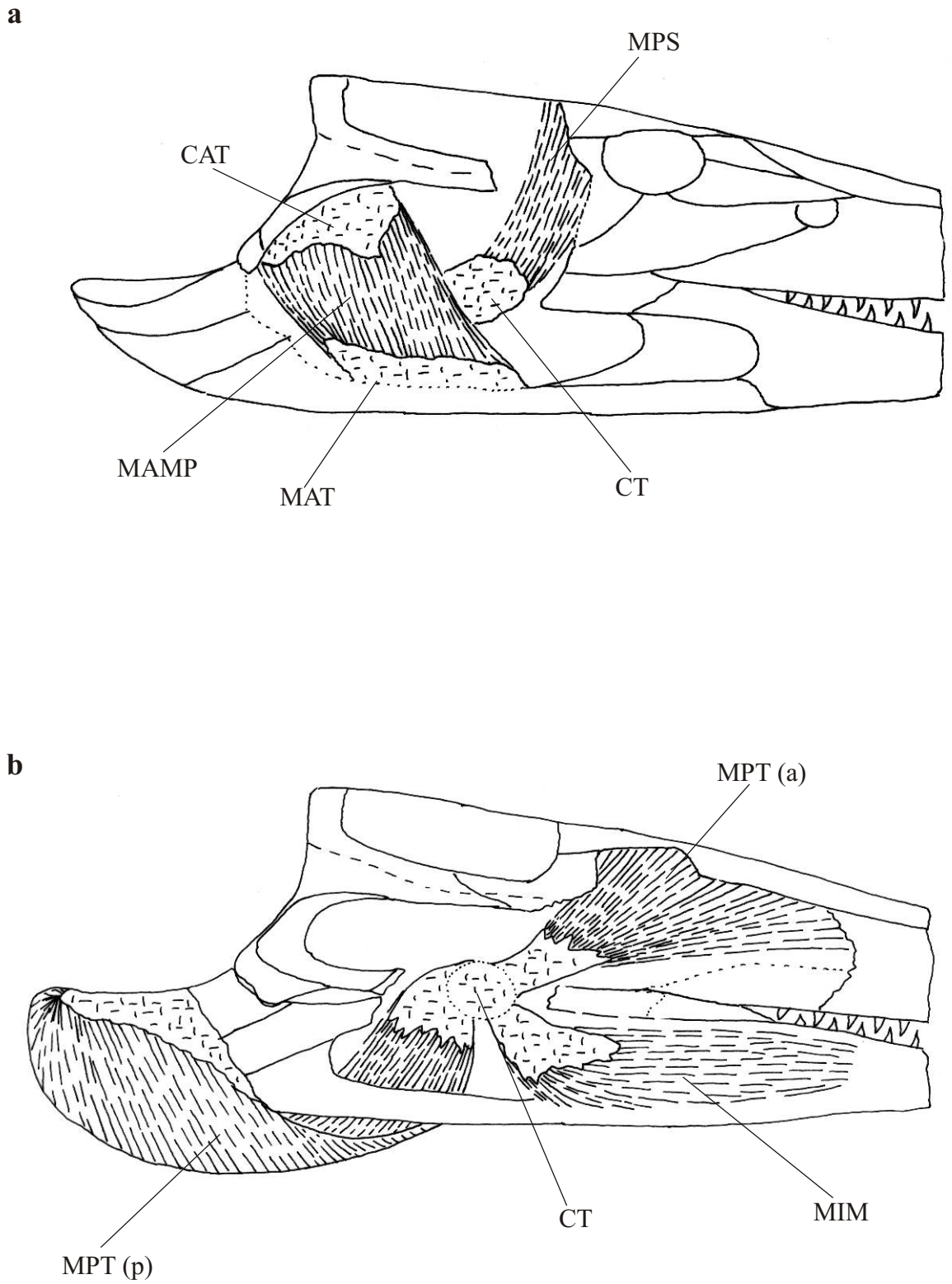

Figure 8.5a-b: Hypothetical reconstruction of the adductor mandibulae posterior muscle (MAMP), the adductor mandibulae internus muscle, and the intramandibularis muscle (MIM). **8.5a-**Origin and insertion of the superficial fibers of the MAMP and the pseudotemporalis muscle (MPS). **8.5b-**Possible run of the anterior and posterior pterygoideus muscles (MPTa/p) and the intramandibularis muscle (MIM). For further explanations and abbreviations see text.

a

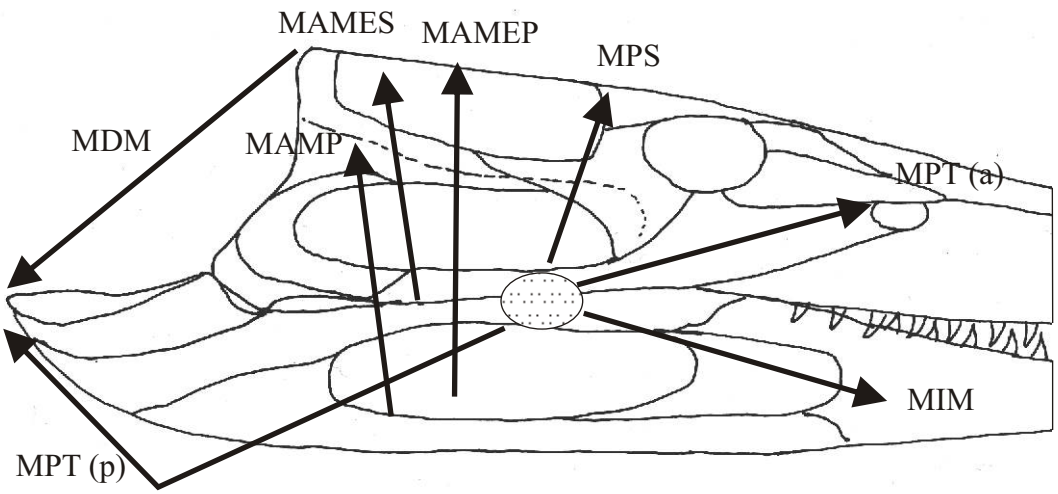

b

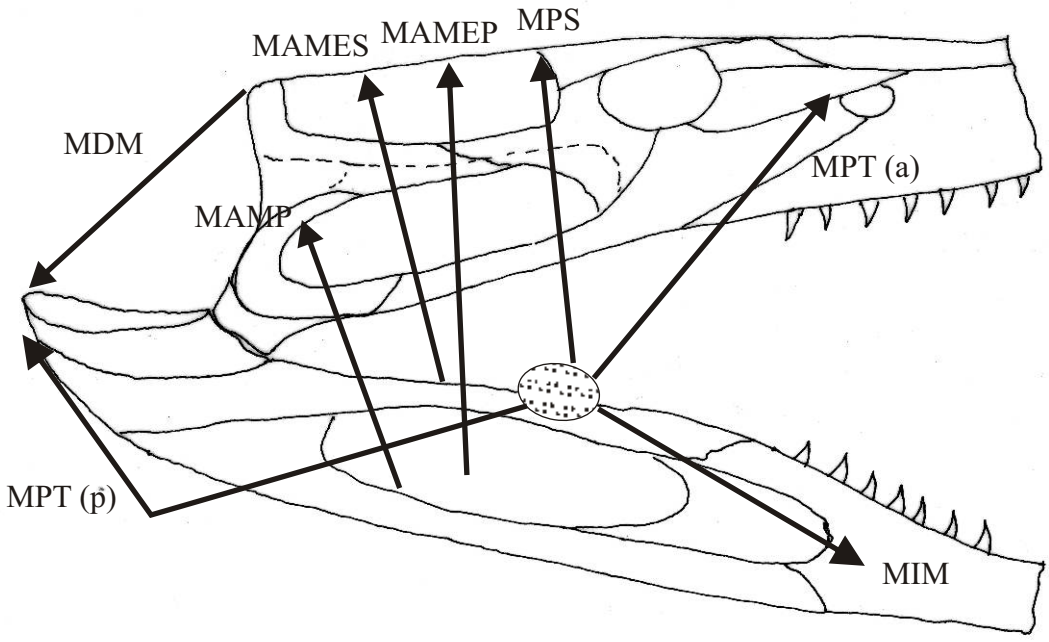

Figure 8.6a-b: Dorsal view of the lines of action of the jaw muscles according to run of the muscle fibers and the muscle itself and the position of the Cartilago transiliensis (CT). **8.6a-**Muscle fibers and postion during closed jaw. **8.6b-**Muscle fibers and position during open jaw.

However, in the suggested hypothetical lever model for the jaw of crocodilians (see above), only the mandible is regarded as movable, and MDM is considered the only jaw abductor muscle.

It is assumed, that during jaw closure, the fibers of the MDM in *Steneosaurus bollensis* inserted approximately in an angle of 55° at the dorsal surface of the retroarticular process (Fig. 8.3). The optimal load transmission would be at an angle of 90° and decreases with a decreasing angle (FASTNACHT pers. comment, RIEPPEL 2002). The angle of insertion in *Gavialis gangeticus* is estimated here with 75° and in *Dyrosaurus* with 80° after the reconstruction by SCHWARZ (2003). *S. bollensis*, thus, probably showed a weaker load transmission compared to *Dyrosaurus* and *Gavialis gangeticus* at least for the MDM. On the other hand; the muscle fibers of the MDM in *S. bollensis* were probably longer compared to those of *Gavialis gangeticus*, because of the more horizontal elongated retroarticular process of *S. bollensis* (Fig.8.1a, d). The probably longer muscle fibers indicate a faster opening of the jaw of *S. bollensis* compared to that of *G. gangeticus*. Thus, the opening of the jaw of *S. bollensis* was probably quicker but weaker compared to the conditions in *G. gangeticus*.

8.1.7 Tooth morphology and dentition (Fig. 8.7)

Steneosaurus bollensis possesses up to 39 teeth on each side of the upper jaw and up to 35 teeth in each dentary (see chapter 3.1 & 5.2.4). The teeth are slender, conical, and apically recurved. The apex is pointed and the tooth crown is covered with a fine vertical striation (see chapter 3 and Fig. 8.7d). This is the common tooth morphology seen in all Liassic thalattosuchians (VIGNAUD 1997). *Steneosaurus bollensis* commonly possesses teeth with one or two low carinae, either on the anterior or posterior side or on both sides of the tooth. The teeth of *S. brevior* are more robust, i.e. possess a larger diameter at the base of their tooth crown, while the teeth of *Pelagosaurus typus* are more slender and mostly without a carina. However, apart from these small differences, all teeth of the Liassic teleosaurids resemble each other. Furthermore, during ontogeny, the teeth increase naturally intraspecifically in thickness and length. Thus, they show all kind of intermediate stages in their length and width, which makes it nearly impossible to refer a single tooth to a specific taxon.

In contrast, the teeth of some other *Steneosaurus* taxa e.g. from the Middle Jurassic are strongly different compared to the Liassic teleosaurid teeth (Fig. 8.7). *Steneosaurus edwardsi,* for example, has robust teeth with a blunt apex and ventral to the tooth crown a small constriction is visible (Fig. 8.7a). *Steneosaurus obtusidens* possesses nearly straight teeth with a blunt apex. The striation of the teeth dissolves and becomes disordered at the apex (Fig.

8.7b). In contrast, the teeth of *S. megistorhynchus* are long, very slender and possess a particular pointed apex.

The Liassic teleosaurid taxa all refer to the Pierce I and Pierce II/General - tooth type defined by MASSARE (1987, 1997). The so-called Pierce I – tooth type includes very slender, sharply pointed, long, delicate teeth. Those teeth are either smooth or show fine longitudinal ridges. This tooth type is found e.g. in the teeth of the Indian gharial (Fig. 8.7e). The Pierce II/ General – tooth type consists of pointed, somewhat slender, curved teeth of moderate length, with usually two carinae or fine longitudinal ridges. These two types are referred to most *Steneosaurus* taxa, which often have slender, slightly apically recurved, more or less pointed teeth with or without carinae and fine vertical striation (Fig. 8.7).

According to MASSARE (1987), the Pierce II / General – type reflects a preference for fleshy prey lacking a hard exterior (while the prey is pierced to capture), and the Pierce I – type is referred to very soft prey or very small vertebrates (while the prey is pierced to capture), or teeth possibly used as sieve.

According to FASTNACHT (2005), a higher tooth crown and a pointed apex increase the efficiency of fixation of food items. The higher the tooth crown is, the deeper it can penetrate into the food item and the more pointed the apex is, the more force is concentrated in this area which is the first to get in contact with the food item (FASTNACHT 2005). "A further effect of a posteriorly curved tooth construction is the restriction of the anterior movement of the food item during jaw occlusion" (FASTNACHT 2005). He postulates that, "the food is transfixed and movement without destruction is only possible in posterior direction [...]". Carinae at the tooth crown are interpreted as cutting edges. However, the more circular the cross-section of the tooth construction gets, the less effect the carinae has, but the puncturing/penetrating capacity is well developed (FASTNACHT 2005).

Thus, the slender, conical, and apically pointed and posteriorly curved teeth of *S. bollensis* had very likely the option to puncture and penetrate the food items and favoured a transportation of the prey in the direction of the pharynx. *S. gracilirostris* has a higher tooth count and probably slightly smaller teeth than *S. bollensis*. This pattern of dentition of *S. gracilirostris* points to that they possibly used their teeth as sieve.

The long and slender rostrum with numerous mostly homodont teeth of teleosaurids is often compared with the similar elongated snout of the extant Indian gharial (*Gavialis gangeticus*) (e.g. BUFFETAUT 1982). *G. gangeticus* possesses up to 110 homodont, very slender teeth with a pointed, slightly recurved apex in the rostrum (Fig. 8.7e). This pattern of dentition resembles that of *Steneosaurus bollensis* (Fig. 8.7d).

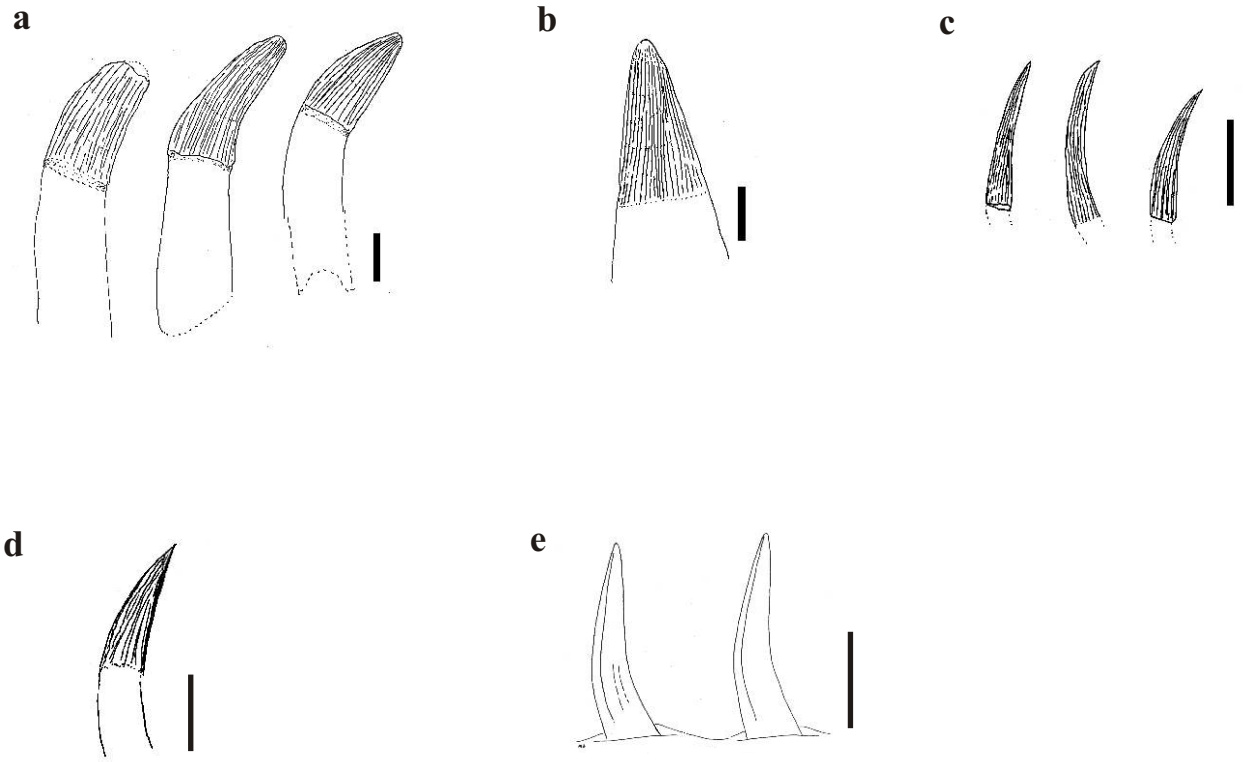

Figure 8.7a-d: Examples for different tooth morphology in different *Steneosaurus* taxa and in *Gavialis gangeticus*. **8.7a-**Sketch of *Steneosaurus edwardsi* teeth (after BMNH R 2865). The tooth crown with thin vertical striation is ventrally constricted. The apex is blunt. A carina is not present. **8.7 b-**Sketch of a tooth of *S. obtusidens* (after BMNH R 3268). The tooth is nearly straight with vertical striations and a relative blunt apex. At the apex, the striation dissolves and become disordered. **8.7c-**Sketch of *S. megistorhynchus* teeth (after BMNH 28497). The teeth are long, very slender, slightly apically recurved with a quite pointed apex. Tooth crown with very fine vertical striation. **8.7-**Sketch of a tooth of *S. bollensis* (after MGUH 1892-234). The tooth is apically recurved with a pointed apex, very fine vertical striations and a single smooth carina at the posterior side of the tooth. **8.7e-** Sketch shows two gavial teeth after MASSARE (1987). The teeth are very slender, slightly apically recurved, and possess only very slight striation. A carina is visible at the lingual side of the teeth. Scale bar is 10 mm.

In fossil thalattosuchians, a long and slender snout with numerous homodont teeth has mostly been interpreted as a sign of piscivory in analogy with the Indian gharial (HUA & BUFFETAUT 1997, HUA & BUFFRÉNIL 1996, FREY 1988b, LEVY 2003). However, the term piscivorous is misleading. Ontogenetic changes in prey preference are known for *Crocodylus porosus*, *Crocodylus niloticu*s, *Alligator mississippiensis*, and are also reported from *Gavialis gangeticus* (COTT 1961, TAYLOR 1979, WHITAKER & BASU 1982, THORBJARNARSON 1990, ERICKSON et al. 2003). Small individuals of *C. porosus* eat mainly crustaceans, whereas only large specimens also add mammals and birds to their diet (TAYLOR 1979). Similar observations are made for *Crocodylus niloticus* and *Alligator mississippiensis*, which changes from insects, crustaceans, and small fish in young specimens to larger fish, mammals, and bird in adults (COTT 1961, ERICKSON et al. 2003). *Gavialis gangeticus* eats mainly fish, but also small vertebrates are reported occasionally. In juvenile specimens, tadpoles and invertebrates are known prey beside fish (WHITAKER & BASU 1982, THORBJARNARSON 1990)

Indian gharials (*Gavialis gangeticus*) are ambush hunters and catch their prey with a sudden lateral stroke of the jaws (WHITAKER & BASU 1982, FREY 1988b, CLEUREN & DE VREE 2000, POOLEY 2002, LEVY 2003). The flat, almost tubular snout and the generally flat skull of *Gavialis gangeticus* decrease the drag in water during such lateral movements (TAYLOR 1987, POOLEY 1989). The reduced drag in all possible directions under water and the elongated jaws with a large number of teeth increasing the chance of catching fast but small prey (BUFFETAUT 1982, CLEUREN & DE VREE 2000). Because of the resembling skull morphology of S*teneosaurus bollensis,* it is assumed that it used a similar method for hunting like *Gavialis gangeticus*. According to RIESS (1986), a quick lateral jaw movement should be connected with a slow approach to the prey in lateral position.

Therefore, most authors assume that teleosaurids had also been ambush hunters like *Gavialis gangeticus*, lying on the bottom of a lagoon environment and waiting for any prey passing by from above (MASSARE 1987, 1988, 1997; MARTILL et al. 1994, HUA & BUFFETAUT 1997). The main argument for this behaviour in *Steneosaurus bollensis* is, beside the assumed similarity with the ecology of the Indian gharial, the anterodorsal position of the orbit, which makes it possible to stalk prey, outlined against the water surface. However, in the skull of *Gavialis gangeticus* the orbit is also dorsally orientated, whereas the eye (i.e. the pupil) in the living animal is more laterally orientated and the eyeball is dorsally covered by skin. If *S. bollensis* had used a similar hunting mode like *G. gangeticus*, it would have been more practically having laterally or anteriorly orientated eyes seeing the prey, before approaching it

with a lateral head movement. However, the orientation of the eyeball in the orbit is pure speculation.

The comparability of the ecology of *G. gangeticus* and *S. bollensis* is anyway questionable. The Indian gharial use to live in freshwater river systems and not in a marine environment like *Steneosaurus bollensis* did.

According to the shape of the skull, the dentition pattern, and the reconstructed jaw muscles of *Steneosaurus bollensis*, it probably preyed on small agile prey, which did not struggle much. Quick bites at the tip of the snout as well as forceful bites close to jaw joint were possible. The bite force was probably higher in *S. bollensis* than in *Gavialis gangeticus* (see paragraph 8.1.6). The general conditions are typical for fish eaters, but most other kind of small prey were possible as well. It is assumed, that size is here a more restrictive factor than the kind of prey. The options for all types of small prey e.g., fish, crustaceans, belemnites, molluscs, cephalopods etc. were given.

8.1.8 Stomach contents of *Steneosaurus bollensis* (Fig. 8.8)

Only little is known about the stomach contents in marine fossil crocodiles, therefore direct evidence of prey is rare. In the present study, several stomach contents are reported in specimens of *Steneosaurus bollensis* from Holzmaden as a black amorphic mass, but also gastroliths and parts of petrified wood are found (e.g. SMNS 51753, SMNS 59736, GPIT Re 1193/1) (Fig. 8.8). In *Platysuchus multiscrobiculatus* and *Pelagosaurus typus,* stomach contents are unknown, neither gastroliths nor wood were observed.

MATEER (1974) investigated a black amorphic mass in the stomach of a *S. bollensis* specimen from Holzmaden (R.161), which is housed at the museum in Uppsala. He describes that the black patch are preserved without any further details and " [...] turned out to be clearly organic, but whether vegetable or animal is difficult to determine" (MATEER 1974; page 54). MATEER (1974) also mentions gastroliths in the same specimen present anterior to the sacral region. Petrified wood, gastroliths, and black amorphic masses were observed in a couple of other *Steneosaurus bollensis* specimens (i.e. SMNS 51753, SMNS 59736), but investigations with a magnifying glass revealed no further details (Fig. 8.8).

In contrast, well-preserved stomach contents are well known from the Holzmaden ichthyosaurs (BÖTTCHER 1989, URLICHS et al. 1994), consisting of belemnite rostrums, hooks from squids, and fish scales (URLICHS et al. 1994). One possible explanation, for the unidentified stomach contents of *S. bollensis*, could be lying in a similar stomach physiology to that of extant crocodilians. The extraordinary acid secretion and gastroliths activity as seen

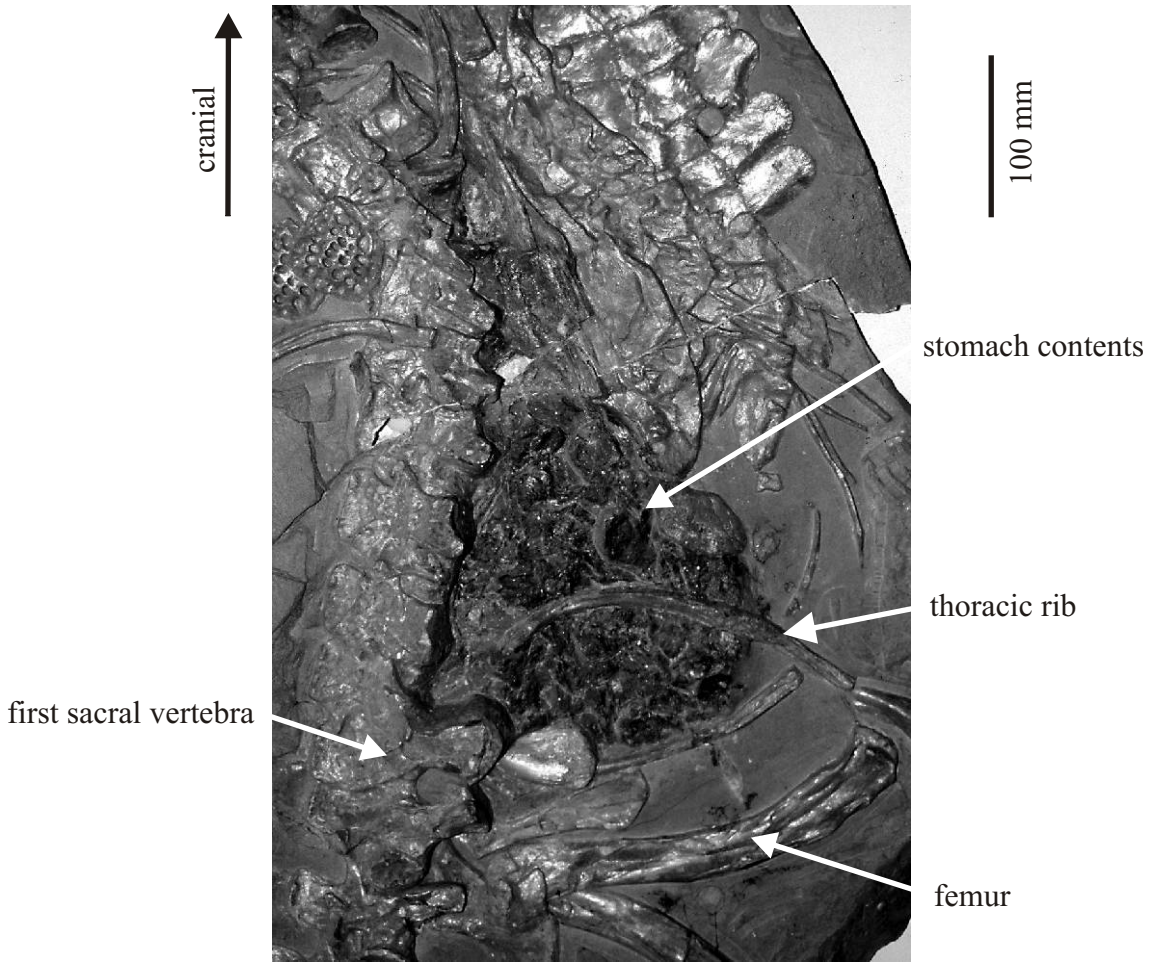

Figure 8.8: Example for preserved stomach contents in *Steneosaurus bollensis* (SMNS 51753). The position of the contents anterior of the sacral vertebra i.e. to the pelvic girdle is typical and indicates probably the position of the stomach. No wood or gastroliths are preserved in this specimen. Due to the flattened preservation a statement about the stomach size is far to speculative.

in the stomach of extant crocodilians makes the digestion of almost anything possible, even bones (POOLEY 2002, LEVY 2003).

One exception from this is probably the thalattosuchian *Metriorhynchus*; MARTILL (1986) and MARTILL et al. (1994) report stomach contents in a *Metriorhynchus* specimen from the Oxford Clay, which contains ammonites, belemnites, pterosaurs bones, and parts of the fish *Leedsichthys* (HUA & BUFFETAUT 1997, WALKER & BRETT 2002). This could be a hint that the stomach physiology of metriorhynchids was different from the teleosaurids or extant crocodilians. However, this assumption is highly speculative and no evidence can be given.

The presence of wood in the stomach of *Steneosaurus bollensis* from Holzmaden is interpreted as a sign of living in a more coastal habitat closer to the shore (URLICHS et al. 1994), even though drifting wood is also known to be sometimes far out in the sea (MASER & SEDELL 1994). Wood and weeds are also reported in the stomach of modern crocodilians (WHITAKER & BASU 1982, WEBB et al. 1982). It is uncertain why crocodiles swallow wood, but most authors agree that it probably occurs only accidentally, as floating wood might be mistaken as prey or accidentally swallowed with the prey (e.g. WHITAKER & BASU 1982, WEBB et al. 1982). In the Holzmaden specimens of *Steneosaurus bollensis*, wood is more common than gastroliths in the stomach contents. It is assumed, that drifting wood was common in the Holzmaden environment, whereas stones had to be ingested at the coast or with prey, which contained the stones in the first place. Therefore, stones occur more rarely in the stomach contents.

The presence of gastroliths in the stomach of extant crocodilians (and various kinds of other animals, e.g. birds) is well known (WEBB et al. 1982, WHITAKER & BASU 1982, LEVY 2003, WINGS 2004). Nevertheless, the function of gastroliths in the stomach of crocodilians is still under discussion. The most common opinion is that gastroliths are used to grind up the stomach contents ("gastric mill"), as it can be seen in many birds (WINGS 2004). Another suggestion is that gastroliths have an effect on the swimming and diving abilities (for buoyancy) (COTT 1961, TAYLOR 1993). However, according to HENDERSON (2003) the possession of relatively small amounts of gastroliths (<2% of the total body mass) has only minor effects on the density and the equilibrium depth of immersion of the body and its inclination. HENDERSON (2003) concludes that "[...] assigning buoyancy control as the principal function to gastroliths in crocodilian is unwarranted."

In this study, gastroliths are only found in a few *S. bollensis* specimens of Holzmaden and only in specimens with a total body length over two meters. It is assumed that gastroliths were not a major component in the stomach of *S. bollensis*. Until the role of gastroliths in

extant crocodilians is completely clarified, any functional statement for fossil crocodilians, whether they were used for digestion or not, remains speculative.

8.2 Aquatic locomotion in teleosaurids

In the following, the aquatic locomotor options in teleosaurids, especially in the Liassic teleosaurids, *Steneosaurus bollensis*, *S. gracilirostris*, *Platysuchus multiscrobiculatus*, and *Pelagosaurus typus,* will be discussed. Because significant parts of the postcranial skeleton of *Steneosaurus brevior* are unknown, this taxon is not considered in the following section.

Osteological differences among the Liassic teleosaurids are compared with extant crocodilians and discussed in detail, regarding their influence on their aquatic locomotion. The discussion is mainly based on the overall body shape and the morphology of the osteodermal shield of teleosaurids.

In addition, the possibility of osmotic regulation as indicated by osteology features is discussed (BUFFETAUT 1982, FERNÁNDEZ & GASPARINI 2000, NAISH 2001).

8.2.1 Body shape and aquatic locomotion (Fig. 8.9)

According to HILDEBRAND & GOSLOW (2004), aquatic adaptations for increasing swimming speed are usually characterized by the decrease of the inertia in water by reduction of bony substance, decrease of the drag in water by change of the body shape and texture of the body surface, and optimization of the buoyancy. To improve the efficiency of aquatic locomotion in the early crocodilians, a reduction of the dermal armour and the fore limbs compared to the terrestrial protosuchians is reported (BUFFETAUT 1980, HUA 2003). Teleosaurids possess reduced fore limbs relatively to the length of the hind limbs, which resemble the limbs of extant crocodilians. In addition, teleosaurids possesses a dorsal and ventral osteodermal shield. In contrast, in certain metriorhynchids, the fore limbs are flattened dorsoventrally and form flippers, while the body lacks an osteodermal shield, and in certain species, a hypocercal caudal fin is developed (ARTHABER 1906, 1907b, AUER 1907, HUA & BUFFRENIL 1996, CALDWELL 2002).

Body shape

The overall bodyshape of teleosaurids resembles the overall body shape of extant crocodilians. The head held horizontally in front of the body, four legs which project from the sides, an osteodermal shield, and a heavy muscular tail (e.g. CARROLL 1993). Besides the osteological differences e.g., vertebra count, osteoderm count, pelvic girdle anatomy (see chapter 4 & 5), the overall body morphology of *Platysuchus multiscrobiculatu*s and

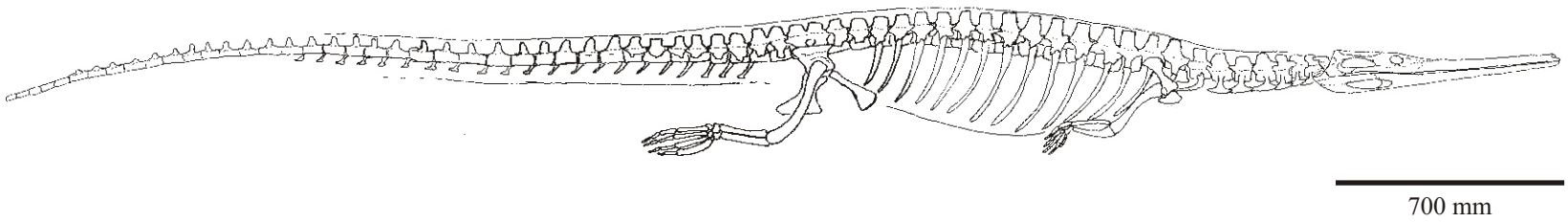

Figure 8.9: Skeletal restoration of *Steneosaurus bollensis* (modified after CARROLl 1994) in the supposed mode of swimming. Dorsal and ventral outlines indicate the position of the dorsal and ventral osteodermal shield.

Steneosaurus bollensis (Fig. 8.9) is similar. Both are sharing typical features with extant crocodilians e.g., a flat skull, held horizontally to the body, a transverse-oval body cross section, shorter fore limbs than hind limbs, and a long and horizontally aligned tail.

In contrast, a slight different body shape is suggested for *Pelagosaurus typus,* compared to that of *Steneosaurus bollensis* (Fig. 8.10). *P. typus* possessed more reduced and more delicate fore limbs compared to *S. bollensis* (see chapter 3.5 & 4), and its skull is more slender and higher, compared to *S. bollensis* (see chapter 4 & 5). This is most likely resulting in a more streamlined skull shape of *P. typus* (see chapter 3.5, 4 & 5). Additionally, the dorsal osteoderms of *Pelagosaurus typus* were arranged in a smaller angle to the neural spine of the vertebrae than in *S. bollensis* (see chapter 3.5. and Fig. 8.10), which resulted most probably in a narrower cross section in the dorsal part of the body compared to that of *S. bollensis* (Fig. 8.10). Due to this, a more streamlined overall body shape for *P. typus* is assumed.

The overall body shape and the flexibility of the spinal column are essential for the reconstruction of the modes of aquatic locomotion. Because the flexibility of the spinal column is influenced by the arrangement of the osteodermal shield in teleosaurids (FREY 1988b), the differences in the arrangement of the osteoderms of the Liassic teleosaurids, compared to the armour of extant crocodilians, is discussed.

The dermal armour of extant crocodilians e.g., alligators consists of osteoderms, which are lacking a peg and socket joint, that underlie the epidermal scales of the dorsal surface of the trunk and anterior part of the tail (REESE 1913). The osteoderms are grouped in two distinct areas the nuchal and the dorsal shields. The former lies just posterior to the head, in the region of the fore limbs, and consists of four to six large and a couple of small plates. The dorsal shield extends over the back in regular longitudinal rows and regular transverse rows. At the widest part of the trunk, there are six or eight of these osteoderms in one transverse row. They become smaller towards the tail (REESE 1913).

Compared to the armour of extant crocodilians, e.g. alligators, most teleosaurids are heavier armoured (see chapter 3). The Liassic taxa possess a paired longitudinal row of dorsal osteoderms covering most of the neck, trunk, and the anterior part of the tail and a well-developed ventral osteodermal shield, which is often lacking or only slightly developed in extant crocodilians (BOLTON 1989). The ventral osteodermal shield is lacking in e.g., *Crocodylus porosus*, *C. acutus*, *Gavialis gangeticus,* and the Alligatoridae (BOLTON 1989).

In *Steneosaurus bollensis*, the dorsal osteodermal shield starts at the level of the third or fourth cervical vertebra and covers the body until the level of the 23rd caudal vertebra (see chapter 3.1, Fig. 3.7a). The ventral osteodermal shield runs in six longitudinal rows from the

sixth thoracic vertebra to the 15th thoracic vertebra, stops there, and starts again with a paired longitudinal row at the level of the third caudal vertebra and terminates individually level with the 10th to 16th caudal vertebra (see chapter 3.1, Fig. 3.8). The osteodermal shields stiffened the body of the teleosaurids and reduced its lateral and dorsoventral movement abilities, in comparison to the body of extant crocodilians (FREY 1988a/b, FREY et al. 1989, HUA 2003). According to FREY (1988b), dorsoventral movement of the trunk is limited in *S. bollensis* and the lateral tail undulation is probably the most important manner for swimming.

Among the Liassic teleosaurids, the degree of stiffness in the trunk area probably varies, because of the different count, shape and arrangement of the osteoderms in their osteodermal shields (see chapter 4 and Fig. 8.10). *Platysuchus multiscrobiculatus* is more heavily armoured than *Steneosaurus bollensis* and *S. gracilirostris* (see chapter 3, Fig. 3.7, 3.8 , 3.29, and 3.30). *Pelagosaurus typus* is the least armoured one among the Liassic teleosaurids (see chapter 3, Fig. 3.43).

For example, *Steneosaurus bollensis* possesses dorsal osteoderms with a pronounced articulation area with a distinct anterolateral peg, to connect the dorsal osteoderms (see chapter 3.1 & Fig. 8.10). The surface of the osteoderms is covered with a pattern of large circular pits and at the level of the pelvic girdle, and a strong keel is visible on the surface of the osteoderm (see chapter 3.1). According to FREY (1988), the osteodermal shield of *Steneosaurus bollensis* allows limited lateral movement, because the osteoderms are not ventrolaterally bent, the keel on the surface is low, and the broad and shallow peg and socket articulation increases the relocalability between the osteoderms.

In contrast, *Platysuchus multiscrobiculatus* possesses thicker and wider osteoderms, anterior without, and level with the lumbar region with smaller peg and sockets joints than those of *S. bollensis*. In addition, the anterior articular area at the osteoderms is smaller but steeper in *Pl. multiscrobiculatus* compared to that of *S. bollensis*, and it has pronounced keels on the external surface of all thoracic osteoderms (see chapter 3.4, Fig. 3.30). It is therefore assumed, that in particular the lateral elongated osteoderms, and the more lateral positioned and higher keels on the osteoderm surfaces in *Pl. multiscrobiculatus* restricted the possibilities for lateral movement of the armour, i.e. the thoracic column, compared to *S. bollensis*.

Pelagosaurus typus is the least armoured teleosaurid. Its dorsal osteodermal shield extends from the third cervical vertebra only until the 10th caudal vertebra. Its thin osteoderms possess only slight anterior articular areas and no peg and socket joints (see chapter 3.5). The thoracic osteoderms are wider than long and slightly overlap each other posteriorly (Fig. 8.10), whereas the posterior 10 caudal osteoderms are not connected to each other. The

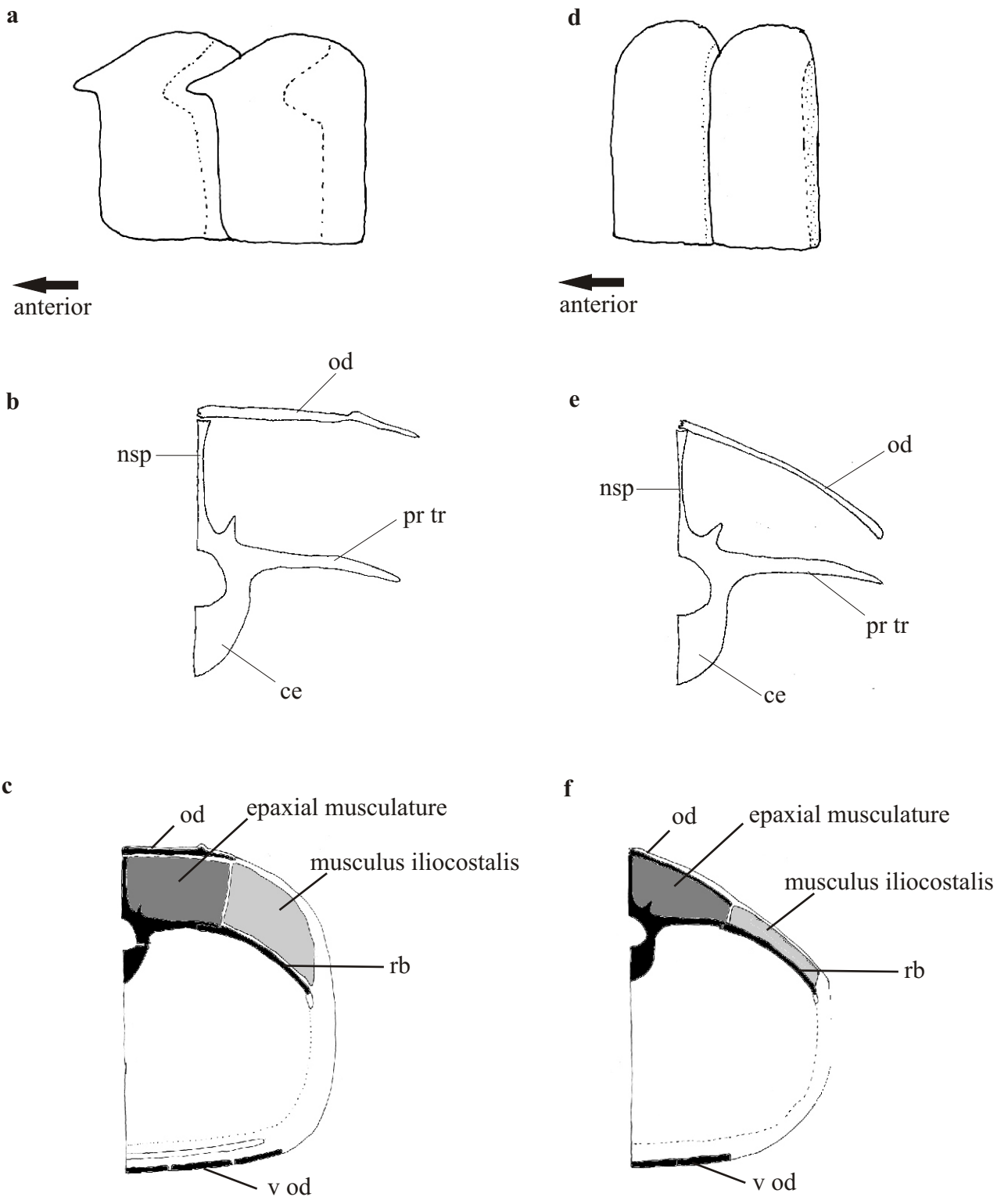

Figure 8. 10a-d: Configuration of osteoderms in ventral view and positions to the vertebra and possible resulting trunk cross section in *Steneosaurus bollenis* (a-c) and *Pelagosaurus typus* (d-f). **8.10a**-Configuration of the dorsal osteoderms to each other in *Steneosaurus bollensis* (after FREY 1988). **8.10b**-Configuration of the dorsal osteoderms to the vertebrae in *S. bollensis* (after FREY 1988). **8.10c-**Assumed trunk cross section for *S. bollensis* (simplified after FREY 1988). **8.10d**-Configuration of the dorsal osteoderms to each other in *Pelagosaurus typus*. **8.10e-**Configuration of the dorsal osteoderms to the vertebrae in *P. typus.* **8.10f**-Assumed trunk cross section for *P. typus*. Abbreviations: ce-centrum, nsp-neural spine, od-osteoderm, pr tr-processus transversus, rb-rib, v od-ventral osteoderm.

external surface of the osteoderms is covered by a pattern of small circular pit, but no keel is developed on the osteoderm surface (see chapter 3.5 & Fig. 8.10). In addition, *P. typus* possesses only four longitudinal rows of ventral osteoderms covering the trunk region instead of six like the *S. bollensis* and *Pl. multiscrobiculatus* (see chapter 3). Therefore, it is assumed that *P. typus* possessed a more flexible trunk region and tail region compared to *S. bollensis* and *Pl. multiscrobiculatus.*

Swimming abilities

According to ELSWORTH et al. (2003), swimming performance is of greater ecological importance in extant crocodilians than terrestrial locomotion, because most ecologically important behaviours, such as prey capture, social interactions, reproduction, and dispersal occur in water. In contrast, FREY (pers. comment) notes that bottom walk is probably the most important locomotion type among extant crocodilians.

For thalattosuchians it is assumed that they spent most, if not all, of their live in the water, and went probably only rarely on land, perhaps for laying eggs (FREY 1988b). Therefore, the aquatic locomotion modes are considered more important for them.

Thalattosuchian and in particular *Steneosaurus* swimming styles have been inferred by analogy with extant crocodilians (MASSARE 1987). In extant crocodilians, swimming is mainly achieved by tail movement, while the limbs are folded against the body (WHITAKER & BASU 1982, FREY 1982, FREY & SALISBURY 2001, SEEBACHER et al. 2003). WILLIS et al. (2004) report that *Alligator mississipiensis* provides hydrodynamic thrust with its tail paired with mediolateral body flexion. Additionally, SEEBACHER et al. (2003) note for *C. porosus* that limbs are only used by very small specimens, or at a low swimming velocity.

Due to the similarities, in general body shape and anatomy between teleosaurids and modern crocodilians, e.g. FREY (1988) and MASSARE (1988) suggested the same use of axial subundulatory mode of swimming. Subundulatory aquatic locomotion is defined as aquatic propulsion using only the posterior half of the trunk (BRAUN & REIF 1982). This implies that most of the aquatic locomotion in teleosaurids was achieved by tail movement. In *S. bollensis,* lateral tail undulation is supposed to be the most important manner for swimming (FREY 1988b).

The tail in extant crocodilians, e.g. *Gavialis gangeticus*, has a laterally flattened cross-section. Therefore, it has a relatively large surface area, which increases the drag in the water as the tail moves laterally in a sinusoidal pattern (Crocodilian Biology Database 2002). The Indian gharial (*G. gangeticus*) uses its tail to accelerate rapidly, when required, and during

fast swimming, as well the trunk undulates sinusoidally (WHITACKER & BASU 1982). According to RIESS (1986), a lateral flattening of the tail is effective but not necessary to achieve propulsion.

S. bollensis possesses a horizontal aligned, long tail similar to the Indian gharial, but the neural spines in the caudal column are much lower than in the Indian gharial. This results most likely in a much lower cross-section of the tail of *S. bollensis*. In *S. bollensis* (as well as all other Liassic teleosaurids), the lack of high neural spines in the tail and the resulting small cross-section of the tail reduced most likely the drag in the water. The limited lateral mobility of the thoracic column of *S. bollensis*, because of its osteodermal shield (see above) compared to that of extant crocodilians, probably limited the option for axial undulation. Therefore, a powerful caudal musculature performing propulsion seems to be necessary.

According to FREY (1988), the lumbar region of *Steneosaurus bollensis* probably hosted enlarged iliocostalis muscles, indicating an integration of the lumbar region in the undulation during swimming. FREY (1988) concludes that the arrangement of the osteoderms of *S. bollensis* allowed an enlargement of certain muscles, like the iliocostalis muscle, which was probably an advantage for swimming performance, but terrestrial high walk was most likely not possible (Fig. 8.10).

In contrast, the observed different arrangement of the osteodermal shield in *Pelagosaurus typus*, probably indicates a smaller iliocostalis muscle according to the suggested conditions in *S. bollensis* by FREY (1988) (Fig. 8.10). The assumed smaller iliocostalis muscle was probably compensated by the suggested more flexible trunk area of *P. typus* (see above). This results probably in a more axial undulatory mode of swimming of *P. typus* compared to *S. bollensis*.

The pelvic girdles in *Steneosaurus bollensis* and *Pelagosaurus typus* have a thinner ilium with a flatter acetabulum compared to extant crocodilians (see chapter 3 and 5, Fig. 3.14, Fig. 3.46, and Fig. 5.3). Furthermore, the ilium of *Steneosaurus bollensis* and *Pelagosaurus typus* lacks a distinct iliac crest. Only *Platysuchus multiscrobiculatus* possesses an ilium with a pronounced iliac crest dorsal to the acetabulum. In extant crocodilians, this crest serves for the origin of the M. iliofemoralis that runs to the lateral femoral shaft (PARRISH 1987). The iliofemoralis muscle is in particular important for walking on land, because it abducts the limb during the swing phase during terrestrial locomotion (CHARIG 1972, HUTCHINSON & GATESY 2000). The pronounced iliac crest in *Platysuchus multiscrobiculatus* indicates larger muscle attachments for the M. iliofemoralis and probably M. iliotibialis than in *Steneosaurus bollensis* and *Pelagosaurus typus,* which might be a hint

for better terrestrial locomotion of *Pl. multiscrobiculatus* compared to *S. bollensis* and *P. typus*.

Additionally, in comparison to extant crocodilians, the femur of teleosaurids is more slender, and especially the femoral head is only moderately developed (see chapter 3.1, 3.4, Fig. 3.18 and Fig. 3.49). Again only *Platysuchus multiscrobiculatus* shows more similarities with extant crocodilians with a slightly more offset femoral head (see chapter 3.4, Fig. 3.33). It is therefore assumed, that the curved femoral head and the well-developed iliac crest in *Platysuchus multiscrobiculatus* indicate an option for a more efficient terrestrial locomotion than it is assumed for *S. bollensis* and *P. typus*.

In this study, the aquatic adaptation of the teleosaurids is not questioned. The abilities for fast swimming were probably not as well developed as in other marine reptiles like ichthyosaurs or mosasaurs, but they were probably efficient swimmers at least like extant crocodilians. The hydrodynamic efficiency during swimming in extant crocodilians is comparable to fully aquatic mammals (SEEBACHER et al. 2003).

As described above *Platysuchus multiscrobiculatus* shows a stronger developed pelvic girdle and femur, additionally a larger osteodermal shield and less reduced fore limbs compared to the other teleosaurids from Holzmaden. It could probably walk better on land than *Steneosaurus bollensis* or *Pelagosaurus typus*. However, its terrestrial locomotion was probably less efficient than that of extant crocodilians. As formerly described by FREY (1988), *Steneosaurus bollensis* was an efficient swimmer and used a subundulatory mode of aquatic locomotion. It possesses a stiffer thorax compared to extant crocodilians, because of the amphicoelous to platycoelous vertebrae (HUA 2003) and the connected osteoderms, and possibly an enlarged, well-developed tail musculature for propulsion. It is assumed, that *Pelagosaurus typus* was the most effective swimmer among the Liassic teleosaurids. It possesses the most reduced and probably most flexible osteodermal shield, a more streamlined skull and body shape, and the most reduced fore limbs compared to the other Liassic taxa. Therefore, it probably used a more undulatory mode of swimming.

8.2.2 Salt glands

Salt glands are necessary for reptiles (and birds), which live in marine or arid environments and do not possess sophisticated kidneys to get rid of nitrogenous waste such as uric acid (SHOEMAKER & NAGY 1977, WILLIAMS 1997). The kidneys of reptiles and birds have lower concentration ability than the kidneys of mammals (SCHMIDT-NIELSEN & FANGE 1958), therefore those animals need salt glands when living in a highly saline environment.

Extant crocodilians possess lingual salt glands, which allow, e.g. the Australian saltwater crocodile (*Crocodylus porosus*) to live in marine and brackish water (TAPLIN & GRIGG 1981). Indeed, seven of eleven existing members of the Crocodylinae have salt glands in their mouth and, to varying degrees, show some capacity for oceanic dispersal (LEVY 2003). The Indian gharial (*Gavialis gangeticus)* also possesses such lingual salt glands, which are in fact modified salivary glands (Crocodilian Biology Database 2002). Alligatorids lack the glands and can therefore only survive in saltwater for a very short time (ROSS 2002, FERNÁNDEZ & GASPARINI 2000). Other reptiles like some desert lizards have modified their nasal glands into salt glands (FERNÁNDEZ & GASPARINI 2000).

Due to the fact, that the thalattosuchians are found in fully marine sediments and show some aquatic adaptations in their osteology, it hast to be assumed that they all were able to survive in a marine environment. There are some hints that at least *Geosaurus* possessed nasal salt glands (FERNÁNDEZ & GASPARINI 2000). FERNÁNDEZ & GASPARINI (2000) describe possible nasal salt glands in two *Geosaurus araucanensis* specimens from Patagonia (Argentina). They describe the remains of these glands, as "[...] a paired protuberance structure, which in dorsal view is shaped like teardrops". The surface of these protuberances is formed by several small lobules. Externally, each protuberance is surrounded by the nasal, lacrimal, prefrontal, jugal, and maxilla (FERNÁNDEZ & GASPARINI 2000).

Whether other taxa including the teleosaurids also possessed nasal or lingual salt glands like modern crocodiles, or lacrimal salt glands like recent sea turtles, cannot be determined.

In this study, no corresponding structures like described by FERNÁNDEZ & GASPARINI (2000) were found in any of the investigated teleosaurid specimens. This does not mean that there were no such glands, but as FERNÁNDEZ & GASPARINI (2000) note, such structures are extremely rare to be preserved in a fossil.

However, in other extinct crocodilians, the antorbital cavity has been sometimes correlated with the presence of salt glands (NAISH 2001, BUFFETAUT 1982). Small antorbital fenestrae are recognized in several specimens of *Pelagosaurus* (see chapter 3.5 Fig. 3.34), *Steneosaurus* (see chapter 3.1, Fig. 3.1), *Metriorhynchus,* and *Geosaurus*, but no further evidence of the existence of salt glands are found. The only exception is a distinct recess between the prefrontal and the lacrimal at the anterior margin of the orbit, observed in some specimens of *Steneosaurus* and *Platysuchus multiscrobiculatus* (see chapter 3.4, Fig. 3.26, 3.27). This feature was interpreted as an opening for the lacrimal duct leading to the lacrimal gland (SHOEMAKER & NAGY 1977). Because marine turtles use modified lacrimal glands as salt glands (SCHUMACHER 1973, SHOEMAKER & NAGY 1977, FERNÁNDEZ & GASPARINI 2000),

this recess in *Steneosaurus* and *Platysuchus multiscrobiculatus* could be at least a hint for possible lacrimal glands or salt glands in teleosaurids, respectively.

8.3 Reproduction in thalattosuchians

Neither eggs nor embryonic materials have been found from any thalattosuchian. Therefore, any statement about the reproductive mechanism of theses animals has to be highly speculative. As far as known, vivipary had never been evolved in crocodilians. As discussed before, the skeletal morphology of teleosaurids was no limiting factor for going ashore to lay eggs (see 8.2.1). The aquatic adaptation was less than for example in the Lower Jurassic ichthyosaurs, with their dolphin-like body shape, or plesiosaurs, with their enlarged shoulder and pelvic girdle and large flippers (CALDWELL 2002, O'KEEFE 2002, MONTANI 2005). Several ichthyosaurs embryos are described from the Holzmaden locality (URLICHS et al. 1994). Therefore, the conditions for a preservation of embryo material were obviously given in these black shale sediments (WILD & ZIEGLER 1986, URLICHS ET AL. 1994). Thus, possible embryonic material should have been preserved also in crocodilians or plesiosaurs by chance, if it would have been there in the first place.

In the Holzmaden area, numerous specimens of *Steneosaurus bollensis* allow to analyse the frequency of occurrence of certain sizes among the animals and this leads to some interesting assumptions about the population structure. The histogram in figure 8.11 shows the occurrence of different skull size of *S. bollensis* in Holzmaden. It is based on 48 skulls; all specimens are from the area of Holzmaden.

Striking is the absence of skulls smaller than 130 mm, respectively of *Steneosaurus bollensis* specimens with a total body length less than 700 mm (see chapter 4 and Fig. 8.11). Excluding taphonomical reasons for this gap as e.g. the lack of preservation, the lack of finds, etc., the answer could be a biological one. The high number of teleosaurid findings in the deposits, and the fact that ichthyosaur embryos are frequently known from the area is an argument against taphonomical reasons. However, taphonomical reasons are possible, and the provided biological explanation is only supposition.

As noted in chapter 4, extant crocodilians with a body length of 700 mm are usually about one to three years old (WESTPHAL 1962, BOLTON 1989). Most extant crocodilians hatch with a total body length of about 250 mm (skull length about 70 mm), considering intra- and interspecific small variations (see chapter 4). Assuming similar hatching size for *S. bollensis*, it leads to two possible reasons for the size distribution of *Steneosaurus bollensis* in Holzmaden: Firstly, the egg laying and hatching of the crocodilians took place somewhere

else on dry land and the baby crocodilians stayed close to that area during their first years. Secondly, *Steneosaurus bollensis* was viviparous and had large newborns with a body size of about 700 mm. This is not impossible but highly unlikely, because vivipary is until now unknown from any other representative of the Crocodylia. Thus, it is more likely that the juveniles lived in a different habitat until they reached a body size of about 700 mm (skull length about 140 mm). From extant juvenile crocodilians it is known that they usually live in other environments than the adults, as a result of different prey preferences and physical needs depending on the body size, such as hiding places (POOLEY 2002, LEVY 2003). Similar behaviour is therefore assumed for *S. bollensis* as well.

Furthermore, gastroliths and wood in the stomach could be a hint that adult steneosaurs swam to costal areas (see 8.1.4). Probably they laid their eggs on the shore and left again for deeper water like e.g. extant sea turtles (CROUSE 1999). Therefore, it is concluded that the youngest states of *S. bollensis* probably lived nearer to the shore or even in a freshwater environment and are therefore absent in the Holzmaden black shale, which represents part of the shelf region of the Tethys (see chapter 1).

Two problems arise from this explanation for the lack of small specimens: Firstly, the high number of finds of *S. bollensis* with a skull size of 150- 250 mm cannot be explained. If those specimens were already two to three years old, the model of a higher mortality rate among hatchlings, as similar observed in extant crocodilians, does not apply. However, it is to consider, that we are not looking on one population of *S. bollensis*, but the finds come from different layers and do not represent a living community. Therefore, we cannot completely exclude a taphonomical factor.

In first diagram (Fig. 8.11), skull sizes of *S. bollensis* from 350 to 900 mm all appear regularly; the fluctuation of skull sizes in *S. bollensis* lies here in normal, expected limits for a population, as it is known in recent populations of crocodilians (ROSS 2002). However, there is another distinct gap at a skull length of about 300 mm (250-350 mm) for *S. bollensis* (Fig. 8.11). Interestingly, the *Pelagosaurus typus* specimens from Holzmaden fill this gap, if they are included in the diagram (Fig. 8.12). Their most common skull size lies exactly in the gap we see here for *Steneosaurus bollensis* (Fig. 8.11 and 8.12).

One possible biological hypothesis is that the immature *S. bollensis* specimens (i.e. skull size smaller than 400 mm) were supplanted by adult *Pelagosaurus typus* specimens, which perhaps won the competition for food resources by being better swimmers (see paragraph 8.2). Another biological hypothesis would be that the *S. bollensis* specimens already reached maturity at a skull length of about 300 mm, and then migrate from the Holzmaden area to

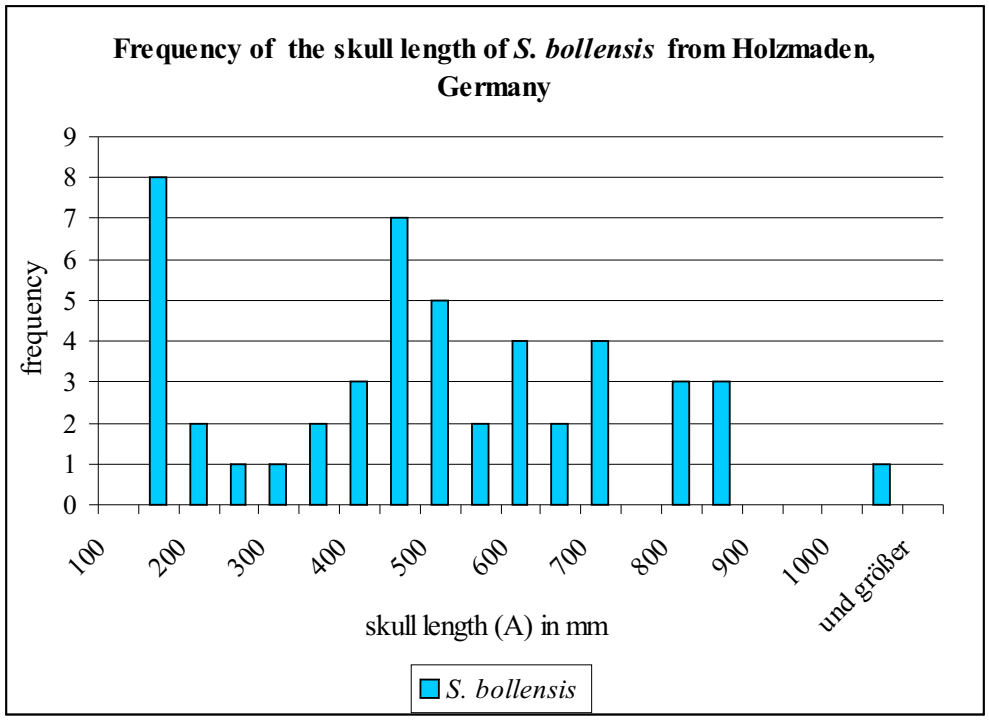

Figure 8.11. The frequency of skull length (A) is an indicator for the frequency of total body length (TL) respectively for the frequence of age of the specimens. *Steneosaurus bollensis* specimens under 130 mm skull length are completely missing, corresponding body sizes less than 700 mm are missing as well. A rare occurrence at a skull length of about 300 mm is visible and a skull length higher than 900 mm is rare, too.

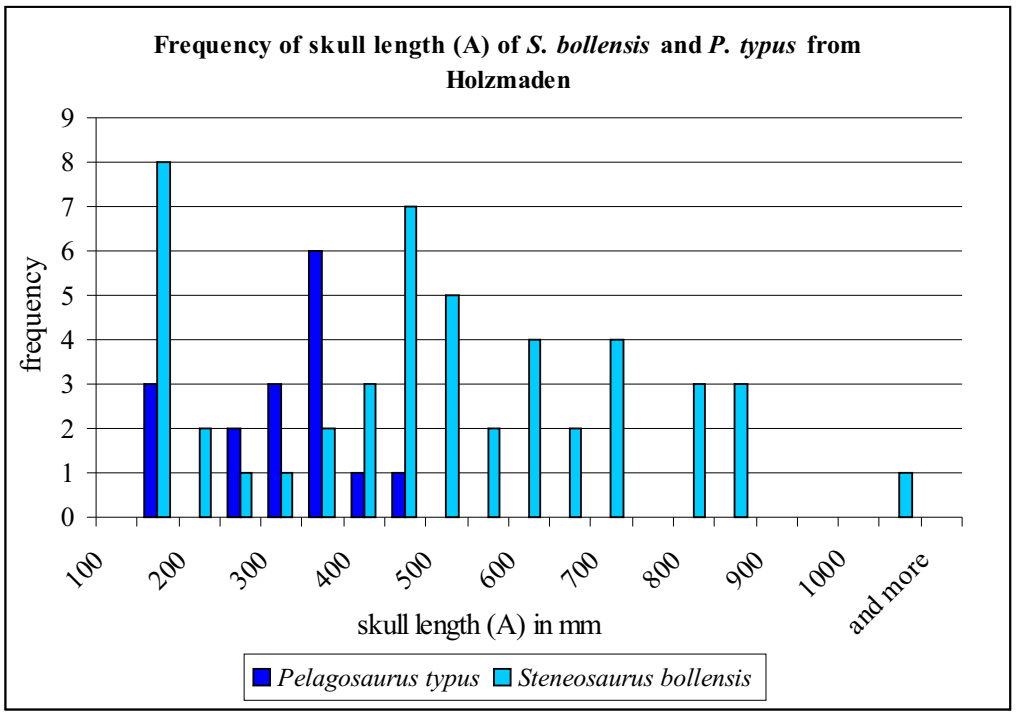

Figure 8.12: Comparison of the frequency of *Steneosaurus bollensis* skull length and *Pelagosaurus typus* skull length. *P. typus* seem to substitute the missing skull sizes of *S. bollensis* between 250-400 mm.

costal areas for mating and egg laying (see above). However, purely taphonomical reasons for this phenomenon cannot be excluded.

Considering, that a fossil community is described, which was collected in different layers of the Posidonia Shale, the number of certain conclusions is limited. However, summarized it seems likely that the earliest juvenile stages of *S. bollensis* (embryos/hatchlings) are missing in the deposits of Holzmaden, because they lived in a different habitat. Furthermore, the lack of specimens with a skull size of about 300 mm, is supposed to show a migration of the mature specimens to the place of reproduction.

Acknowledgements

The present work would not have been possible without the support of a variety of people. First of all, I wish to thank my supervisor [redacted] (Johannes-Gutenberg University Mainz) for his useful advice, all the discussions and support. Special thanks to [redacted] (SMSK), who really helped a lot to improve this work (mostly by going amok with a red pen), and by reminding me that palaeontology is not only a job.

In addition, very special thanks to [redacted] (SMNS), who had the idea for the entire project in the first place.

I would like to thank [redacted] (Humboldt-University Berlin, Museum für Naturkunde) for all the proof-reading, discussions, and the heroic effort to run my bootstrap on a more powerful pc than mine (not successfully, but it was worth a try). Without him, this work would never have been completed.

I am very grateful for the financial support of the project BO 553/13-1 by the Deutsche Forschungsgemeinschaft (DFG).

In addition, my thanks go to the following people, who gave permit to study material in "their" collections: [redacted] (BSGP) with special thanks for taking some photos for me and trust in my ability to bring back a loaned specimen in one piece, [redacted] and [redacted] (both BMNH), who were very kind and helpful in the collection especially with a screwdriver, [redacted] (also BMNH), who saved me, when my camera broke down in the very wrong moment, [redacted] (Université C. Bernard, U.F.R. Sciences de la Terre Lyon - FSL), [redacted] (MNHN) with special thanks for the interesting discussion in the Sushi bar, too, [redacted] & [redacted] (MGUH), [redacted] (NHMUS), with special thanks for the interesting look behind the scenes of the Budapest museum, [redacted] (former SMNS), who allowed me to study and loan teleosaurid specimens, which was the basis of this work, [redacted], Dresden (SNSD); [redacted] (TMH) and [redacted] (Leiden), [redacted] (GPIT), [redacted] (UH), who kindly allowed me to investigate the new juvenile *Platysuchus* specimen, besides all the other help that he offered; and [redacted] (SMF), [redacted] (ZFMK), and [redacted] (ZMUC), who provided extant gharial and other extant crocodilian material for comparative studies.

Furthermore, I would like particularly to thank [redacted] (CNRS), who has provided very useful information, especially about *Pelagosaurus* and the Liassic deposits in France, and who kindly contacted [redacted] in Lyon for me.

Also many thanks to [redacted] (University Mainz) for discussion, technical support, and the help to realize the whole *Pelagosaurus* CT project and to [redacted] (University Hospital Mainz, Klinik für Neuroradiologie), who took all the CT scans of the *Pelagosaurus* skull for us.

In addition, I would like to thank the following people for various discussions and helpful comments (in alphabetical order): [redacted] It is very likely that I forgot to name some people, who also helped. Please accept my apology and ask for a drink next time.

Very special thanks goes to [redacted] (University Copenhagen), most of all for his support and patience (he needed a lot), but also for reading and improving this work.

Last but not least, I thank my family, especially my parents [redacted] (Plettenberg), for all their support (financial & moral) they have given me over the years. You never doubted I could do this. Thank you.

References

ABERHAN, M. 2001. Bivalve palaeobiogeography and the Hispanic Corridor: time of opening and effectiveness of a proto-Atlantic seaway. - Palaeogeography, Palaeoclimatology, Palaeoecology **165**: 375-394.

ABERHAN, M. 2002. Opening of the Hispanic Corridor and Early Jurassic bivalve biodiversity. - [IN] CRAME, J.A. & OWEN, A.W. [EDS.]. Palaeobiogeography and Biodiversity Change: the Ordovician and Mesozoic-Cenozoic Radiations. Geological Society, London, Special Publications **194**: 127-139.

ACHARJYO, L.N., SINGH, L.A.K. & PATTANAIK, S.K. 1990. Age at sexual maturity of gharial *Gavialis gangeticus* (Reptilia: Crocodilia). – Journal of Bombay Natural History Society **87** (3): 458-459.

ADAMS-TRESMAN, S.M. 1987a. The Callovian marine crocodile *Metriorhynchus* from central England. - Palaeontology **30**(1): 179-194.

ADAMS-TRESMAN, S.M. 1987b. The Callovian teleosaurid marine crocodiles from central England. - Palaeontology **30**(1): 195-206.

ANDERSON, H.T. 1936. The jaw musculature of the phytosaur, *Machaeroprosopus*. - Journal of Morphology **59**(3): 549-587.

ANDREWS, C.W. 1909. On some steneosaurs from the Oxford Clay of Petersborough. - Annals and Magazine of Natural History, London **3**(15): 299-308.

ANDREWS, C.W. 1913. A Descriptive Catalogue of the Marine Reptiles of the Oxford Clay. Part II. 206 pp. London.

ANTUNES, M.T. 1967. Um Mesosuquiano do Liásico de Tomar (Portugal). Consideracoes sobre a origem dos crocodilos. – Memoria Servicos Geologicos de Portugal (Nova Serie) **13:** 1-65.

ARTHABER, V., G. 1906. Beiträge zur Kenntnis der Organisation und der Anpassungserscheinung des Genus *Metriorhynchus*. - Beiträge zur Paläontologie und Geologie Österreich-Ungarns und des Orients **19**(4): 287-320.

ARTHABER, V., G. 1907a. Ueber den Anpassungstypus von *Metriorhynchus*. - Centralblatt für Mineralogie, Geologie und Paläontologie 1907: 385-397.

ARTHABER, V., G. 1907b. Ueber die Hinterextremität von *Metriorhynchus*. - Centralblatt für Mineralogie, Geologie und Paläontologie 1907: 502-508.

AUER, E. 1907. Die Extremitäten von *Metriorhynchus*. - Centralblatt für Mineralogie, Geologie und Paläontologie 1907: 536-538.

AUER, E. 1909. Über einige Krokodile der Juraformation. - Palaeontographica **55**: 217-294.

AVERIANOV, A.O. 2000. *Sunosuchus* sp. (Crocodylomorpha, Goniopholididae) from the Middle Jurassic of Kirghisia. - Journal of Vertebrate Paleontology **20**(4): 776-779.

BAILEY, T.R., ROSENTHAL, Y., MCARTHUR, J.M., VAN DE SCHOOTBRUGGE B.& THIRLWALL, M.F., 2003. Paleoceanographic changes of the Late Pliensbachian-Early Toarcian interval: a possible link to the genesis of an Oceanic Anoxic Event. - Earth and Planetary Science Letters **212**: 307-320.

BARDET, N. 1994. Extinction events among Mesozoic marine reptiles. - Historical Biology **7**: 313-324.

BARDET , N. & HUA, S. 1996. *Simolestes nowackianus* Huene, 1938, from the Upper Jurassic of Ethiopia is a teleosaurid crocodile, not a pliosaur. - Neues Jahrbuch für Geologie und Paläontologie, Monatshefte **2**: 65-71.

BASSOULLET, J.-P., ELMI, S. POISSON, A., RICOU, L.E., CEECA, F., BELLION, Y.,GUIRAUD, R. & BAUDIN, F. 1993. Mid Toarcian (184 to 182 Ma). - [IN] DERCOURT, J., RICOU, L.E. & VRIELYNCK, B. [EDS.] Atlas Tethys Palaeoenvironment Maps: 63-80, Gauthir-Villars, Paris.

BEHLER, J.L & BEHLER, D.A. 1998. Alligators & Crocodiles. - 72 pp. Colin Baxter Photography, Grantown-on-Spey, Scotland.

BELLAIRS, A. D`A. & KAMAL, A.M. 1981. The Chondrocranium and the Development of the Skull in Recent Reptiles. - [IN] GANS, C. & PARSONS, T.S. [EDS.]. Biology of the Reptilia Volume **11**: 227-263, Academic Press, London.

BENTON, M.J. & CLARK, J.M. 1988. Archosaur phylogeny and the relationships of the Crocodylia. - [IN] BENTON, M.J. [ED.]. The Phylogeny and Classification of the Tetrapods, Volume 1: Amphibians, Reptiles, Birds. The Systematics Association. Special Volume **35A**: 295-338, Claredon Press, Oxford.

BENTON, M.J. & SPENCER, P.S. 1995. Geological Conservation Review Series. Fossil Reptiles of Great Britain. - 386 pp., London (Chapman & Hall).

BENTON, M.J. & TAYLOR, M.A. 1984. Marine reptiles from the Upper Lias (Lower Toarcian. Lower Jurassic) of the Yorkshire coast. - Proceedings of the Yorkshire Geological Society **44** (4, 29): 399-429.

BERCKHEMER, F. 1928. Untersuchung über die Meerkrokodile des schwäbischen oberen Lias. - Paläontologische Zeitschrift **10**: 60-64.

BERCKHEMER, F. 1929. Beitrag zur Kenntnis der Krokodilier des schwäbischen oberen Lias. - Neues Jahrbuch für Mineralogie, Geologie und Paläontologie, Abteilung B, Beilagenband **64**: 1-60.

BEURLEN, K. 1925. Einige Bemerkungen zur Sedimentation in dem Posidonienschiefer Holzmadens. - Jahresberichte des oberrheinischen geologischen Vereins, neue Folge **14**: 298-302.

BIZZARINI, F. 1995. Sui di Croccodrill del Rosso Ammonitico Veronese di Sasso di Asiago (Altopiano dei Sette Comuni, Prealpi Venete). - Annali Museo Civico Rovereto **11**: 339-348.

BLODGETT, R.B. & FRYDA, J. 2001. Upper Triassic gastropod biogeography of western North America. Cordilleran Section - 97th Annual Meeting, and Pacific Section, American Association of Petroleum Geologists (April 9-11, 2001).

BOLTON, M. 1989. The management of crocodiles in captivity. - FAO Conservation Guide 22. Food and Agriculture Organization of the United Nations, Rome.

BONAPARTE, J.F. 1981.Descripción de Fasolasuchus tenax y su significado el la sistemática y evolución de los Thecodontia. - Rivista del Museuo Argentino de Ciencias Naturales Bernardino Rivadavia **3**: 55-101.

BÖTTCHER, R. 1989. Über die Nahrung eines *Leptopterygius* (Ichthyosauria, Reptilia) aus dem süddeutschen Posidonienschiefer (Unterer Jura) mit Bemerkungen über den Magen der Ichthyosaurier. - Stuttgarter Beiträge zur Naturkunde B **155**: 1-19.

BRAUN, J & REIF, W.-E. 1982. A new terminology of aquatic propulsion invertebrates. - Neues Jahrbuch für Geologie und Paläontologie, Abhandlungen **164**: 162-167.

BROCHU, C.A. 1995. Heterochrony in the Crocodilian Scapulocoracoid. - Journal of Herpetology **29**(3): 464-468.

BROCHU, C.A. 1996. Closure of neurocentral sutures during crocodilian ontogeny: implications for maturity assessment in fossil archosaurs. - Journal of Vertebrate Paleontology **16**(1): 49-62.

BROCHU, C.A., BOUARÉ, M.L., SISSOKO, F., ROBERTS, E.M. & O'LEARY, M.A. 2002. A drysaurid crocodyliform braincase from Mali. - Journal of Paleontology **76**(6): 1060-1071.

BROILI, F. 1932. Weitere Beobachtungen an *Geosaurus*. - Neues Jahrbuch für Mineralogie, Geologie und Paläontologie B **68**: 127-148.

BRONN, H.G. & KAUP, J. J. 1841-1843. Abhandlungen über die gavialartigen Formen der Liasformation. - 47 pp., Verlag Schweitzerbart, Stuttgart.

BRYANT, H.N. & SEYMOUR, K.L. 1990. Observations and comments on the reliability of muscle reconstruction in fossil vertebrates. - Journal of Morphology **206**: 109-117.

BUCKLAND, W. 1836. Geology and Mineralogy **1**: 1-599, **2**: 1-128, London.

BUCKLEY, G.A., BROCHU, C.A., KRAUSE, D.W. & POL, D**.** 2000. A pug-nosed crocodyliform from the Late Cretaceous of Madagascar. - Nature **405**: 941-944.

BUFFETAUT, E. 1977. Sur un crocodilien marin *Metriorhynchus superciliosus*, de l'Oxfordien supérieur (Rauracien) de l`Ile de Ré (Charente-Maritime). - Annales Société Science Naturelles Charente-Maritime **6**(4): 252-266.

BUFFETAUT, E. 1979a. The evolution of the Crocodilians. - Scientific American **241**(4): 124-132.

BUFFETAUT, E. 1979b. Jurassic marine crocodilians (Mesosuchia, Teleosauridae) from Central Oregon, first record in North-America. - Journal of Paleontology **53**(1): 210-215.

BUFFETAUT, E. 1980a. Position systématique et phylogénétique du genre *Pelagosaurus* BRONN, 1841 (Crocodylia, Mesosuchia), du Toarcien d'Europe. - Geobios **13**(5): 783-786.

BUFFETAUT, E. 1980b. Teleosauridae et Metrirorhynchidae: l'evolution de deux families de crocodiliens mesosuchiens marins du Mesozoique. - Comptes-Rendus du Congrès National des Sociétés Savantes - Section des Sciences **105** (3): 11-22.

BUFFETAUT, E. 1981. Die biogeographische Geschichte der Krokodilier, mit Beschreibung einer neuen Art, *Araripesuchus wegeneri*. - Geologische Rundschau **70**(2): 611-624.

BUFFETAUT, E. 1982. Radiation évolutive, paléoécologie et biogéographie des crocodiliens mésosuchiens. - Mémoires Soc. Géologie France **142**: 1-87.

BUFFETAUT, E. 1985. Ein *Steneosaurus* (Crocodylia, Mesosuchia) mit regeneriertem Schwanzende aus dem Lias Epsilon (Toarcium) von Schwaben. – Stuttgarter Beiträge zur Naturkunde, Serie B **113**: 1-7.

BUFFETAUT, E. 1986. Remarks on anatomy and systematic position of *Sunosuchus miaoi* YOUNG, 1948, a mesosuchian crocodilian from the Mesozoic of Gansu, China. – Neues Jahrbuch für Geologie und Paläontologie, Monatshefte 1986: 641-647.

BUFFETAUT, E. & BÜLOW, M., GHEERBRANT, E., JAEGER, J.J., MARTIN, M., MAZIN, J.M.; MILSENT, C. & RIOULT, M. 1985. Zonation biostratigraphique et nouveaux restes de Vertébrés dans les « Sables de Glos » (Oxfordien sup., Normandie). – Comptes Rendus l'Academie des Sciences Paris, Serie II, 300 (18): 929-932.

BUFFETAUT, E. & INGAVAT, R. 1980. A new crocodilian from the Jurassic of Thailand, *Sunosuchus Thailandicus* n.sp. (Mesosuchia, Goniopholididae), and the palaeogeographical history of South-East Asia in the Mesozoic. – Geobios **13**(6): 879-889.

BUFFETAUT, E., TERMIER, G. & TERMIER, H. 1981. A teleosaurid (Crocodylia, Mesosuchia) from the Toarcian of Madagascar and its palaeobiogeographical significance. – Paläontologische Zeitschrift **55**(3/4): 313-319.

BUFFETAUT, E. & THIERRY, J. 1977. Les crocodiliens fossiles du Jurassique Moyen et Supérieur de Bourgogne. - Geobios **10**(2): 151-194.

BUFFRÉNIL, DE V. 1982. Morphogenesis of Bone Ornamentation in Extant and Extinct Crocodilians. - Zoomorphology **99**: 155-166.

BUSCALONI, A.D. & SANZ, J.L. 1988. Phylogenetic relationships of the Atoposauridae (Archosauria, Crocodylomorpha). - Historical Biology **1**: 233-250.

BUSBEY; A.B. III 1989. Form and Function of the Feeding Apparatus of *Alligator mississippiensis*. - Journal Morphology **202**: 99-127.

BUSTARD, H.R. & MAHARANA, S. 1982. Size at first breeding in the gharial [*Gavialis gangeticus* (GMELIN)] (Reptilia, Crocodilia) in captivity. – Journal of Bombay Natural History Society **79**(1): 206-207.

BUSTARD, H.R. & MAHARANA, S. 1983. Growth rates in sub-adult gharial *Gavialis gangeticus* (GMELIN) (Reptilia, Crocodilia). – Journal of Bombay Natural History Society **80**(1): 224-226.

CADBURY, D. 2000. The dinosaur hunters. - 374pp, Fourth Estate, London**.**

CALDWELL, M.W. 2002. From fins to limbs to fins: Limb evolution in fossil marine reptiles. – American Journal of Medical Genetics **112**: 236-249.

CAMP, C.L. & KOCH, J.G. 1966. Late Jurassic Ichthyosaur from Coastal Oregon. - Journal of Paleontology **40**(1): 204-205.

CARROLL, R.L. 1993. Paläontologie und Evolution der Wirbeltiere. – 684pp., Georg Thieme Verlag, Stuttgart.

CHARIG, A.J. 1972. The evolution of the archosaurs pelvis and hindlimb: an explanation in functional terms. - [IN] JOYSEY, K.A. & KEMP, T.S [EDS.]. Studies in Vertebrate Evolution: 121-155, Oliver & Boyd, Edinburgh.

CHOUDHURY, B. C. & BUSTARD, H.R. 1983. Stunted growth in captive-reared gharial. - Journal of Bombay Natural History Society **80**(2): 423-425.

CLARK, J.M. 1986. Phylogenetic relationships of the crocodylomorph archosaurs, Ph.D-Thesis (Unpublished). University of Chicago.

CLARK, J.M. 1994. Patterns of evolution in Mesozoic Crocodyliformes. - [IN] FRASER, N.C. & SUES, H.-D. [EDS.]. In the shadow of the dinosaurs: 84-97, Cambridge University Press, Cambridge.

CLEUREN, J. & VREE, DE F. 2000. Feeding in Crocodilians. - [IN] SCHWENK, K. [ED]. Feeding. Form, Function, and Evolution in Tetrapod Vertebrates: 337-358, Academic Press, San Diego.

COLBERT, E.H. & MOOK, C.C. 1951. The ancestral crocodilian *Protosuchus*. – Bulletin of the American Museum of Natural History **97**: 147-182.

COLLOT, L. 1905. Reptile jurassique (*Teleidosaurus gaudryi*) trouvé à St-Seine-l'Abbaye (Côte d'Or). – Mémoires de l'Académie des Sciences, Arts et Belles-Lettres de Dijon **10**: 41-45.

CORNEE, J.J. & BUFFETAUT, E. 1979. Découverte d'un Téléosauridié (Crocodylia, Mesosuchia) dans le Valanginien sup. du Massif d'Allauch (Sud-Est de la France). – Compte Rendu l'Acadamie des Sciences Paris **288**: 1151-1154.

CORROY, G. 1922.- Les reptiles néocomiens et albiens du Bassin de Paris. - Comptes Rendus de l'Académie des Sciences **174**: 1192-1194.

COTT, H.B. 1961. Scientific results of an inquiry into ecology and economic status of the Nile crocodile (*Crocodilus niloticus*) in Uganda and Northern Rhodesia. - Transaction of the Zoological Society London **133**: 561-572.

COX, P., BETTS, R., BUNTON, C., ESSERY, R., ROWENTREE, P. & SMITH, J. 1999. The impact of new land surface physics on the GCMsimulation of climate and climate sensitivity. - Climate Dynamics **16**: 183-203.

Crocodilian Biology Database 2002.
http://www.flmnh.ufl.edu/natsci/herpetology/brittoncrocs/cbd.html

CROUSE, D.T. 1999. Population modelling and implications for Caribbean Hawksbill Sea turtle Management. – Chelonian Conservation and Biology **3**(2): 185-188.

CUVIER, G. 1812. Sur les ossements fossiles de Crocodiles et particulièrement sur ceux des environs du Havre et de Honfleur, avec des remarques sur les squelettes des sauriens de Thuringe. – Annales du Musee d'Histoire Naturelle de Paris **12**: 73-110.

DANGEARD, L. 1951. La Normandie. - [IN] DE LAPPARENT, A.F [ED.]. Géologie Régionale de la France. Actualités scientifiques et industrielles 1140: 241pp., Paris.

DEBELMAS, J. 1957. Sur la persistence du genere *Dacosaurus* dans le Néocomien de la Haute-Provence. – Compte Rendu l'Academie des Sciences Paris **244**: 1238-1240.

DELAIR, J.B. 1957. The Mesozoic Reptiles of Dorset. – Proceedings of Dorset Natural History and Archaeological Society **79**: 47-72.

DELFINO, M. 2001. The fossil record of the Italian Crocodylomorpha. – Abstracts 6th European Workshop on vertebrate Palaeontology, September 19-22. 2001: 28, Florence-Montevarchi, Italy.

DELFINO, M. & DAL SASSO, C. 2003. Marine "crocodiles" (Thalattosuchia) from the Early Jurassic of Lombardy (northern Italy). -1st EAVP Meeting, July 15th-19th 2003, Abstract volume, Basel, Switzerland.

DE WEVER, P & BAUDIN, F. 1996. Palaeogeography of radiolarite and organic-rich deposits in Mesozoic Tethys. – Geologische Rundschau **85**: 310-326.

D' ORBIGNY, A.D. 1849. Cours élémentaire de paléontologie et de géologie stratigraphiques (1849-1852), 3 volumes, 1146 p., 628 figures, Paris.

DODSON, P. 1975. Functional and ecological significance of relative growth in *Alligator*. – Journal of Zoology London **175**: 315-35.

DUFFIN, C. 1979a. *Pelagosaurus* (Mesosuchia, Crocodylia) from the English Toarcian (Lower Jurassic). – Neues Jahrbuch für Geologie und Paläontologie, Monatshefte **8**: 475-485.

DUFFIN, C. 1979b. The Moore collections of the Upper Liassic crocodiles: a history. – Geological Curators Group Newsletter **2**: 235-252.

DUGUÉ,O., FILY, G. & RIOULT, M. 1998. Le Jurassique des côtes du Calvados: Biostratigraphie, Sédimentologie, Paléoécologie, Paléogéographie et Stratigraphie séquentielle, - Bulletin, Société Géologique de Normandie et des amis du Muséum du Havre **85**(2): 1-134.

EDINGER, T. 1929: Über knöcherne Scleralringe. – Zoologische Jahrbücher, Abteilung Anatomie **51**: 163-222, Jena.

EDINGER, T. 1938. Über Steinkerne von Hirn-und Ohr-Höhlen der Mesosuchier *Goniopholis* und *Pholidosaurus* aus dem Bückeburger Wealden. - Acta Zoologica **14**: 467-503.

EFIMOV, G. & CHKHIKVADZE, V.M. 1987. The review of finds of fossil crocodiles of the USSR. - Izvestiya Akademii Nauk Gruzinskoi SSR, Seriya biologicheskaya **13**: 200–207, [Russian].

ENDO, H., AOKI, R., TARU, H., RIMURA, J., SASAKI, M., YAMAMOTO, M., ARISHIMA, K. & HAYASHI, Y. 2002. Comparative Functional Morphology of the Masticatory Apparatus in the Long-snouted Crocodiles. - Anatomia, Histologia, Embryologia **31**(4): 206-213.

ERICKSON, G.M., LAPPIN, K.A. & VILIET, K.A. 2003. The ontogeny of bite-performance in American alligator (Alligator mississippiensis). - Journal of the Zoological Society London **260**: 317-327.

ETTER, W. & TANG, C.M. 2002. Posidonia Shale: Germany's Jurassic Marine Park. - [IN] BOTTJER, D.J.; ETTER, W.; HAGADORN, J.M. & TANG, C.M. [EDS.] Exceptional fossil preservation: a unique view on the evolution of marine life: 403pp., Columbia University Press, New York.

EUDES-DESLONGCHAMPS, E. 1864. Mémoire sur les Téléosauriens de l'époque Jurassique du Calvados. - Mémoires de la Société Linnéenne de Normandie **13**: 1-138.

EUDES-DESLONGCHAMPS, E. 1867. Note sur un groupe de vertèbres et d'écailles rapportées au Teleosaurus hastifer et provenant des assises kimméridgiennes du Cap de la Hève. - Bulletin de la Societé Linnéenne de Normandie, sér. 2, **1**: 146-156.

FARA, E., OUAJA, M., BUFFETAUT, E. & SRAFRI, D. 2002. First occurrences of thalattosuchian crocodiles in the Middle and Upper Jurassic of Tunisia. - Neues Jahrbuch für Geologie und Paläontologie, Monatshefte **8**: 465-476.

FERNÁNDEZ, M.S. 1997. On the paleogeographic distribution of Callovian and Late Jurassic ichtyosaurs. - Journal of Vertebrate Paleontology **17**(4): 752-754.

FERNÁNDEZ, M. & GASPARINI, Z. 2000. Salt glands in a Tithonian metriorhynchid crocodyliform and their physiological significance. - Lethaia **33**(4): 269-276.

FERNANDEZ, M. & ITURRALDE-VINENT, M. 2000. An Oxfordian Ichthyosauria (Reptilia) from Vinales, Western Cuba: Paleobiogeographic significance. - Journal of Vertebrate Paleontology **20**(1): 191-193.

FRAAS, E. 1901. Die Meerkrokodile (Thalattosuchia) eine Sauriergruppe der Juraformation. - Jahreshefte des Vereins für vaterländische Naturkunde Württemberg **57**: 409–418.

FRAAS, E. 1902. Die Meer-Crocodilier (Thalattosuchia) des oberen Jura unter specieller Berücksichtigung von *Dacosaurus* und *Geosaurus*. – Palaeontographica **49**: 1-71.

FREY, E. 1982. Ecology, locomotion and tail muscle anatomy of crocodiles. – Neues Jahrbuch für Geologie und Paläontologie, Abhandlungen **164**: 194-199.

FREY, E. 1988a. Anatomie des Körperstammes von *Alligator mississippiensis* Daudin. – Stuttgarter Beiträge für Naturkunde, Serie A **424**: 1-106.

FREY, E. 1988b. Das Tragsystem der Krokodile – eine biomechanische und phylogenetische Analyse. - Stuttgarter Beiträge für Naturkunde, Serie A **426**: 1-60.

FREY, E., BUCHY, M.-C., STINNESBECK, W. & JOSE GUADALUPE, L.-O. 2002. *Geosaurus vignaudi* n.sp. (Crocodiliformes: Thalattosuchia), first evidence of metriorhynchid crocodilians in the Late Jurassic (Tithonian) of central-east Mexico. - Canadian Journal of Earth Science **39**(10): 1467-1483.

FREY, E., RIESS, J. & TARSITANO, S.F. 1989. The Axial Tail Musculature of recent Crocodiles and Its Phyletic Implications. - American Zoologist **29**: 857-862.

FREY, E. & SALISBURY, S.W. 2001. The kinematics of aquatic locomotion of *Osteolaemus tetraspis* Cope. [IN] GRIGG, G.C., SEEBACHER, F. & C.E. FRANKLIN [EDS]. Crocodilian Biology and Evolution: 165-179, Surrey Beatty, Chipping Norton, New South Wales, Australia.

GABILLY, J. 1976. Le Toarcien à Thouars et dans le Centre-Ouest de la France. Biostratigraphie. Évolution de la faune (Harpoceratinae, Hildoceratinae). - Série "Les stratotypes français", vol. 3, édit. C.N.R.S., Paris, 217 p.

GALL, J.-C. 1979. Paleoecologie et paleoenviroments de quelques schistes bitumineux. – Documents des Labratoires de Géologie de la faculté des sciences de Lyon **75**: 19-31.

GASPARINI, Z. 1980. Un nuevo cocodrilo marino (Crocodylia, Mesosuchia) del Caloviano del norte de Chile. - Ameghiniana **17**(2): 97-103.

GASPARINI, Z. 1981. Los Crocodylia fosiles de la Argentina. – Ameghiniana **18**(3-4): 177-205.

GASPARINI, Z. 1985. Los reptiles marinos jurásicos de América del Sur. – Ameghiniana **22**(1-2): 23-24.

GASPARINI Z. 1992. Marine reptiles of the Circum-Pacific region. - [IN] Westermann, G.E.G - [Ed.]. The Jurassic of the Circum-Pacific. World and regional Geology 3: 361-364, Cambridge University Press.

GASPARINI Z. 1997. A new pliosaur from the Bajocian of the Neuquen Basin, Argentinia. - Paleontology **40**(1): 135-147.

GASPARINI, Z. & CHONG, D.G. 1977. *Metriorhynchus casamiquelai* n.sp. (Crocodylia, Thalattosuchia), a marine crocodile from the Jurassic (Callovian) of Chile. – Neues Jahrbuch für Geologie und Paläontologie, Abhandlungen **153**(3): 341-360.

GASPARINI, Z., CICHOWOLSKI, M. & LAZO, D.G. 2005. First record of *Metriorhynchus* (Reptilia: Crocodyliformes) in the Bathonian (Middle Jurassic) of the Eastern Pacific. – Journal of Paleontology **79**(4): 801-805.

GASPARINI, Z. & ITURRALDE-VINENT, M. 2001. Metriorhynchid crocodiles (Crocodyliformes) from the Oxfordian of western Cuba. – Neues Jahrbuch für Geologie und Paläontologie, Monatshefte **9**: 534-542.

GASPARINI, Z., POL, D. & SPALLETTI, L.A. 2006. An Unusual Marine Crocdyliform from the Jurassic-Cretaceous Boundary of Patagonia. – Science **311**: 70-73.

GASPARINI, Z., VIGNAUD, P. & CHONG, G. 2000. The Jurassic Thalattosuchia (Crocodyliformes) of Chile: a paleobiogeographic approach. – Bulletin de la Societe geologiques de France **171**(6): 657-664.

GLASVILLE, M. DE (1876). Sur la cavité crânienne et la position du trou optique dans le *Steneosaurus heberti*. - Bulletin de la Société Géologique de France, Paris: 342-348.

GEOFFROY SAINT-HILAIRE, E. 1831. Recherches sur de grands sauriens trouvés à l'état fossile aux confins maritimes de la Basse-Normandie, attribués d'abord au Crocodile, puis déterminés sous les noms de *Teleosaurus* et *Steneosaurus*. - Memoires de l'Academie des sciences **12**: 1-138.

GODEFROIT, P. 1994. Les reptiles marins du Toarcien (Jurassique Inferieur) Belgo-Luxembourgois. – Memoires pour servir a l'explication des cartes geologiques et minieres de la Belgique **39**: 1-98.

GODEFROIT, P., VIGNAUD, P. & LIEGER, A. 1995. Un Teleosauridae (Reptilia) du Bathonien Superieur Lorraine (France). – Bulletin de la Société belge de Géologie **104**(1-2): 91-107.

GRANGE, D.R. & BENTON, M.J. 1996. Kimmeridgian metriorhynchid crocodiles from England. - Palaeontology **39**(2): 497-514.

HALLAM, A. 1979. The Lower Toarcian black shales of England. – Documents des Labratoires de Géologie de la faculté des sciences de Lyon **75**: 91-92.

HALLAM, A. 1987. Mesozoic marine organic-rich shales. - [IN] BROOKS, J. & FLEET, A.J. [EDS.]. Marine Petroleum Source Rocks. Special Publication 26: 251-261, Geological Society, London.

HAUFF, B. 1921. Untersuchungen der Fossilfundstätten von Holzmaden im Posidonienschiefer des Oberen Lias Württenbergs. - Paleontographica **64**: 1-42.

HAUFF, B. & HAUFF, R.B. 1981. Das Holzmadenbuch. - 136 pp., Hauff & Hauff, Holzmaden.

HAUFF, R.B. 1997. Urwelt-Museum Hauff. Leben im Jurameer. - 66pp.,Urwelt-Museum Hauff, Holzmaden.

HENDERSON, D.M. 2003. Effects of stomach stones on the buoyancy and equilibrium of a floating crocodilian: a computational analysis. – Canadian Journal of Zoology **81**: 1346-1357.

HILDEBRAND, M. & GOSLOW, JR. G.E. 2004. Vergleichende und funktionelle Anatomie der Wirbeltiere. – 709pp., 440 pl., Springer Verlag, Heidelberg.

HOHL, R. [ED.] 1985. Die Entwicklungsgeschichte der Erde. - 7th edition, 686 pp., Verlag Dausien, Hanau.

HUA, S. 1999. Le Crocodilien *Machimosaurus mosae* (Thalattosuchia, Teleosauridae) du Kimmeridgien du Boulonnais (Pas de Calais, France). - Palaeontographica A **252**: 141-170.

HUA, S. 2003. Locomotion in marine mesosuchians (Crocodylia): the contribution of the "locomotion profiles". – Neues Jahrbuch für Geologie und Paläontologie, Abhandlungen **227**(1): 139-152.

HUA, S. & ATROPS, F. 1995. Un crâne de *Teleidosaurus* cf. *gaudryi* (Crocodylia, Metriorhynchidae) dans le Bajocien supérieur des environs de Castellane (Sud-Est de la France).- Bulletin de la Société Géologique de France **166**(6): 643-648.

HUA, S. & BUFFETAUT, E. 1997. Crocodylia. [IN] CALLAWAY, J.M. [ED.]. Ancient Marine Reptiles: 357-374, Academic Press, San Diego.

HUA, S., VIGNAUD, P., ATROPS, F. & CLÉMENT, A. 2000. *Enaliosuchus macrospondylus* KOKEN, 1883 (Crocodylia, Metriorhynchidae) du Valanginien de Barret-le-Bas (Hautes Alpes, France): un cas unique de remontée des narines externes parmi les crocodiliens. - Geobios **33** (4): 467-474.

HUA, S., VIGNAUD, P. & EFIMOV, V. 1998. First record of Metriorhynchidae (Crocodylomorpha, Mesosuchia) in the Upper Jurassic of Russia. – Neues Jahrbuch für Geologie und Paläontologie, Monatshefte **8**: 475-484.

HUA, S., VIGNAUD, P., PENNETIER, E. & PENNETIER, G. 1994. Un squelette de *Steneosaurus obtusidens* ANDREWS 1909 dans le callovien de Villers-sur-Mer (Calvados, France) et le problème de la dèfinition des Teleosauridae à dents obtuses. – Compte Rendu hebdomadaire des seances de l'Academie des Sciences Paris **318**, série **2**: 1557-1562.

HUENE, F. von 1938. Ein Pliosaurier aus Abessinien. - Jahrbuch für Mineralogie, Geologie und Paläontologie **147**: 370-376

HUENE, F.VON & MAUBEUGE, P.L. 1952. Sur quelques restes de reptiles du Lias de Jeandelaincourt (M.-et-M.). (Zone à *Amaltheus Margaritatus*). – Bulletin de la Société de France, Serie 6 **2**: 13-17.

HUENE, F. VON & MAUBEUGE, P.L. 1954. Sur quelques restes de Sauriens du Rhétien et du Jurassique lorain. - Bulletin de la Société de France, Serie 6 4(1-3): 105-109.

HUTCHINSON, J.R. & GATESY, S.M. 2000. Adductors, abductors, and the evolution of archosaur locomotion. -Paleobiology 26(4): 734-751.

IORDANSKY, N.N. 1964. The jaw muscles of the crocodiles and some relating structures of the crocodilian skull. - Anatomischer Anzeiger **115**: 256-280.

IORDANSKY, N.N. 1973. The Skull of Crocodilia. - [IN] GANS, C. & PARSONS, T.S. [EDS.]. Biology of the Reptilia, Volume 4, Morphology D: 201-262, Academic Press, London, New York.

JAEGER, G.F. 1828. Über die Fossile Reptilien, welche in Württemberg aufgefunden worden sind. - 48 pp., Stuttgart.

JAIN, S.L., ROBINSON, P.L. & CHOWDHURY, T.K.R. 1962. A new vertebrate fauna from the Early Jurassic of the Deccan, India. – Nature **194**: 755-757.

JENKYNS, H.C. 1988. The early Toarcian (Jurassic) anoxic event: Stratigraphic, sedimentary, and geochemical evidence. – American Journal of Science **288**: 101-151.

JENSEN O. & VICENTE, J.C. 1976. Estudio geológico del área de "Las Juntas" del Río Copiapó (Provincia de Atacama, Chile). - Revista de la Asociacion Geologica Argentina **31**(3): 145-173.

JOUVE, S. & SCHWARZ, D. 2004. *Congosaurus bequaerti*, a Paleocene Dyrosaurid (Crocodyliformes; Mesoeucrocodylia) from Landana (Angola). - Bulletin de l'Institut royal des sciences naturelles de Belgique. Sciences de la terre **74**: 129-146.

KÄLIN, J.A. 1937. Über Skeletanomalien bei Crocodiliden. – Zeitschrift für Morphologie und Ökologie **32**(2): 327-347.

KÄLIN, J.A. 1941. Über die Altersvariation von *Osteolaemus tetrapis* COPE und über „*Osteoblepharon osborni* K.P. SCHMIDT". – Zoologischer Anzeiger **134**(11/12): 295-299.

KÄLIN, J.A. & KNÜSEL, L. 1944. Über die Lokomotion der Crocodiliden. – Revue Suisse de Zoologie **51**(18): 389-393.

KAUP J.J. 1837. Das Thierreich in seinen Hauptformen, systematisch beschrieben. Erste Auflage. 5 Teile in 3 Bänden. Darmstadt, J.P. Diehl.

KLEMBARA, J. 1991. The cranial anatomy of early ontogenetic stages of *Alligator mississippiensis* (DAUDIN, 1802) and the significance of some of its cranial structures for the evolution of tetrapods. - Paleontographica A **215**: 103-171.

KLEMBARA, J. 2001. Postparietal and prehatching ontogeny of the supraoccipital in *Alligator mississippiensis* (Archosauria, Crocodylia). - Journal of Morphology **249**(2): 147-153.

KLEMBARA, J. 2004. Ontogeny of the palatoquadrate and adjacent lateral cranial wall of the endocranium in prehatching *Alligator mississippiensis* (Archosauria: Crocodylia). - Journal of Morphology **262**(2): 644-658.

KRAMER, G. 1955. Über wachstumsbedingte Veränderungen von Körperproportionen bei *Mystriosaurus bollensis*. – Zoologische Jahrbücher **66**: 75-78.

KRAMER, G. & MEDEM, F. 1955. Über wachstumsbedingte Proportionsänderungen bei Krokodilen. – Zoologische Jahrbücher **66**: 62-74.

KREBS, B. 1962. Ein *Steneosaurus*-Rest aus dem Oberen Jura von Dielsdorf, Kt. Zürich, Schweiz. – Schweizerische Paläontologische Abhandlungen **79**: 3-28.

KREBS, B. 1967. Der Jura-Krokodilier *Machimosaurus* H. v. MEYER. - Paläontologische Zeitschrift **41**(1/2): 46-59.
KRISHNA, J. 1987. Biological evidence for better appreciation of the Indian Gondwana. - The Paleobotanist **36**: 268-284.

KUTTY S., JAIN, S.L. & ROY-CHOWDHURY, T. 1987. Gondwana sequences of the northern Pranhita-Godvari valley: its stratigraphy and vertebrate faunas. - The Paleobotanist **36**: 214-229.

LAKJER, T. 1926. Studien über die Trigeminus-versorgte Kaumuskulatur der Sauropsiden.-154 pp., C.A. Reitzel, Copenhagen.

LANGROCK, U. 2003. Late Jurassic to Early Cretaceous Black Shale Formation and Paleoenvironment in High Northern Latitudes. -127pp., PhD Thesis, University Bremen.

LAPPARENT , A.F. DE 1955. Étude paléontologique des vertébrés du Jurassique d'El Mers (Moyen Atlas). – Notes et Memoris du Service Geologique, Maroc, Rabat **124**: 1-36.

LARSSON, H.C.E. 1998. A new method for comparing ontogenetic and phylogenetic data and its application to the evolution of the crocodilian secondary palate. – Neues Jahrbuch für Geologie und Paläontologie, Abhandlungen **210**(3): 345-368.

LENNIER, G. 1887. Description des fossiles du cap de la Hève. - Bulletin de la Société Géologique de Normandy, Le Havre **12**: 17-98.

LEVY, C. 2003. Endangered Species. Crocodiles & Alligators. 128pp, Eagle Editions, Quantum Publishing London.

LI, J. 1993. A new specimen of *Peiphesuchus teleorhinus* from Ziliujing Formation of Daxion, Sichuan. – Vertebrata Palasiatica **31**(2/4): 85-94.

MAGNUSSON, W.E., VLIET, K.A., POOLEY, A.C. & WHITAKER, R. 2002. Fortpflanzung. - [IN] ROSS, C.A.[ED.]. Krokodile und Alligatoren: 118-135, Orbis Verlag, Niedernhausen/Ts.

MAISCH , M.W. & ANSORGE, J. 2004. The Liassic ichthyosaur *Stenopterygius* cf. *quadriscissus* from the lower Toarcian of Dobbertin (northeastern Germany) and some consideration on lower Toarcian marine reptile palaeobiogeography. – Paläontologische Zeitschrift **78**(1):161-171.

MAISCH, M.W., MATZKE, A.T. & STÖHR H. 2003. *Sunosuchus* (Archiosauria, Crocodyliformes) from the Toutunhe Formation (Middle Jurassic) of the Southern Junggar Basin (Xinjiang, NW-China). – Geobios **36**: 391-400.

MARTILL, D. 1986. The diet of *Metriorhynchus*, a Mesozoic marine crocodile. – Neues Jahrbuch für Geologie und Paläontologie, Monatshefte **10**: 621-625.

MARTILL, D., TAYLOR, M.A., DUFF, K.L., RIDING, J.B. & BOWN, P.R. 1994. The tropic structure of the biota of the Peterborough Member, Oxford Clay Formation (Jurassic), UK. – Journal of the Geological Society, London **151**: 173-194.

MARTIN, B.G.H. & BELLAIRS A. 1977. The narial excrescence and pterygoid bulla of the gharial, *Gavialis gangeticus* (Crocodilia). - Journal of Zoology 182: 541-558.

MARTIN, R.B., BURR, D.B. & SHARKEY, N.A. 1998. Skeletal Tissue Mechanics, -392 pp., Springer Verlag Berlin.

MASER C. & SEDELL, J.R. 1994. From the Forest to the Sea: The Ecology of Wood in Streams, Rivers, Esturians, and Oceans. - 200pp., St. Lucie Press.

MASSARE, J. 1987. Tooth morphology and prey preference of Mesozoic marine reptiles. – Journal of Vertebrate Palaeontology 7(2): 121-137.

MASSARE, J. 1988. Swimming capabilities of Mesozoic marine reptiles: implications for method of predation. - Palaeontology **14** (2): 187-205.

MATEER, N.J. 1974. Three Mesozoic crocodiles in the collections of the Palaeontological Museum, Uppsala. – Bulletin geologiske Institute Unversitet Uppsala, N.S. **4** (4): 53-72.

MATEUS, O. 2002. On a large crocodile vertebrae of cf. *Machimosaurus* from the Late Jurassic of Lourinha (Portugal). II Congresso I Ibérico de Paleontologia, Libro de Resúmenes: 73-75, Salamanca.

MEERS, M.B. 2003. Crocodylian forelimb musculature and its relevance to Archosauruia. – The Anatomical Record, Part A **274**: 891-916.

MERCIER, J. 1933. Contribution a l'étude des métriorhynchidés (crocodiliens). – Annales de Paleontologie **22**: 99-119.

MEYER, H. VON. 1830. Achte Versammlung der Naturforscher und Aerzte zu Heidelberg im September 1829, Series B, Mineralogische Abteilung **15**(2): 517–519.

MEYER, H. VON 1840. Mitteilungen an Prof. Bronn. – Neues Jahrbuch der Mineralogie **1840**: 576-584.

MEYER, H. VON 1841. Mitteilungen an Prof. Bronn. – Neues Jahrbuch der Mineralogie **1841**: 96-99.

MEYER, H. VON 1845. Mitteilungen an Prof. Bronn. – Neues Jahrbuch der Mineralogie **1845**: 689-691.

MICHELIN, C., BUFFETAUT, E. & ENAY, R. 1985. Le Crocodilien *Steneosaurus* (Mesosuchia, Teleosauridae) dans le Jurassque Supérieur Franc-Comtois (Jura, France). – Geobios **18**(1): 115-120.

MUELLER-TÖWE, I.J. 2005. Phylogenetic Relationships of the Thalattosuchia. - Zitteliana A **45**: 211-213.

MÜLLER, G.B. & ALBERCH, P. 1990. Ontogeny of the limb skeleton in *Alligator mississippiensis*: Devolpmental invariance and change in the evolution of archosaur limbs. – Journal of Morphology **203**: 151-164.

MÜLLER, J. 2002. A revision of *Askeptosaurus italicus* and other thalattosaurs from the European Triassic, the interrelationships of thalattosaurs, and their phylogenetic position within diapsid reptiles (Amniota, Eureptilia). – 193 pp., PhD Thesis, University Mainz.

MONTAGUE, J.J. 1984. Morphometric Analysis of *Crocodylus novaeguineae* from the Fly River Drainage, Papua New Guinea. - Australian Wildlife Research **11**: 395-414.

MONTANI, R. 2005. Evolution of fish-shaped reptiles (Reptilia: Ichthyopterygia) in their physical environments and constraints. - Annual Review of Earth and Planetary Sciences **33**: 395-420.

MONTEIRO, L.R., CAVALCANTI, M.J. & SOMMER III, H.J.S. 1997. Comparative ontogenetic shape changes in the skull of *Caiman* species (Crocodylia, Alligatoridae). – Journal of Morphology **231**: 53-62.

MONTEIRO, L.R & SOARES, M. 1997. Allometric analysis of the ontogenetic variation and evolution of the skull in *Caiman* SPIX, 1825 (Crocodylia, Alligatoridae). – Herpetologica **53**(1): 62-69.

MOOK, C.C. 1921a. Notes on the postcranial skeleton in the Crocodilia. - Bulletin of the American Museum of Natural History **44**: 67-100

MOOK, C.C. 1921b. Individual and age variations in the skulls of Recent Crocodilia. – Bulletin of the American Museum for Natural History **44**: 51-66.

NAISH, D. 2001. Crocodilians. - Geology Today **17**(2): 71-77.

NESOV, L.A., KAZNYSHKINA, L.F. & CHEREPANOV, G.O. 1989. [Dinosaurs-Ceratopsidae and crocodiles from the Mesozoic of Soviet Central Asia].- Trudy 33 Sessii Vsesoyuznogo Paleontologicheskogo Obshchestva: 144-154.

NEWTON, R.B. 1893. On the discovery of a secondary reptile from Madagascar: *Steneosaurus baroni* (n. sp.). – Geological Magazine **3**(10): 193-198.

O'KEEFE, F.R. 2002. The evolution of plesiosaur and pliosaur morphotypes in the Plesiosauria (Reptilia: Sauropterygia). - Paleobiology **28**(1): 101-112.

OWEN R. 1840. Report on British fossil reptiles. Part I. - Report British Association for the Advancement of Science 1839, Reports: 43-126.

OWEN, R. 1849/1884. A history of British fossils reptiles. Cassel Ed. London.

OWEN, R. 1852. Note on the crocodilians remains accompanying Dr. T.L. Bell's paper on Kotah. - Quaterly Journal of the Geological Society of London **8**: 233.

OWEN, R. 1865. Monograph of the Fossil Reptilia of the Liassic Formations. Part 1: Sauropterygia. - Palaeontographical Society Monograph. London.

PARRISH, J.M. 1987. The origin of crocodilian locomotion. - Paleobiology **13**(4): 396-414.

PARRISH, J.T. 1993. Climate of the supercontinent Pangea. - Journal of Geology **101**: 215–233.

PHIZACKERLEY, P.H. 1951. A revision of the Teleosauridae in the Oxford University Museum (Natural History). – Annals and Magazine of Natural History, Series **12**(4): 1169-1192.

POGLAYEN-NEUWALL, I. 1953. Untersuchungen der Kiefermuskulatur und deren Innervation an Krokodilien. - Anatomischer Anzeiger **16/17**: 259-277.

POL, D. & NORELL, M.A. (2004): A new crocodyliform from Zos Canyon, Mongolia. - American Museum Novitates, **3445**: 1-36.

POMPECKJ, J.E. 1901. Die Jura-Ablagerungen zwischen Regensburg und Regenstrauf. – Geognostische Jahreshefte **14**: 139-220.

POOLEY, A.C. 2002. Nahrung und Ernährungsweise: 76-91. - [IN] ROSS, C.A. [ED.]. German Edition 2002. Krokodile und Alligatoren. Entwicklung, Biologie und Verbreitung. - 239 pp., Orbis Verlag, Niedernhausen.

PREUSCHOFT, H., DEMES, B., MEIER, M. & BÄR, H.F. 1985. Die biomechanischen Prinzipien im Oberkiefer von langschnäuzigen Wirbeltieren. – Zeitschrift für Morphologie und Anthropologie **76**(1):1-24.

QUENSTEDT, F.A. 1852. Handbuch der Petrefactenkunde (first edition) .- 792 pp., H. Laupp Verlag, Tübingen.

QUENSTEDT, F.A. 1858. Der Jura. – H. Laupp Verlag, Tübingen.

REESE, A.M. 1915. The Alligator and its Allies. - 358 pp., GP Putnam's Sons, New York.

RIEGRAF, W. 1985. Mikrofauna, Biostratigraphie und Fazies im Unter Toarcium Südwestdeutschlands und Vergleiche mit benachbarten Gebieten. – Tübinger mikropaläontologische Mitteilungen 3. Tübingen: Institut und Museum für Geologie und Paläontologie der Universität Tübingen.

RIEGRAF, W., WERNER, G. & LÖRCHER, F. 1984. Der Posidonienschiefer: Biostratigraphie, Fauna und Fazies des süddeutschen Untertoarciums (Lias ε). Enke Verlag, Stuttgart.
RIESS, J. 1986. Fortbewegungsweise, Schwimmbiophysik und Phylogenie der Ichthyosaurier. – Palaentographica, Abteilung A, **192**: 93-155.

RIEPPEL, O. 1981. Fossile Krokodilier aus dem Schweizer Jura. – Ecologae Geologica Helvetica **74**(3): 735-751.

RIEPPEL, O.1993. Studies on skeleton formation in reptiles. v. Patterns of ossification in the skeleton of *Alligator mississippiensis* DAUDIN (Reptilia, Crocodylia). – Zoological Journal of the Linnean Society **109**: 301-325.

RIEPPEL, O. 2002. Feeding mechanics in Triassic stem-group sauropterygians: the anatomy of a successful invasion of Mesozoic seas. - Zoological Journal of the Linnean Society **135**: 33-68.

RÖHL, H.-J. 1998. Hochauflösende palökologische und sedimentologische Untersuchungen im Posidonienschiefer (Lias ε) von SW-Deutschland. – Tübinger Geowissenschaftliche Arbeiten A (47) Tübingen: Institut und Museum für Geologie und Paläontologie der Universität Tübingen.

RÖHL, H.-J., SCHMID-RÖHL, A., OSCHMANN, W., FRIMMEL, A. & SCHWARK, L. 2001. The Posidonia Shale of SW Germany: an oxygen-depleted ecosystem controlled by sea level and palaeoclimate. – Palaeogeography, Palaeoclimatology, Palaeoecology **165**: 27-52.

ROMER, A.S. 1956. Osteology of the Reptiles. - 772 pp., The University of Chicago Press, Chicago.

ROSS, C.A. [ED.] 2002. Krokodile und Alligatoren. Entwicklung, Biologie und Verbreitung. German Edition 2002. - 239 pp., Orbis Verlag, Niedernhausen.

SANDER, P.M. 2000. Ichtyosauria: their diversity, distribution and phylogeny. – Paläontologische Zeitschrift **74**(1/2): 1-37.

SATO, I., SHIMADA, K., EZURE, H., MURATAMI, G. & SATO, T. 1994. Morphological Study of Nerve Endings in Jaw Muscles of Post-hatching American Alligators (*Alligator mississippiensis*). – Journal of Morphology **219**: 285-295.

SAUVAGE, H.E 1879. Etudes sur les poissons et les reptiles des treirains crétáces et jurassiques supérieurs de l'Yonne. - Bulletin de la Société des Sciences Historiques et Naturalles de l'Yonne **3**(1): 20-84.

SCHMIDT-NIELSEN, K. & FANGE, R. 1958. Salt glands in marine reptiles. – Nature **182**(4638): 783-785.

SCHUMACHER, G.-H. 1973. The Head Muscles and Hyolaryngeal Skeleton of Turtles and Crocodilians. - [IN] GANS, C. & PARSONS, T.S. [EDS.]. Biology of the Reptilia. Vol. 4, Morphology D: 101-199, Academic Press, London, New York.

SCHWARZ, D. 2003. Konstruktionsmorphologie und evolutionsbiologische Analyse der Dyrosauridae (Crocodilia). - 364 pp., PhD Thesis, FU Berlin

SCOTESE, C. R. 2001. Atlas of Earth History. - Volume 1, - 52 pp., Paleogeography, PALEOMAP Project, Arlington, Texas.

SCOTESE, C.R. 2002. http://www.scotese.com, (PALEOMAP website).

SEILACHER, A. 1982. Posidonia Shales (Toarcian, S.Germany). Stagnant basin model revalidated. - [IN] GALLITELLI, E.M. [ED.]. Paleontology, Essential of Historical Geology: Proceedings of the First International Meeting on Paleontology, Essential of Historical Geology. 279-298, Modena: STEM Mucchi.

SEILACHER, A. 1990. Die Holzmadener Posidonienschiefer – Entstehung der Fossillagerstätte und eines Erdölmuttergesteins. - [IN] WEIDERT, K.W [ED.]. Klassische Fossilfundstellen der Paläontologie.Volume 2: 107-131, Goldschneck-Verlag.

SEILACHER, A., REIF, W.E. & WESTPHAL, F. 1985. Sedimentological, ecological and temporal patterns of fossil Lagerstätten. – Philosophical Transactions of the Royal Society of London B **311**: 5-23.

SELDEN & NUDDS 2004. Evolution of fossil ecosystems. - 160 pp., Manson Publishing, London.
SELENKA, E. 1867. Die fossilen Krokodilinen des Kimmeridge von Hannover. Palaeontographica. **16**(1866-1869): 137-144.

SHA, J. 2002. Hispanic Corridor formed as early as the Hettangian: On the basis of bivalve fossils. – Chinese Science Bulletin **47**(5): 414-417.

SHIMADA, K., SATO, I. & EZURE, H. 1993. Morphological analysis of tendinous structure in the American Alligator jaw muscles. – Journal of Morphology **217**: 171-181.

SHOEMAKER, V.H. & NAGY, K.A.1977. Osmoregulation in amphibians and reptiles. – Annual Reviews of Physiology 39: 449-471.

SHULTZ, M.R., FILDANI, A. & SUAREZ, M. 2003. Occurrence of the Southernmost South American Ichthyosaur (Middle Jurassic—Lower Cretaceous), Parque Nacional Torres del Paine, Patagonia, Southernmost Chile. - Palaios **18** (1): 69-73.

SIMMS, M.J., CHIDLAW, N., MORTON, N. & PAGE, K.N. 2004. British Lower Jurassic Stratigraphy. - Geological Conversation Review Series **30**: 1-458.

SMITH, A.G., SMITH, D.G. & FUNNEL, B.M. 1995. Atlas of Mesozoic and Cenozoic coastlines. - 99 pp., Cambridge University Press, Cambridge.

SOEMMERING, S.T. 1816. Über den *Crocodilus priscus* oder über ein in Baiern versteint gefundes Krokodil, Gavial der Vorwelt. - Denkschriften der Königlichen Akademie der Wissenschaften zu München **5**: 9-82.

STEEL, R. 1975. Die fossilen Krokodile. 76 pp., Die Neue Brehm-Bücherei, Wittenberg Lutherstadt.

STORRS, G.W. 1997. Morphological and taxonomic clarification of the genus Plesiosaurus **-** [In] CALLAWAY, J.M. & NICHOLLS, E.L. [EDS.]. Ancient Marine Reptiles: 145-190, Academic Press, San Diego.

STORRS, G.W. & EFIMOV, M.B. 2000. Mesozoic crocodyliformes of north-central Eurasia. - [IN] BENTON, M., SHISHKIN, M.A., UNWIN, D.M. & KUROCHKIN, E.N. [EDS]. The Age of Dinosauria in Russia and Mongolia: 402-419, Cambridge University Press, Cambridge.

STORRS G.W. & TAYLOR, M.A. 1996. Cranial anatomy of a new plesiosaur genus from the lowermost Lias (Rhaetian/Hettangian) of Street, Somerset, England. - Journal of Vertebrate Paleontology **16**(3): 403-420.

STRICKER, L.S. & TAYLOR, D.G. 1989. A new marine crocodile (Mesosuchia, Metriorhynchidae) from the Snowshoe Formation (Jurassic) Oregon. - Journal of Vertebrae Paleontology **9**(3): 28, 40A.

SWOFFORD, D.L. (2003). Phylogenetic Analysis Using Parsimony*4.0b10. – Sinauer Associates Incorporates, Sunderland.

TALPIN, L.E. & GRIGG, G.C. 1981. Salt glands in the tongue of the estuarine crocodile, *Crocodylus porous*. – Science **212**: 1045-1047.

TATE, R. & BLAKE, J.F. 1876. The Yorkshire Lias. - 474 pp., London.

TAYLOR, J.A. 1979. The Food and Feeding habits of Subadult *Crocodylus porosus* SCHNEIDER in Northern Australia. - Australian Wildlife Research **6**: 347-359.

TAYLOR, M.A. 1987. How tetrapods feed in water: a functional analysis by paradigm. - Zoological Journal of Linnaen Society **91**: 171-195.

TAYLOR, M.A. 1993. Stomach Stones for Feeding or Buoyancy? The Occurrence and Function of Gastroliths in Marine Tetrapods. **-** Philosophical Transactions: Biological Sciences **341**(1296): 163-175.

THORBJARNARSON, J.B. 1990. Notes on the feeding behavior of the gharial (Gavialis gangeticus) under semi-natural conditions. - Journal of Herpetology **24**: 99-100.

THULBORN, R.A. & WARREN, A. 1980. Early Jurassic plesiosaurs from Australia. - Nature **285**: 224-225.

TRUTNAU, L. 1994. Krokodile. – Die Neue Brehme-Bücherei, Bd. 593, - 270 pp., Westarp Wissenschaften, Magdeburg.

TYKOSKI, R.S., ROWE, T.B., KETCHAM, R.A. & COLBERT, M.W. 2002. *Calsoyasuchus valliceps*, a new Crocodyliform from the Early Jurassic Kayenta Formation of Arizona. – Journal of Vertebrate Paleontology **22**(3): 593-611.

URLICHS, M. 1977. The Lower Jurassic in southwestern Germany. - Stuttgarter Beiträge für Naturkunde B **24**: 1-41.

URLICHS, M., WILD, R. & ZIEGLER, B. 1994. Der Posidonienschiefer des unteren Jura und seine Fossilien. – Stuttgarter Beiträge zur Naturkunde B **24**: 1-41.

VIGNAUD, P. 1993. Thalattosuchians from the Callovian of Poitou (Vienne, France). - Revue de Paléobiologique**,** Volume Special **7**: 251-261.

VIGNAUD, P. 1995. Les Thalattosuchia, crocodiles marins du Mésozoique: Systématique phylogénétique, paléoécologie, biochronologie et implications paléogéographiques. Thèse de l'Université de Poitiers. - 410 pp., (Unpublished) Poitiers.

VIGNAUD, P. 1997. La morphologie dentaire des Thalattosuchia (Crocodylia, Mesosuchia). - Palaeovertebrata **26**(1-4): 35-59.

VIGNAUD, P. 1998. Une nouvelle espèce de *Steneosaurus* (Thalattosuchia, Teleosauridae) dans le Callovien du Poitou (France) et la systématique des *Steneosaurus* longirostres du Jurassique Moyen d'Europe occidentale. – Palaeovertebrata **27**(1-2): 19-44.

VIGNAUD, P., DE BROIN, F., BRUNET, M., CARIOU, E., HANTZPERGUE, P. & LANGE-BADRE, B. 1994. Les Faunes de Vertébrés Jurassiques de la Bordure Nord-Orientale du Bassin D`Aquitaine (France): Biochronologie et Environnements. - Geobios **17**: 493-503.

VIGNAUD , P. & GASPARINI , Z. 1996. New *Dakosaurus* (Crocodylomorpha, Thalattosuchia) in the Upper Jurassic of Argentina. - Comptes Rendues de l'Académie de Sciences **322**: 245-250.

WALKDEN, G.M., FRASER, N.C. & MUIR, J. 1987. A new specimen of *Steneosaurus* (Mesosuchia, Crocodilia) from Toarcian of the Yorkshire coast. – Proceedings of the Yorkshire Geological Society **46**(3): 279-387.

WALKER, A.D. 1968. *Protosuchus*, *Proterochampsa*, and the origin of phytosaurs and crocodiles. - Geological Magazine 1**05**(1): 1-94.

WALKER S.E. & BRETT, C. E. 2002. Post-Paleozoic patterns in marine predation: Was there a Mesozoic and Cenozoic marine predatory revolution? - Paleontological Society Papers **8**: 119-193.

WEBB, G.J.W., MANOLIS, S.C. & BUCKWORTH, R. 1982. *Crocodylus johnstoni* in the McKinlay River area, N.T., part 1: variation in the diet, and a new method of assessing the relative importance of prey. - Australian Journal of Zoology **30**(6): 877 - 899.

WESTNEAT, M.W. 2003. A biomechanical model for analysis of muscle force, power output and lower jaw motion in fishes. -Journal of Theoretical Biology **223**: 269-281.

WESTPHAL, F. 1961. Zur Systematik der deutschen und englischen Lias Krokodilier. - Neues Jahrbuch für Geologie und Paläontologie, Abhandlungen **113**: 207-218.

WESTPHAL, F. 1962. Die Krokodilier des deutschen und englischen oberen Lias. – Palaeontographica, Abteilung A **118**: 23-118.

WETTSTEIN, O. von 1937. Crocodilia. - [IN] KÜKENTHAL, W. & KRUMBACH, T. [EDS]. - Handbuch der Zoologie; Sauropsida **7**: 236-320.

WHETSTONE, K.N. & WHYBROW, P. 1983. A cursorial crocodilian from the Triassic of Lesotho (Basutoland), South Africa. – Occasional Paper of the University of Kansas **106**: 1-37.

WHITAKER, R. & BASU, D. 1982. The gharial (*Gavialis gangeticus*): A review. – Journal of Bombay Natural History Society **79**(3): 531-548.

WILD, M.U. & ZIEGLER, B. 1986. Fossilien aus Holzmaden. – Stuttgarter Beiträge zur Naturkunde, Serie C, **11**: 1-34, Stuttgart.

WILLIAMS, M.F. 1997. The adaptive significance of endothermy and salt excretion amongst the earliest archosaurs. – Speculations in Science and Technology **20**: 237-247.

WILLIS, J.S., BIKNEVICIUS, A.R., REILLY, S.M. & EARLS, K.D. 2004. The tail of the tail: limb function and locomotor mechanics in Alligator mississippiensis. - THE JOURNAL OF EXPERIMENTAL BIOLOGY 207: 553-563.

WINCIERZ, J. 1967. Ein *Steneosaurus*-Fund aus dem nordwestdeutschen Oberen Lias. - Paläontologische Zeitschrift **41**(1/2): 60-72.

WINGS, O. 2004. Identification, Distribution, and Function of Gastroliths in Dinosaurs and Extant Birds with Emphasis on Ostriches (*Struthio camelus*). -187pp., PhD Thesis, University Bonn.

WU, X.-C. & SUES, H.-D. 1996. Reassessment of *Platygnathus hsui* Young, 1944 (Archosauria: Crocodyliformes) from the Lower Lufeng Formation (Lower Jurassic) of Yunnan, China. – Journal of Vertebrate Paleontology **16**(1): 42-48.

YOUNG, C.C. 1948. Fossil crocodiles in China, with notes on dinosaurian remains associated with the Kansu crocodilies. - Bulletin of the Geological Society of China **28**(3-4): 255-288.

ZAHER, H., POL, D., CARVALHO, A. B., RICCOMINI, C., CAMPOS, D., & NAVA, W. 2006. Redescription of the Cranial Morphology of *Mariliasuchus amarali*, and its Phylogenetic Affinities (Crocodyliformes, Notosuchia). - American Museum Novitate **3512**: 1-40.

ZIEGLER, P.A. 1990. Geological Atlas of Western and Central Europe. - 2nd edition. - The Hague: Shell International Petroleum Maatschappij.

Appendix I

Material list

Specimen	Taxon	Horizon	Location
BMNH 14438	cf *Steneosaurus bollensis*	Liassic	Whitby, Great Britain
BMNH R 12011	*Steneosaurus bollensis*	Jet Rock Form., Liassic	Whitby, Great Britain
BMNH R 324	cf *Steneosaurus bollensis*	Upper Liassic	Whitby, Great Britain
BMNH R 3936	*Steneosaurus bollensis*	Upper Liassic	Holzmaden, Germany
BMNH R 3937	*Steneosaurus bollensis*	Liassic, Toarcian	Holzmaden, Germany
BMNH R 65	cf *Steneosaurus bollensis*	Liassic, Toarcian	Boll, Germany
BSGP 1949 XV 1a	*Steneosaurus bollensis*	Lias ε , Toarcian	Holzmaden, Germany
BSGP 1949 XV 1b	*Steneosaurus bollensis*	Lias ε , Toarcian	Holzmaden, Germany
BSGP uncatalogued (cabinet)	*Steneosaurus bollensis*	Lias ε, Toarcian	Holzmaden, Germany
BSGP uncatalogued (wall)	*Steneosaurus bollensis*	Lias ε , Toarcian	Holzmaden, Germany
BSGP1972 V 11	cf *Steneosaurus bollensis*	Lias ε, Toarcian	Holzmaden, Germany
GPIM G 23a	*Steneosaurus bollensis*	Lias ε , Toarcian	Holzmaden, Germany
GPIM G 23b (cast)	*Steneosaurus bollensis*	Lias ε , Toarcian	Holzmaden, Germany
GPIM Jur 59	*Steneosaurus bollensis*	Lias ε , Toarcian	Holzmaden , Germany
GPIM Jur 71	*Steneosaurus bollensis*	Lias ε , Toarcian	Holzmaden , Germany
GPIM uncatalogued	*Steneosaurus bollensis*	Lias ε II, 6, Toarcian	Holzmaden, Germany
GPIM uncatalogued	*Steneosaurus bollensis*	Lias ε , Toarcian	Holzmaden, Germany
GPIT Re 1193/1	*Steneosaurus bollensis*	Lias ε II, 6, Toarcian	Ohmden, Germany
GPIT Re 1193/10	*Steneosaurus bollensis*	Lias ε , Toarcian	Germany
GPIT Re 1193/11	*Steneosaurus bollensis*	Lias ε , Toarcian	Holzmaden, Germany
GPIT Re 1193/12	cf *Steneosaurus bollensis*	Lias ε , Toarcian	Germany
GPIT Re 1193/13	*Steneosaurus bollensis*	Lias ε , Toarcian	Holzmaden, Germany
GPIT Re 1193/14	*Steneosaurus bollensis*	Lias ε , Toarcian	Germany
GPIT Re 1193/2	*Steneosaurus bollensis*	Lias ε , Toarcian	Holzmaden, Germany
GPIT Re 1193/3	*Steneosaurus bollensis*	Lias ε , Toarcian	Ohmenhausen, Germany
GPIT Re 1193/4	*Steneosaurus bollensis*	Lias ε , Toarcian	Zell near Holzmaden, Germany
GPIT Re 1193/6	cf *Steneosaurus bollensis*	Lias ε II, 4, Toarcian	Holzmaden, Germany
GPIT Re 1193/7b	cf *Steneosaurus bollensis*	Lias ε , Toarcian	Holzmaden, Germany
GPIT Re 1193/8	*Steneosaurus bollensis*	Lias ε , Toarcian	"Würtemberg", Germany
GPIT Re 1193/9	*Steneosaurus bollensis*	Lias ε , Toarcian	Ohmden, Germany
GPIT RE 209 (6832)	cf *Steneosaurus bollensis*	Lias ε, Toarcian	Germany
GPIT RE 210 + RE 247	*Steneosaurus bollensis*	Lias ε , Toarcian	Germany
GPIT RE 211 (14676)	*Steneosaurus bollensis*	Lias ε , Toarcian	Ohmden, Germany
GPIT RE 219	*Steneosaurus bollensis*	Lias ε , Toarcian	Holzmaden, Germany
GPIT RE 234	cf *Steneosaurus bollensis*	Lias ε , Toarcian	Germany
MGUH 1891-793	*Steneosaurus bollensis*	Liassic, Toarcian	Holzmaden, Germany
MNHN 1885-28	*Steneosaurus bollensis*	Liassic, Toarcian	Holzmaden, Germany
NHMUS M 597 1904	*Steneosaurus bollensis*	Lias ε , Toarcian	Holzmaden, Germany
NHMUSM62 2508	*Steneosaurus bollensis*	Lias ε , Toarcian	Holzmaden, Germany
NHMUS uncatalogued	*Steneosaurus bollensis*	Lias ε II 5,6, Toarcian	Holzmaden, Germany
OUM JZ 176	*Steneosaurus bollensis*	Lias ε, Toarcian	Holzmaden
SMNK I	*Steneosaurus bollensis*	Lias ε , Toarcian	Holzmaden?, Germany
SMNS (cabinet 11.43)	*Steneosaurus bollensis*	Liassic	Germany
SMNS (cabinet 3.5.7)	*Steneosaurus bollensis*	Lias ε II, 6, Toarcian	Holzmaden, Germany
SMNS (cabinet 3.8. 2-4)	*Steneosaurus bollensis*	Lias ε II, 12, Toarcian	Holzmaden, Germany
SMNS (cabinet 3.8.12)	*Steneosaurus bollensis*	Lias ε II, 12, Toarcian	Holzmaden, Germany
SMNS (cabinet 3.8.8-11)	*Steneosaurus bollensis*	Lias ε II, 6, Toarcian	Holzmaden, Germany
SMNS 10000	cf *Steneosaurus bollensis*	Lias ε II, 4, Toarcian	Holzmaden, Germany

Appendix I

Material list

Specimen	Taxon	Horizon	Location
SMNS 107	cf *Steneosaurus bollensis*	Lias ε, Toarcian	Germany
SMNS 10985 (A/B)	*Steneosaurus bollensis*	Lias ε , Toarcian	Frittlingen, Germany
SMNS 15712a	cf *Steneosaurus bollensis*	Lias ε II, 3, Toarcian	Holzmaden, Germany
SMNS 15712b	cf *Steneosaurus bollensis*	Lias ε II, 3, Toarcian	Holzmaden, Germany
SMNS 15816	*Steneosaurus bollensis*	Lias ε II, 4/5, Toarcian	Holzmaden, Germany
SMNS 15951 (a)	cf *Steneosaurus bollensis*	Lias ε II, 8, Toarcian	Holzmaden, Germany
SMNS 15951 (b)	cf *Steneosaurus bollensis*	Lias ε II, 8, Toarcian	Holzmaden, Germany
SMNS 17484a	*Steneosaurus bollensis*	Lias ε , Toarcian	Holzmaden, Germany
SMNS 17484b	*Steneosaurus bollensis*	Lias ε , Toarcian	?Ohmden, Germany
SMNS 18872	*Steneosaurus bollensis*	Lias ε II, Toarcian	Schömberg, Germany
SMNS 18878	cf *Steneosaurus bollensis*	Lias ε , Toarcian	Holzmaden, Germany
SMNS 20280	cf *Steneosaurus bollensis*	Lias ε II, 4, Toarcian	Holzmaden, Germany
SMNS 20281	*Steneosaurus bollensis*	Liassic	Holzmaden, Germany
SMNS 20282	*Steneosaurus bollensis*	Liassic	Holzmaden, Germany
SMNS 20283	*Steneosaurus bollensis*	Liassic, Toarcian	Ohmden, Germany
SMNS 20284	*Steneosaurus bollensis*	Liassic	Germany
SMNS 20286 (115)	cf *Steneosaurus bollensis*	Lias ε , Toarcian	Holzmaden, Germany
SMNS 4168	*Steneosaurus bollensis*	Liassic	Holzmaden, Germany
SMNS 50964	*Steneosaurus bollensis*	Liassic	Holzmaden, Germany
SMNS 51555	*Steneosaurus bollensis*	Lias ε II, 12, Toarcian	Ohmden, Germany
SMNS 51563	*Steneosaurus bollensis*	Lias ε II, 11, Toarcian	Ohmden, Germany
SMNS 51753	*Steneosaurus bollensis*	Lias ε II, 12, Toarcian	Holzmaden, Germany
SMNS 51957	*Steneosaurus bollensis*	Liassic	Holzmaden, Germany
SMNS 51960	*Steneosaurus bollensis*	Lias ε II, 12, Toarcian	Holzmaden, Germany
SMNS 52034	cf *Steneosaurus bollensis*	Liassic epsilon II, 8, Toarcian	
SMNS 52575	cf *Steneosaurus bollensis*	Lias ε II, 5, Toarcian	Ohmden, Germany
SMNS 53422	*Steneosaurus bollensis*	Lias ε II, 4, Toarcian	Ohmden, Germany
SMNS 53661	cf *Steneosaurus bollensis*	Lias ε II, 12	Germany
SMNS 54046	cf *Steneosaurus bollensis*	Lias ε II, 3	Germany
SMNS 56370	*Steneosaurus bollensis*	Lias ε II, 10, Toarcian	Holzmaden, Germany
SMNS 58876	*Steneosaurus bollensis*	Lias ε II, 12, Toarcian	Holzmaden, Germany
SMNS 59558	cf *Steneosaurus bollensis*	Lias ε (*serpentinum*-zone)	Altdorf, Germany
SMNS 59736	*Steneosaurus bollensis*	Liassic	Holzmaden, Germany
SMNS 80235	*Steneosaurus bollensis*	Lias ε II, 6, Toarcian	Holzmaden, Germany
SMNS 80481	*Steneosaurus bollensis*		
SMNS 81699	*Steneosaurus bollensis*	Lias ε , Toarcian	Holzmaden, Germany
SMNS 81825	*Steneosaurus bollensis*	Lias ε *elegantulum-zone,* Toarcian	Hildesheim, Germany
SMNS 849	*Steneosaurus bollensis*	Lias ε II, 6, Toarcian	Bad Boll, Germany
SMNS 9427	*Steneosaurus bollensis*	Lias ε II, 4, Toarcian	Germany
SMNS 9428a/b/c	*Steneosaurus bollensis*	Lias ε , Toarcian	Holzmaden, Germany
SMNS uncataloged	*Steneosaurus bollensis*	Liassic	Germany
SNSD 1 (holotype)	*Steneosaurus bollensis* JAEGER	Lias ε , Toarcian	Bad Boll, Germany
SNSD 2	cf *Steneosaurus bollensis*	Liassic	Bad Boll, Germany
SNSD 3 (cast)	*Steneosaurus bollensis*	Liassic	Germany
SNSD 4 (Zwinger)	*Steneosaurus bollensis*	Lias ε , Toarcian	Holzmaden (Fischer), Germany
TMH 13287	*Steneosaurus bollensis*	Liassic	Holzmaden, Germany
TMH 2741	*Steneosaurus bollensis*	Liassic, Toarcian	Boll, Germany
TMH 2742	*Steneosaurus bollensis*	Liassic, Toarcian	Boll, Germany
TMH 2743	*Steneosaurus bollensis*	Liassic, Toarcian	Boll, Germany

Appendix I

Material list

Specimen	**Taxon**	**Horizon**	**Location**
UH 11	cf *Steneosaurus bollensis*	Lias ε, Toarcian	Holzmaden, Germany
UH 12	*Steneosaurus bollensis*	Lias ε, Toarcian	Holzmaden, Germany
UH 13	*Steneosaurus bollensis*	Lias ε, Toarcian	Holzmaden, Germany
UH 3	cf *Steneosaurus bollensis*	Lias ε, Toarcian	Holzmaden, Germany
UH 5	*Steneosaurus bollensis*	Lias ε , Toarcian	Holzmaden, Germany
UH 6	*Steneosaurus bollensis*	Lias ε , Toarcian	Holzmaden, Germany
Specimen	**Taxon**	**Horizon**	**Location**
BMNH 14792 (holotype)	*Steneosaurus gracilirostris*	Upper Liassic	Whitby, Great Britain
BMNH 15500	*Steneosaurus gracilirostris*	Upper Liassic	Whitby, Great Britain
BMNH R 4	*Steneosaurus gracilirostris*	Liassic	Whitby, Great Britain
BMNH R 757	*Steneosaurus gracilirostris*	Upper Liassic	Whitby, Great Britain
BMNH 33097	*cf Steneosaurus gracilirostris*	Liassic	Whitby, Great Britain
BMNH 33095	cf *Steneosaurus gracilirostris,*	Liassic	Whitby, Great Britain
BMNH 33095 (2)	cf *Steneosaurus gracilirostris*	Liassic	Whitby, Great Britain
BMNH 33095 (3)	cf *Steneosaurus gracilirostris*	Liassic	Whitby, Great Britain
BMNH R 405	cf *Steneosaurus gracilirostris*	Upper Liassic	Yorkshire, Great Britain
BMNH R 63a	cf *Steneosaurus gracilirostris*	Upper Liassic	Yorkshire, Great Britain
Specimen	**Taxon**	**Horizon**	**Location**
BMNH 14436	cf *Steneosaurus brevior*	Upper Liassic	Whitby, Great Britain
BMNH 14781 (holotype)	*Steneosaurus brevior*	Upper Liassic	Whitby, Great Britain
BMNH 20691	*Steneosaurus brevior*	Upper Liassic	Whitby, Great Britain
BMNH 39154	cf *Steneosaurus brevior*	Liassic	Whitby, Great Britain
BMNH R 282 (a)	*Steneosaurus brevior*	Upper Liassic	Whitby, Great Britain
BMNH R 282 a	*Steneosaurus brevior*	Upper Liassic	Whitby, Great Britain
BMNH R 5325	cf *Steneosaurus brevior*	Liassic	Whitby, Great Britain
BMNH R 756	*Steneosaurus brevior*	Upper Liassic	Whitby, Great Britain
BMNH R 78	cf *Steneosaurus brevior*	Great Oolite	Enslaw Bridge, Oxon, Great Britain
UH 7	cf *Steneosaurus brevior*	Lias ε , Toarcian	Holzmaden, Germany
Specimen	**Taxon**	**Horizon**	**Location**
GPIT Re 1193/16	*Platysuchus multiscrobiculatus*	Lias ε , Toarcian	Jurawerk Holzheim near Göppingen
*GPIT Re 1193/7a (cast of SMNS 15919b)	*Platysuchus multiscrobiculatus*	Lias ε , Toarcian	Jurawerk Holzheim near Göppingen
SMNS 50193	*Platysuchus multiscrobiculatus*	Lias ε , Toarcian	Holzheim near Göppingen, Germany
SMNS 9930 (holotype)	*Platysuchus multiscrobiculatus*	Lias ε II, 6, Toarcian	Holzmaden, Germany
SMNS 15391	*cf Platysuchus multiscrobiculatus*	Lias ε II, 6, Toarcian	Holzmaden, Germany
*SMNS 15919a (cast of GPIT Re 1193/16)	*Platysuchus multiscrobiculatus*	Lias ε , Toarcian	Holzheim near Göppingen, Germany
SMNS 15919b	*Platysuchus multiscrobiculatus*	Lias ε , Toarcian	Holzheim near Göppingen, Germany
UH 1	*Platysuchus multiscrobiculatus*	Lias ε , Toarcian	Holzmaden, Germany
UH 2	*Platysuchus multiscrobiculatus*	Lias ε , Toarcian	Holzmaden, Germany
Specimen	**Taxon**	**Horizon**	**Location**
BMNH 14437	*Pelagosaurus typus*	Upper Liassic	Whitby, Great Britain
BMNH 19735 (cast)	*Pelagosaurus typus*	Upper Liassic, Toarcian	Boll, Germany
BMNH 32598	*Pelagosaurus typus*	Upper Liassic	Curcy, Normandy, France
BMNH 32599	*Pelagosaurus typus*	Upper Liassic	Amaye-sur-Orne (Calvados), Normandy

Appendix I

Material list

Specimen	Taxon	Horizon	Location
BMNH 32600	*Pelagosaurus typus*	Upper Liassic	Curcy, Normandy, France
BMNH 32601 (cast)	*Pelagosaurus typus*	Upper Liassic	Curcy, Normandy, France
BMNH 32602	*Pelagosaurus typus*	Upper Liassic	Curcy, Normandy, France
BMNH 32603	*Pelagosaurus typus*	Upper Liassic	Curcy, Normandy, France
BMNH 32604 (2?)	*Pelagosaurus typus*	Upper Liassic	Curcy, Normandy, France
BMNH 32604/5	*Pelagosaurus typus*	Upper Liassic	Curcy, Normandy, France
BMNH 32606	*Pelagosaurus typus*	Upper Liassic	Curcy, Normandy, France
BMNH 32642	*Pelagosaurus typus*	? Liassic	Curcy, Normandy, France
BSGP 1890 I 5	*Pelagosaurus typus*	Upper Liassic, Toarcian	La Caine, Calvados
BSGP 1890 I 501	*Pelagosaurus typus*	Upper Liassic, Toarcian	La Caine, Calvados
BSGP 1890 I 503	*Pelagosaurus typus*	Upper Liassic, Toarcian	La Caine, Calvados
BSGP 1890 I 504	*Pelagosaurus typus*	Upper Liassic, Toarcian	La Caine, Calvados
BSGP 1890 I 505	*Pelagosaurus typus*	Upper Liassic, Toarcian	La Caine, Calvados
BSGP 1890 I 506	*Pelagosaurus typus*	Upper Liassic, Toarcian	La Caine, Calvados
BSGP 1890 I 507	*Pelagosaurus typus*	Upper Liassic, Toarcian	La Caine, Calvados
BSGP 1890 I 508	*Pelagosaurus typus*	Upper Liassic, Toarcian	La Caine, Calvados
BSGP 1890 I 509/1	*Pelagosaurus typus*	Upper Liassic, Toarcian	La Caine, Calvados
BSGP 1890 I 509/10	*Pelagosaurus typus*	Upper Liassic, Toarcian	La Caine, Calvados
BSGP 1890 I 509/11	*Pelagosaurus typus*	Upper Liassic, Toarcian	La Caine, Calvados
BSGP 1890 I 509/6	*Pelagosaurus typus*	Upper Liassic, Toarcian	La Caine, Calvados
BSGP 1890 I 510	*Pelagosaurus typus*	Upper Liassic, Toarcian	La Caine, Calvados
BSGP 1890 I 513	*Pelagosaurus typus*	Upper Liassic, Toarcian	La Caine, Calvados
BSGP 1925 I 34	*Pelagosaurus typus*	Lias ε II, 4, Toarcian	Holzmaden, Germany
BSGP 1973 VII 592	*Pelagosaurus typus*	Lias ε , Toarcian	Holzmaden, Germany
BSGP 1990 XVIII 68	*Pelagosaurus typus*	Lias ε , Toarcian	Holzmaden, Germany
BSGP 7 J2	*Pelagosaurus typus*	Lias ε , Toarcian	Holzmaden, Germany?
BSGP1890 I 509/9	*Pelagosaurus typus*	Upper Liassic, Toarcian	La Caine, Calvados
FSL 530238 (92812)	*Pelagosaurus typus*	Upper Liassic, Toarcian	La Caine, Calvados (Curcy?)
GPIT Re 1193/17	*Pelagosaurus typus*	Lias ε , Toarcian	Ohmenhausen, Germany
GPIT Re 1193/18	*Pelagosaurus typus*	Lias ε , Toarcian	Ohmden, Germany
GPIT RE 213 (5603)	cf *Pelagosaurus typus*	Lias ε , Toarcian	Germany
GPIT RE 214	cf *Pelagosaurus typus*	Lias ε , Toarcian	Bad Boll, Germany
GPIT RE 244	cf *Pelagosaurus typus*	Lower Dogger	Normandy, France
GPIT RE 245 (9537)	*Pelagosaurus typus*	Lias ε , Toarcian	Bad Boll, Germany
MGUH (cast) uncatalogued	*Pelagosaurus typus*	Liassic	Germany
MNHN 1870-11-2	cf *Pelagosaurus typus*	Liassic	Germany
MNHN 1883-14	*Pelagosaurus typus*	Liassic	Curcy, Calvados
MNHN 1883-18	*Pelagosaurus typus*	Liassic	?
MNHN 1914-9-1	*Pelagosaurus typus*	Liassic	Caen, Calvados
MNHN 1914-9-2	*Pelagosaurus typus*	Liassic	Caen, Calvados
MNHN 1914-9-3	*Pelagosaurus typus*	Liassic	Caen, Calvados
MNHN 1914-9-4	*Pelagosaurus typus*	Liassic	Caen, Calvados
MNHN 1914-9-5	*Pelagosaurus typus*	Liassic	Caen, Calvados
MNHN 1914-9-6	*Pelagosaurus typus*	Liassic	Caen, Calvados
MNHN 1914-9-7	*Pelagosaurus typus*	Liassic	Caen, Calvados
MNHN 1914-9-8	*Pelagosaurus typus*	Liassic	Caen, Calvados
MNHN 1914-9-9	*Pelagosaurus typus*	Liassic	Caen, Calvados
NHB M62 2516	*Pelagosaurus typus*	Upper Liassic, Toarcian	Holzmaden
SMNS 11421	*Pelagosaurus typus*	Liassic, Toarcian	?Ohmrnhausen, Germany

Appendix I

Material list

Specimen	**Taxon**	**Horizon**	**Location**
SMNS 17758	*Pelagosaurus typus*	Liassic epsilon II, Toarcian	Holzmaden, Germany
SMNS 19073	cf *Pelagosaurus typus*	Liassic epsilon II, 11, Toarcian	Holzmaden, Germany
SMNS 4554	*Pelagosaurus typus*	Liassic	Swabian Alb, Germany
SMNS 50090	cf *Pelagosaurus typus*	Liassic	Swabian Alb, Germany
SMNS 50148	*Pelagosaurus typus*	Liassic	Swabian Alb, Germany
SMNS 50374	*Pelagosaurus typus*	Liassic	Swabian Alb, Germany
SMNS 51475	*Pelagosaurus typus*	Liassic	Swabian Alb, Germany
SMNS 52461	*Pelagosaurus typus*	Liassic	Swabian Alb, Germany
SMNS 55935* (52034)	cf *Pelagosaurus typus*	Liassic epsilon II, 5/6, Toarcian	Holzmaden, Germany
SMNS 56544 (cabinet??)	*Pelagosaurus typus*	Liassic	Holzmaden, Germany
SMNS 5966???	*Pelagosaurus typus*	Liassic	Holzmaden, Germany
SMNS 80065	*Pelagosaurus typus*	Liassic	Holzmaden, Germany
SMNS 80066	*Pelagosaurus typus*	Lias ε II, 5/6, Toarcian	Ohmden, Germany
SMNS 8666	*Pelagosaurus typus*	Lias ε II, Toarcian	Holzmaden, Germany
SMNS uncataloged	*Pelagosaurus typus*	Lias ε II, 4, Toarcian	Holzmaden, Germany
SMNS uncataloged	*Pelagosaurus typus*	Liassic	Holzmaden, Germany
SMNS uncataloged	*Pelagosaurus typus*	Liassic	Holzmaden, Germany
SMNS cabinet 3.3.4	cf *Pelagosaurus typus*	Lias ε II, 4, Toarcian	Holzmaden, Germany
TMH 13288	cf *Pelagosaurus typus*	Jurassic, Liassic, Toarcian	Holzmaden, Germany
TMH 2744 (holotype)	*Pelagosaurus typus*	Jurassic, Liassic, Toarcian	Nabern near Kirchheim, Germany
UH 10 (X)	*Pelagosaurus typus*	Lias ε , Toarcian	Holzmaden, Germany
UH 4 (IV)	*Pelagosaurus typus*	Lias ε , Toarcian	Holzmaden, Germany
UH 8 (VIII)	*Pelagosaurus typus*	Lias ε , Toarcian	Holzmaden, Germany
UH 9 (IX)	*Pelagosaurus typus*	Lias ε , Toarcian	Holzmaden, Germany
Specimen	**Taxon**	**Horizon**	**Location**
BMNH R 3048	*Steneosaurus boutilieri*	GreatOolite	Kingthorpe, Northampton, Great Britain
BMNH 49126 (holotype)	*Steneosaurus stephani* (*S. boutilieri*)	?	Cornbrash, Closworth, Dorset, Great Britain
OUM J1409	*Steneosaurus boutilieri*	Great Oolite	Enslow Bridge, Oxfordshire
Specimen	**Taxon**	**Horizon**	**Location**
BMNH 3168 (holotype)	*Steneosaurus obtusidens*	Oxford Clay	Peterborough, Great Britain
BMNH R 3169	*Steneosaurus obtusidens*	Oxford Clay	Peterborough, Great Britain
BMNH R 3898	*Steneosaurus obtusidens*	Oxford Clay	Peterborough, Great Britain
Specimen	**Taxon**	**Horizon**	**Location**
BMNH 3320 (holotype)	*Steneosaurus leedsi*	Oxford Clay	Peterborough, Great Britain
BMNH R 2617 (holotype)	*Mycterosuchus nasutus* (*Steneosaurus leedsi*)	Oxford Clay	Peterborough, Great Britain
BMNH R 2619	*Steneosaurus leedsi*	Oxford Clay	?
SMNS 10114	*Steneosaurus leedsi*	"Oxford Clay"	Fletton, England, Great Britain
BMNH R 3806	*Steneosaurus leedsi*	?	?
Specimen	**Taxon**	**Horizon**	**Location**
MNHN 13 1890 (holotype)	*Steneosaurus herberti*	Oxfordian	Villers-sur-mer, Calvados
Specimen	**Taxon**	**Horizon**	**Location**
BMNH 2075	*Steneosaurus edwardsi*	Oxford Clay	Peterborough, Great Britain

Appendix I

Material list

BMNH 2076	*Steneosaurus edwardsi*	Oxford Clay	Peterborough, Great Britain
BMNH 32620	*Steneosaurus edwardsi*	?Oxford Clay	Vaches-Noires, France
BMNH R 2865	*Steneosaurus edwardsi*	?	?
BMNH R 7786	*Steneosaurus edwardsi*	Slate Hill Quarry of Wooton	Woodstock, Oxfordshire, Great Britain
BMNH R 2074 (holotype)	*Steneosaurus hulkei* (*S. edwardsi*)	?	?
BMNH R 3701 (holotype)	*Steneosaurus durobrivensis* (*S. edwardsi*)	?	?
MNHN 8900	*Steneosaurus edwardsi*	Callovian	Vaches-Noires, Calvados
MNHN 8909	*Steneosaurus (edwardsi)*	?	?
Specimen	**Taxon**	**Horizon**	**Location**
BMNH 43086 (holotype)	*Steneosaurus megarhinus*	Kimmeridge Clay	Kimmeridge Bay, Dorset, Great Britain
Specimen	**Taxon**	**Horizon**	**Location**
BMNH 47171	*Steneosaurus lartifrons*	? Upper Liassic	Northampton, Great Britain
Specimen	**Taxon**	**Horizon**	**Location**
BMNH R 1999	*Steneosaurus baroni*	Bathonian	Madagascar
SMNS (cabinet 14.13)	cf *Steneosaurus baroni*	Dogger	Fletton, England, Great Britain
Specimen	**Taxon**	**Horizon**	**Location**
BMNH 33125	*Steneosaurus larteri*	Lower Jurassic, Fuller`s Earth	Caen (Calvados), France
Specimen	**Taxon**	**Horizon**	**Location**
GPIM N VIII (Jur 61)	*Machimosaurus hugii*	Kimmeridgian	Weiser Stein /Harzburg, Germany
GPIM N XV (Jur 63-70)	*Machimosaurus* sp.	Kimmeridgian	Langenberg/Oker, Hannover, Germany
GPIM N XVI	*cf Machimosaurus sp.*	Kimmeridgian	Langenberg/Oker, Hannover, Germany
GPIM N XX (Jur 60)	*Machimosaurus hugii*	Kimmeridgian	Langenberg/Oker, Hannover, Germany
Specimen	**Taxon**	**Horizon**	**Location**
MNHN 1875-321 CAST	*Steneosaurus chapmani*	Bathonian	Oxford, Great Britain
MNHN 8753	*?Crocodile d`Honfleur*	?	?
MNHN 8780	*Steneosaurus*	Callovian	Vaches-Noires, Calvados
MNHN 8785	*Steneosaurus*	Callovian	Vaches-Noires, Calvados
MNHN 89???	*Steneosaurus roissyi* (n..n.)	Callovian	Vaches-Noires, Calvados
MNHN 8908	*?Metriorhynchus?Steneosaurus*	?	?
MNHN 8910	*Steneosaurus?*	?	?
MNHN 8913-89?	*Steneosaurus roissyi* (n..n.)	Callovian	Vaches-Noires, Calvados
MNHN uncatalogued	*Steneosaurus*	Callovian	Poitier
MNHN uncatalogued	*Steneosaurus pepini*	Bathonian	St.Lierre sur Dives, Calvados
TMH 2745	*Steneosaurus nov.sp.*	Liassic	unknown
BMNH 47445	*?Steneosaurus minimus*	Liassic	Whitby, Great Britain
Specimen	**Taxon**	**Horizon**	**Location**
BMNH R 1086	*Steneosaurus priscus*	Kimmeridgian	Daitingen, Monheim, Germany

Appendix I

Material list

Specimen	Taxon	Horizon	Location
BMNH 14439	*Steneosaurus* sp.	Upper Liassic	Whitby, Great Britain
BMNH 47170	*Steneosaurus* sp.	Great Oolite	Belminsthorpe, Stanford, Northants, Great Britain
BMNH R 1091	*Steneosaurus* sp.	Upper Liassic	Whitby, Great Britain
BMNH R 2620	*Steneosaurus* sp.	Oxford Clay	Weymouth, Dorsetshire, Great Britain
BMNH R 4764	Steneosaurus sp.	Oxford Clay	Peterborough, Great Britain
BMNH R 4814	*Steneosaurus* sp.	Oxford Clay	Peterborough, Great Britain
BMNH R 5703	*Steneosaurus* sp.	Liassic	?Runswick Bay, Whitby, Great Britain
BMNH R 6624	*Steneosaurus* sp.	Upper Liassic, *Jurense* zone	River Nene, Stibbington, Great Britain
BMNH R 8668	*Steneosaurus* sp.	Jason zone?	Fletton Pit, ?
BMNH uncatalogued	*Steneosaurus* sp.	Oxford Clay	Peterborough, Great Britain
MNHN 1883-30	*Steneosaurus* sp.	Kimmeridgian	Ruelle
MNHN 1896-6	*Steneosaurus* sp.	Bathonian	Sansac, Charente
BMNH 33105	*Steneosaurus* sp.	Liassic	Whitby, Great Britain
BMNH 47151	*Steneosaurus* sp.	Liassic	Greens Norton, Northants, Great Britain
SMNS 16848	*Steneosaurus* sp.	?	?
MGUH 1892-243	*Steneosaurus sp.*	Liassic	Ohmden, Germany
Specimen	**Taxon**	**Horizon**	**Location**
BMNH 31836	*Teleosaurus* sp.	Great Oolite	Stonesfield, Oxon, Great Britain
BMNH 32595	*Teleosaurus* sp.	Lower Jurassic	Caen (Calvados), France
BMNH 32596	*Teleosaurus* sp.	Lower Jurassic	Caen (Calvados), France
BMNH 32609	*Teleosaurus* sp.	Upper Liassic	Curcy, Normandy, France
BMNH 32610	*Teleosaurus* sp.	Lower Jurassic, Fuller`s Earth	Caen (Calvados) , France
BMNH 32611	*Teleosaurus* sp.	?Upper Liassic	Curcy, Normandy, France
BMNH 32659 (cast)	*Teleosaurus* sp.	Lower Jurassic	Caen (Calvados) , France
BMNH 47155a	*Teleosaurus* sp.	Upper Liassic	Kingsthorpe, Northants, Great Britain
BMNH R 238	*Teleosaurus* sp.	Stonesfield Slate	Stonesfield, Oxon, Great Britain
BMNH R 4143	*Teleosaurus* sp.	?	?
BMNH R 653	cf *Teleosaurus* sp.	Upper Liassic	Robin Hood`s Bay, Whitby, Great Britain
BMNH R 71	cf *Teleosaurus* sp.	Lower Jurassic	Caen (Calvados) , France
BMNH 32611a	cf *Teleosaurus* sp.	Lower Jurassic	Caen (Calvados) , France
BMNH 32680	cf *Teleosaurus* sp.	Lower Jurassic, Fuller`s Earth	Caen (Calvados) , France
BMNH R 2569	cf *Teleosaurus* sp.	Kimmeridgian	Langenberg, Goslar, Hannover
BMNH R 2570	cf *Teleosaurus* sp.	Kimmeridgian	Langenberg, Goslar, Hannover
Specimen	**Taxon**	**Horizon**	**Location**
BMNH 28296	*Teleosaurus cadomensis*	Lower Jurassic, Fuller`s Earth	Caen (Calvados) , France
BMNH 31830	*Teleosaurus cadomensis*	Stonesfield Slate	Stonesfield, Oxford, Great Britain
BMNH 32584 a/b/x	*Teleosaurus cadomensis*	Lower Jurassic, Fuller`s Earth	Caen (Calvados) , France
BMNH 32588	*Teleosaurus cadomensis*	Lower Jurassic, Fuller`s Earth	Caen (Calvados) , France
BMNH 32591	*Teleosaurus cadomensis*	Lower Jurassic, Fuller`s Earth	Caen (Calvados) , France
BMNH 32592	*Teleosaurus cadomensis*	Lower Jurassic, Fuller`s Earth	Caen (Calvados) , France
BMNH 33124	*Teleosaurus cadomensis*	Stonesfield Slate	Stonesfield, Oxford, Great Britain
BMNH 41311	*Teleosaurus cadomensis*	Stonesfield Slate	Stonesfield, Oxford, Great Britain

Appendix I

Material list

Specimen	**Taxon**	**Horizon**	**Location**
BMNH 47997	*Teleosaurus cadomensis*	Stonesfield Slate	Stonesfield, Oxford, Great Britain
BMNH R 4207	*Teleosaurus cadomensis*	Middle Jurassic, Bathonian	Caen (Calvados) , France
BMNH R 880a (CAST)	*Teleosaurus cadomensis*	Lower Jurassic, Fuller`s Earth	Caen (Calvados) , France
MNHN 8745 CAST	*Teleosaurus cadomensis*	Bathonian	Caen (Calvados) , France
MNHN 8746	*Teleosaurus cadomensis*	Bathonian	Caen (Calvados) , France
MNHN 8746 cast	*Teleosaurus cadomensis*	Bathonian	Caen (Calvados) , France
MNHN V289? cast	*Teleosaurus cadomensis*	Bathonian	Caen (Calvados) , France
*SMNS 95 (cast as BMNH 880a)	*Teleosaurus cadomensis*	Bathonian	Caen (Calvados) , France
MNHN uncatalogued	cf *Teleosaurus cadomensis*	Bathonian	Caen (Calvados) , France
MNHN uncatalogued	cf *Teleosaurus cadomensis*	Bathonian	Caen (Calvados) , France
MNHN uncatalogued (cast)	*Teleosaurus cadomensis*	Bathonian	Caen (Calvados) , France
Specimen	**Taxon**	**Horizon**	**Location**
BMNH 33126	cf *Teleosaurus geoffryoi*	Stonesfield Slate	Stonesfield, Oxford, Great Britain
BMNH R 236	cf *Teleosaurus geoffroyi*	?Stonesfield Slate	Stonesfield, Oxford, Great Britain
MNHN uncatalogued	*Teleosaurus geoffroyi*	?	Caen, Calvados
BMNH 39788	cf *Teleosaurus geoffroyi*	Stonesfield Slate	Stonesfield, Oxford, Great Britain
Specimen	**Taxon**	**Horizon**	**Location**
BMNH 28497	cf *Teleosaurus subulidens*	Stonesfield Slate	Stonesfield, Oxford, Great Britain
BMNH 32631	*Teleosaurus superciliousus*	?	Argile des Dives, Vaches Noires, France
BMNH R 236 a	*cf Teleosaurus subulidens*	Stonesfield Slate	Stonesfield, Oxford, Great Britain
GPIM N IV (Jur 62)	*Teleosaurus locurosae* Quenstedt	Upper Portlandian	Holzen/Hils, Germany
MNHN 1908-36 (1-3)	*cf Teleosaurus*	Callovian	Carrieres de Migne, Vienne
MNHN without number (cast)	*cf Teleosaurus*	Bathonian	Caen, Calvados
Specimen	**Taxon**	**Horizon**	**Location**
GPIM N VII	?Teleosauridae	Kimmeridgian	Langenberg/Oker, Hannover, Germany
GPIM N XVII	?Teleosauridae	Kimmeridgian	Langenberg/Oker, Hannover, Germany
GPIM N X (M4687)	Teleosauridae	Kimmeridgian	Langenberg/Oker, Hannover, Germany
GPIM N XI	? Teleosauridae	Kimmeridgian	Langenberg/Oker, Hannover, Germany
GPIM N XII (Jur 50-52)	Teleosauridae	Upper Portlandian	Holzen/Hils, Germany
GPIM N XIII	? Teleosauridae	Kimmeridgian	Langenberg/Oker, Hannover, Germany
GPIM N XIV	Teleosauridae	Kimmeridgian	Langenberg/Oker, Hannover,Germany
GPIM N II	*cf Teleosaurus*	Kimmeridgian	Langenberg/Oker, Hannover, Germany
BMNH 47427	*? Steneosaurus, ?Teleosaurus*	Oxford Clay	? Whittlesea, Great Britain
Specimen	**Taxon**	**Horizon**	**Location**
BMNH R 3015	*Metriorhynchus ?laeve*	Oxford Clay	Peterborough, Great Britain
MNHN 1865-98	*?Metriorhynchus physognathus*	Bathonian	Poitier
MNHN 1872-? (cast)	*Metriorhynchus hastifer*	Kimmeridgian	du Havre
MNHN 1908-6	*Metrirohyncus superciliosus*	?	?

Appendix I

Material list

Specimen	**Taxon**	**Horizon**	**Location**
MNHN 8768	*Metriorhynchus*	Callovian	Vaches-Noires, Calvados
MNHN 8902	*Metriorhynchus moreli*	Callovian	Vaches-Noires, Calvados
MNHN 8903	*Metriorhynchus (superciliosus)*	?	?
MNHN 8923	*? Metriorhynchus (superciliosus)*	?Callovian	? Vaches-Noires
MNHN 8925	*Metriorhynchus superciliosus*	?	?
MNHN 8928	*Metriorhynchus*	Callovian	Vaches-Noires, Calvados
MNHN 8929	*Metriorhynchus*	Callovian	Vaches-Noires, Calvados
MNHN uncatalogued (type)	*Metriorhynchus*	?	?
MNHN uncatalogued (cast)	*Metrirohyncus superciliosus*	Callovian	Villers(-sur-mer, Calvados)
Specimen	**Taxon**	**Horizon**	**Location**
BMNH R 1229 (holotype)	*Geosaurus giganteus*	Kimmeridgian	Monheim, Germany
BMNH R 3948	*Geosaurus gracilis*	Kimmeridgian	Eichstätt, Germany
BSGP AS I 504	*Geosaurus gracilis*	Upper Jurassic	Daiting, Germany
Specimen	**Taxon**	**Horizon**	**Location**
BMNH R 2681 (holotype) (cast)	*Teleidosaurus calvadosi*	Fuller's Earth	Calvados, Normandy
BMNH R 3353 (holotype)	*Teleidosaurus gaudryi*	Lower Jurassic	Sl.Seine-L`Abbaye, Cote d`Or, France
MNHN 1875-17 (cast)	*Teleidosaurus joberti*	Bathonian	Caen, Calvados
MNHN 8747	cf *Teleidosaurus calvadosi*	Bathonian	Caen, Calvados
Specimen	**Taxon**	**Horizon**	**Location**
SMF 1914	*Gavialis gangeticus*	recent	India
SMF 22458 (2448)	*Crocodylus cataphractus*	recent	?
SMF 28132	*Gavialis gangeticus*	recent	India
SMF 28133	*Gavialis gangeticus*	recent	India
SMF 28134	*Tomistoma schlegelii*	recent	Borneo
SMF 28135	*Tomistoma schlegelii*	recent	Sumatra
SMF 36421	*Crocodylus cataphractus*	recent	?
SMF 40144	*Gavialis gangeticus*	recent	India
SMF 49529	*Gavialis gangeticus*	recent	India
SMF 67267	*Tomistoma schlegelii*	recent	Sumatra
SMF 78886	*Gavialis gangeticus*	recent	India
ZFMK (uncatalogued)	*Gavialis gangeticus*	recent	India
ZFMK 21591	*Gavialis gangeticus*	recent	India
ZFMK 21594	*Caiman crocodylus*	recent	?
ZFMK 5246	*Crocodylus niloticus*	recent	Africa
ZFMK 66591	*Tomistoma schlegelii*	recent	?
ZFMK 74533	*Crocodylus cataphractus*	recent	?
ZMUC 36	*Gavialis gangeticus*	recent	Ganges, India
ZMUC 40	*Tomistoma schlegelii*	recent	?Borneo
GPIT Re 1193/19	*?Tomistoma, ?Gavialis*	recent	"Indus", India
OUM 13332	*Crocodylus niloticus*	recent	Africa
GPIM (uncatalogued)	*Crocodylus niloticus*	recent	Africa

Appendix II

Biometric data

Cranial measurements																														
Steneosaurus bollensis	**A**	**B**	**C**	**D**	**E**	**F**	**G**	**H**	**I**	**J**	**K**	**L**	**M**	**N**	**O**	**P**	**Q**	**R**	**S**	**T**	**U**	**V**	**W**	**X**	**W1**	**W2**	**Fm1**	**Fm2**	**C1**	**C2**
Berlin 1921/12 (Westphal 1962)	830	60																												
Berlin 1931/4 (Westphal 1962)	130	89																												
BMNH 14438						47	105		40																					
BMNH R 324			180	105	90	51	126		52	38			3																	
BMNH R 3936																														
BMNH R 3937 (cabinet)	567	410							46																					
BMNH 12011																						337	99							
BSGP uncatalogued (cabinet)	780																							110						
BSGP uncatalogued (wall)	245	181	61,5	31,8	25,5	16,6	37,7		21,3	16,9	15,5	10,4	3,7								260	146,6		25,9						
BSGP1949 XV 1a	470	335	132	80	60	37	85	145	44/44	26/25	35	23	2											59						
Freiburg Geol. L. (Westphal 1962)	608	450							42																					
GPIM G 23a	485	349	135	72	56	39	87		38	24	29	23	3																	
GPIT Re 1193/1	620	470							46															85						
GPIT Re 1193/10	175	133	60				40														202	103		24						
GPIT Re 1193/12			60				42															145	45	26		40°				
GPIT Re 1193/12	220	156																												
GPIT Re 1193/13	390	270	104	68			73		32													220	60							
GPIT Re 1193/2	810	565	260	135/132	115	66	150	250	57/57	45/40	53	39	6,5											150						
GPIT Re 1193/3	1030	735	310	135	125/119	78	225	350	75/72	51/42	72	54	8											155						
GPIT Re 1193/6	148	105	47				27				10	7									158	85	30			30°				
GPIT Re 1193/7b	135	91	39	20	17	13,5	25	35	14,4	11	11	9	4																	
GPIT Re 1193/8			126	77/74	/54		89		37/38	30/28			4																	
GPIT Re 1193/9	417	310	105	58/58	47/43	26	61	144	32/31	25/22	24	16	3											52						
Holzmaden 38a (Westphal 1962)	150	106																												
Holzmaden 68 (Westphal 1962)	595	425																												

Appendix II

Biometric data

Cranial measurements																														
Steneosaurus bollensis	**A**	**B**	**C**	**D**	**E**	**F**	**G**	**H**	**I**	**J**	**K**	**L**	**M**	**N**	**O**	**P**	**Q**	**R**	**S**	**T**	**U**	**V**	**W**	**X**	**W1**	**W2**	**Fm1**	**Fm2**	**C1**	**C2**
MGUH 1891-293		frag. 420									35	27																		
MGUH 1891-793			165										2											83						
NHB M597 1904	530	395	142	78/ 79	37 /58	40	90	205	42,5 /39	29/ 29	31	22	2											69						
NHMUS M62 2508	355	260	94	51	38/ 35	32	63		28/ 29	20/ 22,5	27,5	16,5	3											41						
NHMUS uncatalogued (4)	470 480 c	340	142	81	60	37,5	82	180	36	32	31,5	21	2											66						
SMF R 454 (cabinet)	745	555																												
SMNS uncatalogued	455																													
SMNS 10000	139,5	95	40	24/2 2	14	13	28	30	15/ 15	10/ 10,5	11,5	10	5											16						
SMNS 10985	840	570	265	128	112	85	220	290	62	42	70	50																		
SMNS 15712a	128	91	37																				35	15						
SMNS 15712b	133	93	42	18,5	12,1	13	23	45	13,4	12	13	9									143	76								
SMNS 15816	< 200		76																											
SMNS 15951(a/b)	410	310	100	50	42	28	75	170	30	26	22	11												48						
SMNS 17484a																														
SMNS 17484b																														
SMNS 20280	161	109	45,4	29	20	10	29,6	51,6	15,8	12																				
SMNS 20286 (115)	138,4	99	38,5	22/ 20	16/ 15	12	29	49	13	10	12	11									150	79		12						
SMNS 50964																														
SMNS 51555																														
SMNS 51753	655	495	122	81/ 85	50		85	300	50	35		24												90						
SMNS 51957	590	435	185	93	63	42	97	230	43	32	41	28																		
SMNS 51960																														
SMNS 52034	410	310	108	63,7	48	32	73,3	165	37	30	24,3	16																		
SMNS 53422	500	370	150			42		120			42	26										320	120	80		50°				
SMNS 56370	700	520	118	87			82																							
SMNS 58876	700	500	180																											
SMNS 59736	470	342	145	76	61	43	101, 3	165	43,5	28,3	35,2	21,4																		
SMNS 80235	450	300	130					200														500								
SMNS 849																														

Appendix II

Biometric data

Cranial measurements																														
Steneosaurus bollensis	**A**	**B**	**C**	**D**	**E**	**F**	**G**	**H**	**I**	**J**	**K**	**L**	**M**	**N**	**O**	**P**	**Q**	**R**	**S**	**T**	**U**	**V**	**W**	**X**	**W1**	**W2**	**Fm1**	**Fm2**	**C1**	**C2**
SMNS 9427																														
SMNS 9428a/b/c*																														
SMNS (cabinet 3.8.12)	350			55					35																					
SMNS 18872	650	400		100	100				50	35																				
SMNS 81699	450	300																												
SMNS 51563	570	404, 4	160	98/ 96,5	64/ 67	60	110	220	44	38,5	37	22,4	8																	
SNSD 1 (holotype)																														
SNSD 2	375	260	110	55	52				32	28			8																	
SNSD 3 (cast)	540	380	140	89/ 88	64/ 62	43	100	190	35/ 38	25/ 27	33	27	2																	
SNSD 4 (Zwinger)	585	425	155	83	65	39	100	200	47/ 42	33/ 33	33	22	3																	
TMH 2741	800								67		49	28									980	470		165						
TMH 2742	335								25												375	205		40						
TMH 2743	433	325							31																					
UH 5 (II)	415																													
UH 6 (VI)	180																													
Winterthur A (Westphal 1962)	502	365																						75						
TMH 13288	147	103	38				32				9	8									158	75		16						
SMSN 20281	790 820 c	590	270 295c	130	110				64	43/ 45	71	51		124	22						940	440		130						
SMNS (cabinet 3.8.2-4)	585 595 c	440		76	69				43	32														74						
SMNK I (uncatalogued)	660								64				8																37	
SMNS 53661		356				30		225			20,5	16,5																		
SMNS 54046		> 260									34	21																		
SMNS 55935	255 263 c	185	59	40/4 1	25			74	20	20				39							300			34,5						

Appendix II

Biometric data

Postcranial measurements																														
Steneosaurus bollensis	**H1**	**H2**	**T1**	**T2**	**R1**	**R2**	**U1**	**U2**	**Fi1**	**Fi2**	**Fe1**	**Fe2**	**Sa1**	**Co1**	**P1**	**P2**	**Pu1**	**Pu2**	**Is1**	**Is2**	**S/P-L**	**Tl in meters**								
Berlin 1921/2 (Westphal 1962)	213										368																			
Berlin 1931/4 (Westphal 1962)	31										47																			
BMNH R 3936															68	70	108	42	80	106										
BMNH R 3937	156										256											3,4								
BSGP (cabinet) uncatalogued	180																													
BSGP (wall) uncatalogued	52		50,1				34,1		49,7		84,9		27,8		21,8	29,2	32,4													
BSGP1949 XV 1a/b	195	21			107	11	130	12																						
Freiburg Geol. Land.	124										205																			
GPIM (CAST) G 23b			185						140		222																			
GPIM uncatalogued			117						114		200																			
GPIT Re 1193/1	131										224																			
GPIT Re 1193/10			43	4					41	1	67	4,5							21	23	190									
GPIT Re 1193/12	52	4	51	4	30	2,5	35	2,5	48	2	81	6	25	25			21		25	28	225									
GPIT Re 1193/13	86	8	84	10	50	4	58	5	81,5	4	136	14,5	51	47,5					38	52	400	1,85								
GPIT Re 1193/2	205	28	200	50	123	17	147	15	200	25	345	37	143		85	125					900	4,61/4,5								
GPIT Re 1193/3	227	28	210	27	118		145	17	205	20	395	42			99	125	175	86	145	160	1400	5,17/5,5								
GPIT Re 1193/6	35	3,5	35	4	22	1					51	4	16	19	11,5	17,5	22	10	15	18										
GPIT Re 1193/7b	29	3	33,5	2	19,5	1,5	20,5	1,5	30,5	1	44	3,5		19							175	0,68								
MGUH 1891-793	155													70																
NHMUS M597 1904	120	15	113	14	69	7,5	79	7	115	9,5	205	19	84				82				600									
NHMUS M62 2508	78	6	75		47		52		66		133,5	10	44	45					39	48	360									
NHMUS no number (4)	109	10	105		64	5	76	7,5	105		180		73	75			80	29	65	65	580	2,7								
SMF R 454 (cabinet)	164						105				270											3,85								
SMNS 10000	33	3	34	3	19,5	1,5	23	1	32,5	2,5	48	4	19		12	22					170									
SMNS 10985																														

Appendix II

Biometric data

Postcranial measurements																														
Steneosaurus bollensis	**H1**	**H2**	**T1**	**T2**	**R1**	**R2**	**U1**	**U2**	**Fi1**	**Fi2**	**Fe1**	**Fe2**	**Sa1**	**Co1**	**P1**	**P2**	**Pu1**	**Pu2**	**Is1**	**Is2**	**S/P-L**	**Tl in meters**								
SMNS 15712a	32		30	3,5	20	1,5	23,5	2	30	1	45	4,5	17		13	19					160									
SMNS 15712b																														
SMNS 15816	54	4	55	5	34	2	37	3	55	2	89						33	12,5			280	1,2								
SMNS 15951 (a/b)	85	6	83	6	51	4	56	4	81,8	5	143	13	45			48						1,9								
SMNS 17484a			120	18					115	11	220				54	58	95	38		94										
SMNS 17484b			130	15					122		215																			
SMNS 20280																														
SMNS 20286 (115)																														
SMNS 50964	144	19	140	18					139		235	22			66	60	89	29		87	550									
SMNS 51555																														
SMNS 51753			125						125		220	24	80	91,8			94	10		87	750									
SMNS 51957	162	16,3	165	20	92	11,9	107	11	150	15	270	26	82		60	66	115	47		88	700	3,8								
SMNS 51960													105	165																
SMNS 52034	101	8	98,8	6,5	59,6	4	72	6	98	5,5	180		57,5 /60		32	48					500	2,5								
SMNS 53422	150	13			85	9	100	9					88																	
SMNS 56370											210	24	71			46	91	35		99		3,5								
SMNS 58876	139,4	13,5	123	19	69	6	71	8	120	10	230		84	82						92	700	3,3								
SMNS 59736	139	13	134	15	75	8,4	87	9	127	13	230		80		72,2	58		35,3		83		3								
SMNS 80235	112	13,5			65	6	72	7,5					70	73,2																
SMNS 849	130	18,5	127, 5	15	80	13	89	11	130	7	225	26																		
SMNS 9427			169	21					15,3		290	30					125	14												
SMNS 9428a/b/c*	111	13			68	7	80	8			185		71		50	75	77	22		65										
SMNS (cabinet 3.8.12)			75	7					73	4,5	123	8,5																		
SMNS 18872 (= cabinet 3.8.1a)																						3,2								
SMNS 81699 (= cabinet 3.8.1b)																						2,4								
SMNS 51563 (= cabinet 3.8.6)	150		135		95		100		135		240		102	95																
SNSD 1 (holotype)			175		95		110		175		243	25				98														
SNSD 2			76	9							128	13									450									
SNSD 3 (cast)	128	14	130	16	85		88		128		207		77								600	2,2								
SNSD 4 (Zwinger)	135	15	130		82		92		140		220		85		46	74					610	2,9								

Appendix II

Biometric data

Postcranial measurements																														
Steneosaurus bollensis	**H1**	**H2**	**T1**	**T2**	**R1**	**R2**	**U1**	**U2**	**Fi1**	**Fi2**	**Fe1**	**Fe2**	**Sa1**	**Co1**	**P1**	**P2**	**Pu1**	**Pu2**	**Is1**	**Is2**	**S/P-L**	**Tl in meters**								
TMH 13288	26										43																			
TMH 2741																														
TMH 2742	76		77				52				120																			
TMH 2743	87		87				58				149										690									
UH 5 (II)																														
UH 6																														
Winterthur A (Westphal 1962)	119										196																			
SMNS 55935 (52034)	55	4	58		34	2	39	3,5	58		98				30	32	31		29		275	1,4								
SMNS (cabinet 3.8.2-4)	142				81		96		137		225		85			82	95													
SMF R 454 (cabinet)	164										270																			
Cranial measurements																														
Steneosaurus gracilirostris	**A**	**B**	**C**	**D**	**E**	**F**	**G**	**H**	**I**	**J**	**K**	**L**	**M**	**N**	**O**	**P**	**Q**	**R**	**S**	**T**	**U**	**V**	**W**	**X**	**W1**	**W2**	**Fm1**	**Fm2**	**C1**	**C2**
BMNH 14792 (holotype)	595	460	110	74	58	42	85	280	43/45	36	25	21	3																	
BMNH 15500	700	517	148	86/88	68/63	43	91	270	50/48	39/37	27	20	11																	
BMNH 33095 (2)		>490				51		>275			27	24											110			40°				
BMNH R 757	600	440	121				72		46		35																			
BMNH R 405											22	15																		
MNHNL TU515 (Godefroit 1994)	645	490	128	85	57				52	41																				
MIC 453 (Godefroit 1994)				83	50,5				43,5	39,5																				
Postcranial measurements																														
Steneosaurus gracilirostris	**H1**	**H2**	**T1**	**T2**	**R1**	**R2**	**U1**	**U2**	**Fi1**	**Fi2**	**Fe1**	**Fe2**	**Sa1**	**Co1**	**P1**	**P2**	**Pu1**	**Pu2**	**Is1**	**Is2**	**S/P-L**	**Tl in meters**								
BMNH 14792	124										172										?									

Appendix II

Biometric data

Cranial measurements																														
Steneosaurus brevior	**A**	**B**	**C**	**D**	**E**	**F**	**G**	**H**	**I**	**J**	**K**	**L**	**M**	**N**	**O**	**P**	**Q**	**R**	**S**	**T**	**U**	**V**	**W**	**X**	**W1**	**W2**	**Fm1**	**Fm2**	**C1**	**C2**
BMNH 14781	900	580	300	170	100	85	180	180	69/70	63/65	81	56									880	430				40				
BMNH 14436	650		230	93	73	140	92		46/47	35/36			5	105	14					85										
BMNH R 756	810		270	150	110		165		68/69	53/55			6							110							25	18	36	29
UH 7	700	490	234	131/120	82,3 92,1	70,5	157	222	52,4	42,8	65	40,5	8																	
BMNH R 282a																							110			60				
Cranial measurements																														
Platysuchus multiscrobiculatus	**A**	**B**	**C**	**D**	**E**	**F**	**G**	**H**	**I**	**J**	**K**	**L**	**M**	**N**	**O**	**P**	**Q**	**R**	**S**	**T**	**U**	**V**	**W**	**X**	**W1**	**W2**	**Fm1**	**Fm2**	**C1**	**C2**
SMNS 9930 (holotype)	455	340	125	75	47	60	73,5	185	34	23,5	44,5	22									580			65						
UH 1	400	300,5	107	61,4 / 59,5	43,6 / 45,7	31,6	65,2	179,3	31,8 /29	22,7/ 22,5	35,1	19,6	6																	
UH 2	132	93	37	20	15	10,5	23,5	42	12	12/10,0	11	7	4																	
SMNS 15391	168	122	47	26	17	16	31,5	46	14	13	15,5	12	9																	
Postcranial measurements																														
Platysuchus multiscrobiculatus	**H1**	**H2**	**Ti1**	**Ti2**	**R1**	**R2**	**U1**	**U2**	**Fi1**	**Fi2**	**Fe1**	**Fe2**	**Sa1**	**Co1**	**P1**	**P2**	**Pu1**	**Pu2**	**Is1**	**Is2**	**S/P-L**	**Tl in meters**								
SMNS 9930 (holotype)	140		125		82		95		125		205			93			85			280	950	2,79							
UH 1	109/105		92,6 / 96,2		62,9 / 61,2		74,4 / 71,2				150,4/138		56,4								900	2,7								
UH 2	31		32	2					30	1,5	43	3		17		19			18		170	1,2							
SMNS 15391	40,5	3	42	3,5	26	1,5	30	1	39	2	60	6	20		16	24					220									

Appendix II

Biometric data

Cranial measurements																														
Pelagosaurus typus	**A**	**B**	**C**	**D**	**E**	**F**	**G**	**H**	**I**	**J**	**K**	**L**	**M**	**N**	**O**	**P**	**Q**	**R**	**S**	**T**	**U**	**V**	**W**	**X**	**W1**	**W2**	**Fm1**	**Fm2**	**C1**	**C2**
BGM M 1418a (after Duffin 1979)	107		24																											
SMNS 4554	127,4	95	32	20	12	14	26	49	15	8	7	6																		
SMNS 17758	130	94	31	17	9	10	25	39	14/ 14,5		10		6																	
UH 8	134	99,7	30,9	16,5 / 17,2	10,3 / 10,6	9,1	16,3	46,8	14,3 / 15,4	10,8	7,7	6,7	3																	
GPIT Re 1193/17	250	190	54	30/2 9	18	21,5	45	58	24/ 23	18/ 17	11,5	9,5	15																	
UH 9	250	186, 8	51,1	33,1	19/2 0,4	18,1	39,9	81,3	23,8	15,5	13	11,7	3																	
SMNS 55935 (52034)	263	185	59	40/4 1	25			74	20	20																				
BMNH 19735 (cast)	268	205	55	30	20	18	48	93	21/ 24	10			7																	
Cranial measurements																														
Pelagosaurus typus	**A**	**B**	**C**	**D**	**E**	**F**	**G**	**H**	**I**	**J**	**K**	**L**	**M**	**N**	**O**	**P**	**Q**	**R**	**S**	**T**	**U**	**V**	**W**	**X**	**W1**	**W2**	**Fm1**	**Fm2**	**C1**	**C2**
TMH 2744 (holotype)	270	205	65	33	22	21	43	100	30				10											29						
Berlin 1925/1 (after Westphal 1962)	285	210																												
MNHN 1883-14	285	207	68	40/ 42	27/ 28	20,5	45	90	32/ 29	24/ 29	17	12	4,5								305									
UH 10	300	226, 4	59,2	37,9	21,3 / 24	23,4	39,2	137, 9	27,5 /28	12,5	14,8	12,4	3																	
GPIT Re 1193/18	305	232	73,5	47/ 47	39 /39	25	54		29	22			4																	
BSGP 1990 XVIII 68	312	235	67	40	25	22	52		32		18																			
SMNS 80066	330	240	74			20	50				13	11											62							
SMNS 8666	335	250	69	48/ 48	26	23	55	100	30,5	20	17,5	14,5																		
BSGP 1925 I 34	350	266	70	42	30	22	44	140	33	25	18	12	2											36						
UH 4	380	286, 1	72	50,4	29,2			147, 3	41,2	33,7	18	14	6																	

Appendix II

Biometric data

Cranial measurements																														
Pelagosaurus typus	**A**	**B**	**C**	**D**	**E**	**F**	**G**	**H**	**I**	**J**	**K**	**L**	**M**	**N**	**O**	**P**	**Q**	**R**	**S**	**T**	**U**	**V**	**W**	**X**	**W1**	**W2**	**Fm1**	**Fm2**	**C1**	**C2**
SMNS 19073	420	300	78,6	51		28	68	130	42/36		21	15	3																	
BSGP 1890 I 5	100 frag.		73	46/46	28/30		43		36/34	30/30				34	12					35							13	8	12	
NHB M62 2516	270-275	200	70	35/35	26/24	17,5	50	87	28/29	22	14	10	6								287	148		17						
BMNH 14437				45			45		34	27																				
BMNH 32599			74	45/43	30	24	48		35/36	26/28			4										?	?		30°				
GPIT RE 214			32	20	12				20																					
GPIT RE 244			70	40	25		47		34	30			4																	
GPIT RE 245 9537			72	42	28		55		29				6																	
BSGP 1973 II 592							50,5		35	30																				
MNHN 1914-9-9			79	45	30		52		35	30			3																	
FSL 530238			75	46/45	28/28	>30	50,5		34/34	27/27			4	35	13					37				19						
MGUH uncatalogued (cast)	342 (c)	260	82				50				17	14									374			35						
MNHN 1870-11-2 (cast)			72	42/38	27/25		48		33/32	28/29			5	40	14															
Postcranial measurements																														
Pelagosarus typus	**H1**	**H2**	**T1**	**T2**	**R1**	**R2**	**U1**	**U2**	**Fi1**	**Fi2**	**Fe1**	**Fe2**	**Sa1**	**Co1**	**P1**	**P2**	**Pu1**	**Pu2**	**Is1**	**Is2**	**S/P-L**	**Tl in meters**								
SMNS 17758 (= cabinet 3.8.13)			21	2					18	1	36	3					17	5	13,5	13/13										
SMNS 19073	67	4,8	60	5	35	2	38	3	67	3,5	107	10		42	28	35,5				33	350	1,82								
SMNS 80066					53,5	3	49	2				110			30	35				51										
UH 8	19,3				9		9,8						13,2								140									
UH 9	39																													
UH 4	68,4										106/111						73,5	22,3			420	1,8								
NHB M62 2516	58,5	4	52	5			29	3	50	4	101	9	40	33		28,5	48	13			400	1,8								
TMH 2744 (holotype)	52	3			21		27								19	24	50	14	22		380									

Appendix II

Biometric data

Postcranial measurements																														
Pelagosarus typus	**H1**	**H2**	**T1**	**T2**	**R1**	**R2**	**U1**	**U2**	**Fi1**	**Fi2**	**Fe1**	**Fe2**	**Sa1**	**Co1**	**P1**	**P2**	**Pu1**	**Pu2**	**Is1**	**Is2**	**S/P-L**	**Tl in meters**								
MNHN 1883-14	43		60						60		98				25	31			42	45	400	1,6-1,7								
FSL 530238													46																	
BMNH 32598															28	43														
BSGP 1890 I 504													32																	
MNHN 1914-9-4													45																	
MGUH (cast without number)											108			37			60	20												
SMNS uncatalogued															39	53	82	23		67										
BSGP 1890 I 509/1																			50	45										
BSGP 1890 I 509/6															27	32														
BSGP1890 I 501-508																					400									
MNHN 1914-9-8															28	35			43											
MNHN 1883-18															27			15												
Cranial measurements																														
Steneosaurus leedsi	**A**	**B**	**C**	**D**	**E**	**F**	**G**	**H**	**I**	**J**	**K**	**L**	**M**	**N**	**O**	**P**	**Q**	**R**	**S**	**T**	**U**	**V**	**W**	**X**	**W1**	**W2**	**Fm1**	**Fm2**	**C1**	**C2**
BMNH R 2617	1020	745	240	200	110	75	160	440	55	65	74	43,5	8									590		120		50°				
BMNH R 2619	690*	500	144	115		45	103					32	5								780	425	140	85		45°				
BMNH R 3806	860	610	205	142	82	58	125	340	68	48	47	38	4									495	150	100		45°-48°				
BMNH R 3320 (holotype)	815	600	170	127	70	48	105	350	62	45	36,5	29	7								890	510	160	100		50°				
SMNS 10114																					942	534-555	195	60						

Appendix II

Biometric data

Postcranial measurements																														
Steneosaurus leedsi	**H1**	**H2**	**T1**	**T2**	**R1**	**R2**	**U1**	**U2**	**Fi1**	**Fi2**	**Fe1**	**Fe2**	**Sa1**	**Co1**	**P1**	**P2**	**Pu1**	**Pu2**	**Is1**	**Is2**	**S/P-L**	**Tl in meters**								
BMNH R 2617 (holotype)																														
BMNH R 2619	102	11	115	19						11	250	23			70	76	100	43		90										
BMNH R 3806	127 /129	9	150	21	61	10,5	80	10	140	14	300	29	100	100	90	93	130	67	127	110										
BMNH R 3320 (holotype)																														
Cranial measurements																														
Steneosaurus edwardsi	**A**	**B**	**C**	**D**	**E**	**F**	**G**	**H**	**I**	**J**	**K**	**L**	**M**	**N**	**O**	**P**	**Q**	**R**	**S**	**T**	**U**	**V**	**W**	**X**	**W1**	**W2**	**Fm1**	**Fm2**	**C1**	**C2**
BMNH R 2075											63	51										450	100			55°				
BMNH R 2865	920	570	280				170		80	65	75	53																		
BMNH 32620						50																								
BMNH R 3701	720	450	220	190	90	63		220			59	50	5									370	120	108		60°				
BNMH R 2074	610	340	215	170	82	57	107	155	52/54	39	54	45	3											94						
MNHN 8909		f420				58	115		58	52																				
Postcranial measurements																														
Steneosaurus edwardsi*	**H1**	**H2**	**T1**	**T2**	**R1**	**R2**	**U1**	**U2**	**Fi1**	**Fi2**	**Fe1**	**Fe2**	**Sa1**	**Co1**	**P1**	**P2**	**Pu1**	**Pu2**	**Is1**	**Is2**	**S/P-L**	**Tl in meters**								
BMNH R 2075	139	22	153	25,5							330	33			85	101		49												
BMNH R 2076			174	23,5			117	17	128,5	13	350	39			105	107	155	73,5												
BMNH R 2865			178	27					160	17	390	38					165	79	140	180										
BMNH R 3701 (holotype of *Steneosaurus durobrivensis*)	123	18	139	24	70	12	81	10	132	13	320	30	95	109	77	97			137											
BMNH R 2074 (holotype)															66	80	106	36	88	101										

Appendix II

Biometric data

Cranial measurements																														
Steneosaurus obtusidens	**A**	**B**	**C**	**D**	**E**	**F**	**G**	**H**	**I**	**J**	**K**	**L**	**M**	**N**	**O**	**P**	**Q**	**R**	**S**	**T**	**U**	**V**	**W**	**X**	**W1**	**W2**	**Fm1**	**Fm2**	**C1**	**C2**
BMNH R 3168 (holotype)	1160	710	280	340	130	90	150	450	108	104	92	75	10								1370			160						
Postcranial measurements																														
Steneosaurus obtusidens	**H1**	**H2**	**T1**	**T2**	**R1**	**R2**	**U1**	**U2**	**Fi1**	**Fi2**	**Fe1**	**Fe2**	**Sa1**	**Co1**	**P1**	**P2**	**Pu1**	**Pu2**	**Is1**	**Is2**	**S/P-L**	**Tl in meters**								
BMNH R 3168 (holotype)	192	27	210	35			125	18			455	42	165		140	160	190	90	160	205										
BMNH R 3169													147	160	110	125	200	68												
BMNH R 3898											484	53			175	195			206	256										
Cranial measurements																														
Steneosaurus boutilieri	**A**	**B**	**C**	**D**	**E**	**F**	**G**	**H**	**I**	**J**	**K**	**L**	**M**	**N**	**O**	**P**	**Q**	**R**	**S**	**T**	**U**	**V**	**W**	**X**	**W1**	**W2**	**Fm1**	**Fm2**	**C1**	**C2**
BMNH 49126 (holotype)			250	180	110		152		69	57			8																	
Cranial measurements																														
Steneosaurus priscus	**A**	**B**	**C**	**D**	**E**	**F**	**G**	**H**	**I**	**J**	**K**	**L**	**M**	**N**	**O**	**P**	**Q**	**R**	**S**	**T**	**U**	**V**	**W**	**X**	**W1**	**W2**	**Fm1**	**Fm2**	**C1**	**C2**
BMNH R 1086	168	< 125	48	20	16	15		57			13	9									193	105	35	20						
Postcranial measurements																														
Steneosaurus priscus	**H1**	**H2**	**T1**	**T2**	**R1**	**R2**	**U1**	**U2**	**Fi1**	**Fi2**	**Fe1**	**Fe2**	**Sa1**	**Co1**	**P1**	**P2**	**Pu1**	**Pu2**	**Is1**	**Is2**	**S/P-L**	**Tl in meters**								
BMNH R 1086			27	4,5					27		68	6		23					23	26	190	0,95								
Cranial measurements																														
Steneosaurus lartifrons*	**A**	**B**	**C**	**D**	**E**	**F**	**G**	**H**	**I**	**J**	**K**	**L**	**M**	**N**	**O**	**P**	**Q**	**R**	**S**	**T**	**U**	**V**	**W**	**X**	**W1**	**W2**	**Fm1**	**Fm2**	**C1**	**C2**
BMNH 47171			280	152	135	100	235		70	65			5																	

Appendix II

Biometric data

Cranial measurements																														
Steneosaurus megarhinus	**A**	**B**	**C**	**D**	**E**	**F**	**G**	**H**	**I**	**J**	**K**	**L**	**M**	**N**	**O**	**P**	**Q**	**R**	**S**	**T**	**U**	**V**	**W**	**X**	**W1**	**W2**	**Fm1**	**Fm2**	**C1**	**C2**
BMNH 43086											68	45																		
Cranial measurements																														
Steneosaurus baroni	**A**	**B**	**C**	**D**	**E**	**F**	**G**	**H**	**I**	**J**	**K**	**L**	**M**	**N**	**O**	**P**	**Q**	**R**	**S**	**T**	**U**	**V**	**W**	**X**	**W1**	**W2**	**Fm1**	**Fm2**	**C1**	**C2**
BMNH R 1999																						460	175			60°				
Cranial measurements																														
Steneosaurus herberti	**A**	**B**	**C**	**D**	**E**	**F**	**G**	**H**	**I**	**J**	**K**	**L**	**M**	**N**	**O**	**P**	**Q**	**R**	**S**	**T**	**U**	**V**	**W**	**X**	**W1**	**W2**	**Fm1**	**Fm2**	**C1**	**C2**
MNHN 13 1890	1100	710	340	270/ 270	130/ 125		165		83,5 /84	59/6 6	75	57	~7	213	29			130	43		130 0	560		175		55°				
Cranial measurements																														
Caiman crocodylus	**A**	**B**	**C**	**D**	**E**	**F**	**G**	**H**	**I**	**J**	**K**	**L**	**M**	**N**	**O**	**P**	**Q**	**R**	**S**	**T**	**U**	**V**	**W**	**X**	**W1**	**W2**	**Fm1**	**Fm2**	**C1**	**C2**
ZFMK 21599	30																													
Crocodylus catacphractus	**A**	**B**	**C**	**D**	**E**	**F**	**G**	**H**	**I**	**J**	**K**	**L**	**M**	**N**	**O**	**P**	**Q**	**R**	**S**	**T**	**U**	**V**	**W**	**X**	**W1**	**W2**	**Fm1**	**Fm2**	**C1**	**C2**
ZFMK 74533	370		155																											
SMF 36421	150																													
SMF 22458 (2448)	230																													
Crocodylus niloticus	**A**	**B**	**C**	**D**	**E**	**F**	**G**	**H**	**I**	**J**	**K**	**L**	**M**	**N**	**O**	**P**	**Q**	**R**	**S**	**T**	**U**	**V**	**W**	**X**	**W1**	**W2**	**Fm1**	**Fm2**	**C1**	**C2**
ZFMK 5246	158		80																											
Gavialis gangeticus	**A**	**B**	**C**	**D**	**E**	**F**	**G**	**H**	**I**	**J**	**K**	**L**	**M**	**N**	**O**	**P**	**Q**	**R**	**S**	**T**	**U**	**V**	**W**	**X**	**W1**	**W2**	**Fm1**	**Fm2**	**C1**	**C2**
SMF 40144	222	160	58					55,6													238	145								
SMF 78886	215	149	56,7																		223									
SMF 28132	312		83,8																		344	220								
SMF 1914*	196		87																		333									
SMF 28133	566		205					140													645	350								
SMF 49529	730							150													810									
ZMUC 36	685		210	64	68	61	142		62	64	83									158		447	170	110						
ZFMK 21591	161,5		41,5					42													175, 7	109	40							
ZFMK no number	750		300					200													870	470	185							

Appendix II

Biometric data

Gavialis gangeticus	**A**	**B**	**C**	**D**	**E**	**F**	**G**	**H**	**I**	**J**	**K**	**L**	**M**	**N**	**O**	**P**	**Q**	**R**	**S**	**T**	**U**	**V**	**W**	**X**	**W1**	**W2**	**Fm1**	**Fm2**	**C1**	**C2**
SMF no number	740		295																		840									
Tomistoma schlegelii	**A**	**B**	**C**	**D**	**E**	**F**	**G**	**H**	**I**	**J**	**K**	**L**	**M**	**N**	**O**	**P**	**Q**	**R**	**S**	**T**	**U**	**V**	**W**	**X**	**W1**	**W2**	**Fm1**	**Fm2**	**C1**	**C2**
ZMUC 40	585		120	38	34	46	110		68	44	47									13		327	110	81						
ZMFK 66591	630		245																											
SMF 67267	540		240																		590	280	90							
SMF 28134	565		205																		620									
SMF 28135	545																				610									

Appendix III

Character table

Features / Taxa	***Steneosaurus bollensis***	***Steneosaurus gracilirostris***	***Steneosaurus brevior***	***Platysuchus multiscrobiculatus***	***Pelagosaurus typus***
Total body length (TL)	ca. 5 m	2.5 m	estimated ca. 4.5 m	3 m	1.8 - 2 m
Total number of vertebrae (average)	76	?	?	64	65
% skull length (A) /trunk length (TRL)	51%-65%	67%	?	45%	57%
% tail length/total body length (TL)	ca. 49%	?	?	ca. 49% (holotype)	56%
Number of caudal vertebrae	max. 55	?	?	38	42
Number of cervical vertebrae	9	9	?	9	8
Number of teeth in the premaxilla	3-4	?	3	3	3-4
Number of teeth in the maxilla	26-35	45	23-28	40-44	32
Number of teeth in the dentary	24-35	48	23-28	ca. 40	30-32
Number of dorsal osteoderms	2 lengthwise rows, about 88 osteoderms	2 lengthwise rows, number undetermined	?	2 lengthwise rows, about 92 osteoderms	2 lengthwise rows, 62-64 osteoderms
Number of ventral osteoderms	6 lengthwise rows, 100 (96) osteoderms	?	?	6 lengthwise rows, 102 osteoderms	4 lengthwise rows , 72 osteoderms
Tail armour	until 23. caudal vertebra	?	?	up to 26. caudal vertebra	up to 10. caudal vertebra
Shape of the dorsal osteoderms	slightly broader than long (until square), with "spur" at the anterolateral margin	slightly broader than long (until square)	?	1/3 broader than long, slight “spur” at the anterior margin	1/2 broader than long, very small anterior articulations area
Ornamentation of the dorsal osteoderms	regularly covered with large pits	irregular large pits	?	regularly covered with many small round pits	regularly covered with many small round pits
Keel developed at the dorsal osteoderms	at the level of the pelvic girdle	not exposed	?	slightly from the 3., distinct from 7.	no
Shape of the ventral osteoderms	rectangular until rhombic	?rectangular	?	rectangular or square	rectangular or square
Ornamentation of the ventral osteoderms	regularly covered with many large pits	large pits	?	regularly covered with many small round pits	regularly covered with many small round pits
Ornamentation of the cranial table	f, p, po, sq (l, prf)	f, p, po, sq	f, p, po, (l, prf)	f, p, po, sq, prf, l,	f, p, po, sq, prf, l, in most cases n, j

Appendix III

Character table

Features / Taxa	***Steneosaurus bollensis***	***Steneosaurus gracilirostris***	***Steneosaurus brevior***	***Platysuchus multiscrobiculatus***	***Pelagosaurus typus***
% Supratemporal fenestra length (D) to skull length (A)	15.2% (average)	12.4% (holotype), 12.7% (average)	18.8 % (holotype)	16.5% (holotype) , 15.6% (average)	13.4% (average), 12.2% (holotype)
Shape of the lateral STF margin in dorsal view	thin, with enlargement at the po-sq suture, only slightly ornamented	thin, with slight ornamentation	thin, with slight ornamentation	thin, with pronounced ornamentation	broad with pronounced ornamentation
Shape of the supratemporal fenestra (STF)	2x longer than wide, rectangular	longer than wide, ellipsoid	longer than wide, rectangular	sub-rectangular, longer than wide	ellipsoid, longer than wide
% rostral length (B) to skull length (A) (average)	71.4%	74-76%	65%	75%	74.4%
% skull width (C) to skull length (A) (average)	27-30% (28.57%)	19.9%	33%	27.6%	18-22%
% orbital length (I) to skull length (A)	7.9% (average adult) -9.6% (average juvenile)	average 7.4%	holotype 7.67%	7.5% (adult)-9.1% (juvenile)	average ca. 9.8%
% orbital length (I) to supratemporal fenestra length (D)	adult minimal ca. 40%, juvenile max. 72%, average ca. 55%	average ca. 59.6%	holotype 41.2%, average ca. 44.4%	juvenile 60% , adult ca. 45.5%	holotype 90%, juvenile max. 100%, average ca. 77%
Orientation of the orbit	dorsal	dorsolateral	dorsal	dorsal -anterodorsal	lateral
Orbital shape	small, ellipsoid	large, ellipsoid	small, ellipsoid	small, round	large, round
Scleral rings	no	no	no	no	yes
Paired premaxillae shape (together)	spoon-shaped, various broaden	slightly broadened	spoon-shaped enlargement	spoon-shaped, broad enlargement	only slightly enlarged
Quotient of premaxillae width (K) / narrowing posterior premaxillae (L)	1.46 (average), 1.75 (max.)	1.35 (max.), 1.19 (holotype)	1.45	1.79 (average), 2.02 (max)	1.2 (average)
Orientation of the external naris (en) (W1)	anterodorsal, mainly en about 45° steep	anterior en up to 70° steep	anterior, en up to 70° steep	anterodorsal, en ca. 45° steep	anterodorsal-dorsal, en less than 30° steep
Size & shape of the antorbital fenestra	very small, slit-like or missing	3x longer than high, ellipsoid	2x longer than high, ellipsoid	very small or missing	small, ellipsoid
Size & shape of the prefrontal	small, triangular or rhombic	slender, slightly elongated, rhombic	small, triangular or rhombic	small, triangular or rhombic	largely elongated, rhombic

Appendix III

Character table

Features / Taxa	***Steneosaurus bollensis***	***Steneosaurus gracilirostris***	***Steneosaurus brevior***	***Platysuchus multiscrobiculatus***	***Pelagosaurus typus***
Symphysis angle (W2)	35°-50°	?	40°	?	25-30°
Secondary choana shape	ellipsoid or anterior pointed. posteriorly declining	probably large, anterior pointed	large pointed arch, posteriorly declining	?	longer than wide, anterior pointed, posterior round and deep
Suborbital fenestra shape	circular, small (juvenile), ellipsoid, large (adult)	sigmoid	sigmoid	?	anterior pointed, largely elongated, large
Paired pterygoid shape	broad transverse pterygoid flanges and broad quadrate rami	broad transverse pterygoid flanges, slender quadrate rami	broad, transverse pterygoid flanges, broad quadrate rami	?	broad transverse pterygoid flanges, ventrally flexed, slender quadrate rami
% humerus length (H1) to femur length (Fe1) (average)	(57-65%) 61.6%	72% (WESTPHAL 1962)	?	67.5-72.5% (70.1%)	53.4%
% humerus length (H1) to skull length (A) (average)	23.74%	20.7% (WESTPHAL 1962)	?	27.17%	18.58%
Shape of the humerus	slightly developed humerus head, distinct deltopectoral crest	?	?	slightly developed humerus head, distinct deltopectoral crest	quite slender humerus, humerus head weakly developed, weak deltopectoral crest
Shape of the femur	s-shaped with poorly pronounced femoral head	?	?	s-shaped with well pronounced femoral head, distinctly internally flexed	s-shaped with poorly pronounced femoral head
% tibia length (T1) to femur length (Fe1) (average)	53-62% adult & 68-70% juvenile (60.1%)	?	?	60% adult - 74% juvenile (66.7%)	57.3%
Ilium shape	shallow acetabulum, Iliac crest with short posterior process	?	?	deeper acetabulum, Iliac crest with distinct anterior and posterior process	shallow acetabulum, Iliac crest with very short posterior process and slight recess at the posterior margin
Ischium shape	distinctive groove between the proximal articular facets of the ischium	?	?	shallow groove between the proximal articular facet of the ischium	distinctive groove between the proximal articular facets of the ischium

Appendix III

Character table

Features / Taxa	***Steneosaurus bollensis***	***Steneosaurus gracilirostris***	***Steneosaurus brevior***	***Platysuchus multiscrobiculatus***	***Pelagosaurus typus***
Pubis shape	relatively short, slender with triangular or paddle-shaped broaden distal end, distal margin strongly convex	?	?	relatively short, slender with triangular broaden end, distal margin straight	relatively long, very slender, distal end only slightly enlarged, convex distal margin
Scapula shape	hourglass-shaped, broad shaft similar to coracoid	?	?	hourglass-shaped, shaft broaden, proximal end anterior slightly sloping down	hourglass-shaped, thin with very enlarged proximal end, with strongly convex margin
Coracoid shape	hourglass-shaped, broad shaft similar to scapula		?	hourglass-shaped, shaft very slender, very pronounced glenoid fossa	hourglass-shaped, short and broad
Ratio scapula to coracoid length	1:1	1:1	?	1:1	1:0.75
Phalangal formula pes	2-3-4-4-0	?	?	2-3-3(4)-3-0	?
Phalangal formula manus	2-3-3-4-2	?	?	2-3-4-3-2	?

Appendix IV

Character coding

Geosaurus vignaudi	coded after FREY et al. 2002
Geosaurus giganteus	coded after FRAAS 1902 & after own investigation at the British Museum National History London (BMNH)
Geosaurus gracilis	coded after FRAAS 1902, BROILI 1932 & after own investigation at the BMNH & the Bayrische Staatssammlung für Geologie und Paläontologie Munich (BSGP)
Geosaurus suevicus	coded after FRAAS 1902 & ANDREWS 1913
Machimosaurus hugii	coded after KREBS 1967 & after own investigation at the BSGP
Metriorhynchus hastifer	coded after ANDREWS 1913, VIGNAUD 1995 & after own investigation at the Museum National d'Histoire Naturelle Paris (MNHN)
Metriorhynchus leedsi **(incl. *M. laeve*)**	coded after ANDREWS 1913, VIGNAUD 1995 & after own investigation at the BMNH
Metriorhynchus superciliosus **(incl. *M. moreli*)**	coded after ANDREWS 1913, VIGNAUD 1995 & after own investigation at the MNHN
Pelagosaurus typus	coded after EUDES-DELONGCHAMPS 1864 & after own investigation at the Staatliches Museum für Naturkunde Stuttgart (SMNS), Urweltmuseum Hauff Holzmaden (UH), Natural History Museum Budapest (NHMUS), BSGP, BMNH, & MNHN
Platysuchus multiscrobiculatus	coded after own investigation at the Geologisch-Paläontologisches Institut Tübingen (GPIT), SMNS & UH.
Steneosaurus bollensis	coded after own investigation at the BMNH, BSGP, GPIT, NHMUS, SMNS & the Staatliches Museum für Naturkunde in Karlsruhe (SMNK)
Steneosaurus boutilieri	coded after VIGNAUD 1995 & after own investigation at the MNHN & the Oxford University Museum (OUM)
Steneosaurus brevior	coded after TATE & BLAKE 1876 & after own investigation at the BMNH
Steneosaurus edwardsi	coded after VIGNAUD 1995 & after own investigation at the BMNH & MNHN
Steneosaurus gracilirostris	coded after WESTPHAL 1961 &1962 & after own investigation at the BMNH
Steneosaurus heberti	coded after VIGNAUD 1995 & after own investigation at the MNHN
Steneosaurus leedsi	coded after ANDREWS 1913 & own investigation at the BMNH & SMNS
Steneosaurus baroni	coded after ANDREWS 1913 & own investigation at the BMNH
Steneosaurus pictaviensis	coded after VIGNAUD 1998
Steneosaurus priscus	coded after own investigation at the BMNH
Steneosaurus megarhinus	coded after own investigation at the BMNH
Teleidosaurus calvadosi **(incl. *T. joberti*)**	coded after VIGNAUD 1995 & own investigation at the BMNH & MNHN
Teleidosaurus gaudryi	coded after HUA & ATROPS 1995 & own investigation at the BMNH
Teleosaurus cadomensis	coded after own investigations at the BMNH, MNHN & SMNS
Dakosaurus maximus	coded after FRAAS 1902
Gracilisuchus **(out group)**	coded after CLARK 1994 & POL & NORELL 2004
Protosuchus **(out group)**	coded after COLBERT & MOOK 1951 & CLARK 1994
Dyrosaurus	coded after CLARK 1994 & BROCHU et al. 2002 & JOUVE & SCHWARZ 2004
Pholidosaurus	coded after CLARK 1994

Appendix V

Character list used in the phylogenetic analysis

Character	Description	Character number in the cited references
1	External surfaces of cranial bones smooth (0), or slightly grooved (1) or heavily ornamented, with deep grooves and pits (2) (CLARK 1994)	1 CLARK 1994 modified by POL&NORELL 2004
2	Rostrum narrow anterior to orbits, broading abruptly at orbits (0) or broad throughout (1) (CLARK 1994)	2 CLARK 1994
3	Rostrum higher than wide (0) or nearly tubular (1) or wider than high (2) (CLARK 1994)	3 CLARK 1994
4	Premaxilla forms at least ventral half of internarial bar (0) or forms little, if any, of internarial bar (1) (CLARK 1994)	4 CLARK 1994
5	Premaxilla narrow anterior to nares (0) or broad, similar in breadth to the part lateral to nares (1) (CLARK 1994)	5 CLARK 1994
6	External nares facing: anterolaterally or anterior (0), dorsally not separated by premaxillary bar from anterior edge of rostrum (1), or dorsally separated by premaxillary bar (2) (CLARK 1994)	6 CLARK 1994 modified by POL&NORELL 2004
7	Palatal parts of premaxillae do not meet posterior to incisive foramen (0) or meet posteriorly with maxillae (1) (CLARK 1994)	7 CLARK 1994
8	Premaxilla loosely overlies maxilla on face (0), or premaxilla and maxilla sutured together along butt joint (1) (CLARK 1994)	8 CLARK 1994
9	Ventrally opened notch on ventral edge of rostrum at premaxilla-maxilla contact: absent (0), present as a notch (1), or present as a large fenestra (2) (CLARK 1994)	9 CLARK 1994 modified by POL&NORELL 2004
10	Posterior ends of maxillae do not meet on palate anterior to palatines (0), or ends do meet (1) (CLARK 1994)	10 CLARK 1994
11	Nasals contact lacrimal (0) or do not (1) (CLARK 1994)	11 CLARK 1994
12	Lacrimal contacts nasal along medial edge only (0) or on medial and anterior edges (1) (CLARK 1994)	12 CLARK 1994
13	Nasal takes part in narial border (0) or does not (1) (CLARK 1994)	13 CLARK 1994
14	Nasal contacts premaxilla (0) or does not (1) (CLARK 1994)	14 CLARK 1994
15	Descending process or prefrontal does not contact palate (0), or contacts palate (1) (CLARK 1994)	15 CLARK 1994 modified by POL&NORELL 2004
16	Postorbital anterior to jugal on postorbital bar (0), postorbital medial to jugal (1), or postorbital lateral to jugal (2) (CLARK 1994)	16 CLARK 1994
17	Anterior part of jugal as broad as posterior part (0) or about twice as broad as posterior part (1) (CLARK 1994)	17 CLARK 1994
18	Jugal transversely flattened beneath lateral temporal fenestra (0) or rod-shaped beneath fenestra (1) (CLARK 1994)	18 CLARK 1994
19	Quadratojugal narrows dorsally, contacting only a small part of postorbital (0), or quadratojugal extends dorsally as abroad sheet contacting most of postorbital portion of postorbital bar (1), or quadratojugal does not contact the postorbital at all (2) (CLARK 1994)	19 CLARK 1994 modified by MUELLER-TÖWE
20	Frontals narrow between orbits (similar in breadth to nasals) (0) or are broad, about twice nasal breadth (1) (CLARK 1994)	20 CLARK 1994
21	Frontals paired (0) or fused (1) (CLARK 1994)	21CLARK 1994
22	Dorsal surface of frontal and parietal flat (0) or with narrow midline ridge (1) (CLARK 1994)	22 CLARK 1994
23	Frontal extends well into supratemporal fossa (0) or extends only slightly or not at all (1) (CLARK 1994)	23 CLARK 1994
24	Supratemporal roof with complex dorsal surface (0), or dorsally flat "skull table" developed, with squamosal and postorbital with flat shelves extending laterally beyond quadrate contacts (1) (CLARK 1994)	24 CLARK 1994
25	Postorbital bar lateral surface ornamented (if skull ornamented) (0), or postorbital bar without ornamentation (1) (CLARK 1994)	25 CLARK 1994 modified by MUELLER-TÖWE
26	Postorbital bar transversely flattened (0), or postorbital bar cylindrical (1) (CLARK 1994)	26 CLARK 1994 modified by POL & NORELL 2004
27	Vascular opening on lateral edge of dorsal part of postorbital bar absent (0) or present (1) (CLARK 1994)	27 CLARK 1994
28	Postorbital without or poorly developed anterolateral process (0) or with well-developed anterolateral process ,long and acute (1) (CLARK 1994)	28 CLARK 1994 modified by POL & NORELL 2004
29	Dorsal part of postorbital with anterior and lateral edges only (0) or with anterolaterally facing edge (1) (CLARK 1994)	29 CLARK 1994
30	Dorsal end of postorbital bar broads dorsally, continuous with dorsal part of postorbital (0), or dorsal part of postorbital bar constricted, distinct from dorsal part of postorbital (1) (CLARK 1994)	30 CLARK 1994
31	Bar between orbit and supratemporal fossa broad and solid, with broadly ornamented dorsal surface (0), or bar narrow, with sculpturing on anterior part only (1) (CLARK 1994)	31 CLARK 1994
32	Parietal without broad occipital portion (0) or with broad occipital portion (1) (CLARK 1994)	32 CLARK 1994
33	Parietal with broad, sculpted region separating fossae (0) or with sagittal crest between supratemporal fossae (1) (CLARK 1994)	33 CLARK 1994
34	Postparietal (dermosupraoccipital) a distinct element (0) or not distinct (fused with parietal?) (1) (CLARK 1994)	34 CLARK 1994
35	Posterodorsal corner of squamosal squared off, lacking extra "lobe" (0) or with unsculptured "lobe" (1) (CLARK 1994)	35 CLARK 1994

Appendix V

36	Posterior edge of squamosal nearly flat (0), or posterolateral edge of squamosal extends posteriorly as a long process (1) (CLARK 1994)	36 CLARK 1994
37	Palatines do not meet on palate below narial passage (0), or form palatal shelves that do not meet (1), or meet ventral to narial passage, forming part of secondary palate (2) (CLARK 1994)	37 CLARK 1994 modified by MUELLER-TÖWE
38	Pterygoid restricted to palate and suspensorium, joints with quadrate and basisphenoid overlapping (0), or pterygoid extends dorsally to contact laterosphenoid and form ventrolateral edge of trigeminal foramen, strongly sutured to quadrate and laterosphenoid (1) (CLARK 1994)	38 CLARK 1994
39	Choanal opening: continues with pterygoid ventral surface except for anterior and anterolateral borders (0), or opens into palate through a deep midline depression (choanal groove) (1) (CLARK 1994)	39 CLARK 1994 modified by POL & NORELL 2004
40	Palatal surface of pterygoid smooth (0) or sculpted (1) (CLARK 1994)	40 CLARK 1994
41	Pterygoids separated posterior to choanae (0) or are fused (1) (CLARK 1994)	41 CLARK 1994
42	Depression on primary pterygoidean palate posterior to choana: absent or moderate in size being narrower than palatine bar (0), or wider then palatine bar (1) (CLARK 1994)	42 CLARK 1994 modified by POL & NORELL 2004
43	Pterygoids do not enclose choana (0) or enclose choana (1) (CLARK 1994)	43 CLARK 1994
44	Choanae situated near anterior edge of pterygoids (or anteriorly) (0) or in middle of pterygoids (1) (CLARK 1994)	44 CLARK 1994
45	Quadrate without fenestrae (0), or with single fenestra (1), or with three or more fenestrae on dorsal and posteromedial surfaces (2) (CLARK 1994)	45 CLARK 1994
46	Posterior edge of quadrate broad medial to tympanum, gently concave (0), or posterior edge narrow dorsal to otoccipital contact, strongly concave (1) (CLARK 1994)	46 CLARK 1994
47	Dorsal, primary head of quadrate articulates with squamosal, otoccipital, and prootic (0) or with prootic and laterosphenoid (1) (CLARK 1994)	47 CLARK 1994
48	Venterolateral contact of otoccipital with quadrate very narrow (0) or broad (1) (CLARK 1994)	48 CLARK 1994
49	Quadrate, squamosal, and otoccipital do not meet to enclose cranioquadrate passage (0), enclose passage near lateral edge of skull (1), or meet broadly lateral to passage (2) (CLARK 1994)	49 CLARK 1994 modified by MUELLER-TÖWE
50	Pterygoid ramus of quadrate with flat ventral edge (0) or with deep groove along ventral edge (1) (CLARK 1994)	50 CLARK 1994
51	Ventromedial part of quadrate does not contact otoccipital (0) or contacts otoccipital to enclose carotid artery and form passage for cranial nerves IX-XI (1) (CLARK 1994)	51 CLARK 1994
52	Eustachian tubes not enclosed between basioccipital and basisphenoid (0) or entirely enclosed (1) (CLARK 1994)	52 CLARK 1994
53	Basisphenoid rostrum (cultriform process) slender (0) or dorsoventrally expanded (1) (CLARK 1994)	53 CLARK 1994
54	Basipterygoid process prominent, forming movable joint with pterygoid (0), or basipterygoid process small or absent, with basipterygoid joint closed suturally (1) (CLARK 1994)	54 CLARK 1994
55	Basisphenoid similar in length to basioccipital, with flat or concave ventral surface (0), or basisphenoid shorter than basioccipital (1) (CLARK 1994)	55 CLARK 1994
56	Basisphenoid exposed on ventral surface of braincase (0) or virtually excluded from ventral surface by pterygoid and basioccipital (1) (CLARK 1994)	56 CLARK 1994
57	Basioccipital without well-developed bilateral tuberosities (0) or with large, pendulous tubera (1) (CLARK 1994)	57 CLARK 1994
58	Otoccipital without laterally concave descending flange ventral to subcapsular process (0) or with flange (1) (CLARK 1994)	58 CLARK 1994
59	Cranial nerves IX-XI pass through common large foramen vagi in otoccipital (0), or cranial nerve IX passes medial to nerves X and XI in separate passage (1) (CLARK 1994)	59 CLARK 1994
60	Otoccipital without large ventrolateral part ventral to paroccipital process (0) or with large ventrolateral part (1) (CLARK 1994)	60 CLARK 1994
61	Crista interfenestralis between fenestrae pseudorotunda and ovalis nearly vertical (0) or horizontal (1) (CLARK 1994)	61 CLARK 1994
62	Supraoccipital forms dorsal edge of foramen magnum (0), or otocipitals broadly meet dorsal to the foramen magnum, separating supraoccipital from foramen (1) (CLARK 1994)	62 CLARK 1994
63	Mastoid antrum does not extend into supraoccipital (0) or extends through transverse canal in supraoccipital to connect middle ear regions (1) (CLARK 1994)	63 CLARK 1994
64	Posterior surface of supraoccipital nearly flat (0), or with bilateral posterior prominences (1) (CLARK 1994)	64 CLARK 1994
65	One small palpebral present in orbit (0), or two large palpebrals present (1), or one large palpebral present (2) or palpebral absent (3) (CLARK 1994)	65 CLARK 1994 modified by MUELLER-TÖWE
66	External nares divided (0) or confluent (1) (CLARK 1994)	66 CLARK 1994
67	Antorbital fenestra as large as orbit (0), or about half the diameter of the orbit (1), or much smaller than orbit (2), or absent (3) (CLARK 1994)	67 CLARK 1994 modified by MUELLER-TÖWE
68	Supratemporal fenestrae extension: relatively large, covering most of the surface of skull roof (0), or relatively short, fenestrae surrounded by a flat and extended skull roof (1) (CLARK 1994)	68 CLARK 1994 modified by ORTEGA et al. 2000
69	Secondary choanae confluent (0) or divided by septum (1) or partly divided by midline ridge (2) (CLARK 1994)	69 CLARK 1994 modified by MUELLER-TÖWE
70	Dentary extends posteriorly beneath mandibular fenestra (0) or does not extend beneath fenestra (1) (CLARK 1994)	70 CLARK 1994

Appendix V

71	Retroarticular process: absent or extremely reduced (0), or very short, broad, and robust (1), wit an extensive rounded, wide, and flat (or slightly concave) surface projected posteroventrally and facing dorsomedially (2), posteriorly elongated, triangular-shaped and facing dorsally (3), or posteroventrally projecting and paddle-shaped (4) (CLARK 1994)	71 CLARK 1994 modified by POL&NORELL 2004
72	Prearticular present (0) or absent (1) (CLARK 1994)	72 CLARK 1994
73	Articular without medial process (0), or with short process not contacting braincase (1), or with process articulating with otoccipital and basisphenoid (2) (CLARK 1994)	73 CLARK 1994 modified by POL&NORELL 2004
74	Dorsal edge of surangular flat (0) or arched dorsally (1) (CLARK 1994)	74 CLARK 1994
75	Mandibular fenestra present (0) or absent (1) (CLARK 1994)	75 CLARK 1994
76	Insertion area for M. pterygoideus does not extend onto lateral surface of angular (0) or extends onto lateral surface of angular (1) (CLARK 1994)	76 CLARK 1994
77	Splenial not involved in symphysis (0), or involved slightly in symphysis (1), or involved extensively in symphysis (2) (CLARK 1994)	77 CLARK 1994 modified by MUELLER-TÖWE
78	Posterior two premaxillary teeth similar in size to anterior teeth (0) or much longer (1) (CLARK 1994)	78 CLARK 1994
79	Maxillary teeth homodont, with lateral edge of maxilla straight (0), or teeth enlarged in the middle of tooth row, with edge of maxilla extending outward at these loci (1), or teeth enlarged and edge of maxilla curved in two waves ("festooned") (2) (unordered) (CLARK 1994)	79 CLARK 1994
80	Anterior dentary teeth opposite premaxilla-maxilla contact no more than twice the length of other dentary teeth (0) or more than twice the length (1) (CLARK 1994)	80 CLARK 1994
81	Dentary teeth posterior to tooth opposite premaxilla-maxilla contact homodont (0) or enlarged opposite smaller teeth in maxillary tooth row (1) (CLARK 1994)	81 CLARK 1994
82	Anterior and posterior scapular edges symmetrical in lateral view (0), or anterior edge more strongly concave than posterior edge (1) or dorsally narrow with straight edges (2) (CLARK 1994)	82 CLARK 1994 modified by ORTEGA et al. 2000
83	Coracoid length up to two-thirds of the scapula length (0) or about (sub)equal in length to scapula (1) (CLARK 1994)	83 CLARK 1994 modified by ORTEGA et al. 2000
84	Anterior process of ilium similar in length to posterior process (0) or one-quarter or less the length of posterior process (1), or posterior process absent (2) (CLARK 1994)	84 CLARK 1994 modified by MUELLER-TÖWE
85	Pubis rodlike, without expanded distal end (0) or with expanded distal end (1) (CLARK 1994)	85 CLARK 1994
86	Pubis forms anterior half of ventral edge of acetabulum (0), or pubis at least partially excluded from the acetabulum by an anterior process of the ischium (1) (CLARK 1994)	86 CLARK 1994
87	Distal end of femur with large lateral facet for fibula (0) or with very small facet (1) (CLARK 1994)	87 CLARK 1994
88	Fifth pedal digit with (0) or without (1) phalanges (CLARK 1994)	88 CLARK 1994
89	Atlas intercentrum broader than long (0) or as long as broad (1) (CLARK 1994)	89 CLARK 1994
90	Cervical neural spines: all anteroposteriorly large (0), only posterior ones rodlike (1), or all spines rodlike (2) (CLARK 1994)	90 CLARK 1994 modified by POL&NORELL 2004
91	Hypapophyses in cervicodorsal vertebrae: absent (0), or present only in cervical vertebrae (1), present in cervical and the first two dorsal vertebrae (2), present up to the third dorsal vertebrae (3), or up to the fourth dorsal vertebrae (4) (CLARK 1994)	91 CLARK 1994 modified by POL&NORELL 2004
92	Cervical vertebrae amphicoelous or amphiplatyan (0) or procoelous (1) (CLARK 1994)	92 CLARK 1994
93	Trunk vertebrae amphicoelous or amphiplatyan (0) or procoelous (1) (CLARK 1994)	93 CLARK 1994
94	All caudal vertebrae amphicoelous or amphiplatyan (0), or first caudal vertebra biconvex, with other caudal vertebrae procoelous (1), or all caudal vertebrae procoelous (2) (CLARK 1994)	94 CLARK 1994
95	Dorsal osteoderms rounded or ovated (0), or rectangular, broader than long (1), or square (2) (CLARK 1994)	95 CLARK 1994
96	Dorsal osteoderms without articular anterior process (0), with a discrete convexity on anterior margin (1), or with a well-developed process located anterolaterally in dorsal parasagittal osteoderms (2) (POL & NORELL 2004)	96 POL & NORELL 2004
97	Dorsal osteoderms in two parallel, longitudinal rows (0) or in more than two longitudinal rows (1) (CLARK 1994)	97 CLARK 1994
98	Some or all osteoderms imbricated (0), or osteoderms sutured to one another (1) (CLARK 1994)	98 CLARK 1994
99	Tail with dorsal osteoderms only (0) or completely surrounded by osteoderms (1) (CLARK 1994)	99 CLARK 1994
100	Osteoderms absent from ventral part of trunk (0) or present (1) (CLARK 1994)	100 CLARK 1994
101	Osteoderms with longitudinal keels on dorsal surfaces (0) or without keels (1) (CLARK 1994)	101 CLARK 1994
102	Surangular forms only lateral wall of glenoid fossa (0) or surangular forms approximately one-third of the glenoid fossa (1) (BUCKLEY et al. 2000)	102 TYKOSKI et al. 2002
103	Anterior margin of femur linear (0) or anterior margin of femur bears flange for coccygeofemoralis musculature (1) (BUCKLEY et al. 2000)	103 TYKOSKI et al. 2002
104	Teeth without carinae's, or with smooth carinae's (0) or teeth serrated (1) (BUCKLEY et al. 2000)	104 TYKOSKI et al. 2002
105	Dentary smooth lateral to seventh alveolus (0) or dentary with large occlusal pit lateral to seventh alveolus (1) (Buckley et al. 2000)	105 TYKOSKI et al. 2002
106	Scapular blade no more than twice the length of the scapulocorcoid articulation (0) or scapular blade very broad and greater than twice the length of the scapulocoracoid articulation (1) (BUCKLEY et al. 2000)	106 TYKOSKI et al. 2002
107	Dorsal edge of dentary straight (0) or dorsal edge of dentary sinusoidal, with two concave waves (1) (BUCKLEY et al. 2000)	107 TYKOSKI et al. 2002
108	Compressed dentary (0) or transversely expanded dentary, almost as wide as high (1) (BUCKLEY et al. 2000)	108 TYKOSKI et al. 2002

Appendix V

109	Lateral surface of dentary continuous, without longitudinal groove (0) or lateral surface of dentary with longitudinal groove (1) (BUCKLEY et al. 2000)	109 TYKOSKI et al. 2002
110	Splenial thin posterior to symphysis (0) or splenial robust posterodorsal to symphysis (1) (BUCKLEY et al. 2000)	110 TYKOSKI et al. 2002
111	Prefrontals broad (0), or narrow and short (1), or narrow and long (2) (from BUCKLEY et al. 2000)	111 TYKOSKI et al. 2002
112	Snout long (0), or relatively broad and shorter than the remainder of the skull (1), or narrow and shorter than the remainder of the skull (2) (BUCKLEY et al. 2000)	112 TYKOSKI et al. 2002
113	Posterior cheek teeth not multicusped (0), multicusped with cusped in single row (1), or multicusped with cusps in more than one row (2) (BUCKLEY et al. 2000)	113 TYKOSKI et al. 2002
114	Occipital condyle in posterior position (0) or posteroventral position (1) (BUCKLEY et al. 2000)	114 TYKOSKI et al. 2002
115	Vomer exposed (0) or not exposed (1) on palate (BUCKLEY et al. 2000)	115 TYKOSKI et al. 2002
116	Posterior cheek teeth conical (0), or laterally compressed (1), or strongly spatulate (2) (BUCKLEY et al. 2000)	116 TYKOSKI et al. 2002
117	Cheek teeth not constricted at base of crown (0), or constricted (1) (BUCKLEY et al. 2000)	117 TYKOSKI et al. 2002
118	Maxillary depression absent (0) or present (1) on lateral surface of maxilla (TYKOSKI et al. 2002)	118 TYKOSKI et al. 2002
119	Long anterior processes of pterygoids that contact the maxillae anteromedial to primary choanae absent (0) or present (1) (TYKOSKI et al. 2002)	119 TYKOSKI et al. 2002
120	Jugal participating in margin of antorbital fossa (0), or separated from it (1) (WU & SUESS 1996)	102 POL & NORELL 2004
121	Postacetabular process: directed posteroventrally or posterior (0), or directed posterodorsally and much higher in position than preacetabular process (1) (WU & SUESS 1996)	110 POL & NORELL 2004
122	Prefrontals anterior to the orbits: elongated, oriented parallel to anteroposterior axis of the skull (0), or short and broad, oriented posteromedially-anterolateraly (1) (GOMANI 1997)	111 POL & NORELL 2004 modified from GOMANI 1997
123	Number of sacral vertebrae: two (0) or more than two (1) (BUSCALIONI & SANZ 1988)	115 POL & NORELL 2004
124	Proximal end of radiale expanded symmetrically, similarly to the distal end (0), or more expanded proximomedially than proximolaterally (1) (BUSCALIONI & SANZ 1988)	117 POL & NORELL 2004
125	Dorsal border of external nares: formed mostly by the nasals (0), or by both the nasals and the premaxilla (1), or only by the premaxillae (2) (POL 1999)	124 POL &NORELL 2004 modified by MUELLER-TÖWE
126	Palatine anteromedial margin: exceeding the anterior margin of the palatal fenestrae wedging between the maxilla (0), or not exceeding the anterior margin of palatal fenestrae (1) (POL 1999)	129 POL & NORELL 2004
127	Maxilla-lacrimal contact: partially included in antorbital fossa (0), or completely included (1) (POL 1999)	131 POL & NORELL 2004
128	Jugal posterior process: exceeding posteriorly the infratemporal fenestra (0), or not (1) (POL 1999)	136 POL & NORELL 2004
129	Posteroventral corner of quadratojugal: reaching the quadrate condyles (0), or not reaching the quadrate condyles (1) (POL 1999)	141 POL & NORELL 2004
130	Postorbital process of jugal anteriorly placed (0), in the middle (1), or posteriorly positioned (2) (POL 1999)	143 POL & NORELL 2004
131	Postorbital-ectopterygoid contact: present (0), or absent (1) (POL 1999 & ORTEGA et al. 2000)	144 POL & NORELL 2004
132	Length/height proportion of infratemporal fenestra: higher than wide or equal (0), or very anteroposteriorly elongated (1) (ORTEGA et al. 2000)	159 POL & NORELL 2004
133	Postorbital participation in infratemporal fenestra almost entirely excluded (0), or bordering infratemporal fenestra (1) (WU et al. 1997)	169 POL & NORELL 2004
134	Palatines: form margin of suborbital fenestra (0), or excluded from margin of suborbital fenestra (1) WU et al. 1997)	170 POL & NORELL 2004
135	Vertebra centra: cylindrical (0), or spool-shaped (1) (BUSCALIONI & SANZ 1988)	113 POL & NORELL 2004
136	Basisphenoid : without lateral exposure on the braincase (0) or with lateral exposure (1) (POL 1999)	148 POL & NORELL 2004
137	Dorsal surface of nasals sculptured (0) or smooth (1)	MUELLER-TÖWE
138	Lateral bar of supratemporal fenestra broad in dorsal view (0) or thin (1)	MUELLER-TÖWE
139	Jugal forming large part or all of the lateral margin of the orbit (0), or excluded from the lateral margin of the orbit or only slightly participating (1)	MUELLER-TÖWE
140	Frontal tapers off deeply between the nasals (0) or only slightly or not (1)	MUELLER-TÖWE
141	Choana shape: round (0), anterior pointed (1) or ellipsoid (2) or anterior rectangular (3)	MUELLER-TÖWE
142	Posterior pterygoid wings well developed with broad quadrate contact (0), or very narrow with reduced quadrate contact (1)	MUELLER-TÖWE
143	Pterygoid lateral process not bent posterior (0) or bent posterior (1)	MUELLER-TÖWE
144	Supraoccipital in posterior view paired (0), or with prominent vertical middle ridge and triangular in shape (1), or rhombic shaped and fused (2)	MUELLER-TÖWE
145	Prootic well developed and exposed in lateral view (0), or prootic small and exposed (1), or small prootic mostly hidden by overlaying bones (2)	MUELLER-TÖWE
146	Fused external naris dorsal aligned (0), anterodorsal aligned (1), or anterior aligned (2)	MUELLER-TÖWE
147	Length/width proportion of external naris: wider than long (0), or equal (1), or longer than wide (2)	MUELLER-TÖWE
148	Incisive foramen present (0), or absent (1) in dorsal view	MUELLER-TÖWE
149	Orbits laterally aligned (0), or dorsally aligned (1)	MUELLER-TÖWE
150	Orbits round (0), or ellipsoid (1)	MUELLER-TÖWE
151	External mandibular fenestra restricted by angular, surangular and dental (0), or restricted only by angular and surangular (1)	MUELLER-TÖWE

Appendix V

152	Symphysis angle less than 50° (0), or more than 50° (1)	MUELLER-TÖWE
153	Proximal edge of the scapula broad and flat with convex margin (0), proximal edge of scapula more rectangular flattened (1), or proximal edge of scapula smaller than distal edge (2)	MUELLER-TÖWE
154	Coracoids in the middle part broader than middle part of scapula (0), or equal size (1), or middle part thinner than in scapula (2)	MUELLER-TÖWE
155	The interclavicle has direct contact to the coracoids (0), or not (1)	MUELLER-TÖWE
156	Pubis distal edge paddle-shaped (0), or triangular with convex margin (1), or only slightly enlarged (2)	MUELLER-TÖWE
157	Proximal end of femur with well developed head (0), or without (1)	MUELLER-TÖWE
158	Calcaneum, astragalus and two tarsals (0), or with only one tarsal (1)	MUELLER-TÖWE
159	Calcaneum equal in size of astragalus (0), or nearly double the size (1)	MUELLER-TÖWE
160	9 cervical vertebrae (0), or 8 cervical vertebrae (1), or 7 cervical vertebrae (2)	MUELLER-TÖWE
161	Whole tail is covered by dorsal osteoderms (0), two-thirds are covered by dorsal osteoderms (1), or half the tail (2), less or absent (3)	MUELLER-TÖWE
162	Ventral osteoderms in six longitudinal rows (0), or in four rows (1) or no ventral osteoderms (2)	MUELLER-TÖWE
163	Dorsal osteoderms without keel (0), or keel only developed level with or after the pelvic girdle (1), or with well developed keel anterior to the pelvic girdle (2)	MUELLER-TÖWE
164	Osteoderm surface covered by small round to ellipsoid pits in very dense equal distribution (0), or by large round to ellipsoid pits but in high density (1), or by irregular large pits (2)	MUELLER-TÖWE
165	Ventral osteoderms quadratic in shape (0), or rhombic (1)	MUELLER-TÖWE
166	Dorsal armour starts at the level of the 3. cervical vertebra (0), or at the level of the 4./5. cervical vertebra (1), or after the 7. cervical vertebra (2)	MUELLER-TÖWE
167	Ventral armour present (0), or absent (1)	MUELLER-TÖWE
168	Sclerotic ring (also partly) in orbit present (0), or absent (1)	MUELLER-TÖWE
169	Premaxilla teeth three (0),or four (1), or five (2)	MUELLER-TÖWE
170	Number of teeth in the maxilla: less the fifteen (0), fifteen to twenty (1), twenty-one to thirty (2) thirty-one-forty (3), more than forty (4)	MUELLER-TÖWE
171	Axis with parapophysis and diapophysis for the second cervical rib (0), or only parapophysis for the second cervical rib (1)	MUELLER-TÖWE
172	Cervical centra in ventral view: hourglass-shaped with a well-developed midline ridge in anteroposterior direction (0), or with reduced or absent midline ridge (1)	MUELLER-TÖWE
173	Length/width proportion of supratemporal fenestra: quite longer than wide, shape ellipsoid or rectangular (0) or about equal in size, shape round or quadratic (1)	MUELLER-TÖWE
174	Shape of supratemporal fenestra: mainly ellipsoid (0) or mainly rectangular (1)	MUELLER-TÖWE
175	Percentage of rostral length to skull length: less than 60% (0) or 60-75% (1) or more than 75 % (2)	MUELLER-TÖWE
176	Suborbital fenestra elongated and anterior acute angled (or sigmoid) (0) or round (1)	MUELLER-TÖWE
177	Shape of alveoles in the maxilla: round (0), or ellipsoid (1)	MUELLER-TÖWE
178	Size of prefrontal: half of size of lacrimal (0), equal size of lacrimal (1), or double or more in size than lacrimal (2)	MUELLER-TÖWE
179	Teeth in maxilla without cutting edge (0), or with one smooth (1), or with two smooth (2), or with serrated edge (3)	MUELLER-TÖWE
180	Scapula length: bigger than coracoid length (0), or equal in size (1), or smaller than coracoid length (2)	MUELLER-TÖWE
181	Lateral edge of maxilla in lateral view: smooth (0), or undulating parallel to alveoles (1)	MUELLER-TÖWE
182	Shape of teeth : slender, conical, pointed and apically recurved (0), or blunt and broad (1), or laterally compressed (2)	MUELLER-TÖWE
183	Ilium shape: mainly rectangular with well-developed posterior and anterior process (0), or rectangular with anterior process, but posterior process reduced or absent (1), or mainly triangular (2)	MUELLER-TÖWE
184	Number of teeth in the dental: less than twenty (0), twenty-one to thirty (1) thirty-one to forty (2) more than forty (3)	MUELLER-TÖWE
185	Humerus shape: humerus broadened proximally with well-developed humerus head (0), or humerus slender, slightly s-shaped, without well-developed humerus head (1)	MUELLER-TÖWE
186	Alignation of alveoles in maxilla: strictly ventrally aligned (0), or mainly laterally aligned (1)	MUELLER-TÖWE
187	Ratio humerus length to femur length in percentage: about 100%-80% (0) about 79-55% (1) less than 54% (2)	MUELLER-TÖWE
188	Prefrontal lateral edge is concave to straight and constricted orbit laterally (0), or lateral edge is convex and overlaps orbit (1)	MUELLER-TÖWE
189	Dorsal armour present (0), or absent (1)	MUELLER-TÖWE

Appendix VI

Data matrix Thalattosuchia

#NEXUS begin data; dimensions ntax=30 nchar=189; format missing=? symbols="01234"; ; matrix

ANCESTOR

00000 00000 00000 00000 00000 00000
00000 00000 00000 00000 00000 00000
00000 00000 00000 00000 00000 00000
00000 00000 00000 00000 00000 00000
00000 00000 00000 00000 00000 00000
00000 00000 00000 00000 00000 00000
00000 0000

Geosaurus vignaudi

11(12)?0 (12)?1?? 0111? 101?0 1001? 001?0
?11?0 0???? ????? ????? ????? ?????
????3 0(23)0?? 11??1 ?(12)?0? ????? ?????
?0??? ????0 ?1?00 ?001? 0000? 0????
?1??2 ??1?? ??1?(1?) ?1101 ????? 02?01
????? ????2 32??? ?10?1 0000? ?020?
00??? ??11

Geosaurus giganteus

?10?? ????? 0?11? 1?1?0 10011 10???
?11?? 0???? ????? ????? ????? ?????
????3 120?? ????? ??000 0???? ?????
????? ????0 ???00 ?01?? 0000? 10??0
?1??? ????? ????? ???0(1?) ????? ???00
????? ????2 32??? ?10?? ??00? ?12(12)?
02??? ??11

Geosaurus gracilis

110?0 1?101 0011? 10120 10011 000?0
01111 02001 10000 ?1020 01?10 11101
?1?03 (01)100? 11?11 ?2000 0???? ??1??
????? ????0 ???00 ?0000 00001 0?000
?1?02 01101 ?110? ?1101 21010 02100
?0??? ????2 32??? ?1001 ??001 0?20?
00??? ??11

Geosaurus suevicus

011?0 2?10? 01111 10100 10011 000?0
011?0 02??? 1???? ????? ????? ?11??
?1??3 030?? 1?011 ?2000 01221 1110?
?000? ????0 ?1?00 ?0001 0000? 000??
01002 011(1?)(12) ?1101 ?110(1?) ????? 02101
?002? 11002 32??? ?10(01)2 0?00? ?0222
00??? ??11

Machimosaurus hugii

?0??0 0?111 0011? 111?0 1001? 000?0
01110 02110 1?000 00?21 01?10 111?1
?1?03 1?0?? ????? ??10? ???1? ??1??
?00?? ????? ???0? ????? 10?01 ??000
?0??2 0?1?(1?) (1?)110? ??11(1?) 211?? 10110
????? ????? ????? ?(0?)102 ??011 0001?
?1??? ??00

Metriorhynchus hastifer

111?0 1110? 0011? ??1?0 10011 000?1
0111? 02?0? ????? ???1? ???1? ?1???
?1??3 1(23)01? ????1 ??000 0?0?1 ?11??
?000? ????? ????0 ?000? 0000? ?00??
01002 0?1?(1?) ?110? ???01 31?10 0??0(01)
??20? 11??2 32??? ?100(12) 0000? 0021?
0?2?? ??11

Appendix VI

Metriorhynchus leedsi

011?0	1110?	0111?	??1?0	10011	000?1
0111?	02?0?	?????	???1?	???1?	?1???
?1??3	1(23)01?	?0011	?2000	02021	111??
?000?	?????	???00	?0001	00000	100??
01002	0?1?1	?110?	?1101	31?10	02?01
??20?	11002	32???	?1003	0000?	01210
0?2??	??11				

Metriorhynchus superciliosus

111?0	1110?	0011?	??1?0	10011	000?1
0111?	02?0?	?????	???1?	???1?	?1???
?1??3	1(23)01?	3???1	??000	02(12)21	111??
?000?	?????	???00	?0001	00000	100??
01002	0?1?1	?110?	?0101	31?10	02?01
??20?	11??2	32???	?1002	0000?	0121(12)
0?2??	??11				

Pelagosaurus typus

21(01)10	1?111	00111	11120	10010	000?0
01110	02110	10000	00110	11110	01001
?1?03	12020	(13)1000	?2100	01021	11100
?0001	10001	10000	00100	2000(01)	00000
10002	01101	0110?	00000	11120	1110(01)
0000?	01??1	31000	000(01)3	0000(12)	00100
00121	0200				

Platysuchus multiscrobiculatus

21211	1?111	0011?	11120	10010	001?0
01110	021??	?????	???1?	?????	?1??1
?1?03	1(23)0??	31???	???00	02101	111?0
?0001	10011	0000?	001??	1000?	000?0
00002	?1101	?11??	?(01)101	????0	10110
??02?	10000	10200	0010(34)	1?01(12)	??001
00021	?100				

Steneosaurus bollensis

11211	11111	00111	11120	1(01)010	001?0
01110	02110	10000	00110	01?10	01001
?1?03	1(23)0(02)0	31000	?2100	021(12)1	11100
?0001	20011	(01)0000	00100	10001	00000
10002	01101	0110?	01110	(12)0020	11011
00010	01(01)1(01)	20111	101(012)	(23)11011	000(01)1
00111	0100				

Steneosaurus boutilieri

11211	11111	0011?	11120	10010	000?0
01110	02110	10000	0?110	?1110	01?01
?1?03	12000	31?00	?2100	02121	111?0
?0001	(12)00?1	(01)0000	00100	10001	00000
10002	01101	0110?	01110	(13)1100	?0011
0????	?1???	201??	?01?2	1?011	000??
?0???	1?00				

Steneosaurus brevior

11211	01111	0011?	11120	11010	001?0
01110	02110	11000	0?110	01110	?1?01
?1?03	1(12)020	31?00	?2100	0????	?????
?????	?????	??00?	?01??	10001	00000
?0??2	01101	0110?	01110	100?0	20110
01???	?????	?????	?0102	1?011	00(01)??
0??1?	0?0?				

Appendix VI

Steneosaurus edwardsi

112?1	11111	0011?	11120	10010	00??0
01110	021?0	10000	0?110	01?10	?1?01
?1?03	12000	31?00	?2100	02121	11100
?0001	(12)00?1	(01)0000	?0100	20001	00000
10002	01101	0110?	01110	?(1?)???	11011
01???	?1?1?	??1??	?01?2	??01?	??0??
?0?(12)?	??00				

Steneosaurus gracilirostris

11(01)10	0?111	0011?	11120	10010	001?0
01110	02110	10000	01110	?1?10	?1?01
?1?03	1(12)0(02)0	31?00	?2?00	021??	???00
?0001	(12)00?1	(01)??0?	??1??	10001	00000
?00?2	01101	?110?	01100	100?0	2010(01)
0????	????0	??110	001?4	??002	0?0??
00?3?	0?00				

Steneosaurus heberti

11211	(01)1111	0011?	11120	10010	001?0
01110	021?0	10000	0?110	01?10	?1001
?1?03	120?0	31000	?2100	02121	11100
?0001	?00?1	(01)0?00	00100	10001	00000
10002	01101	0110?	01110	???10	10011
00???	?????	?01??	?01?4	1?011	??0(12)?
(01)0???	0?00				

Steneosaurus leedsi

11211	(01)1111	0011?	11120	10010	001?0
01110	02110	10000	01110	01?10	?1001
?1?03	12000	31000	?2100	02121	11100
?0001	200?1	(01)0?00	00100	10001	00000
10002	01101	0110?	01110	111?0	10011
0022?	11010	?01(01)?	?0114	1?011	0?0?1
?01(23)1	0200				

Steneosaurus baroni

11211	1?111	00111	?1120	10010	00??0
?1110	021?0	10000	00110	11110	01001
?1?03	12000	31000	?2100	02121	11100
?0001	200?1	(01)0000	00100	10001	00000
?1002	?1101	0110?	?1110	?????	???11
?1???	?????	?01??	??1??	1?01?	?0???
1??2?	????				

Steneosaurus priscus

11211	1?111	0011?	11??0	10010	00??0
01110	021?0	1???0	00110	11110	01001
?1?03	12000	31000	?210?	?2121	11100
?0001	200?1	(01)0000	00100	10001	00000
?1002	?1101	?110?	?1?10	?????	???11
?????	????1	(23)01?0	??1(01)?	1?01?	?????
???1?	????				

Steneosaurus megarhinus

??211	11111	0011?	?1???	?????	?????
?????	?2??0	?????	?????	?????	?????
?1???	1????	?1???	??10?	?????	?????
?????	?????	???0?	?0??0	1??01	0????
?1??2	?11?1	?11??	?????	?????	2?1??
?????	?????	?????	???1?	?????	?0???
(01)????	????				

Appendix VI

Steneosaurus pictaviensis

112??	????1	0011?	11120	1?01?	000?0
?1110	02?00	11000	??110	?1010	01001
?1?13	?300?	?????	?2?0?	0????	?????
?000?	?????	???00	?01?0	10001	00000
?0???	0?101	?110?	01100	0111?	???(01)1
?????	?????	?????	????3	??01?	000??
00?2?	0?0?				

Teleidosaurus calvadosi

11??0	0?111	0011?	1?1?0	10011	1?0?1
0111?	02???	?????	?????	?????	?????
?1??3	130?0	31010	?(12)0?0	0????	?????
?????	?????	?0??0	?0000	0000(1?)	?????
?1??2	??1?1	?11??	?1001	?????	12100
00???	?????	?????	???01	??11?	?00??
1??1?	0?1?				

Teleidosaurus gaudryi

11??0	??1?1	0111?	101?0	1?01?	1?0??
01???	02???	?????	???1?	?????	?????
????3	?20??	?????	???0?	0????	?????
?????	????0	?????	?????	000??	0???0
?1??2	011?1	?11??	?1?01	?????	???01
?????	?????	3????	?1?01	???11	?110?
02?1?	??11				

Teleosaurus cadomensis

10211	?11?1	00111	11120	11010	00(01)?0
11110	02000	00000	?1111	01110	01011
?(01)?13	?(23)00?	?????	???0?	?2121	1110?
?0001	100?1	(01)0000	00100	10001	00000
?10?2	0(01)101	1110?	11110	001(01)0	???10
?????	?????	?010?	?01(12)3	??112	010??
0????	0?00				

Dakosaurus maximus

111?1	1?10?	0111?	??1?0	10011	0?0??
011??	0????	?????	?????	?????	?0???
????3	130??	????1	?0000	?????	?????
?000?	?????	???1?	?0010	0(1?)00?	100??
?1??2	??1??	???(1?)?	??101	1????	?0211
0????	?????	?????	?1000	??0(12)0	?1230
?2???	1?11				

Gracilisuchus

00000	0?10?	0000?	00000	00?00	00000
0000?	0??0?	0?000	00?00	0???0	000?0
???00	001?1	10000	?0000	0000?	0???0
000?0	20000	0????	?????	?????	????1
00??0	?1002	?00??	?????	?????	?????
?????	?????	?????	?????	?????	?????
?????	????				

Protosuchus

10000	20110	10000	10021	00100	00001
01010	00101	0?002	01001	11111	00101
01101	011?1	10110	01101	01000	11100
000?1	20001	00000	0000?	0200?	00001
00?01	??000	?01??	??001	?????	02?00
0?1(01)?	20112	100?0	?0110	??10?	??1?0
??0?0	??00				

Appendix VI

Dyrosaurus

011??	1?101	?010?	11?00	10001	1?10?
00110	12?10	10100	11120	11?10	11?10
?10?0	1311?	3?00?	?2?00	0????	????0
?00??	????1	?????	?????	?????	????1
00?12	0000(01)	?110(1?)	1?100	10??1	02001
??02?	?0???	???20	?011?	??011	011?0
121??	0?00				

Pholidosaurus

201??	11101	??11?	11101	10011	1?001
00010	0211?	10000	11121	11?10	1??10
?100?	1300?	300??	?2?0?	??11?	1???0
??0??	2?0??	?????	?????	?????	?????
?????	?????	?????	?????	?????	?????
?????	?????	?????	?????	?????	?????
?????	????				

; endblock;